Reservoir characterisation using macromolecular petroleum compounds including asphaltenes: A case study of the Heidrun oil field in the Norwegian North Sea

von Diplom-Geologin
Katja Theuerkorn
aus Leipzig

von der Fakultät VI – Planen Bauen Umwelt
der Technischen Universität Berlin
zur Erlangung des akademischen Grades

Doktor der Naturwissenschaften
Dr. rer. nat.

genehmigte Dissertation

Promotionsausschuss:

Vorsitzender: Prof. Dr. rer. nat. Gerhard Franz
Berichter: Prof. Dr. Brian Horsfield
Berichter: Prof. Dr. rer. nat. Jan Schwarzbauer

Tag der wissenschaftlichen Aussprache: 30.04.2012

Berlin 2012
D 83

CONTENT

ABSTRACT

The present thesis is part of the industry partnership project “BioPets Flux” between the GFZ Potsdam and the industry partners BG Group, Devon Energy, ExxonMobil, Petrobras, Repsol YPF, Shell, and Statoil. The study aims at improving predictions of reservoir alteration post-filling, and enhancing the understanding of reservoir charge history.

The original composition and the volume of petroleum in reservoirs are often subjected to post-filling alteration processes, in many cases to variable degrees due to the reservoir compartmentalization. Such alteration processes, e.g. biodegradation or water washing, have strong economic consequences since they lead to a decrease in oil quality and producibility.

The focus of this thesis was on the total macromolecular petroleum fraction of reservoir rocks (including asphaltenes) and individual asphaltene fractions separated from oil-stained reservoir rocks. Asphaltenes contain structural and maturity related information of the source, and have been assumed to be unaffected by biodegradation or water washing. Thus, pyrolysis of asphaltenes should provide the unaltered oil fingerprint, allowing the source characterisation as well as the estimation of alteration and charge processes.

The thesis outlines detailed screening results of the Heidrun reservoir (Norwegian North Sea) and a method developed for asphaltene separation with the main focus on reproducibility and linearity. For the screening a sample set comprising 141 reservoir rocks and 31 single asphaltenes was investigated using open system pyrolysis-GC and bulk pyrolysis in order to detect lateral and vertical compositional variabilities in the Heidrun oil field. Parameters known from kerogen typing studies and newly developed parameters were applied to both the total macromolecular petroleum fraction and the single asphaltenes. Direct correlations were found between the aromaticity of the total macromolecular petroleum fraction and biodegradation. Gradients and regularities in the pyrolysate composition could be correlated to differences in the biodegradation level of oil charges achieved in the field, and their mixing. In the northern part of Heidrun a lacustrine source is suspected, while the main part of the oil field shows indications for a marine source.

The asphaltene screening reflects the gradients of their corresponding reservoir rocks and indicate so a possible influence of biodegradation on asphaltenes. MSSV pyrolysis experiments were applied to single asphaltene samples in order to use their compositional kinetic information’s for the delineation of reservoir heterogeneities. The Asphaltene compositional information’s indicate differences concerning the source maturity and mixing effects of oils generated from different sources.

ZUSAMMENFASSUNG

Die vorliegende Arbeit ist Teil des Industriepartner Projektes „BioPets Flux“ zwischen dem GFZ Potsdam und den Industriepartnern BG Group, Devon Energy, ExxonMobil, Petrobras, Repsol YPF, Shell und Statoil. Ziele der Arbeit sind es Vorhersagen von Alterationsprozessen in Erdöllagerstätten zu verbessern sowie das Verständnis über die Befüllung zu vertiefen.

Die ursprüngliche Zusammensetzung sowie das Volumen von Erdöl in einer Lagerstätte sind häufig durch Prozesse, wie Biodegradation oder Auswaschung alteriert und dies oft zu unterschiedlichem Maße in den einzelnen Lagerstättensegmenten. Solche Alterationsprozesse sind von großer ökonomischer Bedeutung, da sie die Qualität und den Wert des Öls mindern.

Im Fokus dieser Arbeit steht das gesamte im Reservoirgestein enthaltene makromolekulare organische Material (inklusive Asphaltene) sowie Asphaltene als separierte Phase. Asphaltene zeigen eine sehr ähnliche Struktur wie das Kerogen aus dem sie gebildet wurden und gelten als resistent gegenüber Alterationsprozessen, wie Biodegradation oder Auswaschung. Mittels der Pyrolyse von Asphaltenen können Teile der ursprünglichen Erdölzusammensetzung der jeweiligen Ölchargen rekonstruiert werden, wodurch sie zur Muttergesteinscharakterisierung sowie zur Charakterisierung des Alterationszustandes und der Befüllung genutzt werden kann.

Die Arbeit präsentiert die Ergebnisse des detaillierten Reservoir-Screenings des Heidrun Ölfeldes (Norwegische Nordsee) sowie eine reproduzierbare und lineare Methode zur Asphalten Fällung. Für das Screening wurden 141 Reservoirgesteinsproben und 31 Asphaltene mittels Pyrolyse-GC und Bulk-Pyrolyse analysiert, um laterale und vertikale Heterogenitäten in der Erdölzusammensetzung zu erfassen. Das makromolekulare organische Material der Reservoirgesteine und die separierten Asphaltene wurden mittels bekannter Parameter zur Kerogentypisierung sowie neu entwickelten Parametern charakterisiert.

Im Norden des Heidrun Ölfeldes gibt es Hinweise auf eine lakustrin beeinflusste Quelle, während der Hauptteil des Erdöls von einem marinen Muttergestein gebildet wurde. Die Aromatizität und Gaszusammensetzung der Reservoirgestein Pyrolysate zeigen einen direkten Zusammenhang zur Biodegradation. Die detektierten Gradienten in der Zusammensetzung der Pyrolysate konnten mit Unterschieden bezüglich des Biodegradationslevel der Ölchargen die das Heidrun Ölfeld erreichten in Verbindung gebracht werden sowie deren Vermischung. Die Pyrolysate der Asphaltene reflektieren die Gradienten ihrer Reservoirgesteine und geben somit Hinweise so auf eine geringere Resistenz gegenüber Biodegradation als angenommen. Um die kompositionelle Kinetik von Asphaltenen zur Profilierung des Muttergesteins und zur Reservoircharakterisierung zu nutzen, wurden MSSV-Pyrolyse Messungen durchgeführt. Die Ergebnisse dieser Experimente zeigen Unterschiede bezüglich der Muttergesteinsreife und/oder deuten auf die Vermischung mit Ölen von anderen Muttergesteinen hin.

ACKNOWLEDGEMENTS

My particular thanks go firstly to my supervisor Prof. Dr. Brian Horsfield for the interesting theme within the “BioPets Flux” project, for his ideas and critical comments on several talks and reports, and for his patience in explaining me a part of the world of organic chemistry. He is especially thanked for his support is the last month of my work. Thoughtful reviews and critical comments by Prof. Dr. Rolando di Primio concerning the kinetic part supported the success of this study. Many thanks go to all Industry Partners for the pleasant cooperation, and in particular to Statoil and Shell for providing sample material. The possibility to present the results of this study at conferences and to publish parts of the work is gratefully acknowledged.

Thanks go to Dr. Raingard Haberer for her helpful suggestions on various drafts for reports, and the nice time we spend on several official trips and to Dr. Eric Lehne for his support at the beginning of my work. This work has benefited from several discussions and help of many colleagues within the Organic Geochemistry Section at GFZ Potsdam, especially Ferdinand Perssen and his support in the Pyrolysis laboratory as well as Anke Kaminsky and Conny Karger for their help in the wet-chemical laboratory. The entire team at GFZ provided an excellent working environment. Thanks to all of you!

I am grateful to my friends Alexandra Vetter, Dr. Clemens Glombitza, and Nicolaj Mahlstedt for their mental and moral support to survive the last years, for their helpful discussions at several beers, and for all the wonderful adventures and great times we had in Berlin. How beautiful that you exist. Thanks go to my room mates Dr. Stefanie Pötz and Phillip “Daniel” Kuhn for the wonderful uncomplicated working atmosphere, helpful comments and funny times we had.

Infinite thanks go to my partner Alexander Schubert who supported me through the whole PhD thesis with his tolerant character to stand all my moods, the confidence, and all the ways he found to keep me going on with the thesis. Special thanks to my parents Peter and Sigrid Theuerkorn, and my sister Conny for their support in the last years.

LIST OF FIGURES

LIST OF TABLES (IN THE TEXT)

LIST OF TABLES (IN THE APPENDIX)

LIST OF PUBLICATIONS AND PRESENTATIONS

JOURNALS

THEUERKORN, K., HORSFIELD, B., WILKES, H., DI PRIMIO, R. AND LEHNE, E. (2008): A reproducible and linear method for separating asphaltenes from crude oil. *Organic Geochemistry, Advances in Organic Geochemistry 2007 - Proceedings of the 23rd International Meeting on Organic Geochemistry 39*, 929-934.

CONFERENCE PAPERS

THEUERKORN, K., HORSFIELD, B., DI PRIMIO, R. AND WILKES, H. (2007): Using Asphaltenes to reconstruct the original charge compositions and volumetrics of petroleum in reservoir compartments. *23rd International Meeting on Organic Geochemistry (IMOG), Torquay/England, (09-14/09/2007).*

THEUERKORN, K., HORSFIELD, B. AND DI PRIMIO, R. (2009): Using asphaltene pyrolysates to build compositional kinetic models of petroleum formation. *11th Norwegian Meeting of Organic Geochemistry (NMOG), Stavanger/Norway, (23-24/10/2008).*

THEUERKORN, K., HORSFIELD, B., DI PRIMIO, R., HABERER, R.M. AND VIETH, A. (2009): Charakterisierung von Heterogenitäten in Erdöllagerstätten mittels Asphaltenen. *DGMK / ÖGEW Spring Meeting, Celle/Germany, (27-28.04.2009).*

THEUERKORN, K., HORSFIELD, B. AND DI PRIMIO, R. (2009): Characterisation of heterogeneities in petroleum reservoirs using the composition of macromolecules *24th International Meeting on Organic Geochemistry (IMOG), Bremen/Germany, (06-11/09/2009).*

PRESENTATION AT INTERNATIONAL SYMPOSIA

THEUERKORN, K., HORSFIELD, B., DI PRIMIO, R. AND WILKES, H. (2007): Petroleum Asphaltenes in Reservoir Compartments - PARC - Using asphaltenes to reconstruct the original charge composition and volumetrics of petroleum in reservoir compartments. *23rd International Meeting on Organic Geochemistry (IMOG), Torquay/England, (09-14/09/2007)* (poster presentation).

THEUERKORN, K., HORSFIELD, B. AND DI PRIMIO, R. (2009): Using asphaltene pyrolysates to build compositional kinetic models of petroleum formation. *11th Norwegian Meeting of Organic Geochemistry (NMOG), Stavanger/Norway, (23-24/10/2008).* (Oral presentation).

THEUERKORN, K., HORSFIELD, B., DI PRIMIO, R., HABERER, R.M. AND VIETH, A. (2009): Charakterisierung von Heterogenitäten in Erdöllagerstätten mittels Asphaltenen. *DGMK / ÖGEW Spring Meeting, Celle/Germany, (27-28.04.2009).* (Oral presentation).

LIST OF PUBLICATIONS AND PRESENTATIONS

THEUERKORN, K., HORSFIELD, B. AND DI PRIMIO, R. (2009): Characterisation of heterogeneities in petroleum reservoirs using the composition of macromolecules *24th International Meeting on Organic Geochemistry (IMOG), Bremen/Germany, (06-11/09/2009)* (poster presentation).

ORAL PRESENTATIONS *(internal)*

THEUERKORN, K., HORSFIELD, B., DI PRIMIO, R. AND LEHNE, E. (2007): BioPets Flux - PARC - Petroleum Asphaltenes in Reservoir Compartments. *1st IPP Meeting Potsdam, 09/07.*

THEUERKORN, K., HORSFIELD, B., DI PRIMIO, R. AND LEHNE, E. (2008): Application of the PhaseKinetics Approach to Asphaltenes and Oil Asphaltene Characterisation from Heidrun Oil field. *2nd IPP Meeting Potsdam, 04/2008.*

THEUERKORN, K., HORSFIELD, B. AND DI PRIMIO, R. (2008): Heterogeneity screening of the Heidrun oil field. *3rd IPP Meeting Potsdam, 10/08.*

THEUERKORN, K., HABERER, R.M., HORSFIELD, B. AND DI PRIMIO, R. (2009): Characterisation of heterogeneities in petroleum reservoirs using the composition and distribution of high molecular weight polar compounds. *4th IPP Meeting Potsdam, 04/09.*

THEUERKORN, K., HORSFIELD, B., DI PRIMIO, R. AND HABERER, R.M., (2009): Using macromolecules for studying heterogeneities in petroleum reservoirs. *5th IPP Meeting Potsdam, 09/09.*

INTERNAL REPORTS FOR THE INDUSTRY-PARTNERS (*unpublished***)**

1st ANNUAL REPORT (10/2007)
2nd ANNUAL REPORT (01/2009)
3rd ANNUAL REPORT (06/2010)

ABBREVIATIONS

A	Frequency Factors
API gravity	Specific Gravity scale developed by the American Petroleum Institute (141.5 / SG at 60°F) - 131.5
ASE	Accelerated Solvent Extractor
ASTM	American Association for Testing Materials
av	Average
b_o	Petroleum Volume Factor
CLD	Alkyl Chain Length Distribution
d	Darcy
DCM	Dichloromethane
Δm/z	Mass/Charge Ratio (dimensionless)
DMN	Dimethylnaphthalene
DST	Drill Stem Test
DT *(Δt)*	Interval Transit Time
EA	Activation Energy
E_{mean}	Mean Activation Energies
FID	Flame Ionisation Detector
Fm.	Formation (geological)
GOC	Gas-Oil Contact
GR	Gamma Ray
H/C	Hyrogen / Carbon Atomic Ratio
HCL	Hydrochloric acid or hydrogen chloride
HF	Hydrofluoric acid or hydrogen fluoride
HI	Hydrogen Index
HMPLC	Heterocompound-Medium Pressure Liquid Chromatography
HMWF	High Molecular Weight fraction
IOR	Improved Oil Recovery
IPP-report	Industry-Partner-Project
K	Permeability
LWD	LoggingWhile Drilling
m	Meter
md	Millidarcy
MeOH	Methanol
MPLC	Medium Pressure Liquid Chromatography
MD-RKB	Measured Depth - Rig Floor Kelly bushing
MN	Methylnaphthalene
mPa*s	Mega Pascal*second
MWD	Measurement While Drilling
N	North
NGL	Narural Gas Liquids
NPD	Norwegian Petroleum Directorate
NPHI (Φ_N)	Neutron Density
NSO-1	Norwegian Standard Oil - 1
NSO compounds	Nitrogen, Sulphur and Oxygen Compounds
NMR	Nuclear Magnetic Resonance

OI	Oxygen Index
OM	Organic Matter
ODT	Oil Down To
OSPP	Organic Sulphur Pyrolysis Products
OUT	Oil Up To
OWC	Oil-Water Contact
Φ(phi)	Porosity
Φ_S	Sonic-Derived Porosity
PEG	Polyethylenglycol
PI	Production Index (S1/S1+S2)
PNA	Paraffinic-Naphthenic-Aromatic
P_{sat}	Saturation Pressure
PVT	Pressure Volume Temparature
RCE	Reservoir Cor Extracts
RHOB (*ρb)*	Bulk Density
R_0	Vitrinite Reflectance
RT	Resitivity
S	South
SP	Spontaneous Potential
SRA	Source Rock Analyzer
STABW	Standard Deviation
STB	Stock Tank Barrel
STDV	Standard Deviation
S_w	Water Saturation
$S_{w\,irr}$	Irreducible Water Saturation
S1	Total Thermovaporised Compounds
S2	Pyrolysis Products
TLC - FID	Thin Layer Chromatography - Flame Ionisation Detector
TOC	Total Organic Carbon
TR	Transfomation Ratio
TVD-SS	True Vertical Depth - Sub Sea Level
UCM	Unresolved Compound Mixture
vol% -	Volume Percentage
WCSB	Western Canada Sedimentary Basin
WUT	Water Up To

1 INTRODUCTION

1.1 PETROLEUM RESERVOIRS

1.1.1 GENERAL CHARACTERISTICS

Petroleum reservoirs are sedimentary rock bodies in the subsurface, which are able to accumulate large volumes of petroleum when specific conditions are fulfilled. Essential prerequisites for reservoir rocks are suitable porosity (typically 10 - 25 %) and permeability (typically 1 - 1000 md), to store and transmit petroleum fluids. The reservoir rock has further to be overlain by a low permeable cap rock, and to be within a trap structure to prevent escape of petroleum. The trap has to be in place before the oil generation commences as well as accessible to hydrocarbons migrating from mature source rocks (described by many authors e.g. Bjørlykke, 1989; Killops & Killops, 2005).

Hydrocarbon traps are usually classified into two main groups, structural and stratigraphic traps (described by many authors e.g. Bjørlykke, 1989; Selley, 1997). Structural traps are very common and primarily formed by tectonic deformation of reservoir beds after their deposition. Typical structural traps are anticlines, folds and faults. The petroleum is trapped below impervious strata because outward flow would require movement opposed to the direction of buoyant forces. Nevertheless, if petroleum is generated in sufficient amounts it can fill the trap and excess volumes can then spill out. A variety of structural traps can be associated with salt domes. Halokinetic movements (salt tectonic) can form very effective traps when the salt deposit thickness exceeds 100 - 200 m, e.g. the Permian Zechstein salt sediments in the Ekofisk area in the North Sea (Bjørlykke, 1989). Stratigraphic traps are depositional features in which the porous reservoir unit is surrounded by less porous and permeable rocks such as shale or limestone preventing the outflow of petroleum. Typical cap rocks such as shale are often slightly leaky with respect to gas and thus the smaller molecules present in gases can escape through narrower pores than oil components (Killops & Killops, 2005).

Well-sorted sandstones with low clay and silt content, fractured carbonates, oolitic limestone or reefs commonly provide suitable reservoir characteristics. More than 60 % of all petroleum occurrences are in clastic rocks, while carbonate reservoirs account for the rest (Killops & Killops, 2005). 40 % of the worldwide oil and gas produced are found in carbonate reservoirs including the large oil fields in the Middle East, e.g. the Ghawar or Burgan field (Bjørlykke, 1989).

Most reservoir rocks were deposited under oxidising conditions in aquatic environments and originally contained little organic material. The mapping of sedimentary facies is vital for delimiting potential prospecting targets. Typical environments for well-sorted sandstone depositions are beaches and shorefaces, tidal flats, deltas or fluvial channel of braided river systems. The depositional environment largely determines the initial vertical and horizontal variability in porosity and permeability, and so consequently the physical extent of the reservoir rock. Carbonate reservoirs largely consist of shallow marine carbonate deposits on shores or shelves, and their extension is mainly depending on ecological sea conditions. Sufficient porosity and permeability are mainly created after deposition by formation of fractures or solution of carbonate minerals, which are more soluble than silicate minerals (Bjørlykke, 1989).

Petroleum reservoirs are commonly far from homogeneous due to lithological differences and unconformities in the strata, and/or they are stressed by tectonic deformation. This may lead to the formation of different compartments in the reservoir, which have a considerable influence on the reservoir filling and the in-reservoir communication. Knowledge of structural compartmentalisation in the reservoir is of paramount importance as it has a large impact on oil and gas production.

1.1.2 PETROLEUM MIGRATION AND RESERVOIR FILLING

The petroleum has to migrate from low porosity fine-grained source rocks into the pores of coarser and more permeable reservoir rocks to create economically viable accumulations. Only in some special cases are source rock and reservoir rock identical, e.g. in the Miocene Monterey Formation in California (Bjørlykke, 1989) and further in many unconventional petroleum systems, e.g. in the Barnett Shale of the Forth Worth Basin in Texas (Jarvie *et al*., 2007). Primary migration is defined as the movement of petroleum from the source rock into adjacent porous and permeable strata. The distance involved is typically up to 1 km (England

et al., 1987). Secondary migration is the subsequent transfer process of petroleum through carrier beds into the reservoir. The expelled petroleum may coalesce into larger stringers or globules within the carrier rock and travel large distances, until it escapes to the surface or is trapped by an impermeable barrier (Tissot & Welte, 1984). Less permeable rock layers hinder upward migration, thus secondary migration generally occurs along permeable strata in the direction of decreasing pressure. The distance involved in secondary migration is usually up to 100 km laterally and 2 km vertically, but depends on volume, type of petroleum and carrier rocks involved (England *et al.*, 1987). Extensive vertical migration generally requires suitable pathways produced by large-scale faulting (Killops & Killops, 2005). The process of petroleum migration into the reservoir is a relatively fast process compared to the time necessary for formation or even storage of hydrocarbons (Tissot & Welte, 1984). The size of an oil accumulation is related to the area of the source rock from which it was generated (the drainage area) and hence to migration distance.

The upward movement of petroleum has strong effects on the petroleum composition and the phase behaviour of the subsurface fluids, due to changes in temperature and pressure conditions. Two phases usually coexist under subsurface conditions: gas-saturated petroleum liquid and oil-saturated petroleum gas. Their phase behaviour mainly determines petroleum fluid properties, density and viscosity. The density is a pressure dependent constant and is mainly influenced by the quantity of gas compounds dissolved in the liquid phase (oil), known as the gas : oil ratio (GOR). With increasing pressure, the dissolution of additional low molecular weight components lowers the average molecular weight of the petroleum liquid and thus its density, which results in increasing GOR. Thus, higher GOR fluids exhibit lower densities and *vice versa*. The density of the subsurface fluids influences the direction of migration, while the stability of the interface between two phases is related to the ratio of their viscosities. The viscosity is a temperature dependent constant and decreases with increasing temperature. It has a major influence on the mobility of petroleum, the speed with which a fluid flows through a rock with a particular pressure gradient, and permeability. Liquid - and gas properties become less similar with increasing vertical migration (England *et al.*, 1987).
The driving forces controlling secondary migration are buoyancy, capillary pressure and hydrodynamic flow (England, 1989; England *et al.*, 1987). On large scale the buoyant rise guiding the petroleum in water-wet porous rocks on average up-dip, because the specific gravities of oil (0.7 - 1.0 kg/m^3) and gas (< 0.0001 kg/m^3) are lower than aqueous pore fluids (Tissot & Welte, 1984). As the mutual solubility for the most hydrocarbons and water is

below < 1 ppm, the petroleum phase will be saturated with respect to water and transported as a separate phase. Only a small proportion is transported dissolved in pore water (Bjørlykke, 1989). On a local scale capillary forces will dictate the migration direction of petroleum as coarser regions of the carrier bed with the lowest pore-entry pressure will be favoured (England *et al.*, 1987). Reservoir rocks commonly exhibit lower capillary pressures than cap rocks preventing the oil from flowing through the cap rock, because the capillary force is stronger than the buoyancy of oil in water.

Migration behaviour further depends on the physical rock properties of the carrier beds and reservoir rocks. Of major importance are the porosity, permeability and water saturation as well as the reservoir rock lithology. The porosity and permeability control the reservoir *in-situ* hydrocarbons volume and are responsible for how easily hydrocarbons will flow in and out of them. The porosity Φ can be defined as the ratio of voids to the total volume of rock and is represented by a decimal fraction or percentage. The *total porosity* describes the total volume of pore space in the rock, while the *effective porosity* is more important for the fluid movement, because it describes the connected pore space in which the fluid might flow through. The permeability K is an expression of the ability of rocks to transmit fluids. It is a rock specific constant depending on the size of pore spaces and the connecting passages between pores, called pore throats or capillaries. K is a proportionality-constant in Darcy's law and is usually measured in Darcys (1 d = $9{,}869*10^{-9}$ cm^2) or millidarcys (md). The *absolute permeability* describes the ability of a rock to transmit a single fluid (single-phase flow), on the condition that it is totally saturated with the given fluid, while the *effective permeability* refers to the ability of a rock to transmit one fluid in the presence of another (multiphase flow) if the two fluids are immiscible (partial saturation). The ratio between both is the *relative permeability*. If the *relative permeability* of formation water is zero the reservoir formation produces water-free hydrocarbons. With increasing *relative permeability,* the reservoir formation produces increasing amounts of water relative to hydrocarbons (Asquith and Krygowski, 2004). In hydrocarbon reservoirs, permeability between 10 - 1000 md describes good to excellent reservoir conditions, while permeability below 10 md is negligible. However, reservoirs with a low permeability might also be exploited commercially, e.g. the Ekofisk field in the Norwegian North Sea due to fractures in the “dense” chalk matrix (Bjørlykke, 1989).

Water saturation and rock lithology mainly influence the poroperm properties. The water saturation S_w is the amount of pore volume in a rock that is occupied by formation water

(connate water). It is represented by a decimal fraction or percentage. Formation water, which is held by capillary forces in the pores and in the connecting passages between pores, may block or reduce the ability of other fluids such as hydrocarbons to move through the rock. When all formation water is adsorbed on grains in the rock or is held in place by capillary pressure, the term *irreducible water saturation* ($S_{w\ irr}$) is used (Asquith and Krygowski, 2004). The lithology describes the solid matrix of a rock in context with its primary mineralogy. For instance, sandstones are primarily composed of quartz grains, limestones are primarily composed of calcium carbonate, and shales mainly comprise clay minerals.

In the petroleum industry these rock properties are routinely and most effectively determined using well log techniques. Measurement while drilling (MWD) or logging while drilling (LWD) techniques are used since the 1980s. By continuous measurements in the uncased portion of the borehole, the rock properties gradual changes from one bed to the next are recorded (logged) (Asquith and Krygowski, 2004). The logs are recorded digitally at intervals of 3 to 15 cm (Bjørlykke, 1989). Different logging tools can be applied for the measurements, which use electric, nuclear or acoustic sources to create the log. The raw log data contains one or more curves related to the characteristic reactions from different rock types, which are subsequently interpreted to define the physical rock properties mentioned above. Logging data are quantitatively used for stratigraphic correlation, identification of the sedimentary facies, and depositional environment etc. (Bjørlykke, 1989). Qualitatively it is possible to evaluate properties of reservoir rocks for production purposes, e.g. to identify productive zones, their depth and thickness, to distinguish between oil, gas, and water in a reservoir, and to estimate hydrocarbon reserves (Asquith and Krygowski, 2004). Different interpretive methods can be used, including charts, cross-plots, and equations, e.g. Archie's equation to calculate S_w.

In the following, the most important logging tools are specified according their primary interpretation target. Spontaneous potential (SP) log and gamma ray (GR) log are both used primarily for the determination of the gross lithology. SP is a measure of the electric potential (current) between drilling fluid and pore water. SP logs in shales are calibrated as baseline, while permeable rocks (sandstones) show negative or positive record variations. Thus, the SP log can be used to distinguish permeable from impermeable beds and to detect bed thickness (Bjørlykke, 1989). GR is a measure of the natural radioactivity, which is elevated in shales (high GR signal). Shale-free sandstones and carbonates usually show low GR readings. However, sandstones with low shale content might also produce a high gamma ray response if

feldspar, glauconite or mica are abundant (Asquith and Krygowski, 2004). SP and GR logs are good indicators for the purity of sandstones, i.e. the degree of sorting or the clay content. They record characteristic coarsening upward and fining upward sequences very efficiently, which can be related to shallow marine and fluvial channels, respectively (Bjørlykke, 1989).
The three common log types generally referred to as porosity logs are the acoustic sonic log, and the nuclear measurements density log and neutron log. The sonic log specifies the interval transit time (Δt = DT) of a compressional sound wave through the borehole, which is dependent upon both lithology and porosity. In the presence of hydrocarbons the DT increases. This *hydrocarbon effect* has to be corrected, otherwise the sonic-drived porosity (Φ_S) is too high (Asquith and Krygowski, 2004). The density log displays the electron density of a formation. This electron density is related to the bulk density (ρ_b = RHOB) of the formation, which in turn is related to the porosity (Asquith and Krygowski, 2004). Neutron logs measure the hydrogen concentration within a formation. In shale-free formations, in which the pores are filled with oil or water, the neutron log defines the liquid filled porosity (Φ_N = NPHI). The logging tool emits neutrons, which will collide and/or become adsorbed on nuclei within the formation. Thereby they lose energy and emit gamma rays. Maximum energy loss occurs when the neutrons collide with hydrogen atoms. The NPHI is further used to distinguish between gas and oil, because gas has a lower hydrogen concentration compared to water and oil (Asquith and Krygowski, 2004).

The most important use of the resistivity log (RT) is the determination of hydrocarbon bearing versus water-bearing zones. As most minerals of the rock matrix as well as hydrocarbons (in particular gas) are nonconductive (high resistivity), the ability of the rock to transmit a current is almost entirely a function of the water (salinity) in the pores (low resistivity). Well-cemented limestones have a very high resistivity. Coal beds have an even higher resistivity, because coals have virtually zero conductivity (Bjørlykke, 1989).
Of further importantance are dipmeter logs, which specify the slope of beds and laminations in rocks, calliper logs that give a record of the borehole diameter, and formation temperature logs.

The mechanisms of reservoir filling are a logical extension to previously discussed mechanisms relevant for secondary migration. The filling process itself is described in detail in England *et al.* (1987) and England (1989). The first petroleum will enter the reservoir structure on a dendritic pathway that only involves coarser regions of the reservoir as

previously mentioned (Figure 1 A). In the initial phase of filling, only small parts of the reservoir are saturated with oil or gas, but as more petroleum migrates into the structure, the buoyant pressure will increase causing the petroleum to displace water from smaller pores (Figure 1 B - D). The most recently generated petroleum will advance the reservoir structure in “fronts” (Figure 1 B). During the filling, there is only a very discontinuous volume of oil-saturated rock, which eliminates any wide scale mixing process and the original fluid composition is preserved. Mixing processes will be able to start if a distinct petroleum saturation (50 % or over) is achieved (Figure 1 D). As a result, the initial petroleum composition in reservoirs frequently shows measurable compositional variations, both laterally (between wells) and vertically (within a single well).

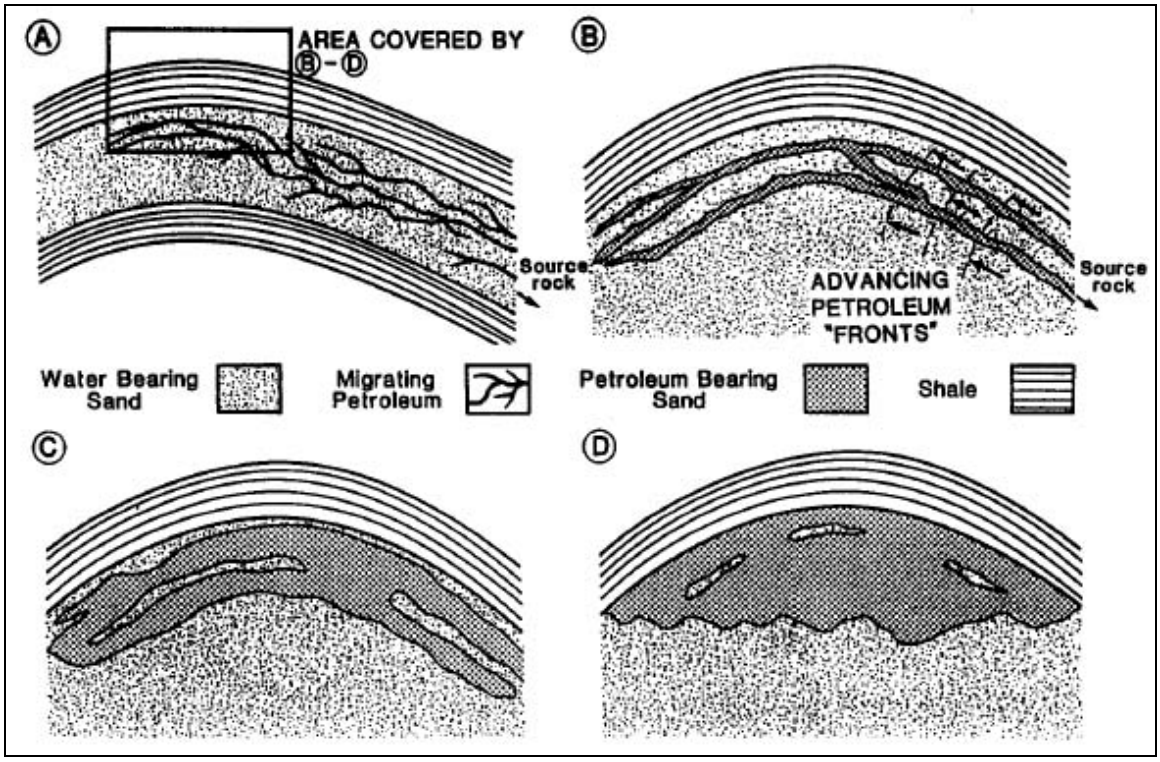

Figure 1 Schematic sequence of the reservoir filling (England, 1989).

For example Leythaeuser *et al.* (2007) detected maturity sequences of individual charges present in a single sample by the sequential extraction of reservoir sandstones. Impregnations in small pores are characterised by a significantly lower maturity level (indicating the first charge) than those observed in larger pores of the sandstone sample. England & Mackenzie (1989) argued that the increasing source maturity will steadily increase the GOR of the petroleum migrating into a reservoir and thus the most recently arrived (most mature)

petroleum will be predominantly found nearest to the source rock kitchen or sourcing direction in general (England, 1989; England *et al.*, 1987).

Initial compositional heterogeneities within a newly filled reservoir are attempted to approach a state of thermodynamic equilibrium, which might occur via a variety of mass-transfers or mixing processes. In the Earth gravitational field, thermodynamically gradients will set up in the oil column, which leads to gravitational segregation during geological time. These effects increase the concentration of denser compounds at the base and lead to a progressive increase of the GOR towards the top of the petroleum column, and a decrease in the subsurface density (England, 1989). Differences in the GOR give a rise to variations in the density (higher GOR = lower fluid density).
Density driven mixing, thermal convection, and diffusive mixing can operate as mixing types on petroleum accumulation. The processes are described in England *et al.* (1987) and England (1989). Thermal convection is unlikely to be a significant mixing process as in many reservoir the magnitudes of thermal gradients (changes in the local temperature) are too low. Density driven mixing is depended on the permeability and was shown to be fast in reservoirs or parts of the reservoir with good (permeability) conditions and *vice versa*. In general, for both mixing processes, reservoir anisotropy plays an important role, because mixing involves vertical and horizontal movements. Except for good to excellent reservoirs England *et al.* (1987) and England (1989) suggest a long time interval for density driven mixing with respect to the time required for the reservoir filling, which will vary considerably depending on reservoir structure, fluid type and viscosity. A typical value for the North Sea was set to 10 Ma. Diffusive mixing reduces or eliminates horizontal chemical potential differences in fluids as a function of differences in the concentration. Vertical diffusion in the oil column is relatively rapid (< 1 Ma) on a geological timescale, but horizontal diffusion is ineffective and slow for large distances between different wells (100 Ma for reservoir with K = 10 md), e.g. as a process for the elimination of variations in the GOR.
Due to distinctly lower viscosity, all mixing processes will be much faster in gas reservoirs.

Assessing the extent of reservoir mixing is important for the comparison and interpretation of fluid analyses from different parts of the reservoir and for the reconstruction of the filling history, because lateral compositional variations are related to the direction from which the field was filled by migrating petroleum generated in the source rock kitchen area. Due to slow

rates (geological time) of intra reservoir mixing the differences may persist to the present day (England *et al.*, 1987).

In many reservoirs, the original petroleum composition is affected by post-filling alteration processes such as cap rock leakage, evaporative fractionation, deasphalting, water washing or biodegradation. Petroleum alteration starts immediately after petroleum formation and has a great influence on the physical fluid properties such as API gravity and viscosity. For instance, biodegradation and water washing are processes initiated at the oil-water interface, which lead to heavy, low API gravity oils depleted in hydrocarbons but enriched in non-hydrocarbons such as NSO compounds and asphaltenes (Killops & Killops, 2005; Palmer, 1993; Peters *et al.*, 2005; Tissot & Welte, 1984).

Petroleum reservoirs commonly have a complex filling history characterised by large and small-scale heterogeneities induced by the filling process itself, in-reservoir mixing, and alteration.

1.2 ASPHALTENES

1.2.1 DEFINITION AND OCCURRENCE

The proportion of aliphatic, aromatic and NSO compounds comprising resins and asphaltenes, define the gross composition of petroleum. The heaviest and most polar fraction of petroleum is named asphaltenes. J.B. Boussingault (1837), who described constituents of bitumen found in the Eastern France and Peru, coined the term asphaltene. Boussingault named the fraction of a distillation residue “asphaltene”, which was insoluble in alcohol but soluble in the essence of turpentine, since it resembled pure asphalt. Nellensteyn (1924) defined the asphaltene fraction of a crude oil as the fraction insoluble in low boiling point paraffinic hydrocarbons, but soluble in carbon tetrachloride and benzene. Marcusson *et al.* (1931) distinguished three petroleum fractions; asphaltenes which precipitated by petroleum ether, resins which are soluble in petroleum ether but are adsorbed on fuller’s earth, and oil constituents which are the ether soluble fraction that does not adsorb on fuller’s earth. Nowadays asphaltenes are defined as that part of the solvent-extractable organic matter, which precipitates upon the addition of excess light hydrocarbons (Hirschberg *et al.,* 1984;

Kawanaka *et al.*, 1989; Leontaris & Mansoori, 1988; Mitchell & Speight, 1973). Asphaltenes belong to the first petroleum products formed during diagenesis, which comprise mainly heteroatomic NSO compounds (Nitrogen, Sulphur, and Oxygen). They are structurally very complex, highly polar and are made up of high molecular weight carbon skeletons, which can be aromatic or aliphatic in character (Tissot & Welte, 1984).
The amount of resins plus asphaltenes ranges from 0 - 40 % in non-degraded crude oils (depending on genetic type and thermal maturation) up to 60 % in heavy degraded oils. Source rock extracted bitumen is richer in asphaltenes and resins compared to crude oils (Tissot & Welte, 1984). The quantity of precipitated asphaltenes varies for a given petroleum with the solvent used, the temperature of mixing and the time elapsed between mixing and separation (Pfeiffer & Saal, 1940).

During crude oil production, asphaltenes give rise to a variety of problems. It is widely recognized that flocculation and deposition of asphaltenes may occur if the thermodynamic equilibrium is disturbed (Hirschberg *et al.*, 1984; Hammami *et. al.*, 2000). This might be triggered by changes in pressure and temperature or by injection of gas during improved oil recovery (IOR) operations. Another possible problem is the adsorption of asphaltenes onto the surface of minerals within the reservoir, whereby the wettability is changed from water-wet to oil-wet thereby reducing the potential oil recovery (Leontaris, 1989; Leontaris & Mansoori, 1988). Thus, from the production point of view, asphaltene enrichments have predominantly negative effects as they represent non-producible oil in place, acting as flow barriers, and introducing oil quality differences in the reservoir (Wilhelms & Larter, 1994a; Wilhelms & Larter, 1994b). Many authors have reported the immense problems initiated by the presence and behaviour of asphaltenes, for instance plugging of wells, deposition on the steel walls in the production line, accumulation of asphaltenes in separators or other fluid processing units, or deactivation of catalysts (e.g. Calemma & Rausa, 1997; Leontaris & Mansoori, 1988). Clean up of deposited asphaltenes in the field may necessitate well shut-in and might lead in the worst case to the loss of producable oil. Hence, preventing asphaltene flocculation is a necessity from both an operational and economical viewpoint.
The understanding of processes leading to asphaltene enrichments is very important for the planning of platforms and safety issues on oil production installations (Leontaris, 1989).

Despite these negative effects, asphaltenes display structural and compositional features, which make them a valuable tool for the geochemical investigations of petroleum reservoirs,

especially if post-filling alteration processes (cf. Chapter 1.1) changed the original petroleum composition. From the oil-water contact (OWC) up to the top of petroleum reservoirs, petroleum alteration zones are often marked by enrichments of asphaltenes, sometimes in the form of tar mats or heavy oils. Asphaltene enrichments can also be found along migration pathways in carrier rocks. Dahl & Speers (1986) investigated a tar mat at the base of the oil column in the southern part of the Oseberg field, which was approximately 13 m thick. The authors showed that the petroleum in the tar mat and in the oil column are closely related and concluded that the tar mat was formed by deasphalting of the oil column accompanied by gravitational segregation.

Thus, the characteristic occurrence of asphaltene enrichments in petroleum reservoirs as well as along migration pathways can reflect both, the original charging history and, if enriched as tar mats, the original column height prior to the process that led to the reduction of the petroleum volume (Wilhelms & Larter, 1994a; Wilhelms & Larter, 1994b).

According to the work of Nellensteyn (1924), petroleum must be looked upon as a colloidal system, with asphaltenes representing the solubilised micelles, hydrocarbons representing the solvent, and resins representing the peptizing agent. The author further described the adsorptive properties of asphaltenes and their interaction with the environment. This theory was modified by Pfeiffer & Saal (1940), who regarded petroleum as a continuum comprising light hydrocarbons as well as heavy asphaltenes. They described the structure of an asphaltene micelle in petroleum as a central bulk of substances exhibiting the greatest molecular weight and highest aromaticity that is surrounded by lighter constituents of less aromatic nature until a continuous transition to the intermicellar phase is formed (Figure 2).

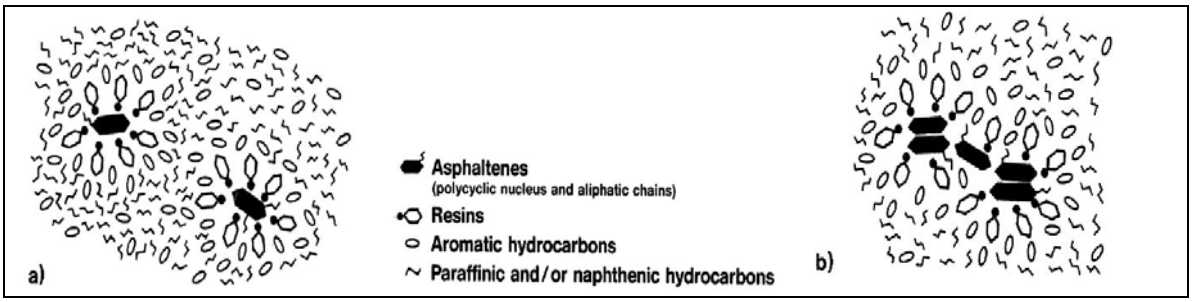

Figure 2 Physical structure of crude oil with a possible micelle structure of asphaltenes and resins according to Pfeiffer & Saal (1940) adapted by Tissot & Welte (1984). (a) Fully dispersed asphaltenes occurs in crude oils with a sufficient amount of resins and aromatic hydrocarbons. (b) Asphaltene-asphaltene combination occurs in crude oils with a depletion of resins and aromatic hydrocarbons compared to asphaltenes.

In their concept petroleum is an equilibrium mixture, which means that if a fraction becomes modified an evolution takes place to recover the equilibrium. Thus, the addition of excess hydrocarbons or the removal of resins causes asphaltene precipitation.
Differences in the physical properties of petroleum compounds are related to size and polarity as well as structure and chemical composition. The latter mainly influence adsorptive properties.

1.2.2 ASPHALTENES IN RESERVOIR GEOCHEMISTRY

It has been reported by several authors that kerogen and asphaltene pyrolysates show close structural and compositional similarities (Behar & Pelet, 1985; di Primio *et al.*, 2000; Eglinton *et al.*, 1991; Muscio, 1991; Pelet *et al.*, 1986). Asphaltenes have been described as "reservoired kerogen moieties", which contain structural and maturity related information of the source rock from which they were generated (Behar & Pelet, 1985; Pelet *et al.*, 1986). Qualitatively, pyrolysis products of asphaltenes and kerogen generate the same type of compounds by thermal evolution (Behar & Pelet, 1985). Horsfield (1997) reported similar alkyl chain length distributions for pyrolysates of kerogen, asphaltenes and heterocomponent fractions (NSO fraction) of Posidonia Shale samples with an oil generating maturity Rm = 0.53 - 0.88 %. Muscio (1991) as well recognised a good correlation of gas-oil ratios (GOR) for these kerogen and related asphaltene samples with increasing maturity.
Both concluded that the organic matter quality can be determined either from kerogens or from genetically related asphaltenes of rock bitumen and/or crude oils. This extends kerogen typing and petroleum prediction concepts from source lithology to petroleum reservoirs (Horsfield *et al.*, 1993). Thus, geochemical techniques and parameters originally developed for kerogen typing studies can be applied for reservoir characterisation using asphaltenes.
From kerogen typing studies, it is already known that pyrolysis yield and pyrolysate composition can be used to characterise the genetic potential, quality and maturity of kerogen (Curry & Simpler, 1988; di Primio & Horsfield, 1996; Eglinton *et al.*, 1990; Horsfield, 1989; Larter, 1984; Senftle *et al.*, 1986; van Graas *et al.*, 1981). Various compound classes have been defined in kerogen pyrolysates e.g. hydrocarbons, ketones, thiols, alcohols or nitriles, which are represented by saturated and unsaturated, cyclic and acyclic carbon skeletons. For instance, phenolic compounds in pyrolysates are a useful indicator for the presence of higher plant debris within the kerogen (Larter, 1984). Alkylated thiophenes are used to estimate the relative content of organic sulphur with respect to organofacies of the source and the thermal

maturity of the organic matter (Eglinton *et al.*, 1991; 1990; 1992; Sinninghe Damste *et al.*, 1989; 1990). Horsfield (1989) demonstrated that the aromaticity of the volatilisable substituents of kerogen can be used as measure of the aromaticity of the total kerogen. It was shown that aromatic compounds can be used to discriminate kerogen types and that the residual organic matter becomes more and more aromatic with decreasing H/C atomic ratio (Horsfield, 1989; Larter, 1984; Muscio & Horsfield, 1996). Proportionately, large gas yields in pyrolysis products are typically generated by hydrogen poor kerogen (Type III) or gas-prone coals. Hydrogen poor kerogens often contain high proportions of lignocellulosic material that is characterised by an increasing tendency to form gas with increasing maturity (Horsfield, 1989; Horsfield, 1997). The ratio of gaseous to liquid compounds (GOR) changes as a function of maturity, whereby higher gas amounts or higher GOR are related to higher maturity levels (Santamaria-Orozco *et al.*, 1998).

The application of thermal analytical methods on asphaltenes, e.g. pyrolysis-GC, for petroleum reservoir characterisation is particularly useful when the oil has been altered or biodegraded. Lehne & Dieckmann (2007) demonstrated that asphaltenes remain unaffected by low temperature alteration processes such as biodegradation or water washing. Although asphaltenes may precipitate during phase separation processes, their major characteristics are preserved. As one constituent of migrating petroleum, asphaltenes in the reservoir can be viewed as fingerprint of the original composition of individual oil charges, and therefore are used as marker for alteration and migration processes.
Appling this concept the relative mass of unaltered petroleum originally present in the Holzener Asphaltkalk of northern Germany could be inferred by micro scale sealed vessel pyrolysis experiments (MSSV) of asphaltenes in the reservoir and its most likely source, the Posidonia Shale (Horsfield *et al.*, 1991). The mass balance calculation revealed that 50 - 90 % of petroleum was lost due to alteration phenomena in the reservoir. Muscio *et al.* (1991) suggested the application of oil asphaltenes for the reconstruction of the original GOR of biodegraded oil accumulations.

Different reservoir compartments are often characterised by highly variable petroleum compositions induced by post-filling alteration processes as documented e.g. for the North Sea (Horstad *et al.*, 1990) or for the Gulf of Mexico (Holba *et al.*, 1996). Unravelling the history of compartmentalized reservoirs with a complex charge and alteration history presents a particularly difficult challenge, because subtle *in-situ* variabilities have to be recognised.

While produced oils present the average product of a thick reservoir interval, reservoir rock samples are useful for identifying small-scale variations within the reservoir. Reservoir rocks enriched in NSO heterocompounds (asphaltene rich) represent residual oil or even organic barriers leading to compartmentalization. They can be sampled in high resolution and used to reconstruct the original oil composition at any place within the reservoir. On the other hand, the labile constituents of asphaltenes still reflect the hydrocarbon fingerprint of the bulk parent oil with which the asphaltenes were generated.

The analysis of reservoir rocks using pyrolysis techniques has been applied in reservoir characterisation studies to delineate complex reservoir compartmentalisation, tracing the movement of the oil in the reservoir, or for studies determining the timing of reservoir filling (Cornford, 1998; Horstad *et al.*, 1995; Karlsen & Larter, 1989). For instance, Karlsen & Larter (1989) combined Iatroscan thin layer chromatography (TLC-FID) and Rock-Eval pyrolysis using reservoir rocks for a petroleum population mapping within individual petroleum reservoirs. Ehrenberg *et al.* (1995) have shown that asphaltenes from reservoir rocks reflect high resolution variations within a reservoir structure due to the specific charging history and that they are very helpful for a better understanding of reservoir heterogeneities defined by the original oil charge. Jarvie *et al.* (2001) detected bypassed pay zones and sand bodies using the Source Rock Analyzer. Bhullar *et al.* (1998) illustrated that the enrichment of asphaltenes and their distribution throughout reservoir rocks can be used as fundamental geomarker for the recognition of oil-water and especially paleo-oil-water contacts in reservoir structures. They also clearly highlighted that petroleum in reservoir structures is much more heterogeneous than previously thought based on studies on produced oils.

Another application for asphaltenes is their use in the assessment of petroleum type organofacies and maturity. Petroleum asphaltenes have been used to determine source rock characteristics of active kitchen areas and to reconstruct the filling histories of reservoirs (Horsfield *et al.*, 1991; Keym & Dieckmann, 2006; Lehne & Dieckmann, 2007). This is important because mature source rocks are usually found at great depth and thus are seldom drilled, and oil accumulations in petroleum reservoirs are often situated in structural heights where the potential source rock is immature and of a different organofacies.

All these findings point to the importance of asphaltenes in petroleum accumulations for the determination of kerogen type and source facies and as well as the gross compositional

characteristics of the original unaltered petroleum expelled from the source. Asphaltenes are a useful tool for correlation studies as substitution for the source rock kerogen. The features of asphaltenes can significantly aid in improving predictions of post-filling reservoir alteration and in enhancing the understanding of compartmentalisation and reservoir filling history.

2 GOALS

The original composition and the volume of petroleum in reservoirs are often modified by post-filling alteration processes, in many cases to a different degree due to the reservoir compartmentalization. Such alteration processes have strong economic consequences since they negatively affect oil quality and producibility. Furthermore, a better understanding of processes leading to reservoir compartmentalisation can enhance drilling strategies when advancing from one reservoir compartment to the next.

The focus of this thesis is on macromolecular compounds in general and specifically single asphaltenes found in reservoir rocks from the oil leg of petroleum accumulations and from the carrier systems. Asphaltenes have been said to be resistant to alteration processes and can therefore be used as markers of source and maturity in different reservoir compartments.

The designated aims of the study are:

- delineation and characterisation of reservoir heterogeneities at high resolution applying and developing new pyrolysis parameters to both, the total macromolecular components and isolated petroleum asphaltenes in oil stained reservoir rocks and carrier systems
- to establish an asphaltene separation method with the main focus on reproducibility and linearity to ensure that subtle changes in composition within reservoirs were real, and not simply artefacts of the separation method
- to establish compositional kinetic models using asphaltenes to reconstruct the petroleum phase that originally charged the reservoir structures

The thesis is subdivided in two major parts.
(1) The first part outlines the results of a detailed screening of the Heidrun reservoir using macromolecular polar constituents from whole reservoir rocks and asphaltenes separated from the residual bitumen of reservoir rocks. Open-system and bulk-pyrolysis techniques were used to delineate vertical and horizontal variabilities at high resolution. The total macromolecular fraction as well as single asphaltenes were characterised by Production Index, pyrolysis yield, and pyrolysate compositional indices, namely aromatic compound ratios, phenol and sulphur

abundances as well as the yield and wetness of gaseous compounds. A series of biodegraded heavy oils from Canada, whose physical properties were known, and Heidrun oil samples with API gravity differences of 10° assisted in the interpretation.

(2) The second part focuses on isolated asphaltenes as a single phase in more detail. A novel linear and reproducible asphaltene separation method is explained. Furthermore, closed-system pyrolysis experiments were applied to asphaltenes from reservoir rock bitumen, produced oil equivalents, and source rock bitumen in order to build compositional kinetic models. The models were used to determine the composition and physical properties of petroleum predicted to be generated. The results can be applied to basin modelling studies in the working area, but no petroleum system modelling was conducted because of time constraints.

3 GEOLOGICAL BACKGROUND AND SAMPLE DETAILS

3.1 HETEROGENEITIES IN THE HEIDRUN OIL FIELD - REGIONAL PERSPECTIVE

The focus of this study was the Heidrun oil field, located in Haltenbanken, a prolific petroleum province on the mid-Norwegian continental shelf about 200 km north-west of the mid-Norwegian coast (Figure 3). The prospect field was discovered in 1985 and is situated in approximately 350 m water depth (Whitley, 1992).

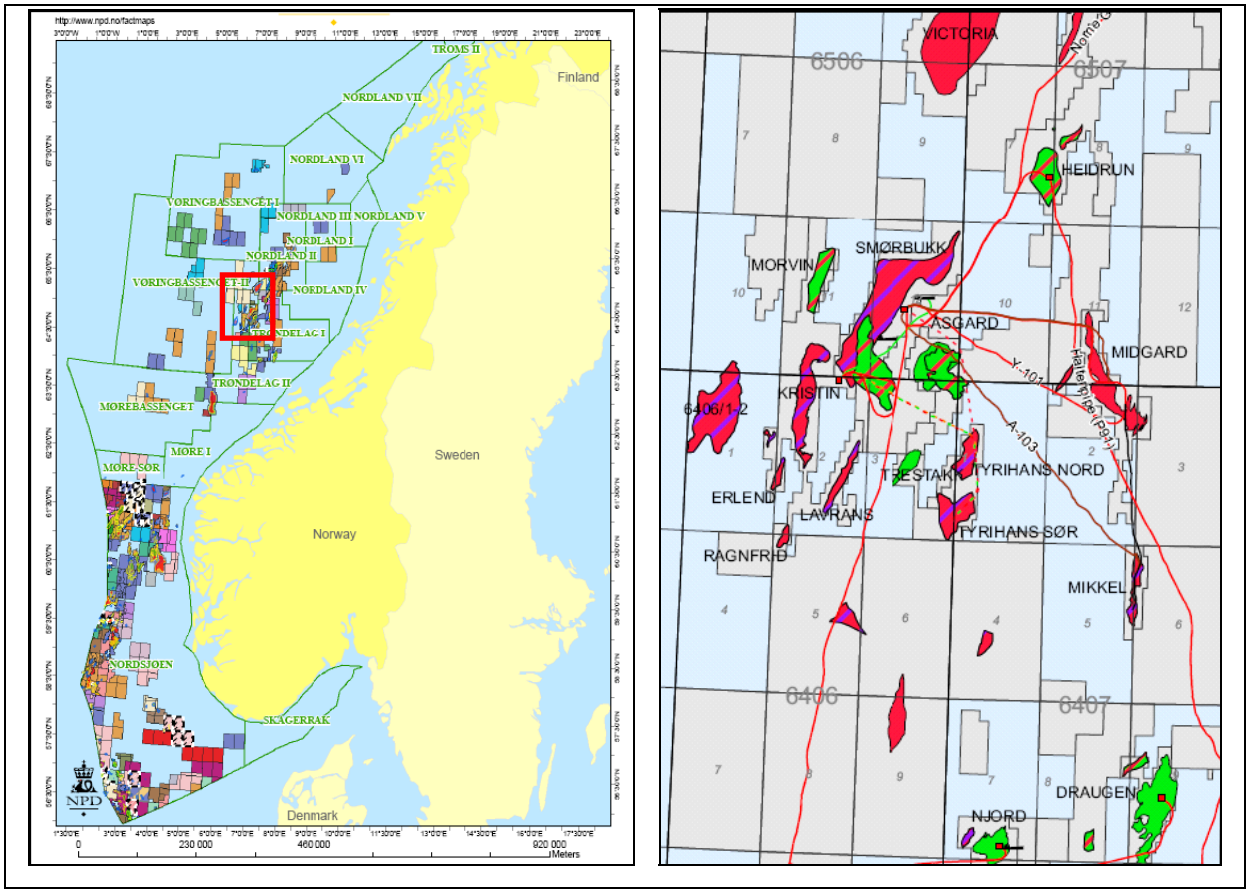

Figure 3 Location map of the study area. *Left:* The oil and gas fields of the Norwegian continental shelf (www.npd.no/factmaps). The red square marks the Haltenbanken area. R*ight:* The oil and gas fields of the Haltenbanken area including the Heidrun oil field.

The Heidrun structure is a large SW-plunging horst block located at the transition between the structurally complex Halten-Terrace and the Nordland Ridge. It is a structural trap, which was

formed during two primary extensional phases. The first phase took place during the Late Palaeozoic and the second phase during the Late Jurassic to Early Cretaceous triggered by Cimmerian tectonics.

The Atlantic rift evolution began in the late Palaeozoic with lithosspheric extension and mantle upwelling between the Caledonian suture zone of Laurentia and Baltica. From the Permian to Triassic extensional tectonics were initiated with downwarping, rifting, erosion, and clastic infill. The rifting culminated in the Late Jurassic with the Cimmerian tectonic phase, when a widespread uplift, erosion and tilting of the Jurassic fault blocks leading to the formation of the Heidrun trap structures (Whitley, 1992).

As a result of the extensional phases, the Heidrun oil field was dissected by a series of north to northeast trending faults with displacements of up to 100 m. They divide the oil field in several structural compartments (segment A - T) (Figure 4).

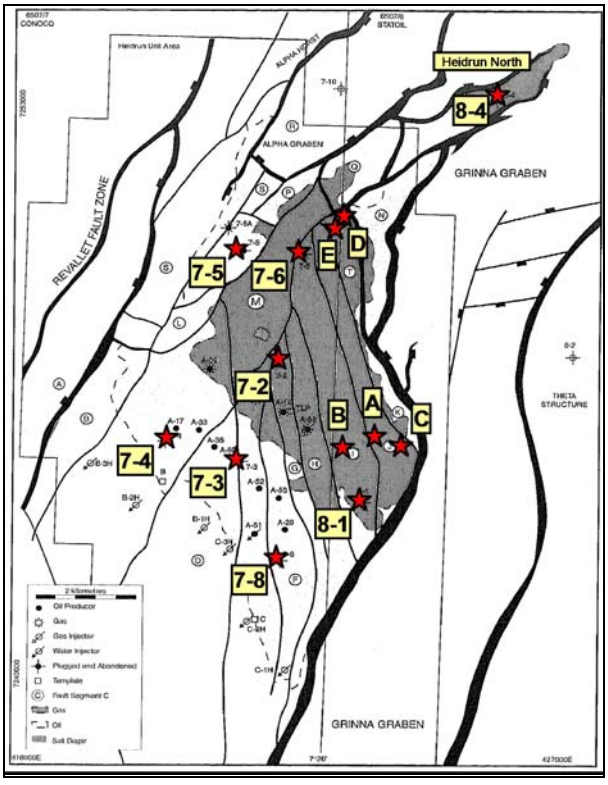

Figure 4 Schematic structure of the Heidrun oil field including the main fault trends and structural compartments (segment A - T), distribution of hydrocarbons (gas/oil) and wells investigated in this study (after Knai & Knipe, 1998).

This fault segmentation induced a heterogeneous fluid system in the Heidrun oil field and created different fluid contacts as well as different fluid types in the single reservoir units (Hemmens *et al.*, 1994; Knai & Knipe, 1998; Whitley, 1992). The distribution of the different contacts are due to partially sealing faults (Hemmens *et al.*, 1994) and/or due to dynamic fault

seals in the Heidrun oil field (Heum, 1996; Welbon *et al.*, 1997). Figure 5 illustrates the various fluid contacts in the Heidrun oil field.

The oil-water contact (OWC) varies in the compartments of the Heidrun oil field between 2400 - 2500 m TVD-SS (true vertical depth - sub sea level) (Figure 5). In Heidrun North in well 6507/7-8, the OWC is in 2225 m TVD-SS. The OWC varies not only across the field, but also within different reservoir levels, several pressure compartments can be distinguished. Of the major reservoir units Garn-, Ile- and Tilje Formation, the latter appears to be the most compartmentalised (internal Statoil report, 2003; www.factpages.npd.no).

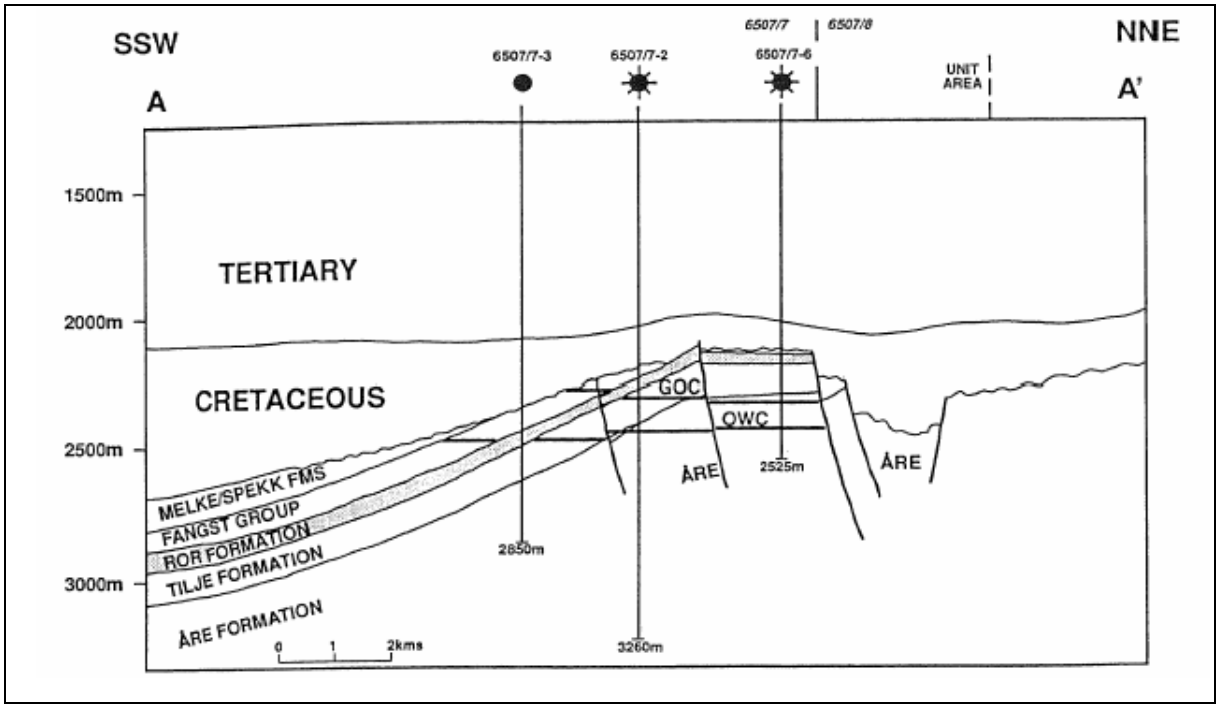

Figure 5 Cross-section through the Heidrun oil field illustrating reservoir units and fluid contacts (Hemmens *et al.*, 1994).

The hydrocarbon accumulation covers an area of 37 km^2. It comprises a saturated oil leg and a separated gas cap with column heights of up to 200 m and 180 m, respectively (Hemmens *et al.*, 1994). The Heidrun oil field is 10.5 km long and maximal 5.5 km wide. In Figure 4 the distribution of hydrocarbons (oil and gas) is shown and well locations from which the reservoir rock- and the oils samples were taken are given. The field produces since 1995. The main operators are Statoil and their partners ConocoPhillips, ENI and Petoro. The estimated recoverable reserves are 170 x 10^6 Sm^3 for oil, 42 x 10^9 Sm^3 for gas, and 2.2 x 10^6 tons for natural gas liquids (NGL). The estimated remaining reserves are 38.1 x 10^6 Sm^3 oil, 29.9 x 10^9 Sm^3 gas and 1.7 x 10^6 tonnes NGL (www.factpages.npd.no).

The hydrocarbons in the Heidrun oil field are trapped in sandstones of the Middle Jurassic Garn- and Ile Formation (Fangst Group), the Early Jurassic Tilje- and the Early Jurassic to Late Triassic Åre Formation (Båt group) (Figure 5, Figure 6). The reservoirs are severely truncated at the northern edge (Hemmens *et al.*, 1994; Knai & Knipe, 1998; Whitley, 1992). The Jurassic reservoir rocks were deposited on the southeastern flank of the developing northeast Atlantic rift domain. The interval was characterised by high coarse clastic influx from the elevated rift shoulders, which were deposited in an overall transgressive regime (Whitley, 1992). The reservoirs are partially sealed by the marine Late Jurassic shales of the Spekk- and Melke Formation, both of which are organic rich rocks of the Viking group, and by Cretaceous shales of the Cromer-Knoll and Shetland Group (Figure 5, Figure 6).

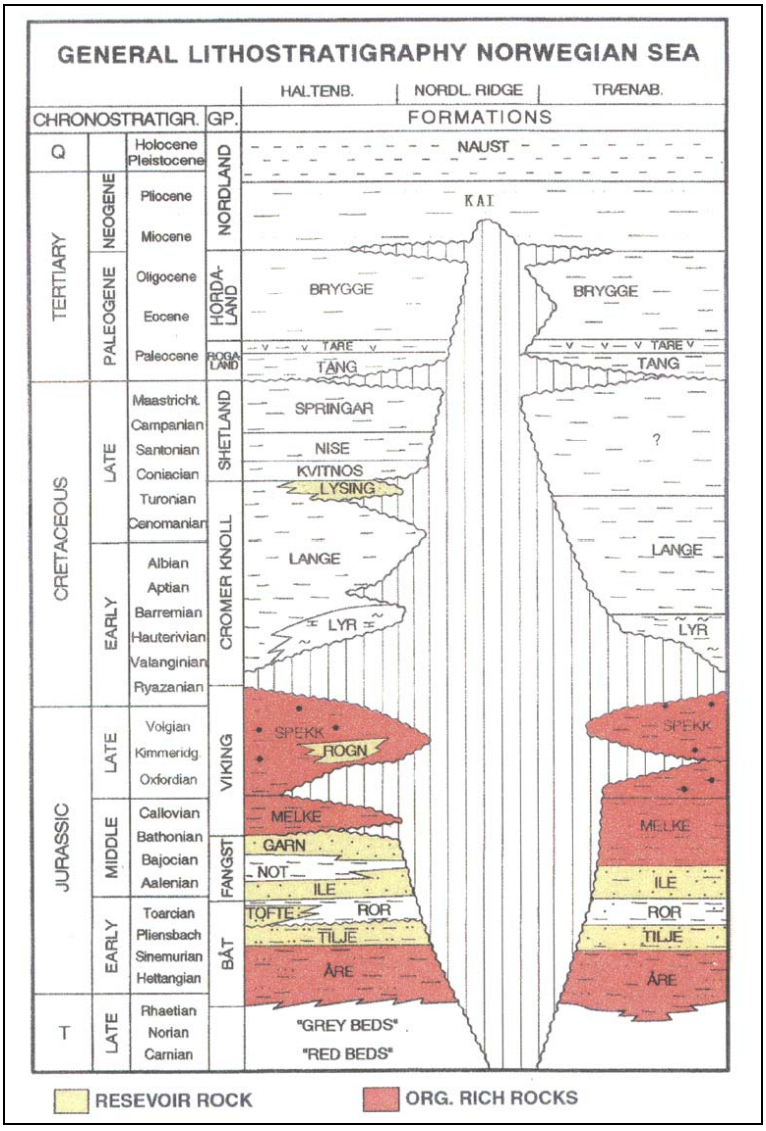

Figure 6 Stratigraphic column of the petroleum province Haltenbanken shows the reservoir units of the Jurassic sandstones in yellow as well as the organic rich rocks in red (from Karlsen *et al.*, 2004)

The Fangst group consists of three units. Two of them, the Garn- and the Ile Formation are regarded as reservoirs. The third, the Not Formation is regarded as non-productive in the Heidrun oil field (internal Statoil report, 2003).
The sandstones of the Fangst Group were mainly deposited in marine environments ranging from shallow shelf to shoreline. The uppermost Fangst subzone, the Garn Formation, lacks indications for marine deposition. The Garn Formation sediments have been deposited in a braided-stream fluvial environment. They represent a mixture of fluvial and tidally influenced deposits with multi-storey channel complexes and contain by far the highest quality reservoir sandstones compared to any other subzone in the Heidrun oil field. Typical are trough cross stratification in this subzone (Hemmens *et al.*, 1994).
The Ile Formation is separated from the overlying Garn by the shallow marine shales and sands of the Not Formation. The Ile Formation consists of two prograding delta / shoreface units (Ile Fm. 1 - 2 and Ile Fm. 3 - 6). They were most likely deposited in a wave-dominated delta on a storm-dominated coastline. The Ile Fm. 1 - 2 represents shallow marine tidally dominated delta deposits and consists of fine to very fine grained cross- or ripple stratified sandstones. They are shaly at the base and coarsen upwards (Hemmens *et al.*, 1994; Whitley, 1992). The Ile Fm. 3 - 6 begins with lower shoreface hummocky cross-stratified sandstone and coarsening upward through the upper shoreface and bay-fill sandstones.
The total thickness of the Fangst group is up to 90 m at the southern flank, while it is thinned or partly completely absent in the crestal part of the field due to erosion (Figure 5) (Hemmens *et al.*, 1994). Compared to the Tilje and the Åre Formation Reservoirs, the Fangst group contains higher quality sandstones concerning porosity, permeability and water saturation. It further contains the largest oil column and oil with a higher API gravity (Whitley, 1992). The physical reservoir parameters of the Heidrun oil field are listed in Table 1.

The Tilje Formation sandstones, with somewhat lower reservoir quality, are one of the four formations of the Båt Group (Figure 6). The Tilje Formation is underlain by the Åre Formation and overlain by the marine mudstones of the Ror Formation. The Tilje Formation sandstones and the upper subzone of the Åre Formation are the products of shallow marine shelf, subtidal, and intertidal environments, which results in highly variable depositional patterns. The sedimentology in the Tilje is therefore very complex and the reservoir subzones are extremely heterogeneous (Hemmens *et al.*, 1994).
Facies associations of the Tilje Formation include *inter alia* storm influenced prodelta, delta front, estuarine, tidal channel, and delta front bars deposited in a wave and storm dominated

environment. In the Heidrun oil field, the Tilje Formation is divided into four reservoir units (Tilje Fm. 1 - 4) with several subunits (internal Statoil report, 2003).
The Tilje Fm. 1 is characterised by silt/mudstones and cross-stratified sandstones, which are intensively burrowed indicating shallow marine depositional environment. The upper part of the Tilje Fm. 1 is a tidal flat sequence with occasional desiccation cracks and rootlets. The Tilje Fm. 2 is composed of a basal muddy unit, which grades upward in a series of five upward coarsening and upward cleaning cycles. They vary from 5 m to 10 m thickness and consist of heterolithic sand- and siltstones. The sands are intensively bioturbated, which indicates a deposition under more marine conditions. The Tilje Fm 3 is typified by tidally influenced deposits (mud rich sediments), which are interbedded with relatively thick sandstones of tidal channel and tidal shoal deposition. These tidal channel sandstones are the highest quality sandstones of the whole Tilje Formation. Sands in the tidal flat deposits are lens-shaped ripples generated by traction transport. Silty shales drape these sand lenses as thin parallel lamina, representing deposition from suspension. As a result, the sands deposited in this environment are more discontinuous. The repeated alternation of traction and suspension indicates dramatic fluctuations in flow intensity, which is a common attribute in tidal environments. The Tilje Fm. 4 comprises a marine shelf to marine shoal sandstone with some shale sandstone sequences. The fine to coarse grained clear sandstones are cemented by siderite, which severely reduces the quality of the reservoir (Hemmens *et al.*, 1994; Whitley, 1992; internal Statoil report, 2003).

The Åre Formation is the lowermost among the reservoir formations of the Heidrun oil field and is divided in 7 reservoir zones (internal Statoil report, 2003). The lower part of the Åre Formation (Åre Fm. 1 - 4) is dominated by fluvial to delta plain deposits, which reflect the overall transgressive development of the formation. This zone is regionally approximately 500 m thick and comprises a series of fluvial channel sands and crevasse splay deposits. Several reservoir subzones are locally capped by peat swamp coal. (Hemmens *et al.*, 1994; Knai & Knipe, 1998).
The sediments of the Åre subzones 1 and 2 were deposited in a mud-dominated delta plain crossed by meandering channels with partly considerably depth (15 m and more) and lateral dimension (several kilometres). The main reservoirs are bar sandstones lying in the meander belts, which generally trend north south. Muddy floodplain deposits with thin coal beds separate the channel sandstones and represent effective lateral and vertical seals. Coal beds

and organic shales may provide a source of hydrocarbons when thermally mature (Hemmens *et al.*, 1994; Whitley, 1992).

The Åre Fm. subzones 3 and 4 are characterised by a slightly increasing marine influence. These sediments represent a complex mixture of bay fill and coastal plain deposits with channel features and marine incursions. Bay fill deposits with minor coastal plain deposits dominate reservoir 3, while coastal plain deposits with minor bay fills dominate reservoir 4. Several reservoir subzones are locally capped by peat swamp coal (internal Statoil report, 2003).

The upper part of the Åre Formation (Åre Fm. 5 - 7) is the most heterogeneous unit in the Heidrun oil field as the sediments have been deposited in varying environments. They range from deltaic and intertidal to shallow marine shelf deposits, where marine, fluvial and tidal forces interact. The highest marine influence can be observed for the middle and the upper parts of the sequence. The total average thickness is about 200 m (Knai & Knipe, 1998; Whitley, 1992).

The base of the upper part comprises sandstones deposited in shallower tidal environments, which consist of flaser-bedded, rippled sand with interbedded mudstones. The upper part comprises burrowed sands with wave ripples, which contain thin zones with interbedded mudstones and ooids, indicating a subtidal environment. A general trend of increasing marine influence can be seen from the transition of the fluvial dominated Åre Fm. 1 and 2 through the bay fill sequences of the Åre Fm. 3 - 6 to the marginal marine sediments at the top of the Åre Fm. 7. The upper boundary of the Åre Fm. 7 to the overlying Tilje Fm. 1 defines the start of the more open marine environment (Whitley, 1992).

Due to the heterogeneous sediment and facies mixture both, the Tilje and the Upper Åre reservoir (Åre Fm. 5 - 7) provide the lowest reservoir quality with respect to porosity and permeability compared to the Fangst group and the lower Åre reservoir (Fm. 1 - 4) (Table 1).

The generally high quality of the reservoir sandstones in all reservoir formations is related to the shallow depth of burial (less than 2500 m) that limited diagenetic changes (Hemmens *et al.*, 1994; Whitley, 1992). Thus reservoir quality is primarily controlled by depositional features and primary porosity the predominant type of porosity. Only minor secondary porosity due to feldspar dissolution is evident. Cemented zones (siderite and calcite) have been noticed but are volumetrically insignificant and restricted to a few relatively thin layers (Hemmens *et al.*, 1994).

Table 1 Physical reservoir data for the Heidrun oil field (from Whitley, 1992).

Parameter or characteristic	Fangst Reservoir	Tilje Reservoir / Upper Åre Reservoir 4.2 - 7.2	Lower Åre Reservoir 1 - 4.1
Porosity in % (average)	29	26	28
Permeability in md			
average	1450	360	1788
range	670 - 19.500	90 - 10.000	30 - 11.000
Water Saturation in % (average)	15	42	24
Oil column in m	195	160	100
Gas cap	yes	yes	yes
° API gravity	29	22 - 28.6	22 - 28.6
GOR in std. ft^3 / STB	628	332 - 641	332 - 641

Haltenbanken is an area with several potential source rocks deposited in both, marine and terrestrial environments. The source rocks of the Heidrun oils are the marine Upper Jurassic Spekk Formation (Kimmeridge Clay equivalent) comprising oil- and gas-prone organic matter (OM), and the Middle Jurassic Melke Formation (Heather equivalent) comprising rather gas-prone to inert OM. Terrestrial source rocks are found in the Lower Jurassic Åre Formation (Brent equivalent) coals (i.e. high TOC) and carbonaceous shales containing gas-prone to inert OM (Hemmens *et al.*, 1994; Karlsen *et al.*, 1995; Mo *et al.*, 1989; Patience, 2003; Whitley, 1992). Geochemical studies of biomarkers (Karlsen *et al.*, 1995) and light hydrocarbons (Odden *et al.*, 1998) indicate a dominantly marine source for the hydrocarbons found in the Haltenbanken area, most likely from the Spekk Formation.

The deposition of the Melke- and Spekk Formation shales represent the start of the marine inundation in the Haltenbanken area (Pedersen *et al.*, 1989). At first, in the initial phase of the Cimmerian tectonics, the Fangst group became partial or totally eroded on major highs resulting in the formation of a widespread unconformity. On this basement, the Melke Fm. shales were deposited. The Late Jurassic transgression culminated with the deposition of the organic-carbon-rich Spekk Fm. black shales in a deeper marine environment with anoxic bottom water conditions (Whitley, 1992).

The Spekk Fm. shale is equivalent in age and facies to the Draupne Formation (Kimmeridge clay) in the North Sea. It is a rich source rock with total organic carbon (TOC) contents up to 13 % (average 4 %) comprising mainly Type II kerogen with some Type III (Cornford, 1998; Whitley, 1992).

A Rock-Eval Hydrogen Index (HI) of up to 700 mg HC / g TOC confirm a high potential for the generation of hydrocarbons (Mo *et al.*, 1989). In the vicinity of the Heidrun oil field, the

Spekk Formation is immature. It is mature near the Smørbukk and Smørbukk Sør fields south-west of the Heidrun oil field (Figure 3, right).

The underlying Melke Formation shows a high variability in organic matter quantity and quality. In general, the Melke Formation can be assumed as being a leaner source rock containing a mixed marine-terrestrial kerogen (Type II/III). TOCs and HIs range from 1 to 4 % TOC and 120 to 200 mg HC / g TOC, respectively (Ehrenberg *et al.*, 1992; Forbes *et al.*, 1991).

Cornford (1998) and references therein describes that Middle Jurassic depositions in the North Sea are limited and generally have a gas-generating potential, but coals are of minor abundance in these sequences. Their gas-prone nature originates in the vitrinitic material dominantly the OM of the mudstone facies.

Pyrolysis studies performed in this study (cf. Chapter 6) indicate a paraffinic-naphthenic-aromatic (P-N-A) low wax petroleum type after Horsfield (1989) for the Spekk Formation. For the Melke Formation the petroleum type organofacies range between gas condensate and P-N-A low wax.

The abundance of coal beds and carbonaceous or siliciclastic shale intervals in the lower part of the Åre Formation (1 - 4.1) are considerable. In total, the coal beds are 30 m - 60 m thick. Hemmens *et al.* (1994) assumed that the coal beds and organic rich shales might locally provide a source of hydrocarbons at sufficient maturation. According to Mo *et al.* (1989), which published average values for the unit as a whole including coal seams, the moderate Rock-Eval HI of 200 mg HC / g TOC points to gas prone Type III OM. In combination with average organic carbon content of about 8.0 wt. %, the data indicates a high potential for hydrocarbon generation.

Hvoslef *et al.* (1988) investigated cores from Haltenbanken with respect to hydrocarbon generation, migration and expulsion processes in the coals of the Åre Formation. They found that hydrocarbon expulsion from the coals associated with some compositional fractionation has taken place in this region. The Åre Formation is mature in all basinal areas of Haltenbanken, even in the eastern proximal basinal regions, which are important for petroleum generation in the drainage area of the Midgard field, where the source rock is immature.

Potential contributions of gas from the Åre Formation to hydrocarbon accumulations in the Haltenbanken area are still under debate. Based on isotopic models Patience (2003) attributed the reservoired gases in Mid-Norway to be predominantly of marine origin (Spekk Fm. ±

Melke Fm.). Only a small proportion is thought to be derived from terrestrial sources such as the coals and shales from the Åre Formation, even though they reach the gas generation window in many areas. The author suggested gas loss to be due to poor expulsion and/or migration routes in the highly heterogeneous Åre Formation. Karlsen *et al.* (2004) argued that the Åre Formation due to its stratigraphic depth has generated petroleum earlier than the Spekk Formation, but that the generated fluids leaked out of the system as traps were either not present at this time or the cap rock was not consolidated. This argument seems to lack substance considering the kinetic behaviour of kerogen as marine source rocks generate petroleum at lower levels of thermal stress than terrestrial sources (e.g. Schenk & Horsfield, 1998).

The Halten Terrace is characterised by two main pressure domains within the Jurassic units, which are divided by the main fault zone, the Revallet Fault Zone (Figure 4). The area exhibiting normal hydrostatic pressure is located east of this fault zone, the area with overpressure is located west of the fault zone (Karlsen *et al.*, 2004).

The filling of the Heidrun oil field started in the Early Cenozoic from the deep parts of the basin west of Heidrun (overpressured area) where the Spekk Formation source rocks reached sufficient maturities. With increasing burial of the Spekk Formation, all reservoirs around Heidrun became charged. In addition to the Spekk Fm., the Melke Fm. may have also acted as a source rock, but higher kinetic stabilities led to a delay in the organic matter transformation in comparison to the overlying Spekk Formation (internal IPP report, 2010). The generated hydrocarbons migrated along the Revallet fault zone into the reservoir structure until its seal-off due to the quartz cementation (Karlsen *et al.*, 2004). This resulted in a cut-off of the Heidrun and Smørbukk oil fields from the western part of the basin. However, only a small part of the first oil directly drained into Heidrun (internal IPP report, 2010). After the migration scheme changed, Heidrun was charged from south-southwest by the mature source rocks in the vicinity of Smørbukk and Smørbukk Sør, which imply long distance migration (> 15 km) (Hemmens *et al.*, 1994). Again, only small proportions of hydrocarbons migrate directly into Heidrun. The main route for hydrocarbons into the Heidrun oil field evolved along a fill-spill pathway along the ridge connecting Smørbukk and Smørbukk Sør to Heidrun from the south-southwest to southwest (Hemmens *et al.*, 1994; internal IPP report, 2010). The latest, probably still ongoing charge to the oil field occurred since the last 2 million years (internal Statoil report, 2003). Leythaeuser *et al.* (2007) reconstructed the accumulation and filling history of different compartments within the Heidrun oil field on the basis of molecular

maturity signatures of sequentially extracted reservoir rocks. They analysed residual oil and documented a significant variability in maturity of the different extracts. It was concluded that the fault compartments studied, which are located in the south- and northwest of the Heidrun oil field, were not filled during the same stages of accumulation history.

Biodegradation and mixing of different charges has severely affected the Heidrun oil composition (Karlsen *et al.*, 1995). Whitley (1992) suggested that the petroleum in certain parts of the field was biodegraded when the field was about 1000 m shallower then today, and that subsequently this biodegraded fluid was mixed with later arriving non-degraded oil. Temperature is one of the factors limiting biodegradation, with little or no biodegradation occurring in reservoirs at temperatures exceeding 80 °C (e.g. Head *et al.*, 2003). Assuming typical geothermal gradients of 25 - 30 °C / km, such temperatures are reached in ~ 2 - 3 km depth.

The present Heidrun reservoir temperature is stated with ~ 85 - 90 °C (internal Statoil report, 2003). Modelling results suggest that temperatures in the Heidrun oil field only exceeded 80 °C in relatively recent times, which in turn suggests an emplacement of non-biodegraded oils within the last million years. One exception is Heidrun North (well 6507/8-4) with present temperature lower than 80 °C. Any oil charge that reached the reservoir before this time is likely to be largely biodegraded (internal Statoil report, 2003).

Hydrocarbons of the later charges are characterised by a higher quality as indicated by unpublished in-house isotopic and biomarker data taken from R. Haberer and A. Vieth. Based on this data, the Heidrun oil field can be roughly subdivided into two dominant parts, a biodegraded part and a mixed part. While biodegraded oil samples are predominantly found in the eastern part of the oil field, oil samples in the western part are biodegraded but altered by mixing with later non-biodegraded oil charges. Furthermore, a third part can be subdivided were signals from both extremes are observed. That means that the biodegradation signature of the later charges can be observed. These wells are found in the central part of the oil field (Figure 7).

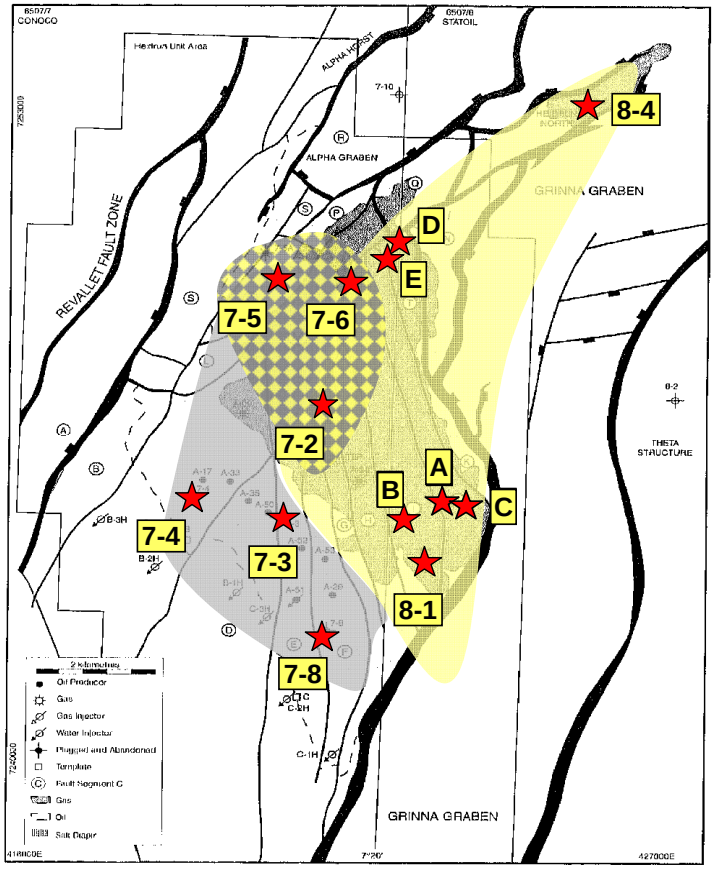

Figure 7 Structure of the Heidrun reservoir shows the present day state of oil alteration. Biodegraded oils without reaching later oil charges are predominantly found in the eastern part (yellow), while biodegraded oils, which have been altered by mixing with a later charge, are predominantly found in the western part of the Heidrun oil field (grey). In the chequered central part, both signals are observed (modified after Knai & Knipe, 1998).

3.2 SAMPLE DETAILS

3.2.1 RESERVOIR ROCK SAMPLES

The sample set consists of 141 plugs (ø 3.5 cm x 3 cm high) comprising 139 reservoir rocks and 2 potential source rocks, and 24 oil samples from drill stem tests (DSTs). Rock- and oil samples analysed within the present thesis are taken from 13 wells in which the following six reservoir formations are present: the Garn-, Not-, and Ile Formation of the Fangst group as well as the Ror-, Tilje- and Åre Formation of the Båt group. The two source rocks are shales from the Melke- and Spekk Formation of the Viking group. The sampled interval ranges from below the present OWC up to the top of the oil column.

Statoil provided most of the reservoir rock samples, namely 106 from the five exploration wells A, B, C, D, and E, and one oil sample from well D. The Norwegian Petroleum Directorate (NPD) provided most of the oil samples (19 oils) and 35 reservoir rock samples from the eight exploration wells 6507/7-2, 6507/7-3, 6507/7-4, 6507/7-5, 6507/7-6, 6507/7-8, 6507/8-1, and 6507/8-4. In the simplified north-south profile in Figure 8 the wells, geological formations, sample intervals and numbers of taken reservoir rock samples and oil samples (DST) are shown. The red numbers represent the number of investigated reservoir rock samples for the individual wells. Rectangles on the right side of the well represent number and depth of the DSTs.

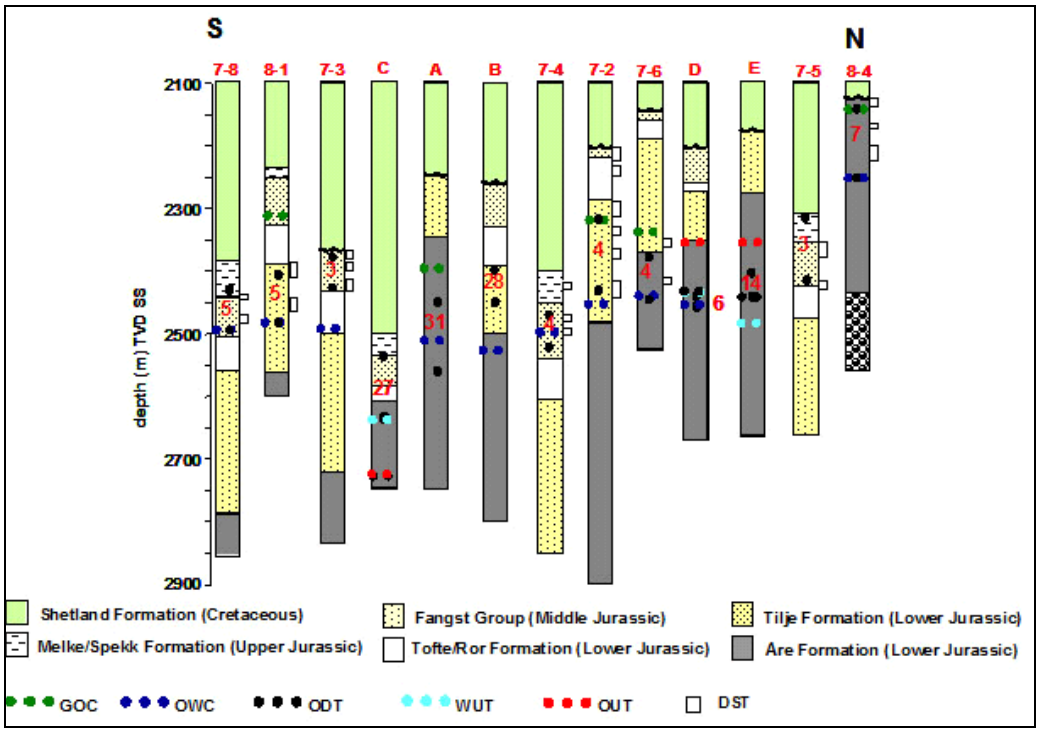

Figure 8 Simplified N-S Profile showing well locations. Red numbers in the profile represent the amount of investigated reservoir rock samples for the individual wells. Rectangles on the right side of the profile represent number and depth of the DST.

GOC - gas/oil contact; OWC - oil/water contact; ODT - oil down to, WUT - water up to; OUT - oil up to.

In the following, the single wells with their appertaining reservoir rock- and oil samples are described in detail, starting with the high-resolution wells from Statoil. The field segment of the wells, sample numbers, their depth and stratigraphical unit, and API gravity for the oil samples are listed in Table 2 - Table 8.

For each profile, well log information complements the description. The logs of the Statoil wells A, B, C, D and E comprise the physical rock properties porosity, permeability, and water saturation. Statoil provided well logs including stratigraphic reservoir zones,

depositional facies, sedimentary structures and lithology. For the investigated NPD well sections the gamma ray log, calliper log, resistivity log, and acoustic log are shown. These logs were taken from the official NPD website (www.factpages.npd.no/factpages). In the individual well log section, the sampled range, the position of the samples in relation to the OWC, as well as barriers (clay, calcite-cemented zones) and coal layers are shown.

3.2.1.1 WELL C

Well C is situated in the southeast of the Heidrun reservoir in field segment J (Figure 4). The 27 analysed reservoir rocks are located deeper than samples of the remaining wells. The samples comprise 25 reservoir rocks of the Middle Jurassic Fangst Group sandstones from the Garn Fm., Not Fm. 1 and Ile Fm. 2 - 6, and two samples from the Early Jurassic Åre Fm. 1 (Båt group) (Table 2, Figure 8). No oil samples are available for well C.

Table 2 Sample numbers, depth and geological formation of reservoir rocks analysed from well C.

well	Field segment	GFZ number	Sample	Sample Type	Stratigraphical Unit	depth
						m MD-RKB
C	J	G004196	reservoir rock	sediment	Garn Fm.	3658.8
C	J	G004197	reservoir rock	sediment	Garn Fm.	3659.6
C	J	G004199	reservoir rock	sediment	Garn Fm.	3661.5
C	J	G004202	reservoir rock	sediment	Garn Fm.	3663.8
C	J	G004203	reservoir rock	sediment	Garn Fm.	3663.9
C	J	G004204	reservoir rock	sediment	Garn Fm.	3665.4
C	J	G004207	reservoir rock	sediment	Garn Fm.	3666.3
C	J	G004208	reservoir rock	sediment	Garn Fm.	3666.4
C	J	G004209	reservoir rock	sediment	Garn Fm.	3667.5
C	J	G004210	reservoir rock	sediment	Garn Fm.	3668.8
C	J	G004213	reservoir rock	sediment	Not Fm. 1	3672.5
C	J	G004215	reservoir rock	sediment	Ile Fm. 6	3674.5
C	J	G004217	reservoir rock	sediment	Ile Fm. 6	3675.9
C	J	G004218	reservoir rock	sediment	Ile Fm. 6	3677.2
C	J	G004219	reservoir rock	sediment	Ile Fm. 6	3677.7
C	J	G004221	reservoir rock	sediment	Ile Fm. 6	3678.9
C	J	G004222	reservoir rock	sediment	Ile Fm. 5	3683.2
C	J	G004223	reservoir rock	sediment	Ile Fm. 5	3685.4
C	J	G004224	reservoir rock	sediment	Ile Fm. 4	3687.3
C	J	G004225	reservoir rock	sediment	Ile Fm. 4	3688.8
C	J	G004226	reservoir rock	sediment	Ile Fm. 4	3692.1
C	J	G004229	reservoir rock	sediment	Ile Fm. 4	3692.8
C	J	G004230	reservoir rock	sediment	Ile Fm. 4	3693.4
C	J	G004234	reservoir rock	sediment	Ile Fm. 3	3696.6
C	J	G004236	reservoir rock	sediment	Ile Fm. 2	3703.7
C	J	G004238	reservoir rock	sediment	Ile Fm. 2	3707.3
C	J	G004240	reservoir rock	sediment	Ile Fm. 2	3709.8
C	J	G004249	reservoir rock	sediment	Åre Fm. 1	3766.8
C	J	G004250	reservoir rock	sediment	Åre Fm. 1	3769.6

Figure 9 shows the well log section of profile C. The ODT contact (oil down to) at 3712 m MD-RKB was used alternativelly for the OWC. The reservoir rocks of the Ile Fm. 2 are in close proximity to the ODT. The Åre Fm. reservoir rocks are below the ODT.

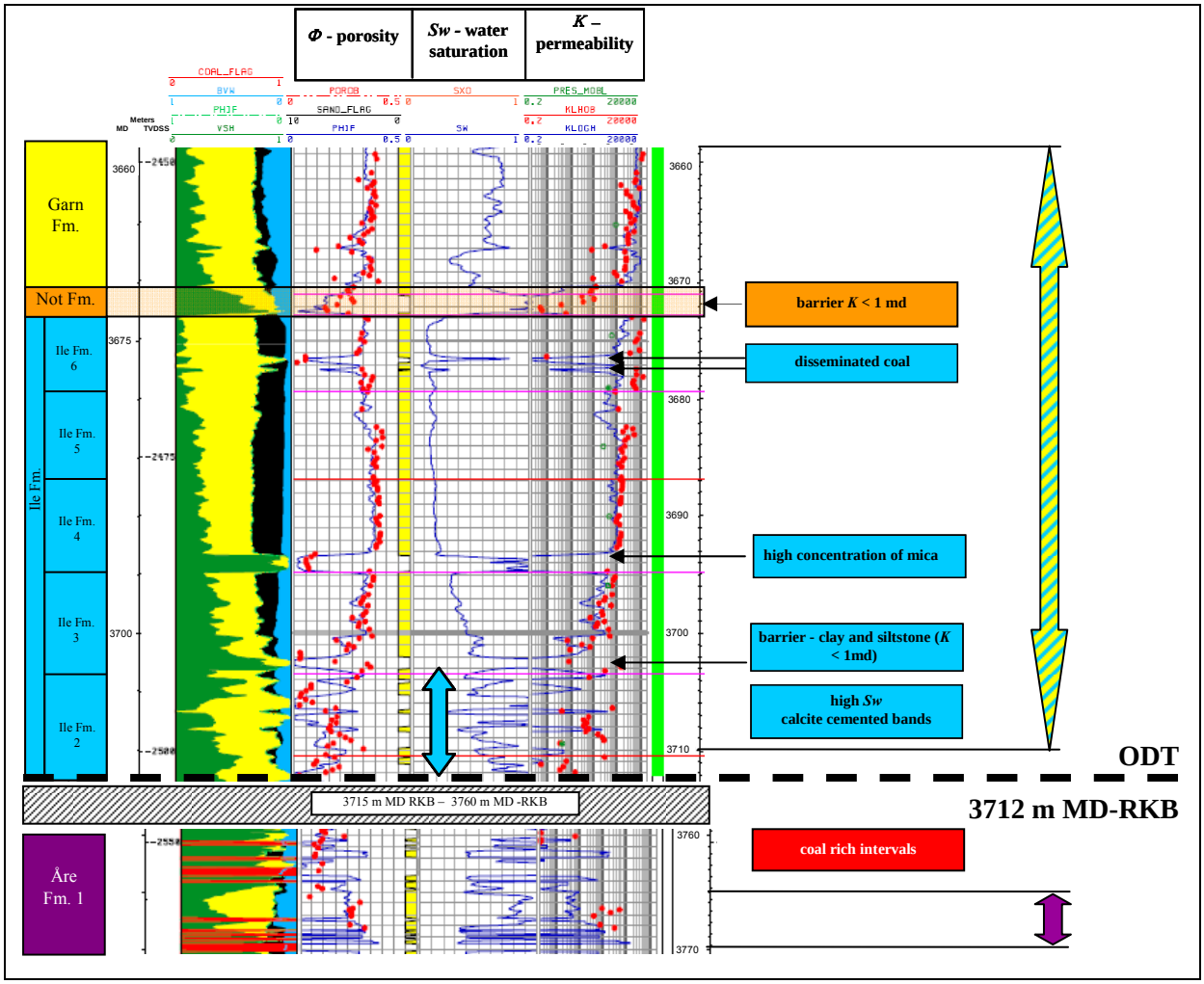

Figure 9 Section of the well log profile C shows the porosity log (left), the water saturation log (middle) and the permeability log (right) as well as barriers and coal layers observed. The sampled interval is marked by the double arrow right beside the log. Zones marked by black arrows are characterised by low porosity, low permeability, and high water saturation. The well log was provided by Statoil.

The Garn Fm. and the Ile Fm. 4 - 6 show good reservoir conditions with relatively uniform poroperm properties compared to the Ile Fm. 2 and 3 near the ODT contact, and the Åre Fm. sediments below the ODT contact. The latter are characterised by several coal-rich intervals (Figure 9).

The Garn Fm. comprises medium- to coarse-grained cross-bedded sandstones, which show the best reservoir properties in the profile (internal Statoil report, 2003), with porosity Φ between 20 % and 40 % and permeability K between 2000 - 20000 md. With increasing depth

both properties slightly decreases. The water saturation (S_w) is relatively high (0.6 - 0.8) in comparison to the water saturation in the Ile Fm. 4 - 6 ($S_w < 0.2$). At the bottom of the Garn Formation the S_w becomes lower (0.3 - 0.6). All rock properties show a sharp contact to the underlying marine shale/sandstones of the Not Formation. Based on Statoil documentations (internal Statoil report, 2003), no communication has to be expected with the Not Fm. as the permeability K is below 1 md (horizontal barrier) (Figure 9).

The analysed reservoir rocks of the Ile Fm. belong to five reservoir zones (Ile Fm. 2 - 6). The sandstones of the Ile Fm. 6 show good reservoir properties with Φ = 30 % - 35 %, K about 2000 md, and a low S_w about 0.1 - 0.2 (Figure 9). Two zones are recognisable at 3676 m and 3677.5 m MD-RKB, with low poroperm signals, and additionally (not shown) low gamma ray signals (no shale), elevated signals for the resistivity and neutron density. Those log signatures are typical for coaly particles. Similar rock properties were observed for coal rich intervals of the Åre Fm at the base of profile C (Figure 9).

The cross-bedded sandstones of the Ile Fm. 5 and 4, and the siltstones of the Ile Fm. 3 represent the upper, middle, and lower parts of a prograding wave-dominated coastline succession. In Ile Fm. 5 and 4, the physical rock parameters show a relatively homogeneous distribution. In comparison to the Ile Fm. 6, the permeability is similar and the porosity is slightly higher. Within both reservoir subzones, Φ and S_w slightly increase with increasing depth. At the base of Ile Fm. 4 (3693 m - 3695 m MD-RKB) a low porosity ($\Phi < 10$ %), low permeability ($K < 1$ md) and high water saturation ($S_w \sim 1$) zone can be observed (Figure 9). A high gamma ray and resistivity signal, as well as a low neutron density signal (not shown) may indicate a shale zone. However, Whitley (1992) observed that the sandstone of the Fangst reservoir 2 (= Ile Fm. 3 - 6) has a high thorium content which gives a high gamma ray log response that could be misinterpreted as a shaly response. In core photos, no shale can be observed but sandstones with high concentrations of mica that also induces by high gamma ray signals. The lowest porosity and highest water saturation of this coastline succession was observed in Ile Fm. 3 which is characterised by clay and siltstone barriers at the base (Figure 9).

The lowermost Ile reservoir (Ile Fm. 2) represents tidally dominated delta sediments with channel sandstones. Here, calcite-cemented bands are typical (internal Statoil report, 2003). Within this unit, the porosity and the permeability decrease down to the ODT contact, while the water saturation increases. Gradually changes in rock properties are reflected by the curve like shapes of the well log (Figure 9).

The Åre Formation is characterised by coal rich intervals. Those coal flags show the lowest signals for porosity and permeability, but high signals for gamma ray, and elevated signals for resistivity and neutron density (not shown).

3.2.1.2 WELL B

This well is situated beside well C in the south-eastern part of the Heidrun oil field in the adjacent segment I (Figure 4). All 28 reservoir rock samples belong to the Early Jurassic Båt group sandstones from the Tilje Formation 2.5 - 3.4 (Table 3, Figure 8). The reservoir rock samples were taken over an interval spanning 55 m, in a distance of 77 m above the OWC at 3356.2 m MD-RKB. A section of well log profile B is shown in Figure 10. No oil samples are available for this location.

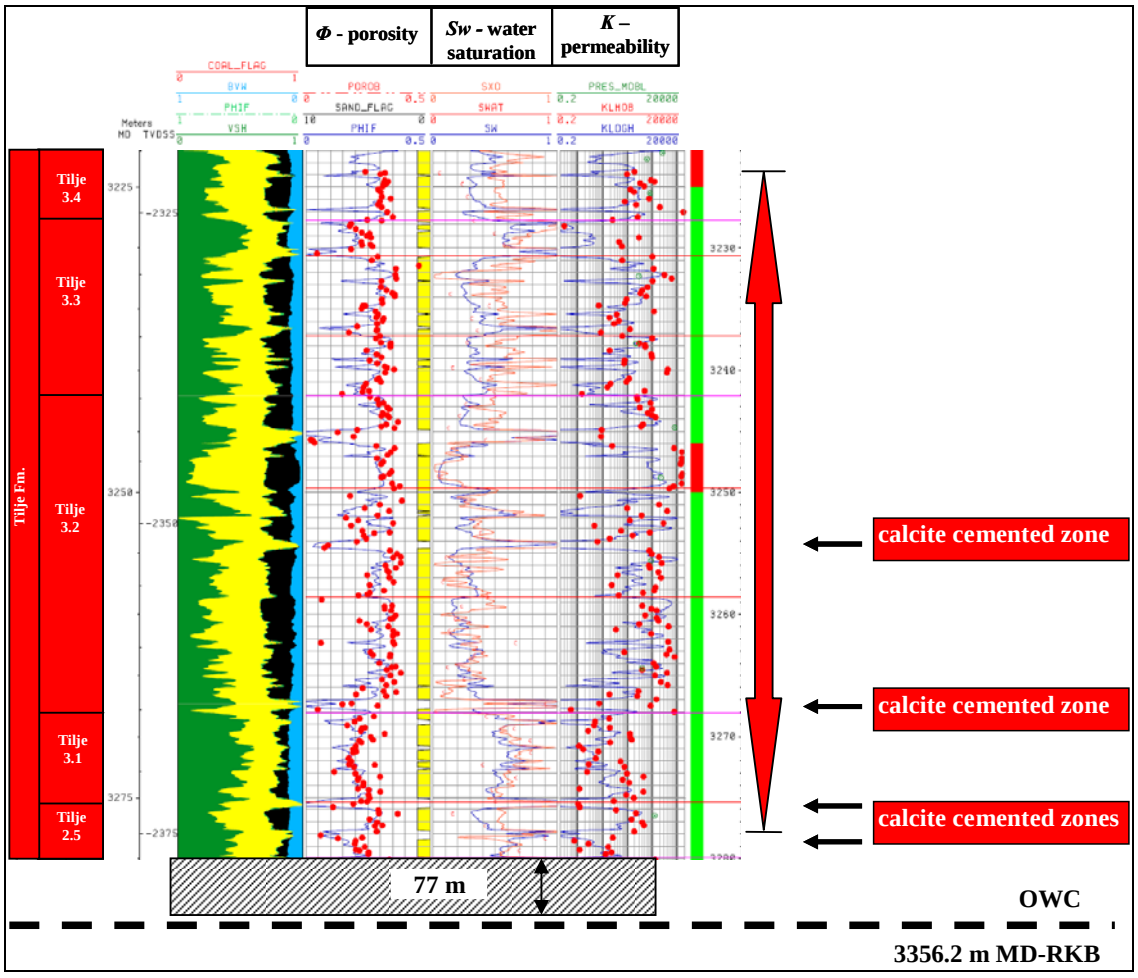

Figure 10 Well log section of profile B showing the porosity log (left), water saturation log (middle) and permeability log (right), and observed calcite cemented zones. The sampled interval is marked by the double arrow right beside the log. The well log was provided by Statoil.

Table 3 Sample numbers, depth and geological formation of reservoir rocks analysed from well B.

well	Field segment	GFZ number	Sample	Sample Type	Stratigraphical Unit	depth
						m MD-RKB
B	I	G004165	reservoir rock	sediment	Tilje Fm. 3.4	3223.9
B	I	G004166	reservoir rock	sediment	Tilje Fm. 3.4	3225.9
B	I	G004167	reservoir rock	sediment	Tilje Fm. 3.4	3226.3
B	I	G004168	reservoir rock	sediment	Tilje Fm. 3.3	3230.0
B	I	G004169	reservoir rock	sediment	Tilje Fm. 3.3	3231.6
B	I	G004170	reservoir rock	sediment	Tilje Fm. 3.3	3232.7
B	I	G004171	reservoir rock	sediment	Tilje Fm. 3.3	3234.4
B	I	G004172	reservoir rock	sediment	Tilje Fm. 3.3	3235.6
B	I	G004173	reservoir rock	sediment	Tilje Fm. 3.3	3237.4
B	I	G004174	reservoir rock	sediment	Tilje Fm. 3.3	3239.5
B	I	G004175	reservoir rock	sediment	Tilje Fm. 3.3	3241.4
B	I	G004176	reservoir rock	sediment	Tilje Fm. 3.2	3242.8
B	I	G004177	reservoir rock	sediment	Tilje Fm. 3.2	3243.6
B	I	G004179	reservoir rock	sediment	Tilje Fm. 3.2	3246.4
B	I	G004182	reservoir rock	sediment	Tilje Fm. 3.2	3250.6
B	I	G004183	reservoir rock	sediment	Tilje Fm. 3.2	3252.3
B	I	G004184	reservoir rock	sediment	Tilje Fm. 3.2	3254.8
B	I	G004185	reservoir rock	sediment	Tilje Fm. 3.2	3257.7
B	I	G004186	reservoir rock	sediment	Tilje Fm. 3.2	3259.4
B	I	G004187	reservoir rock	sediment	Tilje Fm. 3.2	3260.6
B	I	G004188	reservoir rock	sediment	Tilje Fm. 3.2	3263.2
B	I	G004189	reservoir rock	sediment	Tilje Fm. 3.2	3263.9
B	I	G004190	reservoir rock	sediment	Tilje Fm. 3.2	3265.5
B	I	G004191	reservoir rock	sediment	Tilje Fm. 3.1	3272.9
B	I	G004192	reservoir rock	sediment	Tilje Fm. 3.1	3274.2
B	I	G004193	reservoir rock	sediment	Tilje Fm. 2.5	3275.8
B	I	G004194	reservoir rock	sediment	Tilje Fm. 2.5	3276.4
B	I	G004195	reservoir rock	sediment	Tilje Fm. 2.5	3278.9

The Tilje Formation sandstones are characterised by highly variable depositional patterns, which results in very complex and extremely heterogeneous reservoir subzones (Hemmens *et al.*, 1994) (cf. Chapter 3.1). These patterns are reflected in the well log. All reservoir zones are characterised by distinct changes of the porosity, permeability and water saturation at a centimetre to meter scale. The Tilje Fm. 3.4 comprises fine-grained, very clean sandstones. The underlying Tilje Fm. 3.3 comprises two subunits. Both of them are characterised by a distinct upward cleaning and coarsening trend (internal Statoil report, 2003) which is reflected in increasing poroperm properties from the bottom to the top of these zones (Figure 10). Characteristic for the Tilje Fm. 3.2, are stacked distributary channels in shoreface deposits (delta sediments) (internal Statoil report, 2003). A unit with very good reservoir properties (high permeability) is located in the upper part. The fine-grained Tilje Fm. 3.1 and Tilje Fm. 2.5 deposits at the bottom of the profile, show lower porosity and permeability values (Figure 10).

Based on core descriptions and on core photos calcite-cemented zones have been detected, which are characterised by a very low porosity and permeability as well as a high density (not shown) (Figure 10). They might act as flow barrier and/or represent marker for a paleo-OWC. Due to the large distance, a high impact of the present water saturated zone below the OWC can be neglected.

The following three high-resolution wells A, D and E comprise reservoir rocks from the Åre Formation. The Åre Formation is the lowermost reservoir among the reservoir formations of the Heidrun oil field. It belongs to the Lower Jurassic Båt group. The sediments are a heterogeneous mix of channel sands, coals and shales.

3.2.1.3 WELL A

Well A is situated between well C and B in the south-eastern part of the field in segment J (Figure 4). In total 31 reservoir rocks were sampled including the lower Åre subunits 3.1 up to 4.4 (Table 4, Figure 11). The reservoir rock samples were taken over an interval of 117 m. The OWC is observed within the lower part of the sampled well section at 3249.3 m MD-RKB. No oil samples were available for this well.

The very heterogeneous depositional environment of the Åre sediments (cf. Chapter 3.1) is reflected in the well log (Figure 11). While the Åre reservoir 3 is dominated by bay filled deposits with minor coastal plain deposits, characterised by greater variability in the poroperm properties, the Åre reservoir 4 is dominated by coastal plain deposits with minor bay fills. The latter is characterised by slightly lesser heterogeneities and better poroperm properties (Figure 11). Both sediment facies contain channel features with good reservoir conditions (internal Statoil report, 2003). Several reservoir subzones are locally capped by peat swamp coal and show interstratified coal layers, which are marked in the log (Figure 11).

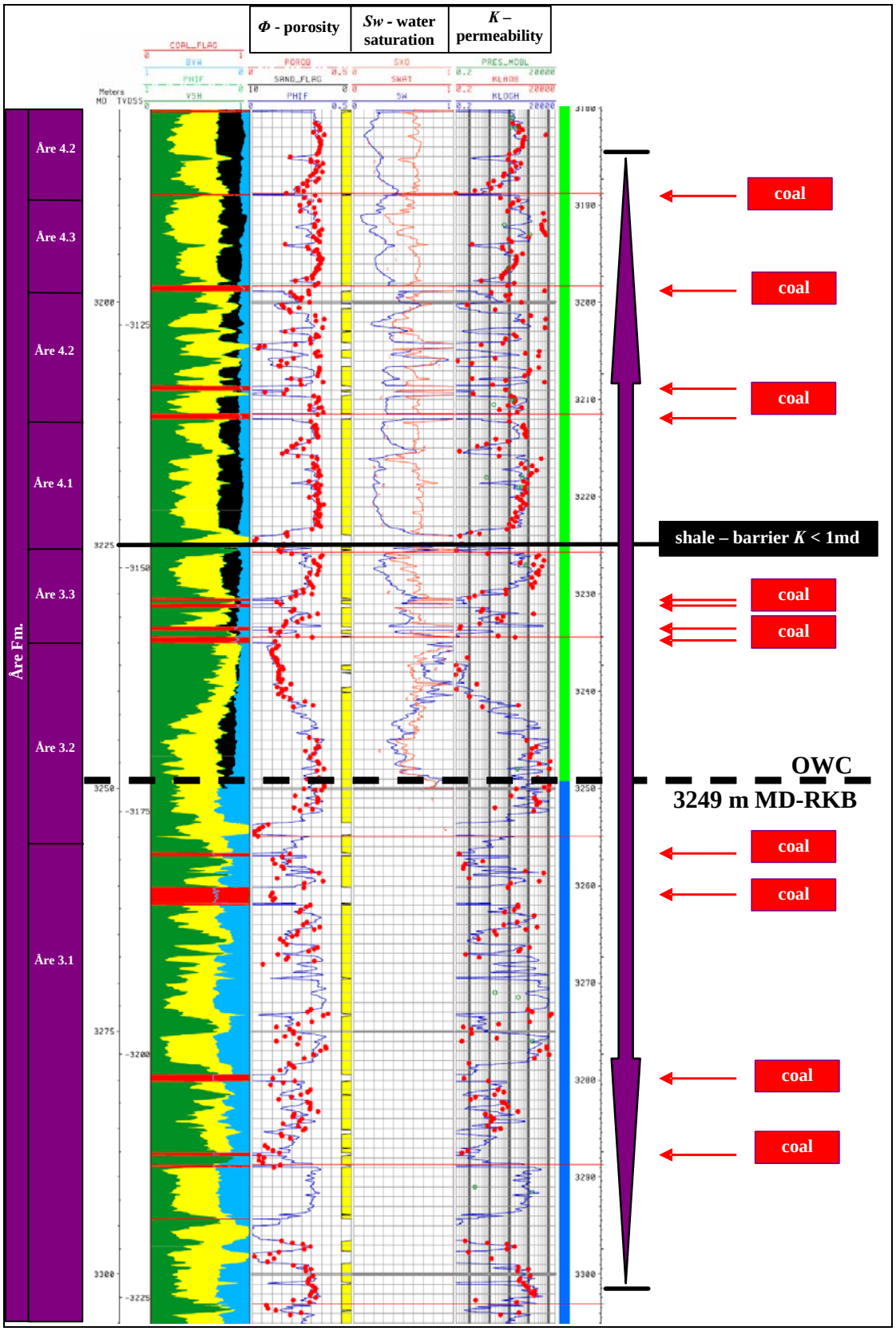

Figure 11 Well log section of the profile A (provided by Statoil) showing the porosity log (left), water saturation log (middle) and permeability log (right). The sampled intervals are marked by the double arrow right beside the log. The coal rich layers and the shale detected between the Åre reservoir zone 3 and 4 are marked in the log.

Table 4 Sample numbers, depth and geological formation of reservoir rocks analysed from well A.

well	Field segment	GFZ number	Sample	Sample Type	Stratigraphical Unit	depth
						m MD-RKB
A	J	G004123	reservoir rock	sediment	Åre Fm. 4.4	3184.3
A	J	G004126	reservoir rock	sediment	Åre Fm. 4.3	3189.5
A	J	G004127	reservoir rock	sediment	Åre Fm. 4.3	3189.9
A	J	G004128	reservoir rock	sediment	Åre Fm. 4.3	3190.3
A	J	G004129	reservoir rock	sediment	Åre Fm. 4.3	3192.5
A	J	G004132	reservoir rock	sediment	Åre Fm. 4.3	3195.8
A	J	G004134	reservoir rock	sediment	Åre Fm. 4.2	3198.6
A	J	G004136	reservoir rock	sediment	Åre Fm. 4.2	3202.4
A	J	G004137	reservoir rock	sediment	Åre Fm. 4.2	3203.9
A	J	G004138	reservoir rock	sediment	Åre Fm. 4.2	3209.5
A	J	G004139	reservoir rock	sediment	Åre Fm. 4.2	3211.3
A	J	G004140	reservoir rock	sediment	Åre Fm. 4.1	3212.5
A	J	G004141	reservoir rock	sediment	Åre Fm. 4.1	3214.5
A	J	G004142	reservoir rock	sediment	Åre Fm. 4.1	3215.5
A	J	G004143	reservoir rock	sediment	Åre Fm. 4.1	3217.9
A	J	G004144	reservoir rock	sediment	Åre Fm. 4.1	3218.6
A	J	G004145	reservoir rock	sediment	Åre Fm. 4.1	3219.8
A	J	G004146	reservoir rock	sediment	Åre Fm. 4.1	3221.3
A	J	G004147	reservoir rock	sediment	Åre Fm. 4.1	3222.3
A	J	G004148	reservoir rock	sediment	Åre Fm. 4.1	3223.3
A	J	G004149	reservoir rock	sediment	Åre Fm. 4.1	3228.4
A	J	G004150	reservoir rock	sediment	Åre Fm. 4.1	3230.3
A	J	G004153	reservoir rock	sediment	Åre Fm. 4.1	3233.6
A	J	G004154	reservoir rock	sediment	Åre Fm. 3.2	3235.5
A	J	G004155	reservoir rock	sediment	Åre Fm. 3.2	3244.5
A	J	G004156	reservoir rock	sediment	Åre Fm. 3.2	3246.1
A	J	G004157	reservoir rock	sediment	Åre Fm. 3.2	3248.6
A	J	G004160	reservoir rock	sediment	Åre Fm. 3.2	3249.7
A	J	G004161	reservoir rock	sediment	Åre Fm. 3.2	3250.8
A	J	G004163	reservoir rock	sediment	Åre Fm. 3.1	3276.5
A	J	G004164	reservoir rock	sediment	Åre Fm. 3.1	3301.5

Both Åre reservoirs are divided by a shale at 3225 m MD-RKB, which might act as a barrier with $K < 1$ md (Figure 11). Sediments of the Åre reservoir subunits 4.4, 4.3 and 4.1, which are located above the shale, show higher porosity and permeability signals indicating good reservoir properties. The Åre Fm. reservoir subunit 4.2 exhibits strong variabilities in rock properties marking it as the most heterogeneous of the Åre reservoir 4 subunits. The poroperm properties in the Åre reservoir subzones 4.4 and 4.3 slightly decrease, while the rock properties in subzone 4.1 are nearly constant. The Åre Fm. subzone 4.1 is characterised by a low porous and permeable layer in the upper part and a sharp contact, in form of the above mentioned shale, to the underlying Åre reservoir zone 3.

In the Åre Fm. reservoir 3 below the shale, the porosity and permeability shows an S-shape down to the OWC. Below the OWC, both rock properties are variable and show significant changes at very small scale. In the Åre reservoir 3.3 the porosity and permeability decreases

with increasing depth, while the water saturation increases. An inverse picture is found in the underlying Åre Fm. reservoir 3.2. The porosity and permeability increases down to the OWC, while the water saturation conspicuously decreases. This zone is finished off by a very dense zone at the bottom (Figure 11). The lowermost Åre Fm. reservoir 3.1 below the OWC shows the greatest variability in poroperm properties and the thickest coal layer.

Typical reservoir rock plugs of the Åre Fm. 4 commonly comprise medium- to coarse-grained, cross-stratified sandstones of light- and dark brown colour (G004137, Figure 12 left). Reservoir rock samples of the Åre Fm. 3 are not stratified. They contain mica in high abundance (micaceous siltstones) and have generally a light brown colour reflecting higher water saturation (G004160, Figure 12 right).

Figure 12 Typical reservoir rocks of the Åre Formation 4 (G004137, left) and the Åre Formation 3 (G004160, right).

3.2.1.4 WELL E

14 Åre Formation reservoir rocks were analysed from well E, which is situated in the northern part of the Heidrun oil field in segment M (Figure 4, Figure 8). These rock samples comprise the lower Åre subunits 4.1, 3.3, and 3.2 (Table 5), shown in the well log section of profile E in Figure 13. They were taken in an interval of 42 m in relatively great depth (> 3500 m MD-RKB). All reservoir rocks are located above the ODT contact, which can be observed directly at the bottom of the profile at 3585 m MD-RKB. Thus, lower reservoir rocks of well E are very close to the water-saturated zone. No oil sample was available for this well.

Table 5 Sample numbers, depth and geological formation of reservoir rocks analysed from well E.

well	Field segment	GFZ number	Sample	Sample Type	Stratigraphical Unit	depth
						m MD-RKB
E	M	G004260	reservoir rock	sediment	Åre Fm. 4.1	3540.5
E	M	G004263	reservoir rock	sediment	Åre Fm. 4.1	3542.8
E	M	G004264	reservoir rock	sediment	Åre Fm. 4.1	3543.2
E	M	G004265	reservoir rock	sediment	Åre Fm. 4.1	3543.8
E	M	G004266	reservoir rock	sediment	Åre Fm. 4.1	3548.2
E	M	G004267	reservoir rock	sediment	Åre Fm. 4.1	3550.5
E	M	G004268	reservoir rock	sediment	Åre Fm. 4.1	3554.5
E	M	G004271	reservoir rock	sediment	Åre Fm. 4.1	3558.8
E	M	G004272	reservoir rock	sediment	Åre Fm. 4.1	3560.8
E	M	G004275	reservoir rock	sediment	Åre Fm. 3.3	3570.5
E	M	G004276	reservoir rock	sediment	Åre Fm. 3.3	3575.2
E	M	G004279	reservoir rock	sediment	Åre Fm. 3.3	3576.3
E	M	G004280	reservoir rock	sediment	Åre Fm. 3.2	3581.7
E	M	G004281	reservoir rock	sediment	Åre Fm. 3.2	3582.6

The sediments of the Åre Formation subzones 4.1 -3.2 were deposited in a mud-dominated delta plain crossed by meandering channels. The main reservoirs are channel sandstones separated by muddy deposits (shales) and coal beds (Hemmens *et al.*, 1994; Whitley, 1992), (cf. Chapter 3.1). These alternations are reflected by varying poroperm properties in the well log (Figure 13). Several interstratified dense and compacted zones, which generally consist of alternating shales and sandstone / siltstones, might act as barriers within the profile.

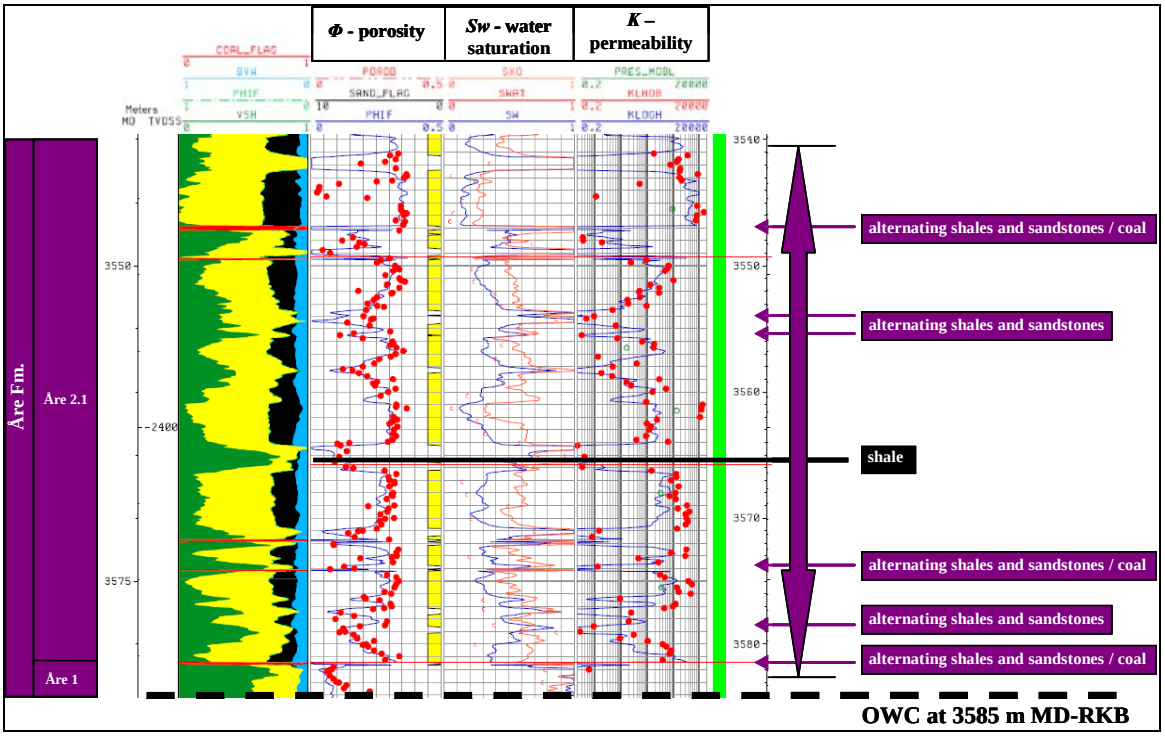

Figure 13 Well log section of profile E showing the porosity log (left), water saturation log (middle) and permeability log (right) as well as observed low permeable zones (= barriers). The sampled interval marked by the double arrow right beside the log. Statoil provided the log.

Based on the core photos and description, sediments of well E consists of fine to medium-grained sandstones with varying oil saturation, and alternating siltstones, mudstones and coals. Most reservoir rocks are from the Åre Fm. 2.1. The upper part of this zone comprises a 5 m thick channel-sandstone interval at 2960 m - 2900 m MD-RKB, that is characterised by a high permeability about 2000 - 20000 md, and porosity between 30 and 40 % (Figure 13). Below this permeable interval, gradients are observed in the sandstone poroperm properties, which are delimited by alternating mudstones and siltstones. These poroperm gradients recognised correlate with the grain size of the sandstone.

3.2.1.5 WELL D

Well D is situated close to well E in Heidrun north in segment Q (Figure 4). In total six reservoir rocks from the lower Åre Fm. subunit 2.1 were investigated. They were taken in a relatively narrow interval over15 m in shallow depth (< 3000 m MD-RKB) (Table 6). Two water legs can be detected in profile D based on well log (Figure 14) and fluid contact reports from Statoil. The first water saturated zone can be seen for the interval from 2890 m MD-RKB (1st WUT) down to the OWC at 2912 m MD-RKB. The second water saturated zone starts at 2937 m MD RKB (2nd WUT). All but the uppermost reservoir rock are taken from the oil-saturated zone in between the two water legs. The second topmost sample is located near the OWC at 2912 m MD-RKB (Figure 14). For well D one oil sample was supplied. The relevant oil data are listed in Table 8.

Table 6: The sample numbers, depth, geological formation of reservoir rocks analysed from well D.

well	Field segment	GFZ number	Sample	Sample Type	Stratigraphical Unit	depth
						m MD-RKB
D	Q	G004251	reservoir rock	sediment	Åre Fm. 2.1	2895.2
D	Q	G004252	reservoir rock	sediment	Åre Fm. 2.1	2912.5
D	Q	G004254	reservoir rock	sediment	Åre Fm. 2.1	2913.1
D	Q	G004255	reservoir rock	sediment	Åre Fm. 2.1	2915.3
D	Q	G004257	reservoir rock	sediment	Åre Fm. 2.1	2920.3
D	Q	G004258	reservoir rock	sediment	Åre Fm. 2.1	2918.4

The Åre Fm. 2.1 contains reservoirs in the form of fluvial channel sandstones separated by floodplain mudstones and peat swamp coal (cf. Chapter 3.1). The well log section in Figure 14 shows this heterogeneous succession of alternating sediments. The whole profile is characterised by numerous interstratified coal layers.

Most of the reservoir rocks are taken from the oil saturated interval, which shows a lower porosity (~ 10 %) and permeability (2 - 200 md) than the Åre Fm. 2.1 in well E. The physical rock properties change at very small scale. An interval in the upper water leg (2890 m - 2900 m MD-RKB), where the uppermost reservoir rock was taken from, is characterised by higher a porosity (20 % - 30 %) and permeabilities between 200 and 2000 md. Both, porosity and permeability increase with increasing depth (Figure 14).

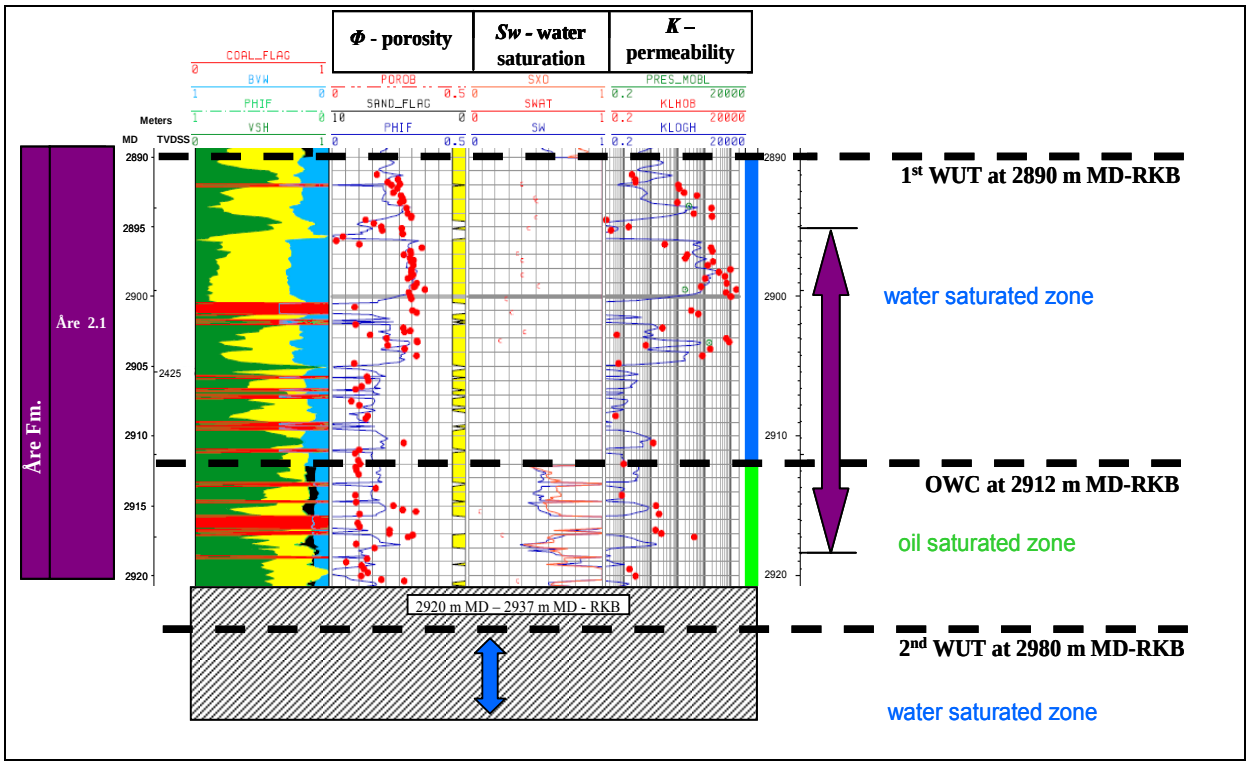

Figure 14 Well log section of profile D showing the porosity log (left), water saturation log (middle) and permeability log (right). The sampled interval marked by the double arrow right beside the log. Coal flags are marked by the red colour left beside the porosity log. The well log was provided by Statoil.

In the following, investigated reservoir rocks, potential source rocks and oil samples (DSTs) taken from the NPD profiles will be described.

3.2.1.6 WELL 6507/7-2

Well 6507/7-2 is situated in segment G, in the central part of the Heidrun oil field (Figure 4). Two reservoir rocks from the Tilje Formation subunits 2.1 and 3.2, and two reservoir rocks of the upper Åre Formation subunits 7.2 and 6.2 were investigated. These four samples were taken over a large interval of 116 m from a relatively shallow reservoir depth as shown in the

section of the well log in Figure 15. All reservoir rock samples are located above the OWC at 2451 m MD-RKB. Important reservoir rock data is listed in Table 7.

Three oil samples (DSTs) are available for this well. They show a distinct gradient in API gravity from 29° to 22 ° (Table 8).

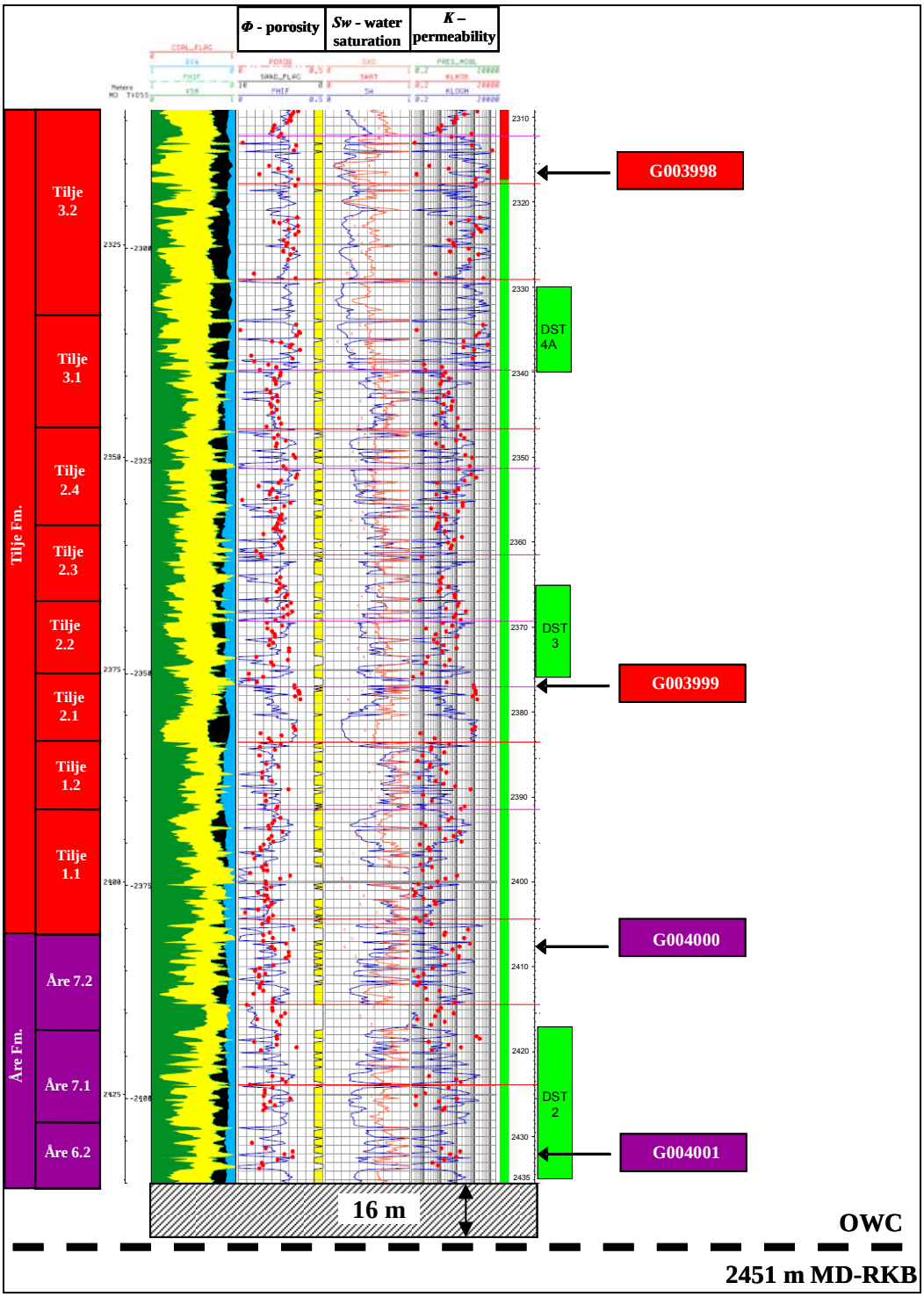

Figure 15 Well log section of profile 6507/7-2 showing the porosity log (left), water saturation log (middle) and permeability log (right). The depth of the analysed reservoir rocks as well as the interval for the oil samples (DSTs) is marked right beside the permeability log. The well log was provided by Statoil.

The Tilje- and the upper Åre Formation reservoirs are characterised by a very complex and heterogeneous sedimentology (cf. Chapter 3.1) that is reflected by strongly alternating rock properties in the well log section (Figure 15).
Both analysed reservoir rocks from the Tilje Fm. 3.2 and 2.1 comprise sandstones deposited in a shallow marine shelf environment with tidal and deltaic influences (cf. Chapter 3.1). These sandstones are characterised by alternating heterolithics and different permeable channels. The uppermost Tilje Fm. 3.2 rock sample belongs to a unit exhibiting good reservoir properties, which consists of deltaic deposits containing high permeable sand channels. This reservoir zone shows a higher porosity (20 - 30 %) and permeability (200 - 20000 md) as well as a lower water saturation than the remaining reservoir zones. The Tilje Fm. 2.1 comprises heterolithic sandstones and siltstones and shows an increase in poroperm properties with increasing depth. Both Åre Fm. reservoirs comprise marginal marine and tidally dominated estuarine deposits with interstratified sand channels.
Interstratified mudstones might act as barriers within all reservoir subunits.

3.2.1.7 WELL 6507/7-3

Well 6507/7-3 is situated in the southwestern part of the Heidrun oil field in segment E (Figure 4). Three reservoir rock samples taken over an interval of 50 m were investigated. These sandstones are from the Garn Fm., the Ile Fm. 4 - 6 and the Ror Fm. 2 (Table 7). All reservoir rocks are located 70 m above the OWC at 2491 m MD-RKB as shown in the well log section in Figure 16.
The three oil samples (DSTs) from the Garn Fm., Ile Fm., and Ror Fm. are characterised by a uniform and relatively high API gravity of 29° (Table 8).

The physical rock properties do not indicate significant differences within the profile. The resistivity and the acoustic signal are very uniform within the sampled interval. The very low resistivity signal (≈ 1 Ω) and low acoustic signal (between 90 and 110 µsec/ft) infer relatively high water saturation. The latter additionally indicates low porosity that is higher in the Garn - and Ile Fm. than in the underlying Ror Formation. The Garn- and Ile Fm. reservoir rocks consist of predominantly medium grained and partly friable sandstones, while the Ror Formation sediments comprise alternating clay stones and siltstones. Within the Ile Fm., the high gamma ray signal indicates a shale zone between 2400 m - 2410 m MD-RKB, which might act as a barrier.

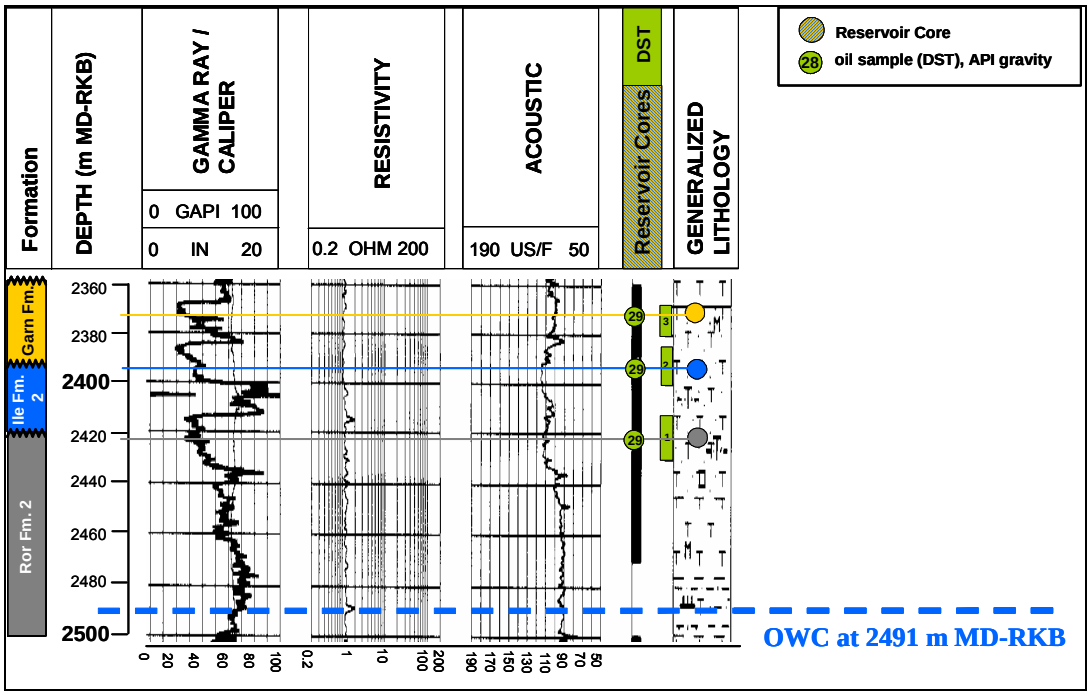

Figure 16 Well log section of profile 6507/ 7-3 showing the gamma ray log (left), resistivity log (middle) and acoustic log (right). The reservoir rocks and the oil samples (DST) with their API gravity are marked by the coloured circles. The numbers in the green rectangles give the DST numbers. The well log is taken from the official NPD website (www.factpages.npd.no/factpages).

3.2.1.8 WELL 6507/7-4

Well 6507/7-4 is the westernmost profile analysed in the Heidrun oil field (Figure 4). From this profile, situated in segment C, four reservoir rock samples were analysed, which consist of Middle Jurassic sandstones from the Fangst group. The subunits comprise the Garn Fm. and the Ile Fm. 5 - 6. The samples were taken over an interval of 45 m. (Table 7). As shown in the well log section in Figure 17, two reservoir rocks from the Ile Fm. are located very close above and below the OWC at 2496 m MD-RKB.

Three oil samples (DSTs) from the Garn- and Ile Formation were available for this well, located above and in the range of the OWC (Table 8, Figure 17).

The Garn Fm. sediments represent a mixture of fluvial and tidally influenced deposits with channel sandstones as reservoirs. The Ile Fm. 5 - 6 sandstones belong to a prograding delta / shoreface unit that comprises bay-fill delta front deposits with less tidally influenced channels. All reservoir rocks in profile 6507/7-4 are well-sorted, pale brown coloured sandstones of a predominantly fine to medium grain-size. They have a carbonaceous and silty matrix, which is partly very friable.

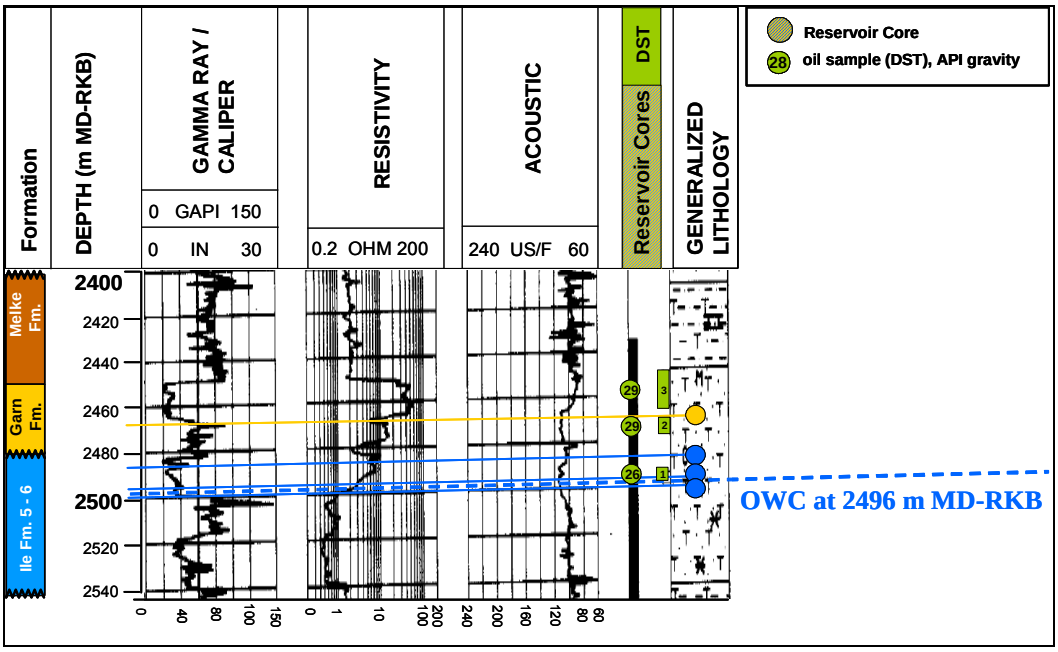

Figure 17 Well log section of profile 6507/7-4 showing the gamma ray log (left), resistivity log (middle) and acoustic log (right). The reservoir rocks and the oil samples (DSTs) with their API gravity are marked by coloured circles. The numbers in the green rectangles are the DST numbers. The well log is taken from the official NPD website (www.factpages.npd.no/factpages).

The oil-saturated zone on the top of the Garn Fm. is characterised by a low gamma ray signal and a high resistivity (Figure 17). The uppermost reservoir rock sample was taken from this zone. In the lower part of the Garn Fm., at 2470 m - 2480 m MD-RKB, the gamma ray signal indicates a zone of alternating shales and sandstones that might act as a barrier system for migrating hydrocarbons. Below the oil-saturated zone down to the OWC, a resistivity decrease indicates the increasing water saturation. The reservoir rocks of the Ile Fm. 5 - 6 are taken from this zone. The acoustic signal is relatively uniform within the sampled interval indicating only slight variabilities in the porosity of the sandstones.

3.2.1.9 WELL 6507/7-5

The samples of profile 6507/7-5, which is situated in segment O in the north-western part of the Heidrun oil field (Figure 4), comprises two reservoir sandstones from the Middle Jurassic Fangst group (Garn Fm. and Ile Fm. 2), and one of the potential source rocks, the shale from the Upper Jurassic Spekk Formation (Viking group). The range over which the rocks were sampled is rather large, in total 104 m as shown in the well log of this profile (Figure 18). All rocks should be unaffected by the OWC, because they were sampled in a distance of 250 m above the OWC at 2661 m MD-RKB.

Two oil samples (DSTs), one of the Garn Fm. and one of the Ile Fm. 2 / 1 are available for this well. Both are characterised by high API gravities of 32° and 28°, respectively (Table 8). The Spekk Formation shale on the top of the profile is characterised by a very high gamma ray signal (Figure 18, left). Below, the two reservoir rocks of the Garn Fm. and the Ile Fm. 2 are within the oil-saturated zone, which is characterised by a high resistivity signal (Figure 18, middle). Both reservoir rocks comprise predominantly medium-grained, oil-stained sandstones and show only slight differences in the resistivity signals, the lower being observed in the Ile Fm. 2.

Gradients in the gamma ray signal can be observed for some intervals within the Garn- and Ile Formation. Each interval is limited by a very dense layer consisting of shales and/or limestones. These dense layers might act as barriers for migrating hydrocarbons.

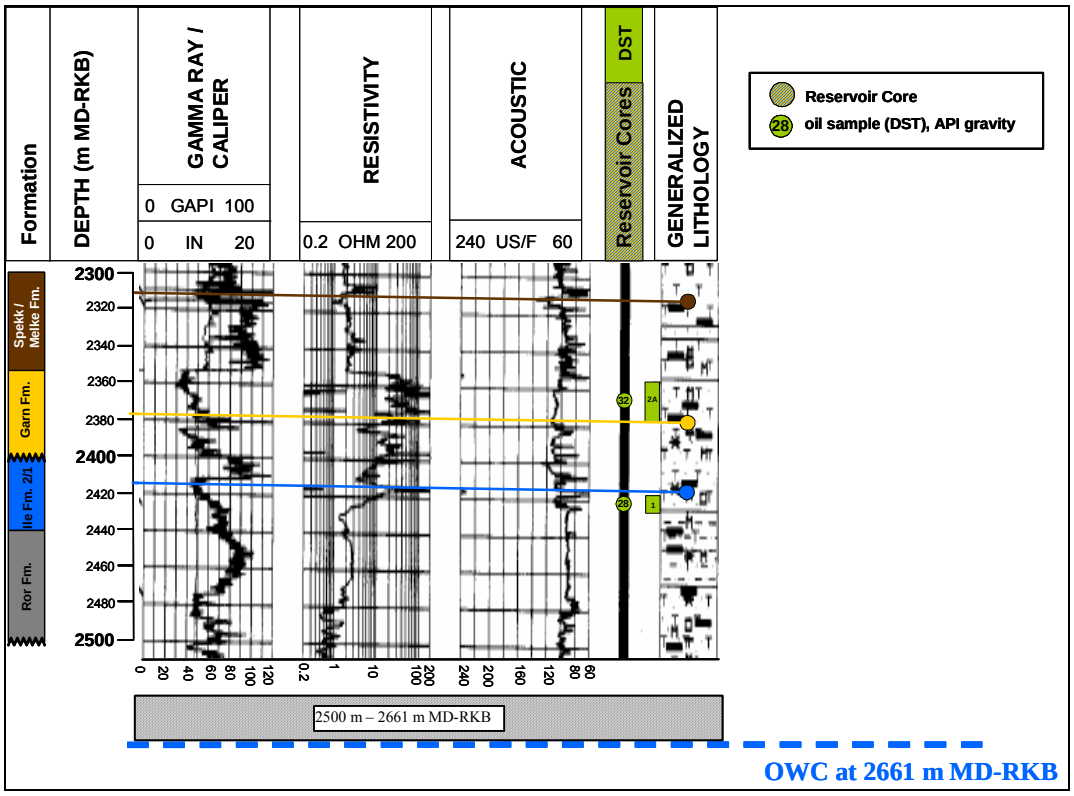

Figure 18 Well log section of the profile 6507/7-5 showing the gamma ray log (left), resistivity log (middle) and acoustic log (right). The reservoir rocks and the oil samples (DSTs) with their API gravity are marked by different coloured circles. The numbers in the green rectangles are the DST numbers. The well log is taken from the official NPD website (www.factpages.npd.no/factpages).

3.2.1.10 WELL 6507/7-6

Well 6507/7-6 is one of two NPD wells in the northern part of the Heidrun oil field (Figure 4). Well 6507/7-6 is located in segment I, together with well B and well 6507/8-1. Four

reservoir rocks from the lower part of the Åre Formation (Båt group) were investigated in a relatively short sample interval spanning 21 m as shown in the log section in Figure 19. The reservoir subunits comprise the Åre Fm. 3.1 - 3.2 and stratigraphic lower units (Åre Fm. 2?), (Table 7). The lowermost three reservoir rocks are located near the OWC at 2438 m MD-RKB, approximately 7 m above and below the OWC.

Both Åre Formation oil samples (DSTs) available for this well are characterised by a distinct drop in API gravity from 27° to 23° with increasing depth (Table 8).

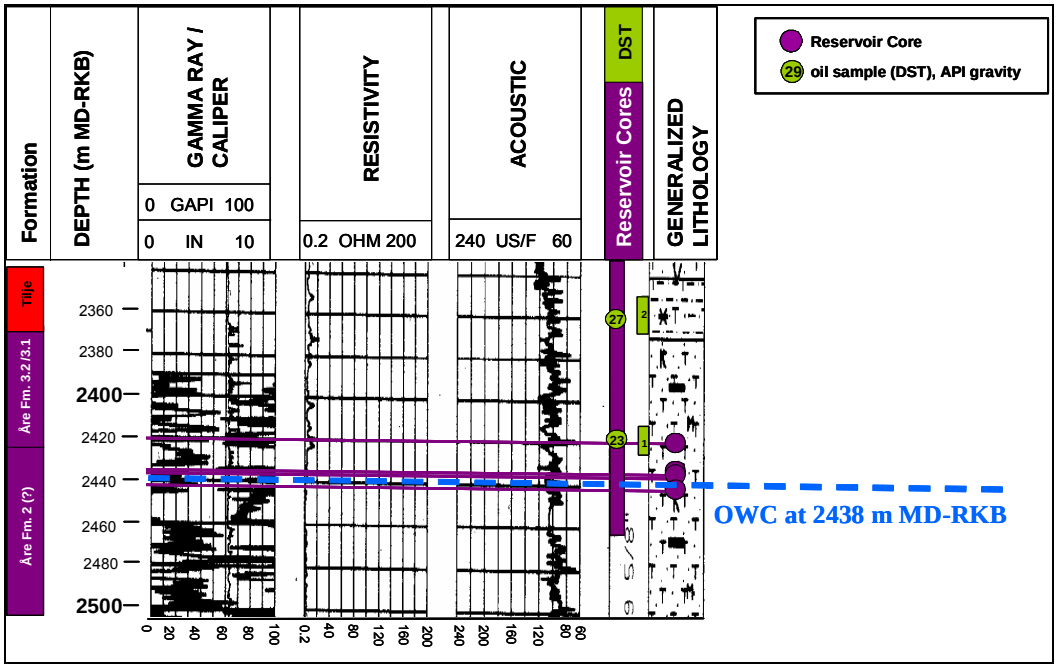

Figure 19 Well log section of the profile 6507/7-6 showing the gamma ray log (left), resistivity log (middle) and acoustic log (right). The reservoir rocks and the oil samples (DSTs) with their API gravity are marked by purple and green circles. The numbers in the green rectangles are the DST numbers. The well log is taken from the official NPD website (www.factpages.npd.no/factpages).

The Åre Fm. subzone 3 is characterised by a slightly increasing marine influence. It comprises a complex sedimentary mixture of bay fill deposits, in which some coastal plain deposits can be found (cf. Chapter3.1). Based on the core photos, core description, and well logs, the sediments of well 6507/7-6 are made up of alternating sandstones and siltstones with thin interstratified zones of clay (mudstone). The analysed reservoir rocks were taken from sandstone zones containing predominantly medium sized grains.

Strong variabilities in the gamma ray signal point to numerous interstratified clay (mudstone) zones in the profile. The resistivity signal is very low (high conductivity) within the evaluated interval. The low resistivity (< 20 Ω) infers high water saturation, which can be expected in the interval close to the OWC. The relatively low and slightly variable acoustic signal

between 80 and 120 µsec/ft is also an indicator for high water saturation and additionally infers a generally low porosity, which might slightly change at small scale (Figure 19).

3.2.1.11 WELL 6507/7-8

Well 6507/7-8 is the southernmost well analysed in the Heidrun oil field (Figure 4). This well is situated in segment F. In total, five rock samples were investigated including the second potential source rock of the Viking Group, the Middle Jurassic shale of the Melke Formation. The reservoir rocks are sandstones from the Fangst Group comprising one sample of the Garn Fm. and three samples of the Ile Fm. (Table 7). Specific subunits are not known for this well. The reservoir rocks were taken over a relatively short interval of 30 m (Figure 8). The two lowermost Ile Fm. reservoir rocks are located very close to the OWC at 2495 m MD-RKB. Two oil samples (DSTs), one of the Garn Fm. and one of the Ile Fm. are available for this well. Both exhibit a relatively high API gravity about 29° and 30° (Table 8).
No log signals were recorded for the investigated interval. One exception is the resistivity signal that decreases in the Ile Formation down to the OWC and indicates an increase in water saturation. Based on core photos and core description, the Ile- and Garn Formation sediments are well-sorted sandstones with a fine to coarse grain size. The Melke Fm. source rock sample is a grey, dense mudstone.

3.2.1.12 WELL 6507/8-1

Well 6507/8-1 is situated in the south south-eastern part of the Heidrun oil field in segment I, southern of well B (Figure 4). Five reservoir rocks from the Tilje Fm. 3.3 - 1 were investigated over an interval of 73 m (Table 7). The last three reservoir rocks are located in a very close distance of only 10 m above the OWC at 2480 m MD-RKB as shown in the well log section in Figure 20.
Two oil samples (DSTs) from the Tilje Fm. 3.3 and 1 are available for this well. Both show lowest API gravity (23° and 20°) of all analysed oil samples (Table 8).

The acoustic log signal is highly variable and indicates significant changes in the porosity at very small scale (Figure 20). Based on the gamma ray signal and the core photos, several thin shale zones (mudstones) are interstratified in the Tilje sandstones. Within the profile, two carbonate- / dolomite-cemented dense, sandstone zones could be detected (high resistivity),

one in the upper part of the profile at 2410 m, and a larger one near the OWC at 2470 m to 2480 m MD-RKB. Both might act as potential barrier. The drop in the resistivity at 2480 m MD-RKB indicates the transition to the water-saturated zone. Both zones are highlighted in Figure 20.

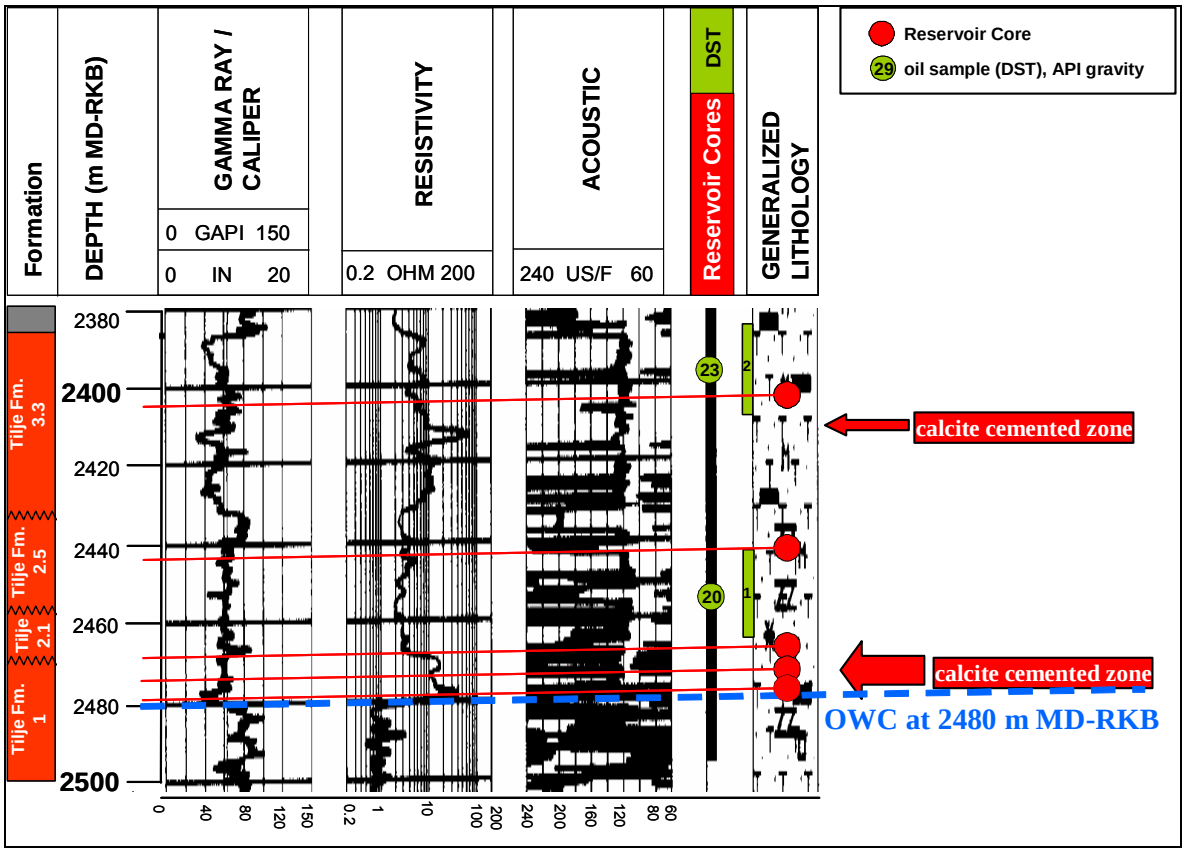

Figure 20 Well log section of profile 6507/8-1 showing the gamma ray log (left), acoustic log (middle), and resistivity log (right). The reservoir rocks and the oil samples (DSTs) with their API gravity are marked by red and green circles. The numbers in the green rectangles are the DST numbers. Dolomite- / calcite-cemented zones are marked by red arrows. The well log is from the official NPD website (www.factpages.npd.no/factpages).

3.2.1.13 WELL 6507/8-4

Well 6507/8-4 is the northernmost profile situated in Heidrun North (Figure 4). In this well, the Åre Formation is in a distinctly shallower reservoir depth than in the remaining analysed wells (Figure 8). Seven reservoir rock samples from the lower part of the Åre Formation were investigated comprising the Åre subunits 2.1 - 1 (similar subunits as in well D and E) (Table 7). The samples cover a large interval of 112 m of the cored section as shown in the well log in Figure 21. The four lowermost reservoir rocks are located approximately 5 m around the OWC at 2251.5 m MD-RKB. Both lowermost reservoir rocks are below the OWC.

Two oil samples (DSTs), one from the Åre Fm. 2.1 and one from the Åre Fm. 1, are available for this well (Table 8). Both are characterised by intermediate API gravities of 24° and 26°.

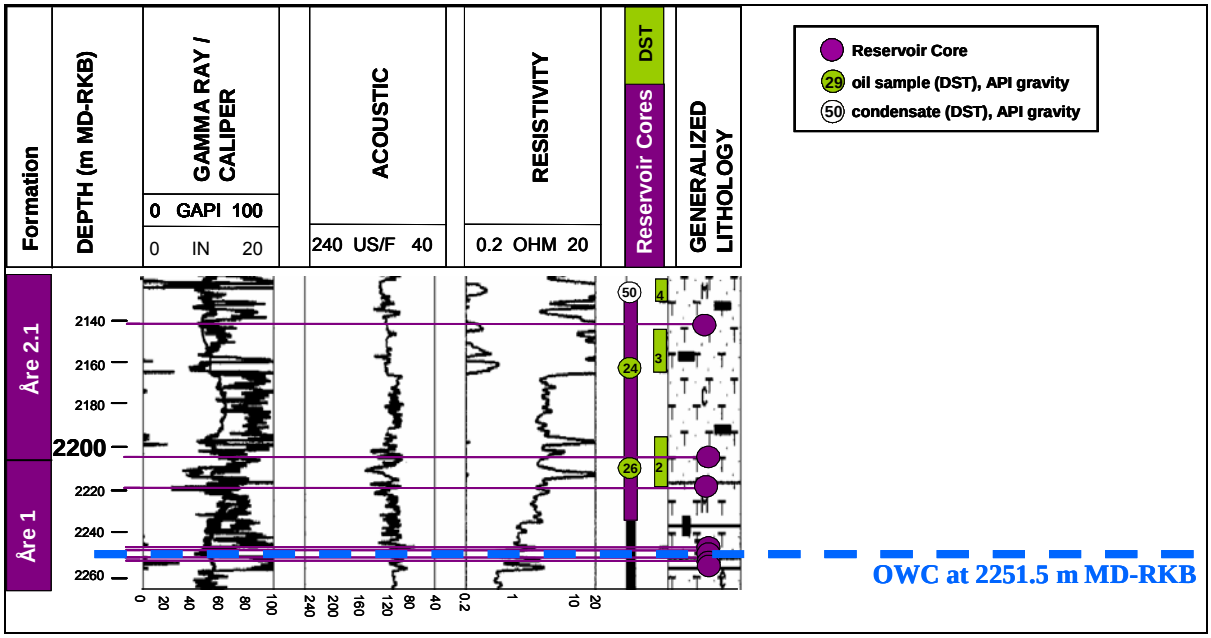

Figure 21 Well log section of profile 8-4 showing the gamma ray log (left), acoustic log (middle), and resistivity log (right). The reservoir rocks and the oil samples (DSTs) with their API gravity are marked by purple and green circles. The numbers in the green rectangles are the DST numbers. The well log is taken from the official NPD website (www.factpages.npd.no/factpages).

The sediments of the Åre Fm. subzones 2.1 and 1 were deposited in a fluvial dominated delta plain crossed by meandering channels. This heterogeneous depositional environment results in channel sandstones acting as main reservoirs, which are separated by muddy deposits (shale) and coal beds (cf. Chapter 3.1). Based on the core photos and description, the reservoir channel sandstones show grains of fine to medium size.

The three upper reservoir rocks were taken from the oil saturated zones, which is characterised by a high resistivity. With increasing depth, a slight decrease in resistivity down to the OWC can be observed (Figure 21, right). Near the OWC, where the four lowermost reservoir rocks were taken from, a lower resistivity indicates higher water saturation. The acoustic log in Figure 21 (centre) infers only small differences in porosity. The gamma ray signal (Figure 21, left) indicates several thin muddy or shaly zones within the profile and reflect so the alternation in the heterogeneous sediment succession.

Table 7 Sample numbers, depth and geological formation of reservoir rocks analysed from the NPD wells.

well	Field segment	GFZ number	Sample	Sample Type	Stratigraphical Unit	depth
						m MD-RKB
6507/7-2	G	G 003998	reservoir rock	sediment	Tilje Fm. 3.2	2316.5
6507/7-2	G	G 003999	reservoir rock	sediment	Tilje Fm. 2.1	2377.0
6507/7-2	G	G 004000	reservoir rock	sediment	Åre Fm. 7.2	2407.7
6507/7-2	G	G 004001	reservoir rock	sediment	Åre Fm. 6.2	2432.2
6507/7-3	E	G 004002	reservoir rock	sediment	Garn Fm.	2371.7
6507/7-3	E	G 004003	reservoir rock	sediment	Ile Fm. 4-6	2394.2
6507/7-3	E	G 004004	reservoir rock	sediment	Ror Fm. 2	2421.4
6507/7-4	C	G 004023	reservoir rock	sediment	Garn Fm.	2465.2
6507/7-4	C	G 004024	reservoir rock	sediment	Ile Fm. 6	2484.2
6507/7-4	C	G 004025	reservoir rock	sediment	Ile Fm. 5	2494.4
6507/7-4	C	G 004026	reservoir rock	sediment	Ile Fm. 5	2499.5
6507/7-5	O	G 004005	source rock	sediment	Spekk Fm.	2310.6
6507/7-5	O	G 004006	reservoir rock	sediment	Garn Fm.	2368.5
6507/7-5	O	G 004007	reservoir rock	sediment	Ile Fm. 2	2414.5
6507/7-6	I	G 004030	reservoir rock	sediment	Åre Fm. 3.2 / 3.1	2419.6
6507/7-6	I	G 004031	reservoir rock	sediment	Åre Fm. 3.2 / 3.1	2433.4
6507/7-6	I	G 004032	reservoir rock	sediment	Åre Fm. (2?)	2435.4
6507/7-6	I	G 004034	reservoir rock	sediment	Åre Fm. (2?)	2440.4
6507/7-8	F	G 004008	source rock	sediment	Melke Fm.	2429.8
6507/7-8	F	G 004009	reservoir rock	sediment	Garn Fm.	2464.5
6507/7-8	F	G 004010	reservoir rock	sediment	Ile Fm.	2486.5
6507/7-8	F	G 004012	reservoir rock	sediment	Ile Fm.	2494.2
6507/7-8	F	G 004013	reservoir rock	sediment	Ile Fm.	2494.6
6507/8-1	I	G 004036	reservoir rock	sediment	Tilje Fm. 3.3	2405.7
6507/8-1	I	G 004037	reservoir rock	sediment	Tilje Fm. 2.5	2442.8
6507/8-1	I	G 004038	reservoir rock	sediment	Tilje Fm. 2.1	2468.7
6507/8-1	I	G 004039	reservoir rock	sediment	Tilje Fm. 1	2476.3
6507/8-1	I	G 004041	reservoir rock	sediment	Tilje Fm. 1	2479.0
6507/8-4	*HDN	G 004021	reservoir rock	sediment	Åre Fm. 2.1	2141.4
6507/8-4	*HDN	G 004020	reservoir rock	sediment	Åre Fm. 2.1	2168.5
6507/8-4	*HDN	G 004019	reservoir rock	sediment	Åre Fm. 2.1	2204.4
6507/8-4	*HDN	G 004015	reservoir rock	sediment	Åre Fm. 1	2248.8
6507/8-4	*HDN	G 004016	reservoir rock	sediment	Åre Fm. 1	2249.3
6507/8-4	*HDN	G 004017	reservoir rock	sediment	Åre Fm. 1	2252.4
6507/8-4	*HDN	G 004018	reservoir rock	sediment	Åre Fm. 1	2253.3

*HDN - Heidrun North

Table 8 Sample numbers, depth interval, geological formation, and API gravities of oil samples analysed from the NPD wells.

well	Field segment	GFZ number	Sample	Sample Type	API°	Group	Stratigraphical Unit	Interval
								m MD-RKB
6507/7-2	G	G003881	DST 4A	oil	29	Båt	Tilje Fm. 3.2	2340-2330
6507/7-2	G	G003882	DST 3	oil	24	Båt	Tilje Fm. 2.2-2.3	2376-2365
6507/7-2	G	G003883	DST 2	oil	22	Båt	Åre Fm. 6.1-6.2	2439-2417
6507/7-3	E	G003884	DST 3	oil	29	Fangst	Garn Fm.	2380-2368
6507/7-3	E	G003885	DST 2	oil	29	Fangst	Ile Fm. 4-6	2400-2385
6507/7-3	E	G003886	DST 1	oil	29	Fangst	Ile Fm. 2- Ror Fm. 2	2430-2413
6507/7-4	C	G003887	DST 3	oil	29	Viking	Melke Fm.	2424-2418
6507/7-4	C	G003888	DST 2	oil	29	Fangst	Garn Fm.	2477-2470
6507/7-4	C	G003889	DST 1	oil	26	Fangst	Ile Fm. 5	2499-2494
6507/7-5	O	G003890	DST 2A	oil	32	Fangst	Garn Fm.	2375-2355
6507/7-5	O	G003891	DST 1	oil	28	Fangst	Ile Fm. 1 - 2	2424-2418
6507/7-6	I	G003892	DST 2	oil	27	Båt	Åre Fm. 5.1-5.2	2365-2348.5
6507/7-6	I	G003893	DST 1	oil	23	Båt	Åre Fm. 3.1-3.2	2424-2411.5
6507/7-8	F	G003894	DST 2	oil	29	Fangst	Garn Fm.	2441-2438
6507/7-8	F	G003895	DST 1	oil	30	Fangst	Ile Fm. 5 - 6	2480-2473
6507/8-1	I	G003896	DST 2	oil	23	Båt	Tilje 3.3 - 4	2406-2386
6507/8-1	I	G003897	DST 1	oil	20	Båt	Tilje 2.2 - 2.4	2462.5-2444
6507/8-4	*HDN	G003899	DST 3	oil	24	Båt	Åre Fm. 2.1	2168-2163.5
6507/8-4	*HDN	G003900	DST 2	oil	26	Båt	Åre Fm. 2.1	2221-2200
*HDN - Heidrun North								
well	**Field segment**	**GFZ number**	**Sample**	**Sample Type**	**API°**		**Stratigraphical Unit**	**Interval**
								m MD-RKB
D	Q	G004653	n.s.	oil	n.s.	Båt	Åre	n.s.
n.s. - not specified								

3.2.2 RESERVOIR ROCK ASPHALTENES

Based on the reservoir formation, geographical position, core photos and core description as well as on the reservoir rock OM composition described later in this report, representative reservoir rocks were selected for asphaltene separation. Samples were taken from seven wells. From north to south, they comprise the following profiles: well D, well E, well 6507/7-5, well 6507/7-2, well B, well C, and well 6507/7-8. The selection of these wells was based on the biodegradation pattern described in Chapter 3.1, which allowed a rough subdivision of the oil field into two parts, the biodegraded eastern part and the biodegraded and mixed western part. The reservoir rock samples were selected along a north-south profile that covers both parts. Altogether 31 reservoir rock asphaltenes were separated. The wells, reservoir rocks, sample depth, and obtained asphaltene yields are listed in Table 9.

Table 9 Depth, field segment, stratigraphical unit, and obtained asphaltene yields of the reservoir rocks selected for asphaltene separation from the Heidrun oil field.

well	Field segment	GFZ no.	sample type	Stratigraphical Unit	depth	Asphaltene amount	
					m MD-RKB	wt.%	mg/g sample
B	I	G004165	reservoir rock asphaltene	Tilje Fm. 3.4	3223.9	3.32	35.94
B	I	G004173	reservoir rock asphaltene	Tilje Fm. 3.3	3237.4	4.08	62.16
B	I	G004179	reservoir rock asphaltene	Tilje Fm. 3.2	3246.4	8.39	20.08
B	I	G004182	reservoir rock asphaltene	Tilje Fm. 3.2	3250.6	4.69	38.04
B	I	G004185	reservoir rock asphaltene	Tilje Fm. 3.2	3257.7	8.55	126.59
B	I	G004188	reservoir rock asphaltene	Tilje Fm. 3.2	3263.2	7.30	39.63
B	I	G004191	reservoir rock asphaltene	Tilje Fm. 3.2	3274.2	5.69	88.47
B	I	G004193	reservoir rock asphaltene	Tilje Fm. 2.5	3275.8	5.53	68.59
C	J	G004199	reservoir rock asphaltene	Garn Fm.	3661.5	6.14	45.43
C	J	G004209	reservoir rock asphaltene	Garn Fm.	3667.5	4.02	18.73
C	J	G004213	reservoir rock asphaltene	Not Fm. 1	3672.5	8.65	73.81
C	J	G004217	reservoir rock asphaltene	Ile Fm. 6	3675.9	4.49	58.52
C	J	G004223	reservoir rock asphaltene	Ile Fm. 5	3685.4	2.81	19.94
C	J	G004230	reservoir rock asphaltene	Ile Fm. 4	3693.4	2.87	45.09
C	J	G004249	reservoir rock asphaltene	Åre Fm. 1	3766.8	16.55	20.71
D	Q	G004254	reservoir rock asphaltene	Åre Fm. 2.1	2913.1	3.13	13.53
D	Q	G004255	reservoir rock asphaltene	Åre Fm. 2.1	2915.3	2.38	27.82
D	Q	G004258	reservoir rock asphaltene	Åre Fm. 2.1	2918.4	0.99	8.58
E	M	G004263	reservoir rock asphaltene	Åre Fm. 2.1	3542.8	6.48	59.49
E	M	G004265	reservoir rock asphaltene	Åre Fm. 2.1	3543.8	6.42	110.27
E	M	G004267	reservoir rock asphaltene	Åre Fm. 2.1	3550.5	2.41	14.90
E	M	G004268	reservoir rock asphaltene	Åre Fm. 2.1	3554.5	6.46	92.77
6507/7-2	G	G 003998	reservoir rock asphaltene	Tilje Fm. 3.2	2316.50	10.84	140.23
6507/7-2	G	G 003999	reservoir rock asphaltene	Tilje Fm. 2.2 / 2.1	2377.00	8.15	74.28
6507/7-2	G	G 004000	reservoir rock asphaltene	Åre Fm. 7.2	2407.65	13.97	177.98
6507/7-5	O	G 004006	reservoir rock asphaltene	Garn Fm.	2368.50	6.79	53.45
6507/7-5	O	G 004007	reservoir rock asphaltene	Ile Fm. 2	2414.50	3.49	29.25
6507/7-8	F	G 004009	reservoir rock asphaltene	Garn Fm.	2464.50	5.63	30.63
6507/7-8	F	G 004010	reservoir rock asphaltene	Ile Fm.	2486.50	4.57	27.95
6507/7-8	F	G 004012	reservoir rock asphaltene	Ile Fm.	2494.20	3.41	12.73
6507/7-8	F	G 004013	reservoir rock asphaltene	Ile Fm.	2494.55	14.15	27.80

3.2.3 OIL ASPHALTENES

Oil asphaltenes were separated from the DSTs. Decisive for the selection of oil samples was mainly the API gravity, because variabilities indicate in-reservoir alteration processes such as biodegradation. In total 16 oil asphaltenes of nine wells were separated. The wells, field segments, depth intervals, API gravities, and obtained asphaltene yields of the selected DSTs are listed in Table 10.

Table 10 Oil samples (DSTs) selected for asphaltene separation, depth interval, field segment, stratigraphical unit, and obtained asphaltene yields.

well	Field Segment	GFZ no.	sample type	Group	Stratigraphical Unit	Interval	API°	Asphaltene amount	
						[m]		wt.%	mg
6507/7-2	G	G003881	oil asphaltene	Båt	Tilje Fm. 3.2	2340-2330	29.0	0.25	47.54
6507/7-2	G	G003882	oil asphaltene	Båt	Tilje Fm. 2.2-2.3	2376-2365	24.0	0.32	62.33
6507/7-2	G	G003883	oil asphaltene	Båt	Åre Fm. 6.1-6.2	2439-2417	22.0	0.53	98.08
6507/7-3	E	G003885	oil asphaltene	Fangst	Ile Fm. 4-6	2400-2385	29.0	0.20	28.68
6507/7-4	C	G003887	oil asphaltene	Fangst	Melke Fm.	2424-2418	29.0	0.24	38.35
6507/7-4	C	G003888	oil asphaltene	Fangst	Garn Fm.	2477-2470	29.0	0.27	43.52
6507/7-4	C	G003889	oil asphaltene	Fangst	Ile Fm. 5	2499-2494	26.0	0.21	
6507/7-5	O	G003890	oil asphaltene	Fangst	Garn Fm.	2375-2355	32.0	0.18	27.65
6507/7-5	O	G003891	oil asphaltene	Fangst	Ile Fm. 1 - 2	2424-2418	28.0	0.16	25.55
6507/7-6	I	G003892	oil asphaltene	Båt	Åre Fm. 5.1-5.2	2365-2348.5	27.0	0.20	33.55
6507/7-6	I	G003893	oil asphaltene	Båt	Åre Fm. 3.1-3.2	2424-2411.5	23.0	0.32	52.68
6507/7-8	F	G003895	oil asphaltene	Fangst	Ile Fm. 5 - 6	2480-2473	30.0	0.24	38.01
6507/8-1	I	G003896	oil asphaltene	Båt	Tilje 3.3 - 4	2406-2386	23.0	0.36	55.59
6507/8-1	I	G003897	oil asphaltene	Båt	Tilje 2.2 - 2.4	2462.5-2444	20.0	0.44	69.89
6507/8-4	*HDN	G003900	oil asphaltene	Båt	Åre Fm. 2.1	2221-2200	26.0	0.17	32.85
D	Q	G004653	oil asphaltene	Båt	Åre Fm.	n.s.	n.s.	2.37	97.47
*HDN - Heidrun North									
n.s. - not specified									

4 METHODOLOGY

4.1 BULK PYROLYSIS FOR SCREENING - SOURCE ROCK ANALYZER

Bulk pyrolysis was performed with all 139 reservoir rocks and two potential source rocks from the Heidrun oil field at a heating rate of 15 °C/min using a modified Source Rock Analyzer© (Humble). Therefore, 25 to 100 mg of crushed reservoir rock and source rock material were weighed into small crucibles. The pyrolysis products were transported to a Flame Ionisation Detector (FID) within a constant helium flow of 50 ml / min. First, at a temperature up to 300 °C, the high volatile hydrocarbons (gas) and free hydrocarbons (gas and oil) are measured by the FID as S0 and S1 peak in mg HC / g rock. Subsequent, the temperature is increased from 300° to 600 °C in order to crack the non-volatile organic matter. Hydrocarbons released from this thermal cracking are measured by the FID as the S2 peak in mg HC / g rock.

4.2 OPEN SYSTEM PYROLYSIS – GAS CHROMATOGRAPHY PY-GC) AND GAS CHROMATOGRAPHY - MASSPECTROMETRY (GC-MS)

Open system pyrolysis was applied to source rocks, reservoir rocks, asphaltenes, and selected oil samples in order to provide compositional and structural characteristics of the complex organic materials. For the reservoir rock samples of the Heidrun oil field, the Py-GC was used as a high-resolution screening tool in order to analyse small-scale variabilities within their composition and molecular structure.

An HP-Ultra 1 dimethylpolysiloxane coated column with 0.52 µm film thickness, 50 m length, and 0.32 mm i.d., was fitted into an Agilent GC 6890A chromatograph equipped with a Quantum MSSV-2 Thermal Analysis System and a FID. Helium served as carrier gas (30 ml / min). Up to 5 mg powdered source rock and between 5 mg and 10 mg finely grounded reservoir rock material was weighed into small glass tubes. Asphaltenes were mixed with thermally pre-cleaned quartz sand in a weight ratio 1 : 10. Up to 5 mg of this asphaltene-quartz sand mix were weighed into the glass tubes. Subsequently, the tubes were plugged with quartz wool at both ends. Isothermal heating at 300 °C for 4 min was used to thermovaporise

and remove volatile products prior to pyrolysis. Then the system is heated from 300 °C up to 600 °C (40 °C / min) and the pyrolysis products were collected in a liquid-nitrogen cooled trap. The pyrolysis products were released from the cold trap by ballistic heating to 300 °C and measured on-line with the GC. The most common pyrolysis products are aliphatic hydrocarbons, aromatic compounds, e.g. alkylbenzenes, alkynaphthalenes, and alkylphenols as well as sulphur containing compounds (alkylthiophenes). *n*-butane was used as an external standard for the peak quantification. The peaks were identified using retention times and quantified based on reference pyrolysis gas chromatograms using Agilent ChemStation® software.

Open system pyrolysis - GC-MS was performed on selected source rocks, reservoir rocks, and asphaltenes. The pyrolysis products were measured by a Thermo Finnigan Trace GC with Trace DSQ-MS (electron energy 70 eV) equipped with a HP-1 MS dimethylpolysiloxane-coated column of 0.25 μm film thickness, 60 m length and 0.25 mm i.d. Peaks were integrated from the total ion current trace using the software Xcalibur (Version 1.3) by Thermo Finnigan.

4.3 THERMOVAPORISATION - GAS CHROMATOGRAPHY (TVAP-GC)

For Tvap-GC, between 25 mg and 35 mg extracted source rock sample, up to 15 mg of ground reservoir rock material, and between 15 mg and 20 mg asphaltene-quartz sand mix (ratio 1 : 10) were weighed into glass capillary tubes plugged with quartz wool at both ends and subsequently sealed. The GC analyses were done using the same instrument configuration as described in Chapter 4.2. Outer tube surfaces were purged at 300 °C and cracked for analysis within the piston device at 300 °C. Mobilized products were collected in a cryogenic trap at -196 °C. Then the trap was heated up to 300 °C and the products were released onto the column. Helium served as carrier gas (30 ml / min) and *n*-butane was used as an external standard for quantification. The peaks were identified using retention times and quantified based on reference pyrolysis gas chromatograms using Agilent ChemStation® software.

4.4 RESERVOIR ROCK AND SOURCE ROCK EXTRACTION

Between 15 and 35 g of the roughly ground reservoir rock, or about 20 g powdered source rock, were extracted using an accelerated solvent extractor (ASE, Dionex GmbH, Idstein,

Germany) to yield the residual bitumen. Both types of rock samples were extracted in four cycles at 100 °C and 50 bar using an azeotropic mixture consisting of chloroform, acetone and methanol in a volume ratio of 32 : 38 : 30. Subsequently the extracts were concentrated using a Turbovap-evaporator, transferred into a 10 ml brown glass vial and dried under a gentle stream of nitrogen. Finally, their weight was recorded when constant.

4.5 ASPHALTENE SEPARATION

Asphaltenes were separated from the oils and reservoir rock extracts by precipitation with *n*-hexane. Between 0.5 ml and 1.5 ml of the reservoir rock extract, and subjected to the API gravity, about 20 ml from the oil samples were used. A detailed description of the asphaltene separation method used is reported in Theuerkorn *et al.* 2008, and in Chapter 7.1. Very briefly, the separation method consists of the following steps. A 40-fold excess of *n*-hexane was added into the oil and extracts dissolved in DCM / MeOH 1 vol. %. The mixture was stirred for 10 min supported by ultrasonic and allowed to settle for 4 h. Thereafter the asphaltenes were separated by vacuum filtration, subsequently washed and the remaining asphaltenes extracted using ASE (method: 80 °C / 100 bar, heat 5 min, static 5 min, 3 cycles). After drying and weighing, the asphaltenes were purified in a second and third step by re-precipitation with *n*-hexane.

5 HETEROGENEITY SCREENING CRITERIA - FROM KEROGEN TO ASPHALTENES

5.1 FIRST SCREENING TOOL – SOURCE ROCK ANALYZER

The Source Rock Analyzer was used to investigate reservoir rock samples in order to assess the quality of the organic matter and to delineate variabilities in organic richness. First, the highly volatile hydrocarbons of the reservoir rocks were thermally desorbed directly in a detector (FID). Then the heavier free hydrocarbons (S1) and pyrolysis products (S2) were detected by temperature programming up to 600 °C. Because there was no compound separation, different areas in the thermogram represent different molecular weight range of the generated products (Figure 22).

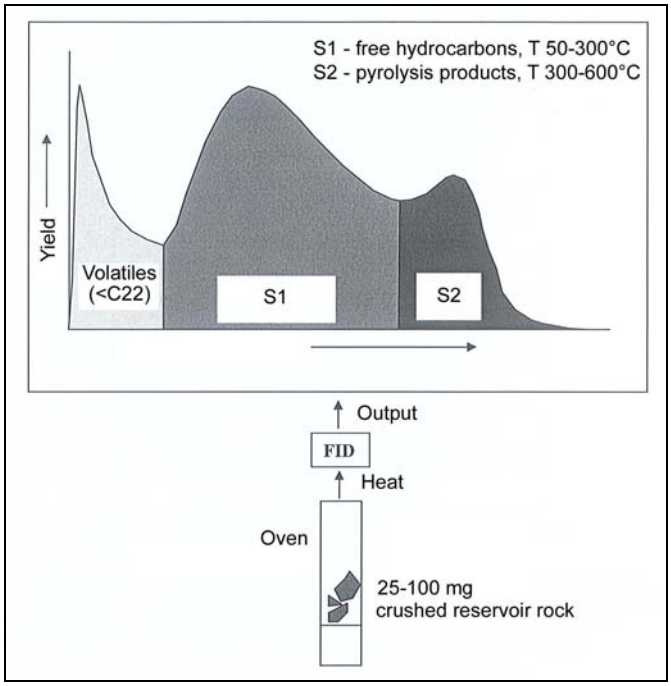

Figure 22 Exemplified illustrations of the thermal distillation and pyrolysis yields from reservoir rock samples. The resulting thermatogram provides a assessment of oil quality based on the distribution of thermally extractable compounds (S1) and pyrolysis products (S2) (modified after Jarvie *et al.*, 2001).

All 139 reservoir rocks and both potential source rocks were evaluated using the Production Index (PI) in order to obtain an idea of hydrocarbons versus non-hydrocarbon ratio. The PI is the ratio of total thermally extractable compounds (S1) to the sum of total thermally

extractable compounds plus pyrolysis products (S1+S2). The S1 represents the free aliphatic and aromatic hydrocarbons released at a temperature between 50 °C and 300 °C. The polar and high molecular weight fraction (NSO compounds including asphaltenes) occur mainly in the S2, which represents the pyrolysis products generated at a temperature between 300 °C and 600 °C. These assignments were based on the analysis of the MPLC separated single fractions (aliphatic hydrocarbons, aromatic hydrocarbons, NSO compounds) of the Norwegian Geochemical Standard North Sea Oil-1 (NGS NSO-1).

A high PI reflect a high hydrocarbon abundance and indicate a good oil quality; on the other hand low PI reflects a high proportion of non-hydrocarbons (NSO compounds and asphaltenes) that may indicate lower oil quality. High hydrocarbon concentrations are typical for free flowing oils, whereas heavier oils (API < 20) will have higher concentrations of non-hydrocarbons. Attention should be drawn when high molecular weight waxes (C_{40+} paraffins) are present as they will elute in the high temperature fraction suggesting a low API gravity oil (Jarvie *et al.*, 2001). The PI can also be an indicator for *in-situ* organic matter in the reservoir rocks if indigenous disseminated kerogen or coal particles are present.

Furthermore, the Source Rock Analyzer was used to delineate variabilities in organic richness. Therefore, the total petroleum hydrocarbon yield (sum S1 + S2) was quantified as mg / g rock for each rock sample. The organic richness reflects the distribution of the total organic matter (OM) within the reservoir and can be a useful marker for oil saturation. Zones with less OM might inversely be water saturated, because high water saturation is commonly correlated to low OM content. Applied vice versa, zones rich in OM can point to oil saturated zones.

5.2 SECOND SCREENING TOOL – PYROLYSIS-GC

Open system pyrolysis - GC (cf. Chapter 4.2) was applied to all 139 reservoir rocks (complete rock including asphaltenes), both potential source rocks, and 31 single asphaltenes separated from the reservoir rock residual bitumen. This analysis highlights compositional and structural heterogeneities in the macromolecular fraction of the OM. The source rocks and the reservoir rock asphaltenes will assist in the comparison of the structural and compositional characteristics of the potential parent kerogen with those obtained from whole reservoir rocks. Prior to pyrolysis, the samples were thermovaporised in order to remove the volatile products (S1).

The term pyrolysis is defined as “chemical degradation reaction that is induced by thermal energy alone” (Ericsson & Lattimer, 1989). High temperature pyrolysis in open systems for short periods (heating rates e.g. 40 °C / min) leads to rapid cracking of OM into smaller molecular fragments at a temperature range of 300 - 600 °C. The volatile pyrolysis products released from kerogen are formed according to the same principles as in natural catagenesis, i.e. thermal cleavage reactions and can be used to predict the composition of petroleum in nature (Horsfield, 1997). Kerogen and asphaltenes due to their structural similarities (Behar & Pelet, 1985; Pelet *et al.*, 1986), degrade upon pyrolysis to yield many compound types including hydrocarbons, ketones, alcohols, nitriles and thiols, which are represented by saturated and unsaturated, cyclic and acyclic carbon skeletons (Rovere *et al.*, 1983; Wilson *et al.*, 1983). The most common and identifiable compounds in the pyrolysis gas chromatograms are aliphatic hydrocarbons (alkane / alk-1ene doublets), aromatic compounds (alkylbenzenes, alkynaphthalenes, alkylphenols) and sulphur containing compounds (alkylthiophenes). It has been reported by many authors that kerogen compositions and hence pyrolysate compositions, depends on the origin of initial organic matter types (I, II and III = marine, lacustrine, deltaic, terrestrial) and evolutionary stage (e.g. Behar & Vandenbroucke, 1987; Curry & Simpler, 1988; Eglinton *et al.*, 1990; Horsfield, 1989; Larter, 1984; Senftle *et al.*, 1986; van Graas *et al.*, 1981). Thus the molecular composition and structure of kerogen and asphaltenes is determined by its biological precursors and the modifications brought about during diagenesis and catagenesis (Rullkötter & Michaelis, 1990). Some views from these authors concerning kerogen typing are adopted in this study and applied to pyrolysates from reservoir rocks including asphaltene.

The most abundant pyrolysis products generated from reservoir rocks are aliphatic hydrocarbons, aromatic compounds and sulphur containing compounds. They were quantified and compared for each single well of the Heidrun oil field using representative geochemical profiles and ternary diagrams to show differences or gradients in their OM composition and to provide an in-field correlation tool.

Different ratios and parameters were applied based on the following resolved peaks in pyrolysis gas chromatograms: C_1 to *n*-C_5 *n*-alkanes, *n*-alk-1-enes and *iso*-alkanes, and in the C_{5+} range *n*-alkanes / *n*-alk-1-enes doublets, benzene, toluene, ethylbenzene, styrene, *meta*- and *para*-xylene (1 peak), and *ortho*-xylene, naphthalene, methylnaphthalenes, dimethylnaphthalenes, phenol, cresols, thiophene, methylthiophenes, ethylthiophene, dimethylthiophene and ethylmethylthiophene. All identified peaks are shown in Figure 23.

The sum of the resolved components makes up on average only 20 % - 50 % of the GC amenable C_{6+} pyrolysates, while the majority is present in the unresolved compound mixture (UCM) or the so called “hump” (Peters & Moldowan, 1993). That is why the bulk pyrolysis yields and the total resolved pyrolysis yields in the boiling ranges C_1 to C_5, C_6 to C_{14} and C_{15+} have been integrated.

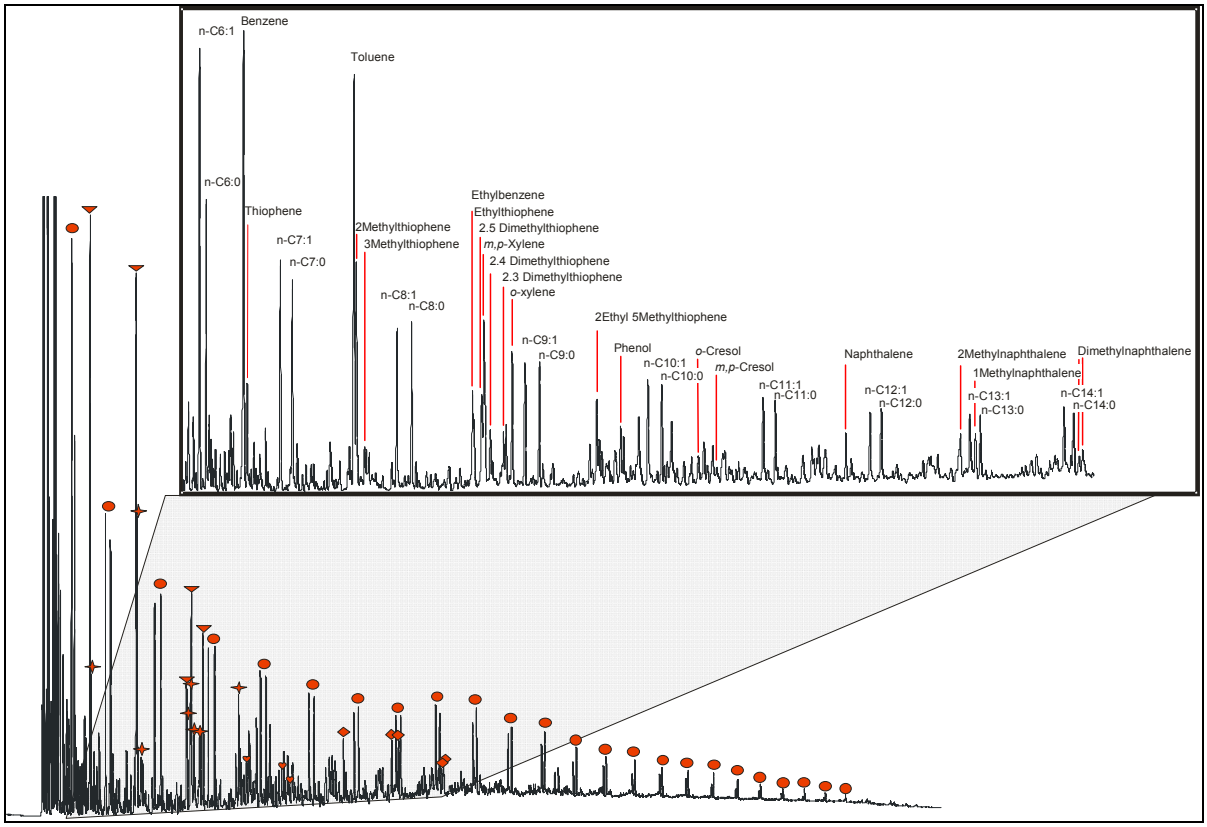

Figure 23 Example pyrolysis gas chromatogram shows pyrolysis products mentioned in the text used for the data interpretation. Main compounds are marked by different red symbols. The *n*-alkene / alkane doublets are marked by dots, monoaromatic hydrocarbons by triangles, diaromatic compounds by rectangles, sulphur compounds by stars and phenol compounds by hearts. Pyrolysis products in the range of C_6 up to C_{14} are enlarged and labelled.

For a detailed structural characterisation the following parameter were used: (A) aromaticity ((C_1-C_2 alkylbenzenes + naphthalene + 2 methylnaphthalene + 1 methylnaphthalene + dimethylnaphthalene) / *n*-C_{5+}). Benzene was not included in this ratio as the alkylbenzenes toluene, ethylbenzene and xylenes are considered to provide a better estimate of the sample aromaticity, because they are more likely associated with indigenous aromatic structures than secondary aromatisation effects during pyrolysis (Larter, 1984). (B) a ratio to differentiate according to the number of aromatic rings (C_1 - C_2 alkylbenzenes / (naphthalene + 2 methylnaphthalene + 1 methylnaphthalene + dimethylnaphthalene)), (C) the relative phenol

content (phenol / *n*-$C_{9:0}$), (D) the gas wetness (C_2 - *n*-C_4 / C_1 - *n*-C_4), and (E) the gas amount in % (C_1 - *n*-C_5 / C_{1+} total resolved).

For bulk characterisation the gas to oil ratio (GOR (mg / mg) = bulk C_1 - C_5 / total resolved C_{6+}) and the amount of unresolved compound mixtures (UCM % = ((bulk C_{6+} - resolved C_{6+}) / bulk C_{1+}*100) were calculated. Concerning the calculation of the GOR, only the resolved components (total) in the C_{6+} boiling range have been used. This approach was shown to be more accurately resemble the generation characteristics of different types of organic matter compared to the approach including the hump using the bulk ratio C_1 - C_5 / C_{6+} (Düppenbecker & Horsfield, 1990; Horsfield, 1997).

Bulk properties of the reservoir rocks and both potential source rocks are displayed by ternary diagrams for (A) the alkyl chain length distribution (CLD) after Horsfield (1989), using at its apices the proportions of total resolved C_1 to *n*-C_5 pyrolysates, summed *n*-alk-1-enes and *n*-alkanes in the *n*-C_6 to *n*-C_{14} range, and summed *n*-alk-1-enes and *n*-alkanes in the *n*-C_{15+} range. Additionally, (B) for the phenol content after Larter (1984) to characterise terrestrial organic matter input using *m,p*-xylene, *n*-octene and phenol at its apices, and (C - D) for the sulphur content. Ternary (C) use the relative amount of 2,3 dimethylthiophene in relation to *ortho*-xylene and *n*-nonane after Eglinton *et al.* (1990), while ternary (D) use the relative amount of 2,5 dimethylthiophene in relation to toluene and the sum of the *n*-nonane and *n*-pentacosan after di Primio & Horsfield (1996)

Another ternary diagram, based on the work of Sinninghe Damste *et al.* (1989) and Eglinton *et al.* (1992) is presented in Chapter 6.6. This ternary diagram is an attempt to identify different lipid precursors (carbon skeletons) using organic sulphur pyrolysis products (OSPP) in order to infer variabilities in the source OM inputs. The analysis of OSPP generated by the macromolecular OM from reservoir- and source rocks, may yield information about the relative content of various sulphur-containing structural moieties and thus, point to contributions from different source organisms. Additionally, connections between different mature source rock formations might be observed. The basic concept is shown in Figure 24.

Analysing OSPP of macromolecular OM, comprising kerogen, coal, and asphaltenes, Sinninghe Damste *et al.* (1989) observed a dominance of specific isomers in the distribution pattern of low molecular weight alkylthiophenes. These substitution patterns are similar to those observed in immature bitumen or crude oils, which suggests a relation of the sulphur containing pyrolysis products to specific alkylthiophene moieties in the kerogen, and additionally, sulphur incorporation into these macromolecules at specific sites in the lipid precursor moieties. The author discriminated four groups of sulphur-containing moieties

based on the substitution patterns of the alkylthiophenes: moieties with linear-, isoprenoid-, branched-, and steroidal carbon skeletons (Figure 24, top left). The structural relationships in which specific OSPP can be grouped according to common "carbon skeletons" are supported by the results from principal component analysis (PCA) from Eglinton *et al.* (1992) (Figure 24, top right). Characteristic carbon skeleton distributions can be observed in the PCA, which vary mainly as a function of kerogen type, but also as a function of kerogen maturity. Sulphur containing products from Type I and Type II kerogens are dominated by OSPP derived from alkylated moieties with linear carbon skeletons, while coals and Type III kerogens shows higher relative abundances of OSPP with branched carbon skeletons (Figure 24, bottom right). Products from Type II-S kerogen have higher relative abundance of OSPP derived from isoprenoid and/or steroidal carbon skeletons, and show generally a higher abundance of all OSPP. Increased maturation results in a depletion of linear relative to branched alkylthiophene precursors (Eglinton *et al.,* 1992).

The most common OSPP analysed in the Heidrun reservoir and source rock samples are 2 ethyl 5 methylthiophene (2E5MT), 3 methylthiophene (3MT), and 2.4 dimethylthiophene (2.4DMT) representing linear, branched and isoprenoid lipid precursor carbon skeletons (Figure 24, bottom left).

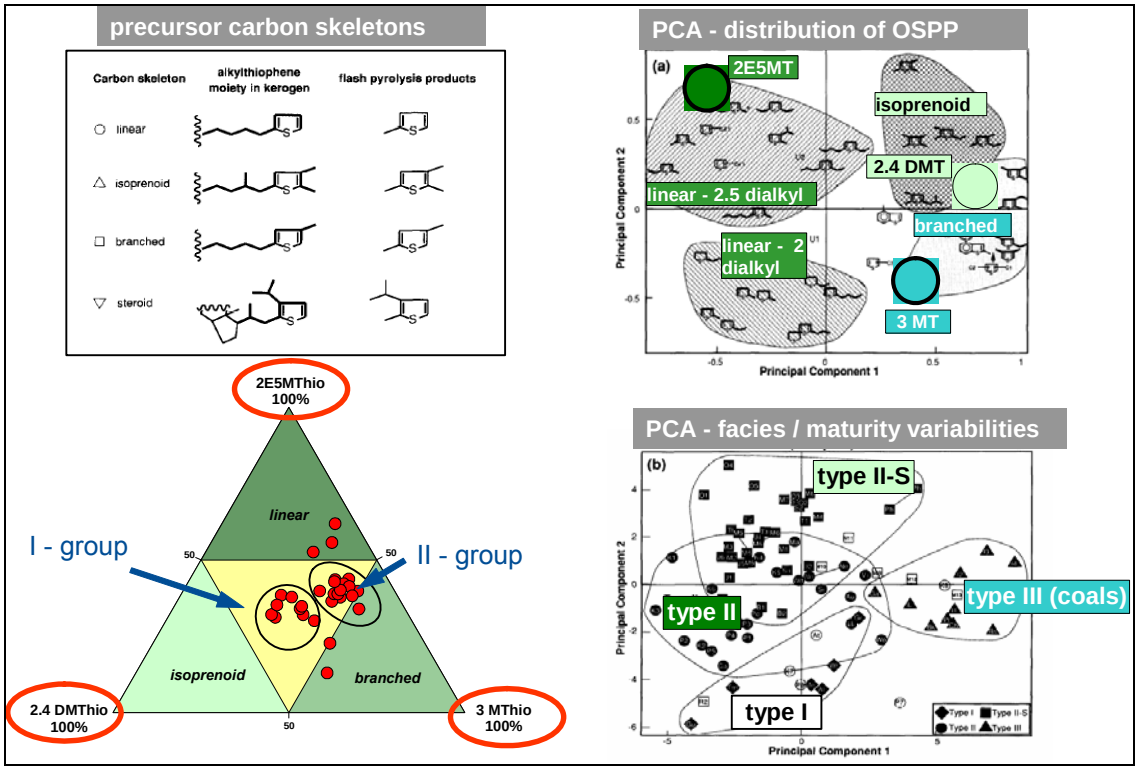

Figure 24 Basis concept of the new sulphur ternary diagram based on work of Sinninghe Damste *et al.* (1989) and Eglinton *et al.* (1992).

6 RESULTS AND DISCUSSION

In the following chapter, the results of the heterogeneity screening are presented and discussed in detail for each single well and individual reservoir formation. At first a general characterisation of the bulk pyrolysis products of all analysed reservoir rocks and some general information about their quality are given. Additionally, general source rock characteristics are presented. In the main part, reservoir rock screening results are described, including OM composition as well as an interpretation with respect to organofacies and maturity. Subsequently, the observed heterogeneities are correlated to physical rock properties from well log data such as permeability, porosity and water saturation as well as to the fluid physical properties viscosity and API° gravity. Concerning the latter, a biodegradation series (heavy oils) from the Western Canada Sedimentary Basin (WCSB) and Heidrun oils with different API gravity were investigated. The heavy oil series was provided by Shell.

6.1 GENERAL CHARACTERISATION

6.1.1 BULK PYROLYSIS PARAMETERS FOR ALL RESERVOIR ROCK SAMPLES

6.1.1.1 PRODUCTION INDEX (PI = (S1 / (S1+S2))

PI bar charts have been used to delineate the heterogeneities of the Heidrun reservoir. Figure 25 shows the PI of all analysed rock samples. Different wells are shown by different coloured bars independent of their geological formation and field position. Within a single well, the PI is shown from the well top to the well bottom with increasing depth. The average (av) and standard deviation (STABW) for the PI are listed in Table X 1 in the appendix.

The average PI of all analysed reservoir rock samples is 0.62 (± 0.13). The NPD wells show a slightly higher PI (0.64 ± 0.06) compared to the wells from Statoil (0.61 ± 0.15).
Excluding the potential source rock samples, variabilities have been detected comparing the PI of the single wells. Especially NPD wells show differences in oil quality. Higher oil quality

was detected in the western part of the oil field in wells 6507/7-3, 6507/7-4 and 6507/7-5. Lower oil quality was observed in Heidrun North in well D, well 6507/7-6, and well 6507/8-4, and in the southern part of the oil field in well 6507/8-1. Reservoir rocks from the central part (well 6507/7-2) and the southwestern part (well 6507/7-8) show both extremes, namely higher oil quality in rock samples on the well top and lower oil quality in reservoir rocks from greater depth of the cored section. These variabilities might by an indication for multiple charging events within the reservoir, whereby most recent charges are characterised by higher oil quality.

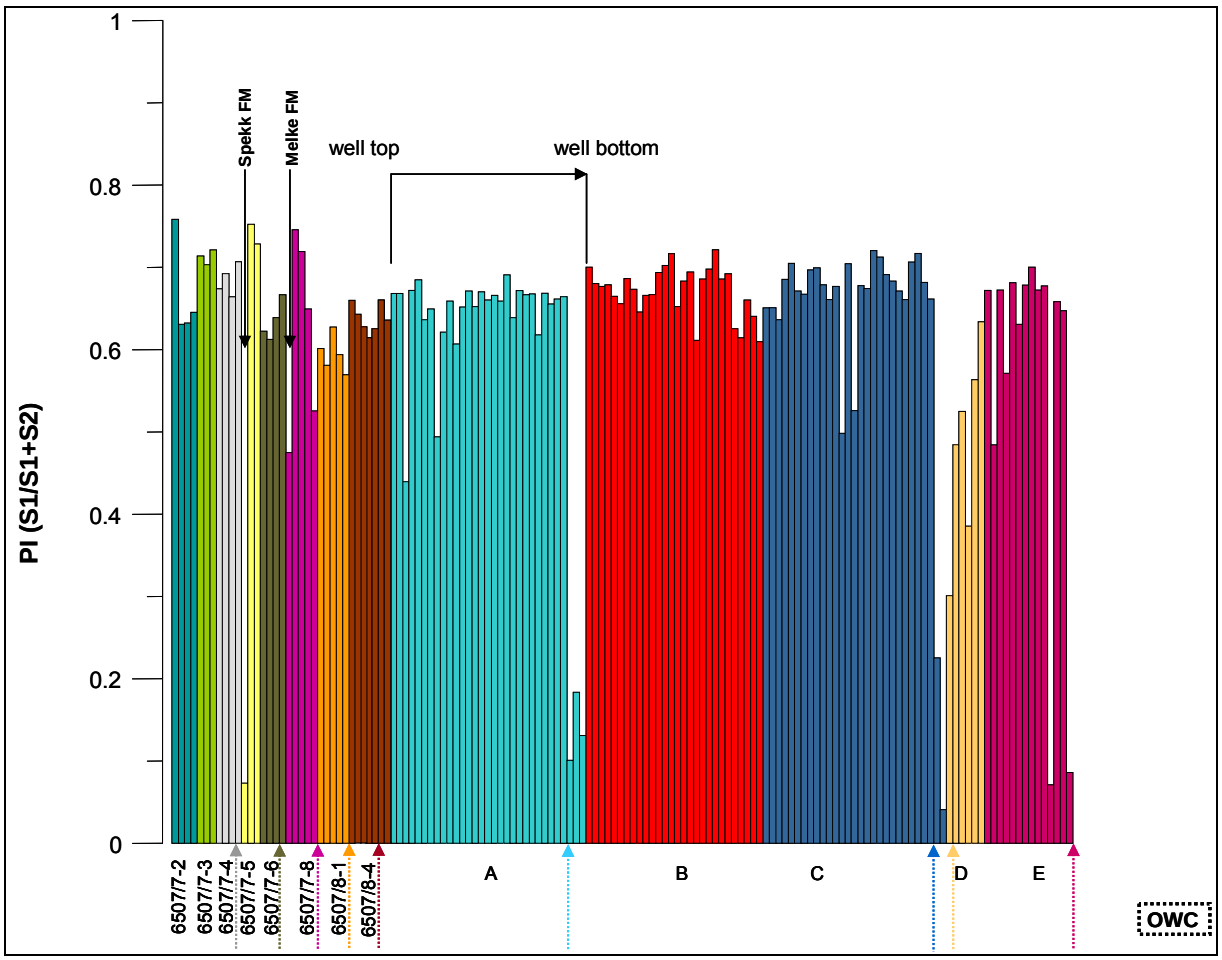

Figure 25 PI (Production Index) for all reservoir rock samples of the Heidrun oil field. Each single well is shown in different coloured bars. The PI within single wells is shown from the well top to the well bottom with increasing depth. Reservoir rock samples from NPD wells named with numbers (6507/7-2, 6507/7-3, 6507/7-4, 6507/7-5, 6507/7-6, 6507/7-8, 6507/8-1, and 6507/8-4). Statoil wells named with the letters A, B, C, D, and E. The dotted lines mark the OWC within the single wells.

Significant heterogeneities in oil quality have been observed comparing single reservoir rock samples within the individual wells, especially in Statoil wells sampled at high resolution. In the upper part of well A and E (both Åre Formation) and in the middle part of well C (Ile Formation), the PI shows variability up to 0.2 at very small scale. Here i*n-situ* organic matter

has to be suspected as being present. The same wells show further an abrupt drop in hydrocarbon abundance (PI < 0.3) at the bottom of their profiles. These samples, which are all from the Åre Formation, are located in the water-saturated zone (well A and C) or in the case of well E in short distance to the OWC (interval of 10 m above the OWC). Similarly low PI (0.3) can be observed in the topmost sample of well D, taken from the upper water leg. Those low hydrocarbon abundance (PI < 0.3) near and in the water saturated zones, is most likely an indication for i*n-situ* organic matter. However, the low PI might also be related to alteration processes such as biodegradation and/or water washing, as both are initiated at the oil-water interface and leading to heavy, low API-gravity oils depleted in hydrocarbons and enriched in non-hydrocarbon NSO-compounds and asphaltenes (Killops & Killops, 2005; Palmer, 1993; Peters *et al.*, 2005; Tissot & Welte, 1984).

The most significant gradient can be seen within reservoir rocks below the topmost sample of well D. Here the aliphatic and aromatic hydrocarbons (S1) strongly increase in relation to the high polar compounds (S2) with increasing depth. Well D shows the greatest variability in the oil quality of the Heidrun oil field.

Different gradients from the well top down to the OWC can be observed in well 6507/7-6, 6507/7-8, 6507/8-1, 6507/8-4 and the lower part of well C. The southwestern well 6507/7-8 reveals greatest differences in oil quality among the NPD wells. While the PI in well 6507/7-8, 6507/8-1 and the lower part of well C shows a stepwise decrease down to the OWC in well 6507/7-6, and the last four reservoir rocks of well 6507/8-4 the PI slightly increase down to the OWC. In both latter wells, situated in Heidrun North, the highest oil quality was found just below the water-saturated zone, which could be an indication for hydrodynamic changes of the recent oil-water interface. The stepwise decreasing PI down to the OWC might be related to alteration processes, as mentioned above.

Slight gradients in the PI independent of the water-saturated zone are observed in the upper part of well B. Conspicuous is the drop in oil quality within the central well 6507/7-2 and the almost identical, but lower oil quality of the reservoir rocks below the top sample. Here a vertical flow barrier might be suspected. Less permeable layers in the form of interstratified heterolithics are typical for the Tilje Formation (cf. Chapter 3.2.1.6).

6.1.1.2 ORGANIC RICHNESS

Organic richness throughout the Heidrun oil field is highly variable and heterogeneous within wells (Figure 26). An overview of the mean organic matter amount is given in Table X 1 in

the appendix. The mean OM amount of all reservoir rock samples is 24.10 mg/g rock (± 16.53). Differences in the distribution alternate up to 10th of mg OM / g rock and change at centimetre to metre scale from very lean to very rich zones.

Most significant differences in the OM amount and distribution can be observed in the high-resolution wells A, B, C, D, and E from Statoil. Within these wells, the OM amount of ranges from 0.4 mg/g rock (well D) up to 112.1 mg/g rock (well C). The average is 26.47 mg/g rock (± 17.78). Well E shows the highest OM content (34.28 mg/g rock ± 20.68), whereas lowest content was observed in well D (17.08 mg/g rock ± 10.98).

Reservoir rocks of the NPD wells 6507/7-2 up to 6507/8-4, show minor OM amounts (16.35 mg/g rock ± 7.58) and a less heterogeneous OM distribution compared to the reservoir rocks from Statoil.

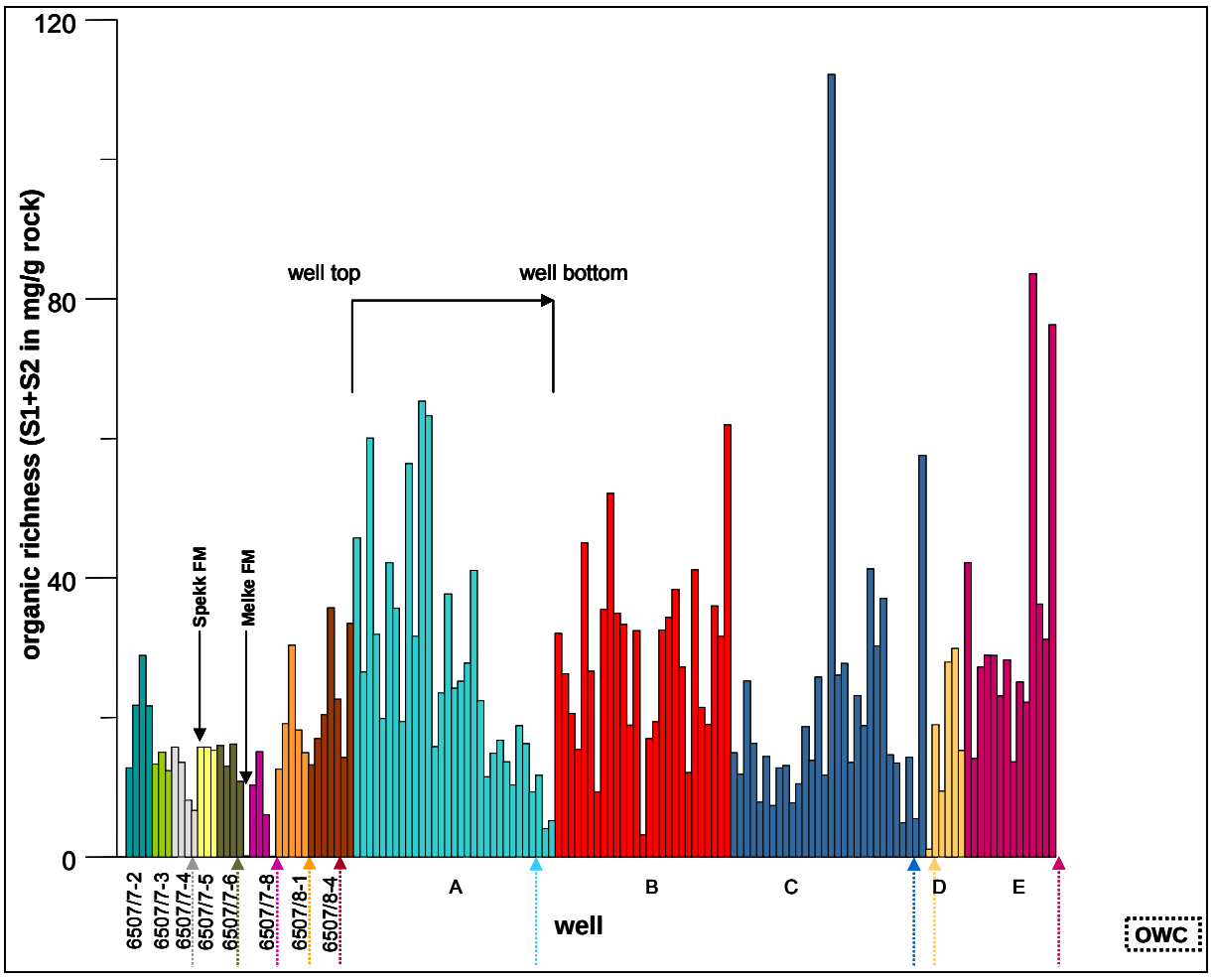

Figure 26 Organic Richness quantified in mg/g organic matter (OM) per sample for all reservoir rocks of the Heidrun oil field. Each single well is shown in different coloured bars. The organic richness within single wells is shown from the well top to the well bottom with increasing depth. Reservoir rock samples of the NPD wells are named with numbers (6507/7-2, 6507/7-3, 6507/7-4, 6507/7-5, 6507/7-6, 6507/7-8, 6507/8-1, and 6507/8-4). Wells from Statoil are named with letters A, B, C, D, and E.

6.1.1.3 INDIGENOUS VERSUS MIGRATED CONTRIBUTIONS

Most reservoir rocks are generally deposited under oxidising conditions and contain little in the way of indigenous organic matter (Bjørlykke, 1989). That means the yields measured by thermal analysis of the reservoir rocks using open system pyrolysis - GC should result from the migrated oil and/or residual bitumen alone and not from *in-situ* organic material deposited during sedimentation such as kerogen or coal. To ensure that this is normally the case, the sample quality of the reservoir rock samples have first been visually checked before analysing, in order to detect macroscopic coal particles. To check for contributions from insoluble organic matter to pyrolysates, namely kerogen, 24 reservoir rocks selected from 9 different wells and 5 different reservoir formations were pyrolysed before and after extraction (Figure 27). The number of samples analysed per well was mainly depending on the sample density, core photos, and first heterogeneities observed concerning PI. The rock samples were taken in defined distances of the cored well section and from different stratigraphical formations and subzones including the Garn-, Not-, and Ile Formation (Fangst group) as well as the Tilje- and Åre Formation (Båt group).

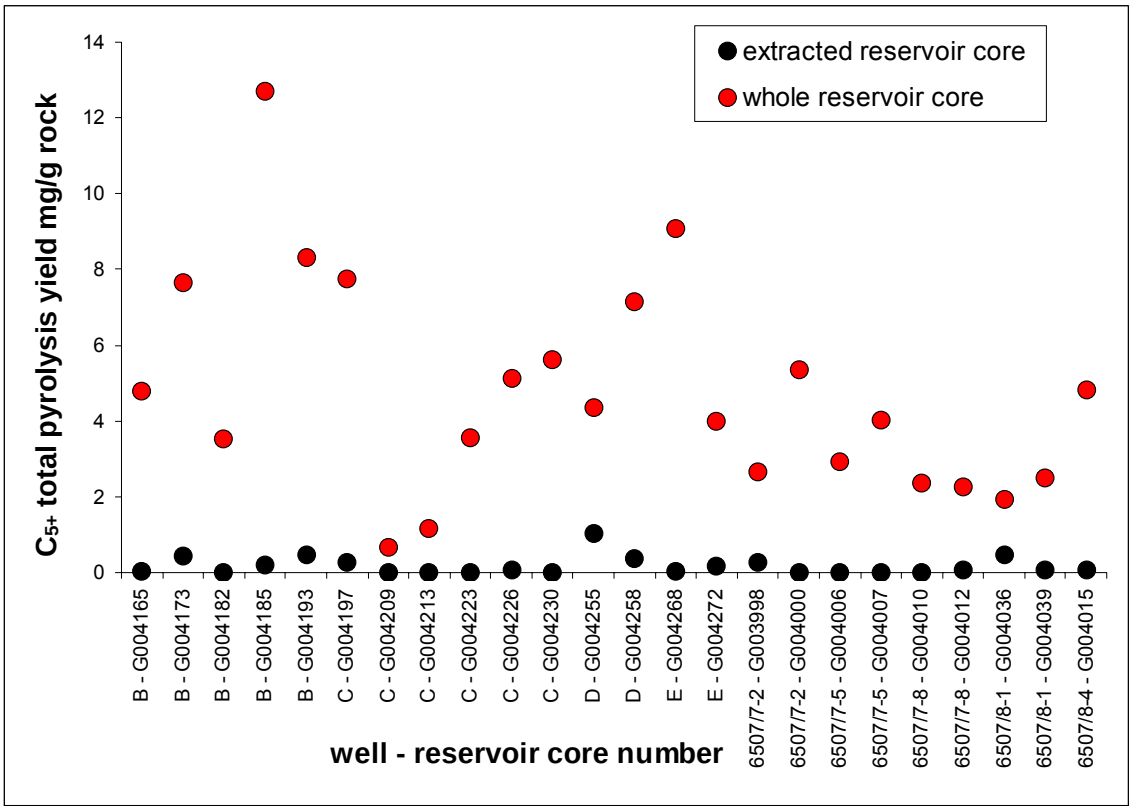

Figure 27 Comparison of the C_{5+} total pyrolysis yield of selected reservoir rocks from different wells and reservoir formations before (red) and after extraction (black). Letters or numbers before the hyphen in the sample name nominate the well the sample was taken from.

Figure 27 shows the comparison of the C_{5+} total pyrolysis yields before and after extraction. Considerable differences can be seen for the pyrolysis yields. Reservoir rocks before extraction exhibit yields between 0.67 mg/g and 12.69 mg/g with an average of 4.76 mg/g (± 2.84), while most extracted reservoir rock samples have pyrolysis yields close to zero (0.17 mg/g ± 0.24). Only one extracted reservoir rock from well D (G004255) show a slightly higher pyrolysis yield (1.02 mg/g).

It was concluded that kerogen content in the analysed reservoir rocks can be excluded and that the results reflect differences in the composition of extractable macromolecular components from the reservoired oil.

6.1.2 SOURCE-RELATED SIGNALS

The Heidrun oil field is mainly sourced from the Upper Jurassic Spekk Formation / Middle Jurassic Melke Formation (Karlsen *et al.*, 2004). Photos of both potential source rocks are shown in Figure 27. The Spekk source rock (Kimmeridge clay equivalent) is a black organic carbon rich shale with TOC values up to 13 % (Figure 28, left). It was deposited under anoxic marine conditions, and has a Type II kerogen composition. Its quality is good to very good as expressed by Rock Eval hydrogen indices up to 700 mg HC / g TOC (Forbes *et al.*, 1991; Mo *et al.*, 1989; Ungerer, 1990). Near the Heidrun oil field, the Spekk Formation is immature.

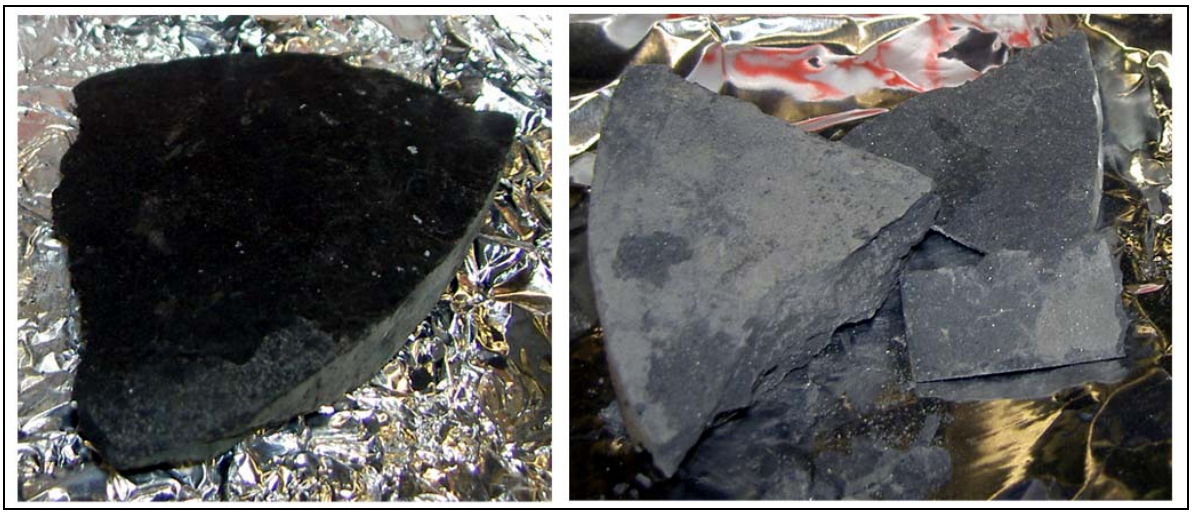

Figure 28 Photos of the two potential source rock shales of the Heidrun reservoir. *Left:* The potential source rock from the Upper Jurassic Spekk Formation, *Right:* The potential source rock from the Middle Jurassic Melke Formation.

The underlying Melke Formation source rock (Heather Formation equivalent) is lighter in colour (Figure 28, right). In general, the Melke Formation is a leaner source rock (lower potential) with a mixed marine-terrestrial Type II / III kerogen, and averaging TOC of ~ 2% and HI of ~ 200 mg HC/g TOC, which are both distinctly lower compared to the Spekk Formation source rock (Forbes *et al.*, 1991).

6.1.2.1 PRODUCTION INDEX

The potential source rocks from the Spekk Formation (well 6507/7-5) and Melke Formation (well 6507/7-8) are characterised by PIs of 0.07 and 0.47, respectively (Figure 25, Table X 1). The Spekk Formation source rock shows lowest PI that is characteristic for its low maturity mentioned above in Chapter 6.1.2. The low S1 reflect low amounts of hydrocarbons that are already present in the source rock in a free or an adsorbed state. Based on the PI alone, the Melke Formation source rock indicates a distinctly higher maturity compared to the Spekk Formation. Additionally, the differences observed point to lithofacies differences in both source rocks.

6.1.2.2 ORGANIC RICHNESS

The organic matter content of the Spekk Fm. source rock (15.74 mg OM/g rock) is comparable to the mean organic matter amount observed in the analysed reservoir rock samples from the NPD wells (15.9 mg/g ± 7.85) (Figure 26, Table X 1). Compared to Spekk Fm., the Melke Fm. source rock shows an organic matter content nearly zero (0.09 mg OM/g rock). This might be explained by quality variability within the underlying Melke Formation mentioned in Chapter 6.1.2.

6.2 CHARACTERISATION OF THE SINGLE PROFILES IN THE EASTERN PART OF THE HEIDRUN OIL FIELD

6.2.1 WELL C IN SEGMENT J (GARN FM., ILE FM. 6-2, NOT FM., ÅRE FM. 1)

6.2.1.1 PRODUCTION INDEX AND ORGANIC RICHNESS

The sampled section in well C comprises the Garn-, Not-, Ile- and Åre Formation (Table 2). The average PI is 0.63 (± 0.15) (Figure 25, Table X 1 in the appendix). The Garn and Ile Formation reservoir rocks show a similar average oil quality with values of 0.67 ± 0.02 and 0.67 ± 0.06, respectively. The Ile samples, G004217 and G004219 from the middle of profile C exhibit lower hydrocarbon abundance with PI of 0.50 and 0.53, which indicate the presence of *in-situ* organic matter. Below these samples, in reservoir rocks from the Ile Fm. 4 and Ile Fm. 2, the PI decreases stepwise. In the latter formation unit, the PI decreases stepwise towards the ODT contact. Both Åre Formation samples at the bottom of the profile show an abrupt drop in oil quality. They are below the ODT contact in the water-saturated zone and show with PI of 0.23 and 0.04 the lowest hydrocarbon abundance within profile C. This low oil quality indicates a significant content of high polar compounds and refers to *in-situ* organic matter present in these reservoir rocks. However, a relation of low PI and higher water saturation cannot be excluded.

Well C is characterised by a lower content of organic matter and minor differences in their distribution in the upper part (Garn Fm. and Not Fm.), compared to the lower part with organic rich samples and significant changes in the organic matter distribution (Ile Fm. and Åre Fm.), (Figure 26). Regarding the stratigraphical units, an increase in organic matter content was observed in the order of Garn-, Ile-, Not- and Åre Formation (Table X 1).
Two reservoir rocks, one in the middle (Ile Fm.) and the last one at the bottom of profile C (Åre Fm.) have very high organic matter contents. The sample in the middle presents the highest content of all analysed reservoir rocks. The lowest organic matter content was found in two reservoir rocks (Ile Fm. and Åre Fm.) near the ODT contact. This might be a pointer to low oil saturation near the water-saturated zone.

6.2.1.2 ORGANIC MATTER COMPOSITION

In Figure 29, exemplary pyrolysis gas chromatograms of the reservoir rock screening from three main sampled Formations Garn, Ile, and Åre are shown. The most abundant compounds generated from the samples are aliphatic hydrocarbons, aromatic compounds, and sulphur containing compounds.

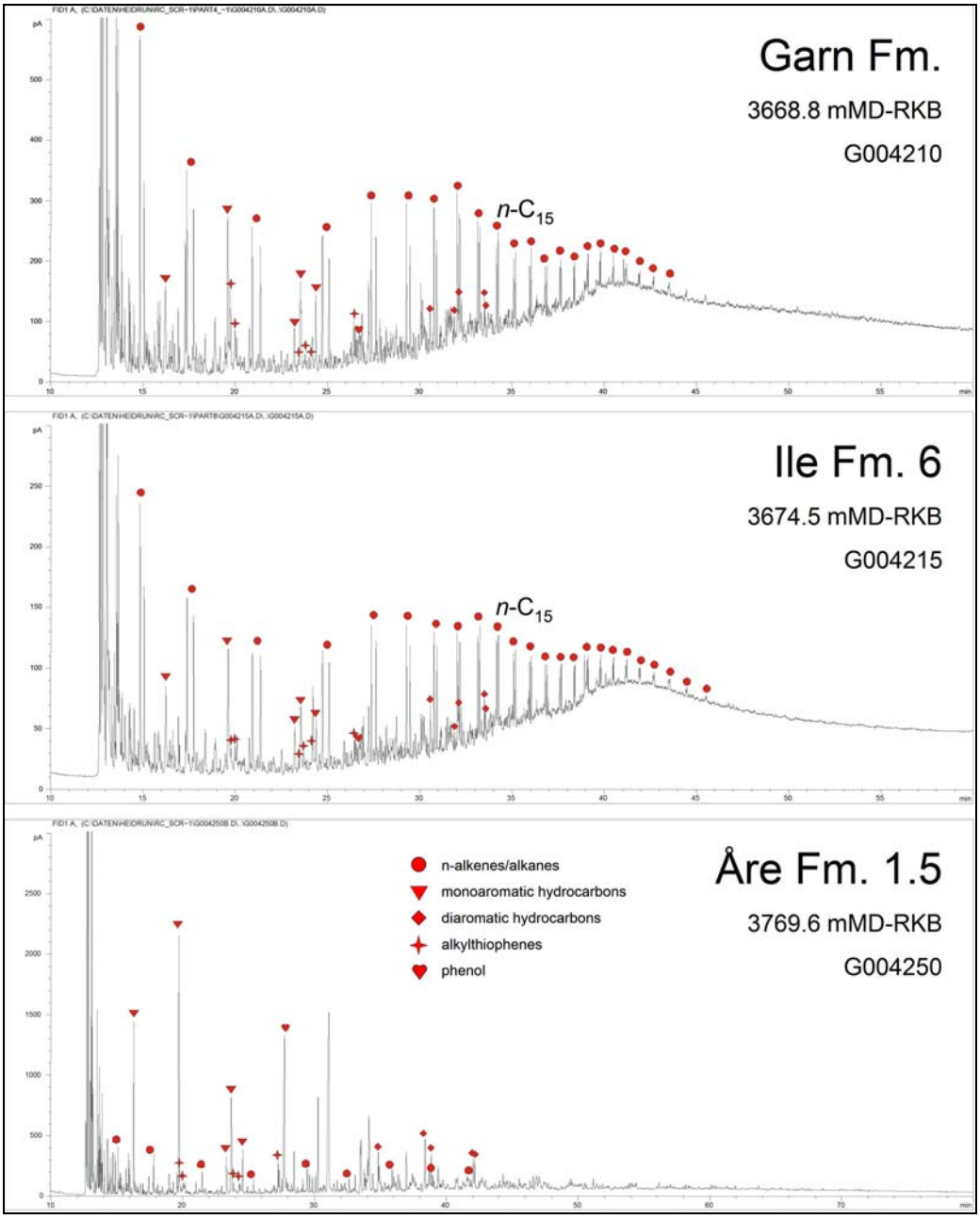

Figure 29 Selected pyrolysis gas chromatograms of well C from the Garn-, Ile- and Åre Formation. Alkene/alkane doublets, mono- and diaromatic hydrocarbons, most abundant alkylthiophenes and phenolic compounds are marked corresponding to retention time from the left to the right. Monoaromatic hydrocarbons: benzene, toluene, ethylbenzene, *m-/p*-xylene and *o*-xylene; diaromatic hydrocarbons: naphthalene, 2 methylnaphthalene, 1 methylnaphthalene and two dimethylnaphthalenes; alkylthiophenes: 2 methylthiophene, 3 methylthiophene, 2.5 methylthiophene, 2.4 methylthiophene, 2.3 methylthiophene, and ethylmethylthiophene.

The Garn and Ile Formation pyrolysis products are dominated by an homologous series of alkene/alkane doublets reaching a maximum chain length of 29 carbon atoms. Both show a bimodal shape underlain by a hump. The latter indicates a relatively high amount of unresolved compound mixture (UCM). The pyrolysis products of the Åre Fm. 1 sample look different. They show a heterogeneous distribution pattern dominated by mono- and diaromatic compounds and phenol. No hump was observed. Those distribution pattern are typical for the dominance of terrigenous organic matter as shown by *inter alia* Horsfield (1989) and Horsfield (1997). Coals are chemically similar to vitrinitic Type III kerogen, which on pyrolysis yield the highest relative amount of total aromatic hydrocarbons compared to Type II and Type I kerogen, so that their pyrolysates are dominated by alkylbenzenes, alkynaphthalenes and alkylphenols (Larter & Senftle, 1985). The high amount of mono- and diaromatic compounds in the pyrolysates results from cracking reactions of the aromatic ring via ß-cleavage during laboratory pyrolysis (Horsfield, 1997).With increasing rank the aromaticity in coals as well as in kerogen increases (Tissot & Welte, 1984).

Figure 30 show the pyrolysis products of well C in geochemical depth plots for the aromaticity (A), monoaromatic/diaromatic hydrocarbon ratio (B), relative phenol content (C), gas wetness (D) and gas amount (E). Within the single profiles, distinct variabilities can be observed with increasing depth, representing heterogeneities in the OM composition of the high molecular weight fraction. The average values and standard deviations for the bulk pyrolysis parameters can be seen in Table X 2, the Py-GC parameter analysed for each single reservoir rock of well C are listed in Table X 3 in the appendix.

Most significant differences in the Py-GC parameters were observed in the Åre Formation. Compared to the Garn- and Ile Formation, the Åre Fm. is characterised by the highest aromaticity (1.29 ± 0.41), highest relative phenol content (19.18 ± 2.75), very high gas yield ($92.9\ \% \pm 1.41$) and low gas wetness (< 0.5) (Figure 30 A, C - E). The enrichment in aromatic compounds and phenol are typical indications for coal as mentioned above, just as the enrichment in gas, especially in methane, because during laboratory pyrolysis and natural maturation of coals mainly methane (CH_4) are liberated (Horsfield, 1997; Tissot & Welte, 1984). The “coal gas” in general, has to be expected to be relatively drier ($> 90\ \%$ methane) than gas from marine source rocks (Patience *et al.,* 2003). In addition, the coaly Åre Fm. reservoir rocks show the lowest proportion of monoaromatic in relation to diaromatic hydrocarbons (Figure 30 B).

Most of the Garn-, Not- and Ile Formation reservoir rocks show phenol ratios below 1, excepting two Garn Fm. samples (G004199, G004202) and two Ile Fm. 6 samples (G004217, G004219). Thus, it was concluded that an elevated phenol ratio > 1 indicates a greater extent of terrestrial organic matter input, and refers to disseminated coal, which was found in six samples of the analysed reservoir rocks in well C (2 x Garn Fm., 2 x Ile Fm., 2 x Åre Fm.).

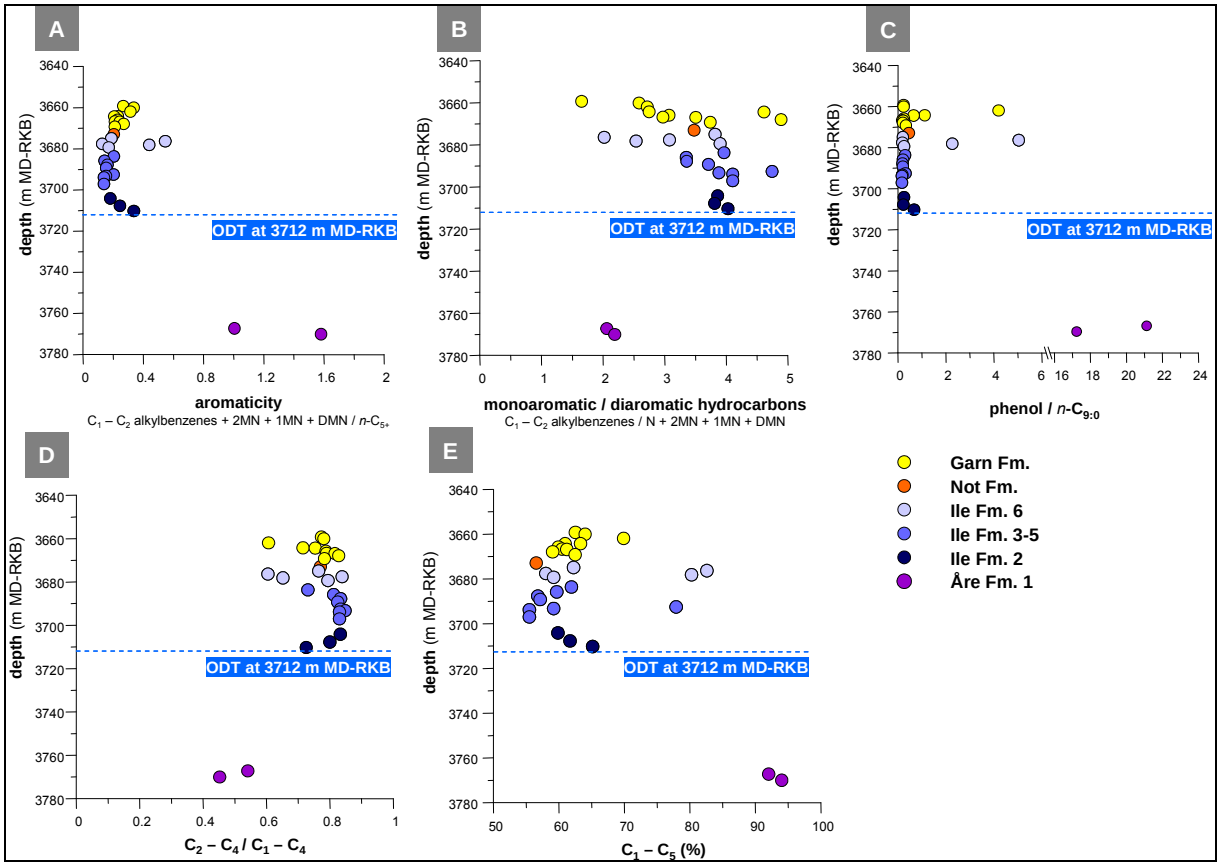

Figure 30 Geochemical profiles showing pyrolysis-GC products from the reservoir rock screening of well C. From A to E the aromaticity (A), monoaromatic/diaromatic hydrocarbon ratio (B), relative phenol amount (C), gas wetness (D) and gas amount (E) are shown.

The aromaticity of all analysed reservoir rocks ranges between 0.12 - 1.57 (Figure 30 A). Highest aromaticity was observed in the Åre Fm. (coals), while reservoir rocks from the Garn Fm. and Ile Fm. present distinctly lower aromaticity. The average aromaticity in the Garn Fm. is about 0.24 (± 0.05). Reservoir rocks from the Ile Fm. present a similar average aromaticity (0.24), but a higher standard deviation (± 0.13) compared to the Garn Formation. Two reservoir rocks from the Ile Fm. 6 (G004217, G004219) exhibit a higher aromaticity about 0.43 and 0.54.

In both formations, an decrease in aromaticity with increasing depth was observed. This might be an indication for changes in maturity, as with increasing rank the aromaticity of coal

and kerogen increases (Tissot & Welte, 1984). Another trend was observed near the ODT contact. Here three Ile Fm. 2 reservoir rocks (G004236, G004238, G004240) display an increase in aromaticity, which is accompanied by an increase in gas % and a decreasing gas wetness, and additionally a stepwise decrease in oil quality (PI) (Figure 25). This trend might be related to alteration processes, which are initiated at the oil-water interface such as biodegradation and/or water washing, and will be discussed below.

Comparing aromaticity and phenol ratio (Figure 30 A and C) most reservoir rocks with higher phenol ratios > 1 show distinct elevated aromaticity. However, both Garn Fm. reservoir rocks with phenol > 1 show low aromaticity.

As far as mono-/diaromatics were concerned, significant changes in the OM composition could be observed (Figure 30 B). The lowest ratios were observed for reservoir rocks with high relative phenol content. Thus, a low mono- versus diaromatic hydrocarbon ratio in this case correlates with the presence of disseminated coal in reservoir rocks.

The Garn Fm. and Ile Fm. 3 - 5 reservoir rocks show trends with increasing depth. Here the amount of monoaromatic hydrocarbon increases with increasing depth relative to the diaromatic hydrocarbons. Within the upper and lower Ile Fm. 6 and Fm. 2, the ratio is nearly constant (Figure 30 B). Disregarding reservoir rock samples with phenol ratio > 1 (coal), the Garn Fm. show an inverse correlation to the aromaticity (Figure 31). With increasing depth, the aromaticity decreases and the relative amount of 1-ring aromatic compounds increases relative to the 2-ring aromatic compounds.

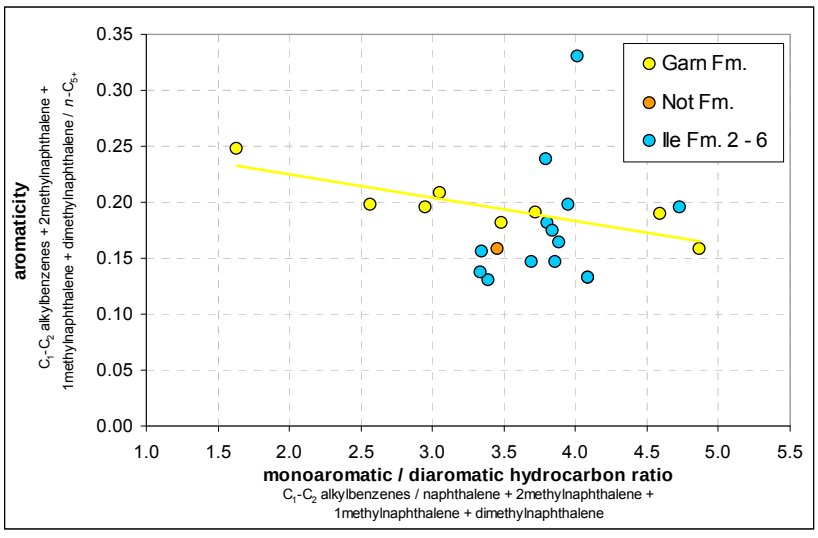

Figure 31 Correlation of aromaticity and monoaromatic versus diaromatic hydrocarbon ratio of well C including reservoir rocks of the Garn Fm., Ile Fm. 2 - 6, and Not Fm. The yellow line marks the trend observed in the Garn Fm.

Reservoir rocks with elevated aromaticity show elevated contributions of gas in their pyrolysis products (Figure 30 E). The Garn Fm. and the Ile Fm. 3 - 6 samples show a decrease in gas percentage with increasing depth, while the three reservoir rocks of the Ile Fm. 2 show an increasing gas amount near the ODT contact. The gas amount and the aromaticity are linearly correlated. Highest gas amounts (90 - 95 %) show the Åre Fm. reservoir rocks with highest phenol content.

Comparing the gas wetness (Figure 30 D) and the aromaticity curve (Figure 30 A), the shapes of both parameters curve look like mirrored. The gas wetness ranges from 0.45 - 0.85. Lowest values exhibit the Åre Fm. reservoir rocks, while samples from the Garn- and Ile Formation have higher gas wetness between 0.60 and 0.85. Both, Garn Fm. and Ile Fm. 3 - 6 display an increase in gas wetness with increasing depth. Near the ODT contact the gas wetness of the Ile Fm. 2 reservoir rocks decreases (0.83 > 0.80 > 0.72). The aromaticity and the gas wetness are apparently linked; both show an inverse correlation (Figure 32). That means, that the higher the aromaticity the dryer the gas and vice versa.

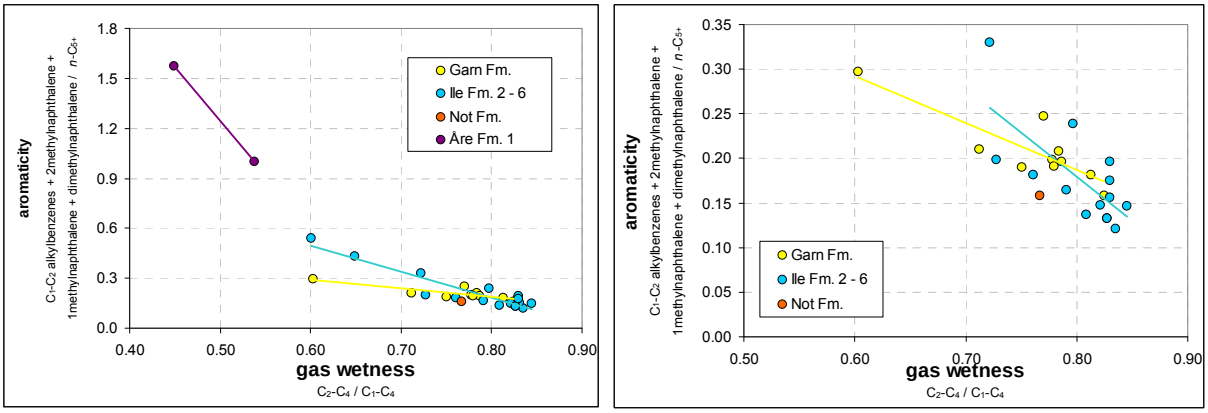

Figure 32 ***Left:*** **Inverse correlation of aromaticity and gas wetness for all reservoir rocks of well C.** ***Right:*** **Inverse correlation of aromaticity and gas wetness without the Åre Fm. coals. Coloured lines mark the trends observed in the individual reservoir formations, blue for the Ile Fm., yellow for the Garn Fm., and purple for the Åre Formation.**

In addition, the gas to oil ratio (GOR) and the percentage of unresolved compound mixture (UCM) show trends related to those observed in the aromaticity (Figure 33). Disregarding the phenol-rich reservoir rocks, the GOR slightly decreases with increasing depth, similar as observed for the aromaticity. Higher GOR can be observed in the Garn Fm. and Ile Fm. 6 compared to the Ile Fm. 3 - 5 and the Ile Fm. 2. Both latter Ile Formations display relatively uniform GOR. Within the Ile Fm. 6, the GOR decreases stepwise with increasing depth.

The percentage of the UCM fraction is different in the individual formations and subunits. However, the UCM of all formations and subunits show decreasing trends with increasing

depth, although with different intensity. The highest amounts of unresolved compounds are observed in the Garn Fm., the lowest in the Ile Fm. 2 near the ODT contact.

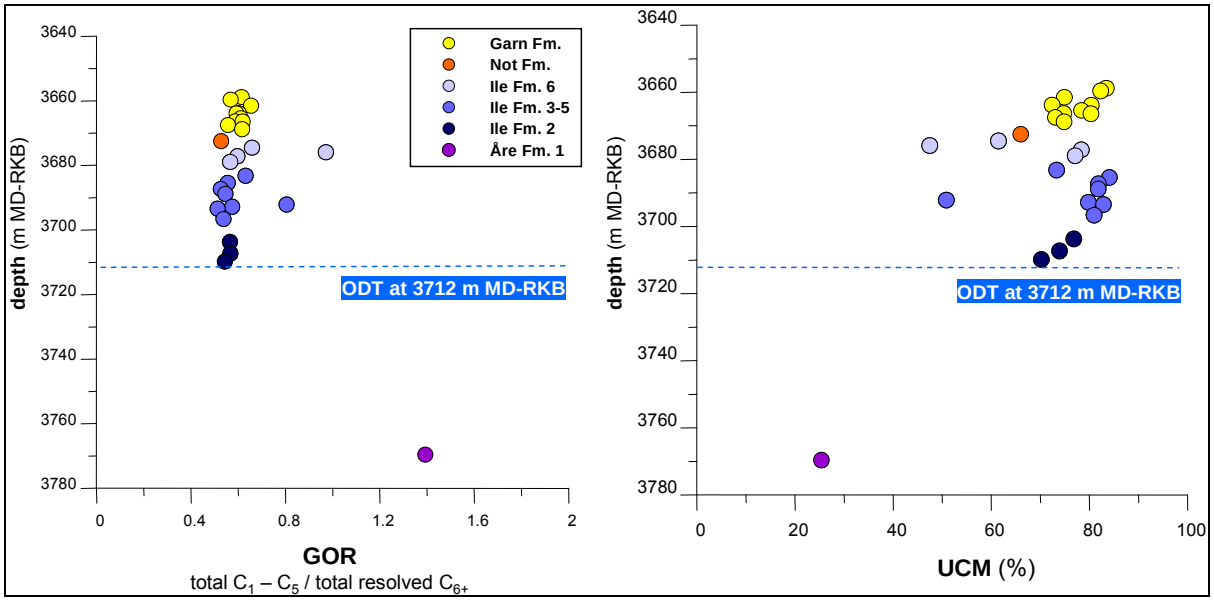

Figure 33 GOR and unresolved compound mixture (UCM) in percent of reservoir rocks from profile C. Samples with phenol ratio > 1 (coal) are disregarded.

In summary, six reservoir rock samples from the Garn Fm. (2), Ile Fm. (2), and Åre Fm. (2) with a phenol ratio > 1 indicate disseminated coal. The type of aromatic hydrocarbon ratio characterises significant changes in the organic matter composition. The Garn Fm. reservoir rocks show a decrease in 1-ring aromatic compounds relative to 2-ring aromatic compounds with increasing aromaticity. Gradients in aromaticity can be observed in the Ile- and Garn Formation. Both formations display a decrease in aromaticity with increasing depth and parallel an increase in gas wetness. Another gradient was observed near the ODT contact. The Ile Fm. 2 reservoir rock samples show an increase in aromaticity and parallel a decrease in gas wetness. That means, the higher the aromaticity the dryer the gas (higher methane content). Both parameters, aromaticity and gas wetness, are inverse correlated. In contrast, increase in the proportion of gas in the reservoir rock pyrolysates occur simultaneously with aromaticity. Additionally, the GOR and the amount of the UCM (in %) show trends related to those observed for the aromaticity.

The enrichment in aromatic compounds in reservoir rock residual bitumen pyrolysis products relative to *n*-C_{5+} is accompanied by depletion in gas wetness. The question is, why? In the

following, three possibilities will be discussed in more detail: (1) organofacies and/or maturity differences, (2) physical rock properties, and (3) physical fluid properties.

6.2.1.2.1 ORGANOFACIES AND/OR MATURITY DIFFERENCES

Heterogeneities in the composition of the reservoir rock pyrolysates can indicate different oil charges, which in turn originate from organofacies and/or maturity variabilities of the generative source rock. The first step in unravelling all fractionation phenomena (alteration affects) is to determine the bulk composition of the petroleum that is first formed in the source rock. All subsequent processes act upon and modify the original composition (Horsfield, 1997).

In order to characterise variabilities in the organofacies and/or maturity of the petroleum charges ternary diagrams, shown in Figure 34 A - D and described in Chapter 5.2, have been used to compare the reservoir rocks to both potential source rock samples from the Upper Jurassic Spekk Formation and the Middle Jurassic Melke Formation.

The Spekk Formation shale generates pyrolysates, which infer a paraffinic-naphthenic-aromatic (P-N-A) low wax oil composition (Figure 34 A). Black shales deposited in marine environments with a Type II kerogen composition typically generate those oils (Horsfield, 1989). Also the Melke Formation pyrolysates fall in the low wax P-N-A field, but compared to the Spekk Formation, distinctly closer to the gas and condensate field, which infer an oil composition with higher proportion of light pyrolysate components (C_1-C_5). Higher proportions of short chains reflect the influence of terrestrial Type III kerogen. Within the phenol and sulphur content characterising ternaries (Figure 34 B - D), pyrolysates of both potential source rocks infer an oil type generated by a marine source. The Spekk Formation generally indicates a Type II kerogen composition, while the Melke Formation source rock pyrolysates indicate a Type II / III kerogen. Pyrolysates of the Melke Formation source rock exhibit higher content of aromatic compounds.
The observed organofacies of the Spekk and Melke Formation source rocks correlate with descriptions in the literature e.g. Mo *et al.*, 1989; Ungerer, 1990; Forbes *et al.*, 1991, Karlsen *et al*. 1995.

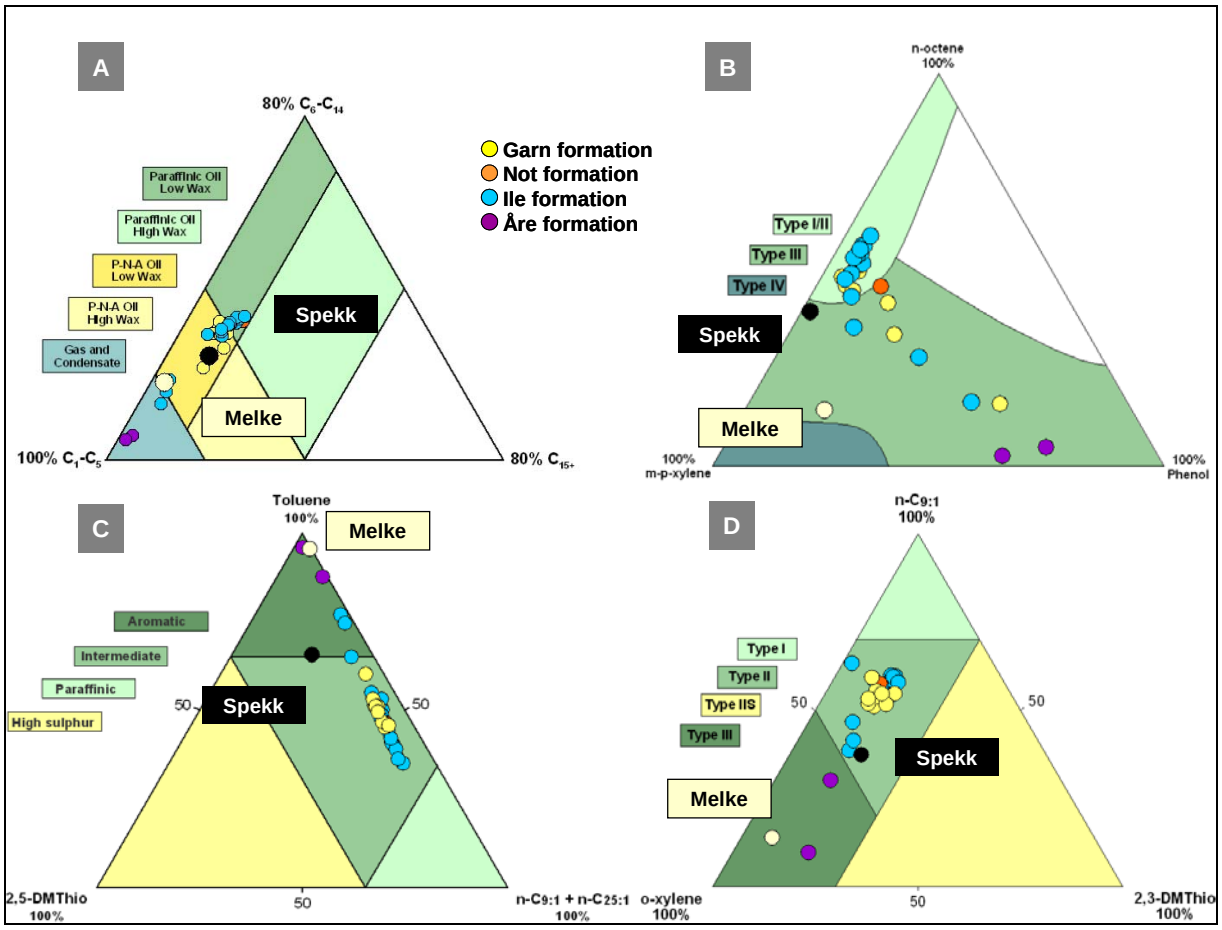

Figure 34 Bulk properties of the reservoir- and source rock pyrolysates concerning (A) alkyl chain length distribution, (B) phenol content, and (C - D) sulphur content.

Most reservoir rocks from the Ile- and Garn Formation show a relatively similar alkyl chain length distribution (CLD) (Figure 34 A). They plot in the P-N-A and the paraffinic low wax oil field, characterising oil generated by kerogen from a marine depositional environment. They show a CLD similar to the marine source rock from the Spekk Formation. However, most reservoir rocks present slightly higher amounts of long chain alkanes (C_{15+}) in there pyrolysis products. Three Ile Fm. reservoir rock samples (G004217, G004219, and G004226) reveal higher proportion of short chains their pyrolysates and plot near the gas and condensate field, closer to the potential source rock from the Melke Formation.

The pyrolysis products of both Åre Formation reservoir rocks present highest amounts of short chains. Thus, they plot in the gas and condensate field characterising the gas-prone nature of coals.

Differences seen in the CLD ternary reflect variabilities observed in the depth plots. Predominantly those reservoir rock pyrolysates with higher phenol content (> 1) are enriched in gas and exhibit higher proportions of short chains. An exception is sample G004226 from the Ile Formation, which display a high proportion of short chain alkanes (73.2 % gas) but

reveal low phenol content (0.28). This reservoir rock plots close to the Melke Formation source rock.

The phenol ternary summarises the distribution observed in the depth plot. In total, 6 reservoir rocks are characterised by higher content of terrestrial organic matter input (Figure 34 B).

The sulphur characterising ternaries in Figure 34 C and D reflect low sulphur contents for all reservoir rocks and large differences in aromaticity, especially in the Åre- and Ile Formation. Most reservoir rock pyrolysates plot in the intermediate field characterising marine sources (Figure 34 C). Two Åre- and two Ile Formation reservoir rocks plot in the aromatic field indicating sources with terrestrial organic matter input. Within Figure 34 D, the reservoir rocks plot relatively close together indicating Type II kerogen composition. Reservoir rocks with high phenol (disseminated coal) reflect a high aromaticity, represented by *o*-xylene, and indicate the composition of a hydrogen poor Type III kerogen and coals.

Distinct differences in maturity and in the depositional environment of the generative source can be excluded, as the observed variabilities result from disseminated coal.

6.2.1.2.2 CORRELATION TO PHYSICAL ROCK PROPERTIES (WELL LOG DATA)

Compound distributions could be related to physical rock properties such as permeability, porosity and the water saturation. The porosity Φ and the permeability K control the *in-situ* hydrocarbons volume and they are responsible how easily hydrocarbons will flow out of them. The water saturation S_w represent the fraction of water in a given pore space. They are very important during the production and migration of oil and further for the microbial live in the subsurface as biodegradation occurs in water-saturated zones. Therefore, well log data can be crucial as different rock properties imply different conditions for microbial activity.

The focus in the next section will be on the relation of these physical rock properties to the aromaticity gradients observed and to the variabilities in the organic matter distribution.

The porosity and permeability distribution of the Garn Fm. and Ile Fm. sandstones seem to be relatively uniform compared to the rock properties of the Åre Fm. sediments, which are characterised by several coal-rich intervals (Figure 9). A comparison of the aromaticity to the physical rock properties porosity, permeability, and water saturation of profile C is shown in Figure 35. Reservoir rocks with coaly particles are not considered in this plot.

In the Garn Fm., which shows good reservoir conditions (cf. Chapter 3.2.1), the permeability and the porosity slightly decrease with increasing depth. The S_w of this reservoir unit is relatively high as compared to the underlying Ile Formation. The reservoir rocks from the Garn Fm. show a relatively low organic matter content between 7.7 - 25.2 mg/g rock and a relatively low aromaticity (0.16 - 0.30). Both parameters slightly decrease with increasing depth parallel to the rock properties (Figure 35).

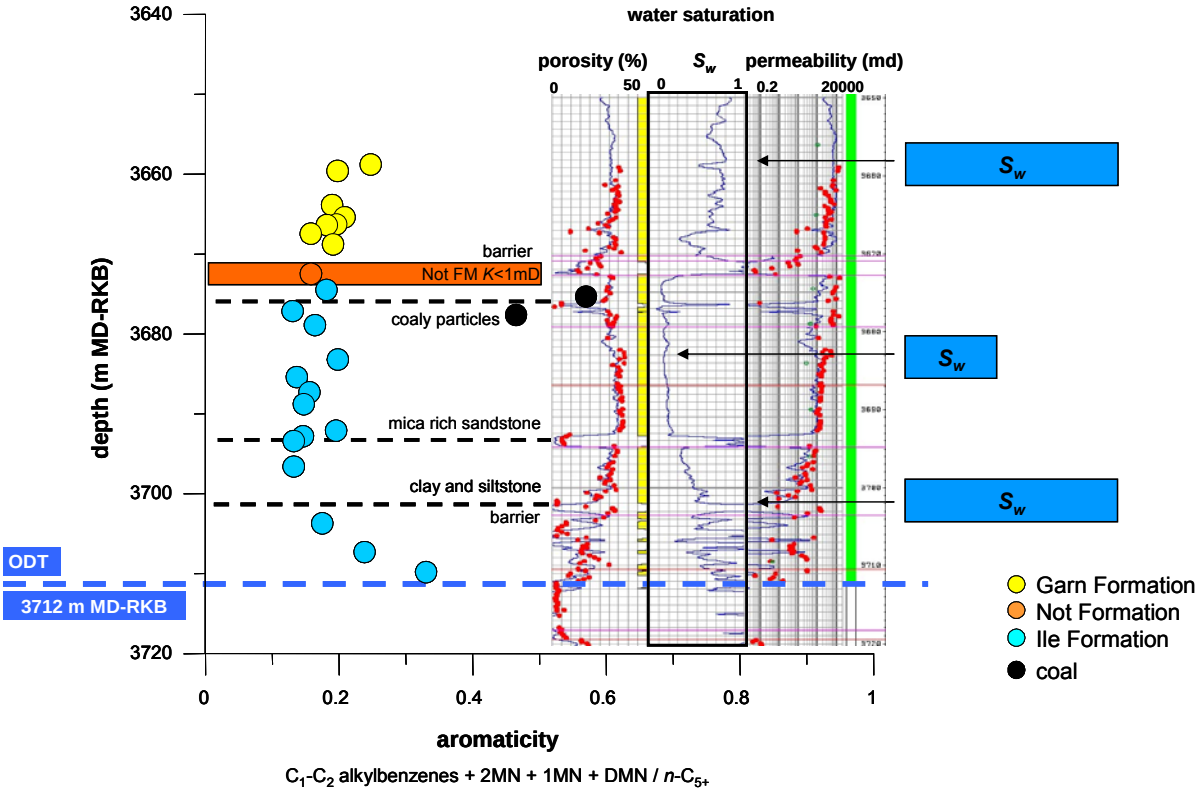

Figure 35 Comparison of the aromaticity (left) analysed in well C to a well log section of the profile (right) including porosity, water saturation, and permeability. Coaly samples are not considered. The well log is provided Statoil.

ODT = oil down to contact

The reservoir rocks analysed from the Ile Fm. are from five reservoir zones (Ile Fm. 2 - 6) (Figure 9). The Ile Formations 4 - 6 (3674 m - 3693 m MD - RKB) shows good poroperm properties similarly to the Garn Fm., but with distinctly lower water saturation S_w (Figure 35). Here the reservoir rocks are characterised by very low aromaticity (< 0.20). Excepted are three zones with low poroperm properties and high S_w. One zone in the upper part of the Ile Fm. 6 shows coaly particles. Here, low poroperm properties correlate to high aromaticity (black dots) and high OM content (not shown). In another zone, at the base of Ile Fm. 4 sandstones at 3693 - 3695 m MD-RKB, a high concentration of mica was observed that additionally result in low poroperm properties. Both reservoir rock samples (G004229,

G004230) analysed here, show higher organic matter content (30.2 and 37.0 mg/g rock), but also very low aromaticity (< 0.15). The third zone at the base of the Ile Fm. 3 (3702 m MD - RKB) comprises clay and siltstones, and may act as a barrier.

In the channel sandstones of the Ile Fm. 2 near the ODT contact, calcite cemented bands are typical (internal Statoil report, 2003). Within this unit, the porosity and permeability decrease, and expectedly the S_w increase down to the ODT contact. The gradually changes in the rock properties can be seen in the curve like shapes in the well log. The three lowermost Ile Fm. reservoir rocks analysed here (G004236, G004238, and G004240), reflect the trend and show an increase in aromaticity from 0.13 up to 0.33 (Figure 35). Thus, the aromaticity is apparently linked to the water saturation. These samples are additionally characterised by a stepwise decrease in the OM content. Thus, the combination of high water saturation, the increase in aromaticity and the diminishing OM content could be an indication for higher microbial activity near the OWC.

In summary, different barrier zones, coal beds and mica rich sandstones were detected, and related to the OM distribution as well as the pyrolysis parameters. Near the ODT contact a decrease in porosity and permeability and an increase in the water saturation was observed, that goes along with an increase in aromaticity and a stepwise decrease in the OM content. The aromaticity is apparently linked to water saturation. However, based on the visual comparison alone no general correlation between the different heterogeneities in the aromaticity and the organic matter distribution was found.

The observed correlation between the aromaticity and the water saturation could be an indication of biodegradation. In other words, biodegradation appears to have resulted in abstraction of hydrogen from the macromolecular components, and thus the enhanced generation of aromatic hydrocarbons on pyrolysis. On the other hand, mineral matrix effects have also to be considered in order to exclude the possibility that analytical artefacts could have led to the aromatic pyrolysis products. Mineral matrix effects for a given mineralogy are more pronounced when organic matter is in low abundance. Therefore, the aromaticity and the whole reservoir rock pyrolysis yields C_{1+} (mg/g rock) of the resolved compounds were compared to see if a relationship between yield and aromaticity could be establihsed. Figure 36 show both parameter versus increasing depth (left) and the C_{1+} (mg/g rock) resolved compounds versus the aromaticity (right). The reservoir rock samples with disseminated coal are excluded.

In Figure 36 a nearly constant aromaticity with increasing pyrolysis yield C_{1+} (mg/g rock) of the resolved compounds can be seen. No correlation of aromaticity and whole reservoir rock pyrolysis yields was found. Thus, a mineral matrix effect can be excluded as a mineral matrix effect would reflect an inverse proportional correlation.

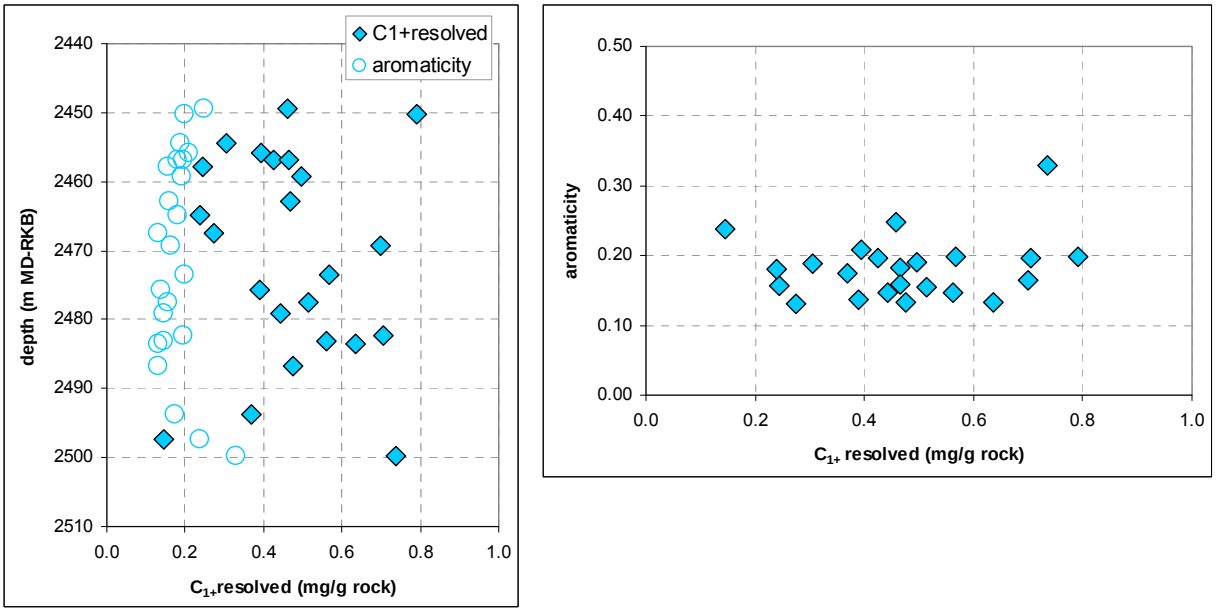

Figure 36 Depth plot of the aromaticity and C_1+ of the resolved compounds (left) and aromaticity versus C_{1+} of the resolved compounds (right) of the reservoir rocks of well C.

6.2.1.2.3 CORRELATION TO PHYSICAL FLUID PROPERTIES

Physical fluid properties such as viscosity and API gravity can reflect the influence of alteration. Alteration processes such as biodegradation preferentially consumes hydrocarbons (saturated are preferred for aromatic) and the residual oil becomes heavier, because of the enrichment in NSO compounds (polar and asphaltene fraction). As result the biodegraded oils are lower in API gravity (increase in oil density), are more viscous, are richer in sulphur, resins, asphaltenes, and metals (e.g. Ni and V), and they show a higher acidity (Connan, 1984; Head *et al.*, 2003; Meredith *et al.*, 2000; Palmer, 1993; Peters *et al.*, 2005; Tissot & Welte, 1984; Volkman *et al.*, 1984).

Based on the oil analysis indications for biodegradation in the Heidrun oil field already exist (cf. Chapter 3.1). Based on this data, the Heidrun oil field can be subdivided in two dominant parts, a biodegraded and a mixed part. The biodegraded oil samples without a second oil charge are predominantly found in the east, while the oils in the western part of the reservoir are biodegraded and altered by a second charge. Further a 3rd part can be subdivided were

signals from both extremes are detected, that means the biodegradation of the second charge can be observed. These wells are in the central part of the field (Figure 7).
In order to observe if the aromaticity trends in reservoir rock pyrolysates reflect an influence of alteration such as biodegradation, a biodegradation series consisting of five heavy oils reservoir rock extracts from the WCSB (Western Canada Sedimentary Basin) and five Heidrun oils with different API gravity (20 - 29°) were analysed using similar parameter as applied for the reservoir rock screening. The Industry partner Shell provided the heavy oil series.

6.2.1.2.3.1 HEAVY OILS (WCSB)

The soxhlet extracted heavy oils are from one well. They represent a sequence of alterated and biodegraded heavy oils. From the well top to the well bottom they show a increase in the PM biodegradation level from moderate to heavy (low 5 up to low 6) (PM after Peters and Moldowan, 1993). The OWC is in the depth range of the lowermost sample at 623.5 m below top. Table 11 lists the five heavy oil extracts analysed, their API gravity, viscosities and asphaltene amount. Original well codes, field codes, and exact sample location are not known for reasons of confidentiality.

Table 11 List of the reservoir rock extracted heavy oils from the biodegradation series of the Western Canada Sedimentary Basin (WCSB). *RCE = reservoir rock extract.

GFZ number	Sample Type	depth	API gravity	viscosity	bitumen	asphaltene
		m below top		(cP)	%	wt %
G005634	heavy oil (*RCE)	604.1	8.2	66368	6.3	18.6
G005635	heavy oil (*RCE)	608.6	7.2	87314	8.1	18.9
G005636	heavy oil (*RCE)	611.3	6.3	365272	9.3	17.9
G005639	heavy oil (*RCE)	621.1	6.0	2359428	9.2	19.5
G005640	heavy oil (*RCE)	623.5	-	2527611	10.3	20.0

Figure 37 (left) shows the viscosity of the heavy oil reservoir rock extracts with increasing depth. The viscosity increases with higher biodegradation level. Viscosities beyond 10000 centipoises (cP) are typical for extra heavy oils or tar sands. They show little or no mobility and already beyond a viscosity of 100 centipoises at reservoir conditions, that correspond to a density of approximately 20° API gravity, those oils are difficult to produce by conventional techniques (Tissot & Welte, 1984).

The differences in the data points result from the jump in viscosity from sample 3 (G005636) to sample 4 (G005639) that is not reflected in the API gravity (Figure 37, middle). The extra heavy oils show API gravity below 8°, which continuously decrease to 6° with increasing depth and with increasing biodegradation level. For the lower most sample (no 5, G005640), no API gravity data are available.

Another typical characteristic of biodegraded oils is the enrichment in asphaltenes and resins as mentioned above. Tissot & Welte (1984) mentioned average values for asphaltenes and resins in heavy oils of 22.9 wt.% and 30.6 wt.% , respectively. In sum, the polar compounds represent 53.5 wt.% in heavy biodegraded oil, compared to conventional oils with 14.2 wt.% for asphaltenes + resins.

The asphaltene wt.% for the heavy oils analysed in these study are shown in Figure 37 (right). With increasing depth the asphaltene amount increases relatively continuously from 18.6 up to 20 wt.%. This corresponds to the average values in the literature. Slightly conspicuous is lower asphaltene amount (17.6 wt.%) of the third sample below top (G005636). However, excluding these sample, the increase in asphaltene wt.% in the profile correlates with the increase in viscosity and specific density (decreasing API gravity). Compared to the heavy oils, the average asphaltene amount in well C is distinctly lower (6.51 ± 4.88; 7 asphaltenes listed in Table 9).

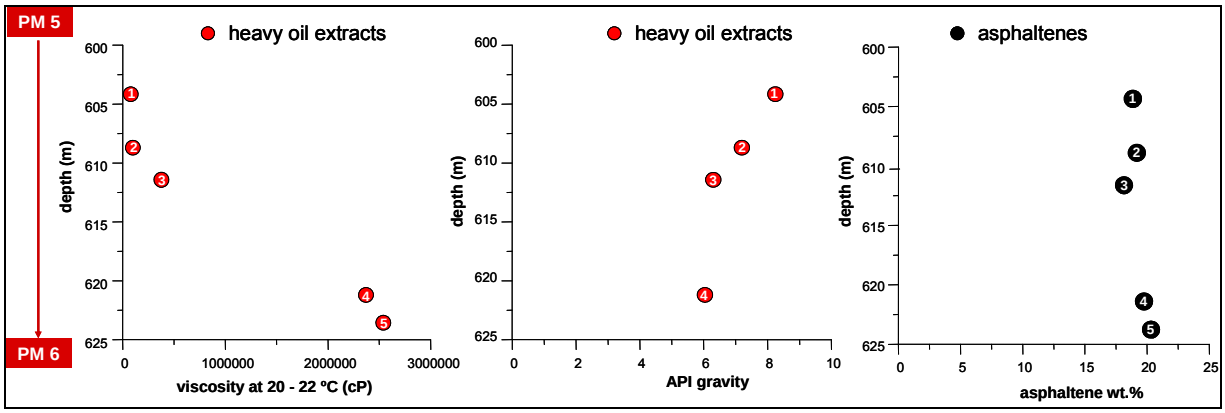

Figure 37 Viscosity (left), API density (middle) and asphaltene wt.% (right) of the heavy oil reservoir rock extracts from the WCSB versus increasing depth. For sample no 5 (G005640) no API density data are available.

Figure 38 show the whole oil chromatograms from the well top to the well bottom with increasing biodegradation level. The large peaks in the middle of the whole oil chromatograms represent the internal standard androstane. In all chromatograms, the *n*-alkanes are completely absent and a significant “hump” occurs, indicating a high amount of

unresolved compound mixture (UCM). It is known that biodegradation of petroleum in reservoir formations results in quite rapid removal of components with alkyl chains, particularly *n*-alkanes (Killops & Al-Jiboori, 1990). The disappearance of these dominant resolved components, in the gas chromatograms of biodegraded petroleum, results in the detection of a "hump" or UCM (Blumer *et al.*, 1973). The UCM consist of bio-resistant compounds, including highly branched and cyclic saturates, aromatic, naphthenoaromatic, and polar compounds (Peters *et al.*, 2005), which may represent either the biodegraded oil fraction or a complex mixture that is always present in crude oils and arise from the removal of major resolved alkylated species by biodegradation (Killops & Al-Jiboori, 1990).

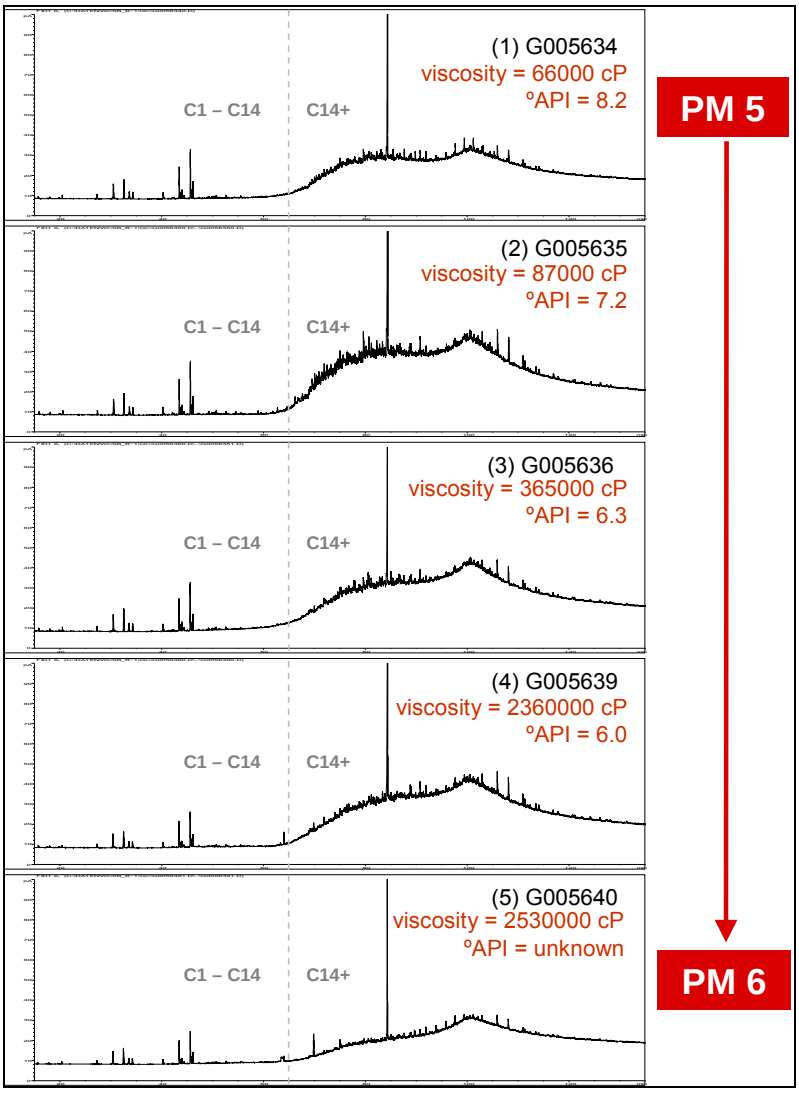

Figure 38 Whole oil chromatograms of the heavy oil extracts, shown from the top to the bottom with increasing biodegradation level.

Differences observed concern the shape of the UCM in the C_{14+} range (Figure 38). In contrast to the bimodal pattern of the four uppermost heavy oils, the UCM of the lower most sample

near the OWC increases nearly continuously and show a single maximum. The distinctions observed refer to differences in the UCM composition. Killops & All-Juboori (1990) reported that multiple maxima in the UCM of biodegraded oils may be due to inputs from different kerogens. The different shape of the lowermost heavy oil (G005640) might further be related to the presence of the water-saturated zone. Thus, both biodegradation and water washing might alter the lowermost heavy oil.

It was concluded that the increase in viscosity, specific density (decrease in API gravity) and asphaltenes amount with in the profile as well as the depletion in *n*-alkanes in combination with the large UCM, indicate that the heavy oils reached high alteration levels probably caused by biodegradation. The trends observed goes along with the increasing biodegradation level from the top to the bottom of the profile.

Pyrolysis products

The PI of the heavy oils is between 0.48 and 0.54. This indicates a relatively low S1, and further a distinctly lower oil quality as observed in well C (0.63 ± 0.15). Table X 4 listed the Py-GC parameters analysed. Within the profile, the PI is nearly uniform. Only a very slight decrease with increasing viscosity can be seen (Figure 39, left). Comparing the PI and the API gravity a linear correlation was found, i.e. despite the small range, the PI directly correlates with the fluid physical properties viscosity and API gravity of the heavy oils and thus, directly with biodegradation (Figure 39 right).

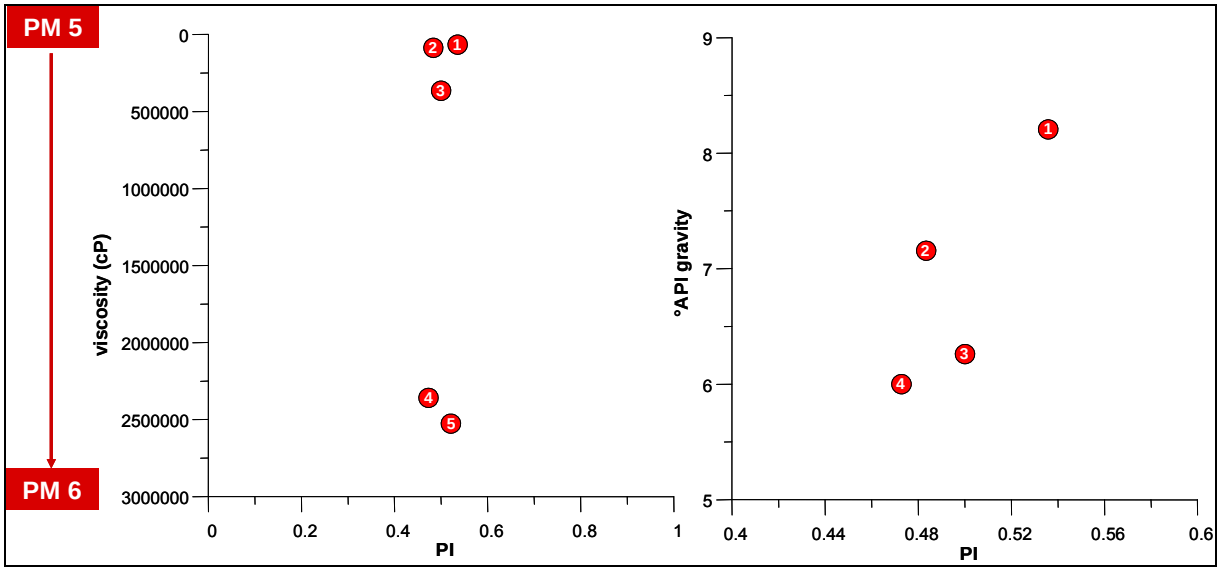

Figure 39 PI of the heavy oil series from the WCSB versus viscosity (left) and versus °API gravity (right). For sample no 5 (G005640) no API density data are available.

The pyrolysis gas chromatograms in Figure 40 (left) show the pyrolysates generated from the heavy oils. The samples illustrated increase in viscosity, °API gravity and biodegradation level from the top to the bottom. The open system Py-GC experiments for the heavy oils show a rather uniform homogeneous alkene/alkane distribution pattern up to C_{25}. All samples show a hump indicating a high amount of unresolved components (UCM). With increasing viscosity, API gravity and biodegradation level, the heavy oil chromatograms look nearly similar. As observed in the whole oil chromatograms (Figure 38), the heavy oil reservoir rock extracts do not reveal great compositional differences in their pyrolysates. Thus, qualitatively, it appears that the macromolecular fraction has not been noticeably altered by biodegradation.

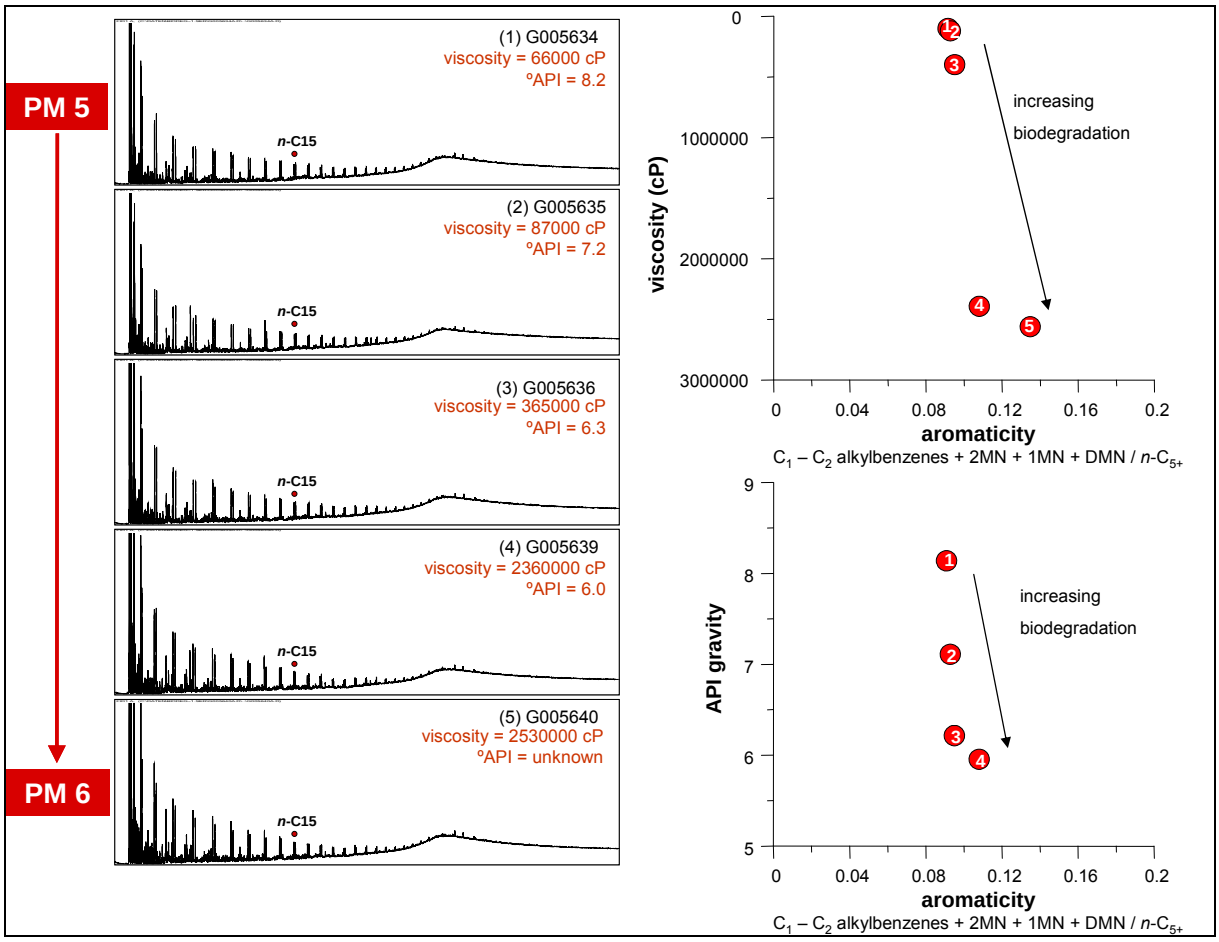

Figure 40 *Left* Heavy oil chromatograms from Pyrolysis-GC experiments. *Right* geochemical depth plots for aromaticity versus viscosity (top), and aromaticity versus API gravity (bottom). Both, the pyrolysis gas chromatograms and depth plots are shown from the top to the bottom of the profile. The difference in the data points of the aromaticity - viscosity plot results from the conspicuous jump in viscosity from sample 3 to sample 4 that is not reflected in the API gravity. For sample no 5 (G005640) no API density data are available.

Nevertheless, the aromaticity of the analysed heavy oils ranges from 0.09 up to 0.13 and a slight increase in aromaticity was observed (Figure 40, right). The differences in the data

points in the viscosity depth plot in Figure 40 (top right) result from the jump in viscosity from sample 3 to sample 4 that is not reflected in the API gravity (Figure 40, bottom right).
As the increase in viscosity of the heavy oils represents the increasing biodegradation level, this refers to an increase in aromaticity with increasing biodegradation. Examining the aromaticity and the API gravity a similar pattern can be seen (Figure 40 bottom right). The aromaticity slightly increases with decreasing API gravity (increase in specific density). The decrease in API gravity represents the increasing biodegradation level and thus the increase in aromaticity with increasing biodegradation. The macromolecular fraction of the heavy oils reservoir rock extracts reveals a direct correlation of aromaticity in the pyrolysates and the biodegradation. Note that the range is much less pronounced for these samples than for the Heidrun cores.

As observed for the aromaticity, the Py-GC monoaromatic / diaromatic hydrocarbon ratio, gas wetness, and gas %, increase too with increasing viscosity and thus, with increasing biodegradation (Table X 4). Different as observed in well C, here the aromaticity and the gas wetness are linearly correlated. Volkmann *et al*. (1984) assessed the susceptibility of different aromatic hydrocarbon classes to biodegradation and showed that the rate of biodegradation decreases with increasing number of aromatic rings in order monoaromatic > diaromatic > triaromatic, and with the number of alkyl substituents. According to this, the monoaromatic / diaromatic hydrocarbon ratio should be decreasing, because diaromatic compounds are more resistant to microbial activity than monoaromatic compounds.

The GOR increases with increasing viscosity. This indicates higher GOR in the pyrolysates with increasing biodegradation level (Figure 41, left). Furthermore, the GOR and the aromaticity show a linear correlation (Figure 41, right). Compared to the GOR, the UCM decreases with increasing viscosity and so with increasing biodegradation level (Figure 42, left), and it shows a inverse correlation to the aromaticity (Figure 42, right).

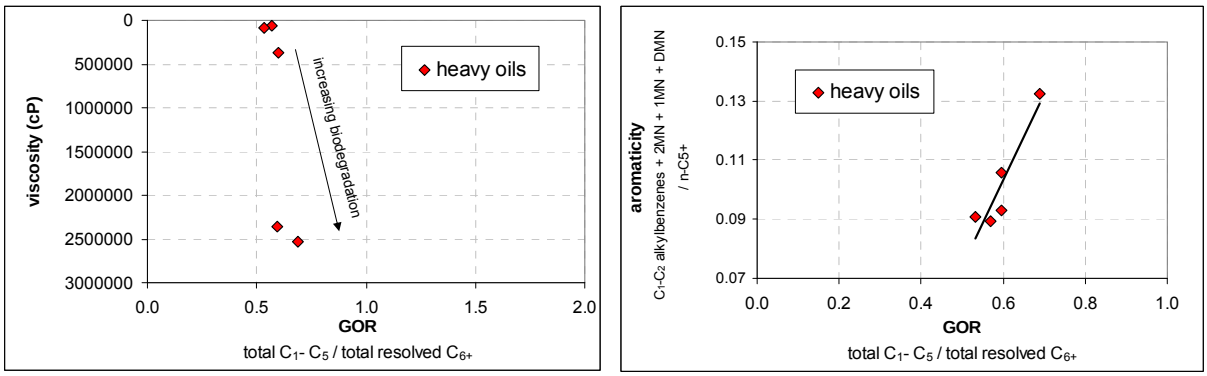

Figure 41 ***Left*** **GOR of the heavy oil series from the WCSB versus viscosity.** ***Right*** **GOR of the heavy oil series correlated to the aromaticity.**

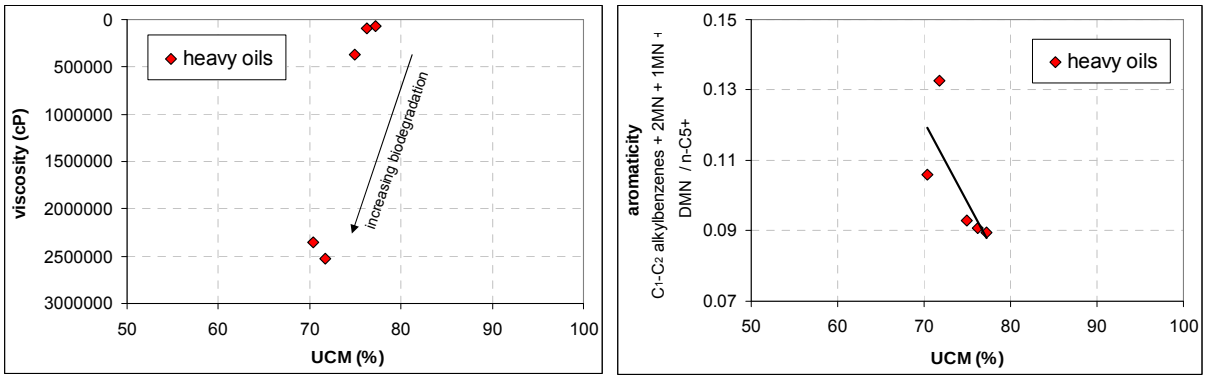

Figure 42 ***Left*** **Unresolved compound mixture (UCM in %) of the heavy oil series from the WCSB versus viscosity.** ***Right*** **UCM (%) of the heavy oil series correlated to the aromaticity.**

6.2.1.2.3.2 HEIDRUN OIL

Five oil samples (DSTs) from two wells were investigated from the Heidrun oil field. Nearly all oils are from the Tilje Formation. They were chosen because they exhibit an API gravity range from 20° up to 29° (Table 12).

Table 12 List of the wells, DST numbers, depth, API gravity and asphaltene amount of Heidrun oil samples used.

well	field segment	GFZ number	sample	sample type	depth interval	stratigraphical unit	API gravity	Asphaltene
					m MD-RKB			wt.%
6507/7-2	G	G003881	DST 4A	oil	2340-2330	Tilje Fm. 3.2	29	0.26
6507/7-2	G	G003882	DST 3	oil	2376-2365	Tilje Fm. 2.2-2.3	24	0.32
6507/7-2	G	G003883	DST 2	oil	2439-2417	Åre Fm. 2.10-2.11	22	0.59
6507/8-1	I	G003896	DST 2	oil	2406-2386	Tilje 3.3 - 4	23	0.33
6507/8-1	I	G003897	DST 1	oil	2462.5-2444	Tilje 2.2 - 2.4	20	0.44

The GOR and API gravity of all Heidrun oils show a very good correlation as well as the GOR and viscosity, similar as observed in the heavy oils from the WCSB. Most degraded or least mixed Heidrun oils show lowest GOR, because microbes consumed the light hydrocarbons. Additionally they show the lowest API gravity.

The oil samples (DSTs) in the Heidrun oil field show two general GOR trends with increasing depth: (1) A decrease in the GOR with increasing depth that is typical in many fields due to fractionation and or gravity segregation, and (2) a "lack" of a trend. The trend 1-oils are predominantly in the northern, central, and southern part of the field. Wells from the western part are characterised by the lack of a trend. The latter are the oils, which received the most recent charge and, which had no time until now to equilibrate (internal Statoil report, 2003).

Thus, the variability in API gravity of 10° is a good indication for variations in the biodegradation level. Another indication is the enrichment in asphaltenes with decreasing API gravity (Figure 43).

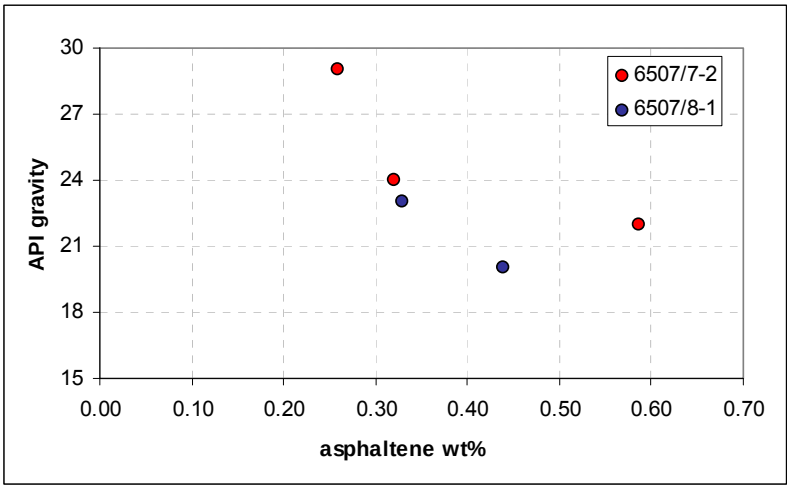

Figure 43 Correlation of API gravity and asphaltene amount in wt.% of selected Heidrun oils with API gravity between 20° and 29°.

Figure 44 show the whole oil chromatograms of well 6507/7-2 and 6507/8-1 from the top to the bottom with decreasing API gravity. With decreasing API gravity, the oils reveal differences in their molecular compositions. In DST 4A, with the highest API gravity (29°), light hydrocarbons, and *n*-alkanes up to *n*-C_{35} are detectable. This is in contrast to the four other oil samples with lower API gravity, where *n*-alkanes are nearly absent. This indicates a higher level of alteration as for DST 4A. These samples further show a significant hump indicating a high amount of unresolved components. Thus, indications were found that these oils reached a high alteration levels probably caused by biodegradation.

Figure 45 show the Production Index (PI) of all oil samples and condensates analysed in the Heidrun oil field versus the corresponding API gravity. The oil samples show a PI between 0.68 - 0.78. Highest PI was observed for the condensate samples (0.95 - 0.97) indicating a high amount of free hydrocarbons (S1). The four selected oil samples from the Tilje Fm. and the oil from the Åre Fm. show PI between 0.69 and 0.77 (Table X 5). Most significant differences in the PI reveal the oil sample G003897 with lowest API gravity of 20° and the oil sample G003881 with the highest API gravity of 29°. The oil samples with API gravity 22°, 23° and 24° present nearly similar PI about 0.72.

The PI and the API gravity show a linear correlation. With decreasing API gravity, the PI decreases. The decrease in API gravity indicates an increase in biodegradation seen before in the whole oil chromatograms. Thus, here a correlation of the PI or the oil quality and the biodegradation was found.

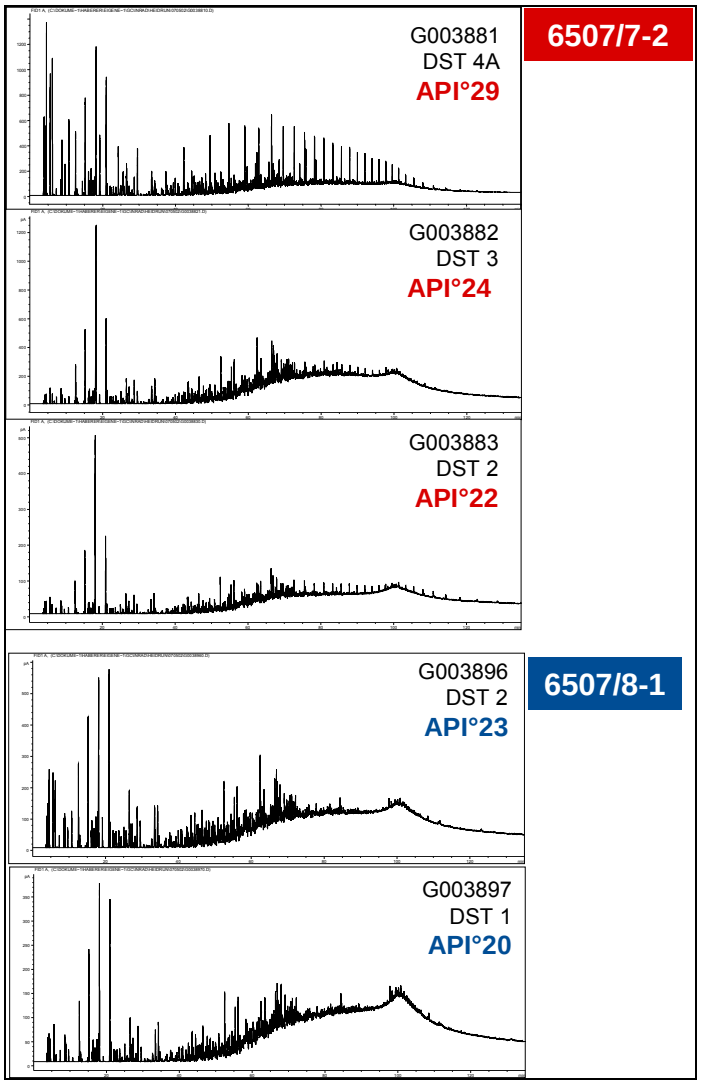

Figure 44 Whole-oil chromatograms of the oil samples of well 6507/7-2 and 6507/8-1 with API gravity between 20° and 29° from the Heidrun oil field.

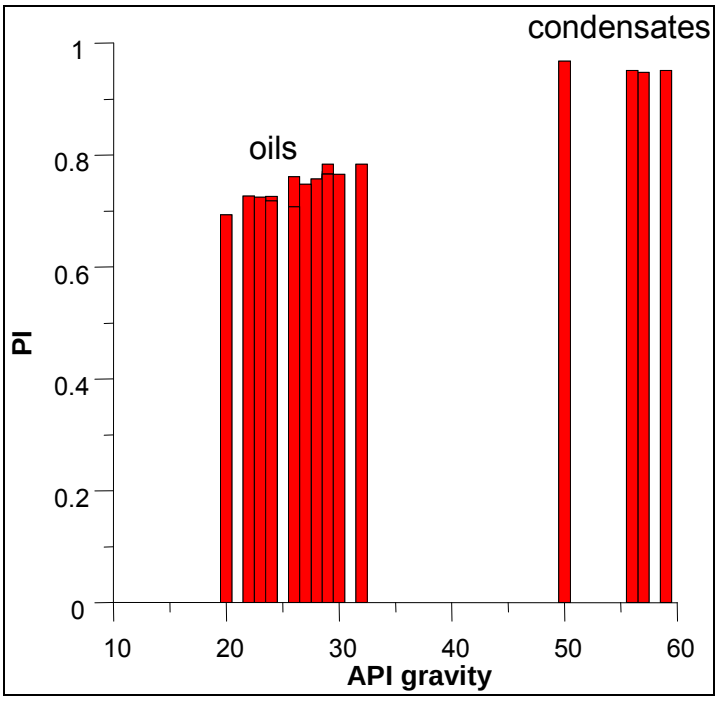

Figure 45 Production Index (PI) of all oil samples and condensates analysed in the Heidrun oil field versus corresponding API gravity.

Pyrolysis products

Table X 5 lists the Py-GC data for macromolecular components in selected Heidrun oils. The pyrolysis gas chromatograms in Figure 46 (right) show the pyrolysates generated from the five oils, from the top to the bottom with decreasing API gravity. All pyrolysis gas chromatograms present a significant hump, indicating a high amount of unresolved compounds. The pyrolysates of the oil G003882 (API 24°), G003896 (API 23°) and G003897 (API 20°), show a relatively constant alkene/alkane distribution pattern with alkyl chain length up to C_{24} and C_{26}, respectively. The pyrolysates of two oils are different. Both, the pyrolysis gas chromatograms of oil sample G003881 (API° 29) and G003883 (API° 22), show a normal distribution of alkene/alkane doublets up to C_{26} and C_{28}, respectively. Afterwards alkanes up to C_{35} and C_{40} were detected. A carryover during the pyrolysis measurements can be excluded, because the samples have been analysed three times. These long chain alkanes represent oil compounds mobilised at higher temperatures.

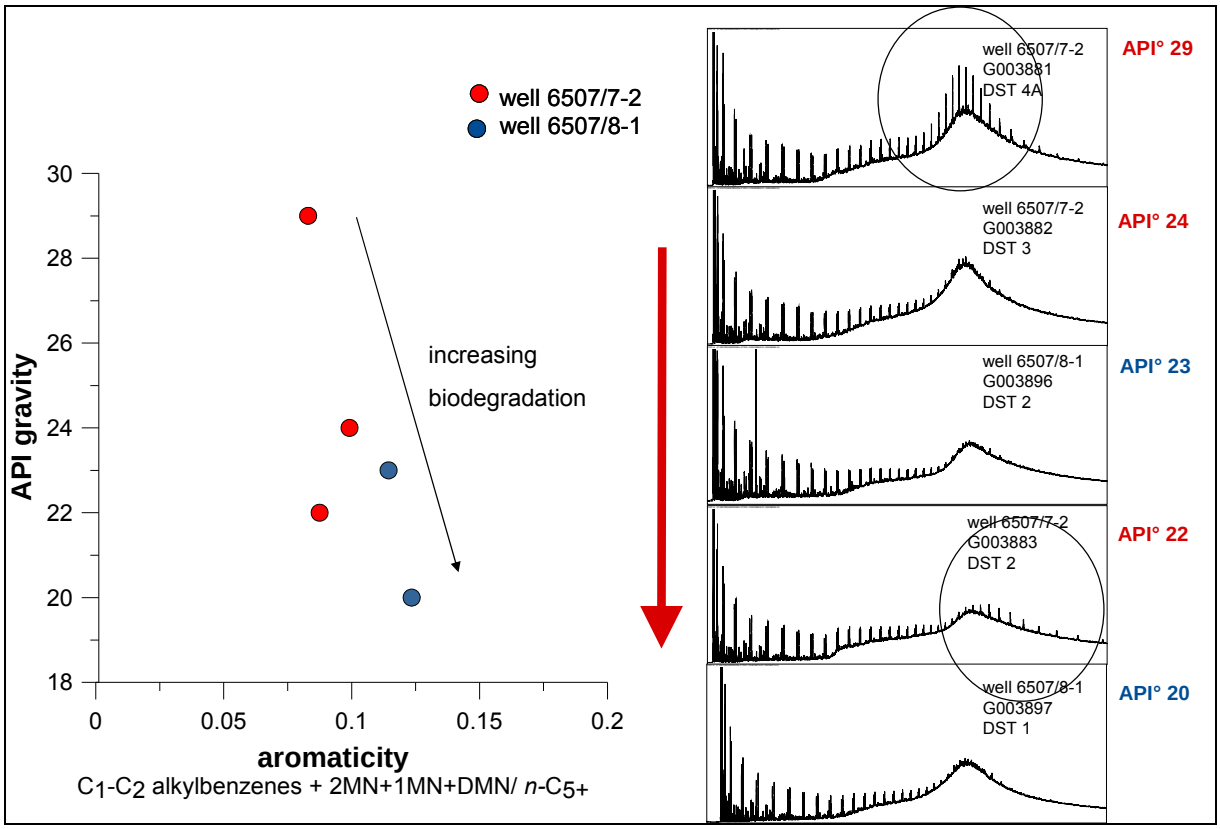

Figure 46 Geochemical depth plots for the aromaticity (left) and the pyrolysis gas chromatograms of the five Heidrun oils (right). From the top to the bottom, the oil pyrolysis gas chromatograms are shown with decreasing API gravity.

The aromaticity of the analysed oils ranges from 0.08 up to 0.12. Examining the aromaticity versus decreasing API gravity (Figure 46, left), a slight increase in aromaticity was observed. As the decreasing API gravity of the oils represents an increasing biodegradation level, this correlation refers to an increase in aromaticity with increasing biodegradation.

Similarly, to the heavy oil series from the WCSB, the macromolecular fraction of the Heidrun oils reveals a direct correlation of aromaticity in the pyrolysates and biodegradation.

To sum up, pyrolysis products from the heavy oil series (WCSB) and the Heidrun oils show an increase in aromaticity with increasing viscosity and decreasing API gravity. Both fluid physical properties appear to be related to different biodegradation levels. A direct correlation of aromaticity and biodegradation was observed within the pyrolysis products.

6.2.2 WELL B IN SEGMENT I (TILJE FM. 3.4 - 2.5)

6.2.2.1 PRODUCTION INDEX AND ORGANIC RICHNESS

The sampled section in well B was from the Tilje Formation only (Table 3). An average PI of 0.67 with very low standard deviation (± 0.03) points to minor changes in oil quality of the reservoir rock samples in profile B (Figure 25, Table X 1). However, a tripartition regarding the PI values could be observed. The middle part of profile B represents highest PI values, five reservoir rock samples in the deeper part show minor PI values of about 0.63 ± 0.02, and reservoir rocks analysed from the well top present intermediate PI values.

Profile B shows a relatively high organic matter content of about 28.29 mg/g rock (± 13.08) and is characterised by a very heterogeneous distribution and significant changes from very lean to very organic rich zones at small scale (Figure 26, Table X 1). In contrast to the PI, the distribution of the OM does not show a tripartition. One sample in the middle part of profile B (G004179) presents significant low organic matter content. This could be an indication for low oil saturation. In the upper part a gradually decrease of the organic matter content was observed.

6.2.2.2 ORGANIC MATTER COMPOSITION

In Figure 47 A - E, the pyrolysis products of well B are shown in geochemical profiles for the aromaticity (A), monoaromatic / diaromatic hydrocarbon ratio (B), relative phenol content (C), gas wetness (D) and gas amount (E). The average values and standard deviations for the bulk pyrolysis parameters can be seen in Table X 2. The Py-GC parameter values for each single reservoir rock of well B are listed in Table X 6.

The pyrolysates of well B show a different picture compared to well C. In well B, an overall increase in aromaticity with increasing depth was observed and the trend consisted of a broad swarm of data points. Significant changes at very small scale within their pyrolysates indicate distinct changes within the organic matter composition of the macromolecular fraction. This might be related to the very complex and heterogeneous lithology of the Tilje Formation. Based on core description, core photos, and well log data, four calcite-cemented zones were detected.

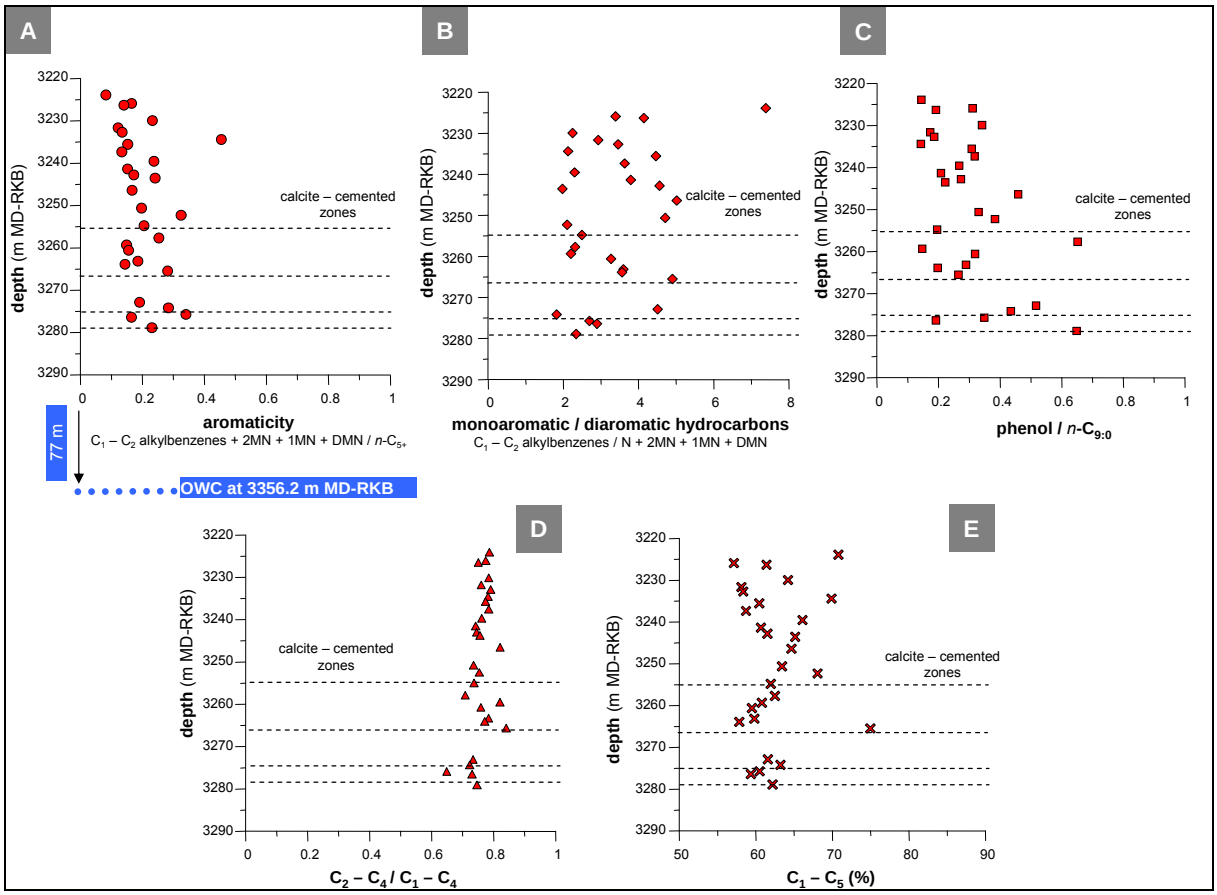

Figure 47 Geochemical profiles of the pyrolysis products from the reservoir rock screening of well B. From A to E the aromaticity (A), monoaromatic/diaromatic hydrocarbon ratio (B), relative phenol amount (C), gas wetness (D) and gas amount (E) are shown. The dashed lines mark the calcite-cemented zones detected.

Reservoir rocks of well B show no indications of disseminated coal (Figure 47 C). The aromaticity (Figure 47 A) ranges from 0.08 to 0.45 and show an average of 0.20 (± 0.08). With increasing depth, more reservoir rock samples are enriched in aromatic compounds.

The grey shaded areas in Figure 48 show an attempt to divide the broad trend into individual cluster, with potentially similar petrophysical properties (Figure 48, left). Additionally, there are possible relations to the calcite-cemented zones, which may act as flow barriers. Within the single Tilje Fm. subunits 3.4, 3.3, and partly 3.2, above the calcite-cemented zone at 3255 m MD-RKB, the aromaticity generally increases. Below this zone, some reservoir rocks of the Tilje Fm. 3.2 are of lower aromaticity. However, reservoir rocks from the Tilje Fm. 3.2., 3.1, and 2.5 below the calcite-cemented zone, show a broader and more heterogeneous distribution (Figure 48, right).

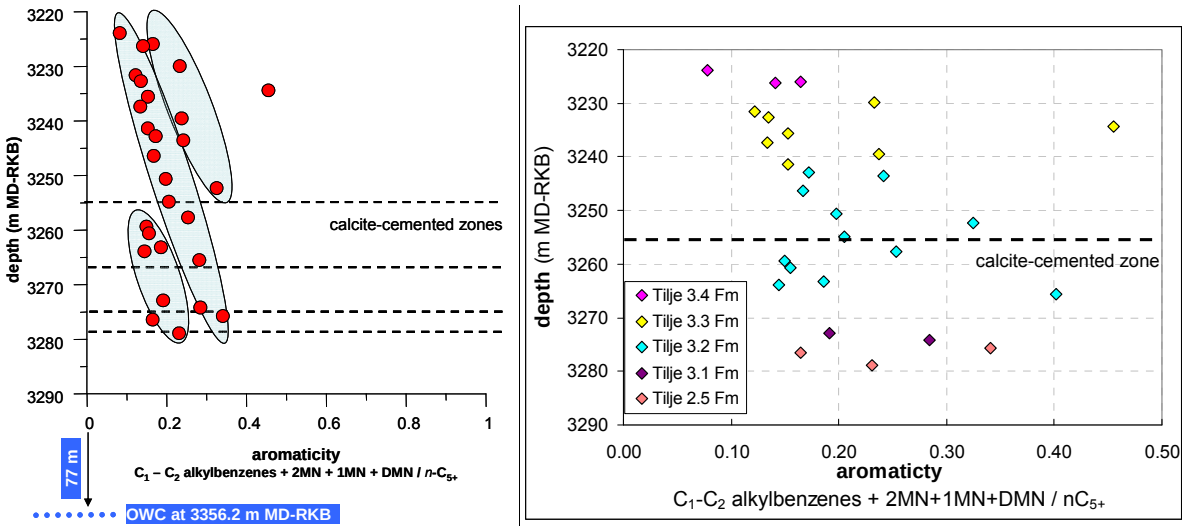

Figure 48 ***Left:*** **Geochemical depth profile for the aromaticity in well B and the calcite-cemented zones detected (dotted lines). The grey shaded areas show a first interpretation of the aromaticity trend.** ***Right:*** **The aromaticity of the single Tilje Fm. subunits is shown.**

Aromatic hydrocarbons show significant changes in the 1-ring and 2-ring aromatic compound ratio (3.39 ± 1.25) (Figure 47 B). The gas wetness (Figure 47 D) reveals a slight decrease with increasing depth. Samples from the upper and lower part (Tilje Fm. 3.4, 3.3, 3.1 and 2.5) present less differences and show relatively homogeneous gas wetness. In the middle part (Tilje Fm. 3.2), located closely beneath the calcite-cemented zone at 3255 m MD-RKB, reservoir rocks with lower methane contents were observed. Comparing gas wetness and aromaticity a correlation was found, similar to the trend observed in well C (Figure 32). Although it is less significant than in well C, the gas wetness decreases with increasing aromaticity. Both parameters are inverse correlated (Figure 49).

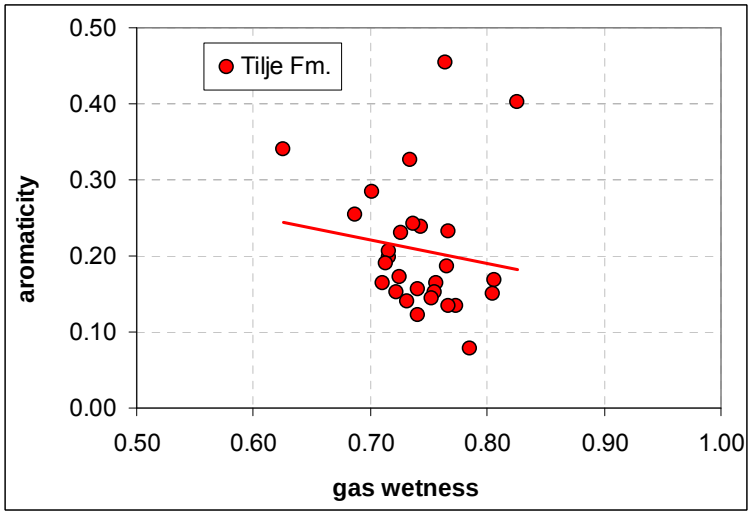

Figure 49 Inverse correlation of the aromaticity and gas wetness for all reservoir rocks of well B. The line mark the trend observed in the Tilje Formation.

The gas amount varies between 57 % and 78 % and shows different gradients. Again, the distribution seems to be related to the calcite-cemented zone at 3255 m MD-RKB. Parallel to the aromaticity, the gas percentage decreases below this zone (Tilje Fm. 3.2). Above the zone, the gas percentage reveals a broad distribution. (Figure 47 E).

The GOR in the Tilje Fm. subunits of well B is slightly higher, compared to the Garn- and Ile Fm. sandstones of well C. With increasing depth down to the calcite-cemented zone at 3255 m MD-RKB, the GOR slightly increases in a similar trend as observed for the aromaticity. Below the calcite-cemented zone, the GOR slightly decreases (Figure 50).

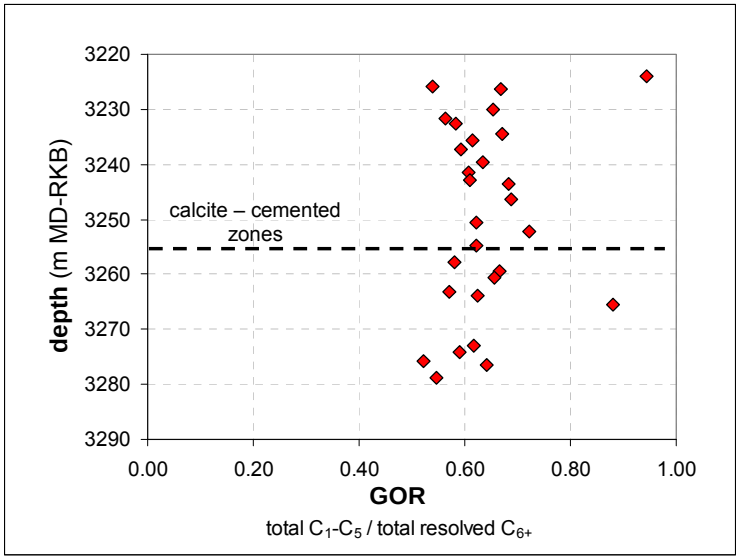

Figure 50 GOR values for the reservoir rocks of well B. The dashed line marks the calcite-cemented zone at 3255 m MD-RKB.

Well B shows another aromaticity trend compared to well C, but again the aromaticity and the gas wetness of the macromolecular fraction show an inverse correlation as found earlier in well C. Thus, at first differences in the organofacies and maturity will be investigated. Subsequently, the trends and their relation to the calcite-cemented zones detected in profile B will be investigated. Therefore, the physical rock properties shown in the well log, will be integrated in greater detail.

6.2.2.2.1 ORGANOFACIES AND / OR MATURITY DIFFERENCES

Within the carbon chain length distribution, the reservoir rocks of well B plot in the P-N-A and the paraffinic low wax oil field indicating low wax oil generated by a kerogen from a

marine depositional environment. Slight differences in the short and medium chain length distribution were observed, but most samples show a similar CLD as the potential source rock from the Spekk Formation. The uppermost rock sample of profile B (G004165) presents a higher content of short chain alkanes and plot more close to the Melke Formation. Compared to the Garn and Ile Formation samples (without disseminated coal) the Tilje shows a similar CLD. The differences observed reflect the variabilities seen in the depth plots (Figure 51). The phenol content is low for all samples analysed. The uppermost rock sample of profile B reflects lowest aromaticity.

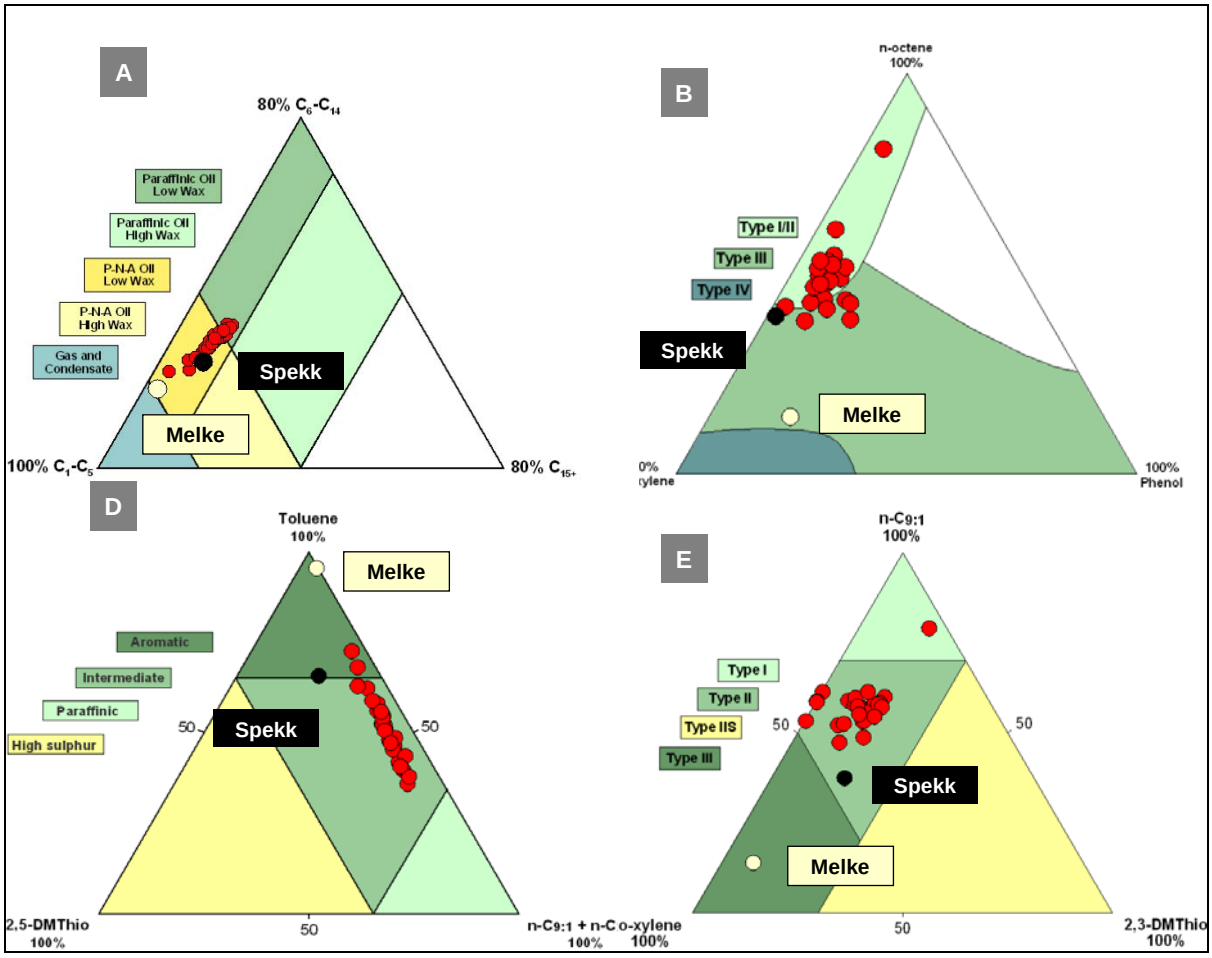

Figure 51 Bulk properties of the reservoir rock pyrolysates of well B and source rock pyrolysis products concerning (A) alkyl chain length distribution, (B) phenol content, and (C - D) sulphur content.

The organic sulphur content is low for all analysed reservoir rocks. Most reservoir rocks pyrolysates indicate a marine source of a classic Type II kerogen. Within Figure 51 C, large differences in the aromaticity can be seen reflecting the gradient observed in the geochemical depth profiles. In Figure 51 D, the uppermost sample with the lowest aromaticity represents a higher content of *n*-octene in the pyrolysates.

No indications for differences related to source material and thermal maturation were observed. An exception is the uppermost reservoir rock that show differences in aromaticity, which are visualised in the ternaries.

6.2.2.2.2 CORRELATION TO PHYSICAL ROCK PROPERTIES (WELL LOG DATA)

The Tilje Formation sandstones are characterised by highly variable depositional patterns, which results in very complex and extremely heterogeneous reservoir subzones (Hemmens *et al.*, 1994) (cf. Chapter 3.1). All reservoir zones in the whole profile are characterised by distinct changes in porosity, permeability and water saturation at centimetre to meter scale. At first glance, the heterogeneities observed in the pyrolysates reflect the variabilities observed in the log.
The calcite-cemented zones detected in profile B (low poroperm properties, Figure 10) might act as a flow barrier resulting in different trends observed in the reservoir rock pyrolysates. These zones might additionally represent marker of Paleo-OWC and thus, potentially zones with higher microbial activity. Thus, biodegradation has to be taken into account as a possible reason for the heterogeneities observed in the pyrolysates, similar as observed before in the macromolecular fraction of the heavy oil from the WCSB and the Heidrun oils with different API gravity.

In Figure 52 the aromaticity is shown on the left side in relation to the porosity log (middle) and the porosity for all reservoir rocks of the whole profile versus depth (right). The samples analysed by screening as part of this thesis are marked with red dots. The porosity changes between 15 and 35 % indicating good to excellent reservoir quality. Interstratified in the profile are zones with low porosity (< 10 %). Predominantly, the calcite-cemented zones are characterised by low porosity. The Tilje Fm. 3.1 and Tilje Fm. 2.5 at the bottom of the profile present lower porosity compared to the upper part (Tilje Fm. 3.4 - 3.2). However, using this data, no direct correlation of aromaticity and porosity was found.

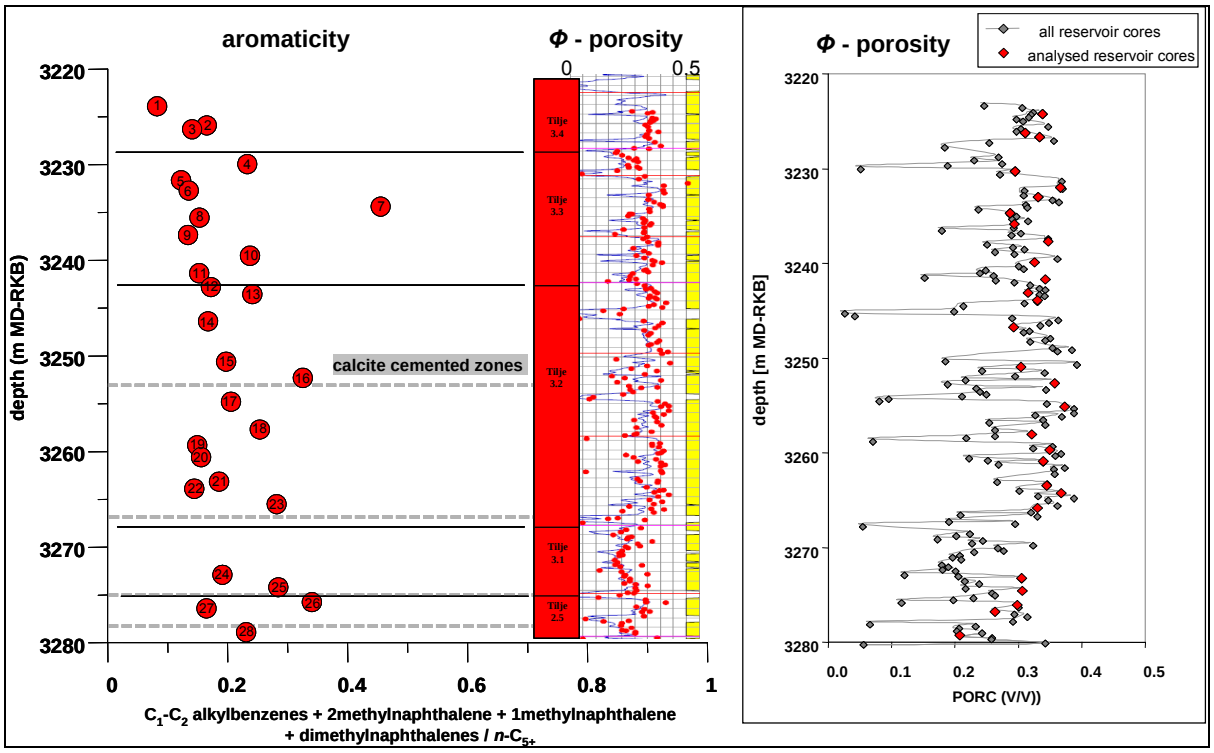

Figure 52 Geochemical depth profile showing aromaticity of well B (left) in relation to the porosity log (middle) and the depth plot of the porosity for all reservoir rocks in the whole profile (right). Statoil provides the porosity log and the single porosity data.

Figure 53 shows the aromaticity (left) in relation to the permeability log (middle) and the permeability for all reservoir rocks in the whole profile versus depth (right). The samples analysed by screening are marked with red dots. Strong variations were observed in the permeability varying between 0 md and 43000 md. Common permeability values for hydrocarbon reservoirs range between 5 md and 2000 md (Bjørlykke, 1989). Several thin zones with very low permeability were observed especially in the Tilje Fm. 3.1 and Tilje Fm. 2.5. Three highly permeable zones have been detected; one in the upper part of the profile (Tilje Fm 3.4), and two in the middle part (Tilje Fm. 3.2). These high permeable zones are marked with yellow circles in Figure 53. From this Figure, it can be seen that high permeable zones and aromaticity shows no direct correlation.

At least the aromaticity is compared to the water saturation of well B. Figure 54 show the aromaticity (left) in relation to the water saturation log (S_w) of profile B. The S_w log shows similar fluctuations as observed for the porosity and permeability log. Within the Tilje Fm. 3.2 minor water saturation are present compared to upper and lower reservoir zones. Here, reservoir rocks showing the highest organic matter content of profile B were found. The lowest two reservoir zones (Tilje Fm. 3.1 and 2.5), reveal the highest water saturation. Both

reservoir zones are characterised by low OM content. However, no direct correlation of the variably aromaticity was found to the water saturation based on visual comparison alone. Therefore, exact water saturation values are needed.

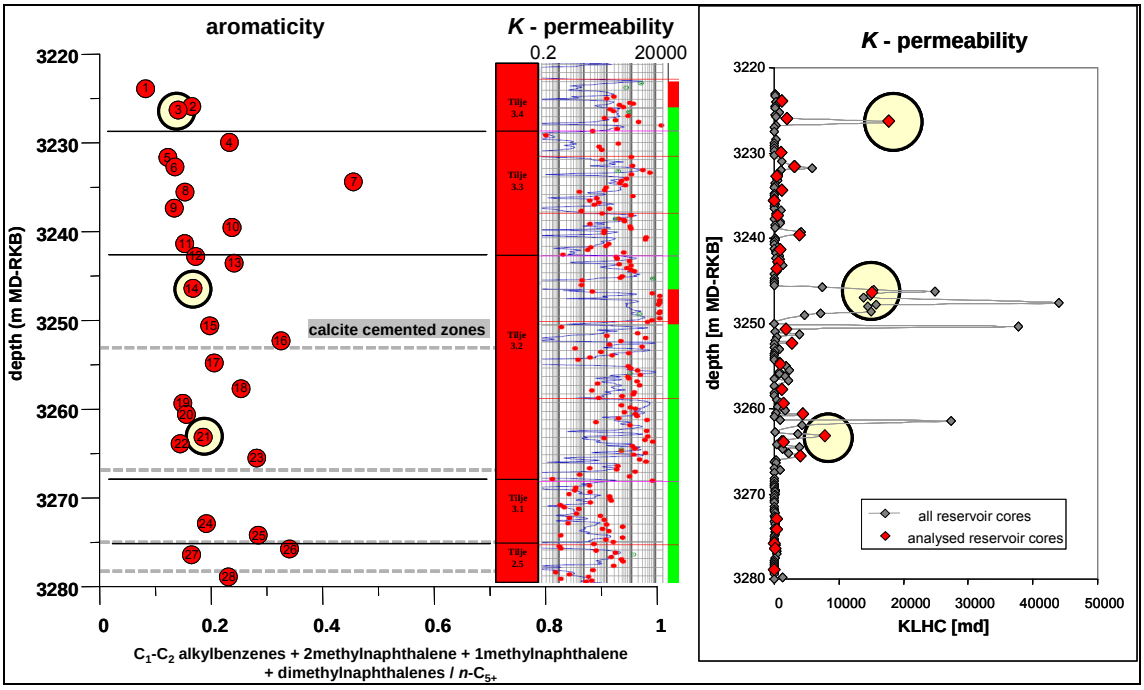

Figure 53 Geochemical depth profile of the aromaticity of well B (left) in relation to the permeability log (middle) and the depth plot of the permeability for all reservoir rocks in the whole profile (right). Statoil provides the permeability log and the single permeability data.

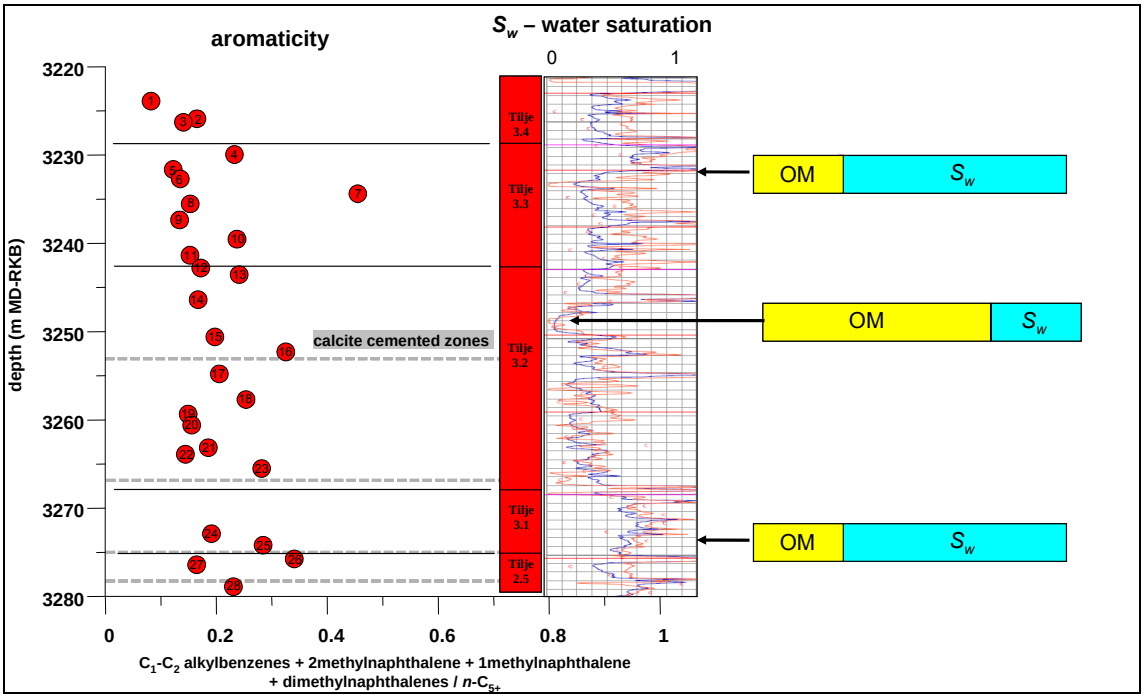

Figure 54 Geochemical depth profile of the aromaticity of well B (left) in relation to the water saturation log (right). Statoil provides the water saturation log.

In order to test whether mineral matrix effects might have caused the heterogeneities in the aromaticity of well B, the aromaticity and the whole reservoir rock pyrolysis yields C_1+ of the resolved compounds were correlated.

Figure 55 shows the C_{1+} resolved compounds versus the aromaticity (left) as well as both parameters versus increasing depth (right). A nearly constant aromaticity with increasing pyrolysis yield C_{1+} of the resolved compounds can be seen. No correlation of aromaticity and pyrolysis yields were found. Thus, a mineral matrix effect can be excluded. The uppermost sample with the lowest aromaticity presents a total pyrolysis yield that is nearly zero. This correlates to the very low organic matter content analysed for this reservoir rock.

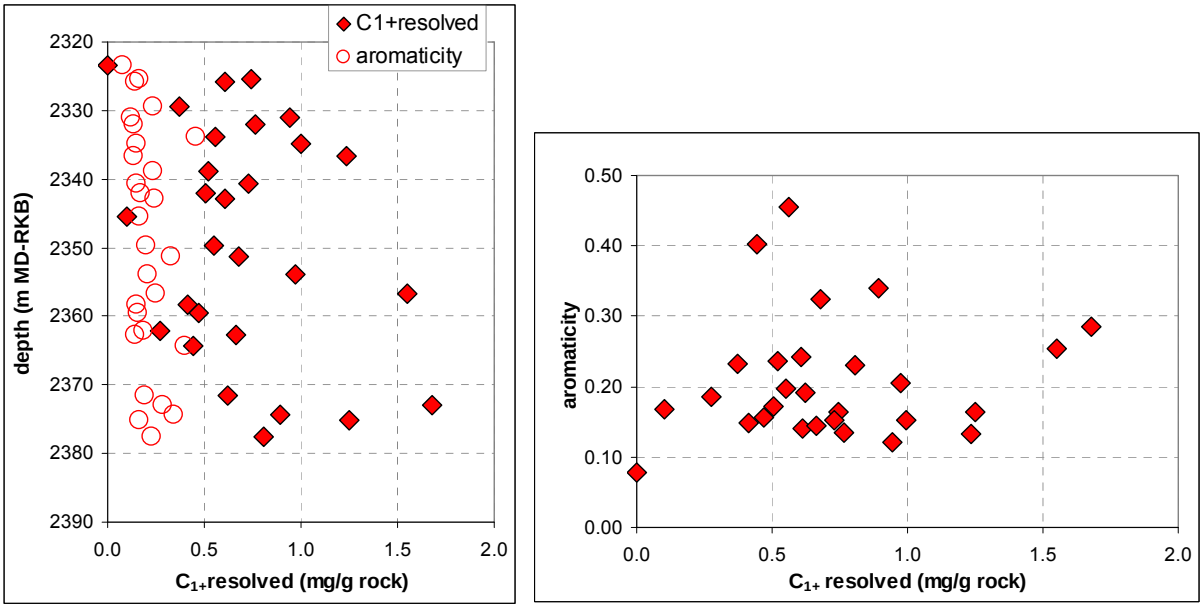

Figure 55 Depth plot of the aromaticity of well B and the C_{1+} of resolved compounds (left) and the aromaticity versus C_{1+} of the resolved compounds (right).

In summary, gradients were observed in the aromaticity of well B, which are different compared to those found in well C. Here again, the aromaticity and the gas wetness correlate inversely. Source and maturity related differences can be excluded for the aromaticity trend observed in well B.

The aromaticity of the macromolecular fraction might be related to biodegradation, as seen before in the heavy oil series and the Heidrun oils with different API gravity. In addition, flow barriers (calcite-cemented zones) might be related to the differences observed in the pyrolysates. However, between the poroperm properties, which indicate different environmental conditions for microbes, and aromaticity no direct correlation was found.

Based on visual correlation alone an inverse relation was found between the organic matter content and the water saturation.
For the interpretation of the heterogeneities observed in aromaticity, an alteration through biodegradation has to taken into account. Therefore, correlations to biomarker parameter and biodegradation ratios are necessary.

6.2.3 WELL A IN SEGMENT J (ÅRE FM. 4.4 - 3.1)

6.2.3.1 PRODUCTION INDEX AND ORGANIC RICHNESS

In well A, reservoir rock samples taken from the Åre Formation were analysed. The Åre Formation is the lowermost reservoir among the reservoir formations of the Heidrun oil field and is characterised by many coal and shale intervals. Reservoir rocks from well A show an average PI of 0.60 (± 0.16) (Figure 25, Table X 1). Similar to observations in well C, a zone (three samples) with low oil quality (PI < 0.18) was found in the lower part of well A (below the OWC). Two other samples in the upper part of well A show low PI of 0.43 and 0.49. The low PI refers to *in-situ* organic matter in these reservoir rocks.

Profile A shows a relative high OM content about 27.33 mg/g rock (± 17.03) (Table X 1) and is characterised by a very heterogeneous distribution as well as significant changes from very lean to very organic rich zones at a small scale (Figure 26). The upper part of profile A shows higher OM content and larger differences regarding the OM distribution compared to the lower part. The reservoir rocks in the upper part have an mean OM content of 35.7 mg/g rock (± 15.4), while the 11 lowermost reservoir rocks contain minor amounts of OM of about 12 mg/g rock (± 4.6).

6.2.3.2 ORGANIC MATTER COMPOSITION

In Figure 56 A - E the pyrolysis products of well A are outlined by geochemical profiles for the aromaticity (A), monoaromatic / diaromatic hydrocarbon ratio (B), relative phenol content (C), gas wetness (D) and gas amount (E). Table X 2 listed the average values and standard deviations for the bulk pyrolysis parameters. The Py-GC parameter values for each single reservoir rock of well A can be seen in Table X 7.

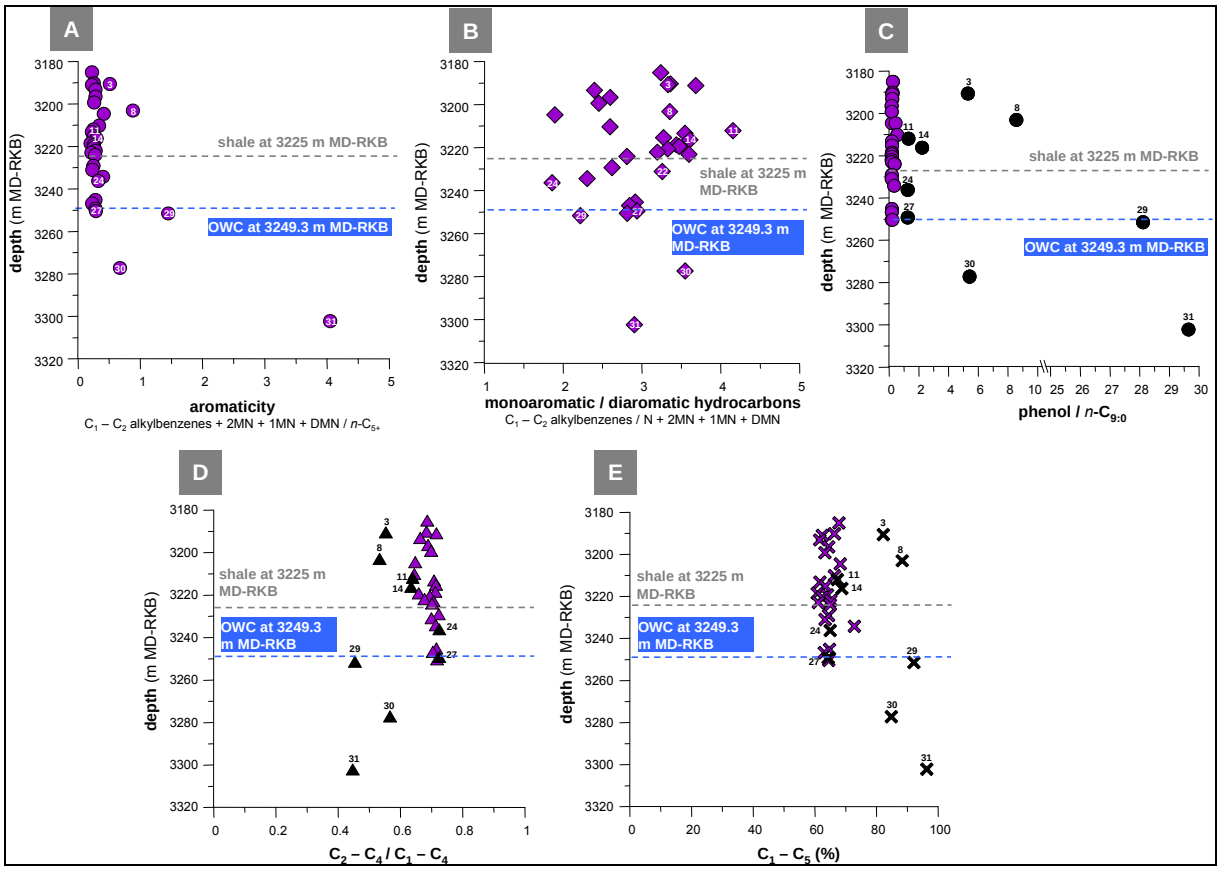

Figure 56 Geochemical profiles of the pyrolysis products from the reservoir rock screening of well A. From A to E the aromaticity (A), monoaromatic/diaromatic hydrocarbon ratio (B), relative phenol amount (C), gas wetness (D) and gas amount (E) are shown. The grey dashed line mark a prominent shale.

The aromaticity reveals a broad distribution and highest values are found below the OWC (Figure 56 A). Five reservoir rock samples have an aromaticity of ≥ 0.50.

Comparing the aromaticity to the phenol depth profile (Figure 56 A and C), the five high aromatic reservoir rocks present the highest phenol ratios ranging from 5.21 to 29.6. The three reservoir rock samples below the OWC are additionally characterised by very low organic matter content.

Four reservoir rock samples show slightly lower phenol ratios in a range of 1.21 to 2.12 and no visible indication for disseminated coal. These samples have a lower aromaticity compared to the phenol rich sample mentioned above. Altogether, nine reservoir rock samples with a phenol ratio > 1 were detected. They exhibit a greater extent of terrestrial OM input and indicate disseminated coaly particles in the analysed reservoir rocks. In Figure 56 C, these samples are marked with black dots and numbers. The remaining reservoir rocks show phenol ratios < 1.

Ignoring the nine coaly samples, the aromaticity shows a distinct lower variability (Figure 57, left). In contrast to the trend observed in well B and well C, the reservoir rocks of well A don't reveal any gradient in aromaticity down to the OWC. Additionally, they are not influenced by the shale observed at 3225 m MD-RKB, which was detected using well log signals. Most of the reservoir rock pyrolysates show aromaticity between 0.18 and 0.26 indicating minor differences with increasing depth. Independent from the shale at 3225 m MD RKB, three samples present higher aromaticity but low phenol ratio. (reservoir rock no. 9 = G004137, reservoir rock no. 10 = G004138, and reservoir rock no. 23 = G004153).

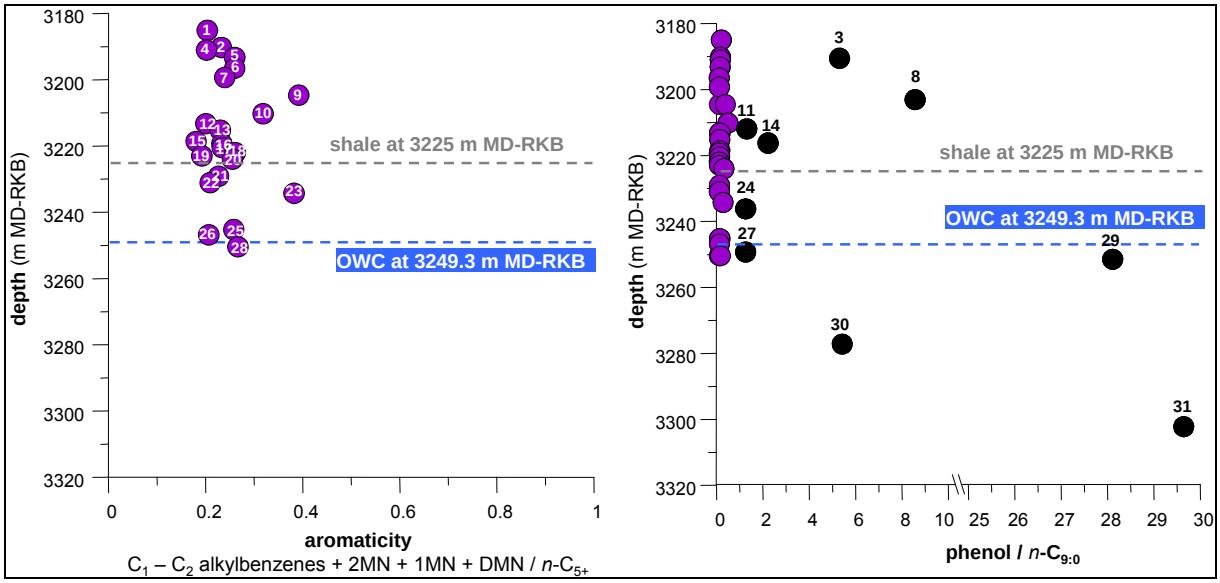

Figure 57 *Left* Geochemical profile for the aromaticity of well A without reservoir rocks containing disseminated coal. *Right* Phenol depth plot indicate the reservoir rocks with disseminated coals. The grey dashed line mark a prominent shale at 3225 m MD-RKB.

Regarding the type of aromatic hydrocarbon ratio, a broad distribution can be seen (Figure 56 B) indicating significant changes within the OM composition. Similar to the Garn Fm. in well C, the ratio is inversely correlated to the aromaticity (not shown). Thus, an increase in aromaticity correlates to the decrease in 1-ring aromatic hydrocarbons relative to the 2-ring aromatic hydrocarbons.

The gas wetness (Figure 56 D) of the pyrolysates ranges between 0.44 and 0.72. The lowest gas wetness was observed in reservoir rocks with disseminated coal. Excluding these samples, the gas wetness show fewer differences with values between 0.64 and 0.74. The lower part of the profile, below the shale a 3225 m MD-RKB, show slightly higher gas wetness.

Comparing gas wetness and aromaticity, the five rock samples with very high aromaticity (high phenol ratio) show an inverse correlation to the gas wetness (Figure 58, left). Excluding these samples, the trend is less significant (Figure 58, right).

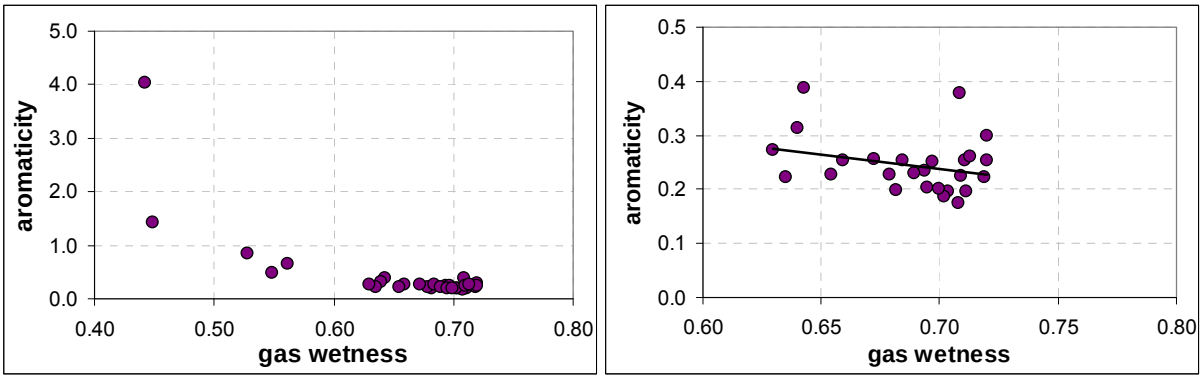

Figure 58 *Left* Correlation of the aromaticity and the gas wetness including all reservoir rocks analysed in well A. *Right* Correlation of the aromaticity and the gas wetness without phenol rich reservoir rocks. The black line indicates the trend observed in well A.

Disregarding the phenol rich samples, the gas amount of the reservoir rock pyrolysates show less differences with increasing depth (Figure 56 E). The reservoir rocks with highest phenol ratio (no. 3, 8, 29, 30, and 31 = G004127, G004136, G004163, G004163, and G004164) showing highest gas amounts between 82 % and 96 %. The reservoir rocks with phenol ratio between 1 and 2.2 (no. 11, 14, 24, and 27 = G004139, G004142, G004154, and G004157) show gas amount between 64 % and 68 %.

Similar to the aromaticity in the upper part of profile A, the GOR show less variability in the Åre Fm. 4.4 - 4.1. Differences are observed in the lower Åre Fm. subzone 3.2 and parts of the subzone 4.1 below the shale and near the OWC. These subunits show higher GOR compared to the Åre Fm. 4.1 - 4.4 in the upper part of profile A (Figure 59, left). Reservoir rocks with phenol ratio > 1 are excluded.

The UCM mirrors the GOR and is lowest near the OWC in reservoir rocks of the lower Åre Fm. 4.1 - 3.2 below the shale. Reservoir rocks of the Åre Fm. 4.1 show a gradient in UCM down to the OWC. (Figure 59, right).

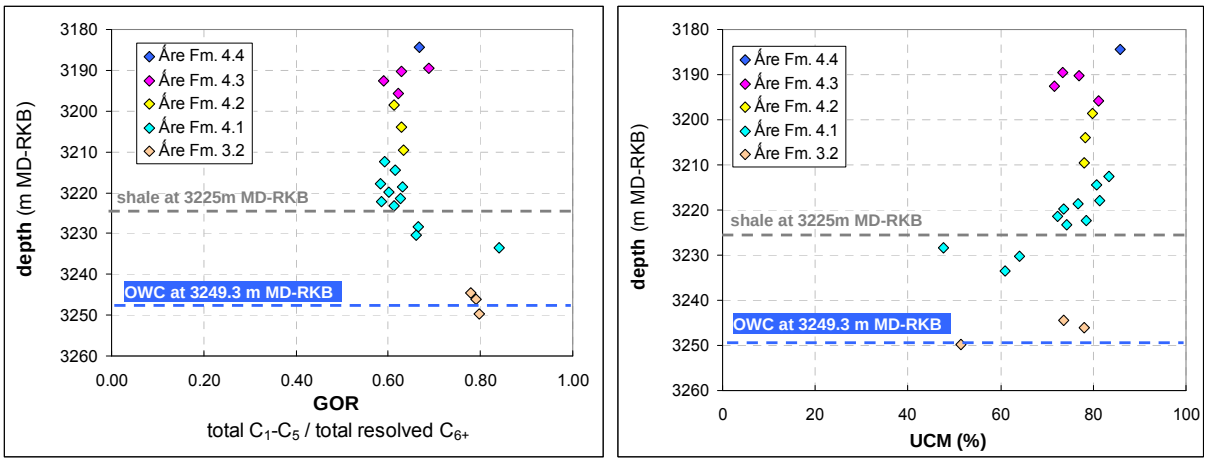

Figure 59 ***Left*** **GOR for the individual Åre Fm. subunits of well A.** ***Right*** **UCM for the individual Åre Fm. subunits of well A. Reservoir rocks with phenol ratio > 1 are excluded in both plots. The grey dashed line mark a prominent shale.**

In summary, nine reservoir rock samples with phenol ratio above one were detected using the phenol content in the pyrolysates. The samples with the highest phenol ratio are characterised by the highest aromaticity, lowest gas wetness and highest gas amount. Significant variabilities in the OM composition of the macromolecular fraction are indicated by the ratio of the 1-ring versus 2-ring aromatic hydrocarbons. The aromaticity is characterised by less variability. Unlike wells B and C, the aromaticity and gas wetness in well A does not show a clear inverse correlation. The GOR and UCM are similar to the aromaticity in the upper Åre Fm. 4.4 - 4.1. In the lower part of the profile below the prominent shale (Åre Fm. 3.2 and parts of subzone 4.1), both parameters show a relation to the increasing water saturation near the OWC (higher GOR and lower UCM).

6.2.3.2.1 ORGANOFACIES AND/OR MATURITY DIFFERENCES

Bulk properties of the reservoir- and source rock pyrolysis products of well A concerning the (A) alkyl chain length distribution, (B) phenol content, and (C - D) the sulphur content are shown in Figure 60 A - E.

Within the carbon chain length distributions most of the reservoir rocks plot in the P-N-A low wax oil field indicating oil generated by a kerogen from a marine depositional environment. Slight differences in the short and medium chain length distribution occur (Figure 60 A); however, most samples show a CLD similar to the potential source rock from the Spekk Formation. Five reservoir rocks reveal higher proportion of short chains in their pyrolysates.

They plot in the gas and condensate field. These pyrolysis products from the Åre Formation consist to 85 - 95% of short chains, characterising the gas-prone nature of coals and reflect the variabilities seen before in the depth plots (Figure 56 C and E).

The phenol ternary support the distribution observed in the depth plot. Most reservoir rocks are low in phenol and show less difference in aromaticity. Nine reservoir rock samples can be identified, which subjected to their phenol content, plot in close distance to the phenol angle. Five reservoir rocks with the highest phenol content show the highest aromaticity.

Both sulphur ternaries indicating very low sulphur content in the pyrolysates (Figure 60 C and D). They reflect the differences in aromaticity caused by the phenol rich reservoir rocks (disseminated coal) seen in the geochemical depth plots before. Excluding the high phenol samples, most reservoir rocks plot in the intermediate field indicating a marine source of a classic Type II kerogen.

No indications for maturity differences or changes in the organofacies of the generating source were found.

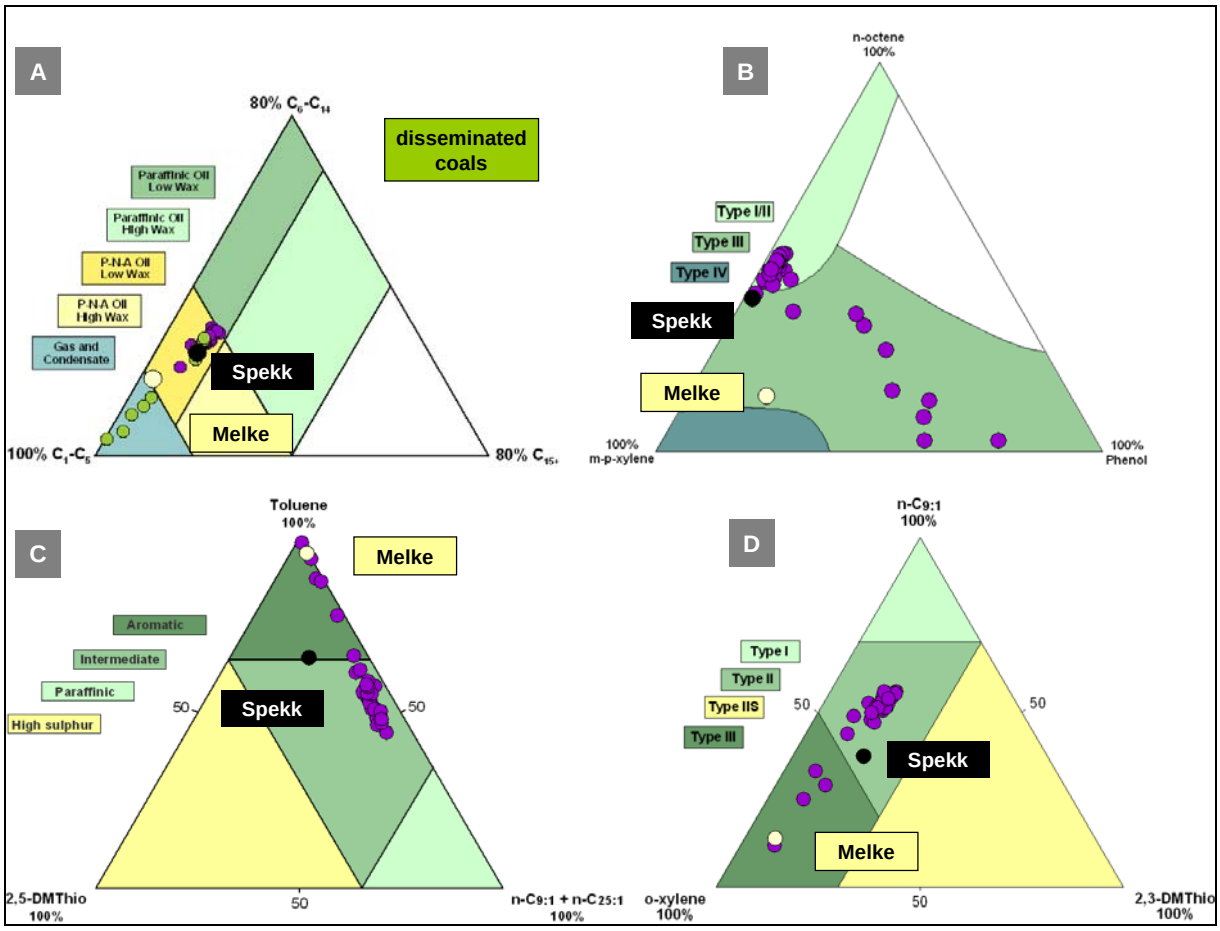

Figure 60 Bulk properties for the reservoir rock- and source rock pyrolysis products of well A, concerning (A) alkyl chain length distribution, (B) phenol content, and (C - D) sulphur content.

6.2.3.2.2 CORRELATION TO PHYSICAL ROCK PROPERTIES (WELL LOG DATA)

In general, the Åre sediments are characterised by a very heterogeneous depositional environment (cf. Chapter 3.1) that is reflected by the well log in Figure 11. The Åre Fm. 3 and 4 contain fluvial channel features with good reservoir conditions. Several of their subzones are locally capped by peat swamp coal (marked in the log).

The micaceous siltstones of the Åre Fm. 3 show greater variability concerning the poroperm properties compared to the medium- to coarse-grained cross-stratified sandstones in the overlying Åre Fm. 4, which shows better reservoir properties (higher porosity, higher permeability, lower water saturation). Both reservoirs are separated by shale at 3225 m MD-RKB, which might act as barrier.

The variabilities in the physical rock properties above and below the shale are reflected in the organic matter content. Distinctly higher organic matter content (35.7 mg/g rock ± 15.4) show reservoir rocks from the Åre Fm. 4 above the shale, compared to reservoir rocks from the Åre Fm. 3, below the shale, which have lower organic matter content (12.0 mg/g rock ± 4.6).

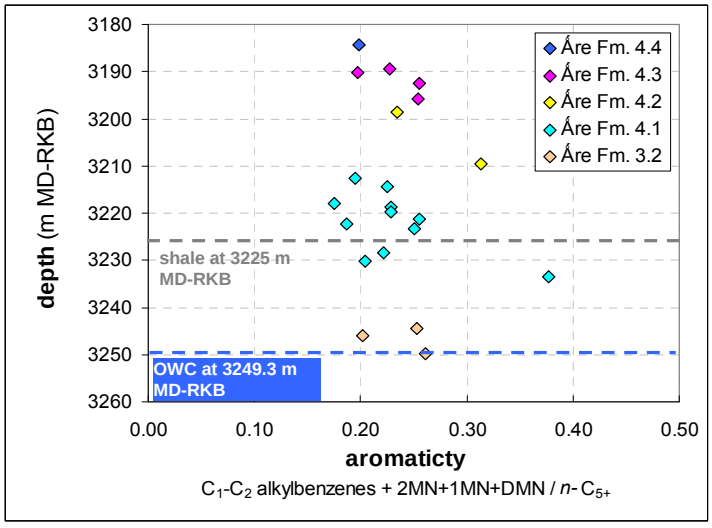

Figure 61 Aromaticity for the reservoir rocks of the individual Åre reservoir subzones of well A. Reservoir rock samples with coal are excluded in the plot. The grey dashed line mark a prominent shale.

Reservoir rocks of the Åre Fm. 3 and parts of the Åre Fm. 4.1 below the shale, show slightly higher gas wetness (Figure 56 D), a distinctly higher GOR (Figure 59, left), and a lower UCM (Figure 59, right) compared to the samples above the shale. These pyrolysis parameters are obviously related to the different porosity and permeability conditions, and in particular to the

higher water saturation. However, comparing the physical rock properties and the aromaticity no distinct correlation was found based on visually correlation alone (Figure 61).

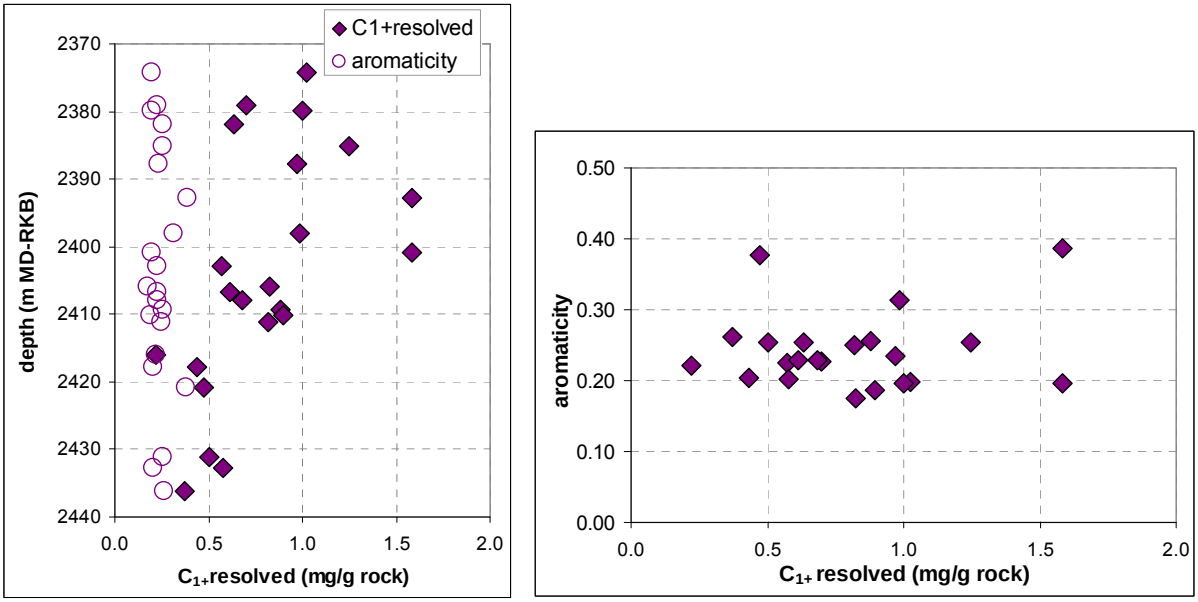

Figure 62 *Left* Depth plot showing the reservoir rock aromaticity of well A and the C_{1+} of the resolved compounds. *Right* Aromaticity versus C_{1+} of the resolved compounds.

Correlating the aromaticity and the total pyrolysis yields (C_{1+}) for all analysed reservoir rocks in well A, a constant aromaticity with increasing pyrolysis yield can be seen and a mineral matrix effect can be excluded (Figure 62 left and right).

In summary, nine reservoir rocks with disseminated coals were detected in profile A. Significant changes are revealed by the type of aromatic hydrocarbon ratio indicating changes within the OM composition of the macromolecular fraction. In contrast to well B and well C, the reservoir rocks of well A does not show significant gradient in aromaticity down to the OWC. Additionally, aromaticity and gas wetness show only a slight correlation trend. The GOR and the UCM are related to increasing water saturation near the OWC. No indications for source and maturity differences were observed.

A direct correlation was found between the OM distribution and the poroperm properties in the Åre Fm. 3 and 4. Both reservoirs are separated by a prominent shale, which might act as barrier. Variability within the physical rock properties are additionally reflected in the GOR and the UCM. However, based on visually correlation alone no relation of the aromaticity to the physical rock properties was found.

6.3 CHARACTERISATION OF THE SINGLE PROFILES IN THE NORTHERN PART OF THE HEIDRUN OIL FIELD

6.3.1 WELL E IN SEGMENT M (ÅRE FM. 4.1-3.2)

6.3.1.1 PRODUCTION INDEX AND ORGANIC RICHNES

The Åre Formation was sampled and evaluated in well E. Significant changes in the PI were observed in well E representing an average PI of 0.56 ± 0.21 (Figure 25, Table X 1). While most reservoir rocks show a PI between 0.65 and 0.70, three reservoir rocks in the upper part and two in the lower part are characterised by distinct differences in the oil quality. In the upper part the oil quality (PI) alternate at a small scale. The lowest PI were found in the two reservoir rock samples at the bottom of profile E (0.09 and 0.07), consistent with the observations made before in well C and A. The low oil quality indicates an elevated content of high polar compounds and might refer to *in-situ* organic matter.

The OM content in well E is between 13.6 and 83.6 mg/g rock (Figure 26, Table X 1). The lower part of well E is characterised by reservoir rocks with higher OM content and significant changes in the OM distribution compared to the upper part. Especially two rock samples show high organic matter content about 83.6 mg/g rock and 75.7 mg/g rock, respectively. These are also the samples with the lowest PI. Two reservoir rocks in the upper and the middle part show low OM content.

6.3.1.2 ORGANIC MATTER COMPOSITION

The reservoir rocks analysed in well E reveal compositional differences regarding their pyrolysates. Bulk properties based on pyrolysis products are shown in geochemical profiles in Figure 63 for the aromaticity (A), monoaromatic / diaromatic hydrocarbon ratio (B), relative phenol content (C), gas wetness (D) and gas amount (E). Table X 2 listed the average values and standard deviations for the bulk pyrolysis parameters. The Py-GC parameter values for each single reservoir rock analysed are listed in Table X 8.

The predominant part of the reservoir rocks are a low in phenol (< 0.34) with some notable exceptions (Figure 63 C). Three reservoir rock samples in the upper part (no. 2, 4, and 6 = G004263, G004265, and G004267) and two reservoir rock samples in the lower part (no. 11, 14 = G004276 and G004281) show phenol ratios between 2.63 up to 16.17 indicating a large extent of terrestrial OM input in form of disseminated coal particles.

Concerning the aromaticity, most reservoir rocks are characterised by a ratio between 0.17 and 0.39. Two highly aromatic reservoir rocks with aromaticity of 1.04 and 0.72 (sample no. 2 and 4 = G004263 and G004265, Figure 63 A) in the upper part of well E also show the highest phenol ratio (Figure 63 C). Reservoir rock samples with phenol ratio between 2.63 and 4.01 present minor aromaticity (sample no. 6, 11, and 14 = G004267, G004276 and G004281).

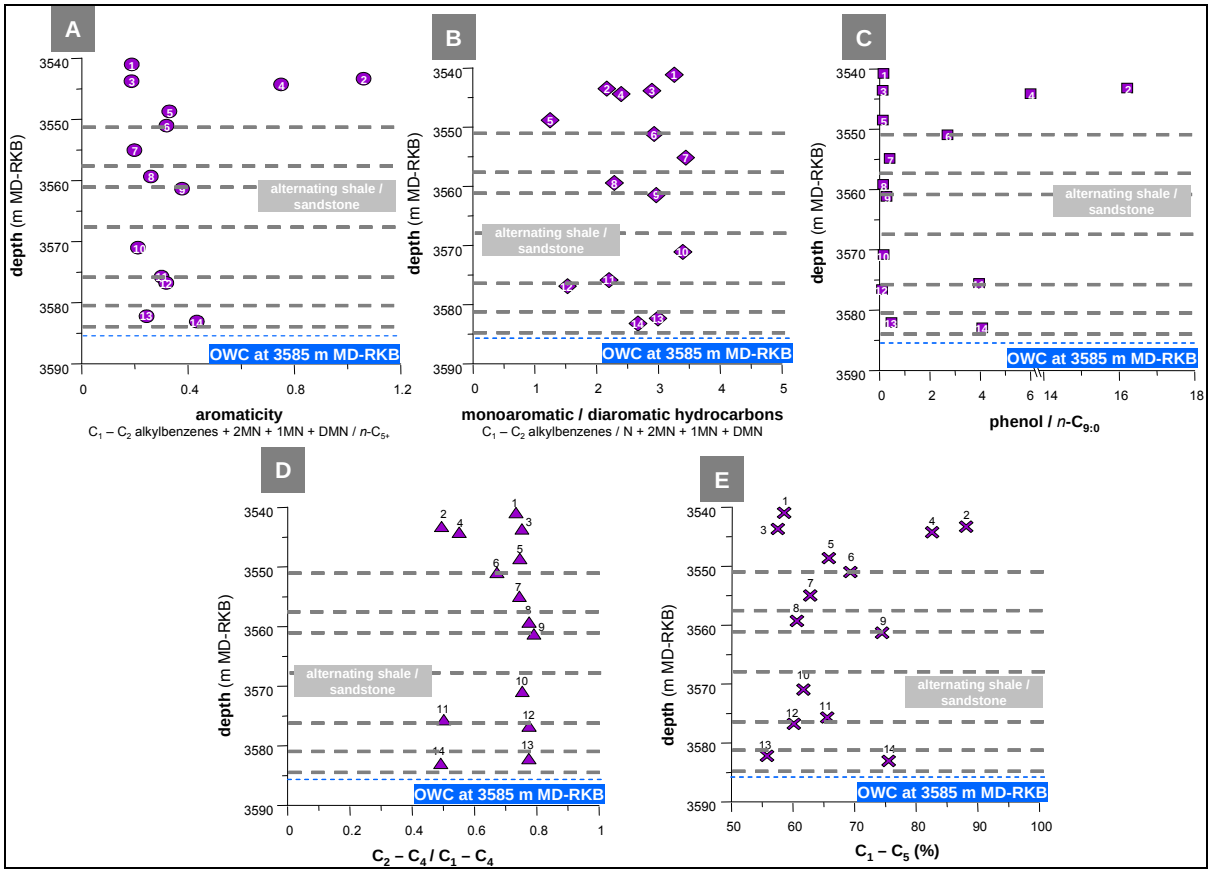

Figure 63 Geochemical profiles of the pyrolysis products from the reservoir rock screening of well E. From A to E the aromaticity (A), monoaromatic/diaromatic hydrocarbon ratio (B), relative phenol amount (C), gas wetness (D) and gas amount (E) are shown. Grey shaded areas indicate zones of alternating shales and sandstones based on the core description and core photos.

Ignoring the five reservoir rock samples (Figure 64, right) three groups with similar gradients in aromaticity can be seen (group 1 = samples no. 1, 3, and 5 (G004260, G004264, G004266),

group 2 = samples no. 7, 8, and 9 (G004268, G004271, G004272), group 3 = samples no. 10, 12, and 13 (G004275, G004279, G004280) (Figure 64, left). Within these groups, the aromaticity increases with increasing depth, sample no. 13 (G004280) close to the OWC excluded. Grey shaded areas indicate zones of alternating shales and sandstones, identified using core description and core photos. A relation of aromaticity trends observed to lithology (shale zones) should be considered.

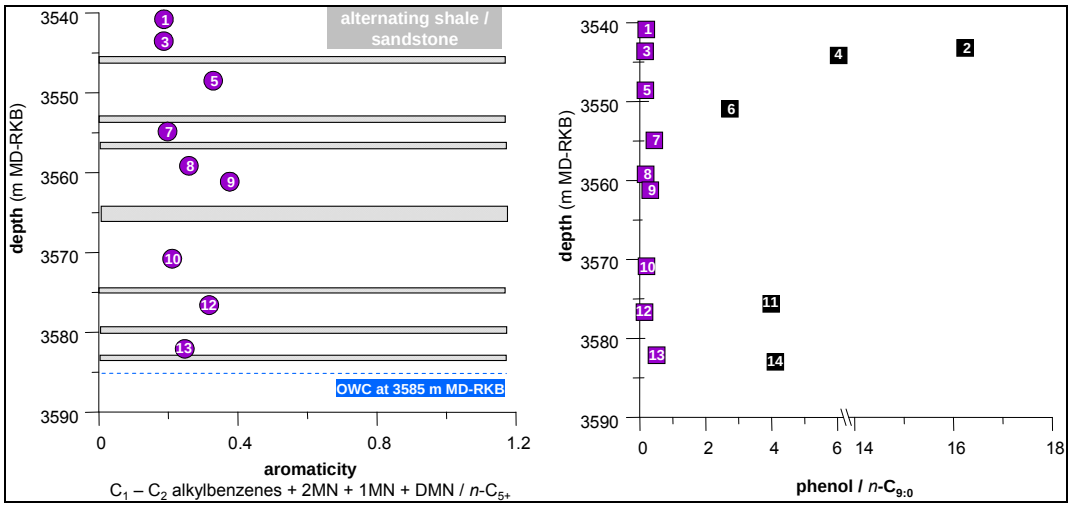

Figure 64 *Left* Geochemical profile for the aromaticity of well E (left). Reservoir rocks with disseminated coal are not considered in the plot. Grey shaded areas indicate zones of alternating shales and sandstones. *Right* Phenol ratio depth plot showing the reservoir rocks with disseminated coals.

The type of aromatic compound ratio is characterised large differences (Figure 63 B). This Py-GC parameter shows a broad distribution between 1.20 and 3.40 and indicates changes within the OM. Comparing the type of aromatic compound ratio to aromaticity an inverse correlation was found, similar as observed in well C (Garn Fm.) and well A (Åre Fm.).

The gas wetness (Figure 63 D) is nearly constant within the profile, disregarding the five phenol rich rock samples, which show higher content of methane in the pyrolysis products. Excluding the phenol rich reservoir rocks three groups can be seen within the remaining samples, similar to those seen in the aromaticity plot (Figure 63 A). Within group 2 (samples no. 7, 8, and 9) and group 3 (samples no. 10, 12, and 13), a very slight increase in gas wetness was observed with increasing depth. A mirrored pattern can be seen for gas percentage (Figure 63 E), considering the variation (66.7 ± 9.8 %).

Comparing aromaticity with gas wetness, the phenol rich samples show an inverse correlation of both parameters (Figure 65, left). The remaining rock samples, especially from group 2 (samples no. 7, 8, and 9) and group 3 (samples no. 10, 12, and 13), show a linear relation of

aromaticity and gas wetness (Figure 65, right). This is contrary to the correlation observed in well C, B and A.

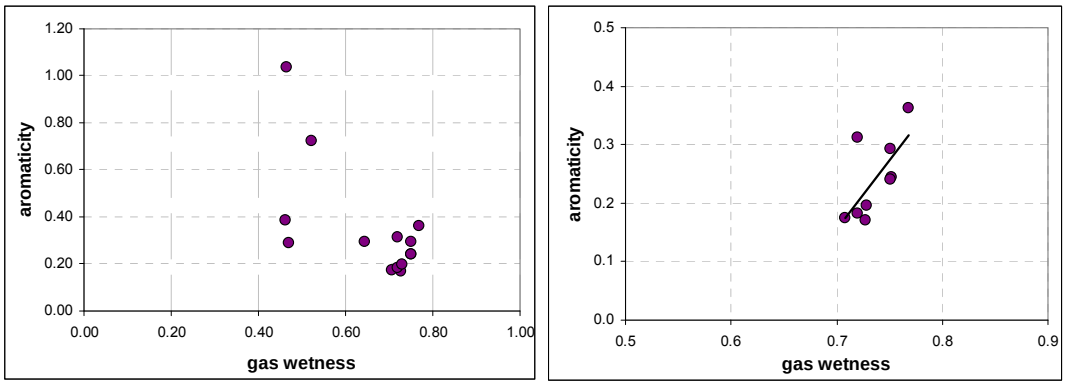

Figure 65 ***Left*** **Correlation of aromaticity and gas wetness including all reservoir rocks analysed in well A.** ***Right*** **Correlation of aromaticity and gas wetness without phenol rich reservoir rocks in well A. The line marks the correlation trend observed.**

The GOR generally increase in the upper part and decrease in the lower part of well E, and seems to be less influenced by the shale zones as well as the Åre formation subzones. Only reservoir rocks of group 3 (samples no. 10, 12 and 13) showing aromaticity trends at the bottom of profile E, are characterised by a significant decrease in GOR. The UCM mirror the GOR trends.

In summary, the analysed reservoir rocks in well E reveal compositional differences in their pyrolysates. Five reservoir rock samples refer to disseminated coal. Three groups with similar aromaticity gradients were observed. The type of aromatic hydrocarbon ratio indicates large differences within the organic matter and shows an inverse correlation to aromaticity. Gas wetness and gas percentage in the reservoir rock pyrolysates are nearly constant within profile E. In contrast to the previous described wells C, B, and A, aromaticity and gas wetness show a linear correlation for samples low in phenol (phenol ratio < 1).
Possibly, there are relations regarding aromaticity trends and variabilities within in the type of aromatic hydrocarbon ratios observed to the lithology (shale zones), which may act as flow barriers.

6.3.1.2.1 ORGANOFACIES AND/OR MATURITY DIFFERENCES

Figure 66 A shows differences in the chain length distribution of the macromolecules within profile E. Most of the reservoir rocks plot in the P-N-A and partly in the paraffinic low wax

oil field, indicating slight differences in the short and medium chain length distribution. They show a CLD relatively similar to the Spekk Formation. The samples no. 12 (G004279) and no. 13 (G004280) from the lower part of well E contain minor amounts of long chains in their pyrolysates.

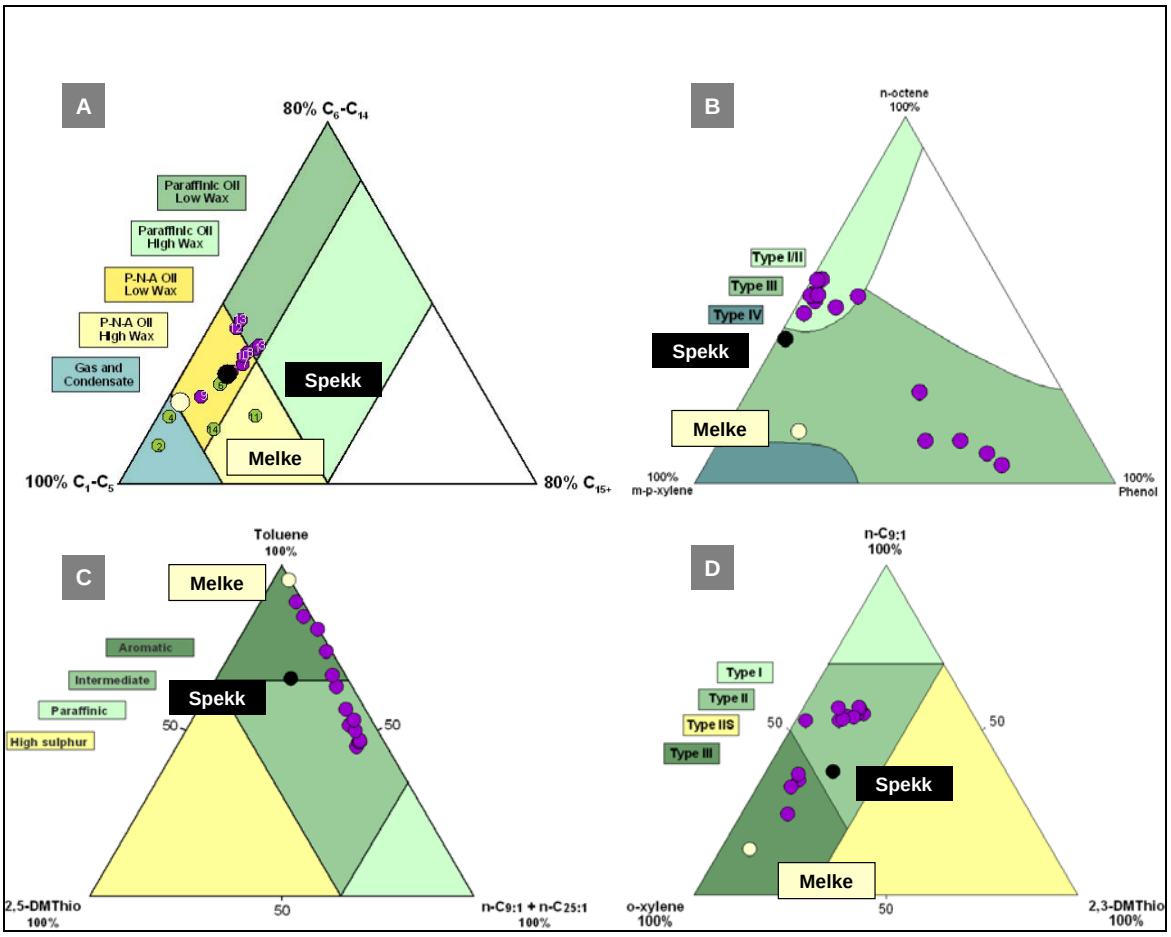

Figure 66 Bulk properties of the reservoir- and source rock pyrolysates of well E concerning (A) alkyl chain length distribution, (B)relative phenol content, and (C - D) relative sulphur content.

The five phenol enriched reservoir rocks show different CLD in their pyrolysates. The high phenol containing samples no. 2 (G004263) and no. 4 (G004265), from the upper part of the profile, show a very high percentage of short chains and plot in the gas and condensate field. Pyrolysates of reservoir rock no. 6 (G004267) plot in the P-N-A low wax oil field close to the Spekk Fm. source rock. Conspicuous are the reservoir rock samples no. 11 (G004281) and no. 14 (G004276). Both plot in the P-N-A high wax oil field. The higher wax content in their pyrolysates refers to a marine source with fluviodeltaic, non-marine influence. Figure 67 shows pyrolysis gas chromatograms of both samples.

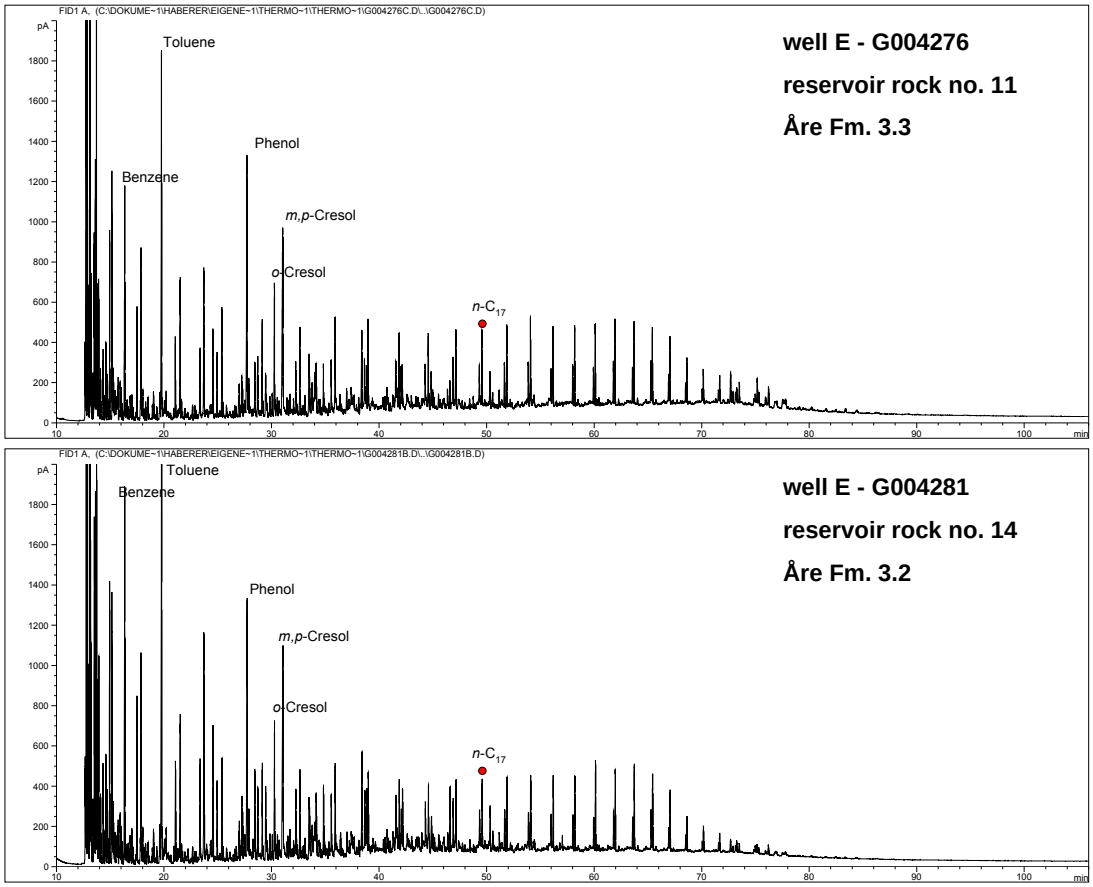

Figure 67 Pyrolysis gas chromatograms of reservoir rock samples no. 11 (G004276) (top) and no. 14 (G004281) (bottom) of well E.

Depending on their phenol content, the five reservoir rocks with disseminated coal plot close to the phenol apex (Figure 66 B). These reservoir rock samples further show the highest aromaticity, represented by the relative *m,p*-xylene content. All remaining reservoir rocks are low in phenol and exhibit less difference in the aromaticity.

All reservoir rock samples are low in sulphur and reflect the differences in aromaticity seen before in the depth plots (Figure 66 C and D). Highest aromaticity is observed in the high phenol containing reservoir rock samples.

6.3.1.2.2 CORRELATION TO PHYSICAL ROCK PROPERTIES (WELL LOG DATA)

The Åre Fm. reservoirs in profile E are mainly channel-sandstones separated by several interstratified compacted zones. The compacted zones, which might act as barriers in the hydrocarbon migration process, consist generally of alternating shales, siltstones, and sandstones, and sometimes coal flags. These sediment sequences are the result of a

fluviodeltaic depositional environment. They are characterised by heterogeneous poroperm properties shown in the log section in Figure 13 (cf. Chapter 3.2.1.4)

Both reservoir rocks of the permeable channel-sandstone zone on the top of the Åre Fm. 4.1 (sample no. 1 and 3 = G004260 and G004264) show lower aromaticity compared to the reservoir rock no. 5 (G004266) from the low poroperm zone at 3547 m - 3549 m MD-RKB, located below the uppermost alternating shale/sandstone zone (Figure 13, Figure 64 left). The channel-sandstones underneath this permeable zone (< 3550 m MD-RKB), show gradients in the rock properties, and parallel gradients in the aromaticity, e.g. in the interval from 3550 m to 3565 m MD - RKB. The porosity and permeability decreases with increasing depth (Figure 13), while the aromaticity of the reservoir rocks increases from 0.18 > 0.24 > 0.36 (group 2 - sample no. 7, 8, and 9 = G004268, G004271, and G004272) (Figure 64 left). Additional poroperm gradients were recognised within other channel-sandstone zones delimited be alternating shales and sand-/siltstones, but no direct correlation of the aromaticity trends to the poroperm signals were found based on visual correlation alone.
However, the core description indicates changes in grain size within in these zones suggesting a correlation of the rock grain size and aromaticity. According to that, the aromaticity in fine-grained sandstones is lower, compared to sandstones with coarse grain size. This refers to a possible relation of the aromaticity and the rock properties porosity and permeability.

In summary, five reservoir rock samples were detected referring to disseminated coal. Three groups with similar gradients in aromaticity were found. Within these groups, the aromaticity increases with increasing depth. Similar as observed in well A, the phenol rich reservoir rock samples show an inverse correlation of aromaticity and gas wetness. Different compared to the previous described wells C, B, and A is the linear correlation of aromaticity and gas wetness for most of the low phenol containing samples. The type of aromatic hydrocarbon ratio indicates changes within the OM and shows an inverse correlation to aromaticity.
No maturity related differences were found. Two reservoir rocks are characterised by higher wax content in their pyrolysates referring to changes in the organofacies of the generative source and indicating a marine source with higher lacustrine influence.
The well log shows zones with gradients in porosity and permeability, which are delimited by alternating shales and sand-/siltstones. However, not all observed gradients in the aromaticity can directly be correlated to the variabilities observed in the rock properties. Based on core

photos and core description changes in the grain size of the oil containing sandstones were recognised, which correlate to the aromaticity. Lower aromaticity was commonly detected in fine-grained sandstones; higher aromaticity in medium- and coarse-grained sandstones. This suggests a potential relation of aromaticity and the rock properties porosity and permeability.

6.3.2 WELL D IN SEGMENT IN SEGMENT Q (ÅRE FM. 2.1)

6.3.2.1 PRODUCTION INDEX AND ORGANIC RICHNESS

Well D is the third well, where the Åre Formation reservoirs have been sampled at high density. The analysed reservoir rocks show the lowest PI (0.48 ± 0.12) of all wells investigated from the Heidrun oil field (Figure 25, Table X 1). The uppermost reservoir rock is characterised by the lowest PI. Within profile D, the PI tends to increase with increasing depth. The changes in the PI refer to *in-situ* organic matter within the reservoir rocks.

The OM content of well D ranges from 1.08 up to 27.85 mg/g rock (Figure 26, Table X 1). The OM distribution in the reservoir rocks is characterised by alteration from high to low OM content at small scale. The uppermost reservoir rock sample is nearly depleted in OM (0.4 mg/g rock).

6.3.2.2 ORGANIC MATTER COMPOSITION

Figure 68 A - E show the pyrolysis products of well D in geochemical profiles for the aromaticity (A), monoaromatic / diaromatic hydrocarbon ratio (B), relative phenol content (C), gas wetness (D) and gas amount (E). Table X 2 summarises the average values and standard deviations for the bulk pyrolysis parameters and Table X 8 the Py-GC parameter values for each reservoir rock analysed from well D.

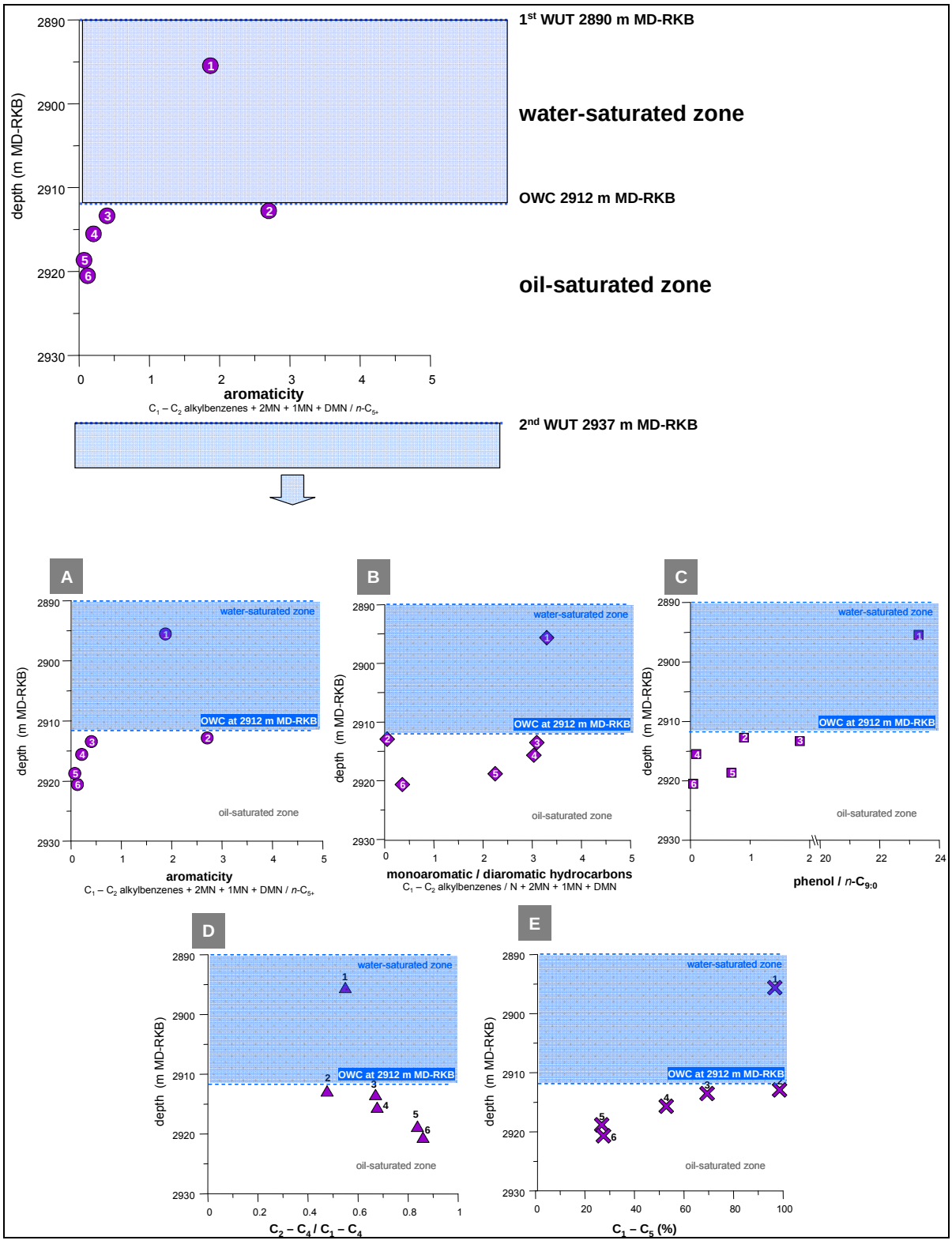

Figure 68 Geochemical profiles of the pyrolysis products from the reservoir rock screening of well D. From A to E the aromaticity (A), monoaromatic/diaromatic hydrocarbon ratio (B), relative phenol amount (C), gas wetness (D) and gas amount (E) are shown.

The analysed reservoir rocks reveal significant compositional differences in their pyrolysates. Based on the pyrolysis products the profile can roughly be subdivided two parts. A phenol

rich and / or aromatic upper part including the three uppermost reservoir rock samples (G004251 above, and G004252 and G004254 in close proximity to the OWC at 2912 m MD-RKB), and a wax enriched lower part including the three reservoir rock samples below the OWC (G004255, G004258, G004257) in the oil saturated zone. The pyrolysis gas chromatograms of the lower three reservoir rock samples show a normal distribution of alkene/alkane doublets up to C_{20}. Afterwards, elevated alkene/alkane doublets up to C_{40} were detected (Figure 69).

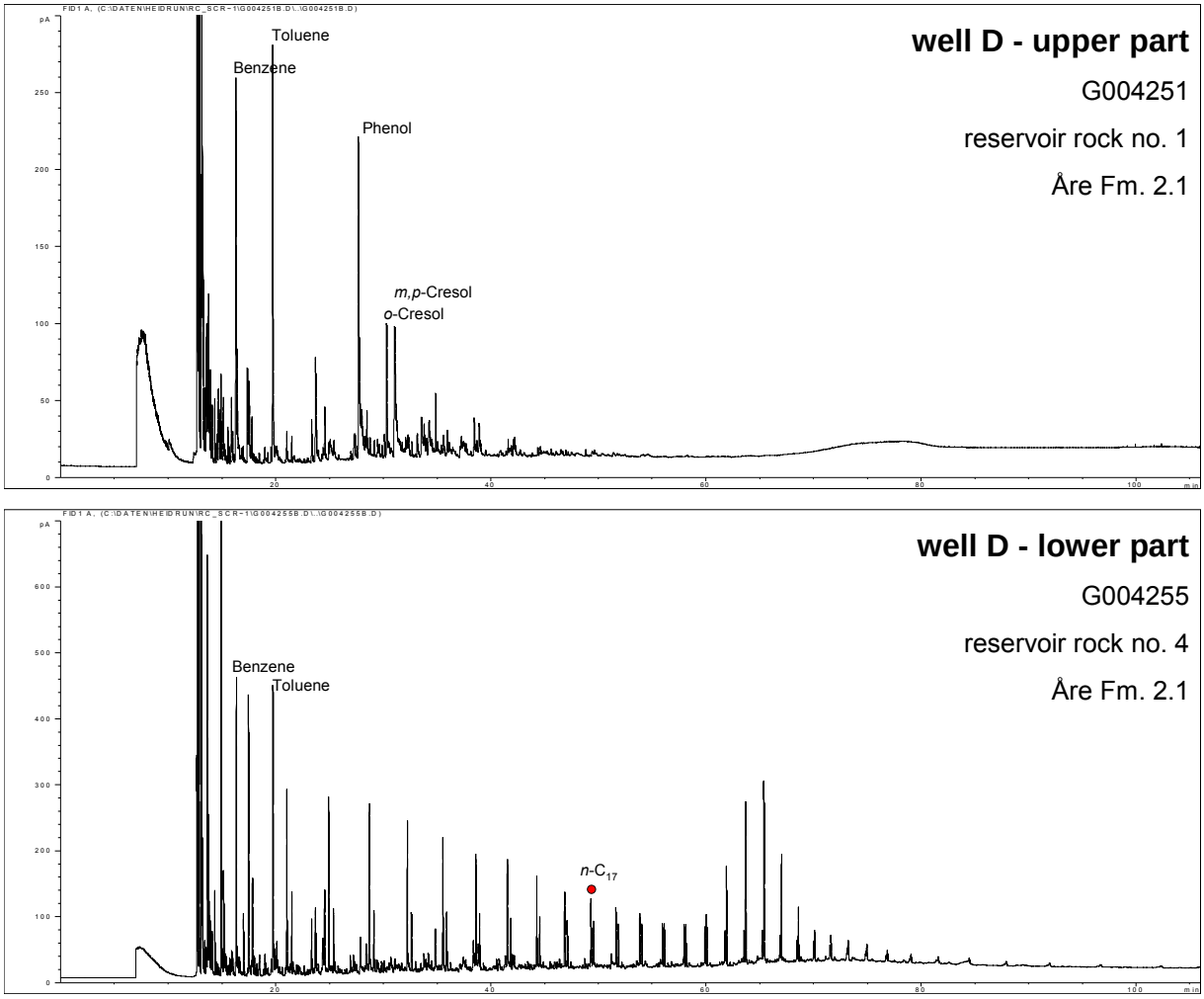

Figure 69 ***Top:*** **Example pyrolysis gas chromatogram for the reservoir rocks from the water-saturated zone of well D near the OWC. These samples are characterised by high phenol content and a significant amount of aromatics in the pyrolysates.** ***Bottom:*** **Example pyrolysis gas chromatogram for the reservoir rocks from the oil-saturated zone of well D. These reservoir rocks are characterised by normal alkene/alkane doublets, minor amounts of aromatic compounds and a high amount of waxy compounds.**

Both upper reservoir rocks in the water-saturated zone and near the OWC (sample no. 1 and 2 = G004251 and G004252) are characterised by the highest aromaticity and gas amount, and lowest gas wetness. The uppermost reservoir rock (no. 1 - G004251) presents additionally the highest phenol ratio referring to disseminated coaly particles within the reservoir rock. Both,

especially the next to the topmost reservoir rock (no. 2, G004252), are highly aromatic and nearly depleted in *n*-alkanes (Figure 69, top). This reservoir rock sample no. 2 is further depleted in 2-ring aromatics and phenol compounds, which is reflected by a very low monoaromatic / diaromatic hydrocarbon ratio and a low phenol ratio (Figure 68 B and C).

Below the OWC in the oil-saturated zone, significant gradients could be observed in the pyrolysis products for all bulk properties (Figure 68 A - E). The aromaticity shows a clear trend with increasing depth (Figure 68 A). Similar gradients are observed in the gas wetness and the gas amount (Figure 68 D and E). The gas wetness increases with increasing depth from 0.44 up to 0.84 and reflects the aromaticity trend. Both parameters show an inverse correlation. The gas amount decreases with increasing depth proportional to the aromaticity from 98 % to 26 %.

A similar trend was observed for the relative phenol content (Figure 68 C). The topmost reservoir rock (G004251) is characterised by an extraordinary high phenol ratio of 23.3. This is additionally observed for the third to top reservoir rock (G004254). Both samples indicate a higher terrestrial input that points to disseminated coal particles. With increasing depth, the phenol amount decreases to 0.02.

Regarding the type of aromatic hydrocarbon ratio, the reservoir rocks show a similar gradient as observed for the aromaticity. Both ratios show a linear correlation. Excluding the heavy depleted second to top reservoir rock sample (no.2, G004252) a decrease in 1-ring aromatic compounds relative to 2-ring aromatic compounds is observed with decreasing depth, indicating variabilities in the average aromatic ring number within the OM. This trend is different from those observed in well C (Garn Fm., Figure 31), well A and well E (both Åre Fm., not shown) indicating differences in the aromatic compounds between these wells as well as within the reservoir formations.

In addition, the GOR decreases with increasing depth and reveal a linear correlation to the aromaticity trend. Similar correlations are observed for the reservoir rocks of well C, A, and E. The UCM mirror the GOR trend and increases with increasing depth.

6.3.2.2.1 ORGANOFACIES AND/OR MATURITY DIFFERENCES

Significant differences in the alkyl chain length distribution of the macromolecules can be seen in Figure 70 A. Both highly aromatic and *n*-alkane depleted uppermost reservoir rocks show a high percentage of short chains and plot in the gas and condensate field indicating high terrestrial organic matter input. Only one reservoir rock, the third to top sample

(G004254), plot in the P-N-A low wax oil field and show a similar CLD as the potential source rock from the Upper Jurassic Spekk Formation (marine Type II kerogen).

The waxy reservoir rocks in the lower part of well D show higher content of long chain alkanes in their pyrolysis products, which increases with increasing depth. Reservoir rock sample no. 4 (G004255) plot in the paraffinic high wax oil field. Both lowermost rock samples (G004257 and G004258) contain > 50 % long chain alkanes (C_{15+}) in their pyrolysis products. The very high wax content within the high molecular weight fraction of these reservoir rocks indicates lacustrine conditions of the deposited source rock. Reservoir rocks in the lower part of well D indicate changes in the organofacies of the generating source.

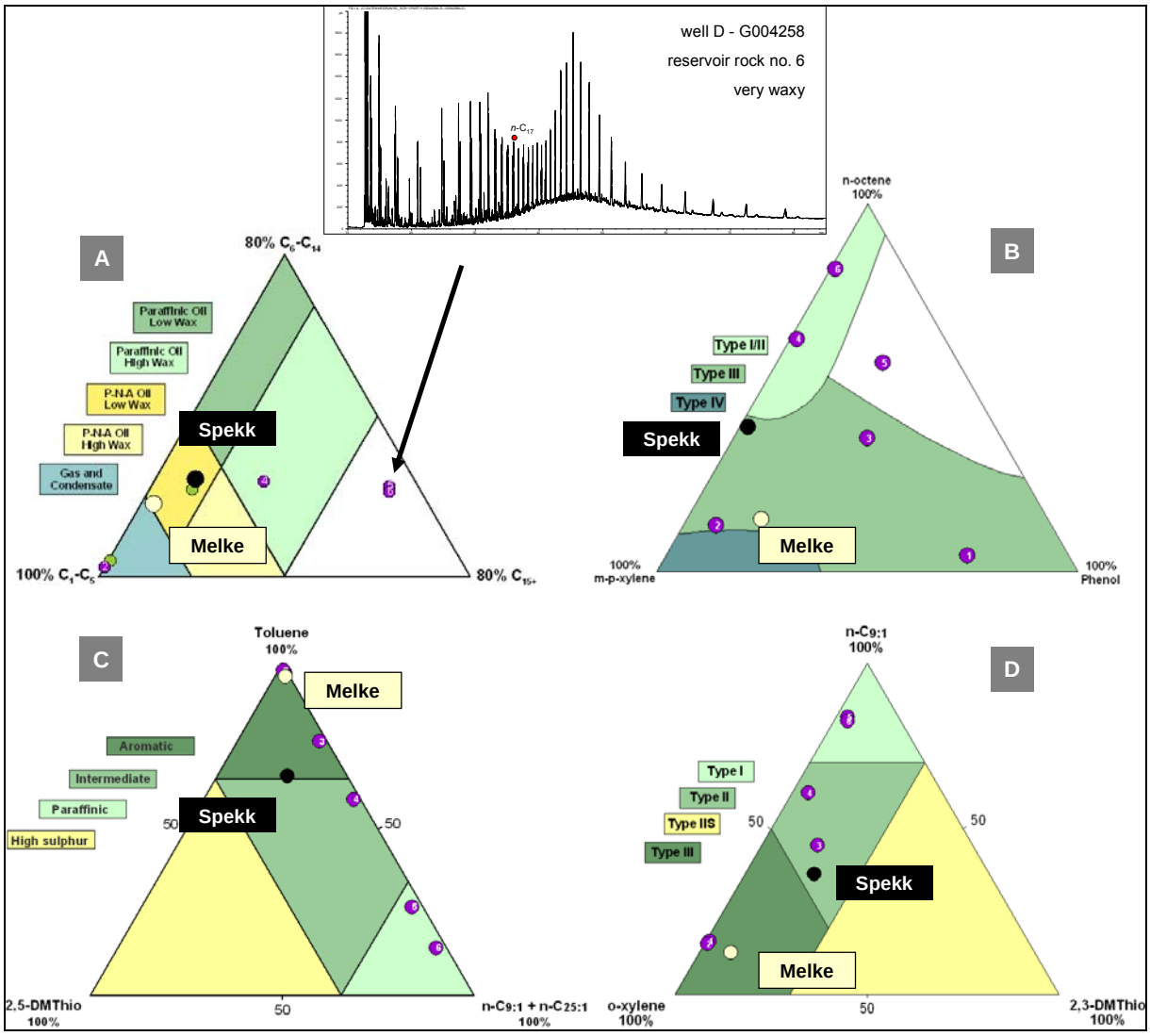

Figure 70 Bulk properties of the reservoir rock and source rock pyrolysates of well D concerning (A) alkyl chain length distribution, (B) phenol content, and (C - D) sulphur content. The pyrolysis chromatogram show the lowermost reservoir rock no. 6 (G004258) characterised by high wax content.

Depending on their phenol content, the reservoir rock samples no. 1 (G004251) and no. 3 (G004254) plot closest to the phenol apex indicating high amount of terrestrial material (Figure 70 B). All reservoir rocks show differences in the aromaticity. As expected, both uppermost rock samples show the highest aromaticity represented by *m, p*-xylene. With increasing depth, the reservoir rock samples become more paraffinic represented by *n*-octene.

Both ternaries in Figure 70 (C and D) indicate low sulphur content for all reservoir rocks and show large differences in aromaticity and paraffinicity.

6.3.2.2.2 CORRELATION TO PHYSICAL ROCK PROPERTIES (WELL LOG DATA)

The fluvial dominated Åre Fm. 2.1 comprises fluvial channel-sandstones (reservoirs) departed by floodplain mudstones and numerous layer of peat swamp coal. The heterogeneous succession of the alternating sediments is reflected by changes in the poroperm properties at very small scale (Figure 14).
The highest aromaticity was observed in the upper water leg and near the OWC (Figure 14, Figure 68 A). Both zones are characterised by different poroperm properties. However, higher aromaticity might be correlated to higher water saturation. The gradient in aromaticity was observed in the oil-saturated zone from 2912 m up to 2937 m MD-RKB. This zone is characterised by generally low poroperm properties (Φ up to 10 % and K = 2 - 200 md), which shows a strong alternation at very small scale. Thus, no direct correlation to the trend observed in the pyrolysis products was found based on visual comparison alone.

In summary, concerning the pyrolysis products, profile D can roughly be subdivided in two parts, a phenol rich and/or aromatic upper part including both uppermost reservoir rock samples, one from the water leg and one near the OWC, and a wax enriched lower part, including the four lowermost rock samples from the oil-saturated zone.
The reservoir rocks within and near the water-saturated zone are additionally characterised by the highest gas amount, lowest gas wetness, a low PI and a low OM content. Both samples are depleted in *n*-alkanes. The next to the top reservoir rock is further depleted in 2- ring aromatic compounds and phenol.
Reservoir rocks in the oil-saturated zone show high proportions of long chain alkane/alkane doublets in their pyrolysates, which are typical for high wax content. These reservoir rocks

show gradients for all bulk properties in their pyrolysates. The aromaticity decreases with increasing depth and shows an inverse correlation to the gas wetness. Additionally, the aromaticity is linear correlated to the 1-ring aromatic / 2-ring aromatic hydrocarbon ratio and the GOR. One reservoir rock refers to disseminated coal.
Reservoir rocks with wax enriched pyrolysis products in the lower part of well D indicate a lacustrine influence of the generating source. No indications for maturity differences were found. The high aromaticity in the reservoir rocks from the upper part might correlate to higher water saturation. However, no direct correlation of the physical rock properties to the trends observed in the pyrolysis products were found based on visual comparison alone.

6.3.3 WELL 6507/8-4 IN HEIDRUN NORTH (ÅRE FM. 2.1 - 1)

6.3.3.1 PRODUCTION INDEX AND ORGANIC RICHNESS

The average PI of the Åre Fm. reservoir rock samples is about 0.64 (± 0.02) (Figure 25, Table X 1). A slight V-shaped gradient was observed in the oil quality within the profile. In the upper part the PI decrease from 0.66 to 0.61; in the lower part the PI rises again up to 0.66 at the OWC. The sample next to last, short below the OWC, present the highest PI, similar as observed in well 6507/7-6 (Åre Fm.). Down to the lowermost reservoir rock, the PI slightly decreases.

The mean organic matter content is about 22.36 mg/g rock (± 8.99) (Figure 26, Table X 1). An inverse V-shaped gradient was observed within the OM distribution. In the upper part, the OM content increases with increasing depth from 13.70 to 35.70 mg/g rock, while reservoir rocks in the lower part of well 6507/8-4 near the OWC are characterised by a decrease in the OM amount to 14.40 mg/g rock. However, the lowermost reservoir rock has a higher OM content of 33.47 mg/g rock.
The organic matter distribution and the oil quality (PI) show an inverse correlation.

6.3.3.2 ORGANIC MATTER COMPOSITION

Figure 71 A - E shows the pyrolysis products of well 6507/8-4 in geochemical depth plots for the aromaticity (A), monoaromatic / diaromatic hydrocarbon ratio (B), relative phenol content

(C), gas wetness (D) and gas amount (E). The average values and standard deviations for the bulk pyrolysis parameters can be seen in Table X 2, the Py-GC parameter values for the individual reservoir rocks are listed in Table X 9 in the appendix.

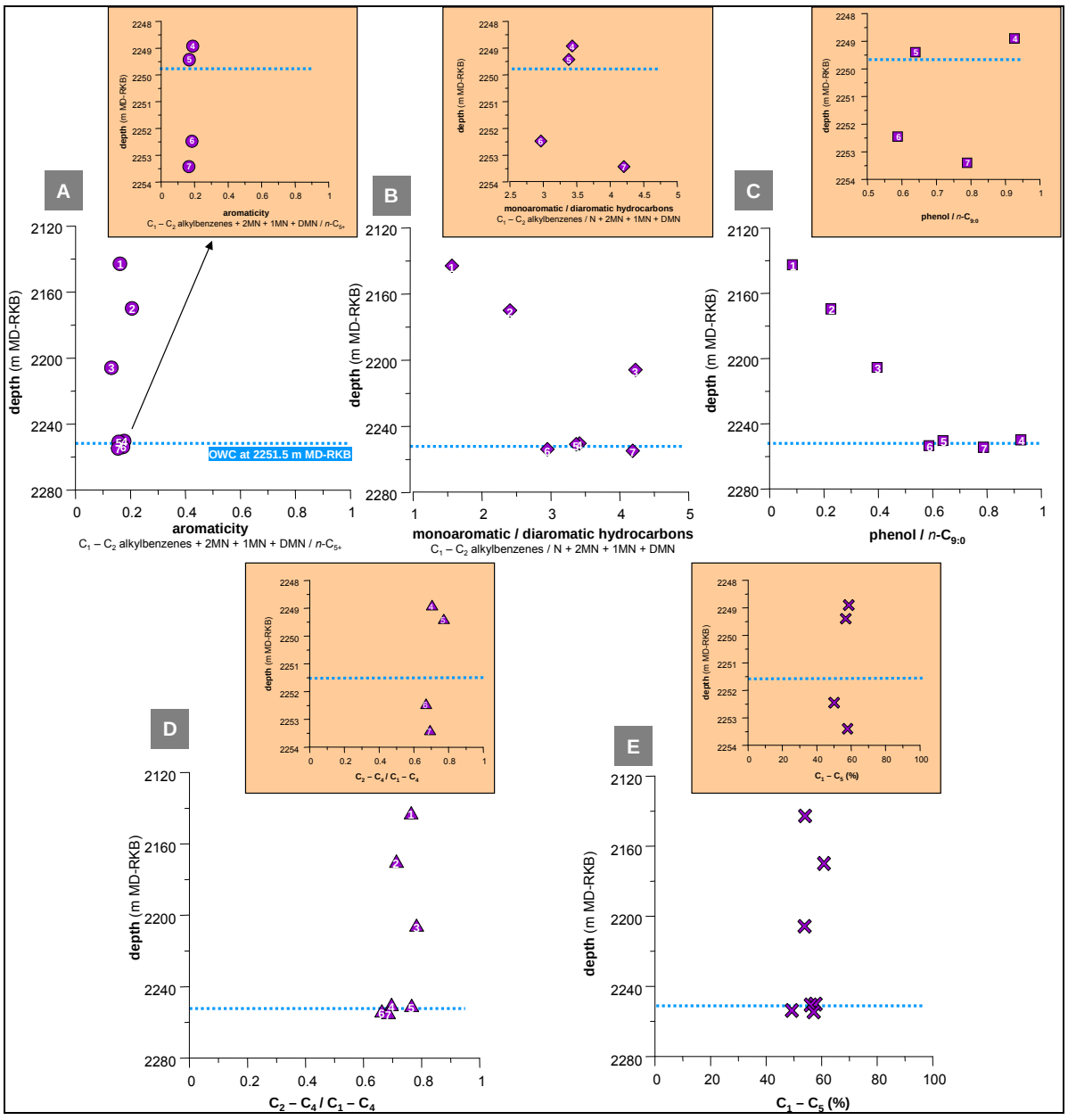

Figure 71 Geochemical profiles of the pyrolysis products from the reservoir rock screening of well 6507/8-4. From A to E aromaticity (A), monoaromatic/diaromatic hydrocarbon ratio (B), relative phenol amount (C), gas wetness (D) and gas amount (E) are shown. The additional plots enlarge the screening results for the reservoir rocks near the OWC.

The aromaticity is low (< 0.20) and shows only marginal changes within profile 6507/8-4 (Figure 71 A). These variabilities are reflected in the gas wetness (Figure 71 D). Reservoir rocks above the OWC show an inverse correlation of aromaticity and gas wetness (Figure 72). Two reservoir rock samples below the OWC (no. 6 and 7 = G004017 and G004018) show

lower gas wetness. The gas percentage reveals similar variabilities as observed for the aromaticity (Figure 71 D). Both parameters are linear correlated.

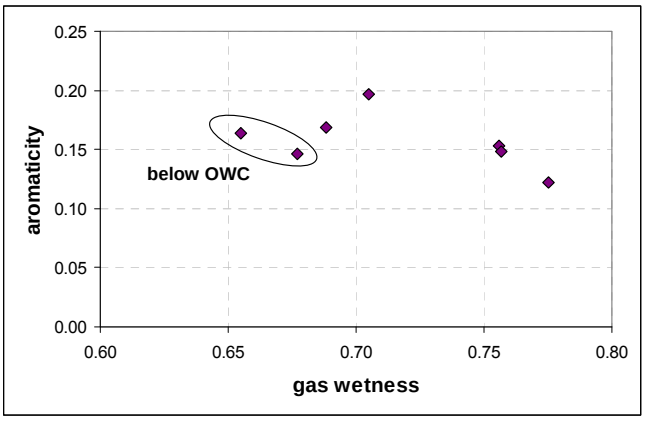

Figure 72 Inverse correlation of the aromaticity and gas wetness for the reservoir rocks of well 6507/8-4 above the OWC. Both reservoir rocks below the OWC show lower gas wetness.

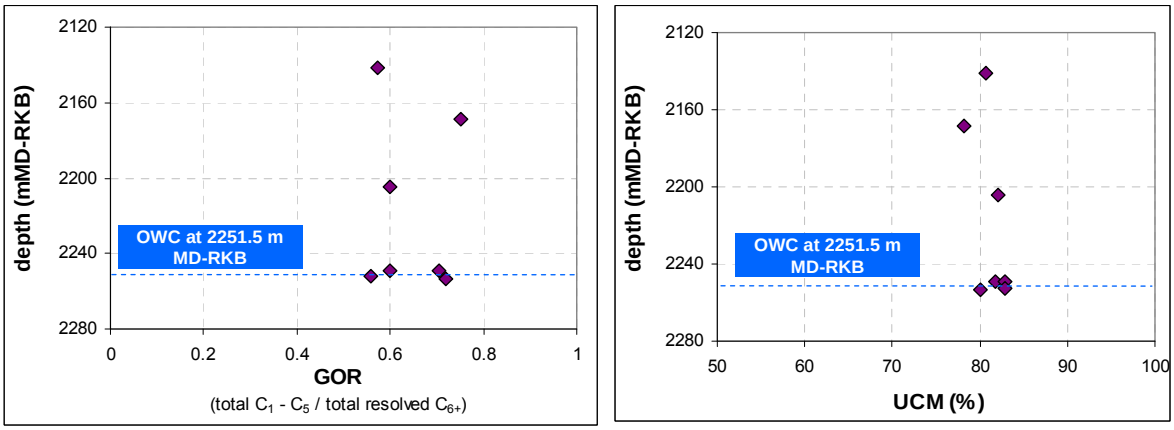

Figure 73 *Left* GOR analysed in the reservoir rocks of well 6507/8-4. *Right* the percentage of the unresolved compound mixture (UCM) of these reservoir rocks.

Gradients were detected within the type of aromatic hydrocarbon ratio indicating changes in the OM composition (Figure 71 B). With increasing depth, the datapoints reveal a V-shaped curve (horizontal) similar to PI and OM distribution (Figure 25, Figure 26). The upper three reservoir rock samples G004019, G004020, and G004021, show an increase in 1-ring aromatics relative to 2-ring aromatic compounds from 1.53 to 4.19. Within the reservoir rocks below, G004015, G004016, and G004017 near the OWC, the ratio decreases to 2.91. The lower most reservoir rock G004018 is different presenting a ratio of 4.15. Similar as observed before in well C, A, and E, the type of aromatic hydrocarbon ratio shows an inverse correlation to the aromaticity.

The phenol ratio shows a similar gradient already observed for the mono/diaromatic hydrocarbon ratio. All reservoir rocks show a phenol ratio below one (Figure 71 C).

Above the OWC, GOR and aromaticity show similar variabilities (Figure 73, left). The amount of unresolved compound mixture (UCM) mirror the GOR (Figure 73, right)

6.3.3.2.1 ORGANOFACIES AND/OR MATURITY DIFFERENCES

Within the CLD ternary, all reservoir rocks plot in the paraffinic high wax oil field and reflect slight variabilities in their proportion of the short and medium chains in their pyrolysates (Figure 74 A). Comparing the reservoir rock CLD with both potential source rocks, the reservoir rocks are more similar to the Spekk Formation, although they have higher proportions of medium- and long alkyl chains in their pyrolysates. This points to higher wax content in the reservoir rocks and could be an indication for a lacustrine influence of the source rock. Well E and well D show similar indication to a lacustrine influenced depositional facies.

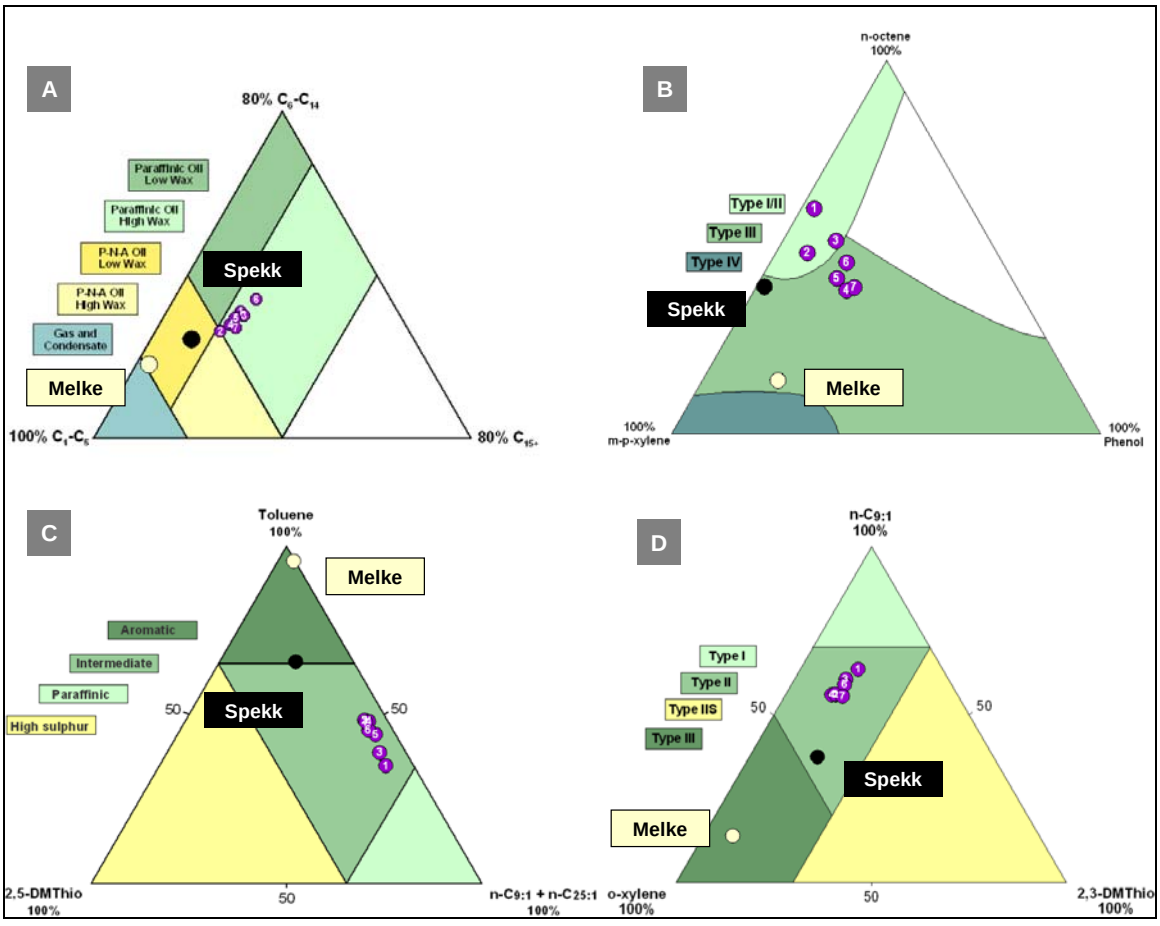

Figure 74 Bulk properties of the reservoir- and source rock pyrolysis products of well 6507/8-4 concerning (A) alkyl chain length distribution, (B) phenol content, and (C-D) sulphur content.

For all but the uppermost reservoir rock, elevated phenol amounts were observed, especially in the reservoir rocks close to the OWC (Figure 74 B).
Both sulphur ternaries indicate low sulphur content for all reservoir rocks. Additionally, the dataset reflects slight differences in the aromaticity (Figure 74 C and D).

6.3.3.2.2 CORRELATION TO PHYSICAL ROCK PROPERTIES (WELL LOG DATA)

The analysed reservoir rocks comprise the lower Åre Fm. subunits 2.1 - 1, as the reservoir sediments of the reservoirs in well D. These sediments represent a succession of fluvial channel sandstones (main reservoirs), which are departed by lacustrine mudstones and peat swamp coal. Figure 21 shows a well log section of profile 6507/8-4 (cf. Chapter 3.2.1.13).
The resistivity signal decreases to the OWC indicating the increase in water saturation, which might influence the OM distribution as well as the composition of the aromatic compounds. Numerous thin muddy or shaly zones are interstratified in the profile, detected by an alternating gamma ray signal. These zones do not directly influence the pyrolysis parameters (no barrier function), in contrast to the observations made in well E. The acoustic log indicates slight variabilities in the porosity, which might be related to slight variabilities in the aromaticity.
No direct correlation of physical rock properties to the composition of the aromatic compounds of the pyrolysis products was found based on visual comparison alone.

In summary, the PI (oil quality) and the OM content are inversely correlated. The aromaticity shows slight changes, which are mirrored in the gas wetness. Both parameters are inversely correlated. Linear correlations were found between aromaticity and GOR as well as between aromaticity and gas amount. Significant changes show the type of aromatic hydrocarbon ratio. This ratio presents a (horizontal) V-shaped trend similar to that observed in the PI and the OM distribution. This trend is further reflected in the phenol ratio.
The higher wax content in the reservoir rocks could be an indication for lacustrine influence of the source rock. Similar indications are visible in the reservoir rocks of well E and well D.
The increase in water saturation near the OWC might have an influence on the decrease in the reservoir rock OM content as well as the decrease in 1-ring aromatic compounds relative to 2-ring aromatic compounds.

6.3.4 WELL 6507/7-6 IN SEGMENT I (ÅRE FM.3.2 - 2)

6.3.4.1 PRODUCTION INDEX AND ORGANIC RICHNESS

All sampled reservoir rocks of well 6507/7-6 are from the Åre Formation 3.2 - 2. The average PI of the reservoir rocks is 0.63 (± 0.02) (Figure 25, Table X 1). With increasing depth down to the OWC, the PI slightly increases. Conspicuously, the highest PI was detected below the OWC.

Well 6507/7-6 is characterised by marginal changes within the organic matter distribution. The mean organic matter content is 13.98 mg/g rock (± 2.56). The reservoir rock below the OWC is characterised by the lowest OM content (10.80 mg/g rock) (Figure 1, Table X 1).

6.3.4.2 ORGANIC MATTER COMPOSITION

Figure 75 A - E shows the pyrolysis products of well 6507/7-6 in geochemical depth plots for the aromaticity (A), monoaromatic / diaromatic hydrocarbon ratio (B), relative phenol content (C), gas wetness (D) and gas amount (E). The average values and standard deviations for the bulk pyrolysis parameters can be seen in Table X 2 the Py-GC parameter values of the individual reservoir rocks are listed in Table X 9.

The reservoir rocks show relatively uniform ratio values for the single pyrolysis parameters shown in Figure 75 A - E. The standard deviation for the aromaticity, phenol ratio and gas wetness is below 0.03 and 1.3 % for the gas amount.

However, slight variabilities are indicated for the aromaticity, which decreases from 0.24 to 0.19 with increasing depth to the OWC. Lowest aromaticity shows the reservoir rock below the OWC. This trend is reflected in the gas wetness, which increases within the profile down to the OWC (Figure 75 A and D). Both pyrolysis parameters show an inverse correlation (Figure 76).
Furthermore, slight fluctuations are observed in the type of aromatic hydrocarbon ratio (Figure 75 B). The phenol ratio is very low for all samples (< 0.10) (Figure 75 C). GOR and UCM are nearly constant within the profile. The latter slightly increases with increasing depth to the OWC reflecting the aromaticity trend.

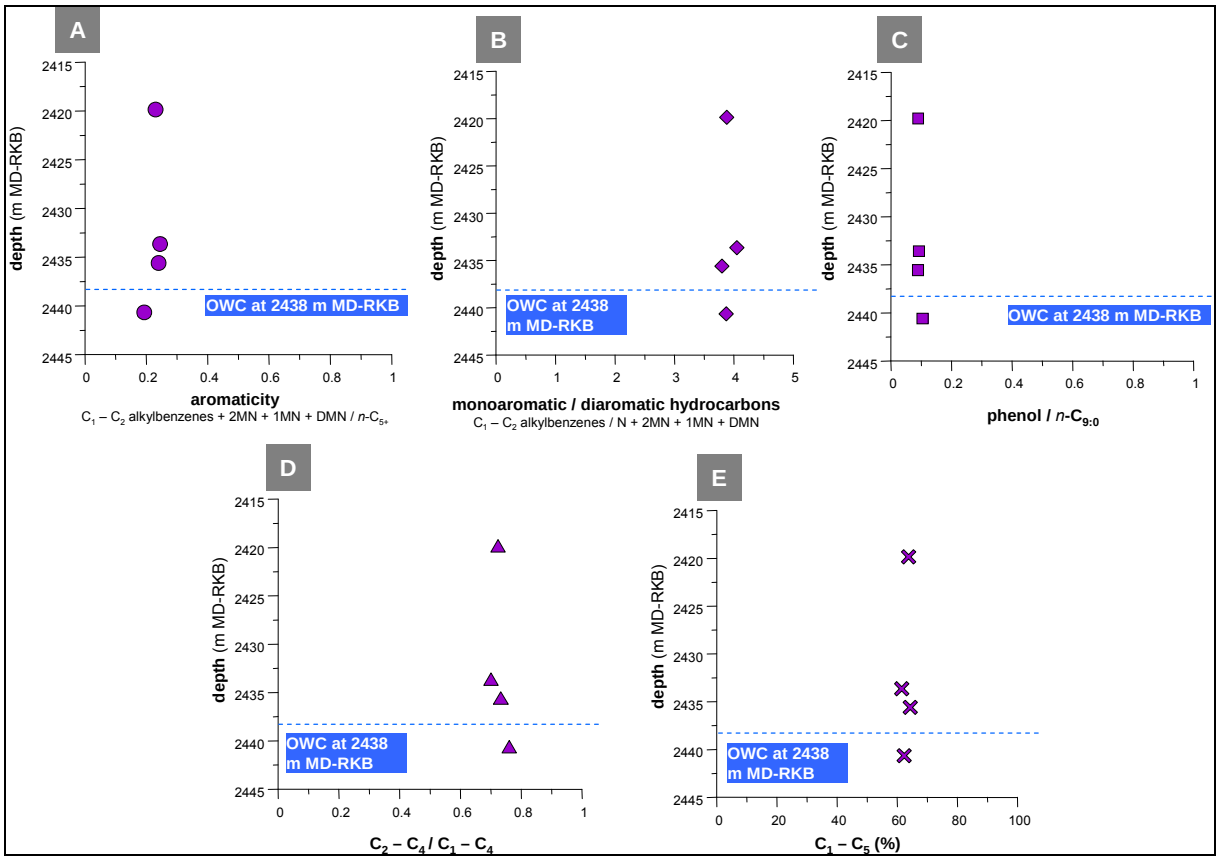

Figure 75 Geochemical profiles of the pyrolysis products from the reservoir rock screening of well 6507/7-6. From A to E the aromaticity (A), monoaromatic/diaromatic hydrocarbon ratio (B), relative phenol amount (C), gas wetness (D) and gas amount (E) are shown.

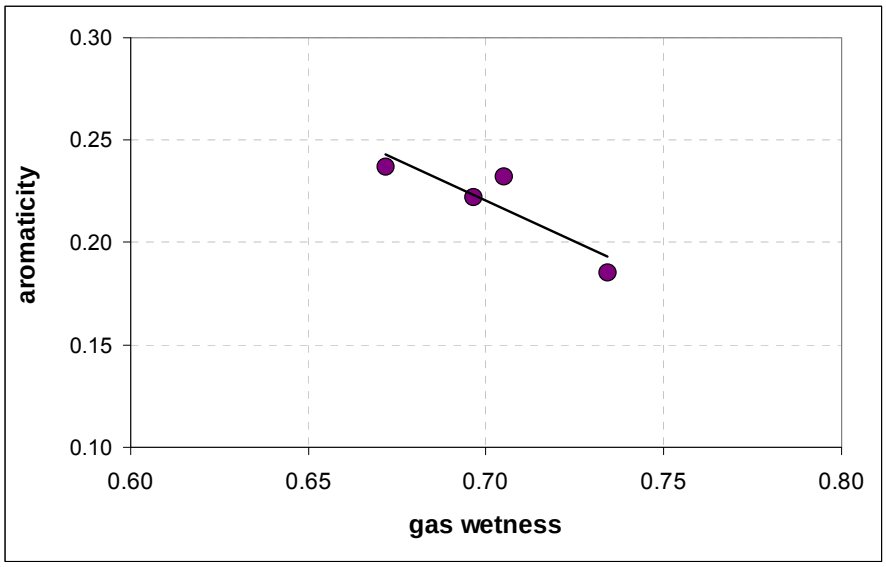

Figure 76 Inverse correlations of the aromaticity and gas wetness observed in the reservoir rock pyrolysates of well 6507/7-6. The line mark the trend observed.

6.3.4.2.1 ORGANOFACIES AND/OR MATURITY DIFFERENCES

Within the CLD ternary, the reservoir rocks plot very close in the P-N-A low wax oil field indicating a similar CLD as the potential source rock from the marine Spekk Formation (Figure 77 A). All reservoir rocks are low in phenol and in sulphur content. Reservoir rock below the OWC reflects the slight differences in the aromaticity (Figure 77 B - D).

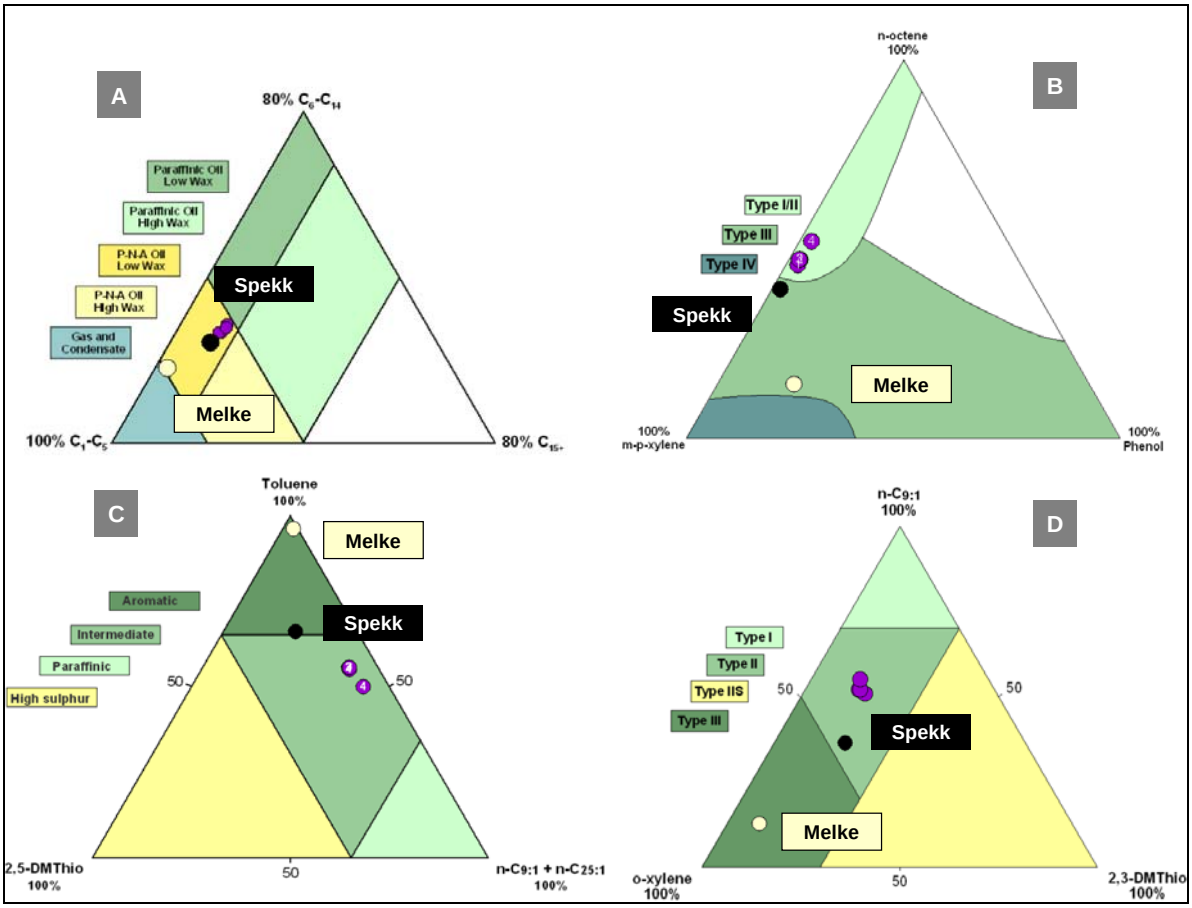

Figure 77 Bulk properties of the reservoir- and source rock pyrolysates of well 6507/7-6 concerning (A) alkyl chain length distribution, (B) phenol content, and (C - D) sulphur content.

6.3.4.2.2 CORRELATION TO PHYSICAL ROCK PROPERTIES (WELL LOG DATA)

The four reservoir rock samples are from the lower part of the Åre Fm. 3.1 - 3.2 and stratigraphic lower units, which are characterised by slight increasing marginal marine influence. The sediments comprise a complex mixture of bay fill deposits with minor coastal plain deposits (cf. Chapter 3.1). All reservoir rocks are in the close vicinity of the OWC. A section of the well log of this profile has shown in Figure 19 in Chapter 3.2.1.10.

The sediments comprise sandstones and siltstones with interstratified thin clay zones. The analysed reservoir rocks were taken from sandstone zones with predominantly medium grain size. The interstratified clays zones do obviously not influence the petroleum composition of these reservoir rocks, which show a relatively homogeneous distribution of the Py-GC parameter. Low resistivity- and low acoustic signals indicate high water saturation over the whole sampled interval.

In summary, the reservoir rocks in well 6507/7-6 present less differences within their pyrolysis products. Marginal changes were observed close to the OWC. The PI slightly increases within the profile to the OWC. Reservoir rock below the OWC represents lowest OM amount. For the aromaticity, a slight decrease with increasing depth is observed that is reflected in the gas wetness. Both pyrolysis parameters show an inverse correlation. No disseminated coaly particles were detected in these Åre Formation reservoir rocks. No indications to organofacies and/or maturity differences of the generative source were found.
No influence of the poroperm properties on the composition of the reservoir rock pyrolysates was found.

6.4 CHARACTERISATION OF THE SINGLE PROFILES IN THE WESTERN PART OF THE HEIDRUN OIL FIELD

6.4.1 WELL 6507/7-5 IN SEGMENT O (SPEKK FM., GARN FM., ILE FM. 2)

6.4.1.1 PRODUCTION INDEX AND ORGANIC RICHNESS

Two reservoir rocks and the potential source rock from the Spekk Formation were analysed in well 6507/7-5. Both reservoir rocks, one from the Garn Fm. and one from the Ile Fm. 2, show very high PI of 0.75 and 0.73, respectively. As described before in Chapter 6.1.2, the potential source rock from the Spekk Formation shows lowest PI with 0.07 (Figure 25, Table X 1).
The organic matter content is very homogeneous within all three samples (15.51 mg/g rock ± 0.34) (Figure 26, Table X 1).

6.4.1.2 ORGANIC MATTER COMPOSITION

The pyrolysis gas chromatograms of both reservoir rocks show a normal distribution of alkene/alkane doublets up to C_{30}. Towards higher retention times, alkanes between C_{30} and C_{40} were detected in the pyrolysates. In Figure 78 A - E, the pyrolysis products of well 6507/7-5 are shown in geochemical depth plots for the aromaticity (A), monoaromatic / diaromatic hydrocarbon ratio (B), relative phenol content (C), gas wetness (D) and gas amount (E). The average values and standard deviations for the bulk pyrolysis parameters can be seen in Table X 2, the Py-GC parameter values for the individual reservoir rocks are listed in Table X 9 in the appendix.

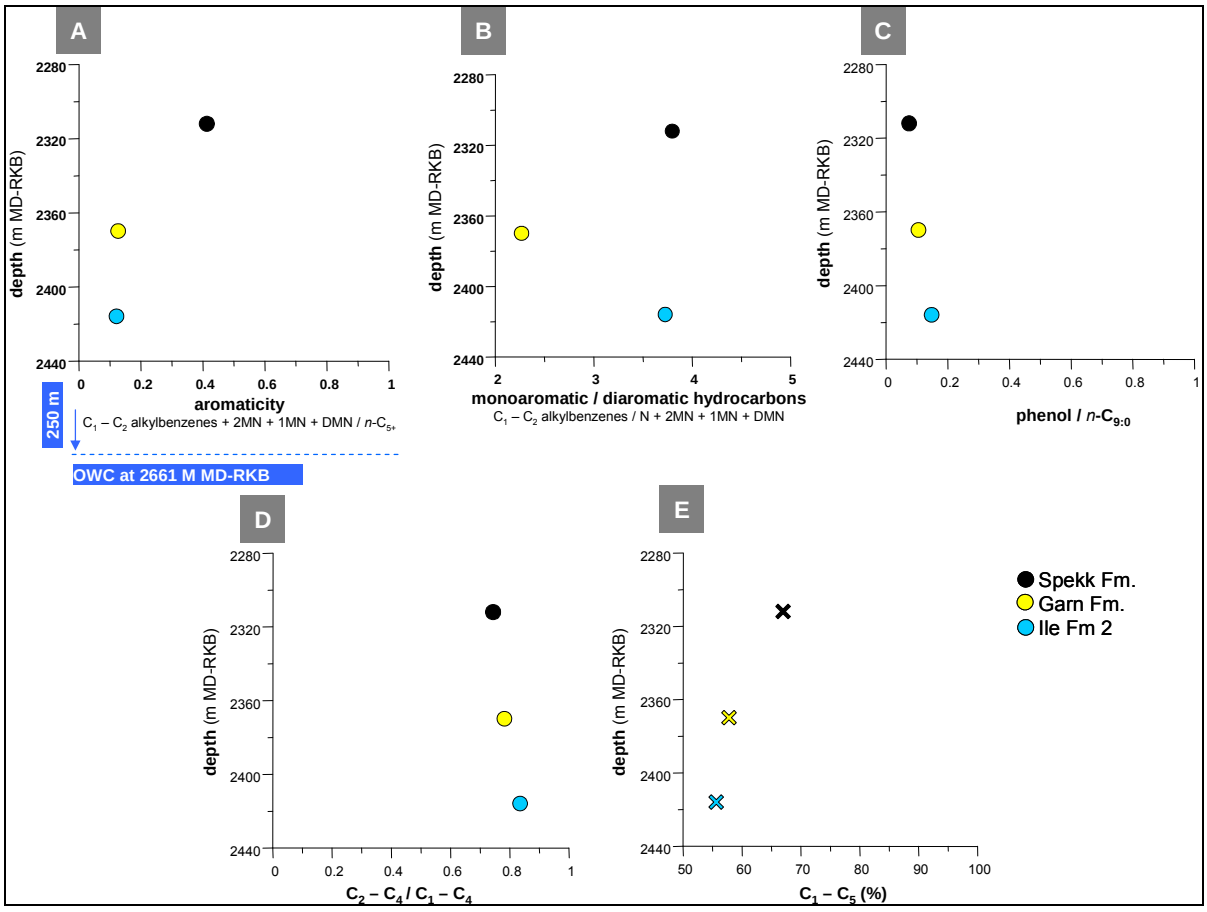

Figure 78 Geochemical profiles of the pyrolysis products from the reservoir rock screening of well 6507/7-5. From A to D aromaticity (A), monoaromatic/diaromatic hydrocarbon ratio (B), relative phenol amount (C), gas wetness (D) and gas amount (E) are shown.

The potential source rock from the Spekk Fm. shows high aromaticity (0.38), lower gas wetness (0.72) and a slightly higher gas amount (67.1 %) in the pyrolysates compared to both reservoir rocks.

The pyrolysates of both reservoir rocks are relatively homogeneous, independent of the different reservoir formations. They are low in aromaticity (0.11 and 0.12) and show only a slight variation in the type of aromatic hydrocarbon ratio and gas wetness, indicating very small changes within the OM of both reservoirs. Gas wetness, gas amount, and phenol ratio are low and nearly constant within profile 6507/7-5. In addition, the GOR and the UCM are nearly constant within profile 6507/7-5.

Well 6507/7-5 is situated in the western part of the Heidrun oil field that was filled by the most recent oil charge (internal Statoil report, 2003). In the Earth gravitational field, thermodynamically gradients will set up in the oil column, which lead to gravitational segregation during geological time (England, 1989). Thus, the homogeneous distribution might be an indication that the mixing processes between the prior biodegraded oil charge(s) and the non-degraded recent oil charge are still going on.

6.4.1.2.1 ORGANOFACIES AND/OR MATURITY DIFFERENCES

Within the CLD ternary, the reservoir rocks plot in the paraffinic high wax oil field (Figure 79 A). The reservoir rocks indicate a higher proportion of long alkyl chains in their pyrolysates compared to the potential source rock from the Spekk Formation. This refers to higher wax content in the reservoir rocks. Thus, it might be an indication for a lacustrine influence of the source rock depositional environment. All reservoir rocks are low in phenol as well as in sulphur and show only slight difference in the aromaticity as observed before in the geochemical depth profiles (Figure 79 B - D).

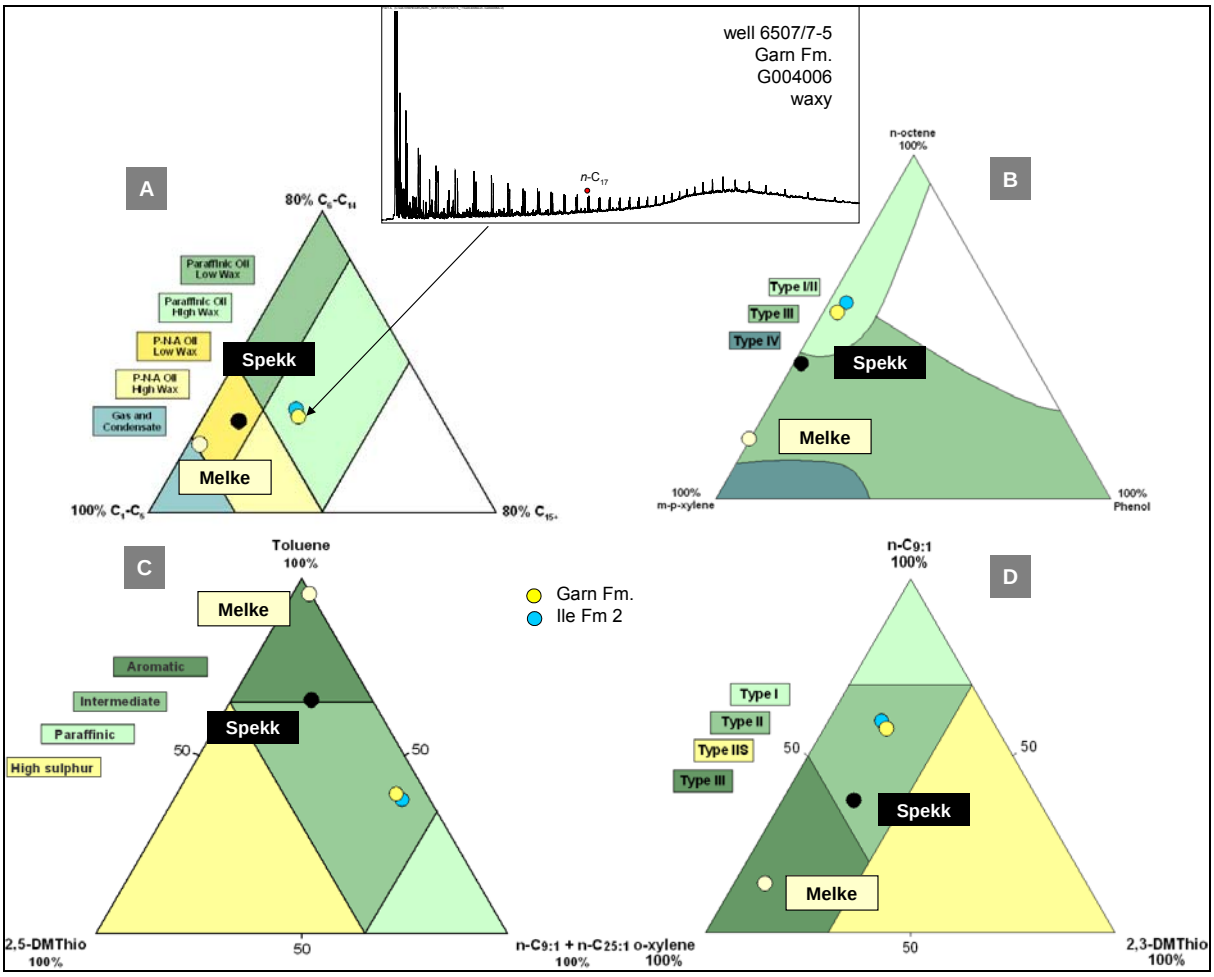

Figure 79 Bulk properties of the reservoir- and source rock pyrolysis products of well 6507/7-5 concerning (A) the alkyl chain length distribution, (B) the phenol content, and (C-D) the sulphur content.

6.4.1.2.2 CORRELATION TO PHYSICAL ROCK PROPERTIES (WELL LOG DATA)

Both reservoir rocks of the Garn Fm. and the Ile Fm. 2 reservoirs comprise predominantly medium-grained, oil stained sandstones and show relatively similar log signals (Figure 18, cf. Chapter 3.2.1.9). The homogeneous physical rock properties are reflected in uniform pyrolysis products. Slight differences in the resistivity signal might indicate better reservoir properties in the Garn Fm. compared to the Ile Fm. 2. However, they are not reflected in the OM composition. The dense shale and/or limestone zones detected in both reservoir formations do not directly influence the pyrolysates composition.

The high gamma ray signal of the potential source rock from the Spekk Formation correlates to high aromaticity.

In summary, both reservoir rocks show uniform bulk properties. They are characterised by high oil quality and low aromaticity. The Spekk Formation shale show very low oil quality (PI), high aromaticity, a lower gas wetness and a slightly higher gas amount in the pyrolysates compared to the Garn and Ile Formation reservoir rock samples. The reservoir rock samples are characterised by slightly higher proportion of medium- and long chains in their pyrolysates compared to the potential source rock from the Spekk Formation. This refers to waxy compounds in the reservoir rocks, which might be an indication to a lacustrine influence of the generating source. Both, the Garn Fm. and the Ile Fm. reservoir rock samples, show nearly similar physical rock properties.
This homogeneous distribution of the pyrolysis products in well 6507/7-5 might be an indication that mixing processes between different oil charges are still going on, as thermodynamically gradients have not yet set up in the oil column.

6.4.2 WELL 6507/7-2 IN SEGMENT G (TILJE FM. 3.2, 2.1, ÅRE FM. 7.2, 6.2)

6.4.2.1 PRODUCTION INDEX AND ORGANIC RICHNESS

The two upper reservoir rock samples from well 6507/7-2 are from the Tilje Formation 3.2 and 2.1, the two lowermost reservoir rock samples belong to the Åre Formation 7.2 and 6.2. The average PI of the reservoir rocks is 0.67 ± 0.06 (Figure 25, Table X 1). The uppermost sample shows higher PI with 0.73 compared to the reservoir rock samples below, which are characterised by a relatively uniform oil quality with PI of 0.63 - 0.65.
The mean organic matter content of the reservoir rocks is 21.23 ± 6.59 (Figure 26, Table X 1). With increasing depth the OM content increases, the lowermost sample G004001 from the Åre Formation excluded.

6.4.2.2 ORGANIC MATTER COMPOSITION

Figure 80 A - E shows the pyrolysis products of well 6507/7-2 in geochemical depth plots for the aromaticity (A), monoaromatic / diaromatic hydrocarbon ratio (B), relative phenol content (C), gas wetness (D) and gas amount (E).. The average values and standard deviations for the bulk pyrolysis parameters can be seen in Table X 2. The Py-GC parameter values for the individual reservoir rocks are listed in Table X 9.

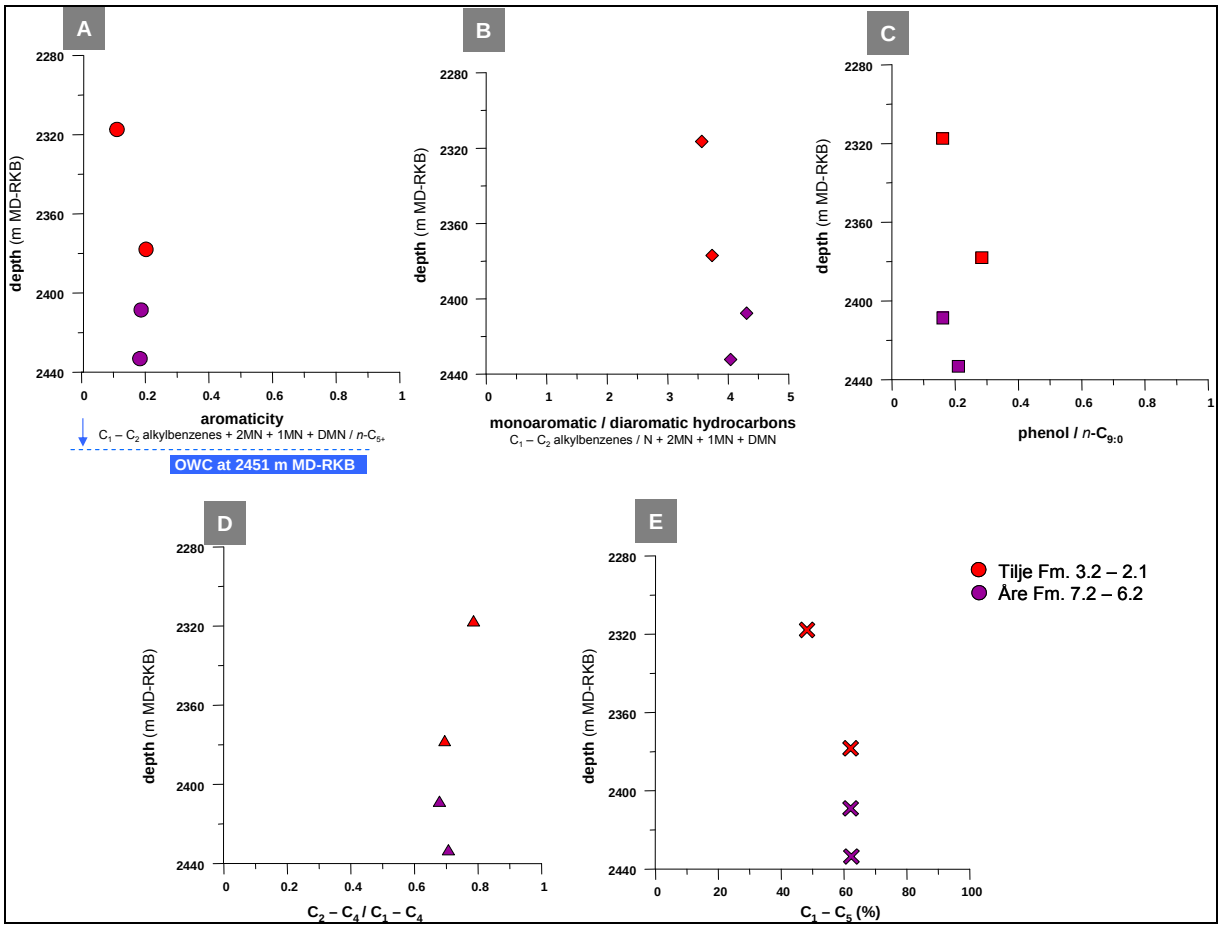

Figure 80 Geochemical profiles of the pyrolysis products from the reservoir rock screening of well 6507/7-2. From A to D the aromaticity (A), monoaromatic/diaromatic hydrocarbon ratio (B), relative phenol amount (C), gas wetness (D) and gas amount (E) are shown.

The uppermost reservoir rock show significant compositional differences in the pyrolysates. This sample shows a normal alkene/alkane distribution up to C_{30}. Afterwards, between C_{30} and C_{40}, elevated alkane peaks were detected (Figure 81).

The aromaticity ranges between 0.11 and 0.20 and shows a slight increase with increasing depth (Figure 80 A). The uppermost reservoir rock has the lowest aromaticity (0.11). This aromaticity trend is reflected in the gas wetness, which shows a slight decrease with increasing depth (Figure 80 D). The uppermost sample presents the highest gas wetness. Both parameters are inverse correlated.

All reservoir rocks exhibit a low phenol content with 0.20 ± 0.06 (Figure 80 C), i.e. no indications for disseminated coal were found. Within the type of aromatic hydrocarbon ratio, a slight increase with increasing depth was observed (Figure 80 B). Excluding the uppermost rock sample, the gas percentage in the pyrolysis products is nearly constant within the profile.

A similar pattern shows the GOR. Here the uppermost reservoir rock is characterised by distinctly lower GOR, compared to the remaining rock samples with nearly constant GOR. Between the GOR and the aromaticity, a linear correlation was found. In addition, the uppermost reservoir rock shows the lowest amount of unresolved compounds (58.9 %) compared to the reservoir rocks below with higher UCM between 71.3 % and 77.3 %. With increasing depth, the UCM slightly increases.

6.4.2.2.1 ORGANOFACIES AND/OR MATURITY DIFFERENCES

Within the ternary for the carbon chain length distribution, both Åre Fm. reservoir rocks and the reservoir rock G003999 from the Tilje Fm. 2.1, plot in the P-N-A low wax oil field near the paraffinic oil field. They show CLD relatively similar to the potential source rock from the Spekk Fm. (Figure 81 A).

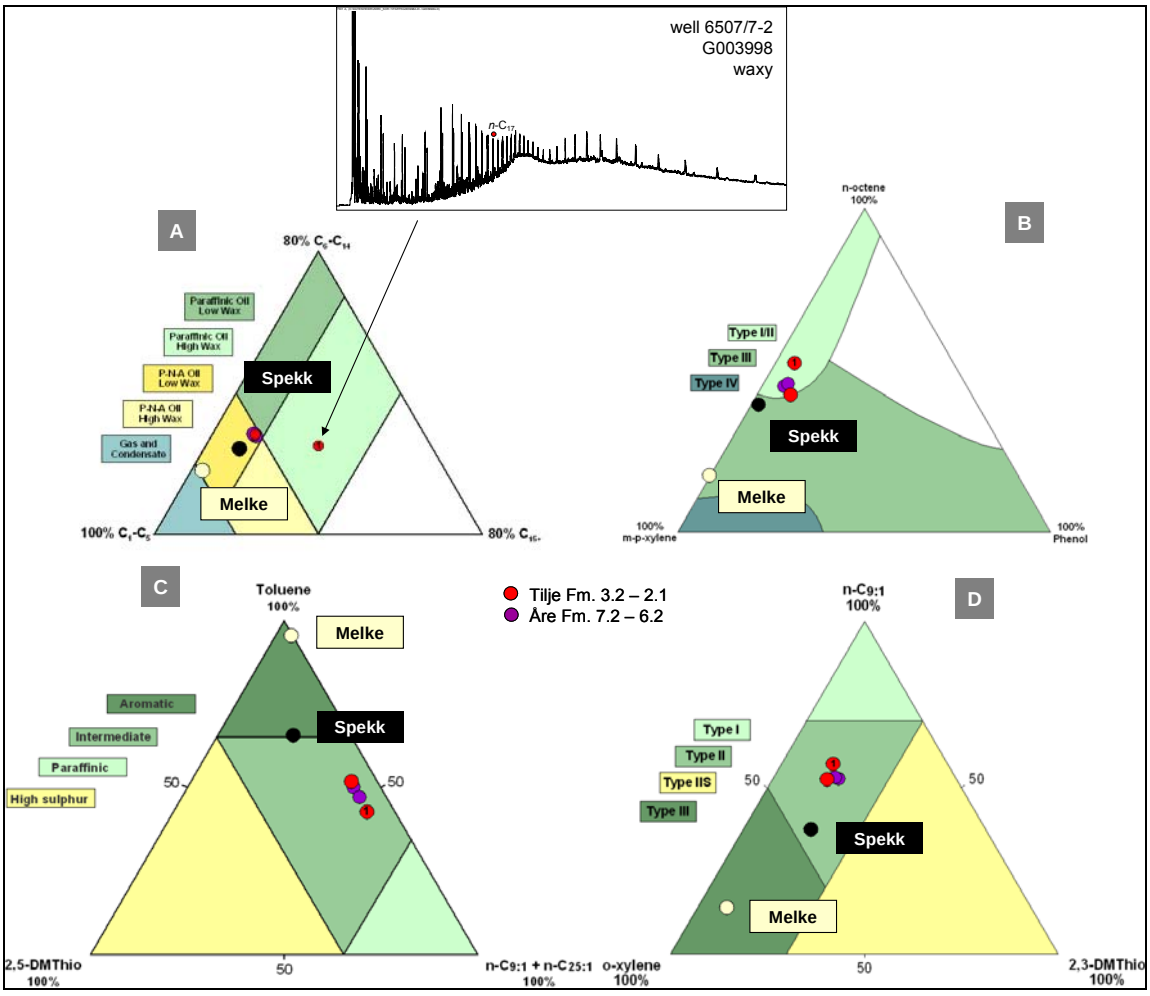

Figure 81 Bulk properties of the reservoir- and source rock pyrolysates of well 6507/7-2 concerning (A) alkyl chain length distribution, (B) phenol content, and (C - D) sulphur content. The pyrolysis gas chromatogram show sample G003998 characterised by large amounts of long alkyl chains.

The uppermost reservoir rock G003998 from the Tilje Fm. 3.2 shows a higher proportion of long chains in the pyrolysates and plot in the paraffinic high wax oil field. Its pyrolysis gas chromatogram is shown beside the CLD ternary in Figure 81 A. The higher content of long chain alkanes in the macromolecular fraction reflect higher wax content in the reservoir rock and might refer to a lacustrine influence of the source rock.

Similar enrichment of waxy compounds show pyrolysates of the oil samples G003881 (DST 4A) and, slightly lesser pronounced, G003883 (DST 2) of well 65077-2 (cf. Chapter 6.2.1.2.3.2, Figure 46). Higher portions of long chains have been observed before in well 6507/7-5 in the western part and well 6507/8-4 as well as in well E and in particular in well D from the northern part of the Heidrun oil field.

The phenol ternary (Figure 81 B) and the two sulphur ternaries (Figure 81 C - D) support the distribution observed before in the depth plots. All reservoir rocks are low in phenol content and in sulphur content, and show slight difference in the aromaticity.

6.4.2.2.2 CORRELATION TO PHYSICAL ROCK PROPERTIES (WELL LOG DATA)

The Tilje- and upper Åre Formation reservoirs are generally characterised by very complex and heterogeneous sedimentology (cf. Chapter 3.1), which is reflected by strong alternating rock properties in the well logs (Figure 15 in Chapter 3.2.1.6). The uppermost reservoir rock from the Tilje Fm. 3.2 belongs to a unit with better reservoir properties (higher poroperm) compared to remaining Tilje Fm. reservoir zones. Thus, the lower aromaticity and higher gas wetness found in this sample might be correlated to better poroperm properties. Interstratified barriers (mudstones) might additionally influence the pyrolysate compositions of the upper reservoir rock and the remaining samples in the profile. However, the reservoir rocks show a large sample distance up to 60 m, thus based on visual comparison alone no direct correlations to the observed differences in the pyrolysis products were found.

In summary, the uppermost reservoir rock from the Tilje Fm. 3.2 indicates significant compositional differences in the pyrolysis products compared to the remaining reservoir rock samples. This sample shows the highest PI and the lowest OM content analysed in well 6507/7-2 as well as a low aromaticity and high gas wetness. The two Py-GC parameters

aromaticity and gas wetness show an inverse correlation. The remaining samples are nearly uniform in their pyrolysates composition. The enrichment in waxy compounds in the uppermost reservoir rock from the Tilje Fm 3.2 indicates differences in the organofacies of the source rock. Similar observations were made in two oil samples (DSTs) of well 6507/7-2.
The uppermost reservoir rock from the Tilje Fm 3.2 is characterised by better poroperm properties and lower water saturation compared to the subunits of the remaining reservoir rocks. An influence of interstratified mudstone barriers on the hydrocarbon distribution might additionally be considered. However, no direct correlations to the observed differences in the pyrolysis products were detected based on visual comparison alone.

6.4.3 WELL 6507/7-3 IN SEGMENT E (GARN FM., ILE FM. 4 - 6, ROR FM. 2)

6.4.3.1 PRODUCTION INDEX AND ORGANIC RICHNESS

The reservoir rocks from well 6507/7-3 are from the Garn- Ile- and Ror Formation (Table 7). The PI is relatively uniform in this profile (0.70 - 0.72) independent of the reservoir formation (Figure 25, Table X 1).
In addition, the OM distribution is relatively homogeneous. Both, the Garn Fm. and the Ile Fm. reservoir rock samples, show a slightly higher OM content of 13.28 and 15.01 mg/g rock, respectively, compared to the reservoir rock from the Ror Fm. presenting an OM content of 12.35 mg/g rock (Figure 26, Table X 1).

6.4.3.2 ORGANIC MATTER COMPOSITION

Independent of the reservoir formation, the analysed reservoir rock samples show relative similar bulk properties with increasing depth regarding the aromaticity (A), monoaromatic / diaromatic hydrocarbon ratio (B), relative phenol content (C), gas wetness (D) and gas amount (E) (Figure 82 A - E). Table X 2 listed the average values and standard deviations for the bulk pyrolysis parameters. The Py-GC parameter values for the individual reservoir rock samples are listed in Table X 9 in the appendix.

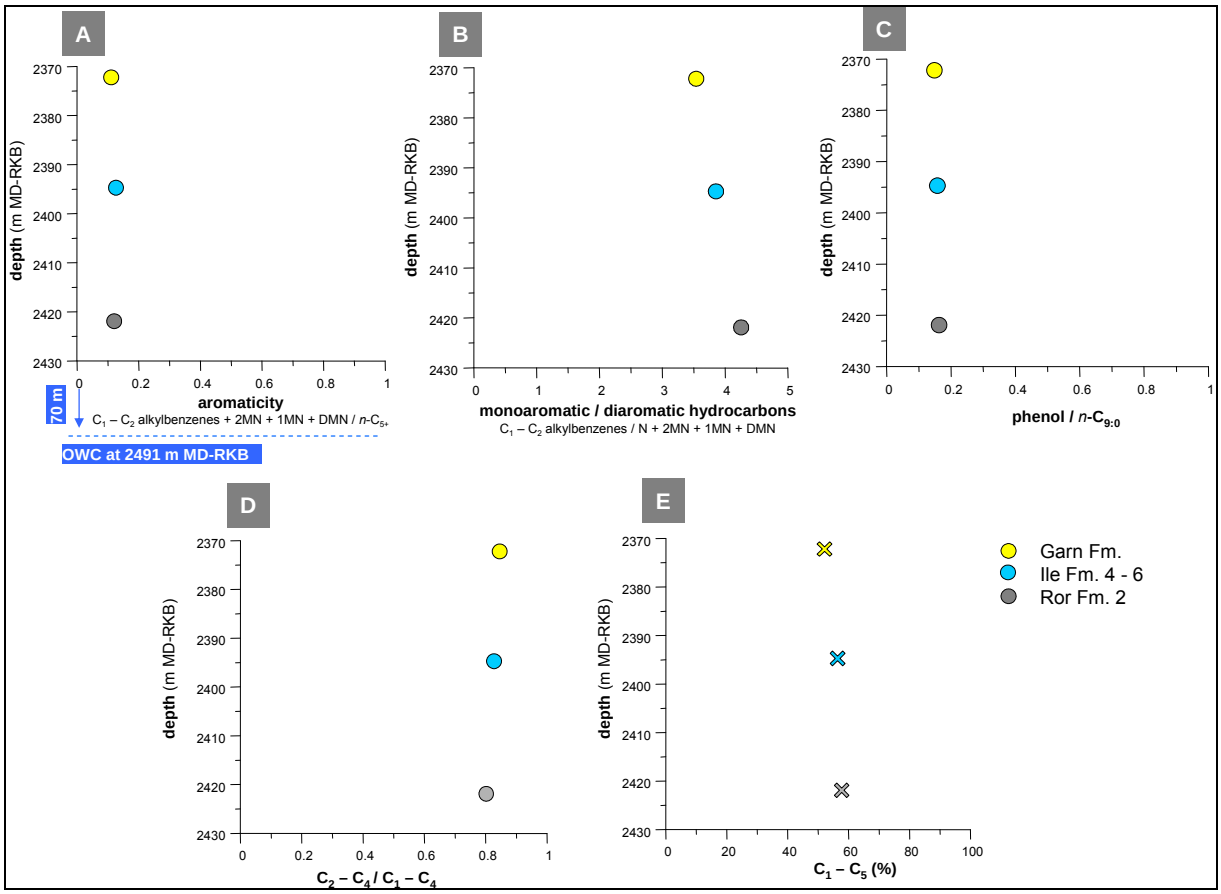

Figure 82 Geochemical profiles of the pyrolysis products from the reservoir rock screening of well 6507/7-3. From A to D the aromaticity (A), monoaromatic/diaromatic hydrocarbon ratio (B), relative phenol amount (C), gas wetness (D) and gas amount (E) are shown.

The pyrolysates of all reservoir rocks show a normal distribution of alkene/alkane doublets up to C_{30}. Towards higher retention times, elevated alkanes up to C_{35} were detected in the pyrolysates. Exemplary the pyrolysis gas chromatogram of reservoir rock sample G004003 (Ile Fm. 4 - 6) is shown in Figure 83.

The aromaticity is low with 0.10 - 0.12 and nearly constant within profile 6507/7-3 (Figure 82 A). Very slight changes were observed for the type of aromatic hydrocarbon ratio, gas wetness and gas amount (Figure 81 B, D, and E). The gas wetness slightly decreases with increasing depth from 0.82 to 0.78, while the type of aromatic hydrocarbon ratio and the gas amount slightly increases. Additionally, GOR and UCM are nearly constant within in the profile.

Similar homogeneity in the pyrolysis products have been observed before in well 6507/7-5 (cf. Chapter 6.4.1.2). Both, well 6507/7-3 and well 6507/7-5 are located in the western part of the Heidrun oil field, which received the most recent non-degraded oil charge (internal Statoil report, 2003). Thus, again the homogeneous distribution might suggest an indication that

mixing processes between the prior biodegraded oil charge(s) and the non-degraded recent oil charge are still going on.

6.4.3.2.1 ORGANOFACIES AND/OR MATURITY DIFFERENCES

Within the CLD ternary, the reservoir rock samples from well 6507/7-3 plot in the paraffinic high wax oil field (Figure 83 A). The samples are characterised by a higher proportion of long alkyl chains in their pyrolysates that decreases from the top to the bottom of the profile from the Garn Fm. to the Ile Fm. 4 - 6, and the Ror Fm. 2.. The reservoir rocks have a slightly different CLD compared to the potential source rock from the marine Spekk Formation. Higher content of long chain alkanes in the high molecular weight fraction reflect higher wax content and might point to a lacustrine influence of the source rock depositional environment. All reservoir rocks have a low phenol- as well as in sulphur content (Figure 83 B - D).

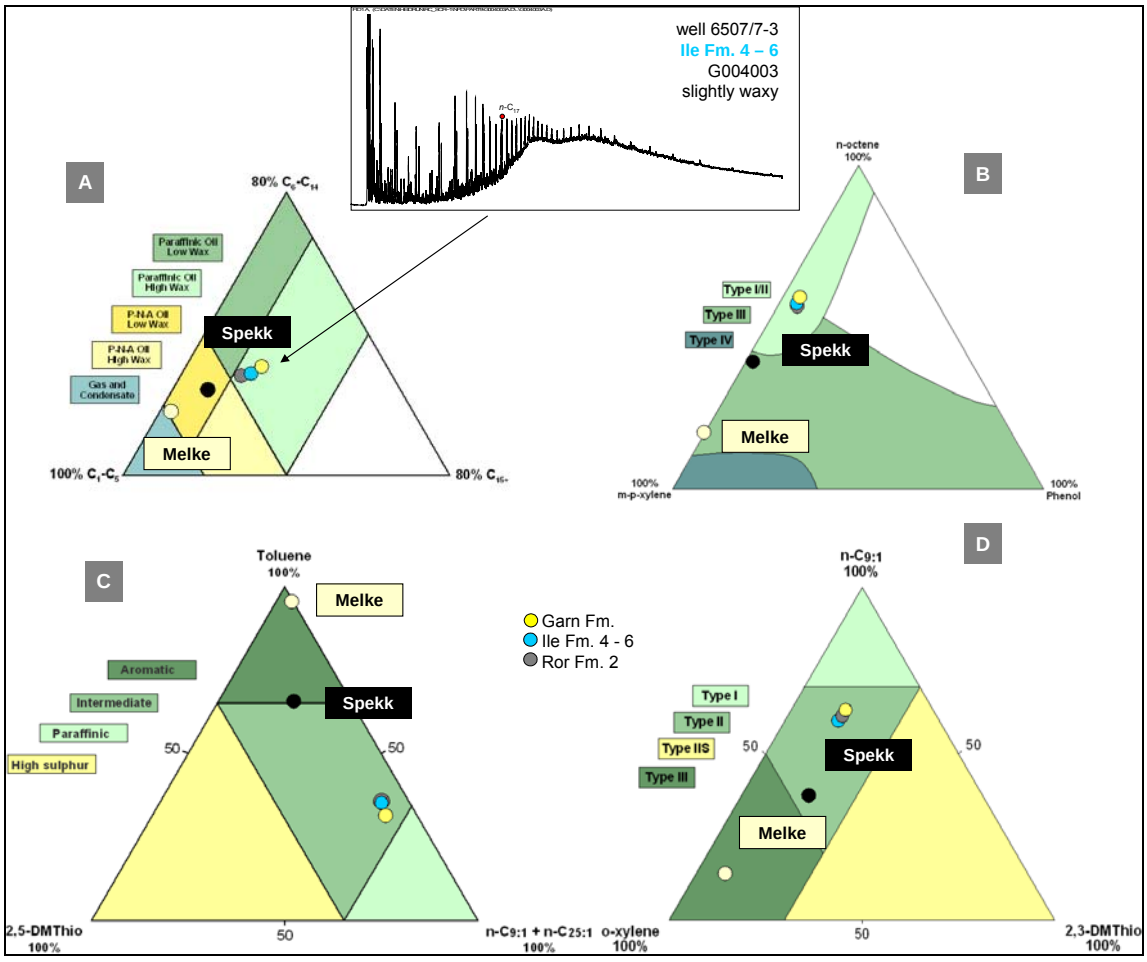

Figure 83 Bulk properties of the reservoir- and source rock pyrolysis products of well 6507/7-3 concerning (A) alkyl chain length distribution, (B) phenol content, and (C - D) sulphur content. The pyrolysis gas chromatogram show reservoir rock sample G004003 from the Ile Fm. 4 - 6) characterised by slightly higher amounts of long alkyl chains.

6.4.3.2.2 CORRELATION TO PHYSICAL ROCK PROPERTIES (WELL LOG DATA)

A section of the well log is shown in Figure 16. The resistivity and the acoustic signal are relatively low and uniform within the sampled interval and refer to relatively high water saturation. Slightly higher porosity of the Garn Fm. and Ile Fm. 4 - 6 sandstones compared to the more fine-grained Ror Fm. 2 mudstones/sandstones, are not reflected in the uniform pyrolysis parameters. Additionally, the shale zone detected in the Ile Fm. at 2400 m - 2410 m MD-RKB shows no influence on the pyrolysates.

In summary, independent of the reservoir formation, the analysed reservoir rock samples are characterised by uniform bulk properties. The reservoir rock samples have a high oil quality and show a homogeneous OM distribution in the profile. The aromaticity is very low. Slight gradients were observed for the type of aromatic hydrocarbon ratio, gas wetness and gas amount. Additionally, the physical rock properties do not indicate significant differences within the profile.

The reservoir rock samples show slightly higher amounts of medium and long alkyl chains (waxy compounds) in their pyrolysates compared to the potential source rock from the Spekk Formation. This could be an indication for a lacustrine influence of the source depositional environment.

This homogeneous distribution of the pyrolysis products in well 6507/7-3 might be an indication that mixing processes between different oil charges are still going on, because thermodynamically gradients have not yet set up in the oil column. Similar homogeneity shows well 6507/7-5 in the western part of the Heidrun field.

6.4.4 WELL 6507/7-4 IN SEGMENT C (GARN FM., ILE FM. 6 - 5)

6.4.4.1 PRODUCTION INDEX AND ORGANIC RICHNESS

The four reservoir rocks analysed from the cored section of well 6507/7-4 are from the Garn Fm. and Ile Fm. 5 - 6. With PI about 0.68 ± 0.02, the reservoir rock samples show a relatively high oil quality, compared to the remaining wells analysed in the Heidrun oil field. Within the well only slight variabilities in the PI were observed (Figure 25, Table X 1). The highest PI was detected below the OWC in the water column.

The OM content decreases stepwise with increasing depth towards the OWC from 15.7 mg/g rock to 6.7 mg/g rock (Figure 26, Table X 1). The reservoir rock from the water column shows lowest OM content.

6.4.4.2 ORGANIC MATTER COMPOSITION

The pyrolysis gas chromatograms of well 6507/7-4 are relatively uniform and present a normal distribution of alkene/alkane doublets up to C_{28}. Towards higher retention times, alkane peaks up to C_{33} were detected in the pyrolysates. Figure 84 A - E show the pyrolysis products of well 6507/7-4 in geochemical depth plots for the aromaticity (A), monoaromatic / diaromatic hydrocarbon ratio (B), phenol content (C), gas wetness (D) and gas amount (E). The average values and standard deviations for the bulk pyrolysis parameters can be seen in Table X 2. The Py-GC parameter values for the individual reservoir rocks are listed in Table X 9 in the appendix.

The aromatic compounds vary between both reservoir formations. The single Garn Fm. reservoir rock show distinctly lower aromaticity with 0.13 and a higher amount of monoaromatic hydrocarbons in its pyrolysates compared to the three Ile Fm. 5 - 6 reservoir rocks located close to the OWC (Figure 84 A and B). In addition, the Garn Fm. reservoir rock sample shows higher gas wetness, lower gas amount and lower amount of phenolic compounds (Figure 84 C - E).

Reservoir rock pyrolysates of the Ile Fm. 5 - 6 present similar gradients for aromaticity, monoaromatic/diaromatic hydrocarbon ratio, phenol compounds and gas wetness. These ratios increase to the OWC and decrease below. They correlate linearly and are obviously related to the increase in water saturation near the OWC.

The differences in aromatic compound composition between both reservoir formations are reflected in the GOR and the UCM. Lowest GOR shows the Garn Fm. reservoir rock sample. The Ile Fm. 5 - 6 reservoir rocks show higher GOR as well as UCM, and mirror the gradient observed in the pyrolysis parameters mentioned above.

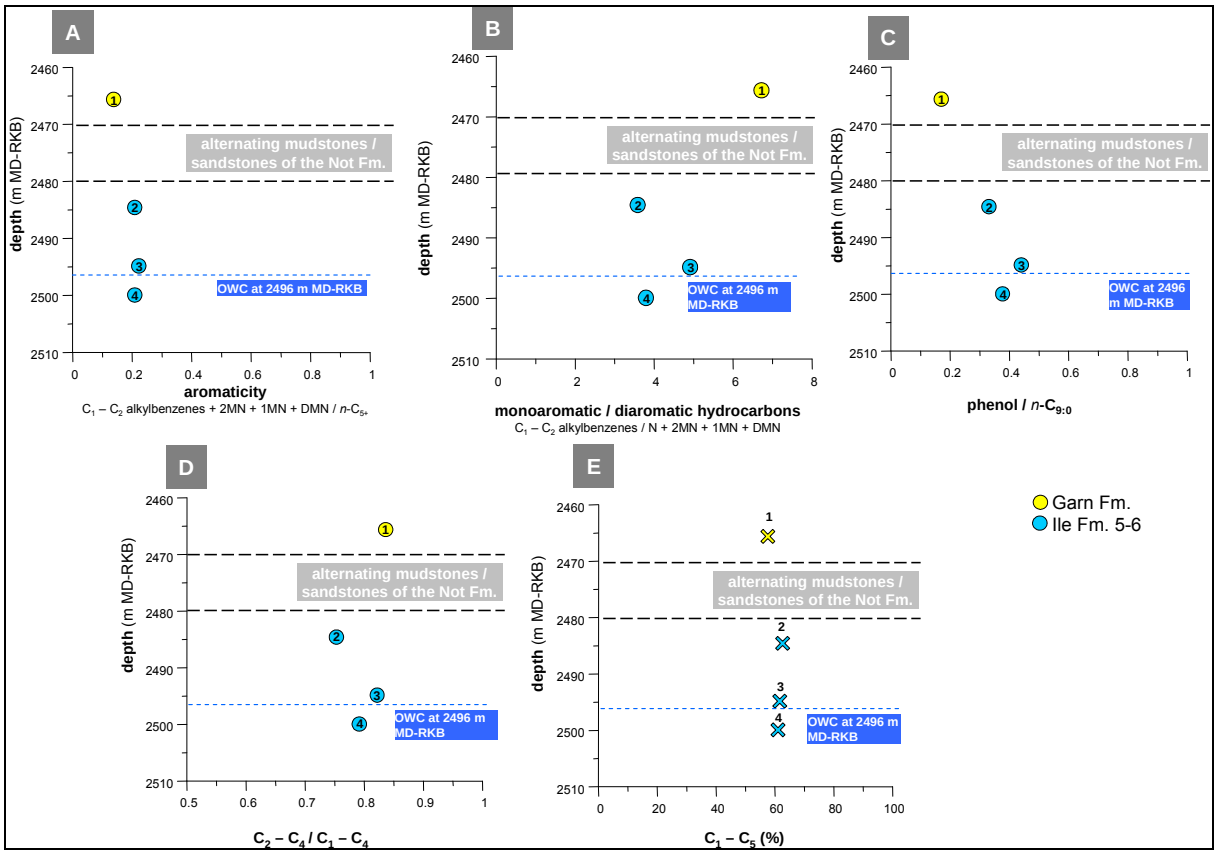

Figure 84 Geochemical profiles of the pyrolysis products from the reservoir rock screening of well 6507/7-4. From A to D the aromaticity (A), monoaromatic/diaromatic hydrocarbon ratio (B), relative phenol amount (C), gas wetness (D) and the gas amount (E) are shown.

6.4.4.2.1 ORGANOFACIES AND/OR MATURITY DIFFERENCES

Within the CLD, all reservoir rock samples plot close together at the transition from the P-N-A to the paraffinic oil field (Figure 85 A). They show relatively similar proportions of short, medium and long chains in their pyrolysates. However, for the Garn Fm. reservoir rock sample the highest proportion of medium alkyl chains was observed. Compared to the potential source rock from the Spekk Formation all reservoir rocks present a slightly higher proportion of medium and long chains in their pyrolysates. This is exemplary shown in the pyrolysis gas chromatogram of sample G004023 from the Garn Fm. (Figure 85 A). All reservoir rocks have additionally a low phenol as well as in sulphur content, and show slight differences regarding the aromaticity (Figure 85 B - D).

The higher content of medium and long alkyl chains in the high molecular weight fraction reflect higher wax content in the reservoir rock pyrolysates and suggest a lacustrine influenced depositional environment of the generative source.

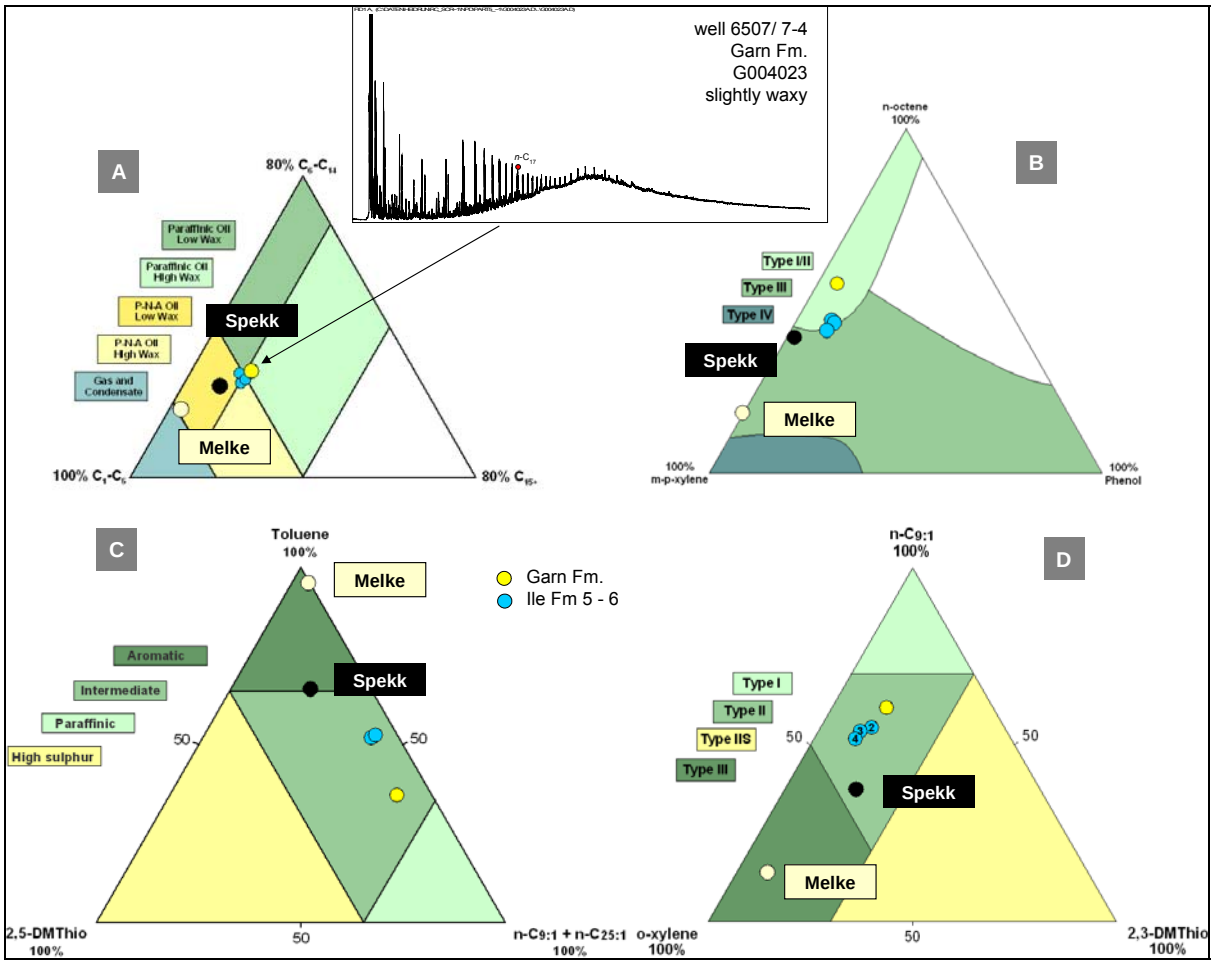

Figure 85 Bulk properties of the reservoir- and source rock pyrolysis products of well 6507/7-4 concerning (A) alkyl chain length distribution, (B) relative phenol content, and (C - D) relative sulphur content. The pyrolysis gas chromatogram of reservoir rock sample G004023 from the Garn Fm. shows exemplary the larger amounts of medium- and long alkyl chains, which are typical for all reservoir rocks within well 6507/7-4.

6.4.4.2.2 CORRELATION TO PHYSICAL ROCK PROPERTIES (WELL LOG DATA)

The Garn Fm. reservoir rock from the oil-saturated zone is characterised by lower water saturation compared to the three underlying Ile Fm. reservoir rocks located close to the OWC, where low resistivity signals indicate higher water saturation. A well log section of profile 6507/7-4 is shown in Figure 17.

Concerning the pyrolysis products, the decrease in resistivity to the OWC correlates to the stepwise decrease in the OM content and a slight increase in aromaticity. Strong variabilities in the porosity between the Garn and the Ile reservoir formations can be excluded due to uniform acoustic signal. Thus, the lower aromaticity in the Garn Fm. compared to the Ile Fm. might be related to better reservoir properties, but especially to the lower water saturation.

The combination of high water saturation, diminishing OM content and increase in aromaticity in the Ile Fm. 5-6 might be an indication for higher microbial activity near the OWC. Similar observations were made in the Ile Fm. of well C.
The zone of alternating shales and sandstones of the Not Fm. may additionally act as barrier between the Garn- and the Ile Formation.

In summary, the reservoir rock samples show slight variabilities in the oil quality (PI) and a stepwise decrease in the OM content with increasing depth. Within the aromatic compounds, gradients and differences between the Garn Fm. and the Ile Fm. 5 - 6 were observed. The Garn Fm. reservoir rocks show lower aromaticity and higher gas wetness compared to the Ile Fm. 5 - 6. Reservoir rocks of the Ile Fm. show similar gradients for all pyrolysis parameters, the gas amount excluded, which is less variable in the profile. The aromaticity and the remaining Py-GC parameters increase down to the OWC and show a slight decrease below the OWC. The differences in the pyrolysis products of the Garn and the Ile Fm. are reflected by the water saturation within the profile (lower aromaticity = lower S_w). Additionally, an influence of the shaly Not Fm. as potential barrier between the Garn- and the Ile Formation has to be considered.
All reservoir rock samples contain slightly higher proportions of medium- and long chains in their pyrolysates compared to the potential source rock from the Spekk Formation. This refers to higher content of waxy compounds in the reservoir rocks, which might be an indication to a lacustrine influence of the generating source.

6.5 CHARACTERISATION OF THE SINGLE PROFILES IN THE SOUTHERN PART OF THE HEIDRUN OIL FIELD

6.5.1 WELL 6507/7-8 IN SEGMENT F (MELKE FM., GARN FM., ILE FM.)

6.5.1.1 PRODUCTION INDEX AND ORGANIC RICHNESS

One reservoir rock from the Garn Fm., three reservoir rocks from the Ile Fm., and the potential source rock form the Melke Fm. were sampled from well 6507/7-8.

The lowest PI with 0.47 and thus the lowest oil quality shows the Melke Fm. source rock sample on top of the profile (Figure 25, Table X 1). The two reservoir Formations Garn and Ile show differences in the oil quality. The Garn Fm. reservoir rock sample shows a PI of 0.75, whereas the Ile Fm. samples presents lower mean PI of 0.63 ± 0.10 and a decreasing gradient to the OWC from 0.73 to 0.53. The very low oil quality of the lowermost Ile Fm. reservoir rock suggests *in-situ* organic matter within in this sample.
The OM distribution is very heterogeneous (Figure 26, Table X 1). The potential source rock from the Melke FM. and the lowermost Ile Fm. reservoir rock show lowest OM contents of 0.09 and 0.07 mg/g rock, respectively. Within the Ile Fm., a gradient was observed. Here, the OM amount decreases with increasing depth from 15.06 mg/g to 0.07 mg/g rock. The Garn Fm. reservoir rock shows organic matter content of 10.28 mg/g rock.

6.5.1.2 ORGANIC MATTER COMPOSITION

The reservoir rocks show compositional differences in their pyrolysates. Profile 6507/7-8 is characterised by a high aromatic layer on the top (G004008, Melke Fm.) and at the base (G004013, Ile Fm.). The remaining reservoir rocks show a normal alkene/alkane distribution pattern up to C_{28}. Between C_{28} and $C_{33,}$ elevated alkane peaks were observed.
In Figure 86 A - E, the pyrolysis products of well 6507/7-8 are shown in geochemical depth plots for the aromaticity (A), monoaromatic / diaromatic hydrocarbon ratio (B), relative phenol content (C), gas wetness (D) and gas amount (E). The average values and standard deviations for the bulk pyrolysis parameters can be seen in Table X 2 and the Py-GC parameter values for the individual reservoir rocks are listed in Table X 9 in the appendix.

The aromatic compounds vary in the Ile Fm. with increasing depth to the OWC. An increase in aromaticity from 0.14 to 1.58 was observed (Figure 86 A), which is similar to the curve like shape seen before in well C (Figure 30 A). Additionally, the type of aromatic hydrocarbon ratio increases from 3.83 up to 6.11 (Figure 86 B). Similar to the observations made before in the Ile Fm. of well C (Figure 31), the aromaticity show a linear correlation to the monoaromatic hydrocarbons, which increase relative to the diaromatic hydrocarbons (not shown). In addition, the gas amount increases with increasing depth parallel to the aromaticity (Figure 86 D). The gas wetness (Figure 86 D) is variable within the Ile Formation. However, the two upper Ile Fm. reservoir rock samples show an inverse correlation to aromaticity.

The lowermost Ile Fm. reservoir rock shows the highest aromaticity, mono/diaromatic hydrocarbon ratio, gas yield and the highest phenol ratio. In combination with the low PI (Figure 25), indications for disseminated coal were found. All remaining reservoir rocks have low relative phenol content

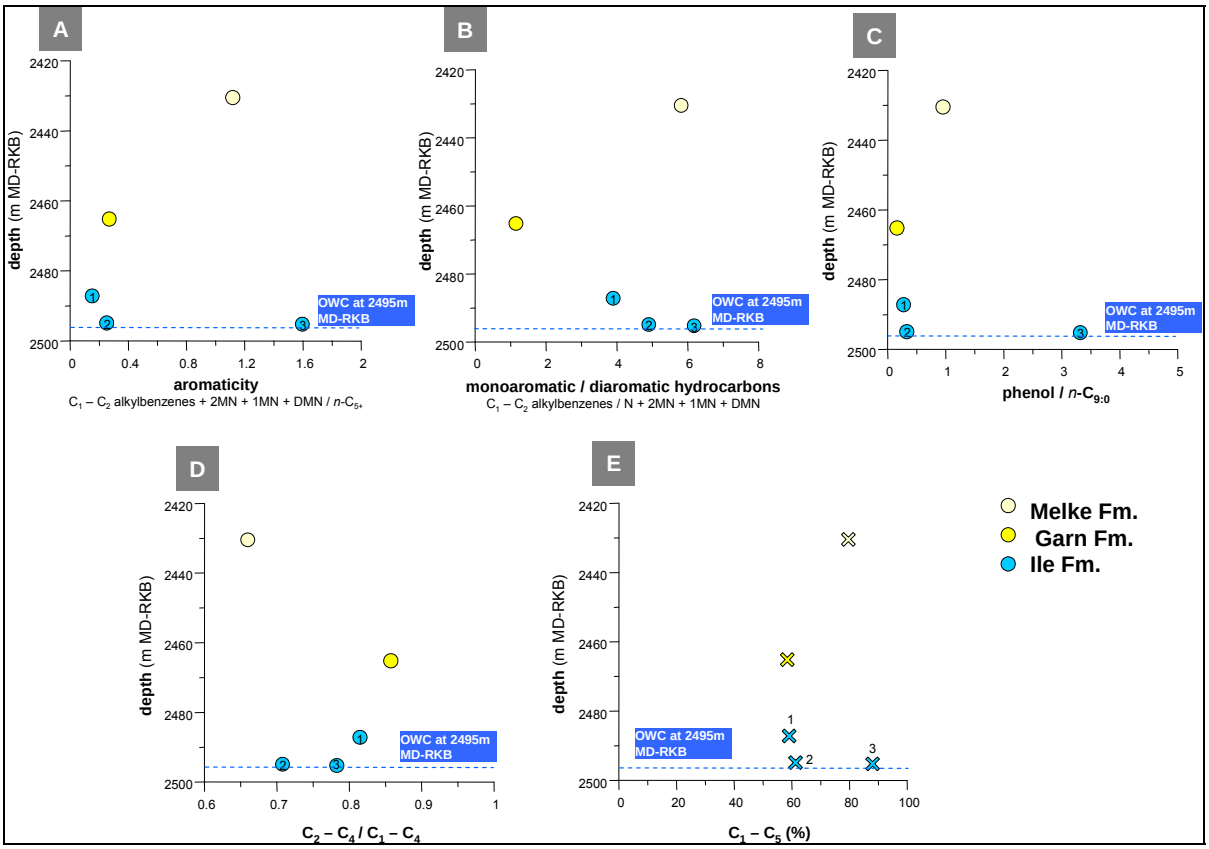

Figure 86 Geochemical profiles of the pyrolysis products from the reservoir rock screening of well 6507/7-8. From A to E the aromaticity (A), monoaromatic/diaromatic hydrocarbon ratio (B), relative phenol amount (C), gas wetness (D) and gas amount (E) are shown.

The potential source rock from the Melke Fm. shows similar bulk parameter ratios as the lowermost Ile Fm. reservoir rock, excepting a lower phenol ratio.

The aromaticity of the Garn Fm. reservoir rock is comparable to the Ile Fm. reservoir rocks no. 1 and 2 = G004010 and G004012. Additionally, it shows the lowest monoaromatic / diaromatic hydrocarbon ratio and the highest gas wetness in well 6507/7-8.

The GOR increases from the Garn Fm. to the Ile Fm. reservoir rocks, the lowermost coaly samples G004013 excluded. The UCM mirror these trend and decreases to the OWC.

6.5.1.2.1 ORGANOFACIES AND/OR MATURITY DIFFERENCES

Within the CLD ternary, the Ile Fm. reservoir rocks no. 1 and 2 (G004010 and G004012) and the Garn Fm. reservoir rock G004009 plot in the P-N-A oil composition field at the transition to the paraffinic oil field (Figure 87 A). These three reservoir rock samples show nearly similar proportions of short, medium and long chains in their pyrolysates compared to the CLD of the Spekk Formation. The lowermost Ile Fm. reservoir rock no. 3 = G004013 shows higher proportions of short chains in its pyrolysates and plot in the gas and condensate field closer to the potential source rock from the Melke Formation.

The phenol ternary (Figure 87 B) reflect higher phenol amounts in the Ile Fm. reservoir rock G004013 and the potential source rock from the Melke Fm. observed before in the depth plots and differences in aromaticity.

The two sulphur ternaries reflect low sulphur content for all rock samples independent of their reservoir formation as well as differences in aromaticity (Figure 87 C and D).

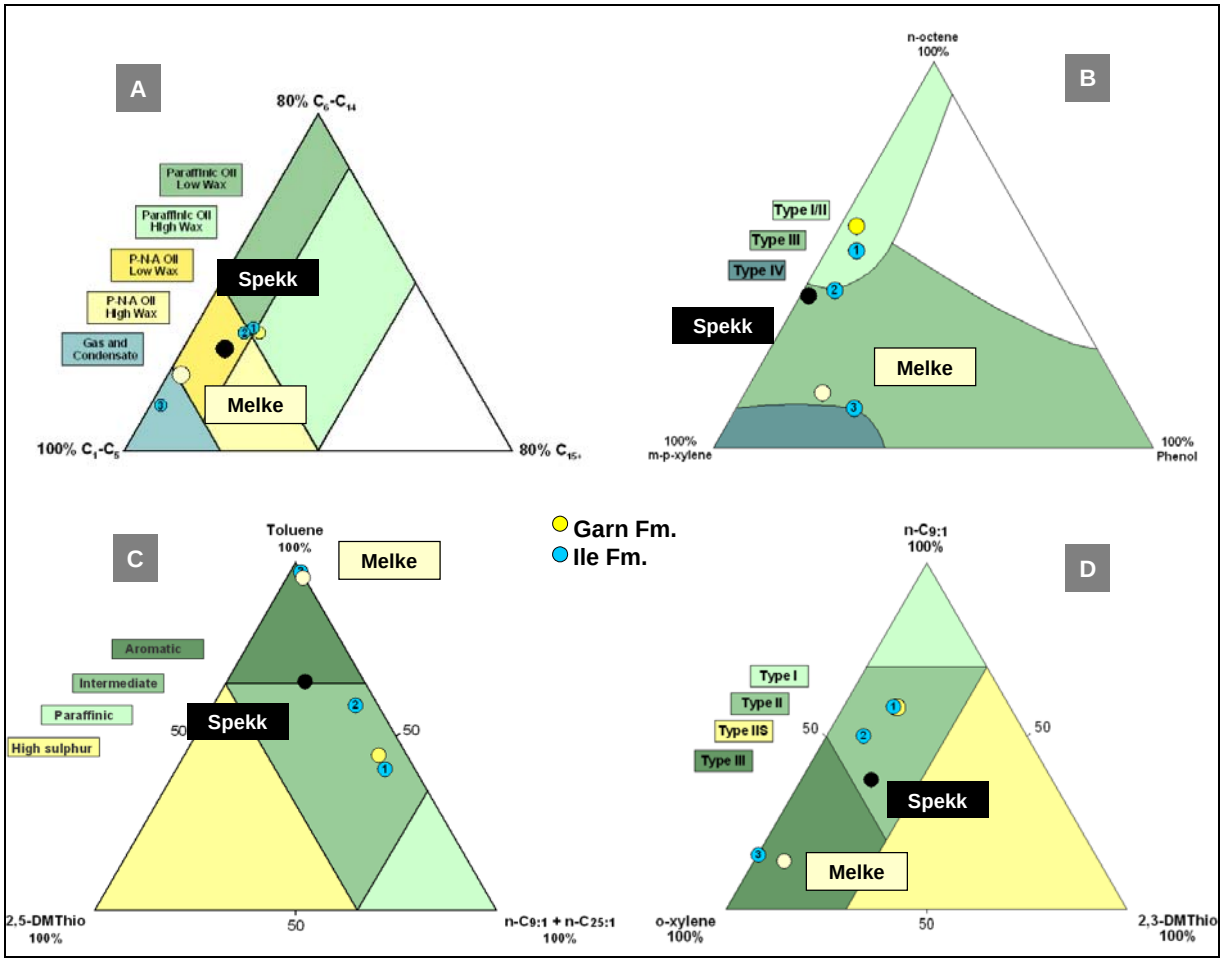

Figure 87 Bulk properties of the reservoir rock and source rock pyrolysates of well 6507/7-8 concerning (A) alkyl chain length distribution, (B) relative phenol content, and (C - D) relative sulphur content.

The potential source rock from the Melke Fm. shows indications for a terrestrial influence of the source depositional environment. The reservoir rocks show no differences concerning the organofacies of the source rock depositional environment.

6.5.1.2.2 CORRELATION TO PHYSICAL ROCK PROPERTIES (WELL LOG DATA)

No well log signals are recorded for the interval of interest, excepting the resistivity signal, which decreases in the Ile Fm. to the OWC and indicate an increase in the water saturation. In combination to the diminishing OM content and the increase in aromaticity, this might be an indication for higher microbial activity around the OWC. Similar observations at the OWC were made in the Ile Fm. of well C and well 6507/7-4.

In summary, the Ile Fm. reservoir rocks shows gradients within the profile to the OWC for PI, OM and aromatic compounds. The aromaticity increases with increasing depth and reflects the curve like shape of the data points observed before for the Ile Fm. reservoir rocks in well C at to the OWC. The type of aromatic hydrocarbon ratio and the gas amount are linear correlated to aromaticity as observed for the Ile Fm. in well C. The gas wetness is variable within the Ile Fm.; however, both upper Ile Fm. reservoir rock samples show an inverse correlation of aromaticity and gas wetness. In the lowermost Ile Fm. reservoir rock sample, disseminated coal particles were detected. The potential source rock of the Melke Fm. shows similar pyrolysis products like the lowermost Ile Fm. reservoir rock.
The potential source rock of the Melke Fm. gives indications to a terrestrial influence of the source depositional environment. The reservoir rocks show no differences in the organofacies of the source rock depositional environment.
The aromaticity and the water saturation are apparently linked within profile 6507/7-8. Indications were found in the Ile Fm. reservoir rocks, where the combination of increasing water saturation, diminishing OM and increasing aromaticity, suggest higher microbial activity near the OWC.

6.5.2 WELL 6507/8-1 IN SEGMENT I (TILJE FM. 3.3 - 1)

6.5.2.1 PRODUCTION INDEX AND ORGANIC RICHNESS

All five reservoir rocks of well 6507/8-1 are from the Tilje Fm. 3.3 - 1. The profile shows slight variabilities in oil quality with mean PI = 0.59 ± 0.02) (Figure 25, Table X 1). In the lower part of the profile, the PI decreases with increasing depth.
The mean OM content is 19.03 mg/g rock ± 6.83 (Figure 26, Table X 1). Within the profile, the OM distribution shows a V-shaped gradient similar as observed before in well 6507/8-4 (cf. Chapter 6.3.3). The OM content increases in the upper part of the profile and decreases in the three lower reservoir rocks down to the OWC. The decrease in OM is parallel to the decrease in the oil quality (PI).

6.5.2.2 ORGANIC MATTER COMPOSITION

In Figure 88 A - E, the pyrolysis products of well 6507/8-1 are shown in geochemical depth plots for the aromaticity (A), monoaromatic / diaromatic hydrocarbon ratio (B), relative phenol content (C), gas wetness (D) and gas amount (E). The average values and standard deviations for the bulk pyrolysis parameters can be seen in Table X 2, the Py-GC parameter values for the individual reservoir rocks are listed in Table X 9 in the appendix. Two calcite-cemented zones were detected in the investigated core section of well 6507/8-1. They are marked in the geochemical depth plots in Figure 88 A - E.

The uppermost reservoir rock sample G004036 shows different values for all bulk parameter ratios. This sample is characterised by the highest aromaticity with 0.60, gas wetness and gas amount as well as the lowest monoaromatic/diaromatic hydrocarbon ratio indicating a higher content of 2-ring aromatic compounds in the pyrolysates, and a very low phenol ratio.
The remaining reservoir rock samples show slight differences in their pyrolysis parameters. The aromaticity is relatively uniform, excluding the penultimate reservoir rock sample (Figure 88 A). The gas wetness and gas amount slightly decreases with increasing depth (Figure 88 D and E).
No indications for terrestrial organic matter were found, as the phenol ratio is low for all reservoir rocks (Figure 88 C). The pyrolysis parameters do not correlate to trends observed regarding PI and OM distribution.

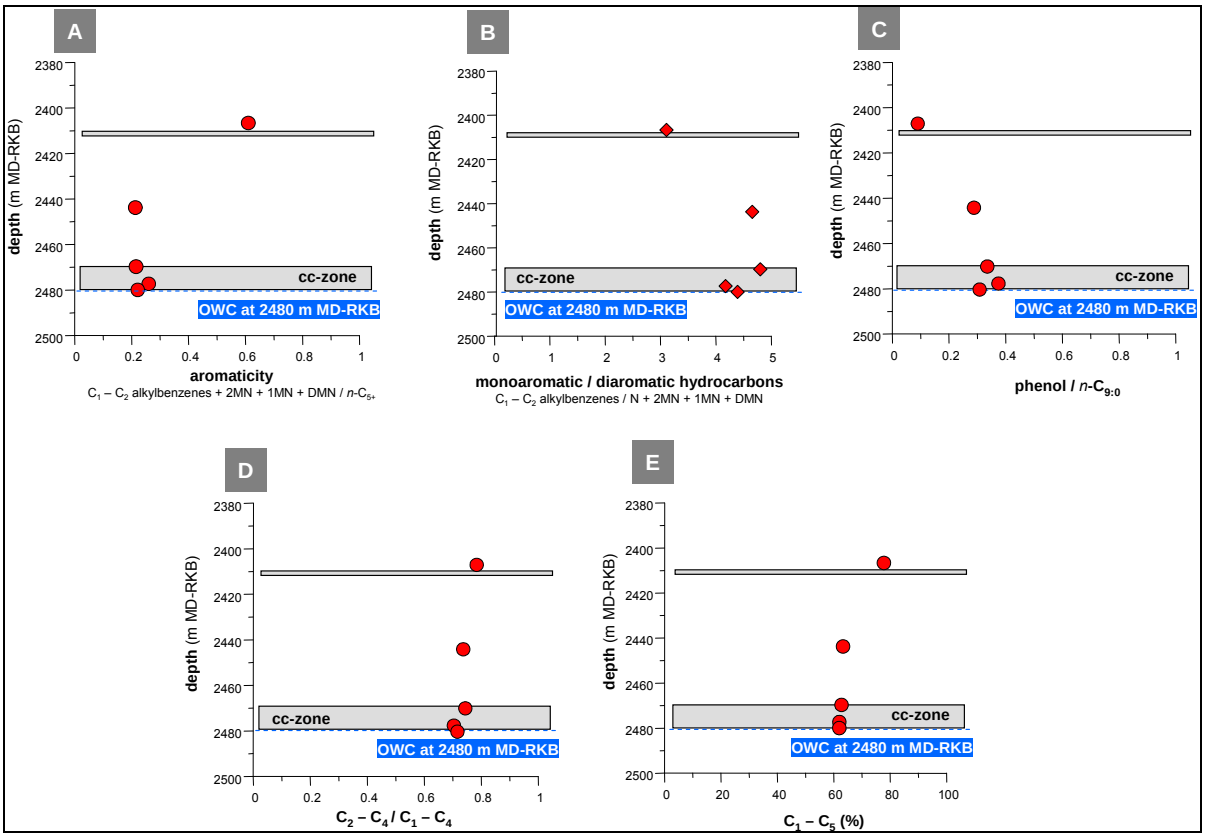

Figure 88 Geochemical profiles of the pyrolysis products from the reservoir rock screening of well 6507/8-1. From A to E the aromaticity (A), monoaromatic/diaromatic hydrocarbon ratio (B), relative phenol amount (C), gas wetness (D) and gas amount (E) are shown.

cc-zone - calcite-cemented zone

The GOR strongly decreases within profile 6507/8-1. However, the uppermost reservoir rock sample reveals distinctly higher GOR compared to the remaining reservoir rocks. The GOR and the UCM are inverse correlated (Figure 89).

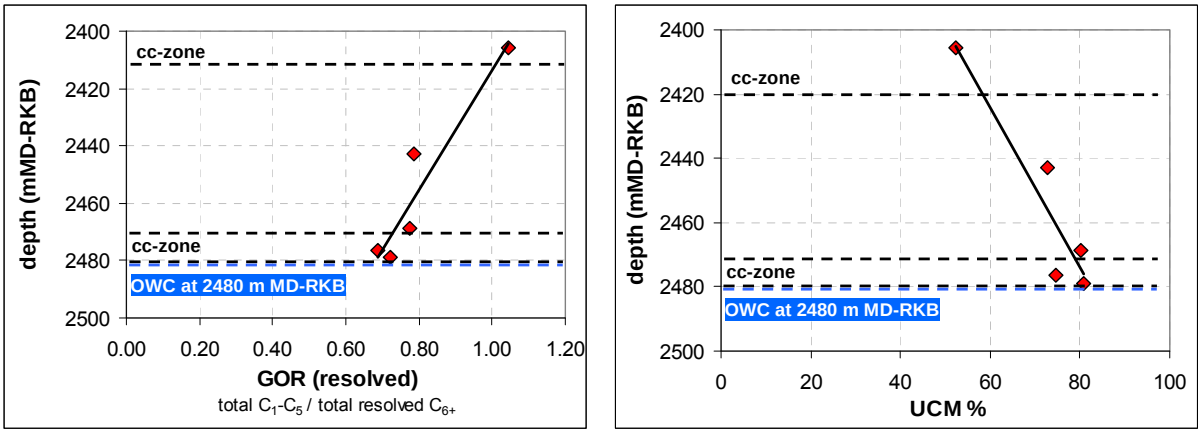

Figure 89 *Left* GOR analysed in the reservoir rocks of well 6507/8-1. *Right* Percentage of the unresolved compound mixture (UCM) of these reservoir rocks.

The differences observed in the uppermost sample might be related to the calcite-cemented zone at 2410 m MD-RKB, which may act as a flow barrier, leading to different compartments within the Tilje Formation.

6.5.2.2.1 ORGANOFACIES AND/OR MATURITY DIFFERENCES

The ternary diagrams in Figure 90 A - D reflect the results seen above in the geochemical profiles. Within the CLD ternary, all reservoir rocks plot in the P-N-A low wax oil field (Figure 90 A). Excepting the uppermost reservoir rock no 1 = G004036, the four remaining samples show relatively uniform proportions of short, medium and long chains in their pyrolysates, which are similar to the CLD of the potential source rock from the Spekk Formation. The CLD of the uppermost reservoir rock G004036 is more similar to the distribution observed in the potential source rock from the Melke Formation.

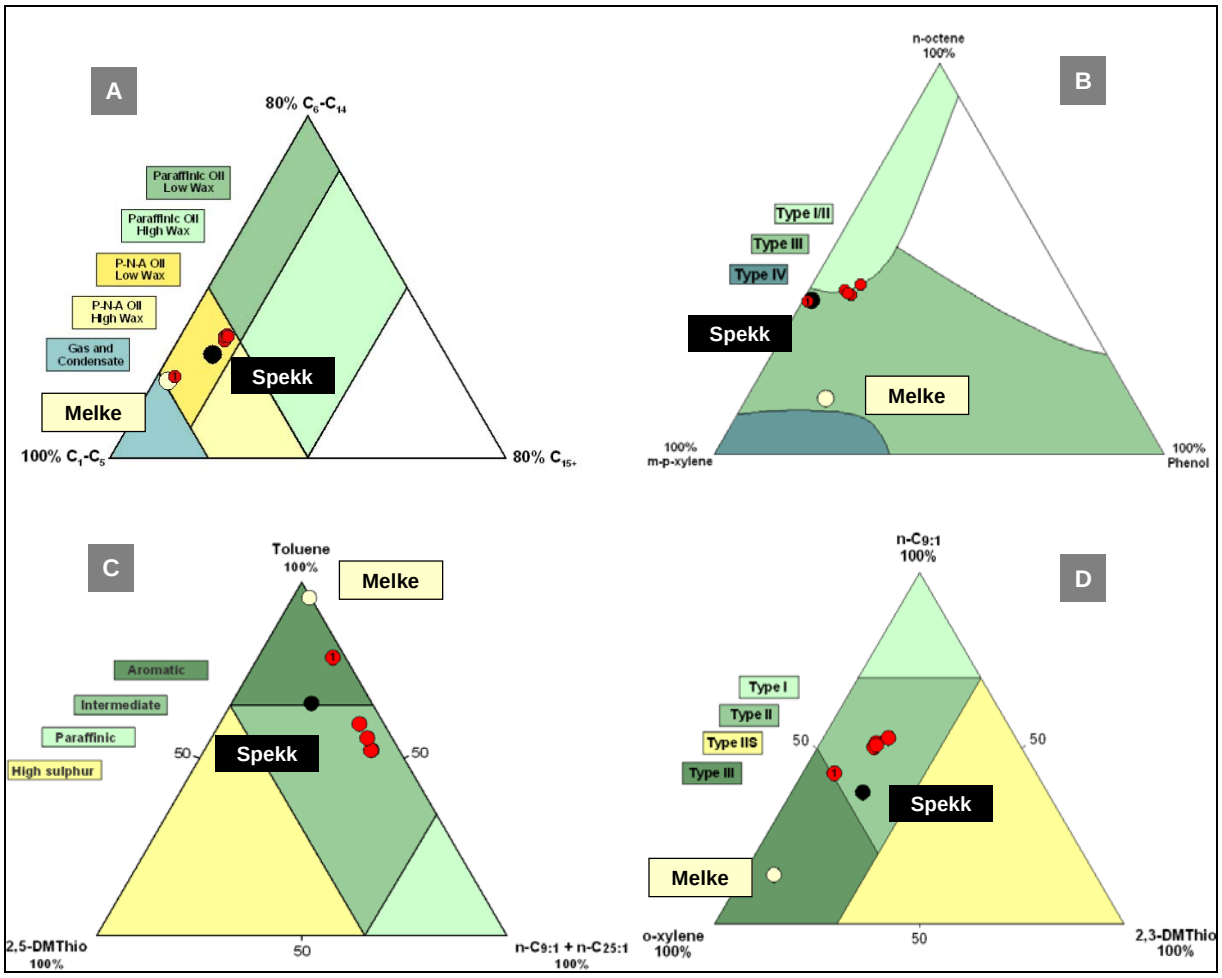

Figure 90 Bulk properties of the reservoir- and source rock pyrolysis products of well 6507/8-1 concerning (A) alkyl chain length distribution, (B) relative phenol content, and (C - D) relative sulphur content.

The relative phenol- and sulphur content are low for all reservoir rocks (Figure 90 B - D). Both, the sulphur and the phenol ternaries indicate differences in the aromaticity seen before in the geochemical profiles.

In-situ terrestrial OM deposited during the sedimentation of the reservoir rocks can be excluded. Thus, the higher proportions of short chains in the pyrolysates of the uppermost reservoir rock G004036 are not generated from the pyrolysis of terrestrial OM. The differences observed in the macromolecular fraction of this sample might be an indication for maturity differences of the potential source rock, because the higher the maturity of the source the higher the aromaticity and the gas content in the generated oil charge (England, 1989).

6.5.2.2.2 CORRELATION TO PHYSICAL ROCK PROPERTIES (WELL LOG DATA)

The dense calcite-cemented zone in the upper part of the profile at 2410 m MD-RKB might act as barrier for the hydrocarbon migration, influencing the heterogeneities observed in the pyrolysates between the upper reservoir rock and the remaining samples. The lower calcite-cemented zone at 2470 m - 2480 m MD-RKB is rather an indication for a paleo-OWC. Thus, the slight differences observed in the aromatic compounds in the lower part of the profile are probably an indication for higher microbial activity in this zone.
No direct influence of porosity changes, based on the acoustic log, and interstratified thin shale layer, based on the gamma ray log, of the pyrolysates has been observed based on exclusively visual comparison.

In summary, the gradient observed in OM content and oil quality (PI) does not correlate with trends observed in the pyrolysis parameters of the reservoir rocks. The uppermost reservoir rock sample of profile 6507/8-1 shows different amounts for all Py-GC parameter ratios. This sample is *inter alia* characterised by the highest aromaticity. The remaining reservoir rocks show slight differences in their pyrolysates. The uppermost reservoir rock presents a CLD similar to the distribution observed in the potential source rock from the Melke Formation. The CLD of the remaining reservoir rocks is more similar to the distribution observed for the potential source rock of the Spekk Formation.
The differences observed in the macromolecular fraction of the uppermost reservoir rock might be an indication for maturity differences of the potential source rock, as the presence of

in-situ terrestrial OM can be excluded. In addition, the calcite-cemented zone in the upper part of the profile might act as barrier and thus generate compartments with variable pyrolysates composition. Slight differences in the aromatic compounds near the OWC are rather the result of higher microbial activity in the water-saturated zone.

6.6 DATA SYNTHESIS FOR THE INDIVIDUAL RESERVOIR FORMATIONS

Many heterogeneities in the OM distribution and composition were detected within the individual wells of the Heidrun oil field using Py-GC. Based on the screening results, significant gradients were found within single wells from eastern (well A, B, and C), northern (well E, D, and 6507/8-4) and southern part (well 6507/7-8 and 6507/8-1) of the oil field. Wells, with relatively homogeneous OM composition and without significant gradients in the Py-GC parameters, were found predominantly in the western part of the Heidrun oil field (well 6507/7-3, 6507/7-4, 6507/7-5, 6507/7-2, and 6507/7-6).

In the following, the focus will be on the heterogeneities in the different reservoir formations. First bar charts are used in order to summarise and compare the observed heterogeneities and to illuminate correlations between the different Py-GC parameters. Subsequently, their distributions over the entire oil field are shown. Therefore, average Py-GC parameter values, analysed in the corresponding reservoir formations of the single wells, are used. The gradients detected in the Py-GC parameters are interpreted with reference to their position in the oilfield and correlated to potential causes leading to the present OM distribution, such as biodegradation, variabilities in the physical rock properties, organofacies and/or maturity differences of the generating source. Additionally, the heterogeneities and their relation to the reservoir age across the whole oilfield are interpreted.

6.6.1 ORGANIC MATTER COMPOSITION

In order to compare and summarise the observed heterogeneities, the bar chart plots in Figure 91 A - D show the Py-GC parameter aromaticity (A), gas wetness (B), gas percentage (C), and the monoaromatic versus diaromatic hydrocarbon ratio (D), from the lowest to the highest value. Each bar in these plots represents a single reservoir rock sample. The bar colour marks the corresponding reservoir formation.

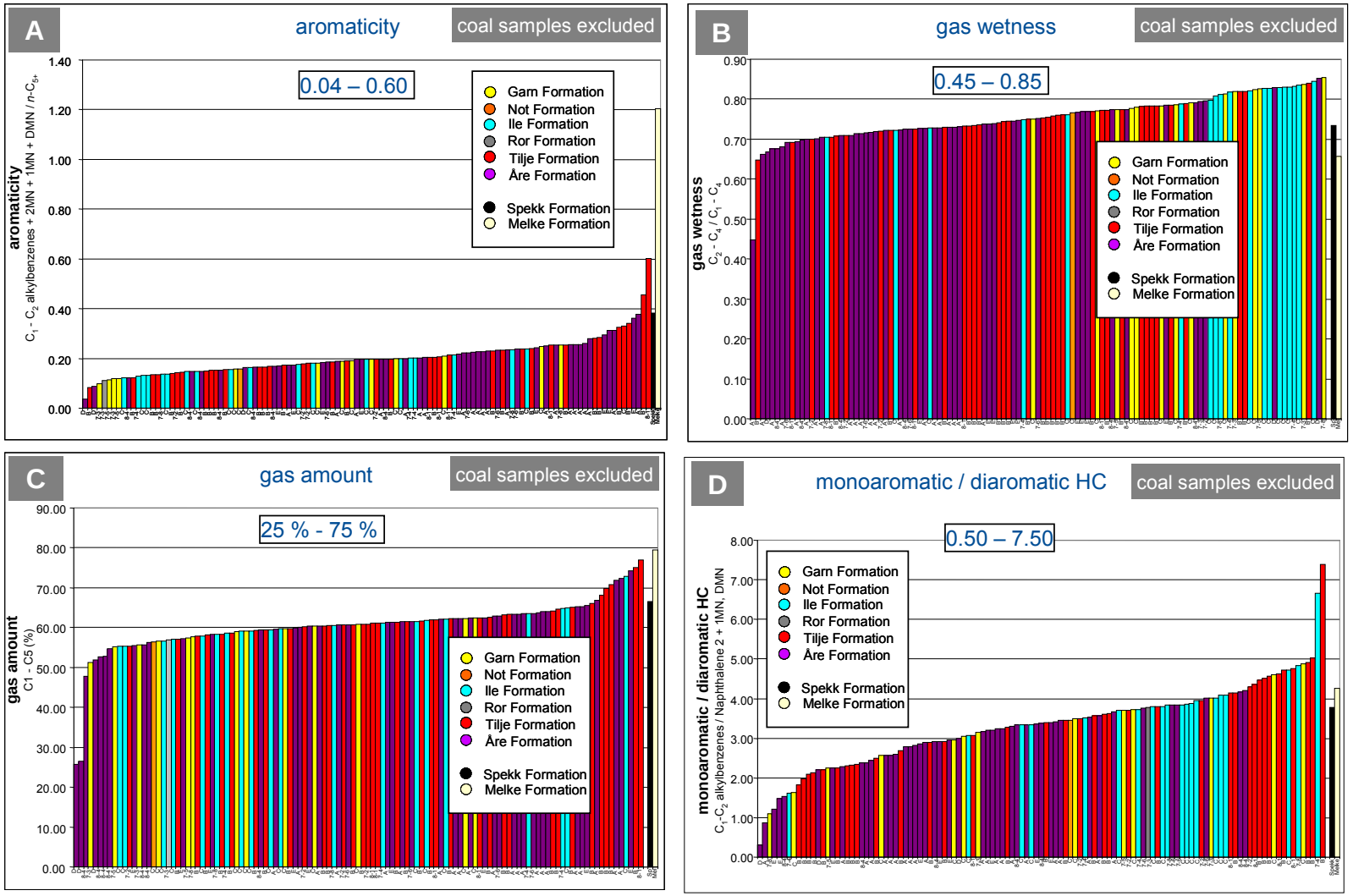

Figure 91 Bar chart diagrams showing the Py-GC parameter from the lowest to the highest value for all reservoir rock and both potential source rock samples analysed in the Heidrun oil field. From A to E the aromaticity (A), gas wetness (B), gas amount in % (C) and monoaromatic/diaromatic hydrocarbon ratio (D) are shown. Reservoir rocks with disseminated coal are disregarded in the plots.

Figure 91 A gives an overview of the aromaticity distribution in the Heidrun oil field. Its values vary between 0.04 and 0.60. Within the plot, the individual reservoir formations fall in discrete fields. Higher aromaticity is typical for the Åre Formation, while the Garn- and the Ile Formation are characterised by lower aromaticity. The greatest variability and the highest aromaticity were observed in the Tilje Formation.

Within the bar chart for the gas wetness, a clearer distribution pattern can be seen (Figure 91 B). All but one reservoir rock sample from the Åre Formation shows gas wetness between 0.65 and 0.85. Most of the Åre Formation reservoir rocks reveal low gas wetness (< 0.75), while the Garn- and especially the Ile Formation reservoir rocks show higher gas wetness (> 0.75). Nearly all rock samples with gas wetness above 0.80 are from the Ile Formation. The greatest variability was observed in the Tilje Formation.

Comparing aromaticity and gas wetness, the results for the individual reservoir formations clearly indicate a general inverse correlation of both parameters (Figure 92). However, most of the wells in the western and the southwestern part of the oilfield did not show a clear inverse correlation. The inverse correlation was predominantly observed in the eastern wells C (Garn- and Ile Fm.) and B (Tilje Fm.), and in the northern wells D, 6507/8-4 and 6507/7-6, all comprising the Åre Formation.

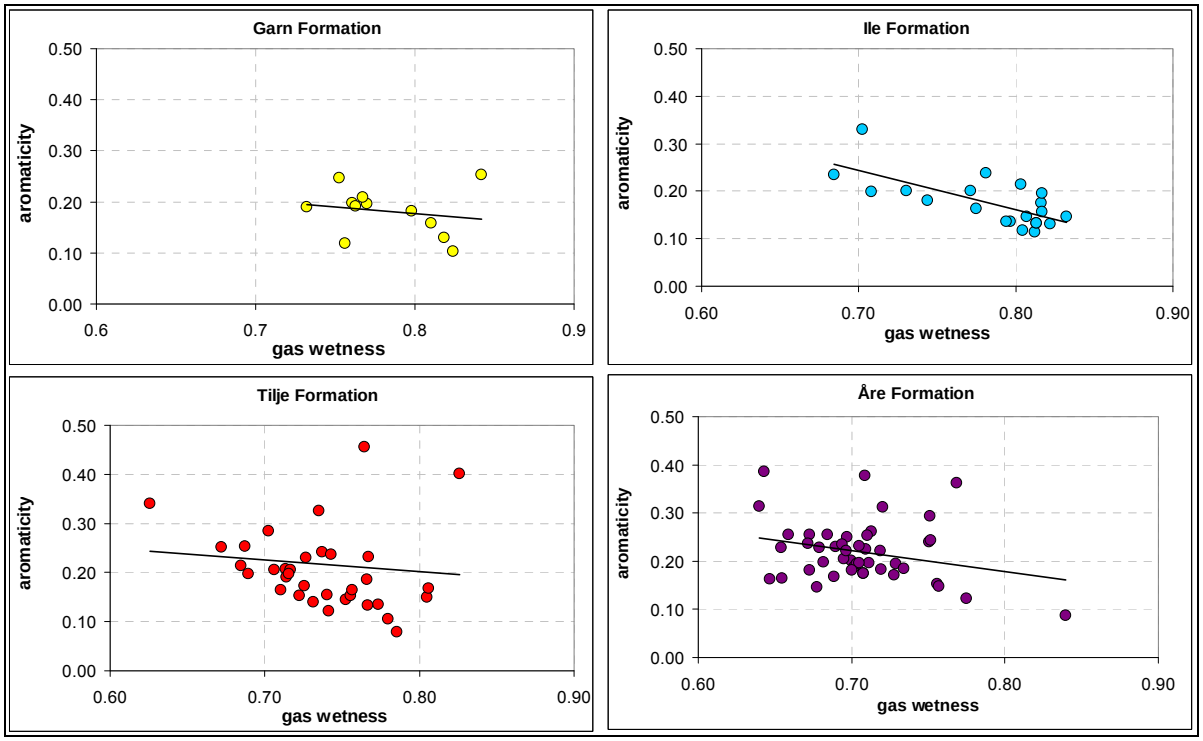

Figure 92 Inverse correlations of aromaticity and gas wetness for the individual reservoir formations Garn, Ile, Tilje and Åre. The two high aromatic reservoir rock samples from the Åre Formation (upper part of well D) are not considered in these plot. The black lines mark the trends observed.

All reservoir formations generate pyrolysis products whose gas contents fall between 25 % and 75 % (Figure 91 C). Two reservoir rocks from the Åre Formation of well D, characterised by large amounts of long alkyl chains, show a very low gas amount. The remaining reservoir rocks exhibit values between 50 % and 75 % and show a similar distribution as compared to the aromaticity (Figure 91 A). The gas amount in the reservoir rock pyrolysates shows a linear correlation to aromaticity (Figure 93). Here, the Åre Formation is characterised by the greatest variability.

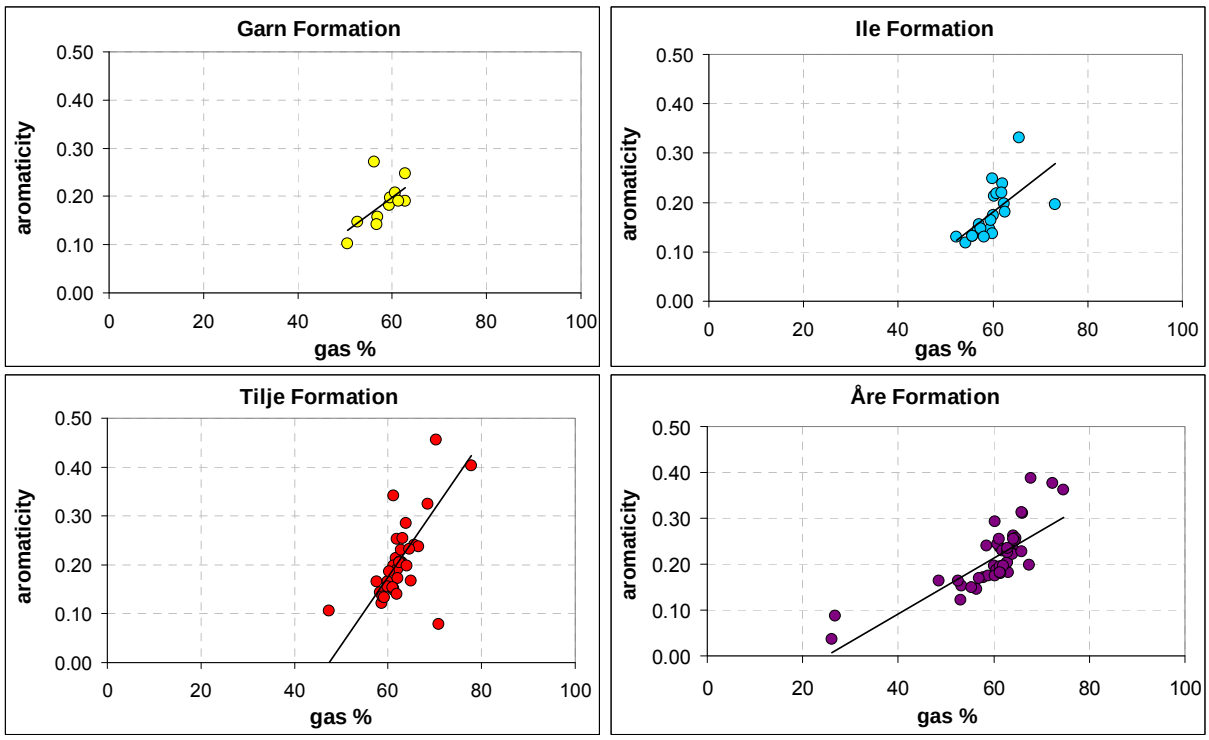

Figure 93 Linear correlations of the aromaticity and the gas percentage for the individual reservoir formations Garn, Ile, Tilje and Åre. The two highly aromatic reservoir rocks (upper part of well D) are not considered in these plot. The black lines mark the trends observed.

The bar chart for the monoaromatic / diaromatic hydrocarbon ratio indicates compositional variabilities in the organic matter (Figure 91 D). Ratios between 0.50 and 7.50 were observed. Predominantly the Tilje reservoir rocks and some reservoir rock samples from the Ile- and Garn Formations show higher ratios.

Comparing the the monoaromatic / diaromatic hydrocarbon ratio to the aromaticity, the Garn-, Tilje-, and Åre Formation show an inverse correlation (Figure 94). In contrast, the monoaromatic / diaromatic hydrocarbon ratio in the reservoir rocks of the Ile Fm. are linear correlated to the aromaticity. Concerning single wells, this comprises the Ile Fm. in well C and well 6507/7-8. The remaining wells comprising Ile Fm. are from the western part of the

oil field (6507/7-3, 6507/7-4 and 6507/7-5). They do not show clear trends due to the low samples density in these wells (1 - 3 reservoir rock samples).

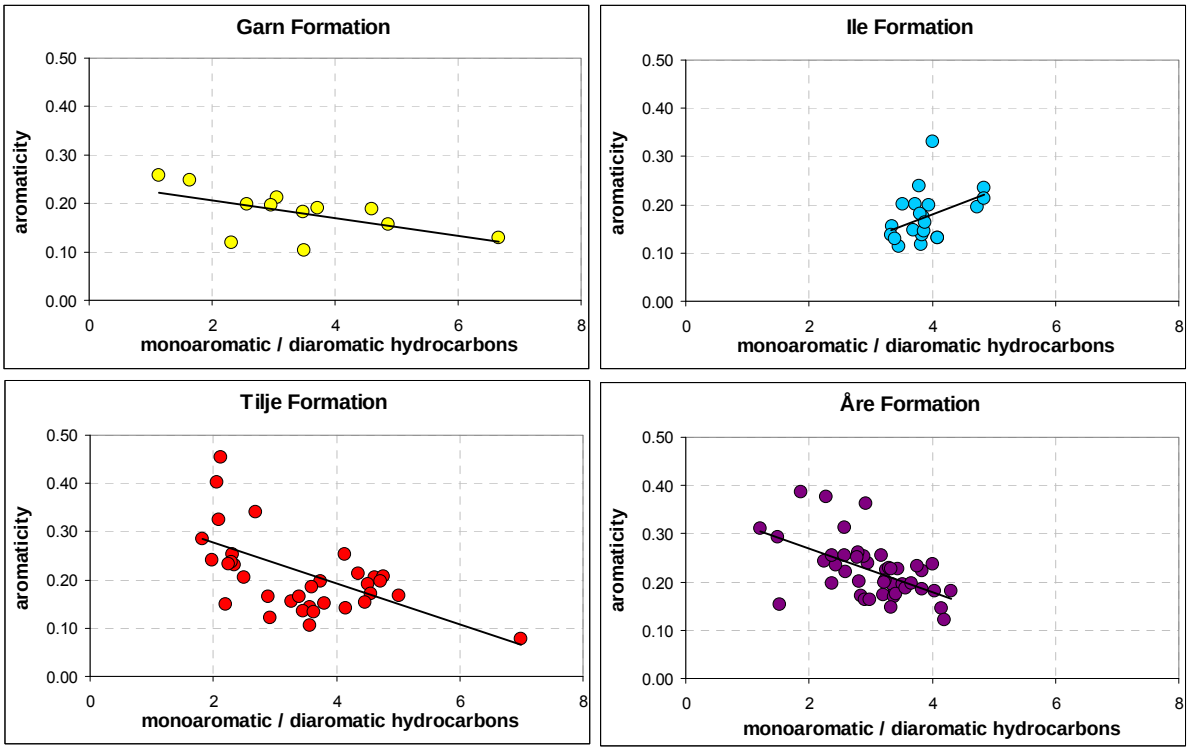

Figure 94 Correlations between of the aromaticity and the monoaromatic / diaromatic hydrocarbon ratio of the individual reservoir formations Garn, Ile, Tilje and Åre. The two high aromatic reservoir rock samples from the Åre Formation (upper part of well D) are not considered in these plot. The black lines mark the trends observed.

The potential source rock sample of the Spekk Formation shows Py-GC parameters that are all within the range of the values observed for the reservoir rock samples analysed. This is in contrast to the Melke Formation source rock, which exhibits the highest aromaticity and the highest gas amount compared to the analysed reservoir rocks. The gas wetness of the Melke Formation is very low and the monoaromatic / diaromatic hydrocarbon ratio is different to the Spekk Formation, but both parameters are within the ranges analysed for the reservoir rocks (Figure 91 A - D).

In order to obtain an overview on the Py-GC parameter distribution in the whole Heidrun reservoir, plots were prepared showing the Heidrun oil field with the average Py-GC parameter values analysed for the corresponding reservoir formations in the single wells. They are shown in Figure 95 A - D including aromaticity (A), gas wetness (B), gas amount (C) and monoaromatic versus diaromatic hydrocarbon ratio (D). The boxes in these Figures show the well name on the top, and below, the average values of the Py-GC parameter and the

standard deviation in brackets. The colour of the box represents the individual reservoir formation. Both, the Not- and the Ror Formation are disregarded in this comparison, because only one sample of each formation was analysed. Additionally, 23 reservoir rock samples with a phenol ratio above one indicating coal contributions are not considered in these plots.

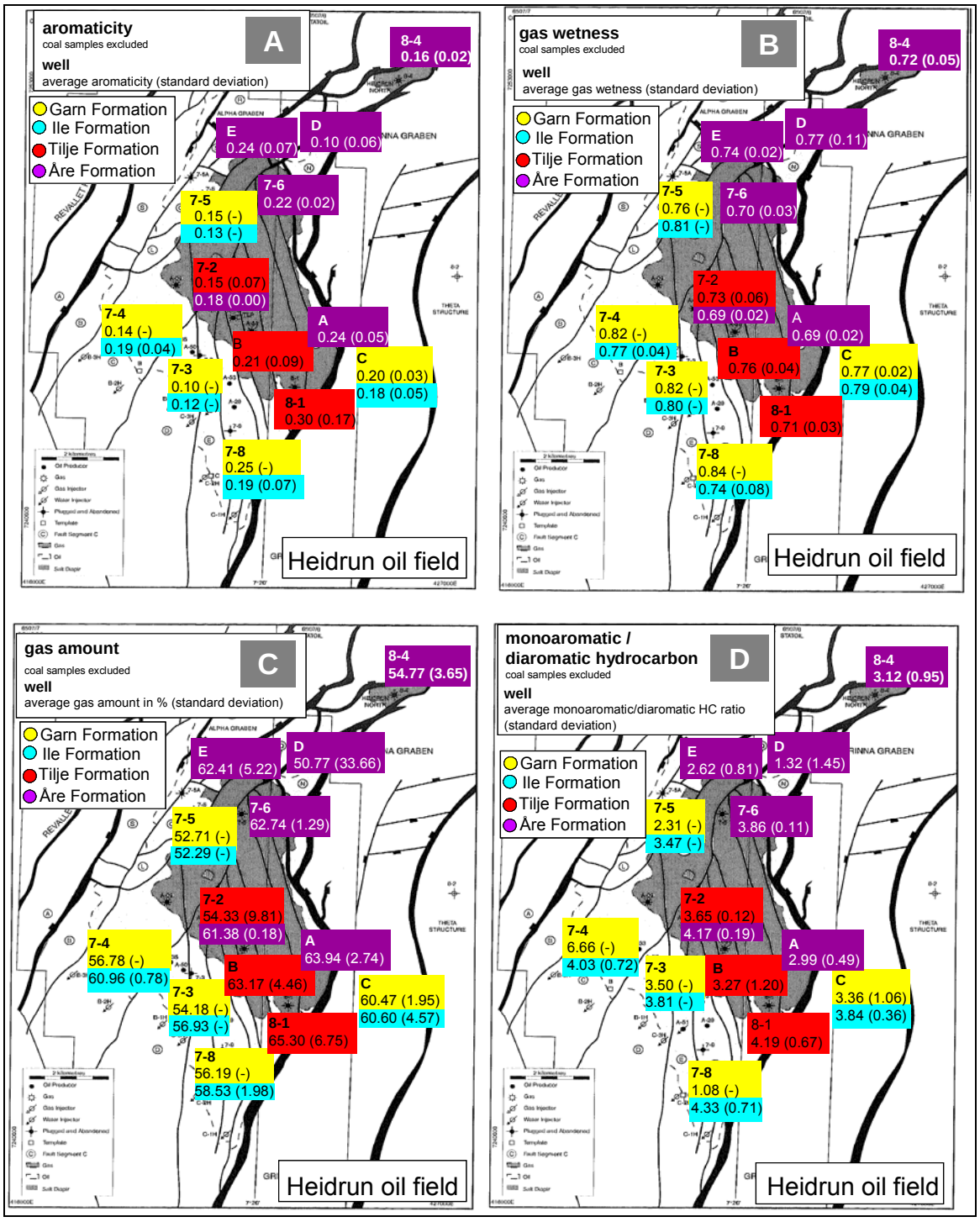

Figure 95 Distributions of the aromaticity (A), gas wetness (B), gas percentage (C), and monoaromatic / diaromatic hydrocarbon ratio (D) in the individual reservoir formations of the Heidrun oil field. The coloured boxes show the well name, the average value of the Py-GC parameter and its standard deviation in brackets. The colours of the boxes represent the individual reservoir formations.

The most prominent parameter for the organic matter composition analysed in this study is the aromaticity. Significant gradients in the aromaticity were found in wells from the eastern and the northern part of the Heidrun oil field (C, B, E and D). Wells in the western part of the oil field are more homogeneous in terms of aromaticity. An overview of the aromaticity distribution in the whole oil field is shown in Figure 95 A.

Two areas can roughly be subdivided, departing the Heidrun oil field along an imaginary N - S axis. One with a higher aromaticity > 0.2 (average values) including wells predominantly found in the eastern part of the field, and one in the western part of Heidrun with average aromaticity < 0.2. Aromaticity above 0.2 was found in the eastern wells A, B, and C, the northern wells E and 6507/7-6, and the southern well 6507/8-1. Lower aromaticity below 0.2 was found in the western and southwestern wells 6507/7-5, 6507/7-4, 6507/7-3, and 6507/7-8 (Ile Fm.), and in the northern wells D and 6507/8-4.

The western and southwestern wells with low aromaticity and a relatively homogeneous aromaticity distribution are closest to the source kitchen or in other words, nearest the present day general filling point at the southwestern margin of the oil field. As with increasing maturity level the aromaticity in the source rock kerogen increases, the oil from the latest charge should be characterised by higher aromaticity and should be found closest to the source (England, 1989). However, no source maturity related variabilities in the oil charges were found in the screening results, one sample in well 6507/8-1 excluded (cf. Chapter 6.2 - 6.5). Thus, maturity related reasons could be disregarded to be responsible for the differences observed in the aromaticity between the western and the eastern part of the oil field. It is known that the western wells achieved the most recent oil charge, comprising fresh and undegraded oil, while wells in the eastern part did not (internal Statoil report, 2003, Chapter 3.1). The recent oil charge composition is distinctly reflected by a better oil quality (PI) in the western wells.

A direct correlation of increasing aromaticity and increasing biodegradation level was found in the pyrolysates of the biodegradation series of the WCSB (heavy oils) and selected Heidrun oils (cf. Chapter 6.2.1.2.3.1 and 6.2.1.2.3.2). Thus, the lower aromaticity in the reservoir rocks of the western Heidrun wells might be an indication to a lower biodegradation level compared to the remaining wells. The homogeneous aromaticity distribution (less or no trends) in the western wells could be an indication for mixing processes.

Additionally, all reservoir rocks in the western wells are Fangst group sandstones comprising the reservoir units Garn- and Ile Formation characterised by the distinctly better poroperm properties compared to Båt group sediments (Tilje- and Åre Formation). However, a direct correlation between the aromaticity and the porosity and permeability was not found in this study. Nevertheless, the aromaticity is apparently linked to higher water saturation. An increase in water saturation accompanied by increasing aromaticity was observed near the OWC in the Ile Fm. of well C and well 6507/7-8.
Both northern wells D and 6507/8-4, and partly well E are different as they show distinctly lower aromaticity compared to the remaining Åre Formation containing wells. In combination with the high wax content found in well D reservoir rocks, here a different source can be assumed.
The Tilje Formation shows an increase in aromaticity from well 6507/7-2 to well B and well 6507/8-1 and indicate so an increase in biodegradation level from the centre of the oilfield to the south. Note that the standard deviation of the average aromaticity increases too.

The gas wetness distribution in the whole oil field shows an inverse distribution pattern to the aromaticity (Figure 95 B). Gas wetness (average values) below 0.80 were predominantly found in the eastern part of the field, while the western (and the northern part) represent higher gas wetness above 0.80. The aromaticity and the gas wetness are inversely correlated, thus lower gas wetness is apparently linked to higher biodegradation.
The following wells, predominantly from the eastern part, show gas wetness below 0.80: well A, B, C, E, 6507/7 2, 6507/7 6 and 6507/8 1. Gas wetness above 0.80 was predominantly found in the western wells 6507/7 3, 6507/7 4, 6507/7 5, and 6507/7 8 (Garn Fm.) and in the northern part in the wells D and 6507/8 4. The wells D and 6507/8-4, both Åre Formation show higher gas wetness compared to the remaining Åre Formation containing wells.

Examining the distribution of the average gas content, higher gas amounts between 60 % - 65 % were predominantly found in the eastern part, while most wells in the western and in the northern part are lower in gas (53 % - 60 %), (Figure 95 C). The gas amount distribution follows the same pattern as the distribution observed in the aromaticity. The aromaticity and the gas percentage are linear correlated, thus, higher gas amount is apparently linked to higher degree of biodegradation.
The Tilje Formation wells show, similar as observed for the aromaticity, an increase in the gas amount from north to south from well 6507/7-2 to well B and well 6507/8-1, and indicate

thus a biodegradation trend. Additionally, the gas amount in the Åre Formation increases from well E to well 6507/7-6 and well A. Note again the high variability (standard deviation) of this Py-GC parameter.

Using the average of the monoaromatic versus diaromatic hydrocarbon ratio of the single wells, no clear distribution patter could be observed within the Heidrun oil field (Figure 95 D). However, the highest ratios were detected in the southern part of the oil field in well 6507/7-8 (Ile Formation) and well 6507/8-1 (Tilje Formation). Low ratios were found in the northern part (well 6507/7-5, well E, and well D). The waxy rock samples in well D represent the lowest ratio.

Concerning the GOR distribution, the Heidrun oil field shows clear variations between the western and eastern part. Wells in the western part, which received the recent undegraded oil charge (internal Statoil report, 2003) are characterised by the lowest GOR in their pyrolysates (Figure 96) and thus, by less indications of biodegradation as compared to the remaining wells. Additionally, their relatively homogeneous Py-GC parameter distribution might be an indication that mixing processes of the older biodegraded oil (primary charge(s)) and the fresher oil of the recent charge are still going on. England (1989) described, that initial heterogeneities in the composition of the newly filled reservoir are attempted to approach a state of thermodynamic equilibrium, which might occur via a variety of mass-transfers or mixing processes. These effects increase the concentration of denser compounds at the base and leads to a progressive increase in GOR towards the top of the petroleum column, and a decrease in the subsurface density. The greatest variability in GOR is observed in the northern wells.

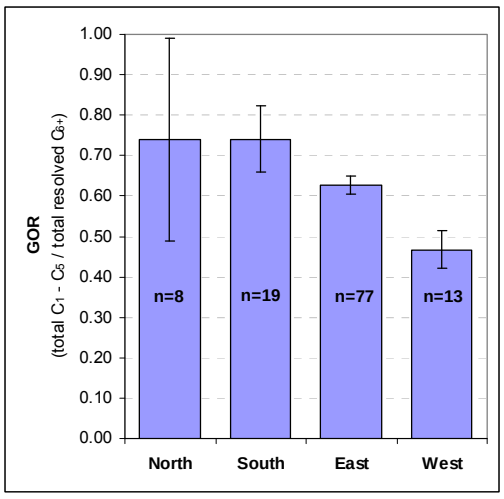

Figure 96 GOR distributions of the reservoir rocks from the northern, southern, eastern, and western part of the Heidrun oil field. n = number of reservoir rock samples.

Taking the age of the single reservoir formations into consideration, additional correlations could be observed among the Py-GC parameters. Especially the aromaticity and the gas wetness of the Fangst group and the Båt group sediments show systematic differences. In the Fangst group, comprising Garn- and Ile Formation sandstones, lower aromaticity and higher gas wetness was recognised compared to the Båt group comprising Tilje- and Åre Formation sediments (Table 13).

Within the single reservoir formations, a slight increase in aromaticity from the younger to the older reservoir was found. The aromaticity increases from the Garn Formation on the top to the underlying Ile Formation, Tilje Formation and Åre Formation (Table 13). This trend is reflected in the gas wetness that shows a slight decrease from the younger to the older reservoir formations. For the Garn- and Ile Formation on the top of the reservoir very similar gas wetness was observed. With increasing reservoir age, the gas wetness decreases from the Garn- and the Ile Formation on the top to the underlying Tilje Formation and the Åre Formation. The latter presents the lowest value and greatest variability.

Table 13 Average values (av) and standard deviation (STABW*) for the Py-GC parameter of the individual reservoir formations evaluated in the Heidrun oil field. * $\sqrt{n\sum x^2 - (\sum x^2)/n^2}$

	aromaticity		**gas wetness**		**monoaromatic / diaromatic HC**		**gas %**	
	av	STABW	av	STABW	av	STABW	av	STABW
Garn Fm.	0.17	0.05	0.80	0.03	3.16	1.09	58.25	3.12
Ile Fm.	0.18	0.05	0.80	0.04	3.88	0.92	60.47	4.03
Tilje Fm.	0.21	0.10	0.75	0.04	3.55	1.16	62.53	4.59
Åre Fm.	0.21	0.06	0.72	0.07	2.90	0.84	60.49	10.42
Spekk Fm.	0.38	-	0.72	-	3.77	-	67.10	-
Melke Fm.	1.20	-	0.63	-	4.25	-	77.51	-

The gas amount (%) increases linearly with the aromaticity from the younger Garn Formation to the older underlying Ile- and Tilje Formation (Table 13). The Åre Formation is different. Here, a gas amount similar to the Ile Formation was found, but with a distinctly higher variability (STABW). This is attributable to the northern wells D and 6507/8-4 (Heidrun North), which are very low in gas (50.41 % and 54.18 %, see Table X 8 and Table X 9). The northern wells are characterised by differences in the organic matter composition.

Comparing the average values of the monoaromatic versus diaromatic hydrocarbon ratio of the particular reservoir formations, no trend in the reservoir age and no correlation to other

Py-GC parameters was found. The lowest ratios are found in the Åre Formation; the highest ratio was found in the Ile Formation (Table 13).

6.6.2 ORGANOFACIES AND/OR MATURITY DIFFERENCES

Ternary diagrams for the alkyl chain length distribution (CLD), the relative sulphur- and the phenol content have been used to detect heterogeneities in the organofacies and/or the maturity of the source rocks compared to the reservoir rock samples. They can indicate variabilities in the oil charges and deliver thus important information with respect to the filling of the reservoir.

Figure 97 A show the CLD of the individual reservoir formations including all reservoir rock sample. Independent of their reservoir formation most of the reservoir rock samples have a CLD that is similar to that of the Spekk Formation source rock sample.

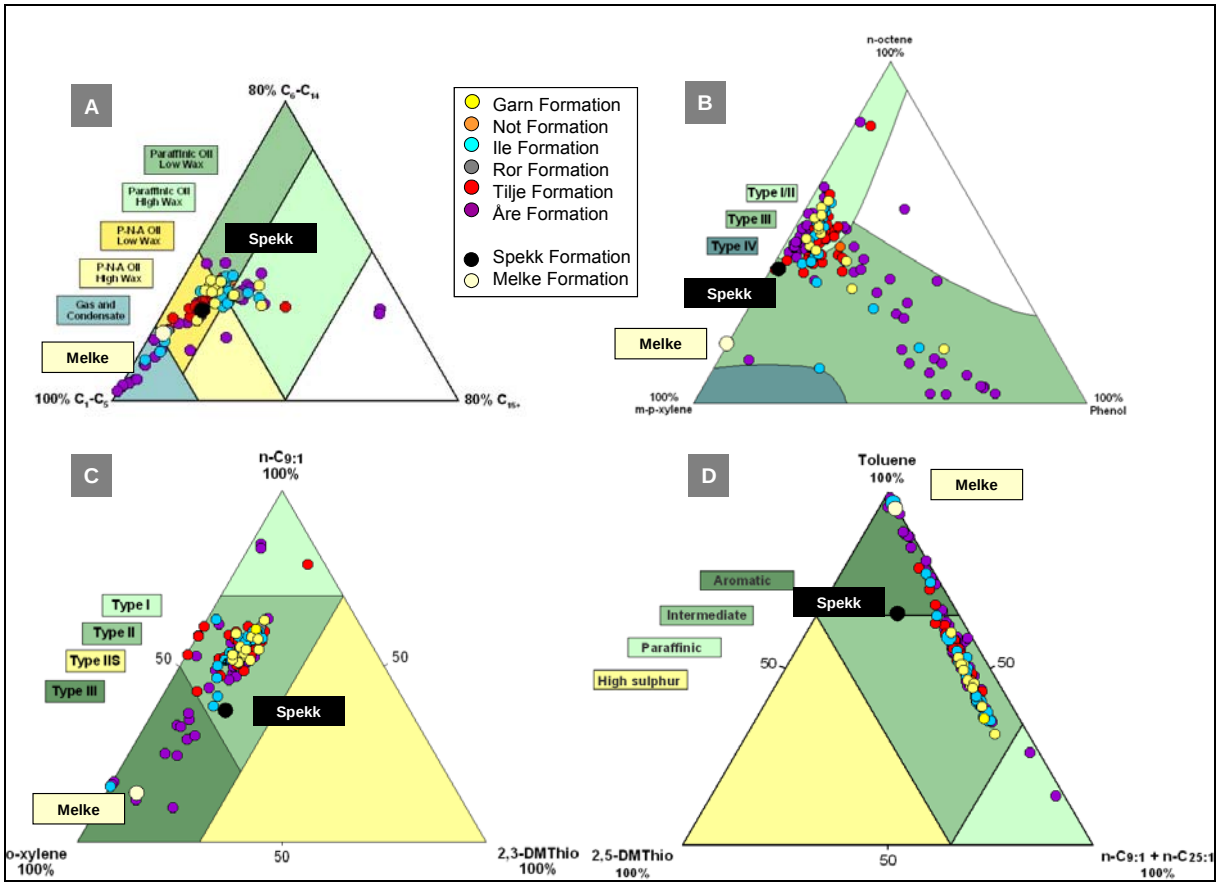

Figure 97 Bulk properties of the individual reservoir formations Garn-, Ile-, Tilje-, and Åre including all reservoir rock and source rock samples analysed in the Heidrun oil field. From A to E the CLD (A), relative phenol content (B) and relative sulphur content (C - D) are shown.

The few reservoir rocks from the Ile- and Åre Formation with large quantities of short alkyl chains in their pyrolysates plot in the gas and condensate field, because they contain *in-situ* coaly particles. Excluding all reservoir rocks containing disseminated coal, several differences within the CLD were observed in the Garn-, Ile-, Tilje- and Åre Formation (Figure 98 A - D). The criterion for the sample exclusion used was a phenol ratio above one.

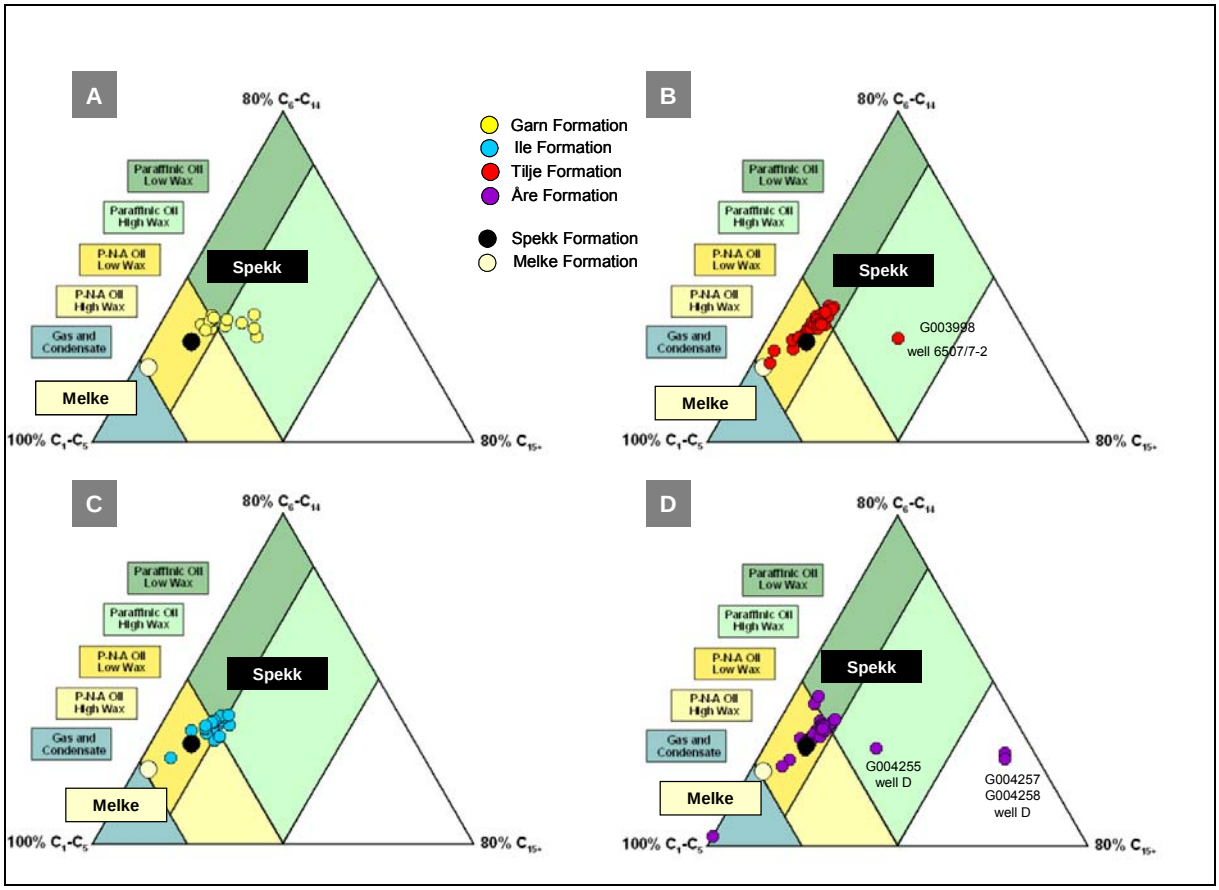

Figure 98 Alkyl chain length distribution of the individual reservoir formations without reservoir rocks containing disseminated coal. The CLD show reservoir rock samples of the Garn (A), Tilje (B), Ile (C) and Åre Formationm (D).

Most significant differences were recognised in the reservoir rocks from the Åre Formation (Figure 98 D). A few of these samples present significant proportions of long chain alkanes in their pyrolysates compared to both potential source rocks from the Spekk- and Melke Formation, and to the remaining reservoir rocks from the Åre Formation. This indicates larger quantities of waxy compounds in the reservoir rocks, which were found in the northern part, especially in well D (G004255, G004257, G004258), but also in well E and well 6507/8-4. Thus, in the northern part of Heidrun, a different source (local?), with a lacustrine influenced depositional environment has to be considered. In well E and well 6507/8-4, the waxy compounds are less pronounced as compared to the lower part of well D. This might indicate

a mixed oil type, comprising oil generated by a lacustrine source and (biodegraded) oil generated by the Spekk Formation that reached the main area of the Heidrun oil field in primary charges.

Reservoir rocks with larger amounts of long alkyl chains in their pyrolysates compared to the Spekk Formation are additionally found in the Garn-, Ile Formation and Tilje Formation. In the Garn Formation, three reservoir rocks were recognised (Figure 98 A). These reservoir rocks are from the western part of the Heidrun oil field of well 6507/7-3, 6507/7-4, and 6507/7-5. Both reservoir rocks recognised in the Ile Formation are also from the western part, from well 6507/7-3 and well 6507/7-5 (Figure 98 C). The differences in the CLD observed, indicate primarily variabilities between the oil compositions generated by the Spekk Fm. and the oil composition analysed in the reservoir rock. Long alkyl chains are typical for waxy compounds, which are usually an indication to a lacustrine influenced source, similar as observed in the reservoir rock samples from the northern part. However, in the western part of the oil field, which received the most recent oil charge, mixing processes between the older biodegraded Spekk Formation generated oil and the fresh undegraded oil from the recent charge (also predominantly generated by the Spekk Formation) are more probable. Additional indications pointing to mixing processes are the homogeneity in the Py-GC parameter distributions in the western wells mentioned before.

Within the Tilje Formation, three reservoir rocks show a different CLD compared to the Spekk Formation source rock (Figure 98 B). Two of them are from the southern part of Heidrun, G004036 from well 6507/8-1 and G004190 from well B. They present a CLD more similar to the distribution observed for the potential source rock from the Melke Formation. The contribution of *in-situ* organic matter in the samples can be excluded (phenol ratio < 1). The Melke Formation source rock plot near the gas and condensate field, because it is more mature than the Spekk Formation (cf. Chapter 6.1.2). Thus, the larger quantities of short alkyl chains in both Tilje Formation reservoir rock pyrolysates compared to the remaining Tilje reservoir rock samples might be an indication to differences in the source maturity.
The third reservoir rock shows large quantities of long chain alkanes in the pyrolysates and plots in the high wax field, similar to the reservoir rock samples from the Åre-, Garn- and Ile Formation from the northern and western part described in the section above. It is the uppermost reservoir rock sample G003998 of well 6507/7-2 located in the western / central part of the oil field and the only sample of this profile showing waxy compounds. An

explanation might be that the recent oil charge achieved here only the upper part of well 6507/7-2 and no mixing with the lower part occurred until now, maybe due to interstratified mudstone layer. However, the greater proportions of waxy compounds could additionally be an indication of a lacustrine influence of the generative source.

The CLD ternaries in Figure 99 A - D show the reservoir rock samples with disseminated coal detected in each reservoir formation. They are marked by green colour. Their phenol ratio representing the relative amount of lignocellulosic OM that increases in linear steps with increasing gas content (Figure 100).

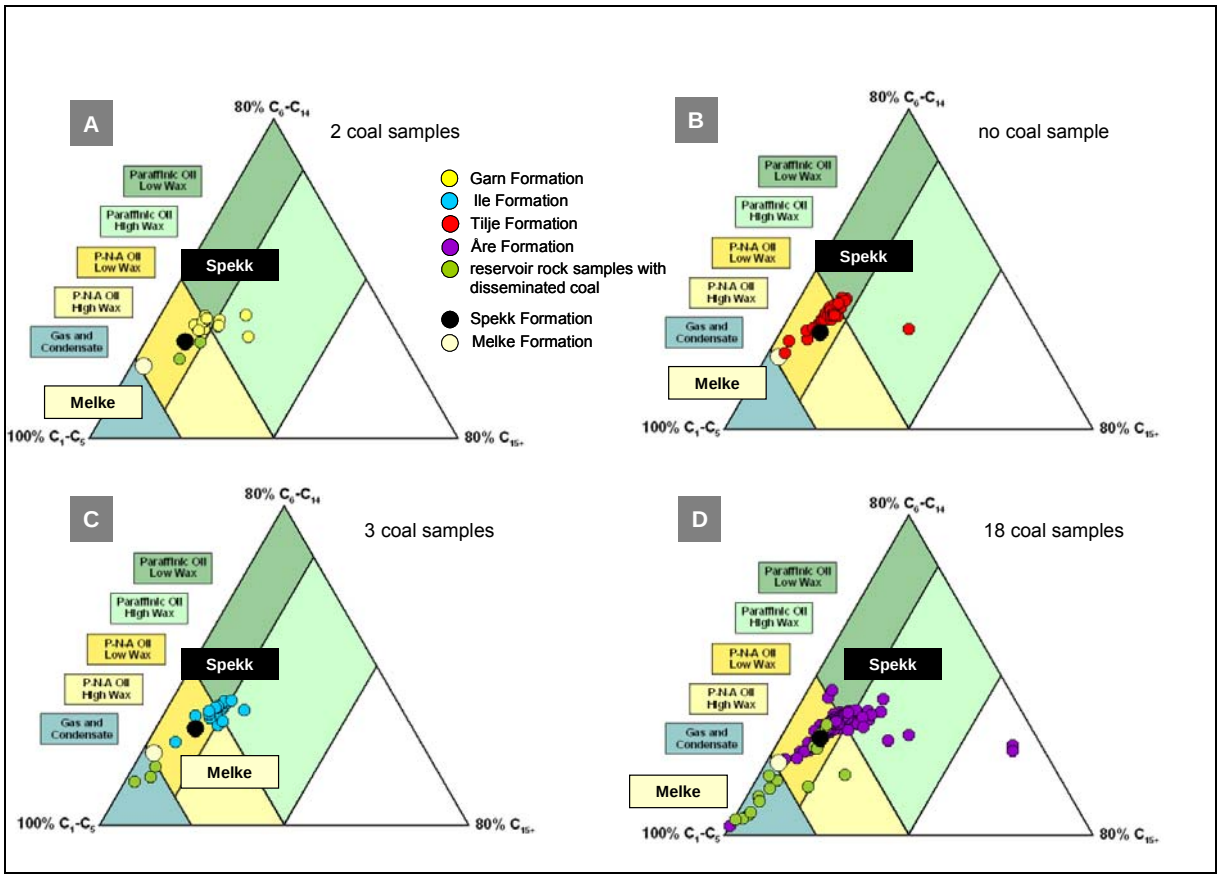

Figure 99 Alkyl chain length distributions of the individual reservoir formations Garn (A), Tilje (B), Ile. (C), and Åre (D). Reservoir rocks containing disseminated coal are green coloured.

Most reservoir rocks with large quantities of coaly particles, which are partly clearly observable, are characterised by a very high phenol ratio and high gas amount in their pyrolysates. Due to the latter, it is obvious that they plot in the gas and condensate field of the CLD ternary closer to the Melke Fm. source rock. Most of the reservoir rocks with lower quantities of disseminated coal, predominantly invisible and finely dispersed, are characterised by a lower phenol ratio and hence a lower gas amount in their pyrolysates.

These reservoir rock samples plot near the Upper Jurassic Spekk Formation in the P-N-A low wax oil field (Figure 101). In total, 23 reservoir rocks with disseminated coal were recognised and as expected, most of are from the Åre Formation (Figure 99 D). No reservoir rocks with disseminated coal were detected in the Tilje Formation.

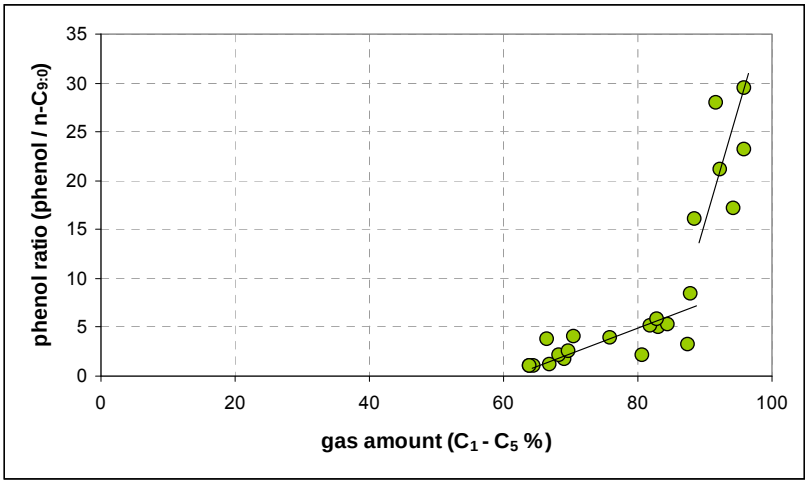

Figure 100 Correlation of the phenol ratio and gas content of the reservoir rocks containing disseminated coal.

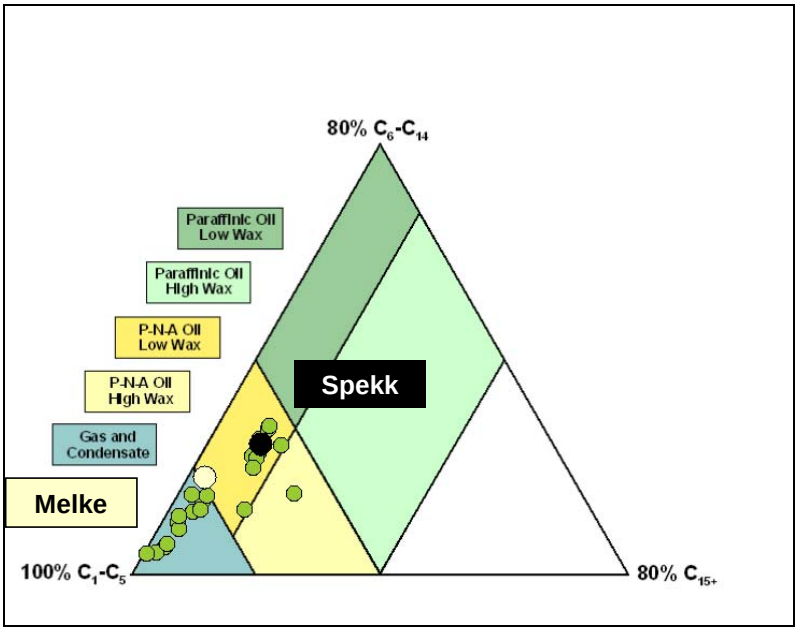

Figure 101 Alkyl chain length distributions of reservoir rocks with disseminated coal only, compared to both potential source rock samples from the Spekk- and Melke Formation.

Both sulphur ternaries in Figure 97 C and D indicate low sulphur amounts for all reservoir formations and correlate with differences in the aromaticity. The potential source rock from the Spekk Formation plots in the intermediate / aromatic field indicating low sulphur oil

generated by kerogen Type II with some Type III deposited under anoxic marine conditions. The potential source rock from the Melke Formation plot in the aromatic field indicating high aromatic and low sulphur oil typically generated by kerogen Type III deposited under terrestrial conditions, or such as in the case of the Melke Formation, by a mature / overmature marine source.

Most of the reservoir rocks from the Garn, Ile, Tilje, and Åre Formation plot in the intermediate field indicating oil generated by kerogen Type II. They represent an organic matter composition more similar to the Spekk Formation source rock than to the Melke Formation source rock. However, several of these reservoir rock samples present higher proportions of paraffinic compounds (lower aromaticity) in their pyrolysates and show lower sulphur contents as compared to the Spekk Formation source rock. Reservoir rocks containing disseminated coal from the Åre- and Ile Formation and reservoir rocks characterised by high aromaticity from the Ile-, Tilje- and Åre Formation (potentially biodegraded) present a composition similar to the Melke Formation. These reservoir rocks plot in the aromatic field that indicates oil generated by terrestrial kerogen Type III.

Significant differences were observed in the Are Formation. Here two reservoir rocks present distinctly higher proportions of paraffinic compounds in their pyrolysates. These are the waxy reservoir rock samples of well D, which is located in the northern part of the Heidrun oil field.

Organic sulphur pyrolysis products (OSPP) have been used as representatives for different lipid precursors with linear, branched and isoprenoid carbon skeletons. The basis concept is given in Chapter 5.2. Figure 102 shows the distribution of the most common OSPP of the reservoir- and potential source rocks in the Heidrun oil field. The aim was to see if the contributions of the various sources could be inferred by relative positions in the diagram. Interestingly, there was invariance as far as the source rock samples were concerned, with both Spekk and Melke source rocks being enriched in 2ethyl 5methylthiophene and plotting in the linear field. Typical petroleum source rocks of marine origin (Type II kerogens) generate relatively high amounts of 2 methyl 5 alkylthiophenes indicating an abundance of moieties possessing linear carbon skeletons (Eglinton *et al.*, 1992). Conspiciously, most of the Åre Formation coals also show large quantities of 2ethyl 5methylthiophene and plot within the linear field (green rectangles Figure 102).

Yet different populations were observed within the single reservoir formations. Most of the reservoir rocks plot in the centre of the ternary indicating similar proportions of the corresponding sulphur compounds. However, it was observed that reservoir rock samples

with high wax content, e.g. from well D, or reservoir rock samples with high gas content, comprising higher amounts of 3 methylthiophene in their pyrolysates and plot thus predominantly in the branched field. Branched carbon skeleton are typical for alkylthiophene-moieties in kerogen Type III or coals according to Sinnighe Damste *et al.* (1989). Most of these reservoir rocks, which indicate differences in the organofacies, were predominantly found in the eastern and the northern part of the Heidrun oil field.

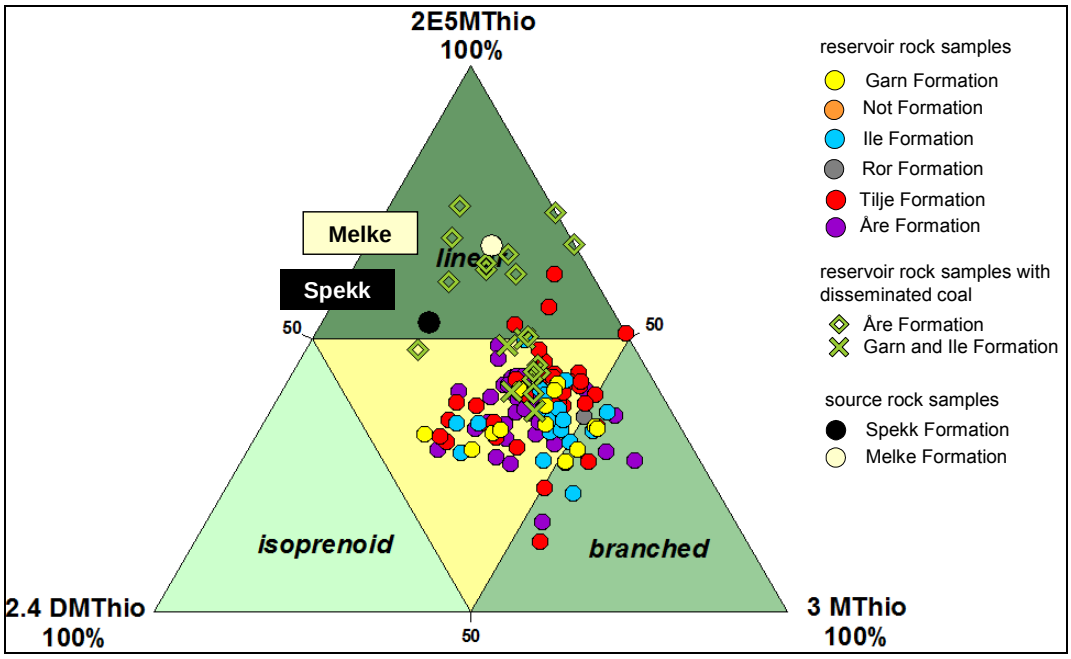

Figure 102 New sulphur ternary using different organic sulphur pyrolysis products (OSPP) on its apices as representatives for different lipid precursors. 2ethyl 5methylthiophene (2E5MT), 3methylthiophene (3MT), and 2.4dimethylthiophene (2.4DMT) representing linear, branched and isoprenoid lipid precursor carbon skeletons, respectively.

Summing up, within the Heidrun field several heterogeneities were found within all Pyrolysis-GC parameters. Comparing the average Py-GC parameter values for each particular reservoir formation an increase in aromaticity and a decrease in the gas wetness was observed. Both parameters are inverse correlated. The gas percentage increases linearly with the aromaticity. An inverse correlation between the aromaticity and the monoaromatic versus diaromatic hydrocarbon ratio was observed in the Garn-, Tilje-, and Åre Formation. This means, a decrease in 1-ring aromatic hydrocarbons relative to 2-ring aromatic hydrocarbons with increasing aromaticity. Conspicuously, the Ile Formation shows a linear correlation of both parameters.

Gradients in the aromaticity, gas wetness, gas amount and monoaromatic versus diaromatic hydrocarbon ratio were found in the reservoir age from the younger to the older reservoirs

(Garn Formation → Ile Formation → Tilje Formation → Åre Formation). An increase in aromaticity and gas content from the north to the south was observed in the Tilje Formation (well 6507/7-2 → well B → well 6507/8-1). Furthermore, in the Åre Formation, the gas content in the pyrolysates increases from the north to the south (well E → well 6507/7-6 → well A).

Based on the screening results, the Heidrun oil field can roughly be separated into an eastern and a western part. The wells in the eastern part (A, B, C, D, E, 6507/8-4, 6507/7-8, and 6507/8-1) show higher aromaticity and gas contents, and lower gas wetness compared to wells in the western part of the oil field. They show additionally significant gradients in the Py-GC parameters. Wells with relatively homogeneous organic matter composition without significant gradients in the Py-GC parameters were predominantly found in the western part of the Heidrun oil field (6507/7-3, 6507/7-4, 6507/7-5, 6507/7-2, and 6507/7-6).
Significant differences in aromaticity and/or the gas compound ratios were found in the northern part, especially in well D, compared to the remaining Åre Formation wells evaluated in the Heidrun oil field.

A direct relation of aromaticity and biodegradation was observed within the pyrolysis products of the heavy oils (biodegradation series) of the WCSB and Heidrun oils. It was shown that with increasing biodegradation level the aromaticity of the macromolecular compounds increases. Thus, variabilities in aromaticity of the reservoir rock pyrolysates are obviously linked to differences in biodegradation. Transferred to the Heidrun oil field, this means in concrete terms a lower level of biodegradation in the western wells, of which one knows that they received the recent undegraded oil charge, and in contrast a higher level of biodegradation in wells of the eastern part.
Comparing the single reservoir formations, the Garn- and the Ile Formation show lower aromaticity compared to the Tilje- and the Åre Formation. Wells comprising Garn- and Ile Formation sediments are predominantly found in the western part of the Heidrun oil field.
Higher aromaticity was additionally observed in zones with higher water saturation, e.g. near the OWC. The presence of water is an essential prerequisite for alteration processes such as biodegradation and/or water washing, as both are initiated at the oil-water interface. Thus, the link between aromaticity and water saturation might *inter alias* refer to higher microbial activity in water saturated zones, and thus additionally to a relationship between aromaticity and biodegradation.

A direct correlation of the Py-GC parameters to the physical rock properties porosity and permeability was not observed based on visual comparison alone using well logs and geochemical depth plots. However, reservoir formations with better rock properties namely higher porosity and higher permeability, such as the Garn- and the Ile Formation, show generally lower aromaticity and higher gas wetness compared to reservoir formations with less well reservoir conditions, such as the Tilje- and the Åre Formation.

In total, 23 reservoir rocks with disseminated coal (phenol ratio > 1) were found. They are generally characterised by low oil quality, high aromaticity and gas percentage, low gas wetness and the presence of more diaromatic hydrocarbons compared to monoaromatic hydrocarbons.
Excluding reservoir rocks with disseminated coal, the alkyl chain length distribution of the majority of the remaining reservoir rocks indicate an identical source rock. They present a CLD comparable to that of the potential source rock from the marine Spekk Formation.

Indications regarding differences in the organofacies of the generative source were observed in several reservoir rocks from the Åre Formation in the northern part (well D, well E, and well 6507/8-4), from the Garn and Ile Formation in the western part (well 6507/7-2, well 6507/7-3, and well 6507/7-4), and in one reservoir rock from the Tilje Formation (well 6507/7-2). Reservoir rocks in these wells show larger quantities of waxy compounds. In the northern part of Heidrun, indications with respect to a different source with a lacustrine influenced depositional environment were found. In well E and well 6507/8-4, the waxy compounds are less pronounced as compared to well D thus, a mixed oil comprising products from a lacustrine source and oil generated by the marine Spekk Formation (biodegraded) are more probable.In the western part, which received the most recent oil charge, mixing processes between the primary Spekk Formation oil (biodegraded) and the recent undegraded oil charge (predominantly also generated by the Spekk Formation) are more probable. Additional indications pointing to mixing processes are the homogeneity in the Py-GC parameter distribution in the western wells.

Potential indications to differences in the source maturity were found in the Tilje Formation in the southern part of the Heidrun oil field. Here two reservoir rocks, one of well 6507/8-1 and one of well B, show a CLD that is similar to the distribution observed for the potential source rock from the Melke Formation, the more mature source rock.

7 SEPARATED ASPHALTENE FRACTIONS – DO THEY YIELD MORE INFORMATION?

Here, the results using single asphaltenes are presented starting with the asphaltene separation method developed and modified to detect small-scale heterogeneities in compartmentalised reservoirs. The article as published in Theuerkorn *et al.* (2008) will be presented followed by some potential problems with contaminations we had using asphaltenes, the screening results based on single asphaltene analysis and finally the compositional kinetic model.

7.1 A REPRODUCIBLE AND LINEAR METHOD FOR SEPARATING ASPHALTENES FROM CRUDE OIL

7.1.1 ABSTRACT

Petroleum asphaltenes exhibit strong structural similarities to their parent kerogen. Thus they can be used to help determine the source rock characteristics of active kitchen areas and to reconstruct the filling histories of reservoirs. The analysis of asphaltenes from compartmentalised reservoirs with complex charging and alteration histories presents a particularly difficult challenge because the *in-situ* compositional variations are sometimes subtle. It is therefore of paramount importance that asphaltene separation methods be utilised, which are highly reproducible and linear, thereby minimising experimental uncertainty and providing high-resolution interpretative capabilities. The asphaltene separation method described here is built on many that have gone before. Different parameters of asphaltene separation were investigated, which influence the asphaltene amount and properties, whereby the focus lay on reproducibility and linearity. Gravimetric and thermal analysis techniques were used to evaluate yields and quality. The developed asphaltene separation method described in detail in this contribution has four sequential steps, first dissolution of the oil in dichloromethane / 1 vol. % methanol, second addition of an excess of n-hexane, third settling time and finally filtration, purging and weighing; this sequence of steps is repeated three times. Within this study the results concerning the reproducibility depending on solvent type,

solvent amount, and aging time as well as the linearity depending on sample amount are presented.

7.1.2 INTRODUCTION

Asphaltenes are defined as that part of solvent-extractable organic matter, which precipitates upon the addition of excess light hydrocarbon (Hirschberg, 1984; Kawanaka, 1989; Leontaris, 1988; Mitchell & Speight, 1973; Speight *et al.*, 1984). Because they exhibit structural similarities to the parent kerogen (di Primio *et al.*, 2000; Muscio & Horsfield, 1996; Pelet *et al.*, 1986), petroleum asphaltenes can provide crucial insights into the organofacies and maturity of undrilled generative source rocks (Horsfield & Dueppenbecker, 1991; Keym *et al.*, 2006; Lehne & Dieckmann, 2007). Unravelling the history of compartmentalised reservoirs with a complex charge and alteration history presents a particularly difficult challenge, because subtle *in-situ* compositional variations have to be recognised, and artefacts associated with separation and analytical procedures have to be minimised. Here we present the detailed description of an asphaltene separation method, which, because it is both highly reproducible and linear, is ideally suited to the task.

Our method was developed with close reference to several standard methods (IP143, NFT60115 and ASTM D3279), employing the Norwegian Geochemical Standard North Sea Oil-1 (NGS NSO-1; 32,9° API gravity, (Dahlgren, 1998). It is already known that precipitant type, precipitant/crude oil ratio, solvent type, solvent/crude oil ratio, aging time, temperature and pressure all influence asphaltene composition (Agrawala & Yarranton, 2001; Alboudwarej *et al.*, 2002; Ancheyta *et al.*, 2002; Gürgey, 1998; Hotier, 1983; Hu & Guo, 2001; Ignasiak *et al.*, 1977; Jones *et al.*, 1988; Parra-Barraza *et al.*, 2003; Rubinstein *et al.*, 1979; Speight, 1999; Speight *et al.*, 1984). Therefore, in a first step, we tested the influence of these parameters on asphaltene composition in the same sequence as mentioned above (which represents the sequence of the analytical steps involved) and then in a second step optimised the linearity of the method. For each investigated parameter a minimum of three asphaltene concentrates were prepared, using identical experimental conditions and analysed by open-system-pyrolysis-GC and thermo vaporisation-GC. In order to evaluate the best separation method, we studied changes in asphaltene properties and compositional variations of their pyrolysates. Standard deviations (STDV) of results from parallel measurements were calculated.

7.1.3 EXPERIMENTAL

7.1.3.1 PRECIPITATION OF ASPHALTENES

In order to assess the influence of solvent type, oil/solvent ratio and aging time on the chemical composition of asphaltenes only one given parameter was changed within each individual set of experiments. A total of 57 asphaltene samples from the NSO-1 oil were isolated. The asphaltene separation method consists of four sequential steps; first, the dissolution of the oil in a minimum amount of polar solvent to etch the resins; second the addition of an excess of short chain alkanes to precipitate the asphaltenes; third allow settling to take place for a fixed time; fourth, vacuum filtration followed by washing in hydrocarbon solvent and drying. All four steps were repeated three times to ensure the removal of entrapped material (Dahlgren, 1998; Gürgey, 1998; Lehne, 2007; Parra-Barraza *et al.*, 2003; Speight *et al.*, 1984). A detailed description is as follows:

For the reproducibility studies, 4ml of the NSO-1 oil were weighed in a pre-weighed 250 ml Erlenmeyer flask. Then a known amount (1, 2 or 4 ml) of dichloromethane (DCM) or dichloromethane with 1 vol. % methanol (DCM/MeOH 1vol %) was added to provide a complete dissolution of the entire oil. Subsequently the solution was stirred for 10min in an ultrasonic bath and a 20-, 40- or 60-fold excess of the total sample volume of n-pentane, n-hexane or n-heptane was added. Then the flask was wrapped with aluminium foil and put aside at ambient temperature for 2, 4, 6, 12, 24 or 48 hours. Thereafter the asphaltenes were separated by filtration through a 0.5 µm Millipore filter. The remaining asphaltenes were transferred into a 11ml cell of an Accelerated Solvent Extraction System (ASE, Dionex GmbH, Idstein, Germany), firstly washed with the same type of solvent used in the precipitation (ASE method: 80°C/100bar, heat 5min, static 4min, 1cycle), and subsequently extracted with DCM/MeOH (1vol%) (ASE method: 80°C/100bar, heat 5min, static 5min, 3 cycles). The asphaltene extracts were concentrated using a Turbovap evaporator, transferred into a 10ml brown glass vial and subsequently dried under a gentle stream of nitrogen. Finally, their weight was recorded when constant. For the linearity test, the NSO-1 oil sample amount was reduced stepwise.

7.1.3.2 ANALYTICAL CHARACTERISATION OF ASPHALTENES

The purity of the different separated asphaltenes was evaluated using thermovaporisation - gas chromatography (Tvap-GC) and open system pyrolysis - GC. Asphaltenes were mixed with thermally pre-cleaned quartz sand in the weight ratio 1:10. The Production Index (PI), here the ratio of thermovaporised bulk hydrocarbons [S1] to the sum of thermovaporised bulk hydrocarbons and pyrolysis products, [S1+S2]) was used to quantify the purity of the separated asphaltenes: the lower the PI, the cleaner the asphaltene sample. Further compositional and structural characteristics are provided by the gas-oil ratio (GOR; C_1-C_5/C_{6+}) and aromaticity (Σ toluene, ethylbenzene, m, p-xylene, o-xylene, 2-methylnaphthalene, 1-methylnaphthalene / Σ C_7 to C_{13} *n*-hydrocarbons) of the pyrolysates.

For Tvap-GC 15 mg asphaltene - quartz sand mix was weighed in glass capillary tubes, plugged with quartz wool at both ends and subsequently sealed. The sealed tubes were introduced into a Quantum MSSV-2 Thermal Analysis System, and the outer surfaces purged at 300°C. For analysis, the tube was cracked at 300°C within the piston device. The mobilized products were collected in a cryogenic trap at -196°C. Then the trap was heated up to 300°C and the products were released onto a dimethylpolysiloxane-coated column (50 m x 32 mm; 0.52 µm film thickness) fitted in an Agilent GC 6890A equipped with a flame ionisation detector (FID). For open system pyrolysis the 5mg asphaltene - quartz sand mix was weighed in glass capillary tubes and held in place with pre-cleaned quartz wool. The measurement was done using the same instrument configuration as described for Tvap-GC. Isothermal heating at 300°C for 4min was used to remove volatile compounds prior to pyrolysis. Then the system was heated from 300°C up to 600°C (40°C/min) and the pyrolysis products were collected in a liquid-nitrogen cooled trap. The products were released from the cold trap by ballistic heating to 300°C and measured on-line with the GC. In both cases, helium served as carrier gas (30 ml/min) and *n*-butane was used as external standard for quantification. The peaks were identified and quantified manually based on reference pyrolysis gas chromatograms using Agilent ChemStation software.

7.1.4 RESULTS

7.1.4.1 SOLVENT TYPE AND OIL/SOLVENT RATIO

In total nine samples were investigated, the main result being that DCM/MeOH 1vol% treated oils yielded slightly more asphaltenes [wt. %] than DCM treated oils. The PI values of the DCM/MeOH 1vol% asphaltenes were lower than PI values using DCM. The asphaltenes precipitated from the DCM/MeOH 1vol% treated oils exhibited a lower aromaticity and higher GOR than the DCM treated oil asphaltenes. All relevant values are listed in Table 14.
To analyse different solvent amounts nine oil samples, 4 ml each, were prepared with the oil [g] / solvent [ml] ratios of 1:0.25, 1:0.5 and 1:1. DCM was used here as solvent. The relevant calculated values are listed in Table 14. Closely similar asphaltene amounts were obtained with the ratios 1:0.25 and 1:0.5 whereas a slight decrease in the asphaltene amount was determined for the oil/solvent ratio 1:1. The PI values did not show strong differences; the lowest PI was detected for the lowest oil/solvent ratio 1:0.25. Decreasing solvent amounts resulted in higher aromaticity of the isolated asphaltenes. A continuous increase from 0.21 to 0.25 with increasing solvent amount was observed for the GOR.
The highest yield of precipitated asphaltenes and lowest PI values were detected for the oil/solvent ratio 1:0.25 and using the slightly more polar solvent mixture (DCM/MeOH 1vol %) rather than DCM alone. Thus, the solvent mixture was used for the consecutive experiments.

7.1.4.2 AGING TIME

The time asphaltenes spent in a multi component mixture of solvent, precipitant and oil within an Erlenmeyer flask is termed aging time in the present paper. In Figure 103 asphaltene compositional data are plotted versus the aging time. The values are also provided in Table 14. It can be seen that the 18 studied asphaltene samples do not show significant variability concerning the asphaltene yield [wt. %] with increasing aging time (Figure 103 A). An exception is the asphaltene amount obtained after 24 hours. In Figure 103 B-D the analysed Tvap- and open system pyrolysis–GC values for PI (Figure 103 B), aromaticity (Figure 103 C) and GOR (Figure 103 D) are plotted versus the aging time. These parameters clearly do not show compositional changes with increasing aging time. However, the PI values show an increase for the aging time of 24 and 48 hours. All parameters, the asphaltene amount, PI

as well as aromaticity values for resolved compounds and GOR remain nearly constant independent of aging time. The highest asphaltene amount and the lowest PI were monitored for an aging time of 4 hours and hence this aging time was used for the separation method.

7.1.4.3 LINEARITY

In Figure 104 the amount of precipitated asphaltenes (A), PI (B), aromaticity (C) and GOR (D) are plotted versus the amount of oil used in the experiments. The data are provided in Table 15. Asphaltene yields for the 0.25 g NSO-1 experiment were too low for Tvap-GC and open system pyrolysis measurements to be made. The data shown is therefore for asphaltenes separated from 0.5 g NSO-1 and higher sample amounts.

As can be seen in Figure 104 A the precipitated asphaltene yield shows an excellent linear correlation to increasing oil amount. This is supported by the correlation coefficient, which is nearly 1. However, slight variations concerning the analysed Tvap- and open system pyrolysis-GC parameters PI (Figure 104 B), aromaticity (Figure 104 C) and GOR (Figure 104 D) were observed. Although these values show a slight increase with the stepwise reduced amount of oil, nearly all values are within the standard deviation and obviously, they do not suggest compositional changes. As all parameters are nearly constant with the stepwise reduced oil amount, it may be concluded that the established asphaltene separation method offers excellent linearity.

7.1.5 CONCLUSION

The proposed method for asphaltene precipitation was developed through the investigation of the influence of solvent type, solvent amount and aging time. The final method shows an excellent reproducibility and linearity for asphaltene separation. The best values for each tested parameter were selected using asphaltene amount in wt. % and thermal analysis parameters PI, aromaticity and GOR for the quality. The method has four sequential steps, which are repeated three times. First the dissolution of the oil with DCM/MeOH 1vol% with an oil/solvent ratio of 1: 0.25; second the addition of a 40fold excess of *n*-hexane; third a short settling time of only 4 hours; fourth vacuum filtration and subsequent purging with *n*-hexane and extraction with DCM/MeOH (1vol%) in the ASE.

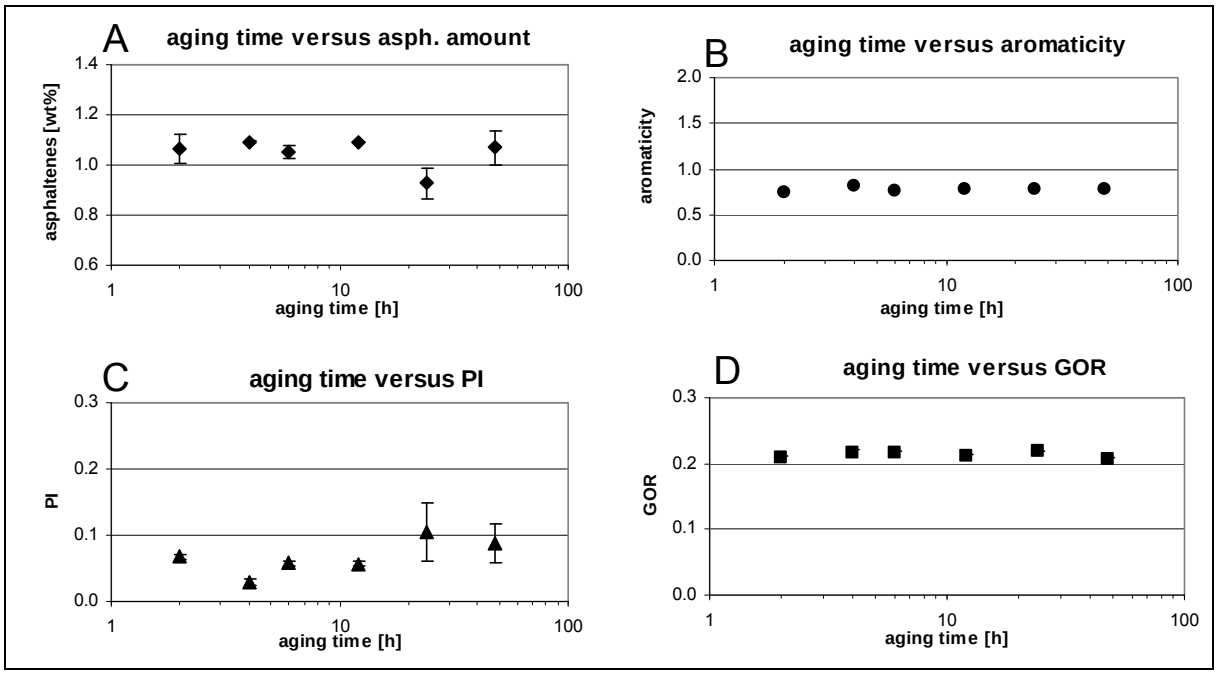

Figure 103 Reproducibility results for the aging time. The asphaltene amount (A), PI (B), aromaticity (C), and GOR (D) are shown versus increasing aging time.

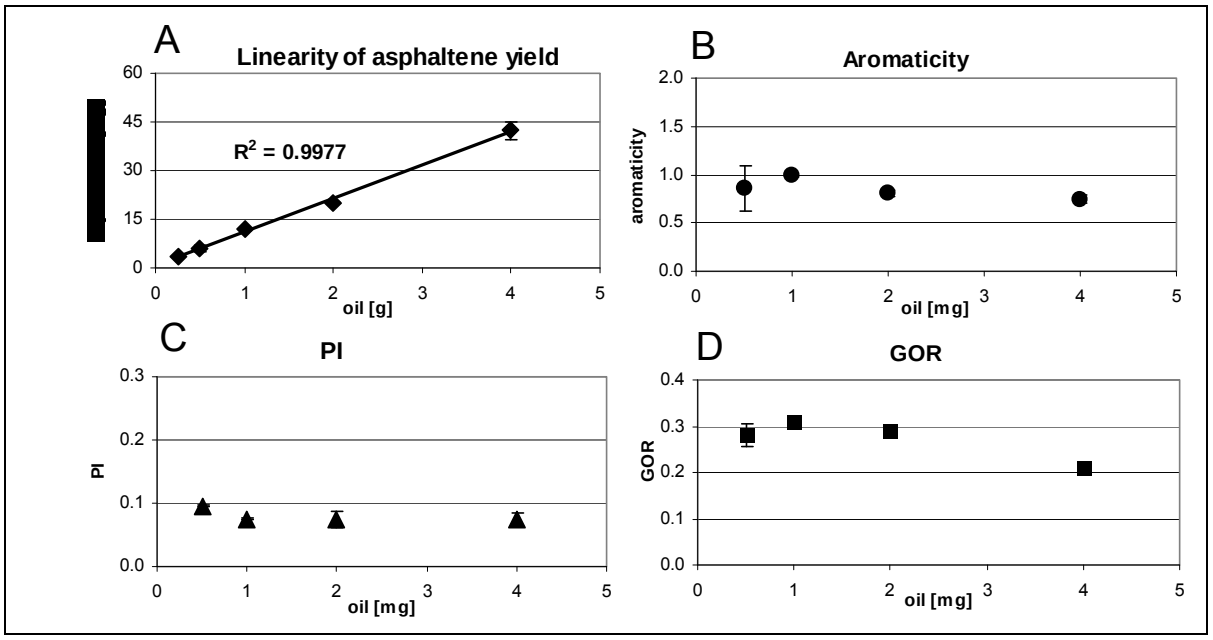

Figure 104 Linearity test results of the investigated method. Precipitated asphaltene yields (A), PI (B), aromaticity (C) and GOR (D) are plotted versus stepwise increased oil sample amounts.

Table 14 Results of the reproducibility tests. For each parameter, 3 samples were analysed. The asphaltene amount [wt. %], PI, aromaticity and GOR are average values of the asphaltene concentrates prepared in triplicate. * $\sqrt{n\sum x^2 - \left(\sum x^2\right)/n^2}$

reproducibility parameter	Asphaltene	STDV*	PI	STDV*	aromaticity	STDV*	GOR	STDV*
	(wt.% oil)	(wt.% oil)						
solvent amount (ml)								
1	0.842	0.006	0.072	0.005	1.006	0.257	0.212	0.003
2	0.848	0.006	0.076	0.002	0.661	0.01	0.23	0.003
4	0.803	0.011	0.076	0.002	0.65	0.01	0.251	0.022
solvent type								
DCM	0.842	0.006	0.072	0.005	1.006	0.257	0.212	0.003
DCM/MeOH 1%	0.873	0.02	0.055	0.004	0.8	0.015	0.231	0.022
aging time (h)								
2	1.066	0.058	0.068	0.003	0.742	0.02	0.209	0.003
4	1.093	0.006	0.029	0.004	0.82	0.002	0.216	0.007
6	1.052	0.024	0.057	0.005	0.769	0.004	0.216	0.003
12	1.09	0	0.057	0.004	0.786	0.017	0.212	0.002
24	0.927	0.06	0.105	0.044	0.775	0.007	0.218	0.002
48	1.068	0.068	0.088	0.029	0.775	0.019	0.207	0.002

Table 15 Results of the linearity tests. For each parameter, 3 samples were analysed. The asphaltene amount [wt. %], PI, aromaticity and GOR are average values of the asphaltene concentrates prepared in triplicate. * $\sqrt{n\sum x^2 - \left(\sum x^2\right)/n^2}$

Linearity parameter	Asphaltene	STDV*	PI	STDV*	aromaticity	STDV*	GOR	STDV*
	(mg/g oil)	(mg/g oil)						
NSO-1 weight (g)								
4	42.288	2.752	0.074	0.011	0.747	0.04	0.212	0.002
2	20.113	0.298	0.075	0.012	0.808	0.039	0.29	0.01
1	11.774	0.223	0.075	0.002	0.99	0.007	0.308	0.008
0.5	6.154	1.03	0.095	0.001	0.855	0.233	0.28	0.024
0.25	3.667	0.1	-	-	-	-	-	-

7.2 POTENTIAL PROBLEMS WITH CONTAMINATION

Some of the reservoir rock asphaltene pyrolysates show very large alkane peaks and conspicuous unknown peaks, which occur in different patterns within the chromatograms. The elevated alkane peaks commonly occur in the range of C_{14}-C_{17} (Figure 105 top and middle); the unknown peaks were mostly detected between C_{18} and C_{30} (Figure 105 bottom). Analysing the asphaltenes using Electro spray-Ionisation – Mass spectrometry (ESI-MS) a

7.2

mass signal was detected that corresponds to that of Polyethylenglycol (PEG), a drilling mud additive. Figure 106 show this mass spectrum. The mass signal shown there and the distance of the mass signals $\Delta m/z = 44$ is typical PEG.

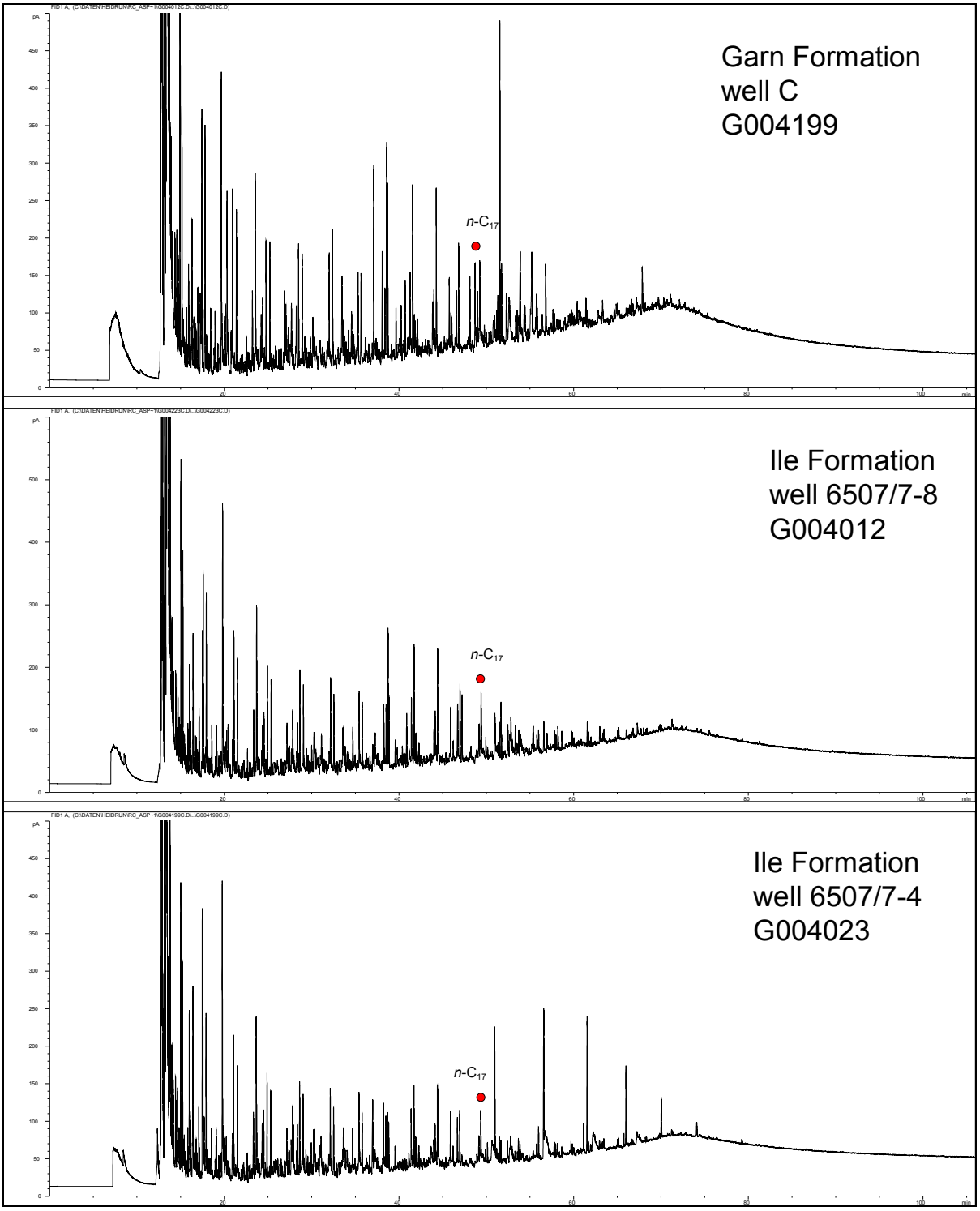

Figure 105 Reservoir rock asphaltene pyrolysis gas chromatograms presenting the form of contamination detected. *Top* G004199 from the Garn Formation in well C; *Middle* G004012 from the Ile Formation of well 6507/7-8; *Bottom* G004023 from the Garn Formation of well 6507/7-4.

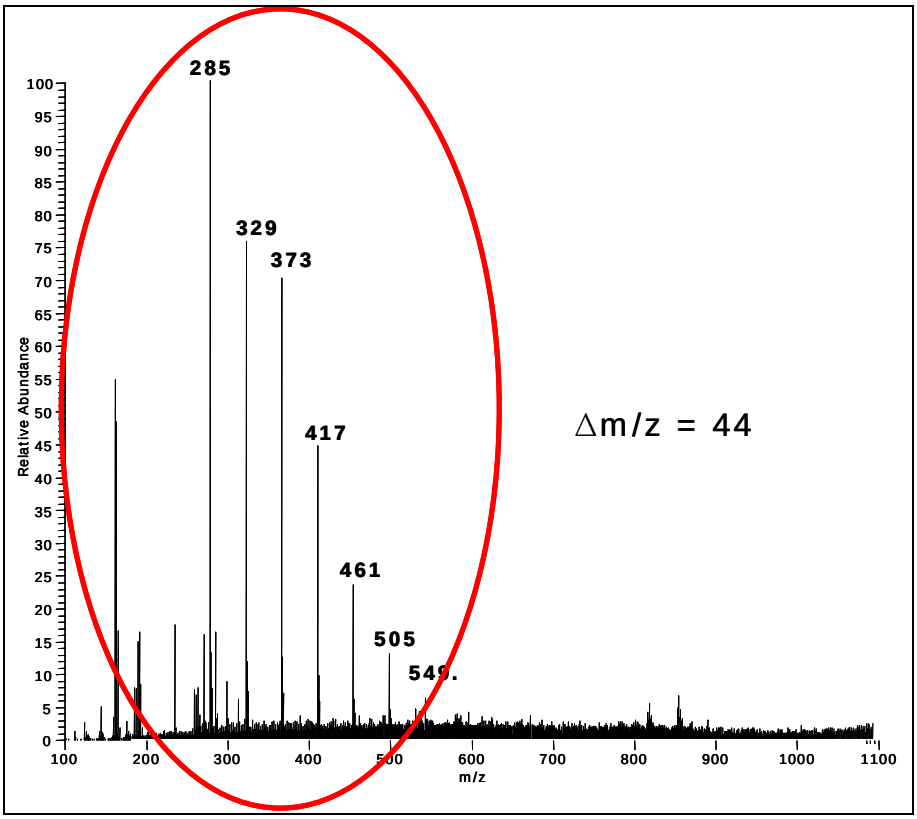

Figure 106 GC-MS spectra of the reservoir rock asphaltene G004199 from the Garn Formation of well C. Polyethylenglycol a drilling mud additive was identified.

7.3 HETEROGENEITY SCREENING USING PURE RESERVOIR ROCK ASPHALTENES

In the following section, the pyrolysis-GC screening parameters received from pure reservoir rock asphaltenes separated from the reservoir rock bitumen extracts are presented. The results obtained from the asphaltenes are presented using similar geochemical profiles and ternary diagrams applied in the reservoir rock screening. Within the diagrams, the asphaltenes are compared to the pyrolysis-GC parameters obtained from the whole rock screening. All pyrolysis-GC parameters of the asphaltenes in comparison to the Py-GC parameters of their corresponding reservoir rock samples are shown in Table X 10 in the appendix.

7.3.1 COMPARISON OF ASPHALTENES AND RESERVOIR ROCKS FROM THE EASTERN PART OF THE HEIDRUN OIL FIELD

7.3.1.1 WELL C IN SEGMENT J (GARN FM, ILE FM. 4 - 6, NOT FM. 1, ÅRE FM. 1)

7.3.1.1.1 ORGANIC MATTER COMPOSITION

In total seven reservoir rock asphaltenes were separated, two from the Garn, three of the Ile, and one from the Not and Åre Formation. Bulk properties based on pyrolysis products are shown in geochemical profiles in Figure 107 A - E for the aromaticity (A), monoaromatic / diaromatic hydrocarbon ratio (B), relative phenol content (C), gas wetness (D) and gas amount (E) and listed in Table X 10.

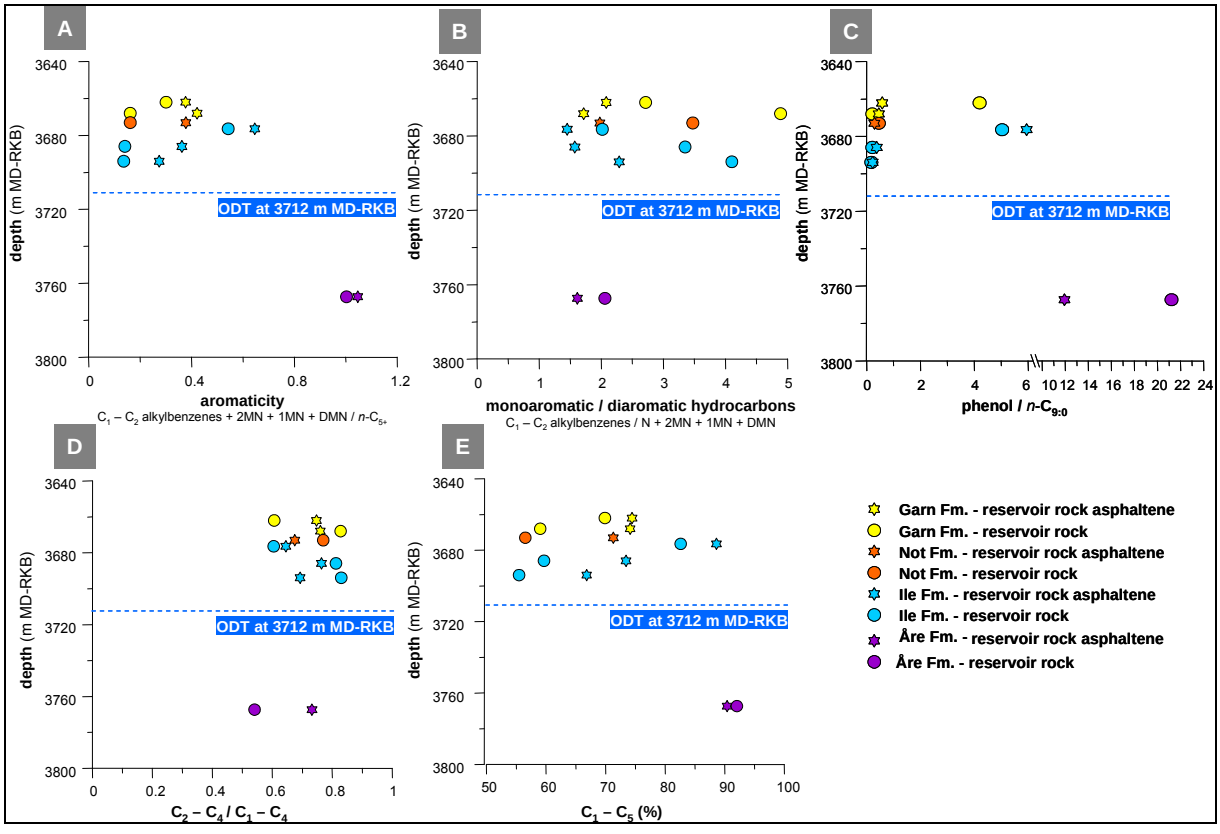

Figure 107 Geochemical profiles obtained from the pyrolysis-GC parameters of the reservoir rock asphaltenes and their corresponding reservoir rock samples from well C. From A to E the aromaticity (A), monoaromatic / diaromatic hydrocarbon ratio (B), relative phenol amount (C), gas wetness (D), and gas amount (E) are shown.

All asphaltene pyrolysates independent of their reservoir formation show higher aromaticity, a lower monoaromatic / diaromatic hydrocarbon ratio and higher gas yields compared to the corresponding reservoir rock samples. The phenol ratio and gas wetness are different within the individual formations. Two asphaltenes from the Ile Formation (G004217) and the Åre Formation (G004249) show a high phenol ratio about 5.9 and 11.9 similar to their corresponding reservoir rocks. Thus, also the asphaltenes indicate terrestrial OM supply. However, both asphaltenes show higher gas wetness, while the remaining asphaltenes present lower gas wetness compared to their reservoir rock samples. The relative phenol content in the upper Garn Formation sample is conspicuous. Here the reservoir rock is very rich in phenol, whereas the asphaltene is very low. Despite these differences, the three Ile Formation asphaltenes show similar trends as seen for the corresponding reservoir rocks with increasing depth.

7.3.1.1.2 ORGANOFACIES AND/OR MATURITY DIFFERENCES

In Figure 108 A - C, the ternary diagrams used for organofacies characterisations are shown. They comprise the reservoir rock asphaltenes in comparison to their corresponding reservoir rock samples.
Within the CLD (Figure 108 A), both high phenol asphaltenes from the Ile – and the Åre Formation plot in the gas and condensate field. All remaining asphaltenes plot in the P-N-A low wax oil field similar to their corresponding reservoir rock samples. They show a CLD similar to the source rock from the Spekk Formation. The relative sulphur content is low for all asphaltenes (Figure 108 C). Additionally, the aromaticity trend observed in the Ile Formation as well as the higher gas amount in all asphaltene pyrolysates is reflected. In general, the asphaltenes shows similar distributions and gradients as observed in the reservoir rock samples.

In summary, compared to the corresponding reservoir rocks the asphaltene pyrolysates show differences in the aromatic compounds (higher aromaticity, lower mono / diaromatic hydrocarbon ratio) and present higher gas yields. In addition, the phenol amount is lower in the asphaltenes, but can be used to indicate terrestrial organic matter input. For the Ile Formation asphaltenes, similar trends were observed with increasing depth.

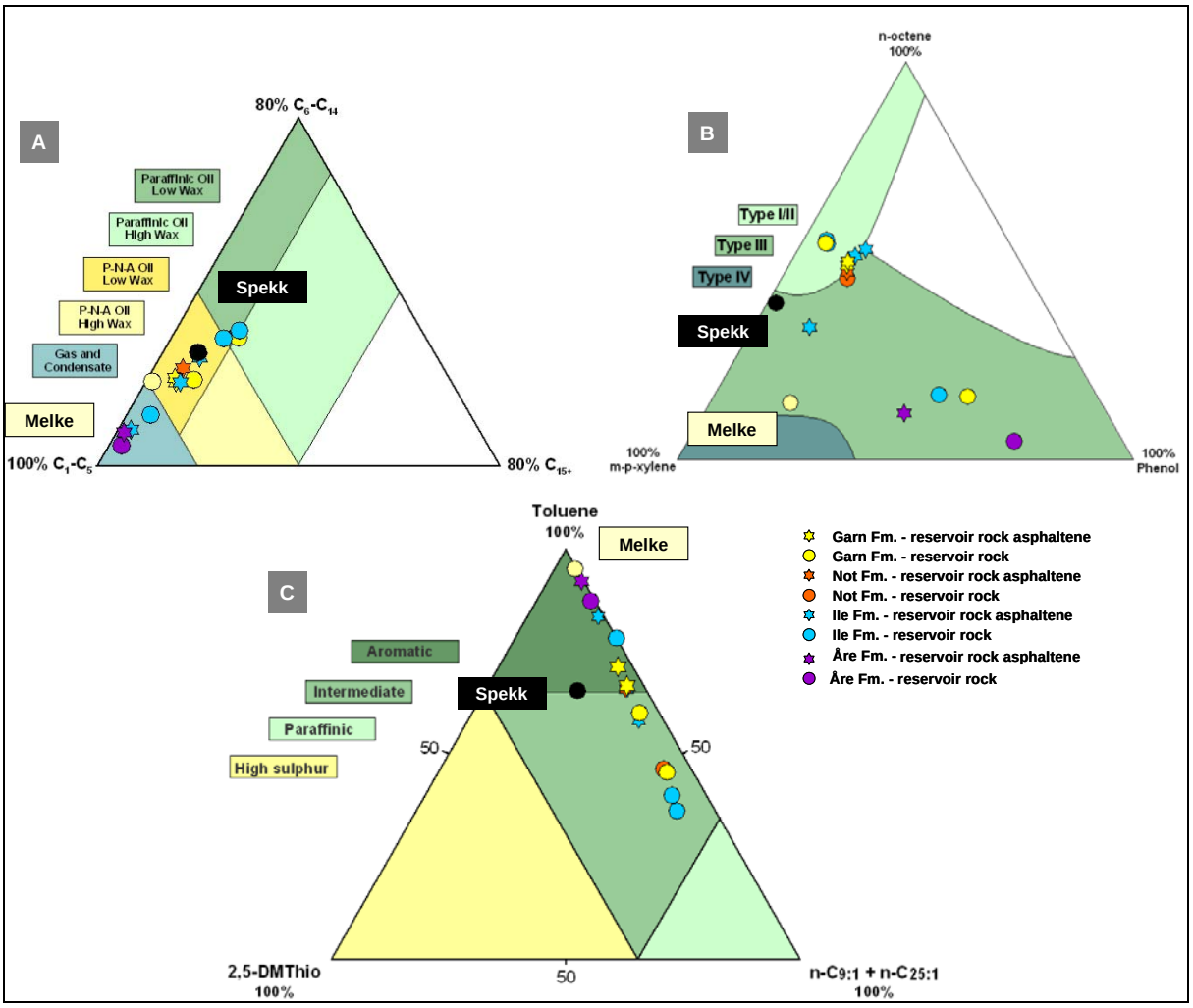

Figure 108 Bulk properties of the reservoir rock asphaltene pyrolysis products of well C in comparison to the pyrolysis products of their corresponding reservoir rock samples and both potential source rock samples analysed in the Heidrun oil field. From A to C the alkyl chain length distribution (A), the phenol content (B), and the sulphur content (C) are shown.

7.3.1.2 WELL B IN SEGMENT I (TILJE FM. 2.5 – 3.4)

7.3.1.2.1 ORGANIC MATTER COMPOSITION

The bulk parameters based on pyrolysis products of eight selected reservoir rock asphaltenes of well B in comparison to their corresponding reservoir rock samples are shown in Figure 109 A - E for the aromaticity (A), monoaromatic / diaromatic hydrocarbon ratio (B), relative phenol content (C), gas wetness (D) and gas amount (E). The corresponding asphaltene and reservoir rock data are listed in Table X 10.

The aromaticity of the asphaltenes (Figure 109 A) range between 0.31 and 0.57 that is twice the value observed for the reservoir rock samples. However, the asphaltenes and reservoir

rock samples show a similar trend in aromaticity with increasing depth. Within the type of aromatic hydrocarbon ratio, the asphaltenes are characterised by less variability in their pyrolysates and the ratio value is half the amount as observed for the corresponding reservoir rock samples (Figure 109 B). The relative phenol content is slightly lower in the asphaltenes (Figure 109 C). Both, gas wetness and gas amount of the asphaltene pyrolysates is higher as compared to the reservoir rock sample pyrolysates (Figure 109 D, E).

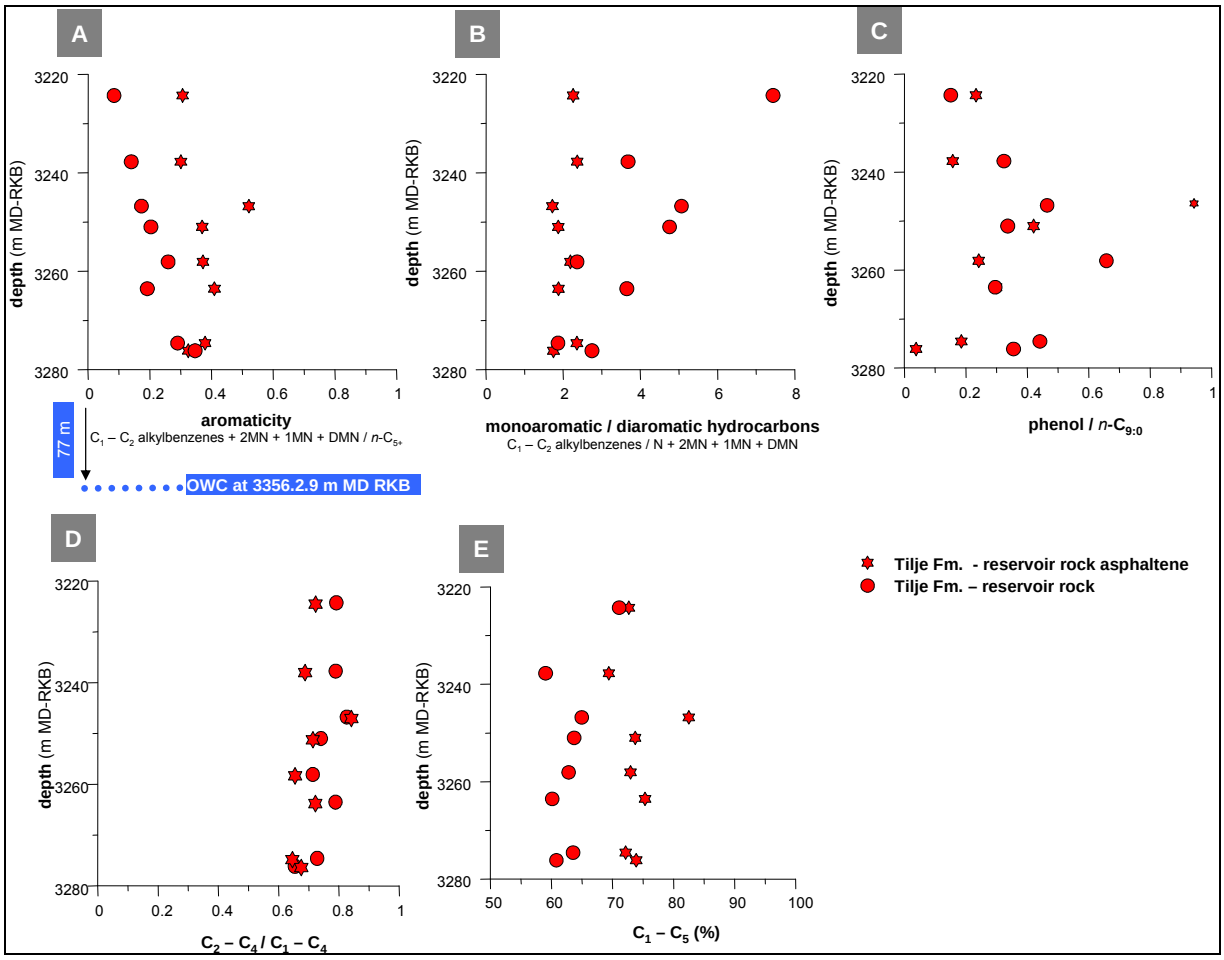

Figure 109 Geochemical profiles using the pyrolysis products of the reservoir rock asphaltenes and their corresponding reservoir rock samples from well B. From A to E the aromaticity (A), monoaromatic / diaromatic hydrocarbon ratio (B), relative phenol content (C), gas wetness (D), and gas content (E) are shown.

7.3.1.2.2 ORGANOFACIES AND/OR MATURITY DIFFERENCES

The ternary diagrams (Figure 110 A - C) reflect higher gas yields in the asphaltene pyrolysates from well B and slight gradients in the aromaticity observed before in the depth plots. Within all ternary diagrams, the asphaltenes plot closer together than the reservoir rock samples. In the CLD ternary nearly all asphaltenes plot in the P-N-A low wax oil field (Figure

110 A) indicating a marine source depositional environment. They show a CLD that is similar to those observed for the Spekk Formation. However, all asphaltenes show higher content of short alkyl chains in their pyrolysates (higher gas content) as compared to the corresponding reservoir rock samples. All reservoir rock asphaltenes are low in sulphur as well as in phenol similar to the reservoir rocks.

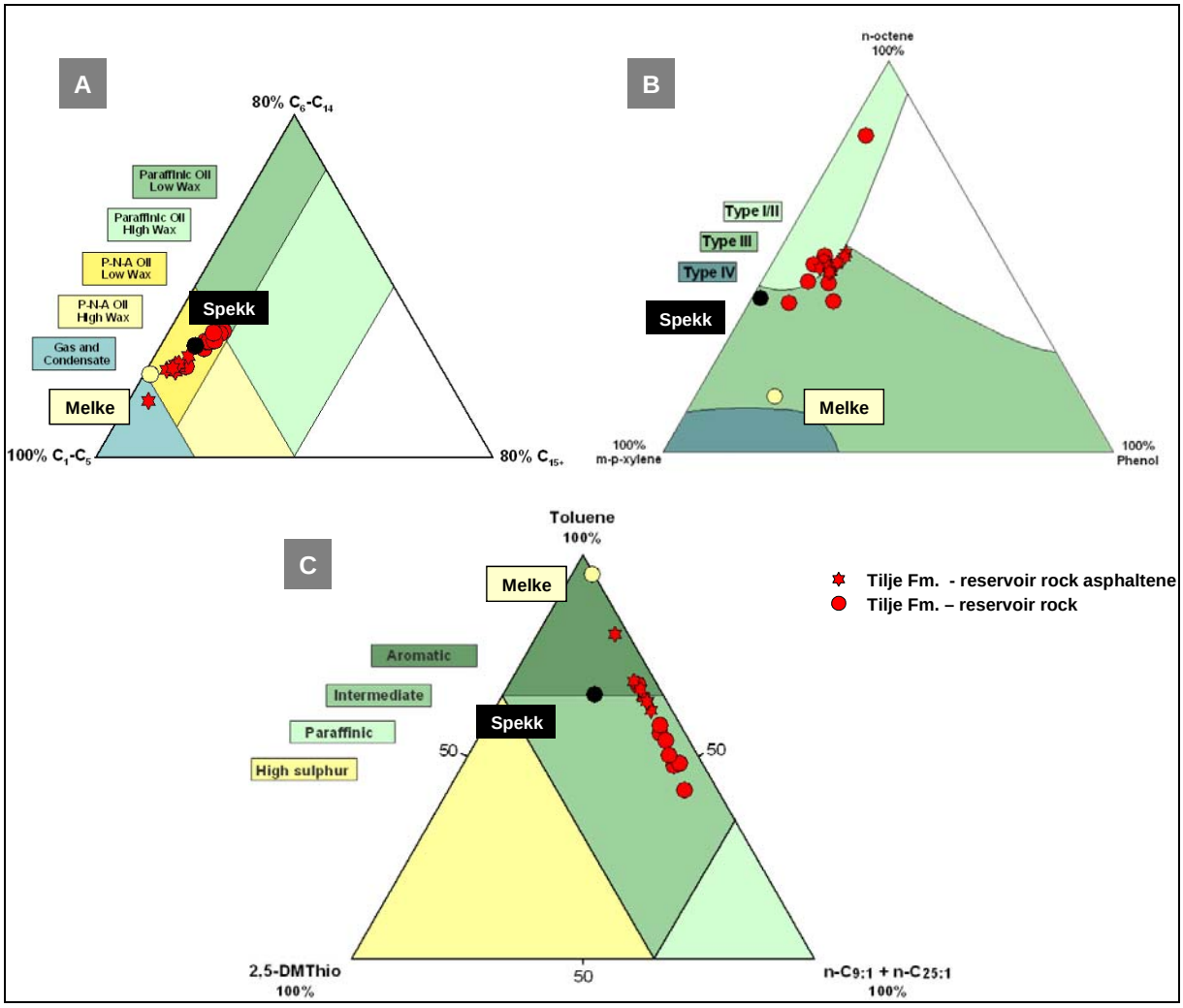

Figure 110 Bulk properties of the reservoir rock asphaltene pyrolysis products of well B in comparison to the pyrolysis products of their corresponding reservoir rock samples and both potential source rock samples analysed in the Heidrun oil field. From A to C the alkyl chain length distribution (A), phenol content (B), and sulphur content (C) are shown.

In summary, compared to the corresponding reservoir rock samples the asphaltene pyrolysates exhibit higher aromaticity and higher gas yields. Furthermore, the asphaltenes do not differ among themselves regarding the individual Py-GC parameters as much as seen for the corresponding reservoir rock samples, but, in general, reflect the gradients observed in the reservoir rock pyrolysates for the individual Py-GC parameters.

7.3.2 COMPARISON OF ASPHALTENES AND RESERVOIR ROCKS FROM THE NORTHERN PART OF THE HEIDRUN OIL FIELD

7.3.2.1 WELL D IN SEGMENT Q (ÅRE FM 2.1)

7.3.2.1.1 ORGANIC MATTER COMPOSITION

In well D, three asphaltenes were separated and analysed from selected reservoir rock samples of the Åre Formation 2.1. Their bulk parameters based on pyrolysis products are compared in Figure 111 A - E concerning the aromaticity (A), monoaromatic / diaromatic hydrocarbon ratio (B), relative phenol content (C), gas wetness (D) and gas amount (E) and listed in Table X 10.

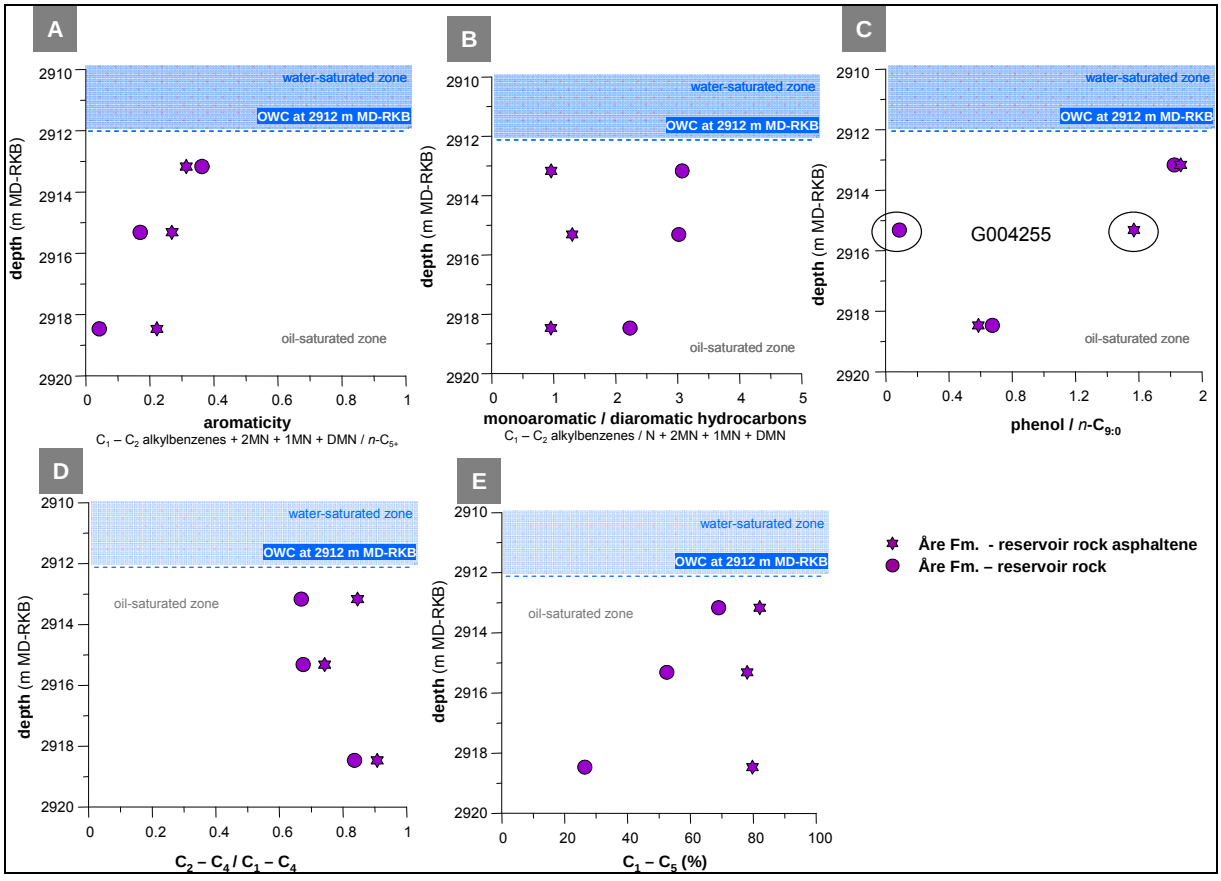

Figure 111 Geochemical profiles using the pyrolysis products of the reservoir rock asphaltenes and their corresponding reservoir rock samples from well D. From A to E the aromaticity (A), monoaromatic / diaromatic hydrocarbon ratio (B), relative phenol amount (C), gas wetness (D), and gas amount (E) are shown.

With respect to aromaticity, the reservoir rock asphaltenes are characterised by slightly higher Py-GC parameter values and a less distinctive but similar trend as observed in the reservoir rock samples (Figure 111 A). Disregarding asphaltene sample G004255 in the middle of the phenol depth plot in Figure 111 C, the relative phenol content in the asphaltenes is similar to the reservoir rock samples and shows the same decrease with depth. Differences could be observed for the mono versus diaromatic hydrocarbon ratio (Figure 111 B). Here most of the asphaltenes show lower ratios and no gradient as observed for the reservoir rocks. The gas wetness and the gas content are higher in the asphaltene pyrolysates compared to the reservoir rocks. Obviously, there are more gas and especially methane generating structures within the asphaltenes.

7.3.2.1.2 ORGANOFACIES AND/OR MATURITY DIFFERENCES

Several differences were observed within the CLD of the asphaltenes compared to the corresponding reservoir rock samples (Figure 112 A). All asphaltenes plot close together in the P-N-A low wax oil field near the gas and condensate field indicating the supply of little lignocellulosic organic matter to the generating source material. They show a similar CLD as compared to the Melke Fm. source rock and indicate oil generated by a marine (mature) source rock Type II / III. The corresponding reservoir rock sample of asphaltenes no. 1 (G004254) present a similar CLD compared to the marine source rock of the Spekk Formation. Significant differences compared to the asphaltenes show reservoir rock samples no. 2 (G004255) and no. 3 (G004258). They present distinctly higher content of long chain alkanes referring to high wax content, which indicates lacustrine conditions of the deposited source rock.

In the phenol ternary diagram (Figure 112 B), asphaltene no 2 (G004255) and its reservoir rock show largest differences concerning the phenol content reflecting the distribution observed in the geochemical depth plot (Figure 111 B).

All asphaltenes are characterised by low sulphur content similar to their corresponding reservoir rock samples. Here, asphaltene no. 3 (G004258) and its waxy reservoir rock sample show large differences in aromaticity and paraffinicity, respectively.

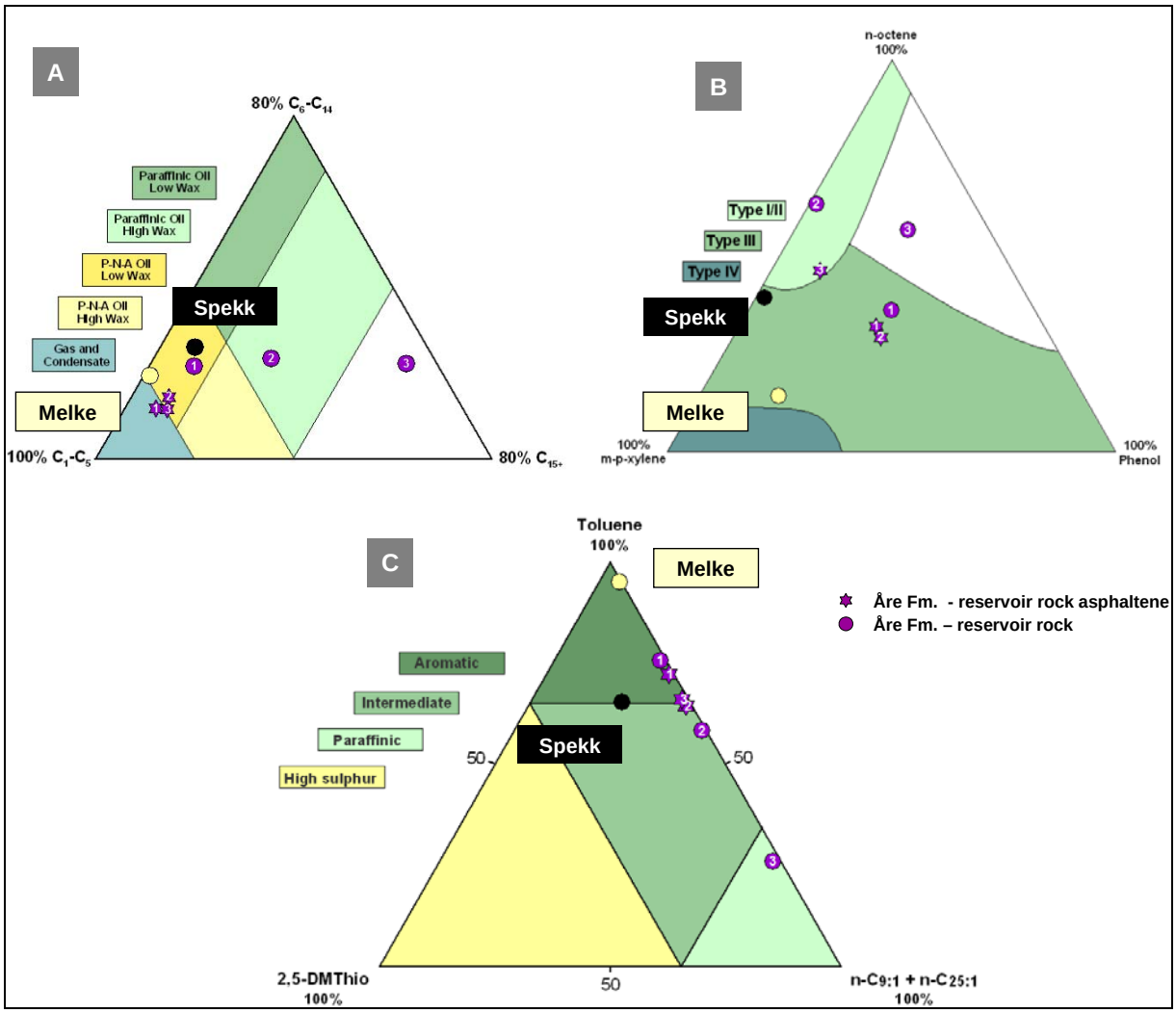

Figure 112 Bulk properties of the reservoir rock asphaltene pyrolysis products of well D in comparison to the pyrolysis products of their corresponding reservoir rock samples and both potential source rock samples analysed in the Heidrun oil field. From A to C the alkyl chain length distribution (A), phenol content (B), and sulphur content (C) are shown.

In summary, similar as observed before in well B and C, the asphaltenes in well D are characterised by differences regarding aromatic and gaseous compounds. They present higher aromaticity, gas yields and gas wetness compared to their corresponding reservoir rock samples. However, phenol ratio and gas amount excluded, the distribution trends of the Py-GC parameters with increasing depth in the profile are similar for asphaltenes and reservoir rock samples. Differences in the organofacies show the lowermost asphaltene and its waxy reservoir rock. While the latter indicates a lacustrine source, the asphaltene indicates a marine kerogen Type II / III.

7.3.2.2 WELL E IN SEGMENT IN SEGMENT M (ÅRE FM 4.1)

7.3.2.2.1 ORGANIC MATTER COMPOSITION

In total, four reservoir rock samples were selected of well E (Åre Formation 4.1) for the asphaltenes separation. The asphaltene and the corresponding reservoir rock bulk Py-GC parameters are shown in Figure 113 A - E for the aromaticity (A), monoaromatic / diaromatic hydrocarbon ratio (B), relative phenol content (C), gas wetness (D) and gas amount (E) and listed in Table X 10.

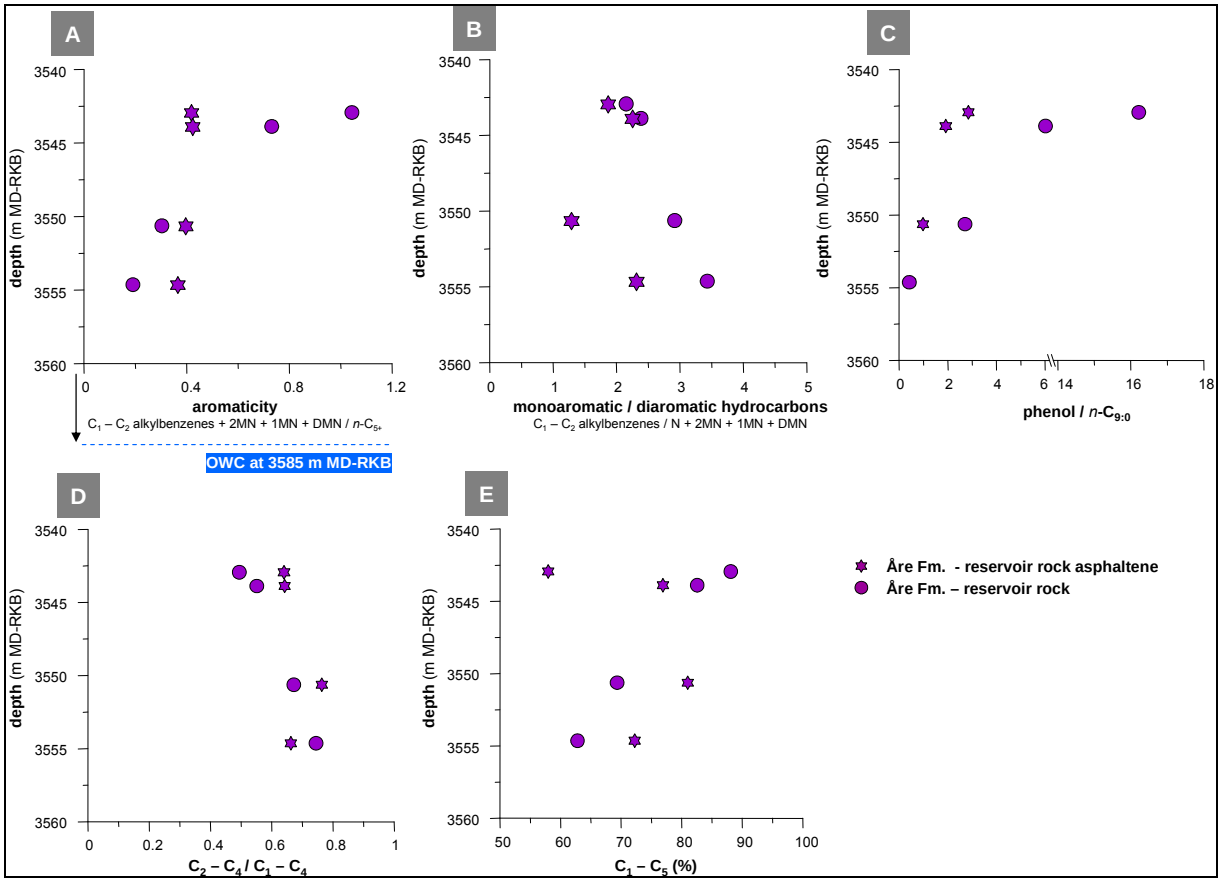

Figure 113 Geochemical profiles using the pyrolysis products of the reservoir rock asphaltenes and their corresponding reservoir rock samples of well E. From A to E the aromaticity (A), monoaromatic / diaromatic hydrocarbon ratio (B), relative phenol amount (C), gas wetness (D), and gas amount (E) are shown.

Both asphaltenes and reservoir rock samples show different distribution pattern concerning the Py-GC parameters. The asphaltenes aromaticity is relatively uniform within the profile in contrast to the corresponding reservoir rock samples presenting a decrease in aromaticity with increasing depth (Figure 113 A). The asphaltenes have a relatively high phenol ratio as they

were separated from phenol rich reservoir rock samples. Concerning the distribution, the asphaltenes present the same trend observed for the reservoir rocks (Figure 113 C). Concerning gradients in the monoaromatic / diaromatic hydrocarbon ratio (Figure 113 B) and gas wetness (Figure 113 D), the asphaltenes do not exactly reflect the distribution observed for the reservoir rock samples. They are characterised by higher gas wetness compared to the corresponding reservoir rock samples. Excluding the lower most asphaltene (G004268), the gas wetness increases with increasing depth and show an inverse correlation to the aromaticity, similar as observed for the reservoir rock samples. The distribution of the gas amount presents largest differences (Figure 113 E).

7.3.2.2.2 ORGANOFACIES AND/OR MATURITY DIFFERENCES

Within the ternary diagrams, showing the Py-GC parameters of well E, the asphaltenes plot closely together (Figure 114 A - C). They plot in the P-N-A low wax oil indicating field and partly in the gas and condensate field. They show differences compared to their corresponding reservoir rock samples. Especially both uppermost asphaltenes no 1 and no 2 (G004263 and G004265) reveal higher amount of short chain alkanes and show a chain length distribution that is more similar to the CLD of the potential source rock from the Melke Formation. The sulphur content is low for all asphaltenes similar to the reservoir rocks. Additionally differences were observed for the phenol content.

In summary, compared to the reservoir rocks the asphaltenes show different values for the investigated parameter and do not differ as much as the reservoir rock pyrolysates. For the asphaltenes separated from phenol rich reservoir rocks, the aromaticity and the gas yields are lower and the gas wetness is higher compared to their corresponding reservoir rocks. The asphaltene with low phenol ratio present a higher aromaticity and gas yields, and lower gas wetness compared to the corresponding reservoir rock samples.

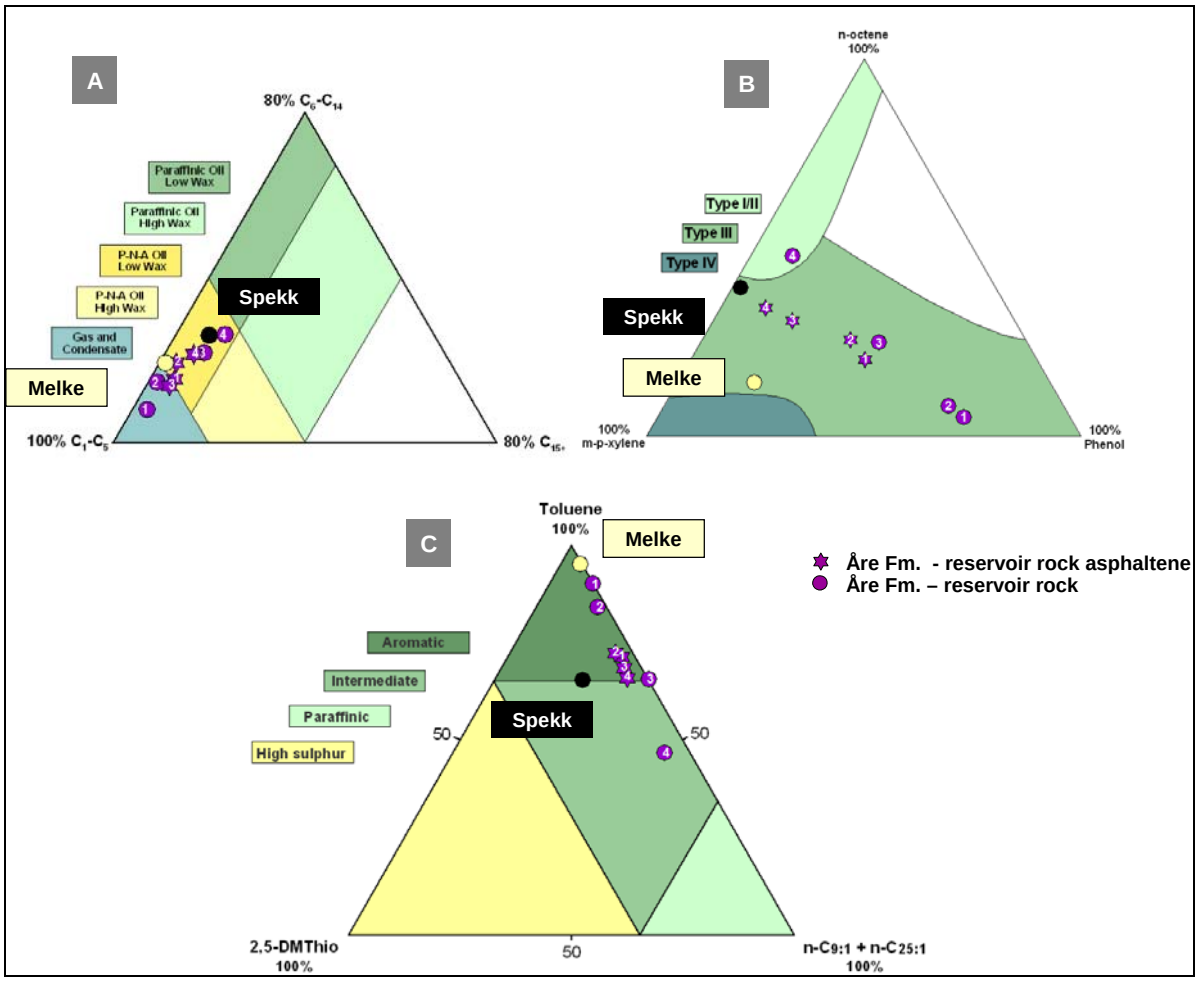

Figure 114 Bulk properties of the reservoir rock asphaltene pyrolysis products of well E in comparison to the pyrolysis products of their corresponding reservoir rocks and both potential source rocks analysed in the Heidrun oil field. From A to C the alkyl chain length distribution (A), phenol content (B), and sulphur content (C) are shown.

7.3.3 COMPARISON OF ASPHALTENES AND RESERVOIR ROCKS FROM THE WESTERN PART OF THE HEIDRUN OIL FIELD

7.3.3.1 WELL 6507/7-2 IN SEGMENT G (TILJE FM. 3.2 AND 2.2/2.1, ÅRE FM. 7.2)

7.3.3.1.1 ORGANIC MATTER COMPOSITION

The bulk Py-GC parameters of the three asphaltenes analysed in well 6507/7-2 shows a very homogeneous distribution. A comparison to their corresponding reservoir rock samples is shown in Figure 115 for the aromaticity (A), monoaromatic / diaromatic hydrocarbon ratio (B), relative phenol content (C), gas wetness (D) and gas amount (E). An overview of the Py-

GC parameters of the investigated asphaltenes and corresponding reservoir rock samples is given in Table X 10.

The aromaticity in the asphaltenes is nearly constant in the profile (0.036 ± 0.02) but the amount is one third higher as compared to the corresponding reservoir rock samples. Within the type of aromatic hydrocarbon ratio, slight differences among the asphaltenes pyrolysis products were observed. In contrast to the reservoir rocks, the ratio for the asphaltenes slightly decreases with increasing depth. Additionally, the ratio is half the amount observed for the reservoir rock samples. The phenol ratio, gas wetness and gas yields are nearly constant within profile 6507/7-2. These Py-GC parameters are similar to the values observed for the reservoir rocks; however, the asphaltenes show about 10 % more gas in their pyrolysates.

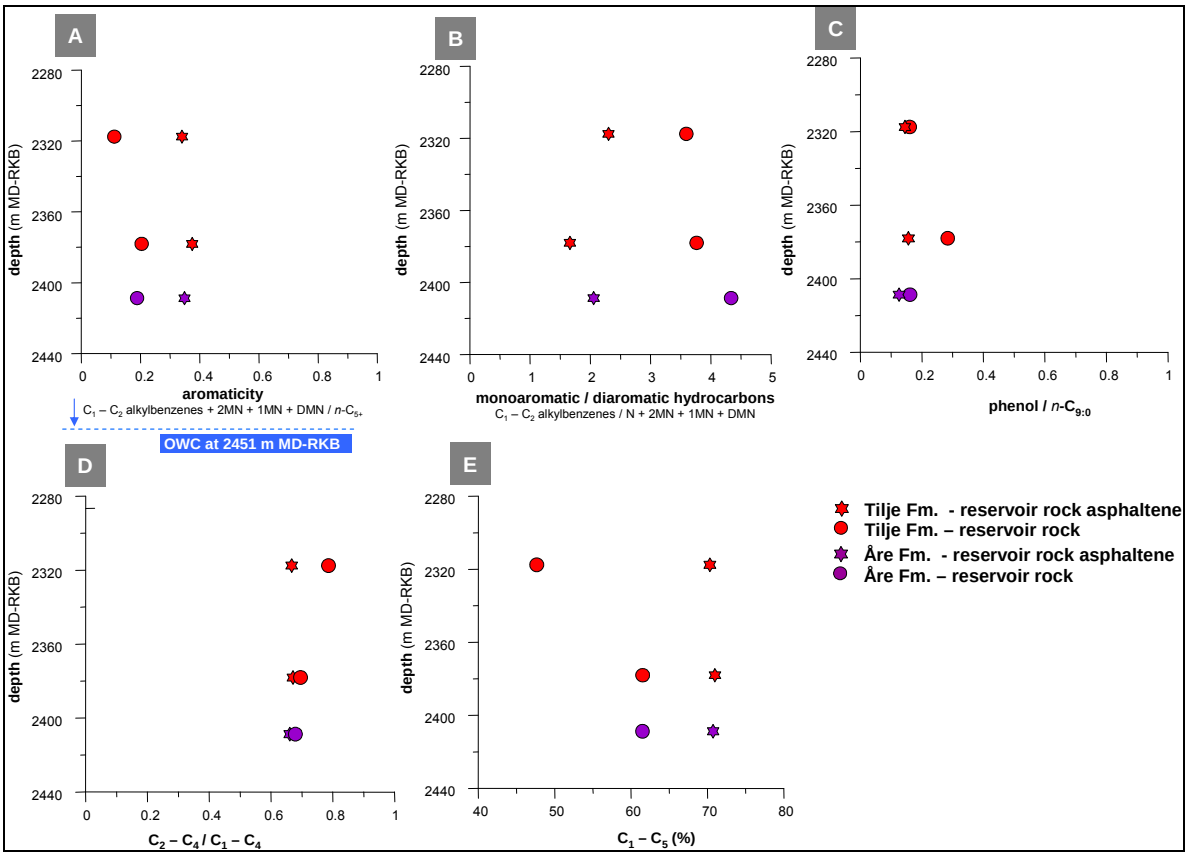

Figure 115 Geochemical profiles using the pyrolysis-GC parameter of the reservoir rock asphaltenes and their corresponding reservoir rock samples from well 6507/7-2. From A to E the aromaticity (A), monoaromatic / diaromatic hydrocarbon ratio (B), relative phenol amount (C), gas wetness (D), and gas amount (E) are shown.

7.3.3.1.2 ORGANOFACIES AND/OR MATURITY DIFFERENCES

The CLD as well as the phenol and sulphur content ternary diagrams (Figure 116 A - C) mirror the differences between asphaltene and reservoir rock pyrolysates seen before in the geochemical depth plots. Largest differences were observed within the chain length distribution (Figure 116 A). Here, all asphaltenes plot very close to the Spekk Formation source rock in the P-N-A low wax oil field, while the corresponding reservoir rock samples, especially the uppermost sample labelled by no. 1 (G003998) show high amounts of waxy compounds in the pyrolysates and plot in the paraffinic high wax field. The sulphur content is low for all asphaltenes similar as observed for their corresponding reservoir rock pyrolysates.

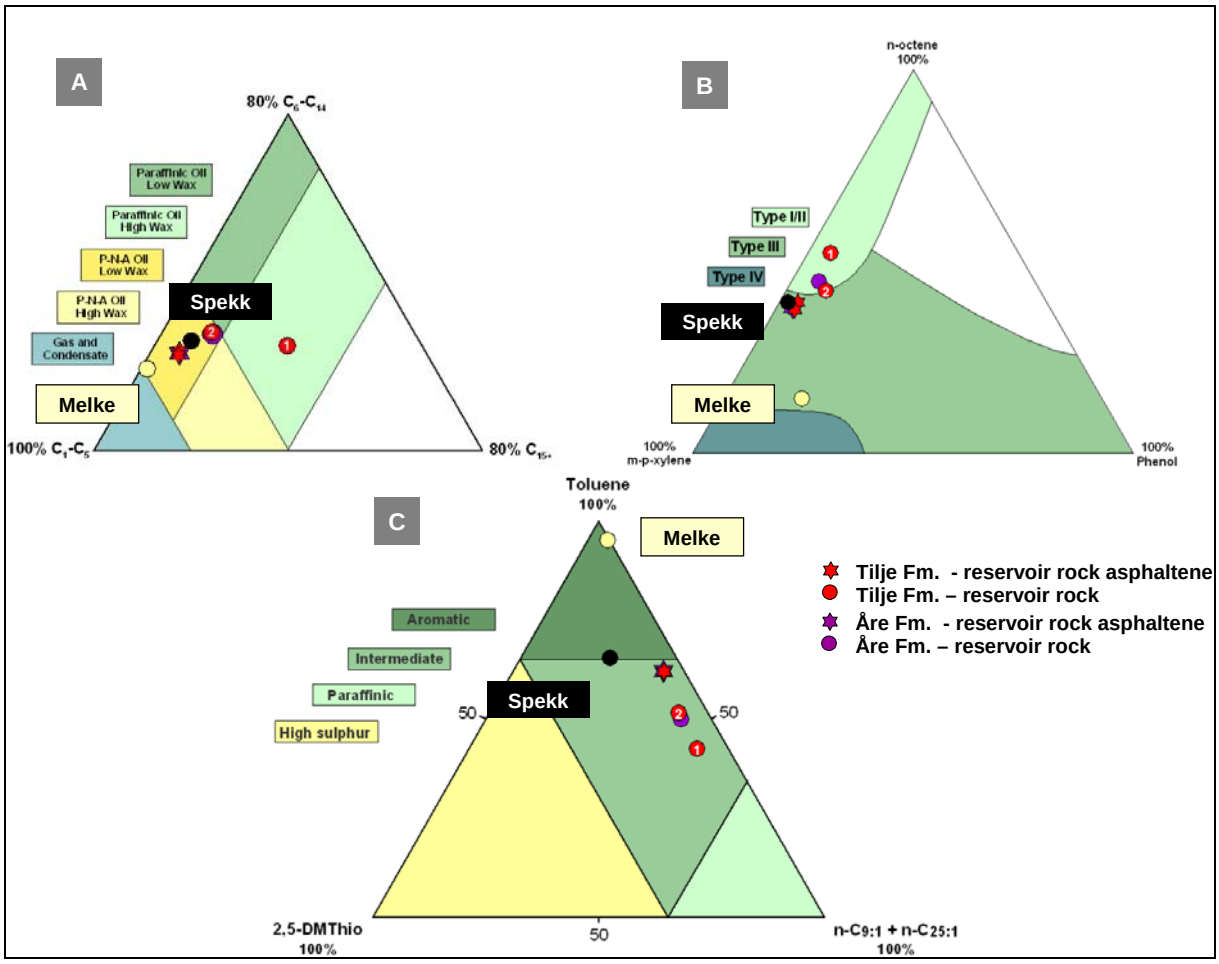

Figure 116 Bulk properties of the reservoir rock asphaltene pyrolysis products of well 6507/7-2 in comparison to the pyrolysis products of their corresponding reservoir rock samples and both potential source rock samples analysed in the Heidrun oil field. From A to C the alkyl chain length distribution (A), relative phenol content (B), and relative sulphur content (C) are shown.

7.3.3.2 WELL 6507/7-5 IN SEGMENT O (GARN FM., ILE FM. 2)

7.3.3.2.1 ORGANIC MATTER COMPOSITION

Both asphaltene samples separated from the Garn and Ile Formation in well 6507/7-5 present relatively uniform pyrolysis parameter similar as observed for the corresponding reservoir rock samples (Figure 117 A - E,). Slight differences were observed for the aromaticity and the monoaromatic / diaromatic hydrocarbon ratio. Compared to their corresponding reservoir rock samples the values of the Py-GC parameters are different. The aromaticity, phenol ratio and gas yield are higher, while the monoaromatic / diaromatic hydrocarbon ratio and gas wetness are lower.

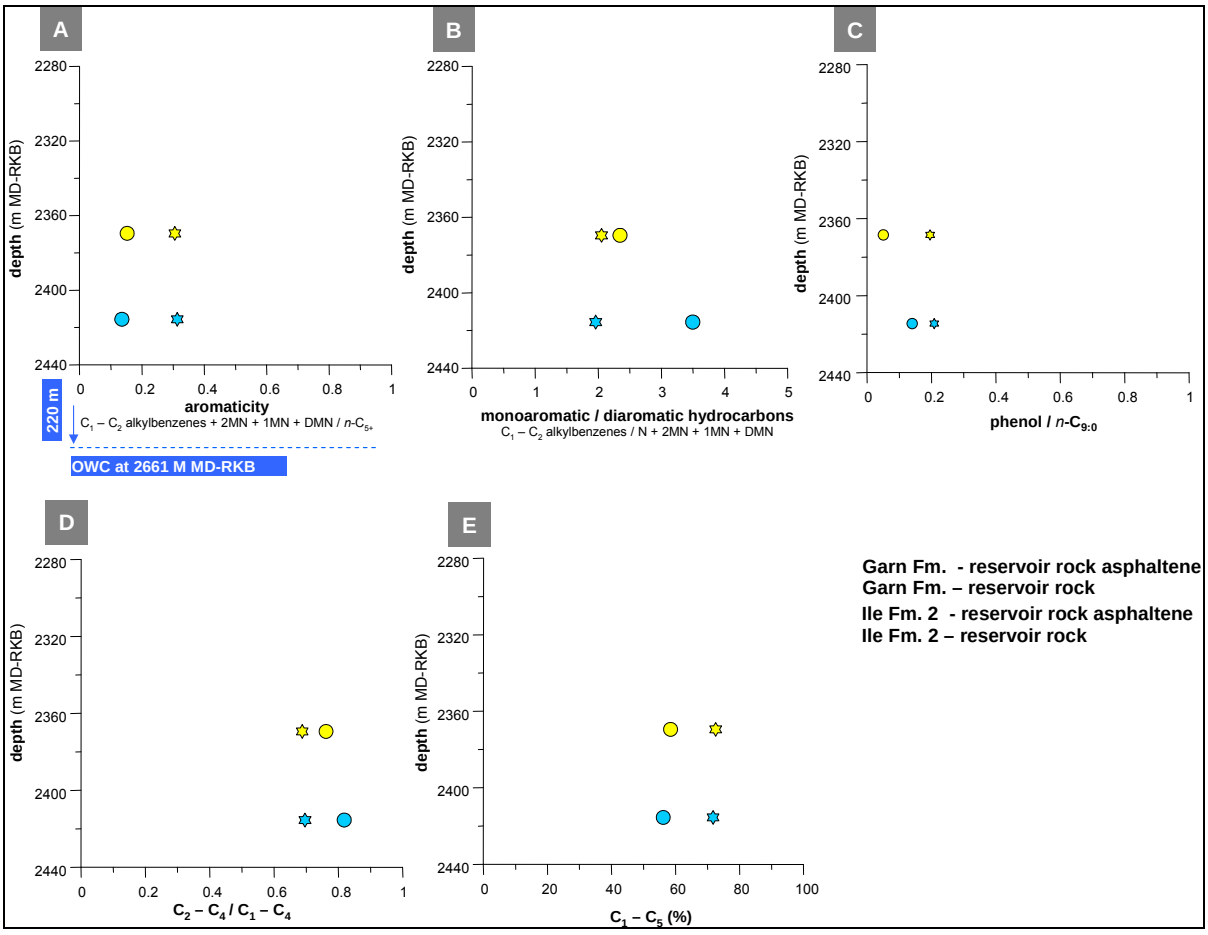

Figure 117 Geochemical profiles using the pyrolysis GC parameters of the reservoir rock asphaltenes and their corresponding reservoir rock samples from well 6507/7-5. From A to E the aromaticity (A), monoaromatic / diaromatic hydrocarbon ratio (B), relative phenol amount (C), gas wetness (D) and gas amount (E) are shown.

7.3.3.2.2 ORGANOFACIES AND/OR MATURITY DIFFERENCES

Differences were observed comparing the alkyl chain length distribution of the Garn and Ile Formation asphaltenes with their corresponding reservoir rock samples (Figure 118 A). The asphaltenes plot in the P-N-A low wax oil field between the marine Spekk- and Melke Formation source rocks, while the corresponding reservoir rock samples plot in the paraffinic high wax oil field. The reservoir rocks show a higher content of long alkyl chains in their pyrolysates, which indicate high wax content and might refer to lacustrine influence of the source, or more probable to mixing processes described in Chapter 6.6.2. The asphaltenes does not reflect these influences. The asphaltenes as well as their corresponding reservoir rock samples are characterised by a low phenol and sulphur content (Figure 118 B and C). The phenol and the sulphur ternary diagram reflects differences regarding the aromaticity between asphaltenes and reservoir rocks as observed in the geochemical depth plot in Figure 117 A).

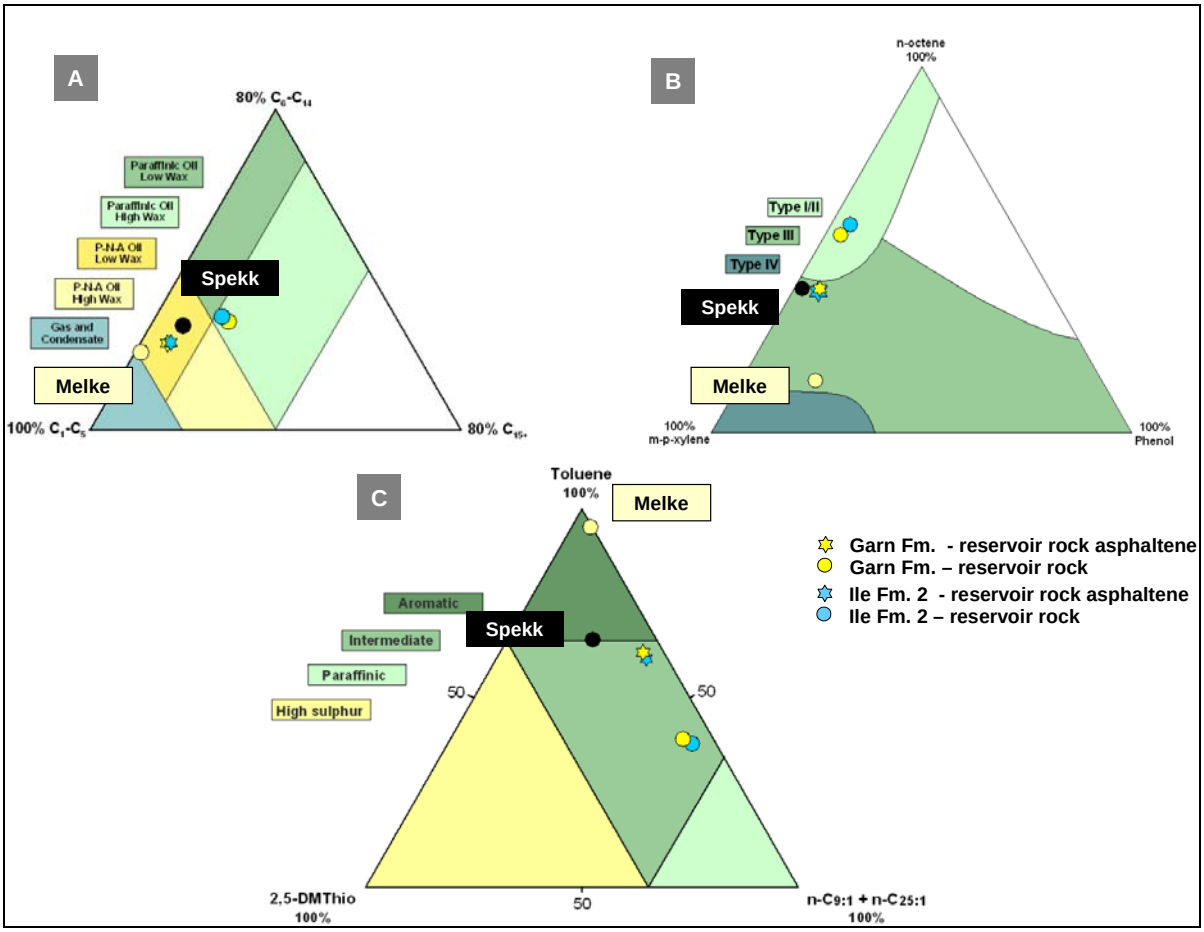

Figure 118 Bulk properties of the reservoir rock asphaltene pyrolysis products of well 6507/7-5 in comparison to the pyrolysis products of their corresponding reservoir rock samples and both potential source rock samples analysed in the Heidrun oil field. From A to C the alkyl chain length distribution (A), relative phenol content (B), and relative sulphur content (C) are shown.

7.3.4 COMPARISON OF ASPHALTENES AND RESERVOIR ROCKS FROM THE SOUTHERN PART OF THE HEIDRUN OIL FIELD

7.3.4.1 WELL 6507/7-8 IN SEGMENT F (GARN FM., ILE FM.)

7.3.4.1.1 ORGANIC MATTER COMPOSITION

Excepting gas wetness, the Garn Formation asphaltene of well 6507/7-8 show Py-GC parameters being higher than those from the corresponding reservoir rock samples (Figure 119 A - E, Table X 10).

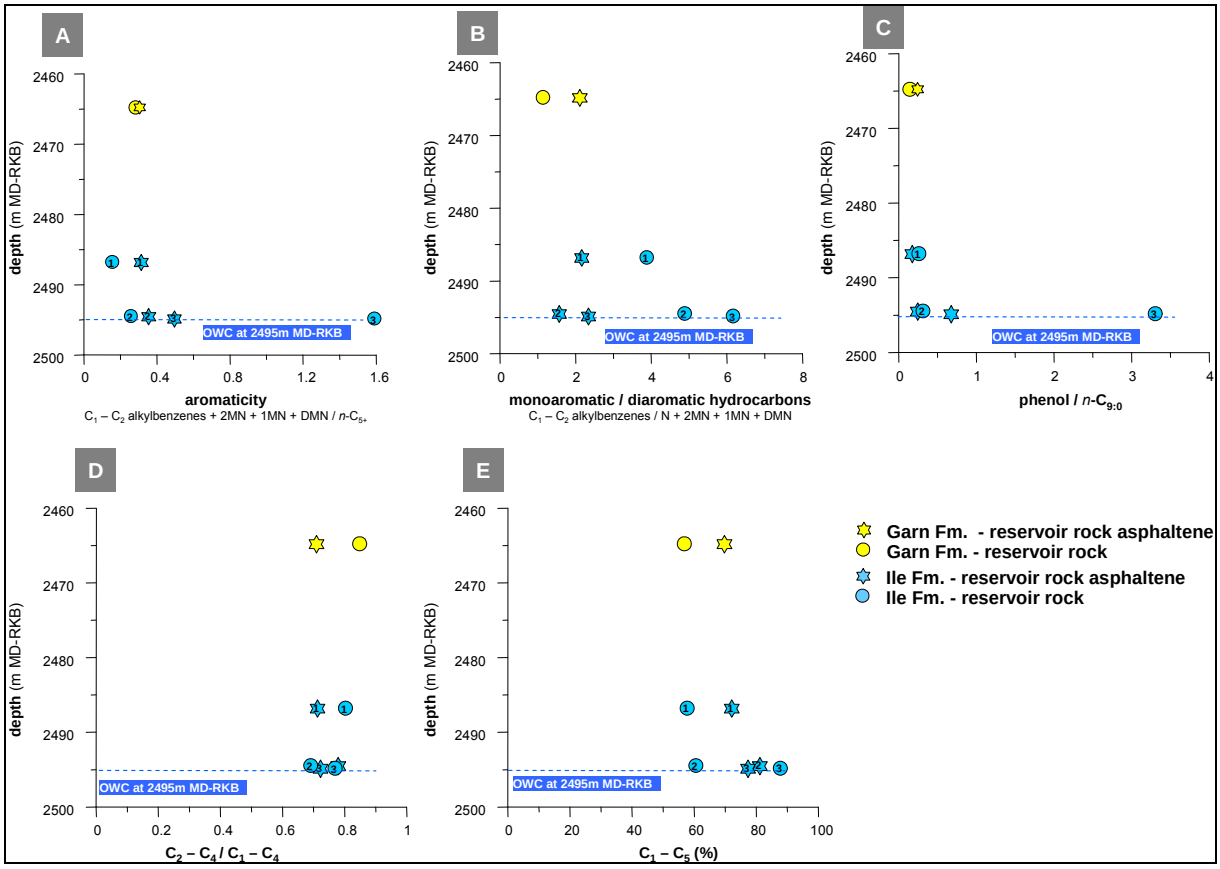

Figure 119 Geochemical profiles using the pyrolysis-GC parameters of the reservoir rock asphaltenes and their corresponding reservoir rock samples from well 6507/7-8. From A to E the aromaticity (A), monoaromatic / diaromatic hydrocarbon ratio (B), relative phenol amount (C), gas wetness (D), and gas amount (E) are shown.

The asphaltenes analysed from the Ile Formation of profile 6507/7-8 exhibit different values for the Py-GC parameters compared to their reservoir rock samples but similar variability

within the aromaticity. With increasing depth, the Ile Formation asphaltenes and reservoir rock samples show an increase in aromaticity (Figure 119 A). The Ile Formation asphaltenes have a lower phenol content and show about 20 % more gas in their pyrolysates compared to their reservoir rocks (Figure 119 C and E). Largest differences were observed for the lowermost asphaltene no. 3 (G004013) separated from a phenol rich reservoir rock (potential coal).

7.3.4.1.2 ORGANOFACIES AND/OR MATURITY DIFFERENCES

The ternary diagrams in Figure 120 A - C for the CLD, relative phenol and sulphur content reflect the differences observed concerning aromaticity and gas content (Figure 119 A and E).

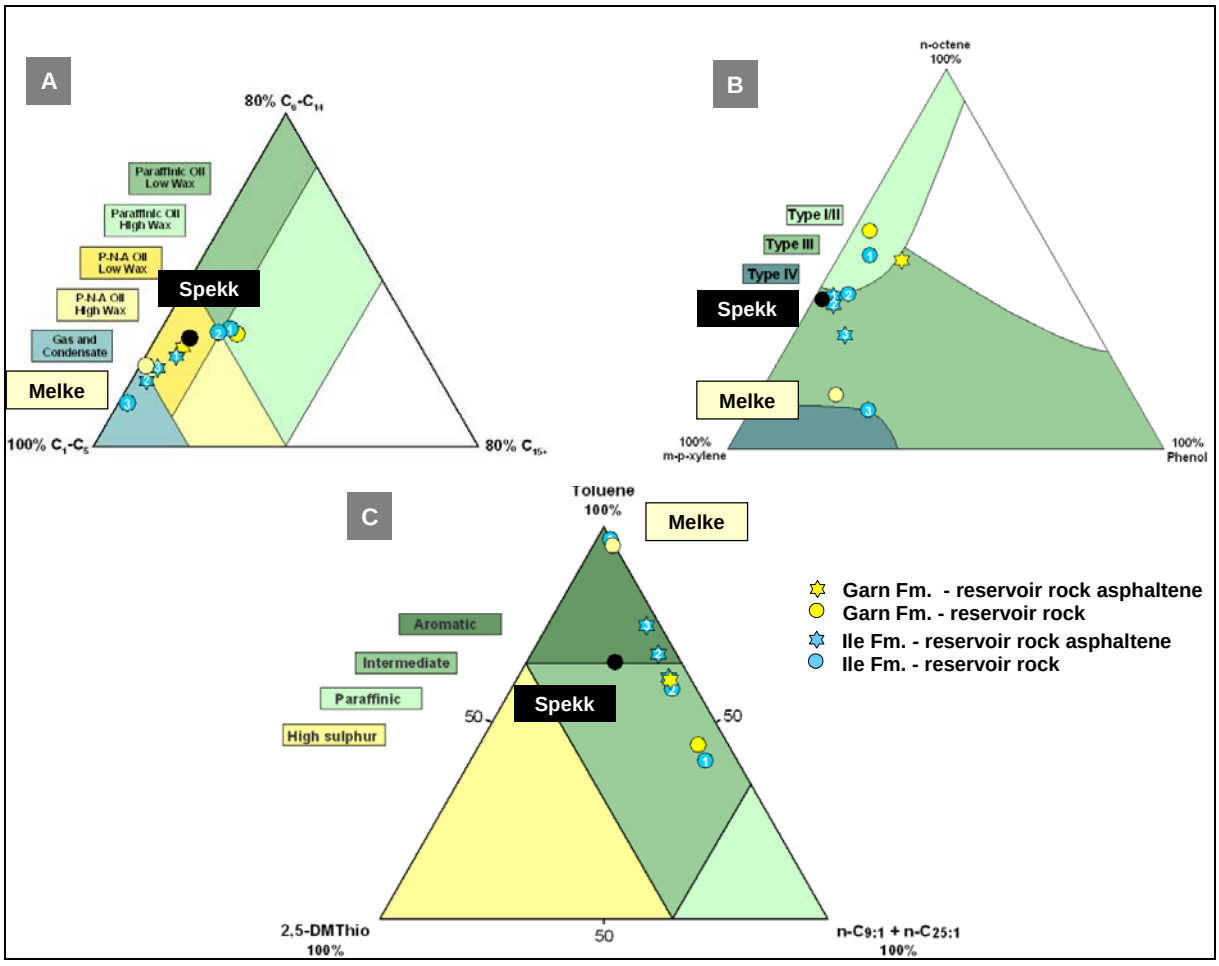

Figure 120 Bulk properties of the reservoir rock asphaltene pyrolysis products of well 6507/7-8 in comparison to the pyrolysis products of their corresponding reservoir rock samples and both potential source rock samples analysed in the Heidrun oil field. From A to C the alkyl chain length distribution (A), relative phenol content (B), and relative sulphur content (C) are shown.

Within the CLD ternary diagram, the Garn- and the uppermost Ile Formation asphaltenes no. 1 (G004010) plot in the P-N-A low wax oil field close to the Spekk Formation source rock shale. The two lower Ile Formation asphaltenes no. 2 and no. 3 (G004012 and G004013) present slightly higher content of short chain alkanes in their pyrolysates and plot close to the Melke Formation source rock sample. Excluding the reservoir rock sample no. 3 (G004013), the reservoir rocks reveal lower amounts regarding short chain alkanes in their pyrolysates than their asphaltenes. All asphaltene and reservoir rock samples are low in sulphur.

7.3.5 SUMMARY

Compared to the reservoir rock samples the corresponding asphaltenes commonly reflect the distribution pattern and gradients observed, but often show different values for the Py-GC parameters. The asphaltenes show differences in the aromatic and gas compounds. Generally, they have a higher aromaticity, lower monoaromatic / diaromatic hydrocarbon ratio, lower gas wetness and a gas yield that is up to 20 % higher as compared to the corresponding reservoir rock samples.
Differences were observed for asphaltenes separated from phenol rich reservoir rocks. These asphaltenes are characterised by higher gas wetness and lower gas content compared to their corresponding reservoir rock samples.

In addition, differences were observed using the organofacies characterising parameters. Within the CLD ternary diagram, most asphaltenes present larger quantities of short chain alkanes in their pyrolysates than their corresponding reservoir rocks. Excluding phenol rich asphaltenes plotting in the gas and condensate field, most of the asphaltenes plot in the P-N-A low wax oil field and partly in the gas condensate field between both potential source rocks from the Spekk- and Melke Formation. This is in contrast to the results obtained from the reservoir rock pyrolysates, where most of the samples present higher quantities of medium and long chain alkanes in their pyrolysates. Most of the reservoir rock samples reveal a CLD that is more similar to the Spekk Formation source rock.
Based on reservoir rock pyrolysis, indications for differences in the organofacies of the source were observed in individual reservoir rock samples from the Garn- and Ile Formation (well 6507/7-2, 6507/7-3, 6507/7-4) from the western part and in reservoir rock samples from the Åre Formation (well D and 6507/8-4) from the northern part of the Heidrun oil field. Within these formations, larger quantities of waxy compounds were found which refer to a lacustrine

influence of the generative source rock or to mixing of oil with different level of biodegradation. Thus, in both the western and especially the northern part of the Heidrun oil field indications to different oil charges were found. In contrast, in the reservoir rock asphaltene pyrolysates no indications for differences in the organofacies are found.

These results indicate that whole reservoir rock analysis provides the most effective means of recognising compositional differences in the macromolecular fraction within reservoirs because of the high sampling densities required. Asphaltene pyrolysates yield similar information on source and maturity, but can only be applied at low resolution because of the time required for the precipitation procedure.

8 COMPOSITIONAL KINETIC MODELS

8.1 INTRODUCTION

It is well established that kinetic parameters from asphaltenes can be used as proxies for the kinetics of the original source rock kerogen (di Primio et al., 2000; Keym & Dieckmann, 2006; Lehne & Dieckmann, 2007). To date bulk or compositional kinetic analysis has been applied to produced oil and tar mat asphaltenes in order to determine source rock characteristics of active kitchen areas (di Primio et al. 2000; Keym & Dieckmann, 2006; Lehne & Dieckmann, 2007), but never within the context of source profiling or the delineation of reservoir heterogeneities. Here especially reservoir rock asphaltenes have a great potential.

The basic principle of using asphaltenes from reservoired oils or reservoir rock extracts for source rock characterisation is the fact that these highly functionalized complex molecules bear close structural similarities to their parent kerogen, and that they are assumed to be not affected by low temperature alteration processes such as biodegradation or water washing as discussed before in detail (cf. Chapter 1.2). Asphaltenes contain the compositional information of the first oil migrated into the reservoir, i.e. they include organofacies and maturity fingerprints of the generating source. Thus, they are useful markers for source rock characterisation as well as for correlation purposes. Obtaining such information from the reservoir is important, because mature source rocks are usually at great depth and thus cannot be drilled, and oil accumulations in petroleum reservoirs are often situated in structural highs where potential source rocks are immature and might be of a different organofacies.

The application of compositional kinetics on asphaltenes is potentially useful for petroleum reservoir characterisation especially when the oil has been altered or biodegraded. Petroleum entering the reservoir carries asphaltenes, which contain fingerprints of the original oil composition and molecular structure of these individual oil charges. In combination with the present day state of alteration, asphaltenes could thus be used as markers for alteration and migration processes.

Within compartmentalized reservoirs, characterised by a complex charge and alteration history, the delineation of vertical and horizontal heterogeneities presents a particularly

difficult challenge, because subtle *in-situ* variabilities have to be recognised. Compared to produced-oil samples, presenting the average product of a thick reservoir interval, reservoir rock samples are useful to identify small scale variations within the reservoir, as they can be sampled at high resolution. Thus, reservoir rock asphaltenes can potentially be used to reconstruct the gross compositional characteristics of the original unaltered petroleum charge at any place within the individual compartments of a reservoir.

The PhaseKinetic approach, which is a well established method using immature source rock samples for the prediction of petroleum compositions generated and expelled (di Primio and Horsfield, 2006) was applied in this study. As kerogen abundance and composition is relatable to depositional settings, kerogen characteristics control the petroleum type and hence the petroleum composition generated, which in turn directly controls the physical behaviour of expelled fluids concerning pressure and temperature dependant changes in phase behaviour and fluid physical properties during secondary migration. With the use of different pyrolysis techniques, it is possible to reconstruct the composition of the oil, which originally was or would be generated. The PhaseKinetic approach uses a combination of bulk kinetic compositional information for characterisation of the reactions leading from kerogen to petroleum and open and closed system pyrolysis techniques for determination of fluid compositions. While liquid compositional evolution is determined directly from closed system pyrolysis results, gas compositions are corrected empirically and finally total fluid corrected compositions integrated with the bulk kinetic results into a compositional kinetic model. The result is a model which allows the prediction of hydrocarbon physical properties such as the GOR (gas : oil ratio), P_{sat} (saturation pressure) and b_o (formation volume factor). The calculation of petroleum phase behaviour under the subsurface conditions of hydrocarbon migration and entrapment is possible using these models in combination with modern basin modelling software, however, no modelling is presented within this thesis.

In order to investigate whether PhaseKinetic parameters calculated on kerogen and asphaltenes are comparable, the approach was first tested on selected source rock kerogens, source rock asphaltenes and reservoir rock asphaltenes from two well-studied areas in Western Canada and the Central Graben. Kerogens of extracted source rocks were analysed and their structural characteristics and PhaseKinetic parameters were compared to these obtained from the source rock asphaltenes and reservoir asphaltenes of genetically related fluids. The main results discussed in the following clearly show that the compositional

information obtained from reservoir asphaltenes are remarkably similar to that obtained from the source rock kerogen at 50 % transformation ratio (TR), and similar bulk fluid properties could be predicted. In contrast to that, source rock asphaltenes present different compositional information at 50 % TR and different bulk property predictions compared to source rock kerogen and reservoir asphaltenes.

Based on these initial test results the PhaseKinetic approach was subsequently applied to the main study area, the Heidrun oilfield, in order to compare and correlate the heterogeneities observed in the residual reservoir rock petroleum composition (cf. Chapter 6.2 - 6.6) with compositional characteristics of an potential source rock, and to improve the understanding of post-filling alteration processes, which have taken place in the oilfield as well as of processes leading to compartmentalisation.

8.2 STUDY AREAS - GEOLOGICAL BACKGROUND AND SAMPLES

8.2.1 TEST I - DUVERNAY FORMATION

The first study area selected to test the PhaseKinetic approach, was the Upper Devonian Duvernay Formation located in the Western Canadian Sedimentary Basin (WCSB). It comprises primarily Type II kerogen and can be regarded as one of the most prolific marine source rocks in this basin (Stoaks & Creaney, 1984; Creaney & Allan, 1990; Chow et al., 1995). The Duvernay Formation was chosen, as it is a homogeneous marine source rock (Dieckmann, 1998, Lehne, 2007). Here four source rocks and the corresponding source rock asphaltenes as well as one oil asphaltene were analysed.

The sample set of the Duvernay Formation comprises 17 source rocks. Rock-Eval data of the whole sample set demonstrates that the Duvernay Formation represents a typical Type II marine source rock (Figure 121). The samples cover a broad maturity range; however, most of them are immature with Tmax values between 414 °C up to 429 °C. The four representative samples selected for further investigations are marked with orange dots (Figure 121). The Rock-Eval data of these selected source rock samples (Lehne, 2007) are shown in Table 16.

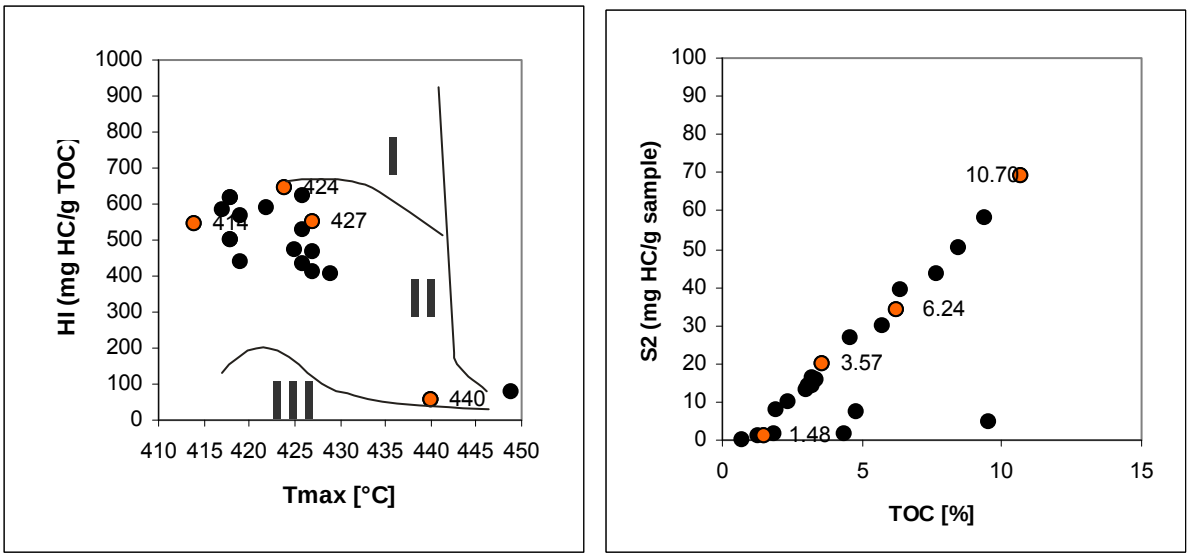

Figure 121 Rock-Eval data of the source rocks from the whole Duvernay Formation sample set. The selected samples for the PhaseKinetic approach are marked with orange dots. *Left* The Pseudo-van-Krevelen diagram with HI versus Tmax data; *Right* Rock Eval S2 versus TOC.

Table 16 Rock-Eval data (Lehne, 2007) and the asphaltene amount for selected source rock samples of the Duvernay Formation for the PhaseKinetic approach. RED - Redwater; CAM - Camrose; IMP 3 - Imperial Armena 3; IMC - Imperial Cynthia.

source rock	well	depth	S1	S2	S3	PI	Tmax	HI	OI	TOC	asphaltene
		(m)	(mg HC/g sample)	(mg HC/g sample)	(mg CO2/g sample)	(S1/S1+S2)	(°C)	(mg HC/g TOC)	(mg CO2/g TOC)	(%)	wt[%]
G000540	RED	1155.6	1.45	33.93	1.76	0.04	414	544	28	6.24	0.30
G000636	CAM	1579.9	5.62	69.11	0.73	0.08	424	646	7	10.70	0.37
G000573	IMP 3	1574.3	1.53	19.69	0.68	0.07	427	552	19	3.57	0.12
G000601	IMC	2971.5	0.71	0.82	0.44	0.46	440	55	30	1.48	0.02

The investigated Duvernay oil is a black oil with an API gravity of 36° from the Redwater well. For the corresponding oil asphaltenes an existing dataset was used, that included the asphaltene amount, bulk compositional information from open-system pyrolysis, bulk kinetics as well as closed system pyrolysis compositional information. Sample comparability should be assumed, firstly as the Duvernay Formation can be seen as a homogeneous petroleum system without facies differences between the wells investigated as demonstrated by the studies of Dieckmann and co-workers (Dieckmann *et al.*, 2004; Dieckmann *et al.*, 2000; Lehne & Dieckmann, 2007) and secondly low mature samples were selected for the investigations.

8.2.2 TEST II - DRAUPNE FORMATION

The second study area selected to test the PhaseKinetic approach is the Upper Jurassic Draupne Formation of the North Viking Graben in the North Sea. The Draupne Formation represents the most important petroleum source rock unit in the North Sea and was deposited during the Oxfordian to Ryazanian in a marine environment with restricted bottom water circulation under anaerobic conditions (Copper & Barnard, 1984; Huc *et al.*, 1985; Isaksen & Ledje, 2001). It consists of two major organic facies, a stratigraphically higher Type II kerogen and a stratigraphically lower, more stable Type II/III facies. The Draupne Formation organofacies are dominated by marine aliphatic-rich organic matter with variable contributions of transported terrestrial organic matter. Numerous authors (Cooper & Barnard, 1984; Huc *et al.*, 1985; Karlsen *et al.*, 1995; Isaksen & Ledje, 2001) have reported heterogeneity in source rock properties for the formation. Keym *et al.* (2006; 2007) and references therein give a good description of the Viking Graben, and regional and geological settings of the Draupne Formation.

An existing dataset from the Draupne Formation was evaluated, where kinetic and MSSV-data of a source rock as well as one reservoir- and one tar mat asphaltenes was available (Erdmann, 1999; Keym, 2007; Keym & Dieckmann, 2006). To ensure sample comparability a source rock and tar mat asphaltene, both from the Eastern Flank of the Viking Graben, were chosen for the application of the PhaseKinetic approach. In Table 17, the Rock-Eval screening data of the source rock are shown. The selected source rock represents a hydrogen-rich marine kerogen Type II. The tar mat asphaltene belong to the Mid-Jurassic Etive Formation (Brent group). Source rock asphaltenes are not available for this study.

Table 17 Sample number, well, depths, and Rock-Eval screening data of the Draupne source rock (Erdmann, 1999).

source rock	well	depth	S1	S2	PI	TOC	Ro	Tmax	OI	HI
		(m)	(mg HC/g sample)		(S1/S1+S2)	(%)	(%)	(°C)	(mg CO2/g TOC)	(mg HC/g TOC)
43254	B	2764.7	2.77	59.76	0.04	11.9	0.37	428	4	502

8.2.3 MAIN STUDY AREA - HEIDRUN OILFIELD

Based on the geochemical parameters analysed in the reservoir rock screening described previously (cf. Chapter 6.2 - 6.6), the geographical well position and the asphaltene amount

(wt. %), seven reservoir rock asphaltenes were selected and compared to the potential source rock from the Upper Jurassic Spekk Formation and the corresponding source rock asphaltene. This marine black shale containing a kerogen Type II with some Type III is immature near the Heidrun oil field, a sample from well 6507/7-5 was used as representative of the Spekk formation.

Background information of the samples is listed in Table 18.

Table 18 - Sample numbers, wells, formation, depths and asphaltene amount of the Heidrun oilfield reservoir rock asphaltenes and the source rock asphaltene used for the compositional kinetic modelling.

well	GFZ no.	sample type	Formation	TVD SS	MD-RKB	Asphaltene amount	
				m	m	wt.%	mg
B	G004165	reservoir rock asphaltene	Tilje 3.4	2396.1	3223.9	2.98	19.1
B	G004192	reservoir rock asphaltene	Tilje 3.1	2372.9	3274.2	5.69	88.47
C	G004207	reservoir rock asphaltene	Garn	2456.8	3666.3	11.92	67.0
C	G004225	reservoir rock asphaltene	Ile 4	2479.1	3688.8	3.20	27.6
E	G004268	reservoir rock asphaltene	Are 2.1	2416.4	3554.5	6.46	92.77
6507/7-2	G 003998	reservoir rock asphaltene	Tilje 3.2	2316.50	2316.50	10.84	140.23
6507/7-2	G 004000	reservoir rock asphaltene	Åre 7.2	2407.65	2407.65	13.97	177.98
6507/7-5	G004005	source rock asphaltene	Spekk	2310.6	2310.6	16.64	95.2
6507/7-5	G004005	source rock	Spekk	2310.6	2310.6	-	-

8.3 ANALYTICAL METHODS

8.3.1 RESERVOIR ROCK AND SOURCE ROCK EXTRACTION

The Duvernay source rocks chosen for the PhaseKinetic approach were extracted for 24 h using a soxhlet apparatus with a DCM / MeOH 1 vol. % mixture (Dichloromethane / Methanol 1 vol. %) in order to yield source rock bitumen. The bitumen extracts were concentrated using a Turbovap-evaporator, transferred into a 10 ml brown glass vial and dried under a gentle stream of nitrogen. Finally, their weight was recorded when constant.

The Draupne source rock was extracted via hydrochloric acid (HCL) and hydrofluoric acid (HF) treatment in order to yield the kerogen concentrate and is described in Erdmann (1999).

Between 15 and 35 g of the roughly grounded Heidrun reservoir rock, and about 20 g powdered Heidrun source rock were extracted using an accelerated solvent extractor (ASE, Dionex GmbH, in Idstein, Germany) to yield the residual bitumen. Both types of rock

samples were extracted in four cycles at 100 °C and 50 bar using an azeotropic mixture consisting of chloroform, acetone and methanol in a mix ratio of 32 : 38 : 30.

8.3.2 ASPHALTENE SEPARATION

The Duvernay- and the Heidrun source rock asphaltenes, and the Heidrun reservoir rock asphaltenes were separated with a 40-fold excess of *n*-hexane using a method detailed described in Theuerkorn *et al.* (2008) (cf. Chapter 7.1). Therefore, 0.5 ml and 1.5 ml of the according rock extract were used. The Duvernay oil asphaltene was separated with a 60-fold excess of *n*-hexane as described in Lehne (2007). The Draupne tar mat asphaltene is *n*-pentane separated and described in Keym (2007).

8.3.3 BULK PYROLYSIS FOR KINETIC MODELING

Bulk pyrolysis was performed on Duvernay and Heidrun asphaltenes and extracted source rocks, and the Draupne tar mat using a modified Source Rock Analyzer© (Humble). For the extracted source rock analysis, three aliquots (slow heating rate ~ 100 mg, medium heating rate ~ 50 mg, fast heating rate ~ 25 mg) of ground material were weighed in small crucibles and measured at the above mentioned heating rates. The asphaltenes were mixed with pre-cleaned quartz sand at a ratio of 1 : 5. About 10 mg of this mixture were used for the fast heating rates; slow heating rates where performed with ~ 60 mg sample material. Products were transported to the FID in a constant helium flow of 50 ml/min. Temperatures from 150 - 700 °C were applied using linear heating rates of 0.7, 2, 5, and 15 K/min.

Bulk flow pyrolysis on the extracted Draupne source rock was performed using an open system pyrolysis-FID bulk flow method (“Rock Eval type” pyrolysis). This method, showing no discrimination of gas versus oil potential, was used to gather data for calculating bulk petroleum kinetic parameters, as described by (Schaefer *et al.*, 1990). Pyrolysis products were removed from the heating zone by a constant argon flow of 45 ml/min, and detection was by FID. Temperatures from 150 - 700 °C were applied using linear heating rates of 0.1, 0.7 and 5 K/min (Erdmann, 1999, Erdmann & Horsfield, 2006).

The discrete activation-energy (Ea) distribution optimisation with a single, variable frequency factor (A) was performed using the KINETICS 2000 and KMOD® programs (Burnham *et al.*, 1987). Slow heating rates were used in order to avoid the influence of heat transfer problems on product evolution curves, kinetic parameters and consequently on geological predictions

(Schenk & Dieckmann, 2004). However, the used heating rates varied enough to ensure a correct iteration of the mathematical model and correctly calculate the frequency factor.

8.3.4 CLOSED SYSTEM PYROLYSIS – MICRO SCALE SEALED VESSEL PYROLYSIS (MSSV)

Artificial maturation experiments were carried out to obtain detailed information regarding the fluid composition generated by the source rock kerogen and the asphaltene fractions at different temperatures. Therefore the micro scale sealed vessel (MSSV) technique developed by Horsfield (1989) was used. Temperatures resulting in 10, 30, 50, 70 and 90 % transformation were determined based on the bulk kinetic data for a heating rate of 0.7 K/min. Aliquots of the source rock and the asphaltenes were weighed into 40 µl seized and 120° bent glass tubes. For the asphaltenes between 5 - 20 mg asphaltene - pre-cleaned quartz sand mixture (ratio 1 : 10) were used. Source rock aliquots of 5 - 8 mg immature extracted kerogen concentrates and because of lower concentration of organic matter, about 20 - 25 mg of finely grounded extracted source rock sample material, was used throughout the MSSV measurement. Both tube ends were filled with quartz sand and quartz wool to keep the sample that is situated in the middle of the tube in place and to reduce the remaining volume in the tube. The tubes were sealed with a hydrogen-oxygen flame. MSSV pyrolysis was conducted at a heating rate of 0.7 K/min using an external GC-oven. The samples were heated using a temperature program that started at 200 °C up to the temperature of the corresponding TR. Subsequently the tubes were removed from the oven, cooled down and finally cracked within a piston device of a Quantum MSSV thermal system to enable the analysis of the maturation products. The products (total and resolved) were quantified using an external *n*-butane standard. Identification of peaks based on reference pyrolysis gas chromatograms was done manually with Agilent ChemStation® software.

8.3.5 METHODOLOGY AND BACKGROUND ON THE PHASEKINETIC APPROACH (PKW TUNING)

The phase behaviour of migrating petroleum fluids is controlled by the fluids composition and the pressure and temperature conditions at which the fluid is found. The geological conditions upon which migrating oil separates into oil and gas are strongly controlled by the gas

(C_1 - C_5) composition of the fluid (di Primio et al., 1998). For petroleum phase behaviour, gas composition plays the dominant role with respect to the fluids saturation pressure and shrinkage behaviour; however, influence of the liquid fraction composition should not be neglected.

The gross description of oil and gas generation from closed system pyrolysis results, and the surface GOR derived there from, are very similar to the GOR distributions observed in nature (di Primio, 2004; di Primio & Horsfield, 2006). Hence, it appears that the relative gas and oil proportions generated as a function of maturity can be estimated based on laboratory experiments.

Compositional predictions are, however, not as straight forward. High methane contents generally result in phase separation at relatively high pressures, i.e. at great depth. A very wet gas composition results in a much lower saturation pressure (P_{sat}) for a given fluid. The sensitivity of gas composition on phase behaviour of migrating hydrocarbons has severe implications for the prediction of petroleum phase behaviour during petroleum generation and migration. As discussed by Mango (1996; 1997) natural fluids display a much stronger predominance of methane in their gas fractions than observed in source rock pyrolysates.

It is commonly known that for genetically related natural fluids saturation pressure correlates linearly to GOR and formation volume factor (B_o). As discussed above the methane content of a fluid is the most important factor controlling its saturation pressure (P_{sat}). Hence, a correction of the gas compositions generated by pyrolysis is possible assuming a linear relationship between the methane proportion of the gas phase (C_1 - C_5) and the fluids GOR. The equation used for methane correction in this study is based on linear regression using a natural dataset from the North Sea representative of the black oil to gas-condensate range (correlation coefficient for the relationship between GOR and C_1 / $C_{2\text{-}5}$ $r^2 = 0.98$). The original GOR used as a starting point for the methane correction is that determined on the MSSV pyrolysates and converted to volumetric data by single stage flash using PVT simulation software.

The characterisation of the generated fluids oil composition (C_{6+}) for phase behaviour assessment is based on the compositional information from MSSV analysis as described by di Primio and Horsfield (2006). The resolved compounds from C_6 onwards were quantified, their proportions converted to molar amounts and these were summed to a total description of the liquid phase which consisted of a pseudo compound C_6 (containing all resolved compounds in the range eluting after pentane until and including hexane) and a C_{7+} fraction (containing the rest of the resolved compounds). The C_{7+} fraction was further characterised by

a molecular weight and density. The molecular weight of the C_{7+} fraction was determined by subdividing the GC hump (MSSV total minus MSSV resolved compounds) into boiling ranges according to the resolved *n*-alkanes, and using the average molecular weights of the resolved compounds as representative of the respective hump range. Quantification of the subdivisions led thus to an averaged molecular weight of the entire hump. The density of the C_{7+} fraction was determined using a C_{7+} molecular weight – density correlation for natural petroleum's from the North Sea. Subsequently the definition of the C_{7+} fraction is used to calculate a distribution of components representing the total liquid phase using a PVT simulator. The determined PVT descriptions of the fluids at different transformation ratios are used for the definition of the compositional kinetic models. The individual potentials per activation energy derived from the bulk kinetic analysis of the samples are subdivided into 14 sub-potentials, one for each compound described.

8.4 RESULTS AND DISCUSSION

In order to show how far PhaseKinetic parameters calculated on kerogen, source rock asphaltenes and reservoir asphaltenes are comparable, all selected samples were characterised in four sequential steps as follows. In a first step the characterisation of structural moieties with open system Py-GC and Tvap-GC was done. This was followed by the analysis of bulk kinetic parameters to predict hydrocarbon generation rates at different temperatures. The heating rates used for this analysis are 0.7, 2.0, 5.0 and 15 K/min. In the third step experimental temperatures were determined, which represent transformation ratios (TR) of 10, 30, 50, 70 and 90 % at 0.7 K/min in order to analyse the oil composition generated at these temperatures via closed system MSSV pyrolysis (Horsfield, 1989). Finally the mol % of particular components was calculated as described by di Primio and Horsfield (2006) in order to predict the hydrocarbon composition under different reservoir conditions. The results of these single characterisation steps will be shown in the following section.

8.4.1 DUVERNAY FORMATION

8.4.1.1 PREDICTING PETROLEUM COMPOSITION

In order to identify structural differences between the kerogen, source rock asphaltene and reservoir asphaltenes, all samples were studied by open system pyrolysis GC. Figure 122 show the resulting pyrolysis gas chromatograms for the four extracted kerogen samples (left) and the corresponding source rock asphaltenes (right). The illustrated samples increase in thermal maturity from the top to the bottom of the relevant figure. In Figure 123 the reservoir asphaltene Py-GC trace is shown.

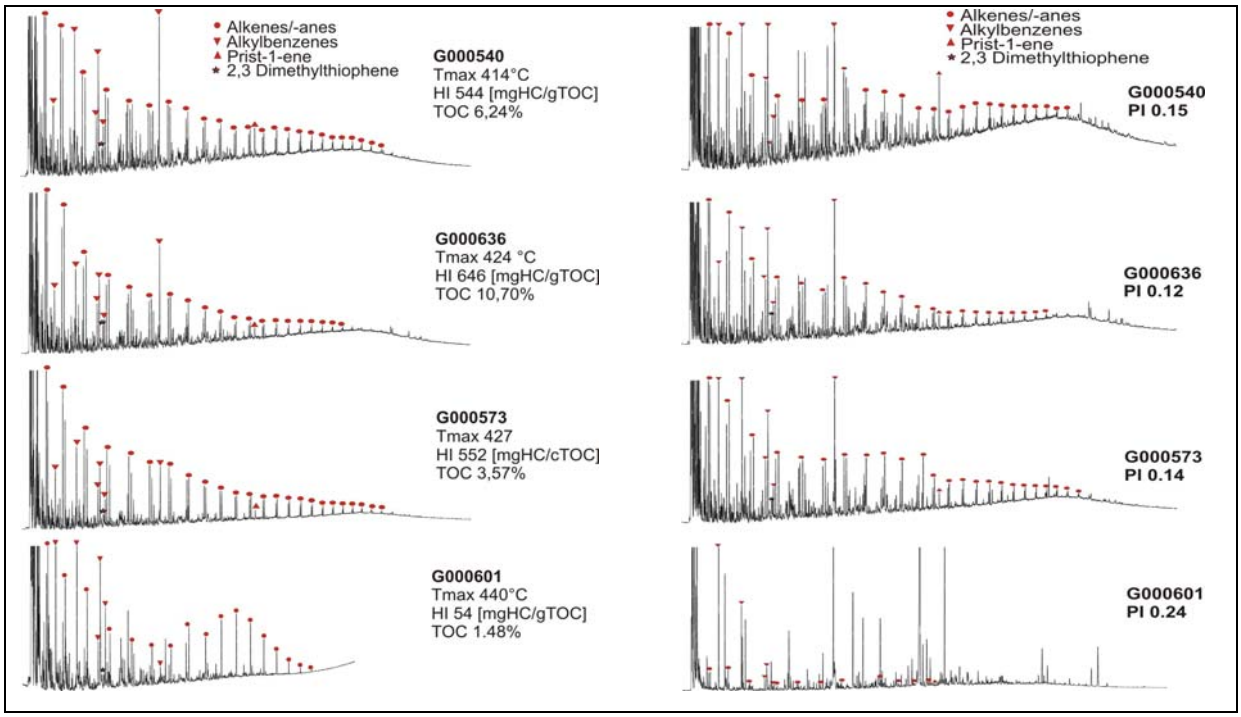

Figure 122 Chromatograms from open system pyrolysis-GC for the kerogen (left) and source rock asphaltene (right) from the Duvernay Formation. The conspicuous peak in the middle part of the GC represents 1, 2, 3, 4 - tetramethylbenzene, marked with an inverted triangle.

The pyrolysis gas chromatograms of the kerogen samples (Figure 122 left) show relatively constant alkene/alkane distribution patterns except for the most mature sample. It is obvious that low mature samples contain significantly higher amounts of aromatic compounds than pyrolysis products formed from more mature samples. A prominent structural moiety for the Duvernay Formation is 1, 2, 3, 4 - tetramethylbenzene (TMB) in natural and pyrolysis products that can be traced to the β-cleavage of diaromatic carotenoid moieties (Clegg *et al.*, 1997; Hartgers *et al.*, 1994; Requejo *et al.*, 1992). This conspicuous 1, 2, 3, 4 - TMB peak

decreases with increasing maturity, but for immature source rocks the concentration of TMB exceeds the concentration of other aromatic compounds. Compared to the kerogen, the source rock asphaltenes (Figure 122 right) are more enriched in aromatic compounds. Additionally they show a higher 1, 2, 3, 4 – TMB content. Even using mass spectrometry, the peaks of the most mature sample at the bottom of Figure 122 are difficult to identify.

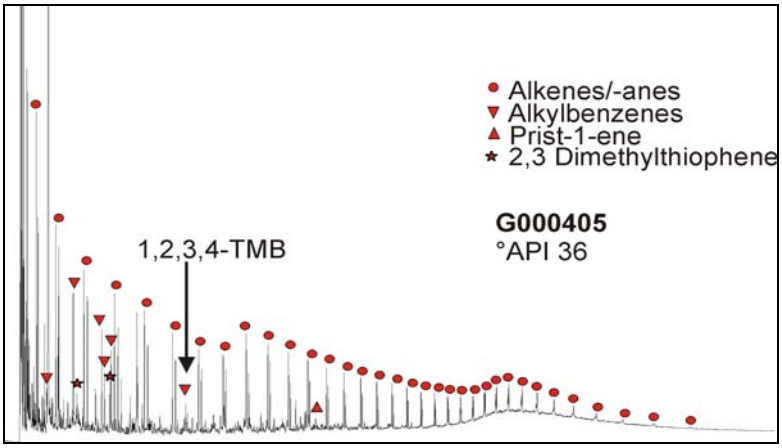

Figure 123 Chromatograms from open system pyrolysis GC for the reservoir asphaltene from the Duvernay Formation. The conspicuous peak in the middle part of the GC represents 1, 2, 3, 4- tetramethylbenzene, marked with an inverted triangle.

The reservoir asphaltene pyrolysates (Figure 123) shows a similar alkene / alkane distribution pattern and a similar content of aromatic compounds as the kerogen pyrolysates (Figure 122 left). Compared to the source rock asphaltenes as well as the kerogen pyrolysates the reservoir asphaltenes show the lowest 1, 2, 3, 4 - TMB content.

Excluding samples of high maturity, the highest aromaticity was observed in pyrolysis products from the source rock asphaltenes, the lowest aromaticity in products from reservoir asphaltenes. A similar feature was observed concerning the content of 1, 2, 3, 4 - TMB. Source rock asphaltenes are most enriched in 1, 2, 3, 4 - TMB compared to kerogen and reservoir asphaltenes, which show the lowest content. In general, it was observed that pyrolysis products from source rock asphaltenes and reservoir asphaltenes show conspicuous differences, while source rock kerogen products are in-between.

The ternary diagrams in Figure 124 A - C show the alkyl chain length distribution (CLD) (A), the sulphur content (B) and the phenol content (C) for the Duvernay sample set. Within the CLD ternary, the low maturity kerogen samples plot in the P-N-A low-wax oil generating field. All source rock asphaltenes show a systematically higher quantity of short chains in their pyrolysates (higher gas amount) as compared to the respective kerogens and the

reservoir asphaltene sample, and therefore plot in the gas condensate field. The reservoir asphaltene shows the lowest gas amount; and the pyrolysis products are more paraffinic. A possible reason for this variability may be seen in the different 1, 2, 3, 4 - TMB content of the pyrolysates (Figure 122, Figure 123). 1, 2, 3, 4 - TMB is a compound which is considered to mark a specific gas precursor in source rocks (Muscio *et al.*, 1994). Figure 124 B and C demonstrate that the Duvernay samples are poor in organic sulphur as well as in phenol. In both diagrams, most kerogen and source rock asphaltenes plot mainly in Type III field based on the high content of *o*-xylene and *m,p*-xylene whereby the source rock asphaltenes contain higher amounts of these aromatic compounds.

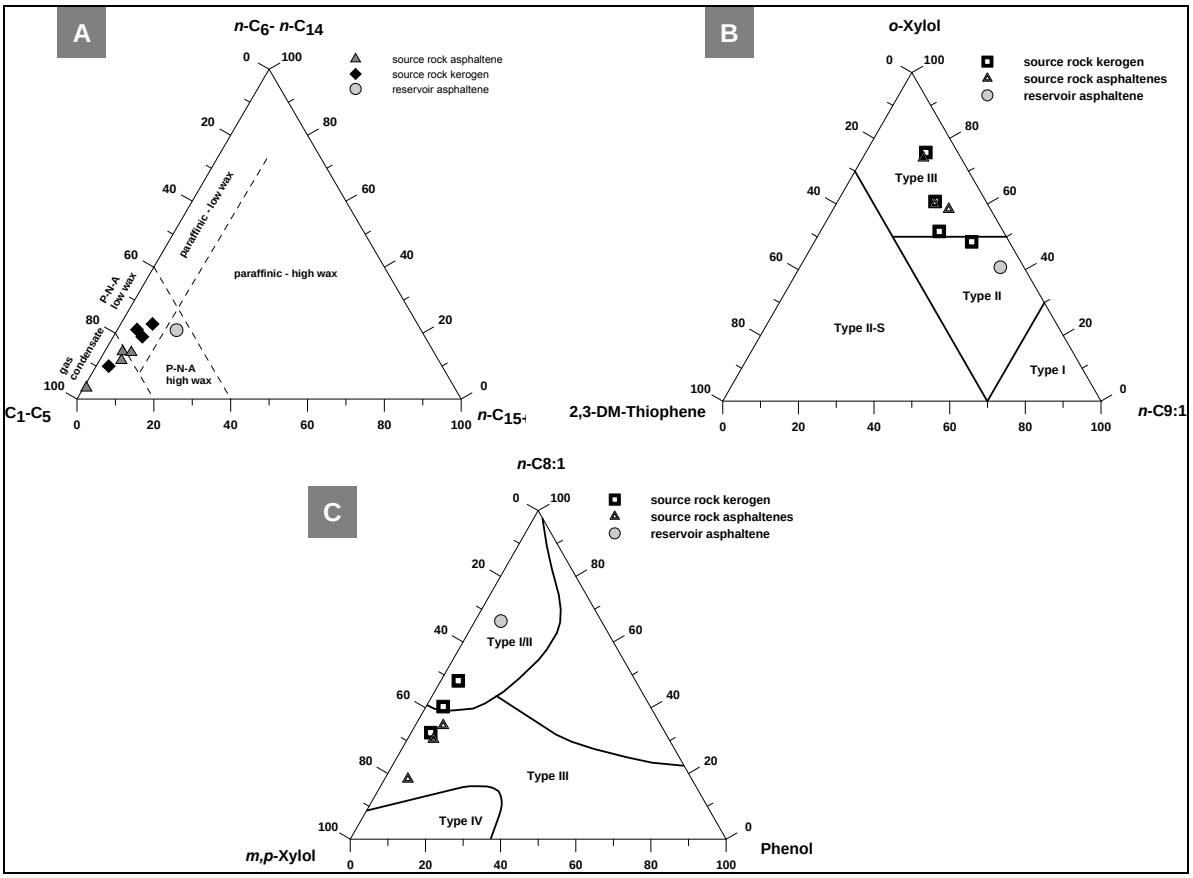

Figure 124 Ternary diagrams for the alkyl chain length distribution (CLD) (A), sulphur content (B) and phenol content (C) for pyrolysates of kerogen and source rock asphaltenes from the Duvernay Formation.

8.4.1.2 BULK KINETIC PARAMETERS

In order to show how far kinetic parameters of source rock kerogen, source rock asphaltenes and reservoir asphaltenes are comparable to each other, Figure 125 illustrates the distribution of activation energies and frequency factors for two selected source rock kerogens with Tmax temperatures of 424 °C (upper row) and 427 °C (lower row), and the corresponding source

rock asphaltenes. The kinetic parameters determined on the source rock asphaltenes are shown on the right hand side, those of the reservoir asphaltene, precipitated from Redwater black oil with API 36°, are shown in the middle of Figure 125.

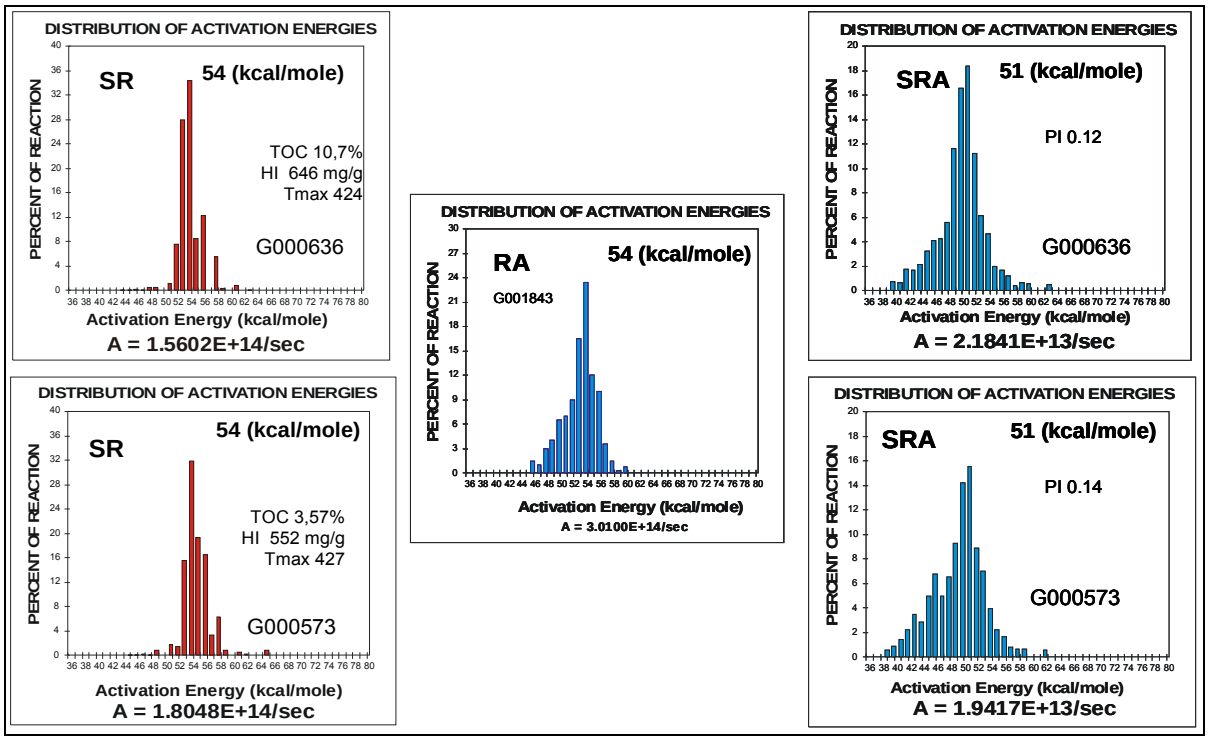

Figure 125 Activation energy distributions (Ea) and frequency factors (A) for the source rock kerogen (left), the reservoir asphaltene (middle), and the source rock asphaltenes (right). *Upper row*: source rock sample with Tmax 424 °C, *Lower row*: source rock sample with Tmax 427 °C.

The kinetics for the source rock kerogens (left) show narrow activation energy distributions (Ea) that indicate a homogeneous organic matter type. Compared to the kerogen, source rock asphaltenes and reservoir asphaltene show a broad Ea distribution that indicates higher content of heterogeneous organic material. The source rock asphaltenes present the broadest Ea distribution. Despite these obviously different Ea distribution patterns, both, kerogen and reservoir asphaltene reveal activation energies from 45 - 60 kcal/mole, have the same mean activation energies (E_{mean}) of 54 kcal/mole and nearly identical frequency factors (A) of 1.56 E - 1.80 + 14 s^{-1} (source rock kerogen Tmax 424 °C and 427 °C) and 3.01 E + 14 s^{-1} (reservoir asphaltene), respectively. Kerogens and reservoir asphaltene show more similarities based on their bulk kinetics than the kerogens and the corresponding source rock asphaltenes. For the latter, the distribution of activation energies ranges from 39 - 63 kcal/mole with E_{mean} values 51 kcal/mole and a frequency factor of 2.18 E + 13 s^{-1} and 1.94 E + 13 s^{-1}, respectively. Source rock asphaltenes show the broadest Ea distribution and lowest E_{mean} and

A, compared to the kerogen as well as reservoir asphaltenes. Lower mean activation energies indicate a higher content of less stable bonds.

In summary, the source rock asphaltenes studied differ significantly in terms of bulk kinetic properties from the kerogens. The reservoir asphaltene bulk kinetic properties are more similar to kerogen.

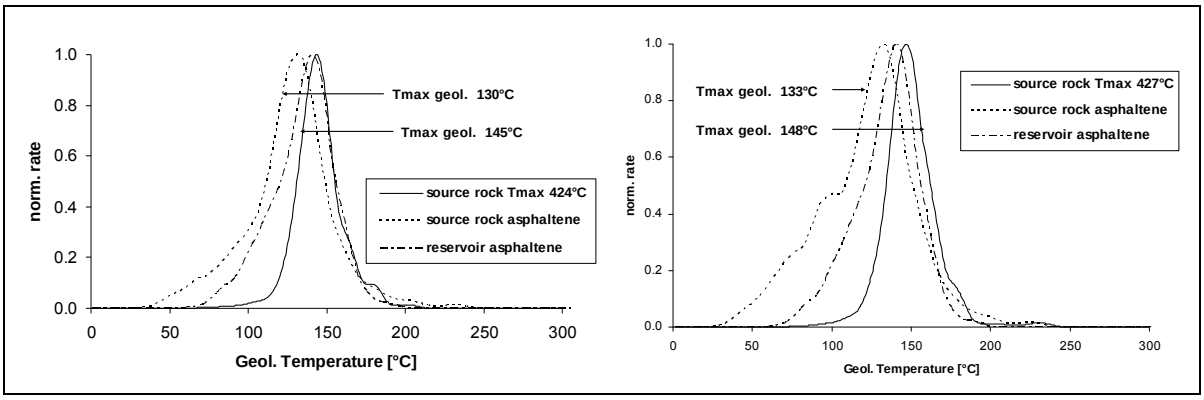

Figure 126 Bulk petroleum generation rates from source rock kerogen, source rock asphaltene and reservoir asphaltene for a geological heating rate of 3 K/my. *Left:* source rock Tmax 424 °C, *Right:* source rock Tmax 427 °C.

The evolution of hydrocarbon generation predicted for a geological heating rate of 3 K/my using the kinetics described above results in significant differences for source rock asphaltene and kerogen with nearly 60 °C difference for the onset and about 15 °C difference for the geological Tmax (Figure 126). The onset of petroleum generation for the source rock kerogen was predicted to begin at nearly 120 °C, while hydrocarbon generation for source rock asphaltenes starts at 65 °C and 53 °C for the source rock samples with Rock Eval Tmax temperatures of 424 °C and 427 °C, respectively. Reservoir asphaltenes represent an intermediate position, they start to generate at 60 °C. The geological Tmax was found at 145 °C for source rock kerogen and reservoir asphaltene, and 130 °C for the source rock asphaltenes. The end of petroleum formation was predicted at about 180 °C in all cases.

Source rock asphaltenes show significantly different generation rate curves as compared to the parent kerogen. They have much earlier onset of hydrocarbon generation than the respective kerogen, with peak generation rates occurring 15 degrees lower than the kerogen. This indicates that the investigated reservoir asphaltenes, although showing an earlier onset of hydrocarbon generation, have larger similarities to the kerogen concerning bulk structural characteristics than source rock asphaltenes. Similar findings are shown previously in Lehne & Dieckmann (2007) and Lehne & Dieckmann (2007).

8.4.1.3 COMPOSITIONAL KINETICS – EVOLVING COMPOSITIONS USING MSSV PYROLYSIS

In order to elucidate evolving hydrocarbon composition with increasing maturation closed system MSSV pyrolysis (Horsfield, 1989) was carried out on the source rock kerogen, source rock asphaltenes and reservoir asphaltenes. The compositional changes were determined for TR steps of 10, 30, 50, 70 and 90 %. The prediction of individual TR stages was based on bulk petroleum generation models (Figure 125) as described in (Düppenbecker & Horsfield, 1990). Figure 127 shows the GOR predicted by MSSV pyrolysis (mass) for the individual samples versus increasing degree of transformation (TR %). In Table 19, the predicted data are summarised.

The source rock kerogen of the sample with a Tmax of 424 °C (Figure 127, left) shows a constant GOR up to 50 % TR followed by increasing GOR up to 90 % TR. The highest GORs were observed for the source rock asphaltenes, which plot in a u-shape and coincide with kerogen GOR from 50 % TR on. The reservoir asphaltene shows the lowest GORs which increase slightly with increasing TR and coincide with kerogen GOR between 30 % and 70 % TR. The greatest differences among the samples were detected for the lowest (10% TR) and the highest (90 % TR) maturity range. For source rock with a Tmax of 427 °C (Figure 127 right), the source rock asphaltene GORs plot again in a u-shape and show conspicuously higher values compared to the kerogen and the reservoir asphaltene. The kerogen GOR presents a linear increase with increasing TR and reveals more similarities to the reservoir asphaltene GOR evolution. Only at TR 90 %, are the kerogen and source rock asphaltene GOR similar.

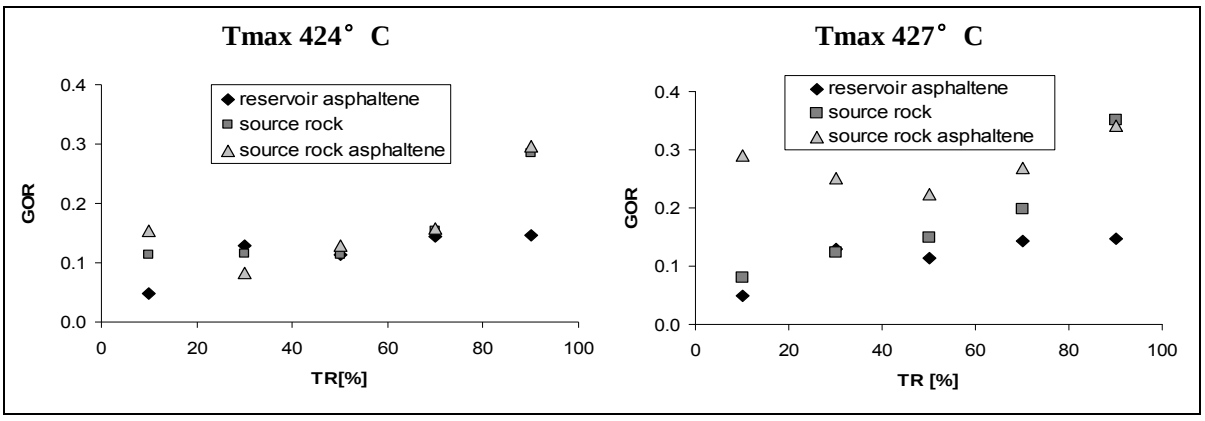

Figure 127 Comparison of the petroleum GOR predicted from the MSSV pyrolysis as a function of increasing maturity (TR %), of the source rock kerogen, source rock asphaltene and reservoir asphaltene. *Left*: source rock with Tmax 424 °C; *Right*: source rock with Tmax 427 °C.

Table 19 Predicted GOR and gas wetness from the MSSV pyrolysis (0,7 K/min) for the reservoir asphaltene and the kerogen and source rock asphaltene of both investigated source rocks with Tmax 424 °C and 427 °C.

	reservoir asphaltene		source rock Tmax 424 °C				source rock Tmax 427 °C			
			SR - Kerogen		SR - Asphaltene		SR - Kerogen		SR - Asphaltene	
TR	GOR	C_1/C_{2-5}	GOR	C_1/C_{2-5}	GOR	C_1/C_{2-5}	GOR	C_1/C_{2-5}	GOR	C_1/C_{2-5}
10	0.049	0.246	0.114	0.481	0.154	0.197	0.081	0.570	0.291	0.073
30	0.130	0.257	0.116	0.418	0.082	0.218	0.123	0.384	0.251	0.079
50	0.114	0.230	0.114	0.399	0.130	0.211	0.150	0.337	0.223	0.152
70	0.143	0.270	0.153	0.375	0.158	0.284	0.198	0.348	0.268	0.217
90	0.147	0.268	0.285	0.371	0.296	0.374	0.351	0.370	0.341	0.330

In summary, the predicted GOR evolution from the kerogens present intermediate values between the source rock asphaltenes, which have shown the highest values and the reservoir asphaltene with the lowest GORs with increasing TR. The greatest similarities were detected for the maturity range from 30 % to 70 % TR, the largest differences at the lowest (10 % TR) and the highest (90 % TR) maturity ranges. Both investigated samples present stronger similarities between the kerogen and the reservoir asphaltene GOR. Kerogen and source rock asphaltene reveal large differences concerning the GOR except for the highest maturity range at 90 % TR.

A possible reason for the higher gas production of the source rock asphaltenes compared to kerogen and reservoir asphaltenes may be due to variability in the 1, 2, 3, 4 - TMB content of the pyrolysates (Figure 122, Figure 123). For differences at the lowest maturity range, we have no explanation until now. The production of higher gas amount at the highest maturity range (90 % TR) could be affected by secondary cracking processes, which are known to take place about or to start at 80 % TR.

8.4.1.4 COMPOSITIONAL KINETIC MODEL

The input for compositional kinetic models consists of the corrected gas composition comprising the molar contents of the C_1 - C_5 alkanes and iso-alkanes and the liquid description consisting of the molecular weight of the C_6 range compounds and 6 pseudo compounds representing the C_{7+} fraction. In summary, the molecular concentrations of 14 compounds for five transformation ratio steps are used to populate the bulk kinetic model

with compositional information (method described in detail in di Primio and Horsfield (2006)).

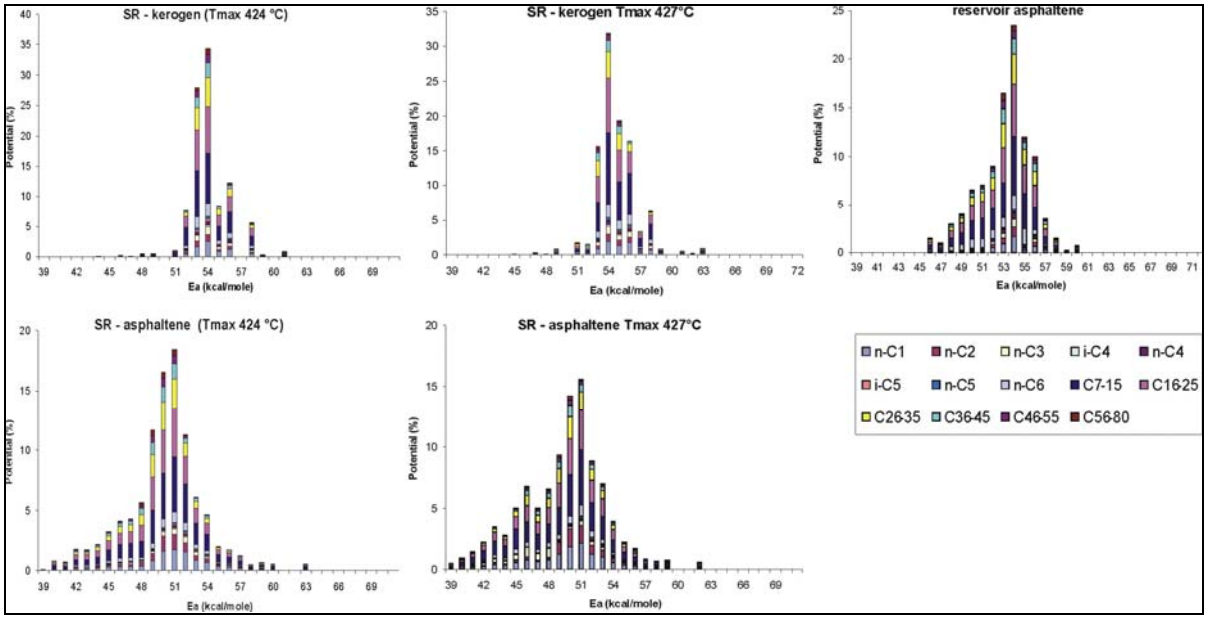

Figure 128 Compositional kinetic models from the PVT simulation of the sample from the Duvernay Formation. *Left*: kerogen (top) and source rock asphaltene (bottom) of the source rock Tmax 424 °C. *Middle:* kerogen (top) and source rock asphaltene (bottom) of the source rock Tmax 427 °C. *Right*: reservoir asphaltene with API 36°.

In the results for the calculated compositional kinetic models for the kerogen, source rock asphaltene of the source rocks with Tmax temperatures of 424 °C and 427 °C, respectively, and the reservoir asphaltene of the oil with an API gravity of 36° are shown. The physical properties of fluids generated from each of the samples studied can be calculated using equation of state based PVT simulators. The predicted GOR, P_{sat} and b_o for the Duvernay Formation samples at the different degrees of transformation studied are shown in Table 20.

Table 20 Predicted GOR, b_o and P_{sat} from the PVT simulation. The range cover the predicted values from 10% - 90% TR.

Predicted data	Tmax 424 °C			Tmax 427 °C		
	GOR	b_o	P_{sat}	GOR	b_o	P_{sat}
	Sm³/Sm³	m³/Sm³	MPa	Sm³/Sm³	m³/Sm³	MPa
SR - kerogen	141-236	1.54-1.83	137-207	111-253	1.56-2.12	191-259
SR - asphaltene	164-336	1.39-1.95	160-180	276-366	1.98-2.16	205-298
reservoir asphaltene	46-169	1.22-1.56	70-218	46-169	1.22-1.56	70-218

In addition to bulk physical properties, the phase behaviour of fluids can be described by its phase envelope, i.e. the location of the bubble and dew point lines of the fluid in a pressure versus temperature diagram as shown in for the Duvernay sample with Tmax 424 °C.

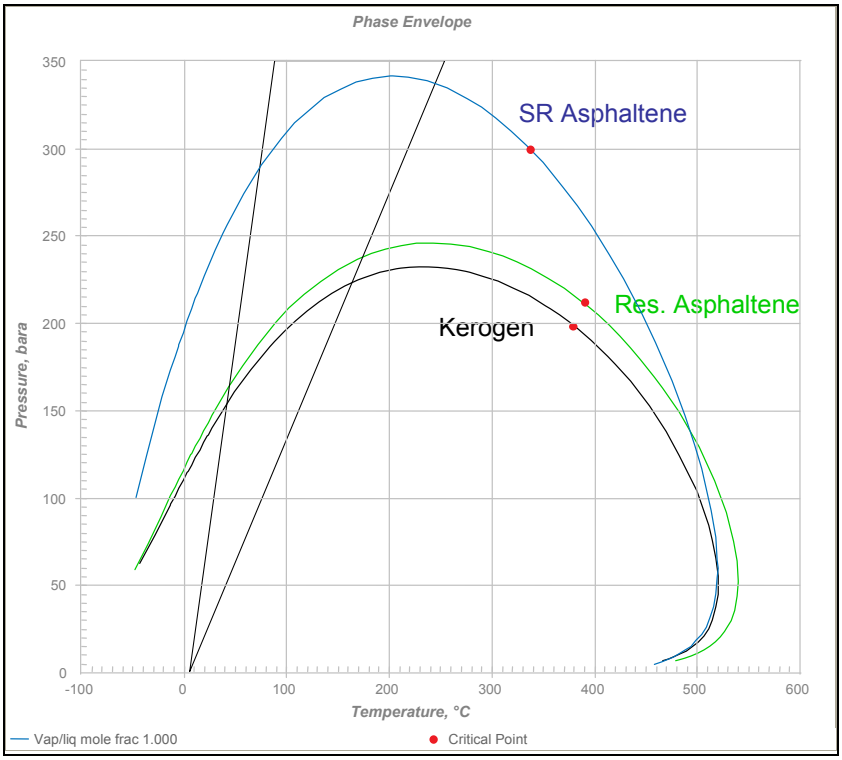

Figure 129 Phase envelopes of the Duvernay sample with Tmax 424 °C from the kerogen, source rock asphaltene and reservoir asphaltene at 50 % TR.

The shape of such a phase envelope strongly depends on the composition of the analysed fluid (di Primio *et al.*, 1998). The liquid composition controls the liquid quality in form of density or API gravity and additionally defines the highest temperature extent of the phase envelope as well as the location of the critical point. It can be seen in Figure 129 that the compositional information from the reservoir asphaltene shows a remarkable similarity to that obtained from kerogen at the same TR (50 %). Kerogen and reservoir asphaltene show both very similar shapes of the phase envelopes, which implies similar physical properties of the fluid that would be generated concerning GOR, P_{sat}, b_o and even API° gravity. Predictions for the source rock asphaltene clearly show a different shape of the phase envelope, characterised by a much higher saturation pressure and a shift of the critical point to lower temperatures. In terms of bulk properties, the source rock asphaltene generated fluid could be described as lighter, high shrinkage oil compared to typical black oil predicted for the kerogen and reservoir asphaltene.

The black triangle in represents roughly the extent of natural pressure and temperature ranges encountered in sedimentary basins.

8.4.2 DRAUPNE FORMATION

In order to show how far PhaseKinetic parameters calculated on kerogen and tar mat asphaltenes are comparable data sets of Erdmann (1999) and Keym (2007) were used. These set comprising data from the open system pyrolysis-GC, bulk kinetic parameters and MSSV pyrolysis data. The same characterisation steps as described for the Duvernay Formation will be presented in this section in a shorter form.

8.4.2.1 PREDICTING PETROLEUM COMPOSITION

Pyrolysis-GC analysis of the tar mat asphaltenes indicates a continuous series of *n*-alkenes/*n*-alkanes and shows a similar pattern as that observed in the Draupne source rock pyrolysate (Keym, 2007). The Draupne source rock kerogen is characterised by the abundance of saturated and monounsaturated aliphatic hydrocarbons and shows the most prominent components in the C_1 - C_7 range. Further a large variety of monoaromatic and diaromatic components and their sulphur-containing counterparts are present (Erdmann, 1999).
The CLD ternary of (Horsfield, 1989) was used to show the composition of hydrocarbons generated in Py-GC based on the alkyl chain length distribution. Here the tar mat as well as the source rock kerogen plot in the P-N-A low wax oil field. The source rock kerogen shows a higher potential for gas and condensate generation as compared to the tar mat asphaltenes. Keym (2007) observed that the investigated tar mat asphaltenes show a very good fit to the source rock kerogen and to the related oil asphaltenes.

8.4.2.2 BULK KINETIC PARAMETERS

In Figure 130 the distribution of activation energies and frequency factors for the source rock kerogen (Tmax 428 °C, left) and the tar mat asphaltene (right) are shown. The narrow Ea distribution of the source rock kerogen kinetics indicates a homogeneous organic matter type.

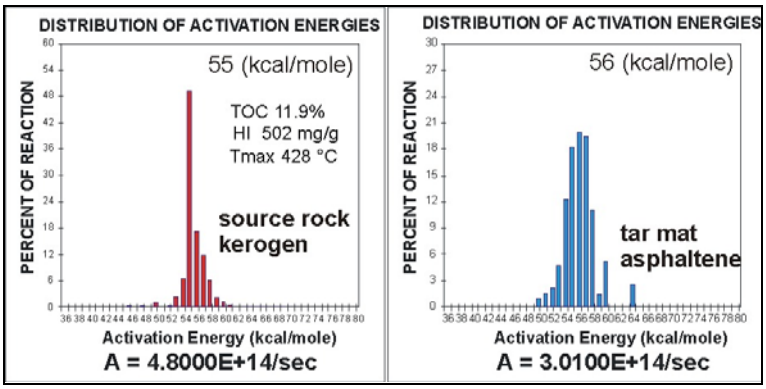

Figure 130 Activation energy distribution and frequency factor (A) for the source rock kerogen (left) and the tar mat asphaltene (right) of the Draupne Formation.

Compared to the kerogen the tar mat asphaltene shows a broader Ea distribution, which indicates higher content of heterogeneous organic material. In spite of these obviously different Ea distribution patterns, kerogen and tar mat asphaltene both show similar activation energies from 50 - 61 kcal/mole and 50 - 64 kcal/mole, have nearly the same mean activation energies (E_{mean}) of 55 and 56 kcal/mole and nearly identical frequency factors (A) of 4.80 E + 14 s^{-1} and 3.01 E + 14 s^{-1}, respectively. Both, kerogen and tar mat asphaltene show similarities based on their bulk kinetics.

The predicted hydrocarbon generation for a geological heating rate of 3 K/my using the kinetics described above is shown in Figure 131. Although the kerogen and tar mat asphaltene show slight differences about 8 - 10 °C for the on- and offset of petroleum generation as well as for the geological Tmax, the generation rates for both are similar. The source rock kerogen and tar mat asphaltene show similar generation rate curves that indicate similarities concerning bulk structural characteristics.

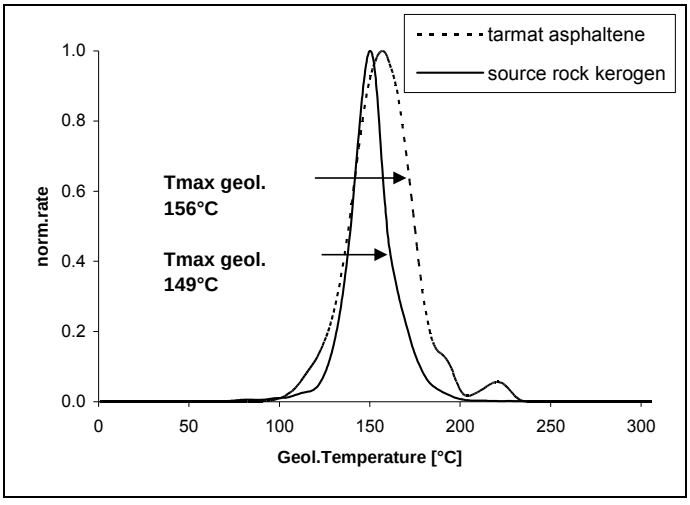

Figure 131 Bulk petroleum generation rates from source rock kerogen, tar mat asphaltene and reservoir asphaltene from the Draupne Formation for a geological heating rate of 3 K/my.

8.4.2.3 COMPOSITIONAL KINETICS – EVOLVING COMPOSITION USING MSSV PYROLYSIS

Figure 132 shows the GOR predicted by MSSV pyrolysis for the individual samples versus increasing degree of transformation (TR %). The Draupne source rock kerogen shows constant GORs up to 50 % TR followed by increasing GOR up to 90 % TR. The highest GORs were found in the TR stages of 70 and 90 %. The Draupne tar mat asphaltene products also show constant GORs up to 50 % TR followed by a less pronounced increase compared to the kerogen up to 90 % TR. Tar mat asphaltene GORs coincide with kerogen GORs between 10 % and 50 % TR. The greatest differences among the samples were detected for the highest (70 % and 90 % TR) maturity range.

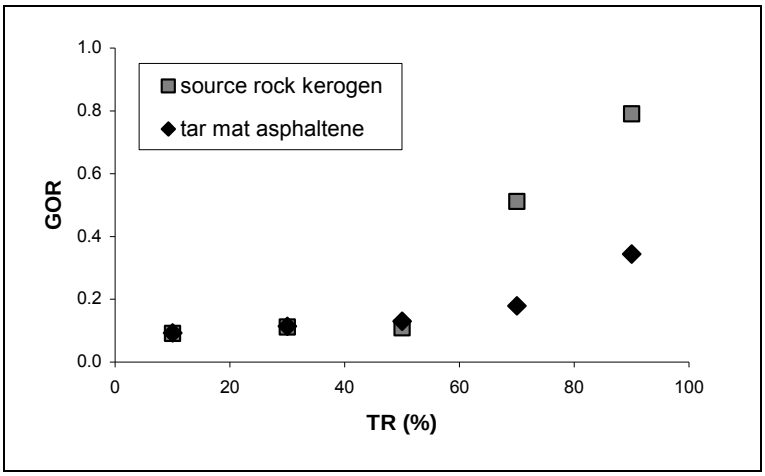

Figure 132 Comparison of the petroleum GOR predicted from MSSV pyrolysis as a function of increasing maturity (TR %), of the source rock kerogen and tar mat asphaltene.

In summary, the predicted GORs from the kerogen show similarities to the tar mat asphaltene GORs for the maturity range from 10 % to 50 % TR and the largest differences at the higher maturity ranges at 70 % and 90 % TR.

8.4.2.4 COMPOSITIONAL KINETIC MODEL

In Figure 133, the results for the calculated compositional kinetic models for the kerogen and tar mat asphaltene based on the MSSV pyrolysis done by Erdmann (1999) and Keym (2007) are presented. The physical properties of fluids generated from the kerogen and tar mat asphaltene studied were calculated using equation of state based PVT simulators and the results for the predicted GOR, P_{sat} and b_o for the Draupne Formation samples at the different degrees of transformation studied are shown in Table 21.

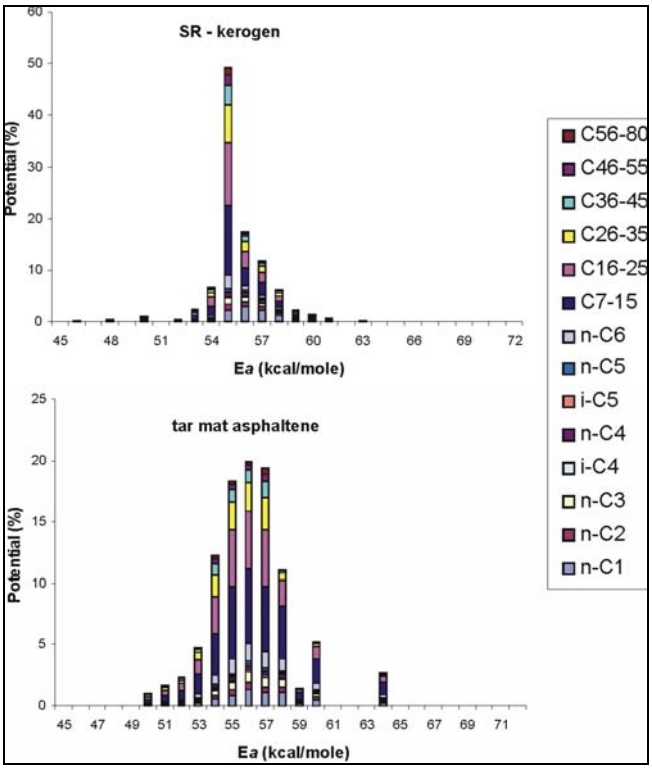

Figure 133 Compositional kinetic models from the PVT simulation for the Draupne Formation kerogen and the tar mat asphaltene.

The predicted GOR, P_{sat} and b_o for the Draupne Formation kerogen and tar mat asphaltene include values calculated for 10 up to 90 % TR. The result for the predicted GORs range from 91 to 543 Sm³/Sm³. The strong increase from 50 up to 70 % TR is conspicuous. The P_{sat} ranges from 130 to 396 MPa and the b_o from 1.34 to 2.64 m³/Sm³. For the tar mat asphaltene, the predicted values are considerably lower. The GOR ranges from 108 to 237 Sm³/Sm³, P_{sat} from 130 to 166 MPa and the formation volume factor b_o ranges from 1.41 to 1.91 m³/Sm³.

Table 21 Predicted GOR, P_{sat} and b_o for the source rock kerogen and tar mat asphaltene from the Draupne Formation.

Predicted data	**source rock Tmax 428 °C (E 43254)**				**tar mat asphaltene (G001279)**			
TR	**GOR**	b_o	P_{sat}	**C_1/C_2-C_5**	**GOR**	b_o	P_{sat}	**C_1/C_2-C_5**
(%)	Sm³/Sm³	m³/Sm³	MPa		Sm³/Sm³	m³/Sm³	MPa	
10	91.10	1.34	130.13	1.34	107.70	1.41	129.6	1.39
30	98.70	1.36	138.25	1.37	108.90	1.40	145.26	1.40
50	98.40	1.36	142.85	1.37	128.40	1.46	157.30	1.45
70	467.70	2.40	391.42	2.44	153.00	1.56	160.34	1.52
90	543.10	2.64	396.71	2.66	237.30	1.91	166.03	1.77

The phase envelopes, which describe the phase behaviour of fluids the Draupne kerogen and tar mat asphaltene would generate, are shown in the pressure versus temperature diagram of Figure 134. It can be seen that the compositional information from the tar mat asphaltene shows a remarkable similarity to that obtained from kerogen at the same TR (50 %). Kerogen and tar mat asphaltene show a similar location of the bubble and dew point lines. The similar shapes of the phase envelopes implies similar physical properties of the fluid that would be generated concerning GOR, P_{sat}, b_o and even API° gravity.

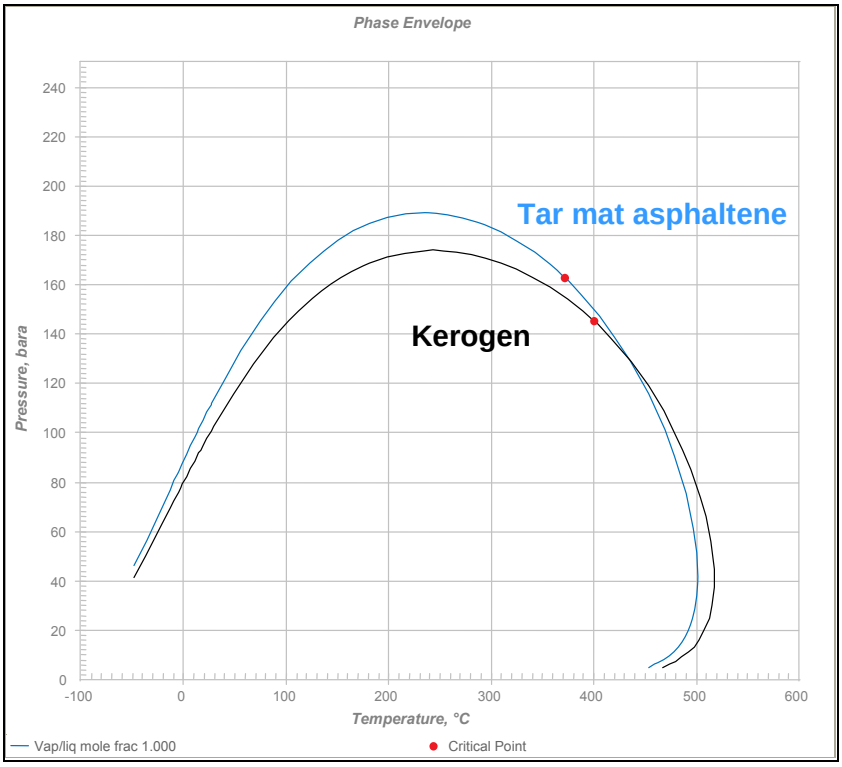

Figure 134 Phase envelopes for the Draupne kerogen and tar mat asphaltene at 50 % TR.

8.4.3 MAIN STUDY AREA - HEIDRUN OILFIELD

8.4.3.1 PREDICTING PETROLEUM COMPOSITION

Seven reservoir rock asphaltenes as well as the source rock kerogen and the corresponding source rock asphaltenes were analysed using pyrolysis – GC in order to characterise structural differences of the samples. The pyrolysis gas chromatograms are shown in Figure 135, which includes the geographical well position where the samples were taken around a greatly simplified sketch of the Heidrun oilfield. Biodegradation and mixing of different charges has

severely affected the Heidrun oils in the reservoir, which can, based on in-house data, roughly be subdivided in two dominant parts, a biodegraded and a mixed part (shown also in Figure 133). The biodegraded oil samples, which were not influenced by a later fresh oil charge, are found in the east, while the oils in the western part of the reservoir are biodegraded and refreshed by mixing with a secondary (later) charge. Further a third part can be subdivided were signals from both extremes were observed. These wells are found in the central part of the field (cf. Chapter 3.1)

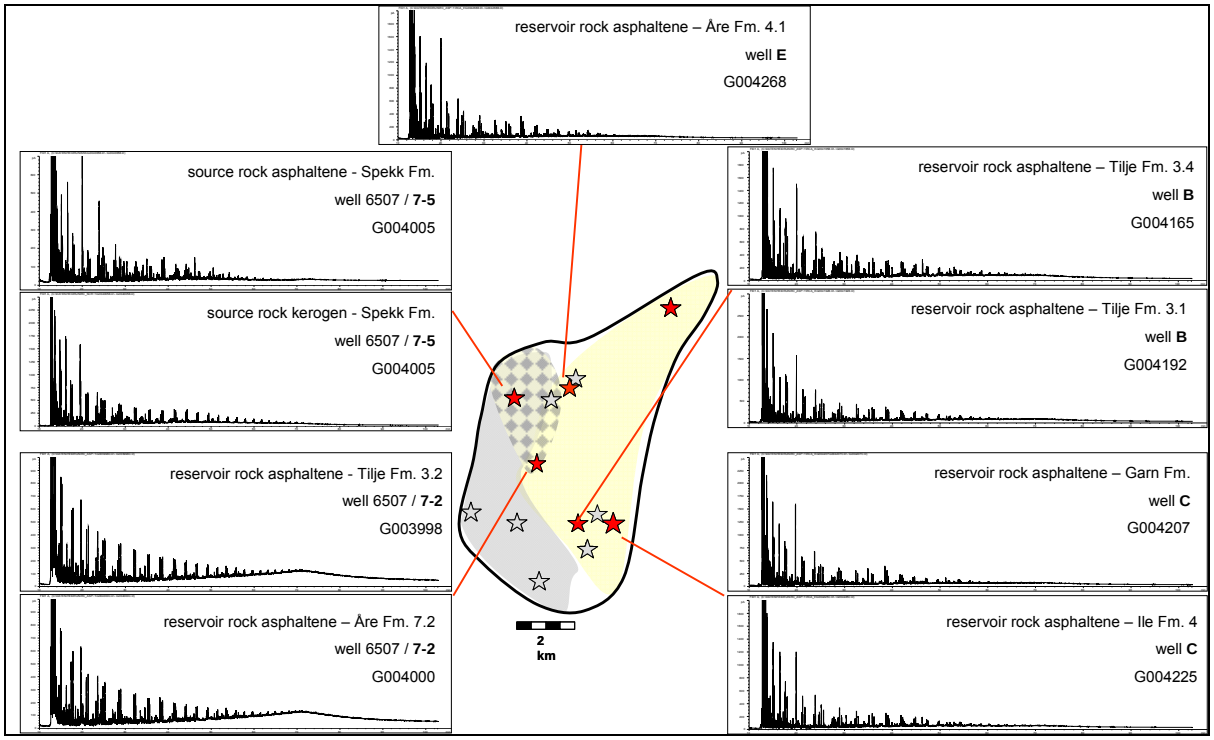

Figure 135 Chromatograms from open system Py- GC for the reservoir rock asphaltenes, the source rock kerogen and the corresponding source rock asphaltene analysed are shown concerning there geographical well position around a greatly simplified sketch of the Heidrun oilfield. The colours in this sketch mark the rough division of the oil field into a biodegraded eastern part (yellow) and a biodegraded and mixed part (grey) in the west. In the chequered central part, both signals were observed.

The GC trace of the source rock kerogen presents a relatively constant *n*-alkene/*n*-alkane distribution pattern and relatively high quantities of monoaromatic compounds (Figure 135, top left). The most prominent aromatic structures monitored are benzene and toluene. Compared to the kerogen, the corresponding source rock asphaltene is more enriched in aromatic compounds, present low amounts of *n*-alkenes /*n*- alkanes and large peaks in the gas range.

Both reservoir rock asphaltenes pyrolysates of well 6507/7 -2 (Figure 135, bottom left) reveal a similar *n*-alkene/*n*-alkane distribution pattern as observed for the source rock kerogen, but

distinctly minor amounts of monoaromatic and diaromatic hydrocarbons in their chromatograms. These samples were the only ones in which a hump was detected.
Both reservoir rock asphaltenes of well C, the lowermost reservoir rock asphaltene of well B (G004192), and the reservoir rock asphaltene of well E from the eastern and northern part of the reservoir present at the first view a relatively similar *n*-alkene/*n*-alkane distribution patterns as well as similar contents of aromatic pyrolysis products (Figure 135, right and top). In general, the monitored compositions are more similar to the source rock kerogen than to the source rock asphaltene. In the chromatogram of the upper reservoir rock asphaltene of well B (G004165) a multitude of unknown peaks were observed.

Within the CLD ternary (Figure 136 A) all reservoir rock asphaltenes plot in the P-N-A low wax oil generating field as does the source rock kerogen of the Spekk Formation. The reservoir rock asphaltenes of well 6507/7-2 show nearly identical alky chain length distributions as compared to the source rock kerogen, while the remaining reservoir rock asphaltenes of well B, C and E have slightly higher quantities of gaseous compounds. The source rock asphaltene CLD is clearly different. It shows the largest quantities of gas compounds of all samples analysed and plots in the gas and condensate field.

All asphaltenes and the kerogen analysed are low in phenol, indicating a low input of terrestrial organic matter (Figure 136 C). All samples studied, with exception of the source rock asphaltene, plot relatively close together and indicate so the composition of Type II / III kerogen. The organic sulphur content is low for the reservoir rock asphaltenes (Figure 136 B), while the source rock kerogen and the source rock asphaltenes present slightly higher amounts of sulphur-containing pyrolysis products. Differences in aromaticity among the samples are reflected in both ternaries, especially the highly aromatic character of the source rock asphaltene. The reservoir rock asphaltenes and the kerogen show a lower and relatively similar aromaticity. It was observed that reservoir rock asphaltenes from the Tilje Formation, especially of well 6507/7-2, reveal the lowest aromaticity, compared to the remaining asphaltenes, which is most similar to the aromaticity of the kerogen (Figure 136 C and B).

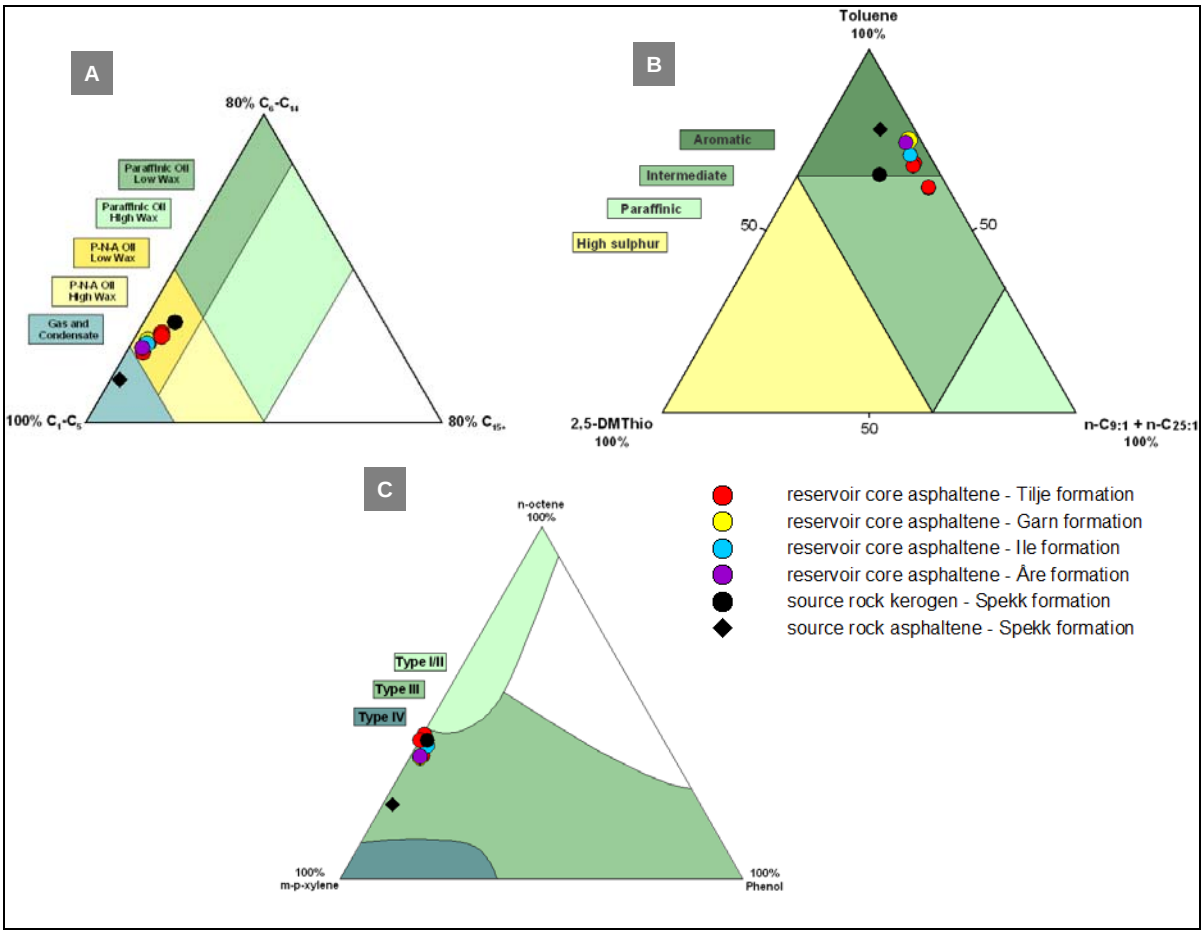

Figure 136 Ternary diagram of the alkyl chain length distribution (A), relative sulphur content (B) and relative phenol content (C) for pyrolysates of the reservoir rock asphaltenes, source rock asphaltene and the source rock kerogen of the Spekk Formation selected from the Heidrun oilfield.

8.4.3.2 BULK KINETIC PARAMETERS

Before the kinetic analysis, all asphaltenes samples were thermally extracted for 20 min at 300 °C to remove potential solvent residues. Despite this cleaning step, the source rock asphaltene and the reservoir rock asphaltene G004165 of well B showed a very heterogeneous S2, characterised by two maxima in the measured generation rate curve. Obviously, the macromolecular asphaltene fraction of these two samples contains a distinct proportion of "free" hydrocarbons, which are not extractable at 300 °C (Tvap). These compounds are removed at higher temperatures and result so in augmented S2 measurements. For coals those processes are known, where due to their strong adsorptive properties some of the "free" hydrocarbons are not thermally extractable at 300°C (Orr, 1983).

High molecular weight waxes (C_{40+} paraffins) could be responsible for those effects, but in this case, no waxy compounds are detected in the asphaltenes (Figure 135). However, many

unknown peaks have been observed especially in these two chromatograms, thus other high molecular weight compounds have to be considered.

Consequently, both, the source rock asphaltene and the reservoir rock asphaltene G004165 of well B, were excluded from further analyses. In Figure 137, the activation energy distribution (Ea) and the frequency factors (A) for the six remaining reservoir rock asphaltenes (blue) and the source rock kerogen (red) are shown.

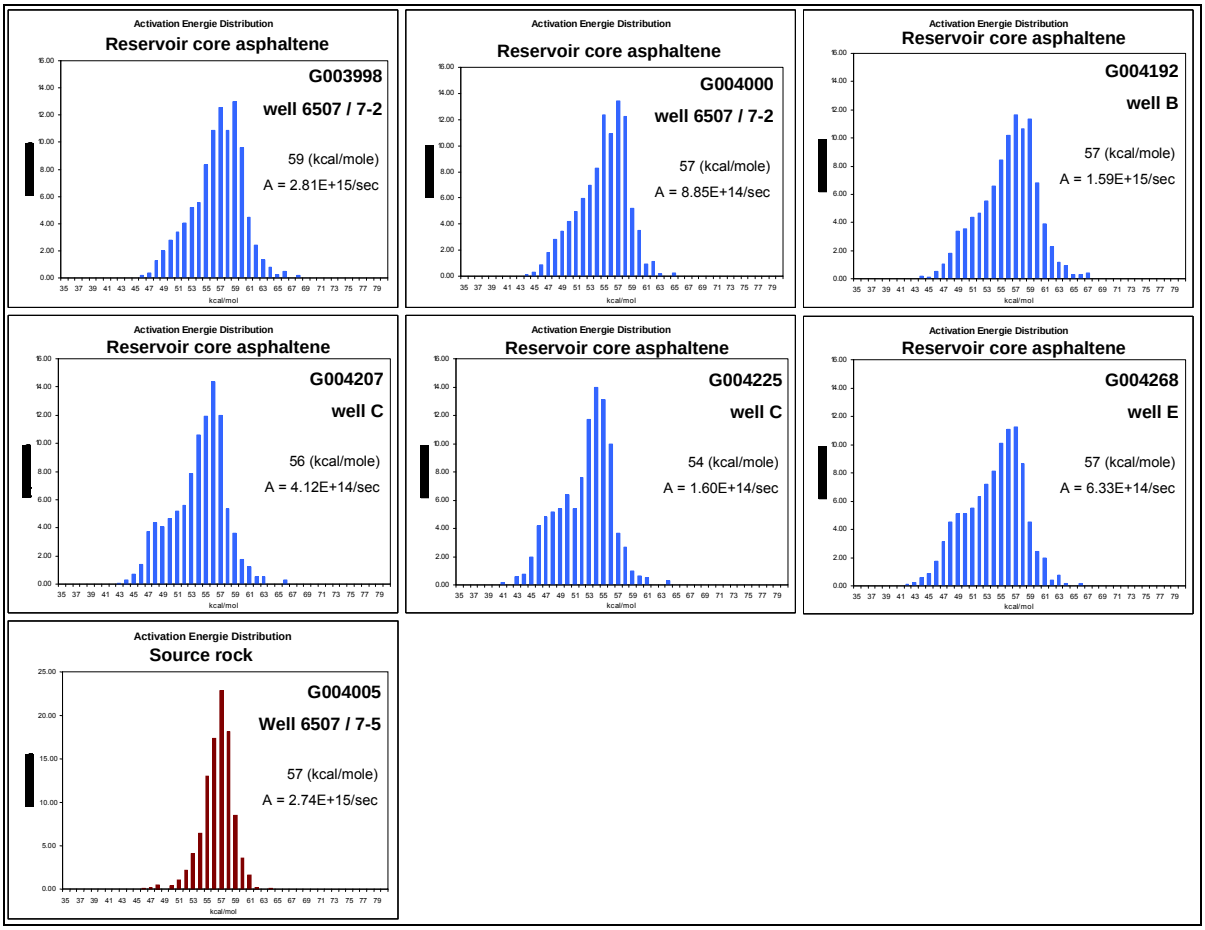

Figure 137 Activation energy distribution (Ea) and frequency factor (A) for the reservoir rock asphaltenes (blue) and the source rock kerogen (red) from the Heidrun oil field.

The source rock kerogen show a relatively narrow Ea distribution indicating a more homogeneous organic matter type compared to the reservoir rock asphaltenes. They present a very broad Ea distribution that indicates a relatively heterogeneous organic matter composition. The Ea distribution of the kerogen is between 46 - 64 kcal/mole, those of the reservoir rock asphaltenes between 41 - 68 kcal/mole.

Slight differences were observed for the main activation energy E_{mean} and the frequency factor A. The kerogen shows E_{mean} = 57 kcal/mole and frequency factor A = 2.74 E + 15 s^{-1}. The

reservoir rock asphaltene E_{mean} ranges between 54 and 59 kcal/mole, the frequency factor A between 1.60 E + 14 s^{-1} and 2.81 E + 15 s^{-1}. However, compared to the clear defined single E_{mean} observed for the kerogen, most of the reservoir rock asphaltenes show more than one potential main activation energies. Considering these, greatest differences were observed in well 6507/7-2 from the western / central part and well C from the eastern part of the Heidrun field. Asphaltene G003998 (well 6507/7-2) shows the highest E_{mean} = 59 kcal/mole of all samples analysed and a similar frequency factor as compared to kerogen, while the asphaltenes of well C, G004207 and G004225, are characterised by the lowest E_{mean} = 56 and 54 kcal/mole and the lowest frequency factor A = 4.12 E + 14 s^{-1} and 1.60 E + 14 s^{-1}. The remaining asphaltenes G004000 (well 6507/7-2), G004268 (well E) and especially G004192 (well B) show similar kinetic parameters as compared to the kerogen.

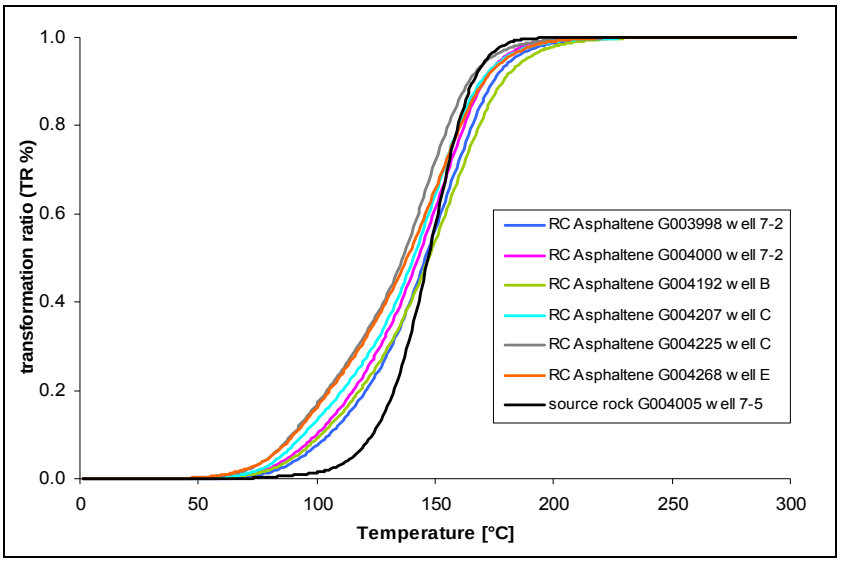

Figure 138 Bulk petroleum transformation ratio curves of the source rock kerogen and reservoir rock asphaltenes for a geological heating rate of 3 K/my.

Figure 138 shows the predictions for a geological heating rate of 3 K/my for the kerogen and the reservoir rock asphaltenes. The differences in the shape of the transformation ratio curves imply differences in the bond stability of their organic matter. The asphaltenes are characterised by a higher content of instable bonds compared to kerogen. Within the profiles 6507/7 -2 and C, a decrease in the bond stability of the organic matter was observed from the upper to the lower asphaltene. Concerning the geographic well positions in the Heidrun oil field, the asphaltenes of the western / central part (well 6507/7-2) are characterised by more stable bonds compared to most of the asphaltenes from the eastern and northern part, which indicate a lower content of stable bonds in their organic matter.

The petroleum formation windows predicted for geological heating conditions of 3 K/my result in an earlier onset of up to 33 °C, different temperatures at 50 % transformation and an later offset of up to 14 °C for the reservoir rock asphaltenes as compared to the kerogen (Figure 138, Table 22). At 50 % conversion the reservoir rock asphaltenes G003998 and G004192 of well 6507/7-2 and B, respectively, and the kerogen shows similar temperatures (147 - 149 °C), while the remaining asphaltenes shows lower temperatures between 137 - 144 °C. The onset of petroleum generation (10 % TR) of the asphaltenes ranges between 90.5 °C and 108.1 °C, which corresponds to calculated vitrinite reflectance (R_0 %) between 0.5 and 0.62. The source rock kerogen of the Spekk Formation starts to generate hydrocarbons at a distinctly higher temperature of 123.5 °C, which corresponds to higher maturity of 0.72 R_0 % (Table 22). Differences can be seen comparing the onset of hydrocarbon generation of the single asphaltenes. Within wells a vertical trend was found in well 6507/7-2 and well C. In both profiles, the temperature for the onset of hydrocarbon generation decreases with increasing depth, indicating so a decrease in maturity with increasing depth. Laterally (between wells) the latest onset and so the highest maturity was observed for the upper asphaltene G03998 of well 6507/7-2 in the western / central part, while asphaltenes of well C (G004225) and well E (G004268) from the eastern and the northern part of the Heidrun oilfield start earlier and are characterised by distinctly lower maturity.

Table 22 Calculated temperatures (°C) and calculated vitrinite reflectance (R_0 %) for the hydrocarbon generation at a heating rate of 3 K/my of the reservoir rock asphaltenes and source rock kerogen from the Heidrun oilfield.

well	sample	formation	asphaltene type	10%TR (onset)		50 % TR		90%TR (offset)		Tmax	
				T °C	R_0 %	T °C	R_0 %	T °C	R_0 %	T °C	R_0 %
6507/7-2	G003998	Tilje 3.2	reservoir rock	108.1	0.621	148.9	0.969	177.4	1.47	151.6	1.015
6507/7-2	G004000	Åre 7.2	reservoir rock	100.8	0.559	143.7	0.897	171.5	1.361	149.2	0.973
B	G004192	Tilje 3.1	reservoir rock	102.8	0.577	148.3	0.959	179.5	1.511	154.8	1.073
C	G004207	Garn	reservoir rock	96.3	0.527	142.8	0.887	171.2	1.355	153.5	1.05
C	G004225	Ile 4	reservoir rock	90.5	0.495	137.2	0.828	165.2	1.237	146	0.926
E	G004268	Åre 4.1	reservoir rock	92.5	0.506	140.2	0.859	172.5	1.381	152.2	1.026
6507/7-5	G004005	Spekk	source rock	123.5	0.721	147.1	0.941	165.9	1.25	150.1	0.989

To summarise, asphaltenes are more instable compared to kerogen. Indicators of the second (later) charge have been found in asphaltenes from the western part of the Heidrun oilfield, which are characterised by more stable bonds and a higher maturity compared to asphaltenes from the eastern and northern part. Indications of earlier charge have been found in

asphaltenes from the eastern and northern part. These asphaltenes are characterised by less stable bonds and lower maturity compared to the western asphaltenes.

8.4.3.3 COMPOSITIONAL KINETIC – EVOLVING COMPOSITION WITH MSSV PYROLYSIS

As the phase behaviour is mainly controlled by the gas amount and its composition, the GOR (left) and the gas wetness (right) predicted by MSSV pyrolysis for all reservoir rock asphaltenes and the source rock kerogen (black dots) are shown in Figure 139 as a function of increasing maturity (TR %). Table 23 and Table 24 summarise the predicted data. During the MSSV pyrolysis the vessel of the reservoir rock asphaltene G004225 of well C was broken for the analysis of composition at 50 % TR, hence their GOR and gas wetness are not known.

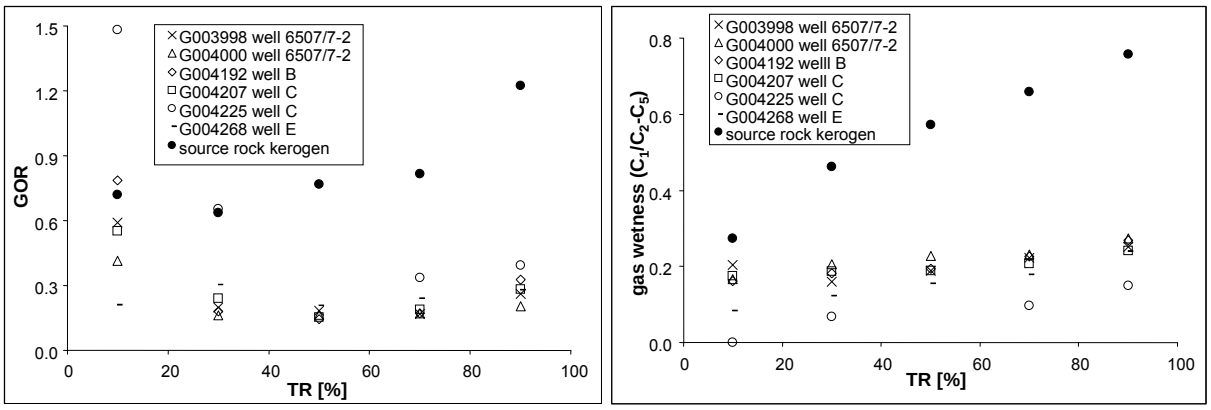

Figure 139 Comparison of the petroleum GOR (left) and the gas wetness (right) predicted from MSSV pyrolysis as a function of increasing maturity (TR %), of the reservoir rock asphaltenes and the source rock kerogen from the Heidrun oil field.

The source rock kerogen shows an increasing GOR between 10 % and 70 % TR and a distinct rise up to 90 % TR (Figure 139 left). For the reservoir rock asphaltenes, which plot in a slight u-shape, distinctly lower GORs were determined. Between 30 % and 70 % TR, the predicted GOR of the Spekk Formation kerogen is nearly twice that predicted for the reservoir rock asphaltenes. The largest differences between asphaltenes and kerogen were observed at 90 % TR.

Comparing the GOR of the individual reservoir rock asphaltenes the greatest variability was observed at 10 % TR. Between 30 % TR up to 90 % TR slightly lower GORs were observed for the three asphaltenes from the Tilje and Åre Formation (well 6507/7-2 and well B), which are characterised by the highest calculated vitrinite reflectance (maturity) (cf. Chapter8.4.3.2,

Table 22). Highest GORs are monitored for the Ile Formation asphaltene (G004225) of well C and the Åre Formation asphaltene of well E (G004268).

Considering lateral variabilities, lowest GORs are predicted mainly for the western part of the Heidrun field (10 % TR excluded), while the eastern and northern part of the field are characterised by higher GORs. Considering vertically variabilities, in well 6507/7-2 the GOR decreases from top to the bottom, while the GOR in well C is characterised by large differences between the Garn and the Ile Fm. asphaltenes, but generally increases with depth.

Table 23 Predicted GOR from the MSSV pyrolysis (0.7 K/min) for the reservoir rock asphaltene and the source rock kerogen of the Heidrun oil field.

	reservoir rock asphaltenes						**source rock kerogen**
	G003998	**G004000**	**G004192**	**G004207**	**G004225**	**G004268**	**G004005**
TR %	GOR	GOR	GOR	GOR	GOR	GOR	GOR
10	0.590	0.414	0.786	0.552	1.483	0.209	0.721
30	0.197	0.163	0.180	0.239	0.655	0.303	0.637
50	0.182	0.164	0.144	0.153	-	0.207	0.769
70	0.169	0.170	0.172	0.190	0.337	0.239	0.817
90	0.261	0.203	0.326	0.283	0.392	0.278	1.225

The gas wetness increases stepwise with increasing TR from 10 % up to 90 % (Figure 139, right). The source rock kerogen shows a distinctly higher gas wetness as compared to the reservoir rock asphaltenes. Most similar gas wetness predictions for kerogen and asphaltenes are observed at 10 % TR. Greatest differences can be seen at 90 % TR, where the reservoir rock asphaltene gas wetness is one-fourth the amount of the gas wetness predicted for the kerogen. Comparing the gas wetness predictions for the individual reservoir rock asphaltenes, between 30 % TR up to 90 % TR slightly higher amounts were observed for the three asphaltene samples from the Tilje Formation of well 6507/7-2 and well B (G003998, G004000 and G004192). The lowest gas wetness was observed in the Ile Formation asphaltene of well C (G004225).

Considering lateral variabilities, higher gas wetness are predicted mainly for the western part of the Heidrun field, while the eastern and northern part of the field are characterised by slightly lower gas wetness. Considering vertically variabilities, well 6507/7-2 shows a increase in gas wetness from top to the bottom, while the gas wetness in well C decreases (Table 24).

Table 24 Predicted gas wetness from the MSSV pyrolysis (0.7 K/min) for the reservoir rock asphaltene and the source rock kerogen of the Heidrun oil field.

	reservoir core asphaltenes						source rock
	G003998	G004000	G004192	G004207	G004225	G004268	G004005
TR	C_1 / C_2-C_5	C_1 / C_2-C_5	C_1 / C_2-C_5	C_1 / C_2-C_5	C_1 / C_2-C_5	C_1 / C_2-C_5	C_1 / C_2-C_5
10	0.203	0.166	0.162	0.174	0.000	0.082	0.274
30	0.160	0.205	0.181	0.186	0.069	0.122	0.462
50	0.188	0.228	0.194	0.188		0.154	0.573
70	0.223	0.231	0.225	0.208	0.097	0.179	0.659
90	0.252	0.274	0.269	0.241	0.150	0.240	0.758

In summary, the predicted GOR as well as the gas wetness from the kerogen show remarkably differences to the predictions for the reservoir rock asphaltenes for the maturity range from 30 % TR up to 90 % TR. At 10 % TR, the GOR predictions show the greatest variability, while the gas wetness predictions for the kerogen and the reservoir rock asphaltenes show the greatest resemblance. The largest differences for both predicted parameter were observed at 90 % TR. Laterally, lower GOR and higher gas wetness are predicted for the western part of the Heidrun oilfield. Vertically variable trends have been observed.

8.4.3.4 COMPOSITIONAL KINETIC MODEL

In Figure 140, the results for the calculated compositional kinetic models for the reservoir rock asphaltenes and the source rock kerogen are shown. The predicted GOR, gas wetness (C_1/C_2 - C_5), P_{sat} and b_o for the Heidrun sample set analysed at different degrees of transformation are shown in Table X 11 in the appendix. As mentioned before, during the MSSV pyrolysis, the vessel of the reservoir rock asphaltene G004225 for the analysis of composition at 50 % TR was broken, hence a gap in the Ea of the compositional kinetic model of can be seen.

In the gas range (C_1 - C_5) the compositional kinetic model of the source rock kerogen is dominated by methane, while the liquid part of the predicted petroleum composition is dominated by relatively low weight molecular compounds in the range of C_7 - C_{15} and only a minor part of compounds > C_{16}.

Compared to the kerogen the compositional kinetic models for the asphaltenes predict a more mixed gas composition (C_1 - C_5) and a heavier liquid petroleum composition, which is mainly composed of low and medium weight molecular compounds in the range of C_7 up to C_{35}. In

addition, each of the analysed asphaltenes shows a significant amount of high molecular weight compounds in the range > C_{35}, typically waxes. The latter were not observed in the source rock kerogen.

The predicted petroleum composition based on the source rock kerogen of the Spekk Formation and the reservoir rock asphaltene from the Heidrun oilfield are thus different.

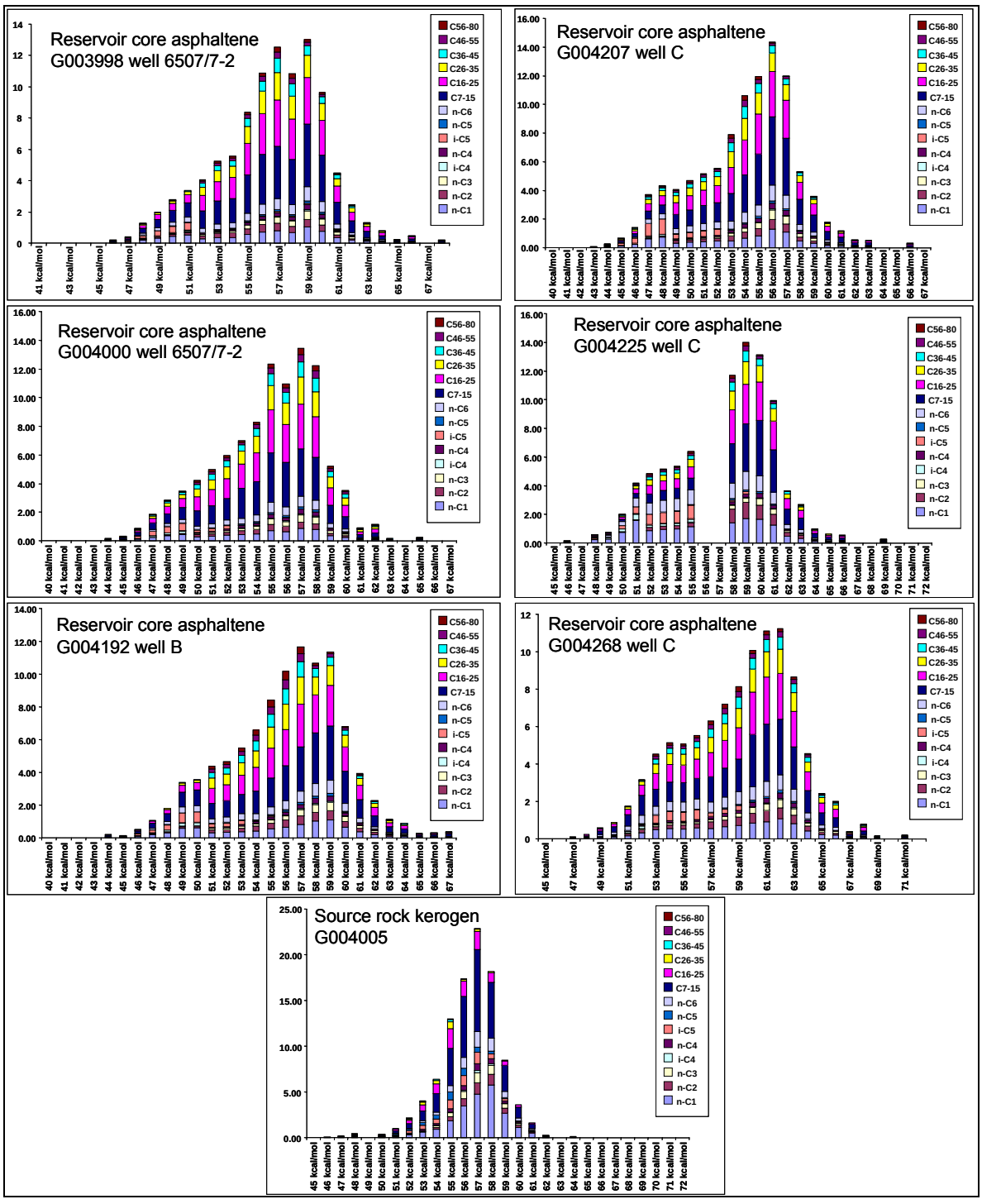

Figure 140 Compositional kinetic models from the PVT simulation for the reservoir rock asphaltenes and the source rock kerogen from the Heidrun oil field.

The phase envelopes commonly used to describe the phase behaviour of fluids the source rock kerogen and the reservoir rock asphaltenes would generate are shown in Figure 141. In this pressure / temperature diagram, the phase envelopes at 50 % transformation are shown.
At the first view, it is obvious that the reservoir rock asphaltenes and the source rock kerogen have remarkably different phase envelopes, which implies different properties for the fluids generated concerning GOR, P_{sat}, b_o and API gravity. The kerogen is characterised by a lower P_{sat} compared to the asphaltenes of well B, C and E, and a shift of the critical point to lower temperatures (200 °C) compared to all reservoir rock asphaltenes.

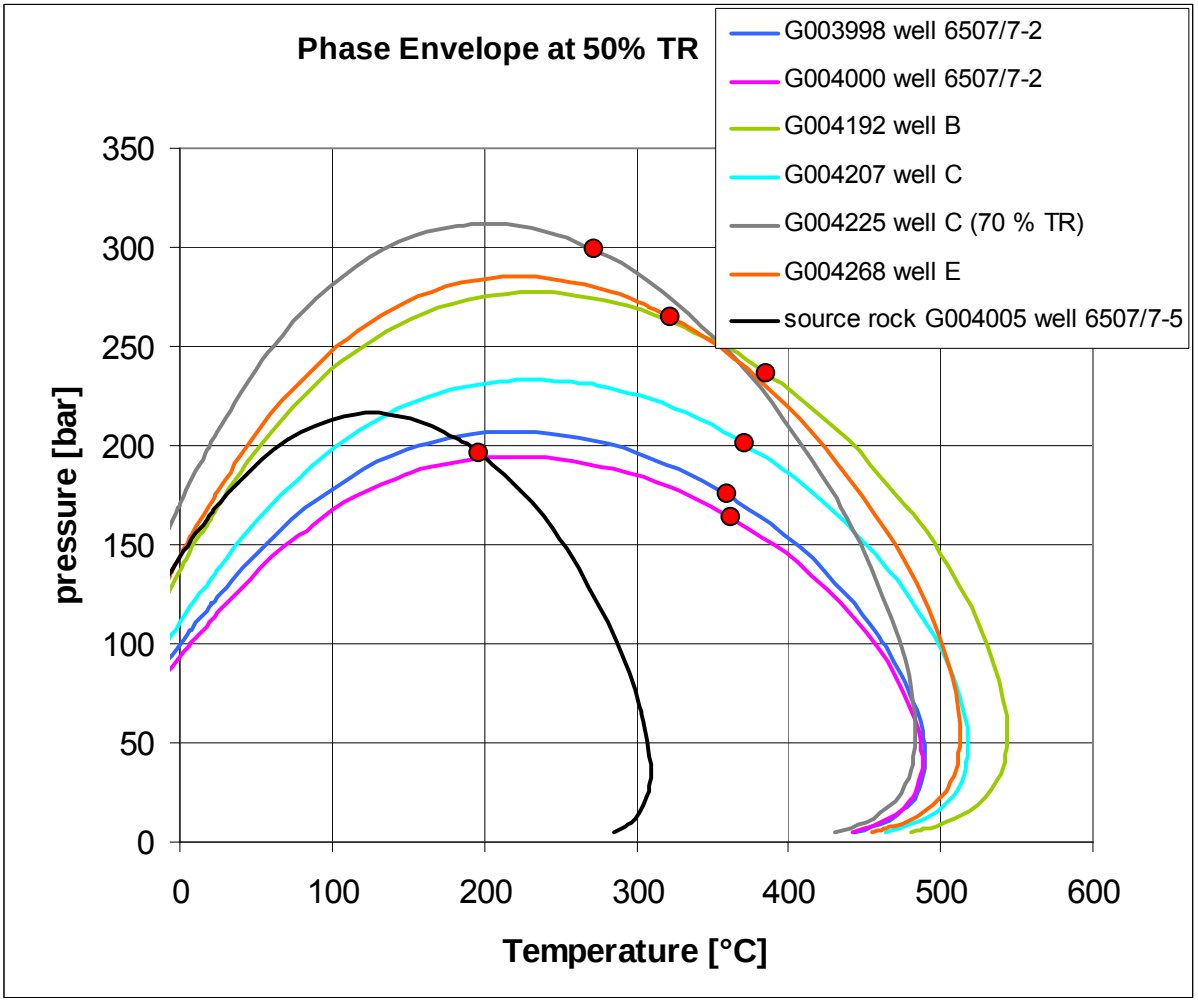

Figure 141 Phase envelopes of the reservoir rock asphaltenes well 6507/7-2, well B, well C (G004207), well E and the source rock kerogen analysed from the Heidrun reservoir at 50 % TR. The phase envelope of asphaltene G004225 of well C is shown for 70 % TR. The critical points are indicated by red dots.

Comparing the single reservoir rock asphaltenes differences in the shape of the phase envelope are obvious. The predicted P_{sat} and cricondentherm temperatures of the asphaltenes (highest temperature extent of the phase envelope) ranges from 195 bar to 285 bar and 480 °C

to 545 °C, respectively. Lowest P_{sat} and cricondentherm temperatures were predicted for both asphaltenes of well 6507/7-2 in the western / central part of the Heidrun oilfield. Although both show relatively similar phase envelopes, slightly higher P_{sat} and a shift of the critical point to lower temperatures was observed for the upper reservoir asphaltene of well 6507/7-2. Relatively high P_{sat} and cricondentherm temperatures were observed for the asphaltenes of well B and well E, from the eastern and northern part of the reservoir. Both show relatively similar predictions, however, the well E asphaltene G004268 has slightly higher P_{sat} but a lower cricondentherm temperature compared to well B and shows the lowest temperature of the critical point.

The most significant differences regarding fluid composition are those predicted for the asphaltenes of well C from the eastern part of the oilfield. This is caused by the difference in the TR of the shown phase envelopes, 70 % TR for this sample as compared to 50 % TR for the other sample. Thus, these two asphaltenes present a variability in P_{sat} predictions of nearly 100 bar, which corresponds to a difference in reservoir depth of circa 1 km (10 m water column ~1 bar). The asphaltene of the Ile Fm. (G004225) shows the highest predicted P_{sat} and will not be considered for further analysis. The pressure / temperature predictions for the Garn Fm. asphaltene (G004207) are in between the remaining asphaltene predictions.

The amount and composition of gas in the fluid strongly influence its P_{sat} and GOR, whereby a methane-rich gas composition results commonly in a higher P_{sat} than a comparably "wetter" gas composition (di Primio *et al.*, 1998). Beside the Ile Fm. asphaltene G004225 of well C, the lowest gas wetness was observed in the asphaltene of well E, characterised by the highest $P_{sat.}$ at 50 % TR. The highest gas wetness was observed in well 6507/7-2 presenting the lowest P_{sat}.

Concerning the critical point the asphaltenes of well 6507/7-2, well C and well B show relatively similar temperatures. A distinct shift of the critical point to lower temperatures was observed for the asphaltenes of well E (and the lower asphaltene of well C albeit representing a higher TR than the other samples). Phase envelopes of samples with increasing maturity show a systematic decrease in their cricondentherms with increasing cricondenbars, and the locations of the critical points move systematically towards lower temperatures and higher pressures (di Primio *et al.*, 1998). Thus the high P_{sat} of the well E asphaltene and the distinctly lower temperature of the critical point compared to the remaining asphaltene samples could be

an indication of higher maturity of the source which generated the petroleum in well E (Heidrun north).

In terms of bulk properties, the fluid that would be generated by the reservoir rock asphaltenes of well 6507/7-2 could be described as petroleum with higher proportions of high molecular weight material and densities compared to the lighter oil predicted by the source rock kerogen. Within well 6507/7-2, the slight shift of P_{sat} and the critical point temperature between both asphaltenes might indicate changes in the source maturity.

The critical points of the asphaltene samples of well 6507/7-2, well B and well C seem to remain at nearly constant temperatures independent of the shift of the bubble point curves to higher pressures. A similar behaviour was observed in natural fluids where the observed vertical shift in critical point temperatures was attributed to mixing of fluids from two different sources in the reservoir (di Primio *et al.*, 1998). Thus, the different physical properties of petroleum fluids observed are possibly not only controlled by maturity, but may reflect also reservoir charging and mixing dynamics.

The large difference in predicted source rock fluid properties as compared to the asphaltenes may additionally indicate that the source rock present on the Heidrun structure, which is thermally immature, is likely not a good representative of the deep and mature generating kitchen.

The compositional information derived from the reservoir rock asphaltenes indicate differences in the maturity of the source and could further be influenced by mixing of oils from sources of different maturity or organofacies.

9 CONCLUSION

Vertical and lateral variabilities in the organic matter composition and distribution were delineated in the Heidrun reservoir screening applying known and new pyrolysis parameter to the macromolecular polar fraction in reservoir rocks.

Using the phenol content in the reservoir rock pyrolysates in 23 reservoir rock sample *in-situ* organic matter was found in form of finely dispersed coaly particles.

Great variabilities were observed for aromatics and gas compounds in the macromolecular fraction. The 1-ring versus 2-ring aromatic hydrocarbon compound ratio indicates differences in the organic matter composition in all wells and individual reservoir formations.
Different gradients were found in the aromaticity with increasing depth. Similar trends were observed in the gas amount. The enrichment in aromatic compounds relative to the *n*-C_{5+} in reservoir rock pyrolysis products is accompanied by depletion in the gas wetness. In most of the wells, we observed an inverse correlation of aromaticity and gas wetness. Both parameters are apparently linked.

A direct correlation of aromaticity and biodegradation was observed within the pyrolysis products from the heavy oil series (WCSB) and the Heidrun oils, which show an increase in aromaticity with increasing viscosity and decreasing API gravity. Both fluid physical properties appear to be related to different biodegradation levels. However, the range is much less pronounced for these samples than for the Heidrun cores.
Based on visual comparison a correlation of the aromaticity and the water saturation was observed in a few wells, especially near the OWC. The water saturation of in the reservoir zones is important as biodegradation occurs in water-saturated zones.

In a lateral direction higher aromaticity, higher gas amount, and lower gas wetness predominantly in the eastern part of the Heidrun reservoir compared to the western part were found. These findings correlate to the biodegradation pattern based on the oil analysis in the Heidrun field that already exists. The Heidrun field can be subdivided in two dominant parts, a biodegraded eastern and a mixed western part.

Furthermore, we observed a trend in the reservoir age. From the younger to the older reservoir formation (Garn Fm. - Ile Fm. - Tilje Fm. - Åre Fm.) the aromaticity and gas content in the pyrolysates increase, and the gas wetness decreases.

Differences in the alkyl chain length distribution within the reservoir rocks have been used in order to detect heterogeneities in the organofacies and/or the maturity of the source rock, which in turn can indicate variabilities in the oil charges and deliver thus information for the filling history reconstruction.
Both potential source rocks show differences in the source organofacies and indications to different maturity. The Spekk Formation indicates a low maturity and a marine depositional environment; the Melke Formation show higher maturity and indicates a marine depositional environment with terrestrial influence.
Independent of their reservoir formation most of the reservoir rocks shows an alkyl chain length distribution that is broadest the same as that of the Spekk Formation. A few reservoir rocks predominantly from the western part of the Heidrun reservoir were detected showing slightly higher amount of long alkyl chains compared to the potential source rock from the Spekk. They show greater proportions of waxy compounds that could be an indication to a lacustrine influence of the generative source. Great quantities of waxy compounds were found in reservoir rocks from Heidrun north. Here a lacustrine influence of the generative source has to be considered.

A new asphaltene separation method was developed in order to evaluate small-scale heterogeneities in the Heidrun reservoir based on single asphaltene fractions. The proposed method for asphaltene precipitation was developed through the investigation of the influence of solvent type, solvent amount and aging time. The final method shows an excellent reproducibility and linearity for asphaltene separation.

As far as the screening is concerned, it could be concluded that asphaltenes do not yield noticeably more information on the geochemical parameter used. Compared to the corresponding reservoir rocks the asphaltene pyrolysates exhibit higher aromaticity and higher gas yields. They further do not differ among themselves as much as seen for the corresponding reservoir rock samples, but reflect the gradients observed in the reservoir rock pyrolysates for the individual parameter.

The analysis is additionally time consuming, and thus not appropriate for screening of large sample sets. The best results for heterogeneity screening were obtained using whole reservoir rock Py-GC.

However, it is well established that kinetic parameters from asphaltenes can be used as proxies for kinetics for source rock kerogen. To date such compositional kinetics has been applied to produced oils and tar mats, but never within the context of source profiling and the delineation of reservoir heterogeneities. Here we use compositional kinetics for that purpose.

In both test study areas, the Duvernay and the Draupne Formation, it was observed that kerogen and reservoir asphaltene show both very similar shapes of the phase envelopes, which implies similar physical properties of the fluid that would be generated concerning GOR, P_{sat}, b_o and even API gravity. Predictions for the source rock asphaltenes clearly show different shapes of the phase envelopes, characterised by a much higher P_{sat} and a shift of the critical point to lower temperatures.

Within the main study area, the Heidrun reservoir, reservoir rock asphaltenes and source rock kerogen show different compositional information. They show different shapes of the phase envelope that imply different physical properties of the fluid generated. The kerogen is characterised by a lower P_{sat} compared to most of the reservoir rock asphaltenes analysed and a shift of the critical point to lower temperatures compared to all reservoir rock asphaltenes. The large difference in predicted source rock fluid properties as compared to the asphaltenes indicate that the source rock present on the Heidrun structure, which is thermally immature, is likely not a good representative of the deep and mature generating kitchen.

The compositional information of individual reservoir rock asphaltene samples indicate differences in the maturity of the source and / or mixing effects of oils generated from different sources.

10 APPENDIX

Table X 1 Average (av) and standard deviation (STABW)* for the PI and organic richness of the reservoir rock samples and potential source rock samples of the Heidrun oil field. * $\sqrt{n\sum x^2 - \left(\sum x^2\right)/n^2}$

Reservoir rocks					
Statoil wells	**stratigraphical unit**	**PI**		**organic richness (mg / g rock)**	
		av	**STDV***	**av**	**STDV***
A	Åre Fm. 3.1 - 4.4	0.60	0.16	27.33	17.03
B	Tilje Fm. 2.5 - 3.4	0.67	0.03	28.29	13.08
C	Garn/Not/Ile/Åre Fm.	0.63	0.15	26.47	17.78
	Garn Fm.	0.67	0.02	12.70	5.32
	Not Fm. 1	0.66	-	18.66	-
	Ile Fm. 2 - 6	0.67	0.06	26.77	24.80
	Åre Fm. 1	0.13	0.13	31.52	36.84
D	Åre Fm. 2.1	0.48	0.12	17.08	10.98
E	Åre Fm. 4.1 - 3.2	0.56	0.21	34.28	20.68
NPD wells					
6507/7-2	Tilje/Åre Fm.	0.67	0.06	21.23	6.59
	Tilje Fm. 2.1 / 3.2	0.69	0.09	17.24	6.35
	Åre Fm. 6.2 / 7.2	0.64	0.01	25.22	5.13
6507/7-3	Garn/Ile/Ror Fm.	0.71	0.01	13.54	1.35
	Garn Fm.	0.71	-	13.28	-
	Ile Fm. 4 - 6	0.70	-	15.01	-
	Ror Fm. 2	0.72	-	12.35	-
6507/7-4	Garn/Ile Fm.	0.68	0.02	11.02	4.32
	Garn Fm.	0.67	-	15.74	-
	Ile Fm. 5 - 6	0.69	0.02	9.45	3.63
6507/7-5	Garn/Ile Fm.	0.74	0.02	15.51	0.34
	Garn Fm.	0.75	-	15.75	-
	Ile Fm. 2	0.73	-	15.27	-
6507/7-6	Åre Fm. 2 (?) - 3.2	0.63	0.02	13.98	2.56
6507/7-8	Garn/Ile Fm.	0.62	0.13	7.86	6.37
	Garn Fm.	0.75	-	10.28	-
	Ile Fm.	0.50	0.24	7.05	7.55
6507/8-1	Tilje Fm. 1 - 3.3	0.59	0.02	19.03	6.83
6507/8-4	Åre Fm. 1 - 2.1	0.64	0.02	22.36	8.99
Statoil wells		0.61	0.15	26.47	17.78
NPD wells		0.65	0.06	16.35	7.58
all wells		0.62	0.13	24.10	16.53

Source rocks					
6507/7-5	Spekk Fm.	0.07	-	15.74	-
6507/7-8	Melke Fm.	0.47	-	0.09	-

Table X 2 Average (av) and standard deviation (STABW)* for the Py-GC parameters applied to the reservoir rocks for each individual well and both source rocks from the Heidrun oil field. * $\sqrt{n\sum x^2 - \left(\sum x^2\right)/n^2}$

Reservoir rock samples															
Statoil wells	**stratigraphical unit**	**aromaticity**		**mono/diaromatic hydrocarbons**		**phenol**		**gas wetness**		**gas %**		**GOR**		**UCM**	
		C_1-C_2 alkylbenzenes + 2MN + 1MN + DMN / *n*-C_{5+}		C_1-C_2 alkylbenzenes / N + 2MN + 1MN + DMN		phenol / *n*-$C_{9:0}$		C_2-C_4 / C_1-C_4		C_1-C_5		bulk C_1- C_5 / total resolved C_{6+}		%	
		av	**STDV***	**av**	**STDV***	**av**	**STDV***	**av**	**STDV***	**av**	**STDV***	**av**	**STDV***	**av**	**STDV***
A	Åre Fm. 3.1 - 4.4	0.45	0.71	2.99	0.55	2.74	7.23	0.66	0.08	68.12	9.55	0.19	0.19	67.50	17.57
B	Tilje Fm. 2.5 - 3.4	0.21	0.09	3.27	1.20	0.30	0.15	0.74	0.04	63.17	4.46	0.63	0.07	76.59	5.55
C	Garn/Not/Ile/Åre Fm.	0.28	0.30	3.39	0.83	1.94	4.94	0.74	0.10	64.60	10.32	0.64	0.18	72.85	13.13
	Garn Fm.	0.21	0.04	3.23	0.97	0.73	1.24	0.74	0.07	61.80	3.66	0.59	0.04	77.48	3.97
	Not Fm. 1	0.16	-	3.46	-	0.42	-	0.75	-	56.88	-	0.66	-	66.01	-
	Ile Fm. 2 - 6	0.21	0.12	3.65	0.64	0.64	1.27	0.77	0.08	63.25	8.41	0.61	0.13	73.38	11.42
	Åre Fm. 1	1.29	0.41	2.11	0.09	19.18	2.75	0.47	0.06	93.19	1.39	1.07	0.46	25.40	-
D	Åre Fm. 2.1	0.85	1.11	2.05	1.44	4.47	9.22	0.65	0.16	61.32	31.93	1.00	1.36	38.75	13.94
E	Åre Fm. 4.1 - 3.2	0.35	0.24	2.61	0.70	2.43	4.41	0.66	0.12	67.47	9.59	0.66	0.21	61.93	16.86
NPD wells															
6507/7-2	Tilje/Åre Fm.	0.17	0.04	3.91	0.33	0.20	0.06	0.71	0.05	57.86	6.98	0.46	0.05	70.28	7.99
	Tilje Fm. 2.1 / 3.2	0.15	0.07	3.65	0.12	0.22	0.09	0.73	0.06	54.33	9.81	0.49	0.00	66.32	10.54
	Åre Fm. 6.2 / 7.2	0.18	0.00	4.17	0.19	0.18	0.03	0.69	0.02	61.38	0.18	0.43	0.08	74.24	4.20
6507/7-3	Garn/Ile/Ror Fm.	0.11	0.01	3.84	0.36	0.15	0.01	0.80	0.02	53.89	3.20	0.43	0.08	70.84	9.88
	Garn Fm.	0.10	-	3.50	-	0.14	-	0.82	-	50.56	-	0.35	-	59.44	-
	Ile Fm. 4 - 6	0.12	-	3.81	-	0.15	-	0.80	-	54.18	-	0.41	-	76.50	-
	Ror Fm. 2	0.11	-	4.21	-	0.15	-	0.78	-	56.93	-	0.51	-	76.59	-
6507/7-4	Garn/Ile Fm.	0.19	0.04	4.69	1.44	0.32	0.12	0.78	0.04	59.92	2.18	0.57	0.03	80.72	3.38
	Garn Fm.	0.13	-	6.66	-	0.16	-	0.82	-	56.78	-	0.60	-	79.28	-
	Ile Fm. 5 - 6	0.20	0.01	4.03	0.72	0.37	0.06	0.77	0.04	60.96	0.78	0.56	0.02	81.20	3.97
6507/7-5	Garn/Ile Fm.	0.12	0.00	2.89	0.82	0.10	0.06	0.78	0.04	52.50	0.30	0.59	0.27	77.76	6.15
	Garn Fm.	0.12	-	2.31	-	0.05	-	0.76	-	52.71	-	0.40	-	73.41	-
	Ile Fm. 2	0.11	-	3.47	-	0.14	-	0.81	-	52.29	-	0.78	-	82.10	-
6507/7-6	Åre Fm. 2 (?) - 3.2	0.22	0.02	3.86	0.11	0.09	0.01	0.70	0.03	62.74	1.29	0.92	0.24	77.79	1.76
6507/7-8	Garn/Ile Fm.	0.18	0.06	3.54	0.63	0.09	0.03	0.73	0.05	59.33	5.38	0.87	0.23	62.19	36.93
	Garn Fm.	0.25	-	1.08	-	0.12	-	0.84	-	56.19	-	0.65	-	83.94	-
	Ile Fm.	0.65	0.81	4.93	1.15	1.27	1.74	0.75	0.06	68.06	16.58	0.94	0.22	54.94	41.60
6507/8-1	Tilje Fm. 1 - 3.3	0.30	0.17	4.19	0.67	0.27	0.11	0.71	0.03	65.30	6.75	0.71	0.09	72.14	11.54
6507/8-4	Åre Fm. 1 - 2.1	0.16	0.02	3.12	0.95	0.56	0.27	0.72	0.05	54.77	3.65	0.66	0.08	81.22	1.68
Source rock samples															
6507/7-5	Spekk	0.38	-	3.77	-	0.48	-	0.72	-	67.10	-	0.44	-	42.84	-
6507/7-8	Melke	1.20	-	4.25	-	0.91	-	0.63	-	79.31	-	0.57	-	1.53	-

Table X 3 Py-GC parameters for each reservoir rock analysed in well C. Blue coloured reservoir rock samples were selected for asphaltene separation.

Statoil					aromaticity	mono/diaromatic hydrocarbons	phenol	gas wetness	gas %	GOR	UCM
well	GFZ no.	stratigraphical unit	depth in m TVD-SS	depth in m MD-RKB	C_1-C_2 alkylbenzenes + 2MN + 1MN + DMN / *n*-C_{5+}	C_1-C_2 alkylbenzenes / N + 2MN + 1MN + DMN	phenol / *n*-C_{9-0}	C_2-C_4 / C_1-C_4	C_1-C_5	bulk C_1- C_5 / total resolved C_{6+}	
			m	m							%
C	G004196	Garn Fm.	2523.5	3658.8	0.25	1.64	0.20	0.75	62.84	0.61	83.43
C	G004197	Garn Fm.	2524.3	3659.6	0.20	2.57	0.20	0.76	59.51	0.57	82.28
C	G004199	Garn Fm.	2526.2	3661.5	0.30	2.70	4.16	0.58	70.50	0.65	74.91
C	G004202	Garn Fm.	2528.5	3663.8	0.21	2.73	1.08	0.69	63.76	0.60	72.42
C	G004203	Garn Fm.	2528.6	3663.9	0.19	4.59	0.62	0.73	61.32	0.59	80.36
C	G004204	Garn Fm.	2530.1	3665.4	0.21	3.06	0.21	0.77	60.21	0.61	78.37
C	G004207	Garn Fm.	2531.0	3666.3	0.20	2.96	0.14	0.77	60.78	0.59	74.77
C	G004208	Garn Fm.	2531.1	3666.4	0.18	3.49	0.18	0.80	59.43	0.62	80.32
C	G004209	Garn Fm.	2532.2	3667.5	0.16	4.87	0.17	0.81	56.89	0.56	73.07
C	G004210	Garn Fm.	2533.5	3668.8	0.19	3.72	0.30	0.76	62.80	0.62	74.84
C	G004213	Not Fm. 1	2536.9	3672.5	0.16	3.46	0.42	0.75	56.88	0.53	66.01
C	G004215	Ile Fm. 6	2538.9	3674.5	0.18	3.80	0.17	0.74	62.57	0.66	61.45
C	G004217	Ile Fm. 6	2540.3	3675.9	0.54	2.00	4.99	0.58	82.97	0.97	47.46
C	G004218	Ile Fm. 6	2541.6	3677.2	0.13	3.39	0.15	0.82	58.20	0.60	78.35
C	G004219	Ile Fm. 6	2542.1	3677.7	0.43	2.52	2.23	0.63	80.62	-	-
C	G004221	Ile Fm. 6	2543.3	3678.9	0.16	3.88	0.21	0.77	59.49	0.57	77.07
C	G004222	Ile Fm. 5	2547.6	3683.2	0.20	3.95	0.26	0.71	62.33	0.63	73.31
C	G004223	Ile Fm. 5	2549.8	3685.4	0.14	3.33	0.18	0.79	59.91	0.56	84.07
C	G004224	Ile Fm. 4	2551.6	3687.3	0.16	3.34	0.15	0.82	56.99	0.53	81.83
C	G004225	Ile Fm. 4	2553.1	3688.8	0.15	3.69	0.17	0.81	57.37	0.55	81.80
C	G004226	Ile Fm. 4	2556.4	3692.1	0.20	4.73	0.28	0.82	73.18	0.80	50.85
C	G004229	Ile Fm. 4	2557.1	3692.8	0.15	3.86	0.15	0.83	59.38	0.57	79.80
C	G004230	Ile Fm. 4	2557.7	3693.4	0.13	4.09	0.13	0.81	55.71	0.51	82.84
C	G004234	Ile Fm. 3	2560.8	3696.6	0.13	4.09	0.13	0.81	55.71	0.54	80.94
C	G004236	Ile Fm. 2	2567.8	3703.7	0.17	3.84	0.21	0.82	60.05	0.57	76.83
C	G004238	Ile Fm. 2	2571.4	3707.3	0.24	3.79	0.19	0.78	61.96	0.57	73.93
C	G004240	Ile Fm. 2	2573.9	3709.8	0.33	4.01	0.64	0.70	65.54	0.54	70.20
C	G004249	Äre Fm. 1	2630.4	3766.8	1.00	2.04	21.13	0.51	92.21	-	-
C	G004250	Äre Fm. 1	2633.1	3769.6	1.57	2.17	17.23	0.43	94.17	1.39	25.40

Table X 4 Py-GC parameters for the heavy oil series of the Western Canada Sedimentary Basin (WCSB). The Industry Partner Shell provides the samples.

Heavy oil Reservoir Rock Extracts									
GFZ no.	**depth**	**PI**	**aromaticity**	**mono/diaromatic hydrocarbons**	**phenol**	**gas wetness**	**gas %**	**GOR**	**UCM**
	m below top	S1/(S1+S2)	C_1-C_2 alkylbenzenes + 2MN + 1MN + DMN / *n*-C_{5+}	C_1-C_2 alkylbenzenes / N + 2MN + 1MN + DMN	phenol / *n*-$C_{9\text{-}0}$	C_2-C_4 / C_1-C_4	C_1-C_5	bulk C_1- C_5 / total resolved C_{6+}	%
G005634	604.1	0.54	0.089	2.933	0.129	0.755	52.74	0.57	77.2
G005635	608.6	0.48	0.091	3.168	0.080	0.749	51.87	0.53	76.2
G005636	611.3	0.50	0.093	3.211	0.143	0.758	54.16	0.60	75.0
G005639	621.1	0.47	0.106	3.390	0.102	0.762	55.74	0.60	70.4
G005640	623.5	0.52	0.133	3.900	0.165	0.778	59.01	0.69	71.7

Table X 5 Py-GC parameters for the Heidrun oil samples with different API gravity from 29 to 20°.

Heidrun oil samples											
well	**GFZ no.**	**depth interval**	**stratigraphical unit**	**PI**	**aromaticity**	**mono/diaromatic hydrocarbons**	**phenol**	**gas wetness**	**gas %**	**GOR**	**UCM**
		m MD-RKB		S1/(S1+S2)	C_1-C_2 alkylbenzenes + 2MN + 1MN + DMN / *n*-C_{5+}	C_1-C_2 alkylbenzenes / N + 2MN + 1MN + DMN	phenol / *n*-$C_{9\text{-}0}$	C_2-C_4 / C_1-C_4	C_1-C_5	bulk C_1- C_5 / total resolved C_{6+}	%
6507/7-2	G003881	2340-2330	Tilje Fm. 3.2	0.77	0.08	2.40	0.09	0.79	39.80	0.31	89.2
6507/7-2	G003882	2376-2365	Tilje Fm. 2.2-2.3	0.72	0.10	2.06	0.13	0.78	52.17	0.42	91.9
6507/7-2	G003883	2439-2417	Åre Fm. 2.10-2.11	0.73	0.09	2.07	0.11	0.77	46.60	0.35	88.89
6507/8-1	G003896	2406-2386	Tilje 3.3 - 4	0.72	0.11	2.45	0.09	0.80	56.64	0.49	87.2
6507/8-1	G003897	2462.5-2444	Tilje 2.2 - 2.4	0.69	0.12	1.83	0.11	0.78	53.72	0.44	90.6

Table X 6 Py-GC parameters for each reservoir rock analysed in well B. Blue coloured reservoir rock samples were selected for asphaltene separation.

Statoil					aromaticity	mono/diaromatic hydrocarbons	phenol	gas wetness	gas %	GOR	UCM
well	GFZ no.	stratigraphical unit	depth in m TVD-SS	depth in m MD-RKB	C_1-C_2 alkylbenzenes + 2MN + 1MN + DMN / *n*-C_{5+}	C_1-C_2 alkylbenzenes / N + 2MN + 1MN + DMN	phenol / *n*-$C_{9:0}$	C_2-C_4 / C_1-C_4	C_1-C_5	bulk C_1- C_5 / total resolved C_{6+}	
			m	m							%
B	G004165	Tilje Fm. 3.4	2323.4	3223.9	0.08	6.99	0.00	0.79	70.79	0.94	72.64
B	G004166	Tilje Fm. 3.4	2325.4	3225.9	0.16	3.39	0.31	0.76	57.62	0.54	79.36
B	G004167	Tilje Fm. 3.4	2325.8	3226.3	0.14	4.14	0.19	0.73	61.92	0.67	79.31
B	G004168	Tilje Fm. 3.3	2329.4	3230.0	0.23	2.24	0.34	0.77	64.64	0.65	69.87
B	G004169	Tilje Fm. 3.3	2331.1	3231.6	0.12	2.92	0.17	0.74	58.63	0.56	81.43
B	G004170	Tilje Fm. 3.3	2332.1	3232.7	0.13	3.46	0.19	0.77	58.81	0.58	83.03
B	G004171	Tilje Fm. 3.3	2333.8	3234.4	0.45	2.12	0.14	0.76	70.31	0.67	58.90
B	G004172	Tilje Fm. 3.3	2334.9	3235.6	0.15	4.46	0.31	0.76	60.92	0.62	81.24
B	G004173	Tilje Fm. 3.3	2336.7	3237.4	0.13	3.63	0.32	0.77	59.18	0.59	74.82
B	G004174	Tilje Fm. 3.3	2338.8	3239.5	0.24	2.30	0.27	0.74	66.58	0.63	77.91
B	G004175	Tilje Fm. 3.3	2340.6	3241.4	0.15	3.80	0.21	0.72	61.22	0.61	80.80
B	G004176	Tilje Fm. 3.2	2342.0	3242.8	0.17	4.56	0.27	0.73	62.04	0.61	82.04
B	G004177	Tilje Fm. 3.2	2342.8	3243.6	0.24	1.98	0.22	0.74	65.65	0.68	72.41
B	G004179	Tilje Fm. 3.2	2345.6	3246.4	0.17	5.02	0.46	0.81	65.01	0.69	75.63
B	G004182	Tilje Fm. 3.2	2349.7	3250.6	0.20	4.71	0.33	0.72	63.96	0.62	75.92
B	G004183	Tilje Fm. 3.2	2351.4	3252.3	0.33	2.10	0.38	0.73	68.54	0.72	69.73
B	G004184	Tilje Fm. 3.2	2353.8	3254.8	0.21	2.49	0.20	0.72	62.50	0.62	79.85
B	G004185	Tilje Fm. 3.2	2356.7	3257.7	0.25	2.31	0.65	0.69	63.11	0.58	77.48
B	G004186	Tilje Fm. 3.2	2358.3	3259.4	0.15	2.20	0.15	0.80	61.18	0.67	70.06
B	G004187	Tilje Fm. 3.2	2359.5	3260.6	0.16	3.27	0.32	0.74	60.01	0.66	83.98
B	G004188	Tilje Fm. 3.2	2362.1	3263.2	0.19	3.60	0.29	0.77	60.27	0.57	80.06
B	G004189	Tilje Fm. 3.2	2362.8	3263.9	0.14	3.56	0.20	0.75	58.33	0.62	74.65
B	G004190	Tilje Fm. 3.2	2364.4	3265.5	0.40	2.05	0.26	0.83	77.84	0.88	68.79
B	G004191	Tilje Fm. 3.1	2371.6	3272.9	0.19	4.51	0.52	0.71	62.12	0.62	78.99
B	G004192	Tilje Fm. 3.1	2372.9	3274.2	0.28	1.82	0.43	0.70	63.80	0.59	75.12
B	G004193	Tilje Fm. 2.5	2374.5	3275.8	0.34	2.69	0.35	0.63	61.26	0.52	79.17
B	G004194	Tilje Fm. 2.5	2375.1	3276.4	0.16	2.90	0.19	0.71	59.92	0.64	82.48
B	G004195	Tilje Fm. 2.5	2377.6	3278.9	0.23	2.34	0.65	0.73	62.72	0.55	78.74

Table X 7 Py-GC parameters for each reservoir rock analysed in well A.

Statoil					aromaticity	mono/diaromatic hydrocarbons	phenol	gas wetness	gas %	GOR	UCM
well	GFZ no.	stratigraphical unit	depth in m TVD-SS	depth in m MD-RKB	C_1-C_2 alkylbenzenes + 2MN + 1MN + DMN / *n*-C_{5+}	C_1-C_2 alkylbenzenes / N + 2MN + 1MN + DMN	phenol / *n*-$C_{9:0}$	C_2-C_4 / C_1-C_4	C_1-C_5	bulk C_1- C_5 / total resolved C_{6+}	
			m	m							%
A	G004123	Åre Fm. 4.4	2374.3	3184.3	0.20	3.22	0.16	0.68	67.35	0.67	85.79
A	G004126	Åre Fm. 4.3	2379.1	3189.5	0.23	3.34	0.13	0.68	65.83	0.69	73.38
A	G004127	Åre Fm. 4.3	2379.5	3189.9	0.49	3.31	5.21	0.55	81.74	0.94	41.19
A	G004128	Åre Fm. 4.3	2379.9	3190.3	0.20	3.66	0.12	0.71	61.97	0.63	77.04
A	G004129	Åre Fm. 4.3	2382.0	3192.5	0.25	2.37	0.12	0.66	61.08	0.59	71.51
A	G004132	Åre Fm. 4.3	2385.1	3195.8	0.25	2.57	0.07	0.68	64.05	0.62	81.11
A	G004134	Åre Fm. 4.2	2387.7	3198.6	0.23	2.43	0.08	0.69	62.82	0.61	79.88
A	G004136	Åre Fm. 4.2	2391.4	3202.4	0.86	3.33	8.47	0.53	87.90	1.10	17.63
A	G004137	Åre Fm. 4.2	2392.8	3203.9	0.39	1.87	0.07	0.64	67.75	0.63	78.33
A	G004138	Åre Fm. 4.2	2398.1	3209.5	0.31	2.57	0.45	0.64	65.91	0.63	78.03
A	G004139	Åre Fm. 4.2	2399.8	3211.3	0.22	4.13	1.21	0.63	66.84	0.65	81.63
A	G004140	Åre Fm. 4.1	2400.9	3212.5	0.20	3.52	0.09	0.70	61.21	0.59	83.34
A	G004141	Åre Fm. 4.1	2402.8	3214.5	0.23	3.25	0.10	0.71	62.91	0.62	80.72
A	G004142	Åre Fm. 4.1	2403.8	3215.5	0.27	3.59	2.12	0.63	68.30	0.66	75.78
A	G004143	Åre Fm. 4.1	2406.0	3217.9	0.18	3.41	0.10	0.71	60.32	0.58	81.30
A	G004144	Åre Fm. 4.1	2406.7	3218.6	0.23	3.45	0.07	0.65	63.59	0.63	76.73
A	G004145	Åre Fm. 4.1	2407.8	3219.8	0.23	3.30	0.09	0.69	61.91	0.60	73.51
A	G004146	Åre Fm. 4.1	2409.3	3221.3	0.26	3.17	0.07	0.67	64.69	0.63	72.30
A	G004147	Åre Fm. 4.1	2410.2	3222.3	0.19	3.57	0.08	0.70	60.66	0.59	78.55
A	G004148	Åre Fm. 4.1	2411.1	3223.3	0.25	2.79	0.27	0.70	64.53	0.61	74.30
A	G004149	Åre Fm. 4.1	2416.0	3228.4	0.22	2.60	0.08	0.72	63.97	0.67	47.67
A	G004150	Åre Fm. 4.1	2417.8	3230.3	0.20	3.23	0.08	0.69	62.87	0.66	64.02
A	G004153	Åre Fm. 4.1	2420.8	3233.6	0.38	2.28	0.24	0.71	72.35	0.84	61.00
A	G004154	Åre Fm. 3.2	2422.7	3235.5	0.30	1.84	1.15	0.72	64.48	0.67	68.36
A	G004155	Åre Fm. 3.2	2431.2	3244.5	0.25	2.89	0.09	0.71	64.31	0.78	73.68
A	G004156	Åre Fm. 3.2	2432.7	3246.1	0.20	2.82	0.08	0.70	62.62	0.79	78.02
A	G004157	Åre Fm. 3.2	2435.1	3248.6	0.25	2.91	1.15	0.72	63.86	0.72	72.96
A	G004160	Åre Fm. 3.2	2436.2	3249.7	0.26	2.79	0.08	0.71	64.03	0.80	51.47
A	G004161	Åre Fm. 3.2	2437.2	3250.8	1.42	2.19	28.06	0.45	91.65	1.35	25.98
A	G004163	Åre Fm. 3.1	2461.6	3276.5	0.65	3.52	5.32	0.56	84.37	1.13	50.30
A	G004164	Åre Fm. 3.1	2485.3	3301.5	4.0	2.88	29.60	0.44	95.85	1.45	36.91

Table X 8 Py-GC parameter s for each reservoir rock analysed in well E and D. Blue coloured reservoir rock samples were selected for asphaltene separation.

Statoil					aromaticity	mono/diaromatic hydrocarbons	phenol	gas wetness	gas %	GOR	UCM
well	GFZ no.	stratigraphical unit	depth in m TVD-SS	depth in m MD-RKB	C_1-C_2 alkylbenzenes + 2MN + 1MN + DMN / *n*-C_{5+}	C_1-C_2 alkylbenzenes / N + 2MN + 1MN + DMN	phenol / *n*-C_{9-0}	C_2-C_4 / C_1-C_4	C_1-C_5	bulk C_1- C_5 / total resolved C_{6+}	
			m	m							%
D	G004251	Åre Fm. 2.1	2438.9	2895.2	1.82	3.25	23.25	0.52	95.88	0.74	44.34
D	G004252	Åre Fm. 2.1	2454.8	2912.5	2.67		0.87	0.44	97.73	3.74	28.76
D	G004254	Åre Fm. 2.1	2455.4	2913.1	0.36	3.04	1.81	0.64	69.00	0.71	26.89
D	G004255	Åre Fm. 2.1	2457.5	2915.3	0.16	2.98	0.07	0.65	52.58	0.59	25.02
D	G004257	Åre Fm. 2.1	2462.5	2920.3	0.04	0.66	0.82	0.82	26.04	0.23	48.21
D	G004258	Åre Fm. 2.1	2460.7	2918.4	0.09	0.31	0.02	0.84	26.71	0.21	59.28
E	G004260	Åre Fm. 4.1	2404.4	3540.5	0.17	3.21	0.09	0.71	58.85	0.54	79.81
E	G004263	Åre Fm. 4.1	2406.8	3542.8	1.04	2.12	16.17	0.46	88.31	1.00	31.70
E	G004264	Åre Fm. 4.1	2407.2	3543.2	0.17	2.85	0.06	0.73	57.78	0.49	74.27
E	G004265	Åre Fm. 4.1	2407.7	3543.8	0.72	2.35	5.93	0.52	82.87	0.74	53.17
E	G004266	Åre Fm. 4.1	2410.1	3548.2	0.31	1.20	0.07	0.72	66.03	0.59	76.74
E	G004267	Åre Fm. 4.1	2412.4	3550.5	0.30	2.89	2.63	0.64	69.66	0.68	69.34
E	G004268	Åre Fm. 4.1	2416.4	3554.5	0.18	3.40	0.34	0.72	63.04	0.64	74.31
E	G004271	Åre Fm. 4.1	2420.7	3558.8	0.24	2.24	0.07	0.75	60.82	0.60	49.51
E	G004272	Åre Fm. 4.1	2422.7	3560.8	0.36	2.92	0.21	0.77	74.54	0.90	50.35
E	G004275	Åre Fm. 3.3	2432.4	3570.5	0.20	3.35	0.10	0.73	61.90	0.62	70.12
E	G004276	Åre Fm. 3.3	2437.1	3575.2	0.29	2.16	3.88	0.47	66.31	0.65	41.76
E	G004279	Åre Fm. 3.3	2438.2	3576.3	0.29	1.49	0.04	0.75	60.30	0.48	80.92
E	G004280	Åre Fm. 3.2	2437.6	3581.7	0.24	2.95	0.41	0.75	58.42	0.43	75.48
E	G004281	Åre Fm. 3.2	2438.5	3582.6	0.39	3.35	4.01	0.46	75.79	1.12	39.62

Table X 9 Py-GC parameter s for each reservoir rock analysed from the NPD wells. Blue coloured reservoir rock samples were selected for asphaltene separation.

NPD					aromaticity	mono/diaromatic hydrocarbons	phenol	gas wetness	gas %	GOR	UCM
well	GFZ no.	stratigraphical unit	depth in m TVD-SS	depth in m MD-RKB	C_1-C_2 alkylbenzenes + 2MN + 1MN + DMN / *n*-C_{5+}	C_1-C_2 alkylbenzenes / N + 2MN + 1MN + DMN	phenol / *n*-C_{9-0}	C_2-C_4 / C_1-C_4	C_1-C_5	bulk C_1- C_5 / total resolved C_{6+}	
			m	m							%
6507/7-2	G 003998	Tilje Fm. 3.2	2316.5		0.11	3.56	0.15	0.78	47.39	0.37	58.87
6507/7-2	G 003999	Tilje Fm. 2.2 / 2.1	2377.0		0.20	3.73	0.28	0.69	61.26	0.48	73.78
6507/7-2	G 004000	Åre Fm. 7.2	2407.7		0.18	4.31	0.15	0.67	61.26	0.49	77.21
6507/7-2	G 004001	Åre Fm. 6.2	2432.2		0.18	4.04	0.20	0.70	61.51	0.49	71.27
6507/7-3	G 004002	Garn Fm.	2371.7		0.10	3.50	0.14	0.82	50.56	0.38	59.44
6507/7-3	G 004003	Ile Fm. 4-6	2394.2		0.12	3.81	0.15	0.80	54.18	0.35	76.50
6507/7-3	G 004004	Ile Fm. 2 / Ror Fm. 2	2421.4		0.11	4.21	0.15	0.78	56.93	0.41	76.59
6507/7-4	G 004023	Garn Fm.	2465.2		0.13	6.66	0.16	0.82	56.78	0.51	79.28
6507/7-4	G 004024	Ile Fm. 6	2484.2		0.20	3.52	0.32	0.73	61.81	0.60	83.01
6507/7-4	G 004025	Ile Fm. 5	2494.4		0.21	4.85	0.43	0.80	60.82	0.56	76.64
6507/7-4	G 004026	Ile Fm. 5	2499.5		0.20	3.73	0.37	0.77	60.26	0.59	83.94
6507/7-5	G 004005	Spekk Fm.	2310.6		0.38	3.77	0.48	0.72	67.10	0.54	42.84
6507/7-5	G 004006	Garn Fm.	2368.5		0.12	2.31	0.05	0.76	52.71	0.44	73.41
6507/7-5	G 004007	Ile Fm. 2	2414.5		0.11	3.47	0.14	0.81	52.29	0.40	82.10
6507/7-6	G 004030	Åre Fm. 3.1-3.2	2419.6		0.22	3.84	0.08	0.70	63.55	0.78	75.33
6507/7-6	G 004031	Åre Fm. 3.1-3.2	2433.4		0.24	4.01	0.09	0.67	61.31	0.78	77.91
6507/7-6	G 004032	Åre Fm. (2?)	2435.4		0.23	3.76	0.08	0.71	64.07	0.84	78.45
6507/7-6	G 004034	Åre Fm. (2?)	2440.4		0.19	3.83	0.10	0.73	62.04	0.78	79.47
6507/7-8	G 004008	Melke Fm.	2429.8		1.20	4.25	0.91	0.63	79.31	1.28	1.53
6507/7-8	G 004009	Garn Fm.	2464.5		0.25	1.08	0.12	0.84	56.19	0.57	83.94
6507/7-8	G 004010	Ile Fm.	2486.5		0.14	3.83	0.23	0.80	57.13	0.65	78.17
6507/7-8	G 004012	Ile Fm.	2494.2		0.24	4.83	0.29	0.68	59.93	0.69	79.74
6507/7-8	G 004013	Ile Fm.	2494.6		1.58	6.11	3.28	0.76	87.14	1.09	6.91
6507/8-1	G 004036	Tilje Fm. 3.3	2405.7		0.60	3.07	0.08	0.76	77.33	1.04	52.40
6507/8-1	G 004037	Tilje Fm. 2.5	2442.8		0.21	4.62	0.28	0.71	63.03	0.79	72.86
6507/8-1	G 004038	Tilje Fm. 2.1	2468.7		0.21	4.76	0.32	0.71	62.53	0.78	80.08
6507/8-1	G 004039	Tilje Fm. 1	2476.3		0.25	4.14	0.36	0.67	61.81	0.69	74.65
6507/8-1	G 004041	Tilje Fm. 1	2479.0		0.21	4.35	0.30	0.68	61.80	0.72	80.71

Table X 9 (continued) Py-GC parameters for each reservoir rock sample from the NPD wells. Blue coloured reservoir core samples were selected for asphaltene separation.

NPD					aromaticity	mono/diaromatic hydrocarbons	phenol	gas wetness	gas %	GOR	UCM
well	GFZ no.	stratigraphical unit	depth in m TVD-SS	depth in m MD-RKB	C_1-C_2 alkylbenzenes + 2MN + 1MN + DMN / *n*-C_{5+}	C_1-C_2 alkylbenzenes / N + 2MN + 1MN + DMN	phenol / *n*-C_{9-0}	C_2-C_4 / C_1-C_4	C_1-C_5	bulk C_1- C_5 / total resolved C_{6+}	
			m	m							%
6507/8-4	G 004021	Åre Fm. 2.1	2141.4		0.15	1.53	0.08	0.76	53.26	0.57	80.71
6507/8-4	G 004020	Åre Fm. 2.1	2168.5		0.20	2.37	0.55	0.71	60.03	0.75	78.21
6507/8-4	G 004019	Åre Fm. 2.1	2204.4		0.12	4.19	0.39	0.78	53.06	0.60	82.05
6507/8-4	G 004015	Åre Fm. 1	2248.8		0.17	3.38	0.92	0.69	56.98	0.70	81.71
6507/8-4	G 004016	Åre Fm. 1	2249.3		0.15	3.33	0.63	0.76	55.26	0.60	82.84
6507/8-4	G 004017	Åre Fm. 1	2252.4		0.16	2.91	0.58	0.65	48.47	0.56	82.93
6507/8-4	G 004018	Åre Fm. 1	2253.3		0.15	4.15	0.78	0.68	56.33	0.72	80.12

Table X 10 Pyrolysis-GC parameters of the reservoir rock asphaltenes (RCA) compared to their corresponding reservoir rock (RC) Py-GC parameters.

Reservoir rock (RC) - reservoir rock asphaltene (RCA)					aromaticity		mono/diaromatic hydrocarbons		phenol		gas wetness		gas %		GOR		UCM	
well	GFZ no.	stratigraphical unit	depth (m MD-RKB)		C_1-C_2 alkylbenzenes + 2MN + 1MN + DMN / n-C_{5+}		C_1-C_2 alkylbenzenes / N + 2MN + 1MN + DMN		phenol / n-$C_{9\cdot0}$		C_2-C_4 / C_1-C_4		C_1-C_5		bulk C_1- C_5 / total resolved C_{6+}		(%)	
			TVD SS	MD	RC	RCA	RC	RCA	RC	RCA	RC	RCA	RC	RCA	RC	RCA	RC	RCA
B	G004165	Tilje Fm. 3.4	2323.44	3223.9	0.08	0.32	6.99	2.22	0.00	0.23	0.79	0.71	70.79	72.40	0.94	1.35	72.6	60.4
B	G004173	Tilje Fm. 3.3	2336.68	3237.4	0.13	0.31	3.63	2.32	0.32	0.15	0.77	0.68	59.18	69.15	0.59	0.95	74.8	60.8
B	G004179	Tilje Fm. 3.2	2345.57	3246.4	0.17	0.57	5.02	1.68	0.46	0.94	0.81	0.83	65.01	82.21	0.69	1.64	75.6	51.3
B	G004182	Tilje Fm. 3.2	2349.72	3250.6	0.20	0.39	4.71	1.83	0.33	0.42	0.72	0.70	63.96	73.46	0.62	1.15	75.9	59.2
B	G004185	Tilje Fm. 3.2	2356.68	3257.7	0.25	0.38	2.31	2.15	0.65	0.24	0.69	0.65	63.11	72.68	0.58	0.89	77.5	65.3
B	G004188	Tilje Fm. 3.2	2362.05	3263.2	0.19	0.43	3.60	1.84	0.29	0.29	0.77	0.71	60.27	75.05	0.57	2.86	80.1	72.3
B	G004191	Tilje Fm. 3.1	2372.92	3274.2	0.19	0.33	4.51	2.31	0.52	0.18	0.71	0.64	62.12	71.88	0.62	1.03	79.0	62.7
B	G004193	Tilje Fm. 2.5	2374.45	3275.8	0.34	0.44	2.69	1.71	0.35	0.03	0.63	0.67	61.26	73.60	0.52	0.92	79.2	63.7
C	G004199	Garn Fm.	2452.04	3661.5	0.30	0.40	2.70	2.07	4.16	0.55	0.58	0.74	70.50	74.31	0.65	1.21	74.9	73.7
C	G004209	Garn Fm.	2457.95	3667.5	0.16	0.45	4.87	1.70	0.17	0.42	0.81	0.76	56.89	73.99	0.56	1.15	73.1	54.2
C	G004213	Not Fm. 1	2462.92	3672.5	0.16	0.40	3.46	1.96	0.42	0.26	0.75	0.67	56.88	71.17	0.53	0.91	66.0	60.5
C	G004217	Ile Fm. 6	2466.29	3675.9	0.54	0.67	2.00	1.44	4.99	5.91	0.58	0.64	82.97	88.49	0.97	1.32	47.5	65.6
C	G004223	Ile Fm. 5	2475.70	3685.4	0.14	0.38	3.33	1.56	0.18	0.34	0.79	0.76	59.91	73.30	0.56	1.22	84.1	57.6
C	G004230	Ile Fm. 4	2483.62	3693.4	0.13	0.29	4.09	2.27	0.13	0.19	0.81	0.69	55.71	66.70	0.51	0.87	82.8	59.8
C	G004249	Åre Fm. 1	2556.31	3766.8	1.00	1.15	2.04	1.60	21.13	11.86	0.51	0.73	92.21	90.26	-	1.63	-	56.7
D	G004254	Åre Fm. 2.1	2431.51	2913.1	0.36	0.34	3.04	0.93	1.81	1.85	0.64	0.84	69.00	81.53	0.71	1.77	26.9	49.2
D	G004255	Åre Fm. 2.1	2433.33	2915.3	0.16	0.29	2.98	1.27	0.07	1.56	0.65	0.74	52.58	77.53	0.59	1.64	25.0	57.3
D	G004258	Åre Fm. 2.1	2436.00	2918.4	0.09	0.25	0.31	0.93	0.02	0.58	0.84	0.90	26.71	79.23	0.21	1.95	59.3	45.6
E	G004263	Åre Fm. 4.1	2383.38	3542.8	1.04	0.43	2.12	1.84	16.17	2.78	0.46	0.63	88.31	57.69	1.00	1.11	31.7	65.9
E	G004265	Åre Fm. 4.1	2384.16	3543.8	0.72	0.44	2.35	2.22	5.93	1.85	0.52	0.64	82.87	76.65	0.74	0.93	53.2	65.3
E	G004267	Åre Fm. 4.1	2389.75	3550.5	0.30	0.42	2.89	1.26	2.63	0.91	0.64	0.76	69.66	80.75	0.68	1.75	69.3	50.4
E	G004268	Åre Fm. 4.1	2393.05	3554.5	0.18	0.37	3.40	2.28	0.34	0.38	0.72	0.66	63.04	71.99	0.64	0.97	74.3	62.9
6507/7-2	G 003998	Tilje Fm. 3.2	2316.50	2316.50	0.11	0.35	3.56	2.28	0.15	0.14	0.78	0.66	47.39	70.11	0.37	0.81	58.9	61.3
6507/7-2	G 003999	Tilje Fm. 2.2 / 2.1	2377.00	2377.00	0.20	0.38	3.73	1.63	0.28	0.15	0.69	0.67	61.26	70.78	0.48	0.84	73.8	63.7
6507/7-2	G 004000	Åre Fm. 7.2	2407.65	2407.65	0.18	0.35	4.31	2.03	0.15	0.12	0.67	0.66	61.26	70.54	0.49	0.80	77.2	62.6
6507/7-5	G 004006	Garn Fm.	2368.50	2368.50	0.12	0.30	2.31	2.02	0.05	0.20	0.76	0.68	52.71	72.08	0.44	0.91	73.4	61.9
6507/7-5	G 004007	Ile Fm. 2	2414.50	2414.50	0.11	0.31	3.47	1.93	0.14	0.21	0.81	0.69	52.29	71.25	0.40	1.00	82.1	61.6
6507/7-8	G 004009	Garn Fm.	2464.50	2464.50	0.25	0.31	1.08	2.06	0.12	0.22	0.84	0.70	56.19	69.08	0.57	0.91	83.9	63.1
6507/7-8	G 004010	Ile Fm.	2486.50	2486.50	0.14	0.32	3.83	2.11	0.23	0.15	0.80	0.71	57.13	71.44	0.65	0.98	78.2	62.1
6507/7-8	G 004012	Ile Fm.	2494.20	2494.20	0.24	0.38	4.83	1.51	0.29	0.22	0.68	0.77	59.93	80.51	0.69	1.56	79.7	53.0
6507/7-8	G 004013	Ile Fm.	2494.55	2494.55	1.58	0.52	6.11	2.29	3.28	0.65	0.76	0.72	87.14	76.67	1.09	1.21	6.9	52.2

Table X 11 Predicted GOR, gas wetness (C_1 / C_2 - C_5), *bo* and *Psat* from the PVT simulation of the Heidrun oil field reservoir rock asphaltenes and the source rock kerogen samples.

PVT simulation					
reservoir rock asphaltene	**TR**	**GOR**	**C_1/C_2-C_5**	***b_o***	***P_{sat}***
G003998	10	398.90	2.24	2.49	219.45
	30	159.20	1.54	1.54	188.09
	50	152.10	1.52	1.53	176.66
	70	148.40	1.51	1.51	183.73
	90	184.20	1.61	1.66	178.25
G004000	10	293.00	1.93	2.08	210.05
	30	146.40	1.50	1.51	186.04
	50	140.50	1.49	1.50	164.83
	70	136.90	1.48	1.48	170.02
	90	155.50	1.53	1.52	197.69
G004192	10	477.20	2.46	2.89	207.53
	30	171.60	1.58	1.57	220.43
	50	159.20	1.54	1.50	236.50
	70	177.40	1.59	1.58	225.99
	90	238.50	1.77	1.83	210.65
G004207	10	490.50	2.50	2.69	308.04
	30	190.50	1.63	1.67	194.5
	50	151.90	1.52	1.51	196.19
	70	165.20	1.56	1.58	178.44
	90	217.10	1.71	1.79	183.19
G004225	10	1859.80	6.47	0.00	636.62
	30	539.70	2.65	0.01	347.97
	50	-		-	-
	70	314.20	1.99	2.01	279.87
	90	316.30	2.00	2.08	238.78
G004268	10	244.50	1.79	1.95	166.15
	30	258.50	1.83	1.89	236.19
	50	222.70	1.73	1.73	245.99
	70	200.80	1.66	1.68	207.98
	90	235.10	1.76	1.79	225.45
source rock kerogen					
G004005	10	364.60	2.14	2.35	222.24
	30	350.70	2.10	2.31	208.46
	50	542.60	2.65	3.14	211.54
	70	578.30	2.76	3.28	214.4
	90	1055.70	4.14	5.18	252.4

11 REFERENCES

Agrawala, M., Yarranton, H.W., (2001) An asphaltene association model analogous to linear polymerization. *Industrial & Engineering Chemistry Research*, 40(21), 4664-4672.

Alboudwarej, H., Beck, J., Svrcek, W.Y., Yarranton, H.W., Akbarzadeh, K., (2002) Sensitivity of Asphaltene Properties to Separation Techniques. *Energy Fuels*, 16(2), 462-469.

Ancheyta, J., Betancourt, G., Centeno, G., Marroquin, G., Alonso, F., Garciafigueroa, E., (2002) Catalyst deactivation during hydro processing of Maya heavy crude oil. 1. Evaluation at constant operating conditions. *Energy & Fuels*, 16(6), 1438-1443.

Behar, F., Pelet, R., (1985) Pyrolysis-gas chromatography applied to organic geochemistry; Structural similarities between kerogens and asphaltenes from related rock extracts and oils. *Journal of Analytical and Applied Pyrolysis*, 8, 173-187.

Behar, F., & Vandenbroucke, M., (1987) Chemical modelling of kerogens. *Organic Geochemistry*, 11(1), 15-24.

Bhullar, A.G., Karlsen , D.A., Holm, K., Backer-Owe, K., Le Tran, K., (1998) Petroleum Geochemistry of the Frøy field and Rind discovery, Norwegian Continental Shelf. Implications for reservoir characterisation, compartmentalisation and basin scale hydrocarbon migration patterns in the region. *Organic Geochemistry*, 29(1-3), 735-768.

Bjørlykke, K., (1989) *Sedimentology and Petroleum Geology*. Springer-Verlag, Berlin Heidelberg New York

Blumer, M., Ehrhardt, M., Jones, D.M., (1973) The environmental fate of stranded oil. *Deep-See Res*, 20, 239-250.

Burnham, A.K., Braun, R.L., Gregg, H.R., Samoun, A.M., (1987) Comparison of methods for measuring kerogen pyrolysis rates and fitting kinetic parameters. *Energy Fuels*, 1(6), 452-458.

Calemma, V., Rausa, R., (1997) Thermal decomposition behaviour and structural characteristics of asphaltenes. *Journal of Analytical and Applied Pyrolysis*(40-41), 569-584.

Clegg, H., Horsfield, B., Stasiuk, L., Fowler, M., Vliex, M., (1997) Geochemical characterisation of organic matter in Keg River Formation (Elk point group, Middle Devonian), La Crete Basin, western Canada. . *Organic Geochemistry*, 26, 627-643.

Connan, J., (1984) Biodegradation of crude oils in reservoirs. In: J. Brooks, D.H. Welte (Eds.), *Advances in Petroleum Geochemistry* (Ed. by J. Brooks, D.H. Welte), pp. 299-335. Academic Press, London.

Cornford, C., (1998) Source rocks and hydrocarbons of the North Sea. In: K.W. Glennie (Ed.), *Petroleum Geology of the North Sea, Basic Concepts and recent advances.* (Ed. by K.W. Glennie), pp. 376-462. Blackwell Science.

Curry, D.J., Simpler, T.K., (1988) Isoprenoid constituents in kerogens as a function of depositional environment and catagenesis. *Organic Geochemistry*, 13(4-6), 995-1001.

Dahlgren, S., Hanesand, T., Mills, N., Patience, R., Brekke, T., Sinding-Larsen, R., (1998) NIGOGA - Norwegian Geochemical Standard samples: North Sea Oil - 1 (NGS NSO-1). Norwegian Geochemical Standard Newsletter, vol.3.

di Primio, R., (2004) Surface Exploration Case Histories. Applications of Geochemistry, Magnetics, and Remote Sensing: Dietmar Schumacher and Leonard A. LeSchack (Eds.); AAPG Studies in Geology No. 48, Tulsa, OK, USA, 2002, 486 pages, soft

back, ISBN 0-89181-055-2, US$98 ($79 for AAPG members). *Organic Geochemistry*, 35(2), 215-216.

di Primio, R., Dieckmann, V., Mills, N., (1998) PVT and phase behaviour analysis in petroleum exploration. *Organic Geochemistry*, 29(1-3), 207-222.

di Primio, R., Horsfield, B., (1996) Predicting the generation of heavy oils in carbonate/evaporitic environments using pyrolysis methods. *Organic Geochemistry - Proceedings of the 17th International Meeting on Organic Geochemistry*, 24(10-11), 999-1016.

di Primio, R., Horsfield, B., (2006) From petroleum type organofacies to hydrocarbon phase prediction. *AAPG Bulletin*, 90(7), 1031-1058.

di Primio, R., Horsfield, B., Guzman-Vega, M.A., (2000) Determining the temperature of petroleum formation from the kinetic properties of petroleum asphaltenes. *Nature*, 406(6792), 173-176.

Düppenbecker, S., Horsfield, B., (1990) Compositional information for kinetic modelling and petroleum type prediction. *Organic Geochemistry*, 16, 259-266.

Eglinton, T.I., Larter, S.R., Boon, J.J., (1991) Characterisation of kerogens, coals and asphaltenes by quantitative pyrolysis--mass spectrometry. *Journal of Analytical and Applied Pyrolysis*, 20, 25-45.

Eglinton, T.I., Sinninghe Damsté, J.S., Kohnen, M.E.L., de Leeuw, J.W., (1990) Rapid estimation of the organic sulphur content of kerogens, coals and asphaltenes by pyrolysis-gas chromatography. *Fuel*, 69(11), 1394-1404.

Eglinton, T.I., Sinninghe Damsté, J.S., Pool, W., de Leeuw, J.W., Eijk, G., Boon, J.J., (1992) Organic sulphur in macromolecular sedimentary organic matter. II. Analysis of distributions of sulphur-containing pyrolysis products using multivariate techniques. *Geochimica et Cosmochimica Acta*, 56(4), 1545-1560.

Ehrenberg, S.N., Gjerstad, H.M., Hadler-Jacobsen, F., (1992) Smørbukk Field—A Gas Condensate Fault Trap in the Haltenbanken Province, Offshore Mid-Norway. In: M.T. Halbouty (Ed.), *Giant Oil and Gas Fields of the Decade 1978–1988* (Ed. by M.T. Halbouty). AAPG, Tulsa.

Ehrenberg, S.N., Skjevrak, I., Gilje, A.E., (1995) Asphaltene-rich residues in sandstone reservoirs of Haltenbanken province, mid-Norwegian continental shelf. *Marine and Petroleum Geology*, 12(1), 53-69.

Elias, R., Vieth, A., Riva, A., Horsfield, B., Wilkes, H., (2007) Improved assessment of biodegradation extent and prediction of petroleum quality. *Organic Geochemistry*, 38, 2111-2130.

England, W.A., (1989) The organic geochemistry of petroleum reservoirs. *Organic Geochemistry*, 16(1-3), 415-425.

England, W.A., (2007) Reservoir geochemistry -- A reservoir engineering perspective. *Journal of Petroleum Science and Engineering*, 58(3-4), 344-354.

England, W.A., Mackenzie, A.S., (1989) The geochemistry of petroleum. *Geologische Rundschau*, Special Volume: Evolution of Sedimentary Basins. 78 (1).

England, W.A., Mackenzie, A.S., Mann, D.U., Quigley, T.M., (1987) The movement and entrapment of petroleum fluids in the subsurface. *Journal of Geological Society, London*, 144, 327-347.

Erdmann, M., (1999) Gas generation from over mature Upper Jurassic source rocks, Northern Viking Graben. In: *Berichte4 des Forschungszentrum Jülich*, pp. 198. Forschungszentrum Jülich, Jülich.

Espitalié, J., Laporte, J.L., Madec, M., Marquis, F., Leplat, P., Paulet, J., Boutefeu, A., (1977) Méthode rapide de caractérisation des roches mères de leur potentiel pétrolier et de leur degré d`évolution. *Rev. Inst. Fr. Pétrole*, 32, 23-42.

Forbes, P.L., Ungerer, P.M., Kuhfuss, A.B., Riis, F., Eggen, S., (1991) Compositional modelling of petroleum generation and expulsion: Trial application to a local mass balance in the Smørbukk Sør Field, Haltenbanken Area, Norway. *AAPG Bulletin*, 75(5), 873-893.

Gürgey, K., (1998) Geochemical effects of asphaltene separation procedures: changes in sterane, terpane, and methylalkane distributions in maltenes and asphaltene co-precipitates. *Organic Geochemistry*, 29(5-7), 1139-1147.

Hartgers, W.A., Damste, J.S.S., de Leeuw, J.W., (1994) Geochemical significance of alkylbenzene distributions in flash pyrolysates of kerogens, coals, and asphaltenes. *Geochimica et Cosmochimica Acta*, 58(7), 1759-1775.

Head, I., Jones, D.M., Larter, S.R., (2003) Biological activity in the deep subsurface and the origin of heavy oil. *Nature*, 426, 344-352.

Hemmens, P.D., Hole, A., Reid, B.E., Leach, P.R.L., Landrum, W.R., (1994) The Heidrun oil field. In: J.O. Aasen, E. Berg, A.T. Buller, O. Hjelmeland (Eds.), *North Sea Oil and Gas Reservoirs*, *III* (Ed. by J.O. Aasen, E. Berg, A.T. Buller, O. Hjelmeland), pp. 1-23. Kluwer Academic publishers, Dordrecht.

Heum, O.R., (1996) A fluid dynamic classification of hydrocarbon entrapment. *Petroleum Geoscience*, 2, 145-158.

Hirschberg, A., de Jong, L.N.J., Schipper, B.A., Meijer, J.G., (1984) Influence of temperature and pressure on asphaltene flocculation. *Society of Petroleum Engineers Journal*, 283-293.

Holba, A.G., Dzou, L.I.P., Hickey, J.J., Franks, S.G., May, S.J., Lenney, T., (1996) Reservoir Geochemistry of South Pass 61 Field, Gulf of Mexico: compositional heterogeneities reflecting filling history and biodegradation. *Organic Geochemistry*, 24(12), 1179-1198.

Horsfield, B., (1989) Practical criteria for classifying kerogens: Some observations from pyrolysis-gas chromatography. *Geochimica et Cosmochimica Acta*, 53(4), 891-901.

Horsfield, B., (1997) The bulk composition of the first formed petroleum in source rocks. In: D.H. Welte, B. Horsfield, D.R. Baker (Eds.), *Petroleum and Basin Evolution. Insights from Petroleum Geochemistry, Geology and Basin Modelling* (Ed. by D.H. Welte, B. Horsfield, D.R. Baker), pp. 535. Springer, Berlin Heidelberg.

Horsfield, B., Dueppenbecker, S.J., (1991) The decomposition of Posidonia Shale and Green River Shale kerogens using microsclae sealed vessel (MSSV) pyrolysis. . *Journal of Analytical and Applied Pyrolysis*, 20, 107-123.

Horsfield, B., Dueppenbecker, S.J., Schenk, H.J., Schaefer, R.G., (1993) Kerogen typing concepts designed for the quantitative geochemical evaluation of petroleum potential concepts designed for the quantitative geochemical evaluation of petroleum potential. *Basin modelling; advances and applications; proceedings of the Norwegian Petroleum Society conference*, 3, 243-249.

Horsfield, B., Heckers, J., Leythaeuser, D., Littke, R., Mann, U., (1991) A study of the Holzener Asphaltkalk, northern Germany: observations regarding the distribution, composition and origin of organic matter in an exhumed petroleum reservoir. *Marine and Petroleum Geology*, 8(2), 198-211.

Horstad, I., Larter, S.R., Dypvik, H., Aagaard, P., Bjørnvik, A.M., Johansen, P.E., Eriksen, S., (1990) Degradation and maturity controls on oil field petroleum column heterogeneity in the Gullfaks field, Norwegian North Sea. *Organic Geochemistry*, 16(1-3), 497-510.

Horstad, I., Larter, S.R., Mills, N., (1995) Migration of hydrocarbons in the Tampen Spur area, Norwegian North Sea: a reservoir geochemical evaluation. In: J.M. Cubitt, W.A. England (Eds.), *The geochemistry of reservoirs*, *Special Publication 86* (Ed. by J.M. Cubitt, W.A. England), pp. 159-183. The Geological Society, London.

Hotier, G., Robin, M., (1983) Action de divers diluants sur les produits pétroliers lourds: mesure interprétation et prévision de la floculation des asphaltenès. *Revue de l`Institut Français du Pétrole*, 38(1), 101-120.

Hu, Y.F., Guo, T.M., (2001) Effect of temperature and molecular weight of n-alkane precipitants on asphaltene precipitation. *Fluid Phase Equilibria*, 192(1-2), 13-25.

Hvoslef, S., Larter, S.R., Leythaeuser, D., (1988) Aspects of generation and migration of hydrocarbons from coal-bearing strata of the Hitra formation, Haltenbanken area, offshore Norway. *Organic Geochemistry*, 13(1-3), 525-536.

Ignasiak, T., Kemp-Jones, A.V., Strausz, O.P., (1977) The molecular structure of Athabasca asphaltene. Cleavage of the carbon-sulphur bonds by radical ion electron transfer reactions. *J. Org. Chem.*, 42(2), 312-320.

Jarvie, D.M., Morelos, A., Han, Z., (2001) Detection of pay zones and pay quality, Gulf of Mexico: Application of Geochemical Techniques. *Golf Coast Association of Geological Society Transactions*, 151-160.

Jones, D.M., Douglas, A.G., Connan, J., (1988) Hydrous pyrolysis of asphaltenes and polar fractions of biodegraded oils. *Organic Geochemistry*

Proceedings of the 13th International Meeting on Organic Geochemistry, 13(4-6), 981-993.

Karlsen, D.A., Larter, S.R., (1989) A rapid correlation method for petroleum population mapping within individual petroleum reservoirs - application to petroleum reservoir description. In: J. Haresnape (Ed.), *Correlation in Hydrocarbon Exploration* (Ed. by J. Haresnape), pp. 77-85. Graham and Trotman.

Karlsen, D.A., Nyland, B., Flood, B., Ohm, S.E., Brekke, T., Olsen, S., Backer-Owe, K., (1995) Petroleum geochemistry of the Haltenbanken, Norwegian continental shelf. In: J.M. Cubitt, W.A. England (Eds.), *The Geochemistry of Reservoir*, *86* (Ed. by J.M. Cubitt, W.A. England), pp. 203-256. Geological Society Special publication, London.

Karlsen, D.A., Skeie, J.E., Backer-Owe, K., Bjørlykke, K., Olstad, R., Berge, K., Cecchi, M., Vik, E., Schaefer, R.G., (2004) Petroleum migration, faults and overpressure; Part II, Case history; the Haltenbanken petroleum province, offshore Norway. In: J.M. Cubitt, W.A. England, S.R. Larter (Eds.), *Understanding petroleum reservoirs; towards an integrated reservoir engineering and geochemical approach.*, *237*, *Geological Society Special Publications* (Ed. by J.M. Cubitt, W.A. England, S.R. Larter), pp. 305-372. Geological Society of London, London.

Kawanaka, S., Leontaris, K.J., Park, S.J., Mansoori, G.A., (1989) Thermodynamic and colloidal models of asphaltene flocculation. In: *American Chemical Society, Symposium Series 396 Oil-Field Chemistry, Enhanced Recovery and Production Stimulation*, pp. 442-458, Washington, DC.

Keym, M., (2007) Asphaltenes as geochemical markers: A case study in the Norwegian North Sea. In: *GFZ-Potsdam*. TU-Berlin, Potsdam.

Keym, M., Dieckmann, V., (2006) Predicting the timing and characteristics of petroleum formation using tar mats and petroleum asphaltenes: A case study from the Northern North Sea. *Journal of Petroleum Geology*, 29(3), 273-296.

Keym, M., Dieckmann, V., Horsfield, B., Erdmann, M., Galimberti, R., Kua, L.C., Leith, L., Podlaha, O., (2006) Source rock heterogeneity of the Upper Jurassic Draupne Formation, North Viking Graben, and its relevance to petroleum generation studies. *Organic Geochemistry*, 37(2), 220-243.

Killops, S.D., Al-Jiboori, M.A.H.A., (1990) Characterisation of the unresolved complex mixture UCM in the gas chromatograms of biodegraded petroleum. *Organic Geochemistry*, 15, 147-160.

Killops, S.D., Killops, V.J., (2005) *An introduction to organic geochemistry -2nd ed*. Blackwell Publishing.

Knai, T.A., Knipe, R.J., (1998) The impact of faults on fluid flow in the Heidrun oil field - 10.1144/GSL.SP.1998.147.01.18. *Geological Society, London, Special Publications*, 147(1), 269-282.

Larter, S.R., (1984) Application of analytical pyrolysis techniques to kerogen characterisation and fossil fuel exploration/exploitation. In: K.J. Vorhees (Ed.), *Analytical pyrolysis* (Ed. by K.J. Vorhees), pp. 212-275, Colorado.

Larter, S.R., Senftle, J.T., (1985) Improved kerogen typing for petroleum source rock analysis. *Nature*, 318, 277-280.

Lehne, E., (2007) Geochemical study on reservoir and source rock asphaltenes and their significance for hydrocarbon generation. In: *GFZ-Potsdam*, pp. 361.

Lehne, E., Dieckmann, V., (2007) The significance of kinetic parameters and structural markers in source rock asphaltenes, reservoir asphaltenes and related source rock kerogens, the Duvernay Formation (WCSB). *Fuel*, 86(5-6), 887-901.

Leontaris, K.J., (1989) Asphaltene deposition: a comprehensive description of problem manifestation and modelling approaches *Soc. Petrol. Engin. AIME, SPE Pap. No. 18892*.

Leontaris, K.J., Mansoori, G.A., (1988) Asphaltene deposition: a survey of field experiences and research approaches. *Journal of Petroleum Science and Engineering*, 3(1), 229-239.

Leythaeuser, D., Keuser, C., Schwark, L., (2007) Molecular memory effects recording the accumulation history of petroleum reservoirs: A case study of the Heidrun oil field, offshore Norway. *Marine and Petroleum Geology*, 24(4), 199-220.

Mango, F.D., (1996) Transition metal catalysis in the generation of natural gas. *Organic Geochemistry*, 24(10-11), 977-984.

Mango, F.D., (1997) The light hydrocarbons in petroleum: a critical review. *Organic Geochemistry*, 26(7-8), 417-440.

Meredith, W., Kelland, S.-J., Jones, D.M., (2000) Influence of biodegradation on crude oil acidity and carboxylic acid composition. *Organic Geochemistry*, 21, 1059-1073.

Mitchell, D.L., Speight, J.G., (1973) The solubility of asphaltenes in hydrocarbon solvents. *Fuel*, 52(2), 149-152.

Mo, E.S., Throndsen, T., Andresen, P., Backstrom, S.A., Forsberg, A., Haug, S., Torudbakken, B., (1989) A dynamic deterministic model of hydrocarbon generation in the Midgard Field drainage area offshore Mid-Norway. *Geologische Rundschau*, 78(1), 305-317.

Muscio, G.P.A., Horsfield, B., (1996) Neoformation of Inert Carbon during the Natural Maturation of a Marine Source Rock: Bakken Shale, Williston Basin. *Energy & Fuels*, 10(1), 10-18.

Muscio, G.P.A., Horsfield, B., Welte, D.H., (1994) Occurrence of thermogenic gas in the immature zone--implications from the Bakken in-source reservoir system. *Organic Geochemistry*, 22, 461-476.

Muscio, G.P.A., Horsfield, B., Welte, D.H., (1991) Compositional changes in the macromolecular organic matter (kerogens, asphaltenes, and resins) of a naturally matured source rock sequence from northern Germany as revealed by pyrolysis methods. In: D. Manning (Ed.), *Organic geochemistry advances and applications in energy and the natural environment* (Ed. by D. Manning), pp. 447-449. Manchester University Press, Manchester.

Odden, W., Patience, R.L., van Graas, G., (1998) Application of light hydrocarbons (C4-C13) to oil/source rock correlations; a study of the light hydrocarbon compositions of source rocks and test fluids from offshore Mid-Norway. *Organic Geochemistry*, 28, 823-847.

Palmer, S.E., (1993) Effects of biodegradation and water washing on crude oil composition. In: M.H. Engel, S.A. Macko (Eds.), *Organic Geochemistry* (Ed. by M.H. Engel, S.A. Macko), pp. 511-533. Plenum Press, New York.

Parra-Barraza, H., Hernandez-Montiel, D., Lizardi, J., Hernandez, J., Herrera Urbina, R., Valdez, M.A., (2003) The zeta potential and surface properties of asphaltenes obtained with different crude oil/*n*-heptane proportions. *Fuel*, 82(8), 869-874.

Patience, R.L., (2003) Where did all the gas go? *Organic Geochemistry*, 34, 375-387.

Pedersen, T., Harms, J.C., Harris, N.B., Mitchell, R.W., Tooby, K.M., (1989) The role of correlation in generating the Heidrun oil field geological model. In: J.D. Collison (Ed.), *Correlation in Hydrocarbon Exploration* (Ed. by J.D. Collison), pp. 327-338. Graham & Trotman.

Pelet, R., Behar, F., Monin, J.C., (1986) Resins and asphaltenes in the generation and migration of petroleum. *Organic Geochemistry*, 10(1-3), 481-498.

Peters, K.E., Moldowan, J.M., (1993) *The biomarker guide: Interpreting molecular fossils in petroleum and ancient sediments.* Englewood Cliffs, Prentice Hall, NJ (United States).

Peters, K.E., Walters, C.C., Moldowan, J.M., (2005) *The Biomarker Guide - 2nd ed.* Cambridge University Press.

Requejo, A.G., Allan, J., Creaney, S., Gray, N.R., Cole, K.S., (1992) Aryl isoprenoids and diaromatic carotenoids in Palaeozoic source rocks and oils from the Western Canada and Williston Basins. *Organic Geochemistry*, 19(1-3), 245-264.

Rovere, C.E., Crisp, P.T., Ellis, J., Bolton, P.D., (1983) Chemical characterisation of shale oil from Condor, Australia. *Fuel*, 62, 1274-1282.

Rubinstein, I., Spyckerelle, C., Strausz, O.P., (1979) Pyrolysis of asphaltenes: a source of geochemical information. *Geochimica et Cosmochimica Acta*, 43(1), 1-6.

Rullkötter, J., Michaelis, W., (1990) The structure of kerogens and related materials. A review of recent progress and future trends. In: B. Durand, F. Behar (Eds.), *Advances in Organic Geochemistry* (Ed. by B. Durand, F. Behar), pp. 829-852. Pergamon Press, Oxford.

Santamaria-Orozco, D., Horsfield, B., di Primio, R., Welte, D.H., (1998) Influence of maturity on distributions of benzo- and dibenzothiophenes in Tithonian source rocks and crude oils, Sonda de Campeche, Mexico. *Organic Geochemistry*, 28(7-8), 423-439.

Schenk, H.J., Dieckmann, V., (2004) Prediction of petroleum formation: the influence of laboratory heating rates on kinetic parameters and geological extrapolations. *Marine and Petroleum Geology.*, 21, 79-95.

Schenk, H.J., Horsfield, B., (1998) Using natural maturation series to evaluate the utility of parallel reaction kinetics models: an investigation of Toarcian shales and Carboniferous coals, Germany. *Organic Geochemistry*, 29(1-3), 137-154.

Selley, R.C., (1997) *Elements of Petroleum Geology*. Academic Press, New York.

Senftle, J.T., Larter, S.R., Bromley, B.W., Brown, J.H., (1986) Quantitative chemical characterisation of vitrinite concentrates using pyrolysis-gas chromatography. Rank variation of pyrolysis products. *Organic Geochemistry*, 9(6), 345-350.

Sinninghe Damste, J.S., Eglinton, T.I., De Leeuw, J.W., Schenck, P.A., (1989) Organic sulphur in macromolecular sedimentary organic matter: I. Structure and origin of sulphur-containing moieties in kerogen, asphaltenes and coal as revealed by flash pyrolysis. *Geochimica et Cosmochimica Acta*, 53(4), 873-889.

Sinninghe Damsté, J.S., Rijpstra, W.I.C., De Leeuw, J.W., Schenck, P.A., (1990) The occurrence and identification of series of organic sulphur compounds in oils and sediment extracts: II. Their presence in samples from hypersaline and non-hypersaline palaeoenvironments and possible application as source, palaeoenvironmental and maturity indicators. *Geochimica et Cosmochimica Acta*, 53(6), 1323-1341.

Speight, J.G., (1999) *The chemistry and technology of petroleum*, Marcel Dekker, New York.

Speight, J.G., Long, R.B., Trowbridge, T.D., (1984) Factors influencing the separation of asphaltenes from heavy petroleum feedstocks. *Fuel*, 63(5), 616-620.

Theuerkorn, K., Horsfield, B., Wilkes, H., di Primio, R., Lehne, E., (2008) A reproducible and linear method for separating asphaltenes from crude oil. *Organic Geochemistry Advances in Organic Geochemistry 2007 - Proceedings of the 23rd International Meeting on Organic Geochemistry*, 39(8), 929-934.

Tissot, B.P., Welte, D.H., (1984) *Petroleum formation and occurrence.* Springer-Verlag.

Ungerer, P., (1990) State of the art of research in kinetic modelling of oil formation and expulsion. *Organic Geochemistry*, 16(1-3), 1-25.

van Graas, G., de Leeuw, J.W., Schenck, P.A., Haverkamp, J., (1981) Kerogen of Toarcian shales of the Paris Basin. A study of its maturation by flash pyrolysis techniques. *Geochimica et Cosmochimica Acta*, 45(12), 2465-2474.

Volkman, J.K., Alexander, R., Kagi, R.I., Rowland, S.J., Sheppard, P.N., (1984) Biodegradation of aromatic hydrocarbons in crude oils from the Barow Sub-basin of West Australia. *Organic Geochemistry*, 6, 619-632.

Welbon, A.L., Beach, A., Brockbank, P.J., Fjield, O., Knorr, S.D., Pederson, T., Thomas, S., (1997) Fault seal analysis in hydrocarbon exploration and appraisal: examples from offshore mid-Norway. In: P. Møller-Peddersen, A.G. Koestler (Eds.), *Hydrocarbon seals - Importance for Exploration and Production*, *7* (Ed. by P. Møller-Peddersen, A.G. Koestler), pp. 125-138. Norsk Petroleumsforening/NPF (Norwegian Petroleum Society) Special publications

Whitley, P.K., (1992) The geology of Heidrun; A giant oil and gas field on the mid-Norwegian shelf. In: M.T. Halbouty (Ed.), *Giant oil and gas fields of the decade 1978-1988*, *Memoir 54* (Ed. by M.T. Halbouty), pp. 383-406. AAPG, Tulsa.

Wilhelms, A., Larter, S.R., (1994a) Origin of tar mats in petroleum reservoirs. Part I: introduction and case studies. *Marine and Petroleum Geology*, 11(4), 418-441.

Wilhelms, A., Larter, S.R., (1994b) Origin of tar mats in petroleum reservoirs. Part II: formation mechanisms for tar mats. *Marine and Petroleum Geology*, 11(4), 442-456.

Wilson, M.A., Philp, R.P., Gillam, A.H., Gilbert, T.D., Tate, K.R., (1983) Comparison of the structures of humic substances from aquatic and terrestrial sources by pyrolysis gas chromatography-mass spectrometry. *Geochim. Cosmochim. Acta* 47, 497-502.